

**Phenomics and transcriptomics applied in  
mode-of-action analyses for developmental  
neurotoxicity of several compound classes *in vitro***

Dissertation to obtain the degree

Doctor rerum naturalium (Dr. rer. nat.)

at the Heinrich-Heine-University Düsseldorf

submitted by

**Jördis Klose**

from

Wolfsburg

Düsseldorf, June 2021





**Phenomik und Transkriptomik angewendet in  
Wirkmechanismus-Analysen für die  
Entwicklungsneurotoxizität mehrerer  
Substanzklassen *in vitro***

Inaugural-Dissertation

Zur Erlangung des Doktorgrades  
der Mathematisch-Naturwissenschaftlichen Fakultät  
der Heinrich-Heine-Universität Düsseldorf

vorgelegt von

**Jördis Klose**

aus

Wolfsburg

Düsseldorf, Juni 2021



Angefertigt am IUF – Leibniz-Institut für umweltmedizinische Forschung gGmbH (IUF)  
an der Heinrich-Heine-Universität Düsseldorf

Gedruckt mit der Genehmigung der  
Mathematisch-Naturwissenschaftlichen Fakultät der  
Heinrich-Heine-Universität Düsseldorf

Referentin: Prof. Dr. Ellen Fritsche

Korreferentin: Prof. Dr. Vlada Urlacher

**Tag der mündlichen Prüfung: 11.10.2021**



***Was wir wissen, ist ein Tropfen,  
was wir nicht wissen, ein Ozean.***

(Isaac Newton)



## Table of Contents

<b>1</b>	<b>Introduction</b> .....	<b>1</b>
1.1	Brain development.....	1
1.2	Developmental Neurotoxicity (DNT).....	3
1.2.1	DNT testing.....	4
1.3	Alternative toxicity testing .....	6
1.3.1	Paradigm shift in toxicology .....	6
1.3.2	New Approach Methodologies.....	7
1.3.3	<i>In vitro</i> DNT testing.....	11
1.4	The 'Neurosphere Assay' as an <i>in vitro</i> model for DNT testing.....	12
1.5	Exemplary compound classes with unknown DNT potential .....	16
1.5.1	Flame retardants .....	16
1.5.2	Chinese Herbal Medicines .....	17
1.7	Aim of this thesis .....	19
<b>2</b>	<b>Manuscripts</b> .....	<b>20</b>
2.1	Development of the Concept for Stem Cell-Based Developmental Neurotoxicity Evaluation.....	22
2.2	Current Availability of Stem Cell-Based <i>In Vitro</i> Methods for Developmental Neurotoxicity (DNT) Testing .....	32
2.3	The Neurosphere Assay as an <i>In Vitro</i> Method for Developmental Neurotoxicity (DNT) Evaluation.....	44
2.4	A transcriptome comparison of time-matched developing human, mouse and rat neural progenitor cells reveals human uniqueness.....	74
2.5	Rabbit neurospheres as a novel <i>in vitro</i> tool for studying neurodevelopmental effects induced by intrauterine growth restriction.....	100
2.6	Neurodevelopmental toxicity assessment of flame retardants using a human DNT <i>in vitro</i> testing battery.....	117
2.7	TBBPA Targets Converging Key Events of Human Oligodendrocyte Development Resulting in Two Novel AOPs.....	158

2.8	Application of the Adverse Outcome Pathway concept for investigating developmental neurotoxicity potential of Chinese Herbal Medicines by using human neural progenitor cells <i>in vitro</i> .....	182
<b>3</b>	<b>Discussion</b> .....	225
3.1	The ‘Neurosphere Assay’ as part of a DNT <i>in vitro</i> testing battery (DNT-IVB).....	226
3.2	From scientific validation to compound classification and prioritization.....	231
3.2.1	Scientific validation of DNT- <i>in vitro</i> assays .....	231
3.2.2	<i>In vitro</i> data analysis .....	232
3.2.3	Compound classification .....	233
3.2.4	Compound prioritization.....	235
3.3	Mechanistical investigations for developing AOPs .....	236
3.4	Moving from hazard characterization to risk assessment .....	239
<b>4</b>	<b>Abstract</b> .....	242
<b>5</b>	<b>Zusammenfassung</b> .....	243
	Abbreviations.....	245
	References .....	253
	Danksagung.....	271
	Eidesstattliche Erklärung/Declaration .....	273

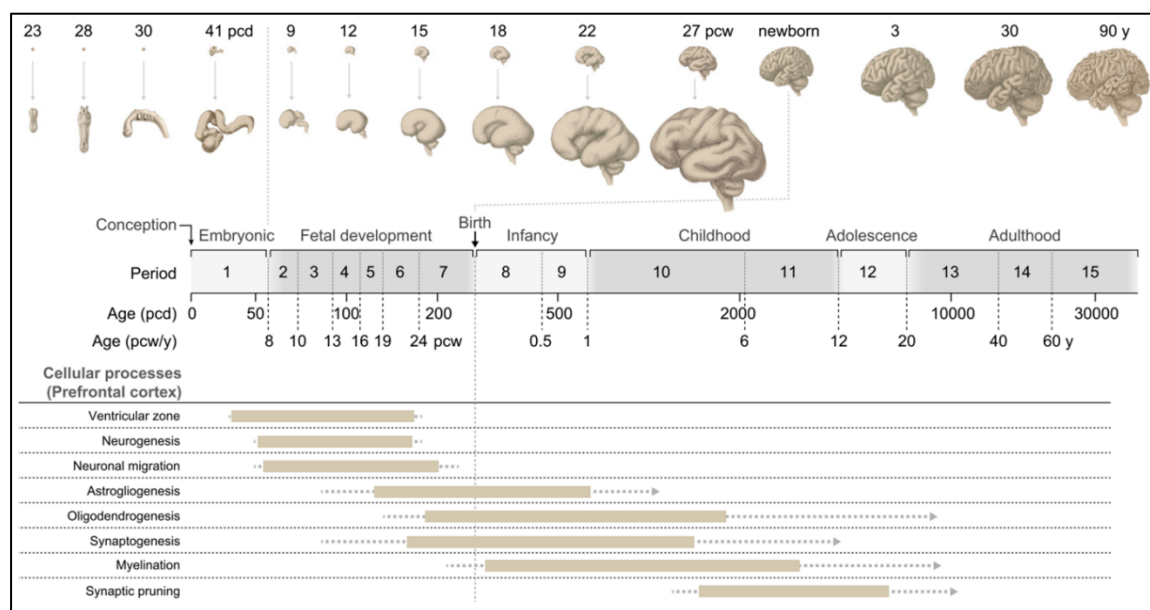


# 1 Introduction

## 1.1 Brain development

The human central nervous system (CNS) is the most complex biological tissue in the body comprising on average 100 billion neurons, ten times more glial cells (Kandel et al. 2000; Azevedo et al. 2009) and approximately 620 trillion to several quadrillion synapses (Silbereis et al. 2016). In order to ensure proper brain function, these cell types have to interact intensively and need to further develop into neuronal subtypes defining inhibitory and excitatory neurons as well as glial cells, further separated into astrocytes, microglia and oligodendrocytes, finally establishing a complex neuronal network (Kandel et al. 2000).

Individual processes of human brain development are highly complex, strictly regulated and continue/last from the early embryonic phase until the mid-20s (Fig. 1).



**Figure 1: Stages of human brain development.** Cellular processes of human brain development are depicted in a time-dependent manner and last from early embryonic phase to adulthood (adapted from Silbereis et al. 2016).

To be exact, human brain development starts three weeks after fertilization with the formation of the neural plate into the neural tube, which represents the first defined brain structure (Stiles and Jernigan 2010; Silbereis et al. 2016). During a phase of enormous cell proliferation, the neural tube expands further to form the five brain vesicles, thereby establish the primary organization of the central nervous system (Linderkamp et al. 2009). In the late embryonic phase, on day 42 post conception, neurogenesis begins. It continues throughout the fetal phase and postnatally in certain brain regions (Stiles and Jernigan 2010). During neurogenesis neural progenitor cells start

to differentiate into neurons and radial glia cells in symmetric or asymmetric divisions. Here, the symmetrical mode of cell division generates pairs of neurons, while during asymmetrical division one daughter cell remains a progenitor cell and the other one become a neuron or a glial cell (Noctor et al. 2004; Huttner and Kosodo 2005). The issue whether divisions are symmetric or asymmetric is intimately linked to the polarized organization of the progenitor itself, the equal versus unequal inheritance of cell fate determinants by the daughter cells, as well as to cell cycle length (Huttner and Kosodo 2005). Differentiation is followed by cell migration to the final position in the brain. Here, radial glia cells migrate to the outer ventricular zone where they are radially orientated to the neocortex (Borrell and Götz 2014). The radial glia migration leads to the development of a scaffold that is used by neurons to migrate along these glial fibers and reach their final cortical position (Borrell and Götz 2014; Fernández et al. 2016). While early-developed neurons settle in a narrow zone above the ventricular zone, lately-developed neurons reach the cerebral cortex, the outer layer of the brain that is composed of up to six layers (Bronner and Hatten 2013; Fernández et al. 2016). Once neurons finish migration and detach from the radial fiber, they differentiate and mature into several subtypes of inhibitory or excitatory neurons. Finally, they begin to extend dendrites and axons and establish connections (synapses) with other neurons in order to form a neuronal network (Sidman and Rakic 1973; Silbereis et al. 2016). Dendritic outgrowth and synaptogenesis begin prenatally but continue into adulthood (Fig. 1). Specifically, synaptogenesis is accompanied by regular strengthening and elimination/pruning (Jung and Bennett 1996; Andersen 2003; Silbereis et al. 2016). Shortly after the beginning of neurogenesis, radial glial cells start to differentiate into astrocytes and oligodendrocytes - a process which is persistent throughout life. Oligodendrocytes are necessary for myelination. They form myelin protein sheets around neighboring axons to isolate them and ensure a higher axonal conduction velocity. During human brain development the process of myelination generally starts around birth and is similar to synaptogenesis characterized by regular pruning during life, depending on individual learning processes (de Hoz and Simons 2015; Marinelli et al. 2016; Kuhn et al. 2019).

All processes are guided by an interplay of several proteins that operate as signaling molecules, receptors, messengers or transcription factors which expression is regulated by genetic, epigenetic and environmental factors. Overall, many cellular and molecular factors determine the correct development of a healthy and functional brain and it is mandatory that all processes take place in spatiotemporal orchestration (Kandel et al. 2000). Therefore, the brain is especially vulnerable towards the adverse effect of chemicals and even small adverse effects might lead to massive adverse outcomes (Volpe 2000; Grandjean and Landrigan 2014; Fernández et al. 2016).

## 1.2 Developmental Neurotoxicity (DNT)

Disturbance of any of the above described processes of brain development, e.g. by chemical action, might lead to cellular, structural, and in the end to functional impairment of the brain is called 'developmental neurotoxicity' (DNT; EPA 1998; OECD 2007). DNT is an important issue that can result in severe biological, social, and economic implications. According to the World Health Organization (WHO), 5 % of the world's children under the age of 15 have some type of moderate to severe neurophysical or cognitive developmental disability (World Health Organization 2008), e.g. lower intelligence quotient (IQ), learning disability, dyslexia, Attention Deficit Hyperactivity Disorder (ADHD) or some kind of autism spectrum disorder. On the basis of the mean IQ of a population, the Mt. Sinai Children's Environmental Health Care Center impressively demonstrated that a reduction of five IQ points leads to an increase of 57 % in the number of mentally retarded (IQ < 70) and a likewise decrease in the very gifted (IQ < 130) parts of the population (Schmidt 2013). Thereby, the cause of the reduced IQ, e.g. environmental chemicals or by medical events such as preterm birth, traumatic brain injury, tumors or congenital heart disease, is irrelevant (Bellinger 2012). Altogether, such socioeconomic consequences can be enormous, causing diminished economic productivity, higher costs due to medication, education and individual support (Grandjean and Landrigan 2006; Bellanger et al. 2013). Along those lines, Bellanger (2013) assessed that methylmercury exposure leads to a cumulative IQ loss of 600,000 IQ points in Europe and 264,000 IQ points in the United States accompanied by socioeconomic costs of several billion US\$ per year. Recently, Gaylord (2020) analyzed data from the National Health and Nutrition Examination Surveys (United States) and revealed known exposure-IQ relationships of polybrominated diphenyl ethers (PBDEs), organophosphates, lead and again methylmercury. During the period from 2001 to 2016, these chemicals led to a loss of 243 million IQ points in total, which can be directly associated with mental retardation in more than 1 million cases. Here, the compound class of PBDEs had the highest impact, as 162 million IQ points were reduced, resulting in more than 700,000 cases of less gifted people. The ranking was followed by lead, organophosphates and finally methylmercury.

In addition to these compounds studied by Gaylord (2020), also arsenic, polychlorinated biphenyls, toluene, fluoride, manganese and tetrachloroethylene (environmental-, or industrial chemicals) have been identified as developmentally neurotoxic to humans. Chlorpyrifos, DDT and DDE (pesticides), valproic acid (medical drug) as well as ethanol and cocaine (drugs of abuse) complement the list of known DNT compounds (Giordano and Costa 2012; Kadereit et al. 2012; Grandjean and Landrigan 2014; Aschner et al. 2017). Considering the fact, that there are more than 180 million substances circulating worldwide (CAS Registry 2021), the DNT potential for the

majority of chemicals has not been evaluated. In accordance, there is still a large data gap especially in the mechanistic understanding of chemically-induced adverse neurodevelopmental outcomes (Grandjean and Landrigan 2006; De Felice et al. 2015; Sachana et al. 2019). In comparison to DNT, more than 200 compounds are known to cause neurotoxicity (NT) in humans. Furthermore, there are experimental data for more than 1000 compounds on their neurotoxic potential in animal *in vivo* or *in vitro* studies (Grandjean and Landrigan 2006).

So far, DNT testing is only mandatory in Europe for pesticides and biocides, while it is required in the United States only for pesticides, upon triggers, that have a known neurotoxic mode-of-action (MoA), a compound structure-activity alert or for substances that cause neurotoxicity or endocrine disruption observed in standard *in vivo* adult, developmental or reproduction studies (Schmidt et al. 2016; Pistollato et al. 2021). Therefore, European regulations do not specifically address more physiologically complex toxicity effects as it is the case for DNT (Pistollato et al. 2021). In general, it is assumed that the developing nervous system is especially susceptible to adverse chemical actions, as the blood brain barrier (BBB) is not fully developed. Thus, hydrophilic chemicals and ionic substances can enter the developing brain more easily than the adult brain (Pardridge 1998; Claudio et al. 2000). Another reason is based on the extremely high plasticity of the developing brain characterized by highly coordinated molecular and cellular changes taking place during neurodevelopment, which are mostly completed in adulthood.

Considering the high vulnerability of the developing brain, there is a high probability that additional chemicals affect human brain development. Hence, the current safety margins derived from NT or other toxicity studies do not necessarily protect the developing brain and the current triggers for DNT studies are insufficient (Radonjic et al. 2013; Terron and Bennekou Hougaard 2018). Moreover, it is to note, that not only intoxications with high chemical exposure raise concerns for brain development, but also chronic low dose and especially the exposure towards a mixture of compounds is thought to contribute to the increasing incidence of neurodevelopmental disorders (Grandjean and Landrigan 2014; Bennett et al. 2016). Therefore, European regulators are currently considering DNT studies as regulatory requirements not only for pesticides, but also for other chemicals and drugs (Sachana et al. 2019).

### 1.2.1 DNT testing

Current DNT testing is performed according to the available United States Environmental Protection Agency (US EPA) and the Organization for Economic Co-operation and Development (OECD) *in vivo* guideline studies, EPA 870.6300 DNT guideline (EPA 1998) and the draft OECD guideline 426 (OECD 2007). These guideline studies are conducted preferably in rats, and

compounds are tested over a period from early gestation until the end of lactation. They are focused on observations of neurologic and behavioral abnormalities in neonatal and young animals, as they include tests describing physical development, behavioral ontogeny, motor and sensory function, motor activity, learning and memory as well as the assessment of brain weights and neuropathology.

Compared with the thousands of chemicals that humans may be exposed to, including everyday products and those released into the environment by external sources, only approximately 150 chemicals have been assessed by using these guideline studies, most of them being pesticides (Sachana et al. 2019). This huge data gap is mainly due to the not sufficiently sensitive triggers (Radonjic et al. 2013; Terron and Bennekou Hougaard 2018) for requesting the *in vivo* guideline studies. In addition, these studies are highly demanding with regard to time and money, as they take about one year per compound and cost up to one million US\$ (Rovida and Hartung 2009; Crofton et al. 2012). Moreover, they are of particular ethical concern, since approximately 140 dams and 1,000 juvenile rats are needed just for evaluating one compound (Lein et al. 2005; Crofton et al. 2012). Thus, they are not suited for testing large amounts of chemicals (Tsuji and Crofton 2012; Fritsche et al. 2018c). Further limitations include their high variability and lack of reproducibility as well as the uncertainty of extrapolation from animals to humans (Tsuji and Crofton 2012; Leist and Hartung 2013; Terron and Bennekou Hougaard 2018; Sachana et al. 2019). Especially the mechanistic understanding of chemically-induced adverse neurodevelopmental outcomes cannot be provided and despite many tested endpoints, they may not sufficiently mirror human health outcomes, for example with regard to cognitive functions (Terron and Bennekou Hougaard 2018; Sachana et al. 2019). Therefore, regulators, academic, and industrial scientists recently agreed on a need for a new testing strategy to assess the DNT potential of chemicals, which is supposed to be faster and less expensive, as well as more relevant to humans, e.g. by using human cell-based models (EFSA 2013; Crofton et al. 2014; Bal-Price et al. 2015a, 2018; Fritsche et al. 2015, 2017, 2018c, a).

Since 2005, in the field of DNT, a number of workshops and stakeholder meetings took place with the aim to illustrate the need for a new framework to develop and use *in vitro*, *in silico* and alternative species test methods that deliver useful data for regulatory decision-making (Sachana et al. 2019). Based on the international efforts described more in detail in Sachana et al. (2019) the OECD and EFSA organized a workshop in 2016 (Fritsche et al. 2017). Here, scientific consensus emerged that a proposed draft *in vitro* testing battery should be applied instantly to screen and prioritize chemicals, be harmonized by an international acceptance process through OECD and eventually be used for hazard characterization. Thus, this workshop formed the basis of a number

of global projects, including a US EPA supported project to develop and validate *in vitro* DNT methods (US EPA 2020), an EFSA funded project for generating data from a DNT *in vitro* testing battery (DNT-IVB; see 1.4, 3.1; Masjosthusmann et al. 2020), a project led by the Danish EPA (DK EPA, grant number MST-667-00205) to test high priority pesticides, as well as another project, funded by the US NTP (Behl et al. 2019), regarding the development of a rapid and cost-effective screening strategy to prioritize replacements for specific compound classes (e.g. flame retardants). Moreover, another important response to this workshop was the initiation of an OECD project, which is currently developing a guidance document that will introduce a framework to facilitate the regulatory use of DNT *in vitro* data derived from a time-and cost-efficient testing battery through an integrated approach to testing and assessment (IATA). This OECD guidance document is expected to be finalized in fall 2021.

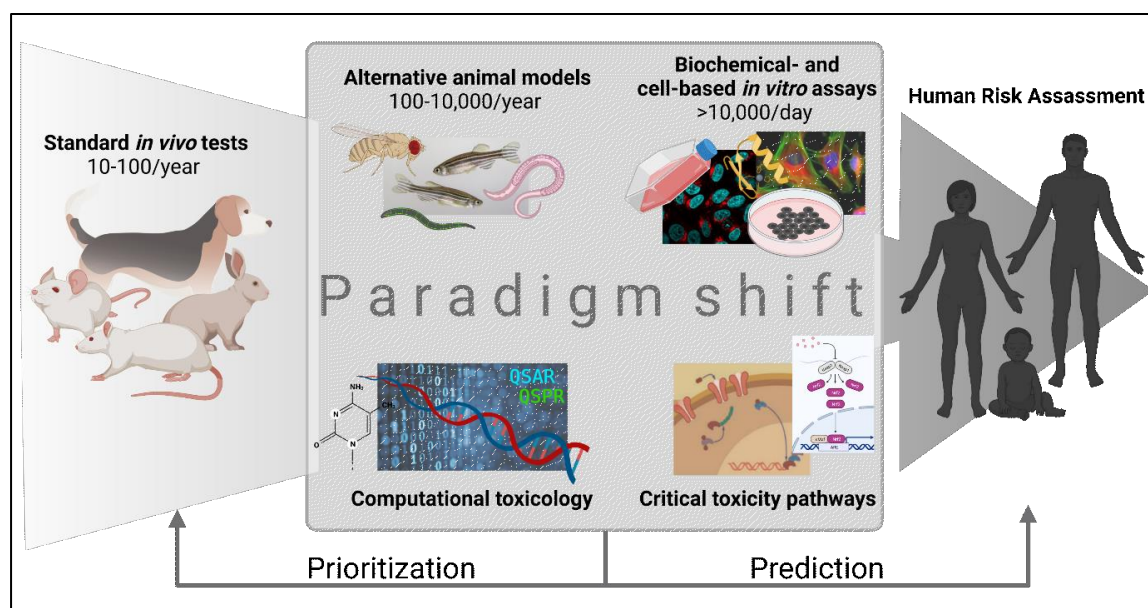
### 1.3 Alternative toxicity testing

The aim of classical toxicological risk assessment is to establish safety factors for human exposure based on the evaluation of the outcome of animal tests. The dose, which causes no toxicologically relevant effect in the animal studies is extrapolated to the no-effect dose in humans based on the application of appropriate safety factors that account for toxicodynamic and toxicokinetic inter-species differences as well as inter-individual susceptibilities (EFSA 2012; Konietzka et al. 2014). However, the current toxicological testing for human risk assessment is particularly questionable due to low prediction, known species differences and especially the increasing societal awareness of animal testing, illustrating the need to advance alternative testing approaches (Russell and Burch 1959; Dorman et al. 2001; Kaufmann 2003; Tsuji and Crofton 2012; Leist and Hartung 2013).

#### 1.3.1 Paradigm shift in toxicology

In 2007 the US National Research Council (NRC) published the report 'Toxicity Testing in the 21<sup>st</sup> Century: A Revision and a Strategy' (NRC 2007). They recommended a paradigm shift for toxicity testing by using alternative, toxicity pathway-based high throughput methods for human hazard and risk assessment instead of apical endpoint measurements in *in vivo* studies. Here, the new testing strategy is focused on the application of alternative methods, e.g. *in vitro*-based cell models or model organisms, like *Caenorhabditis elegans* (*C. elegans*), *Danio rerio* (zebrafish) and *drosophila melanogaster*, in combination with molecular and computational biology or biotechnology, such as toxicogenomics and bioinformatics. The obtained data can be analyzed by using *in silico* methods like quantitative structure-property and structure-activity (QSPR and

QSAR), followed by read across structure-activity relationship (RASAR) with other compounds and their known underlying MoA, which is useful for compound prioritization for further testing in *in vivo* studies. Overall, the recommendations from the NRC allow a time- and cost-efficient screening of large amounts of compounds with a more mechanism-based hazard identification (Collins et al. 2008; Gibb 2008; Krewski et al. 2009, 2020; Ginsberg et al. 2019). To date, the progress has confirmed the integrity and fidelity of the NRC vision, which is well on its way to becoming reality, since e.g., internationally government agencies are beginning to incorporate the new approach methodologies envisioned in the original NRC report into regulatory practice (Krewski et al. 2020). Figure 2 visualizes the new toxicity testing approach envisioned by the NRC.



**Figure 2: Paradigm shift in toxicology.** The combination of high throughput *in vitro* cell-based methods and alternative organisms with computational toxicology will allow the screening of a large amount of substances, the prioritization of chemicals for further testing and can assist in prediction of human risk assessment (adapted from Collins et al. 2008). Figure created with BioRender.com.

### 1.3.2 New Approach Methodologies

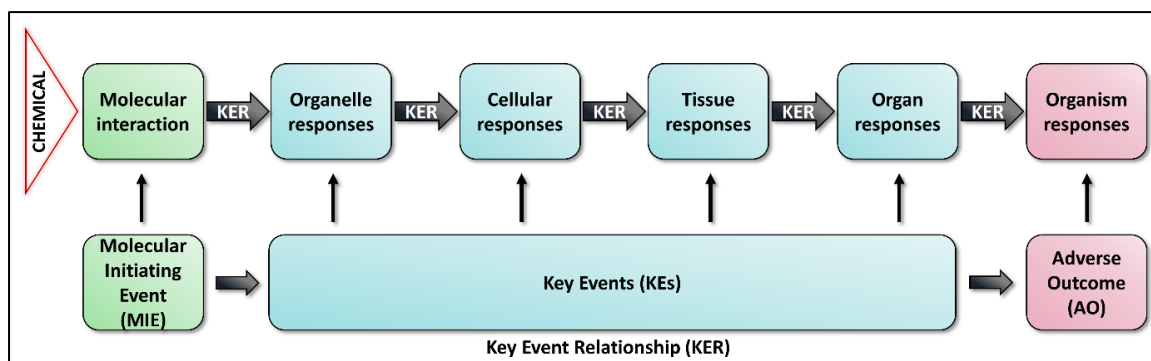
New approach methodologies (NAMs) are non-animal-based methods, which can be used to provide information on chemical hazards. NAMs generate data on the toxicodynamic of a compound to support the proposed paradigm shift in toxicology - moving from the sole use of apical endpoints generated in animals towards a mechanistic understanding and more human-relevant approaches for regulatory applications (NRC 2007; Collins et al. 2008).

Currently, many testing approaches, irrespective of the particular methodology used, do not result in a mechanistic understanding of the induced toxicity. Especially, non-animal testing approaches

exhibit a real challenge to understand the relationship between what is tested and the apical toxicity endpoint being predicted. Therefore, results from novel approaches are not yet widely used for regulatory purposes. From the regulatory point of view, there is a clear need for an objective and systematic framework, which characterizes the individual biological and toxicological relevance of novel methods for predicting an adverse effect. The same framework can be combined with other tools and methods to benefit from an integrated approach (OECD 2020). Therefore, the 'Integrated Approaches to Testing and Assessment' (IATA) concept has been proposed by the OECD member states to embed alternative testing strategies into weight of evidence assessment for decision-making by using data from various information sources (OECD 2016, 2020). IATA information can comprise results from one or the combination of many methodological approaches (QSAR, QSPR, RASAR, *in silico*, *in chemico*, *in vitro*, *ex vivo*, *in vivo*) as well as '-omic' technologies (e.g. toxicogenomics). Thereby, the construction of IATAs is highly flexible, depending on the regulatory need and respective assessment context. However, IATAs should be mechanistically informed, thus illustrating the knowledge of the mechanisms through which chemicals exert their toxicity (Tollefsen et al. 2014). Mechanistic understanding offers a frame for the analysis of information from methods that target different levels of biological organization, enabling the contribution of results in deciding on the possibility of the adverse outcome (Tollefsen et al. 2014; OECD 2015, 2020; Patlewicz et al. 2015). Such mechanistic understanding might arise from Adverse Outcome Pathways (AOPs).

AOPs are structured organizations of causally related biological events leading to adverse effects relevant for the human organism and population (Fig. 3). More in detail, they provide mechanistic information on the molecular initiating event (MIE), molecular, cellular, structural and functional key events (KEs) and associated key event relationships (KER), finally end in an adverse outcome (AO) that can be common to different MIEs (Ankley et al. 2010; OECD 2016). Thereby, AOPs serve as a knowledge assembly and communication tool between research and regulatory communities involved e.g. in regulatory and systems toxicology, biomedical challenges, in safety evaluations associated with drug development and clinical trial simulations (Carusi et al. 2018), thus covering a broad biomedical application domain. An essential platform for AOP documentation, that is currently most developed, is the AOP-Wiki (<http://aopwiki.org>), which provides a formalized, transparent and quality-controlled data documentation and hence facilitates knowledge exchange between research and regulatory communities (Kandel et al. 2000; Vinken et al. 2017).





**Figure 3: Schematic illustration of the 'Adverse Outcome Pathway' concept.** An AOP is based on a sequence of molecular, cellular, structural and functional key events (KEs), triggered by a molecular initiating event (MIE) in which a chemical interacts with a biological target(s), resulting in an adverse outcome (AO) relevant for the human organism and population. Single KEs are associated to KE relationships (KER; adapted from Bal-Price and Meek 2017).

In order to realize a consistent, scientifically rigorous and transparent AOP development, there are some principles and strategies to consider: (1) AOPs are not chemical specific; (2) AOPs are modular and composed of reusable components, notably KEs and KERs; (3) An individual AOP, composed of a single sequence of KEs and KERs, is a pragmatic unit of AOP development and evaluation; (4) Networks composed of multiple AOPs that share common KEs and KERs are likely to be the functional unit of prediction for most real world scenarios; and (5) AOPs are living documents that will evolve over time as new knowledge is generated (Villeneuve et al. 2014).

The overall aim of the AOP concept is to obtain a more predictive hazard characterization and classification of chemicals as it is currently the case. For example, MIEs shared by different compounds can be used for read across approaches which will facilitate compound prioritization for further testing (Bal-Price et al. 2015b). The organization of mechanistical information will automatically generate more AOPs, identifying connections between the AO in the applied alternative models compared to the AO in populations. This allows for a better interpretation of findings *in vitro* or in alternative organisms. To obtain physiologically relevant data, which are ideally based on KEs defined in an AOP, the applied *in vitro* system should reflect the human *in vivo* situation as precisely as possible (Bal-Price et al. 2015b). The number and diversity of AOPs continues to grow, illustrating the necessity to create AOP networks (Pollesch et al. 2019). An AOP network can be generated whenever, e.g. a MIE or KE is linked to more than one AOP. This is important to avoid that AOP developers describing only linear paths and enables data connections clearly displayed (Knapen et al. 2018).

So far, development of AOPs for DNT is extremely challenging, since spatiotemporal orchestration of molecular and cellular processes is essential for proper human brain development (Bal-Price et al. 2015b; Bal-Price and Meek 2017). Due to the manifold KEs that occur in a time- and brain region-specific manner, creation of AOPs for DNT that cover the whole DNT-sensitive period of

time will be a continuous effort that is far from being completed at the moment. To date, seven AOPs are endorsed by the OECD, eleven were submitted to the AOP Wiki (<https://aopwiki.org/>) and quite a few were published in the scientific literature (Bal-Price et al. 2016; Bal-Price and Meek 2017; Barenys et al. 2019; Li et al. 2019; Spinu et al. 2019; Chen et al. 2020; Manuscript 7 - Klose et al. 2021b).

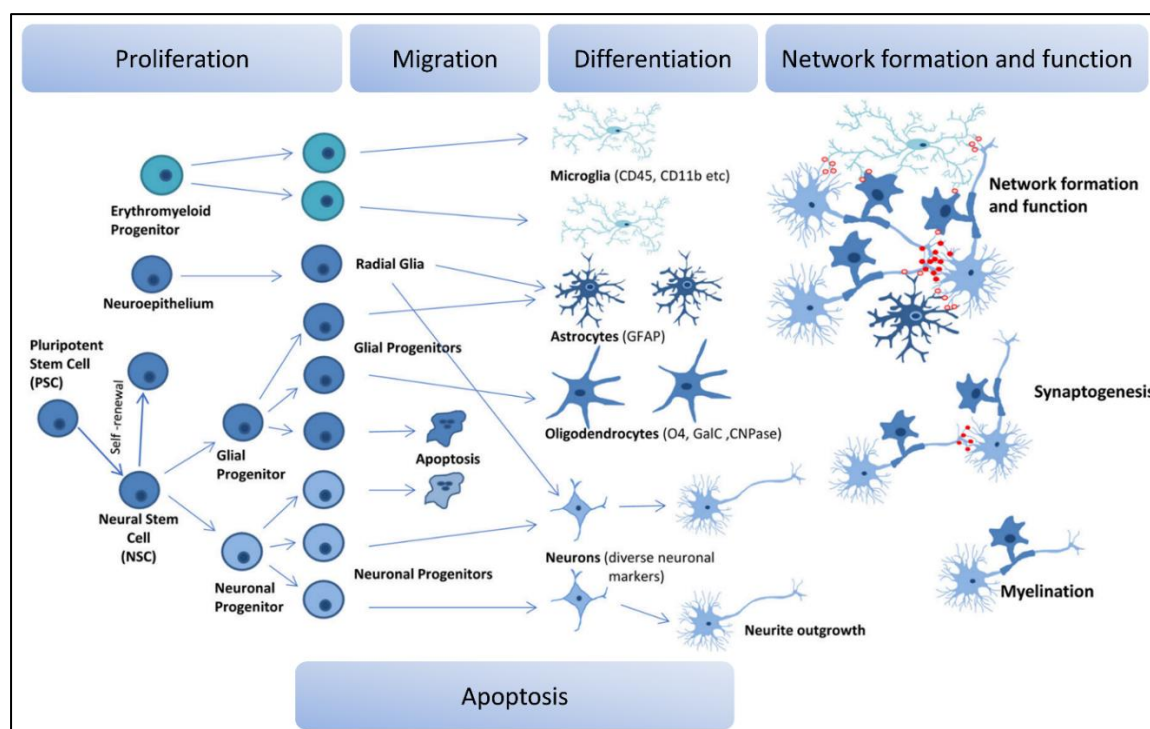
Another approach with high relevance for the paradigm shift is the 'ToxCast Screening Project' (EPA's *Toxicity Forecaster*), which was evolved by the US EPA. The ToxCast program uses high-throughput screening methods and computational toxicology approaches to evaluate chemical properties and bioactivity profiles, that can be finally used for their ranking and prioritization (Dix et al. 2007). Therefore, ToxCast screens chemicals in more than 700 high-throughput assay (HTA) endpoints, covering an enormous range of high-level cell responses. To date, information for approximately 1,800 chemicals from a broad range of sources including industrial and consumer products, food additives, and potentially green chemicals that could be safer alternatives to existing chemicals, are available (Status May 2021; <https://www.epa.gov/chemical-research/toxicity-forecasting>). Similar to the AOP concept, ToxCast data are publicly available, ensuring knowledge sharing, and can be used for AOP building from 'data mining' (Villeneuve et al. 2014) as exemplified in Knudsen and Kleinstreuer (2011). In addition, the ToxCast Dashboard offers the possibility to compare non-ToxCast with ToxCast data when the identical chemicals were studied (manuscript 2.6 - Klose et al. 2021a).

A further approach, specialized on the DNT potential of environmental chemicals, offers the 'Developmental NeuroToxicity Data Integration and Visualization Enabling Resource' (DNT-Diver) generated by the US National Toxicology Program (NTP; Behl et al. 2019). The NTP provides a platform for collecting, bio statistically analyzing and presenting data of a battery of *in vitro* (primarily human) and alternative animal assays (mainly zebrafish) to quantify chemical effects on a variety of neurodevelopmental processes. Therefore, the NTP is a highly collaborative project with approximately 40 participants spanning across domains of academia, industry, government and regulatory agencies. To close the gap of compound uncertainties, like impurities or concentration variabilities, and for better comparison of single data, collaborators that generated data with cell-based assays and alternative organisms use a targeted set of compounds provided by the NTP. In order to be able to compare results across the applied assays, the NTP analyzed all assay results by using benchmark concentration (BMC) modelling. In comparison to the traditionally used NOAEL (No Observed Adverse Effect Level), the value where the level of exposure (dose or concentration) indicates no biological or significant observation of an adverse effects, the BMC modelling is largely independent of the chosen study design. Thereby, the BMC

is based on the fitting of various mathematical models and identifies a dose or a concentration that produces a predetermined change, commonly percentage, in the response rate of an adverse effect, called the benchmark response (BMR; Davis et al. 2011). The NTP then shares the respective results with the contributing researchers and subsequently provides them online (Behl et al. 2019; <https://ntp.niehs.nih.gov/>).

### 1.3.3 *In vitro* DNT testing

Due to the limitations of current DNT testing *in vivo*, coupled with an increasing need to assess the hazards of thousands of compounds, there is a clear need to for a more efficient and predictive DNT testing strategy (EFSA 2013; Crofton et al. 2014; Bal-Price et al. 2015a, 2018; Fritsche et al. 2015, 2017, 2018c, b). For such an *in vitro* testing strategy, different alternative DNT assays need to be set up in a test battery, covering a large scale of major KEs necessary for brain development (Fig. 4). A single *in vitro* test system alone is not able to fully mimic the immense complexity of human brain development and its maturation.

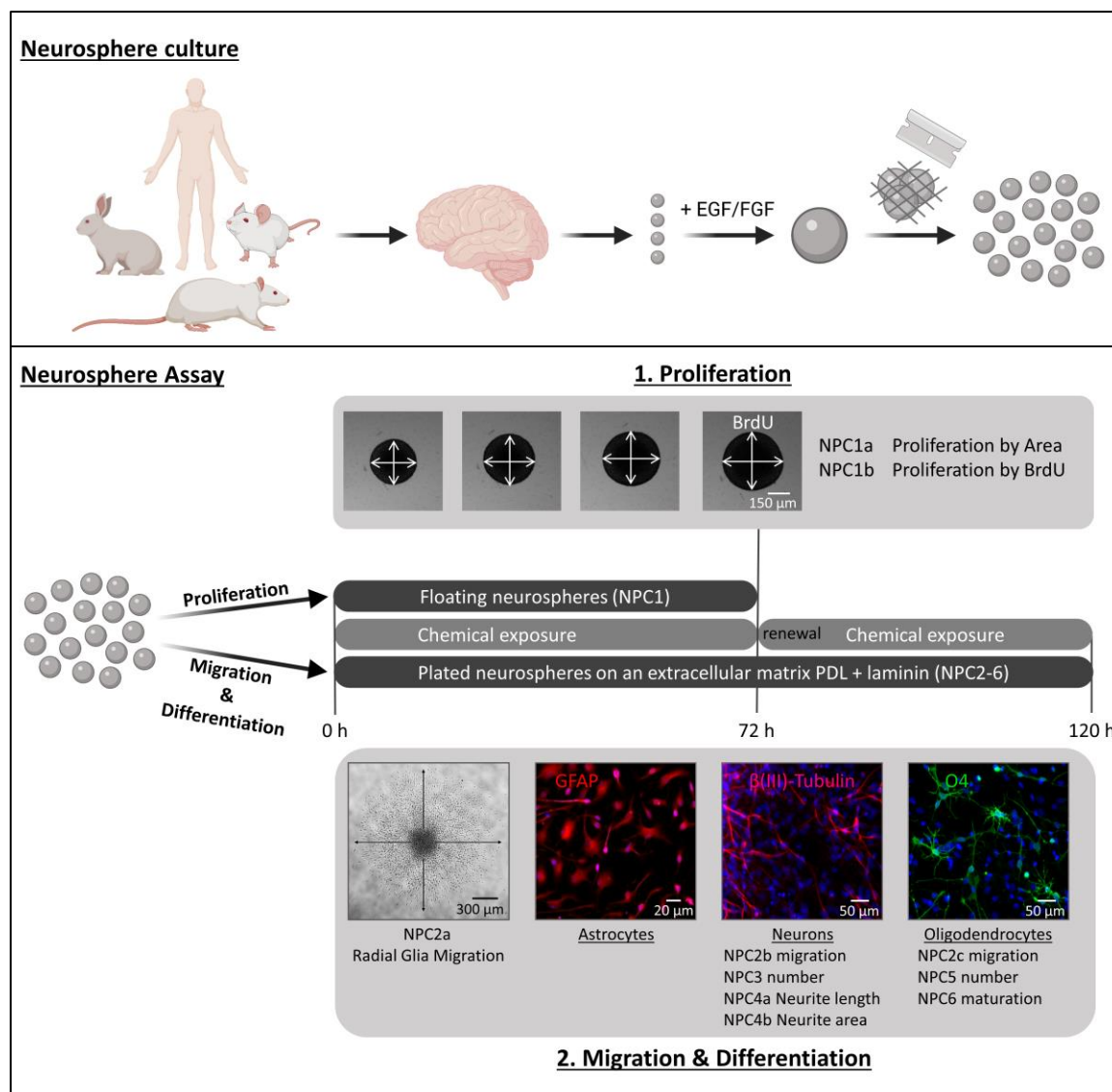


**Figure 4: Overview of neurodevelopmental processes essential for brain development.** Several processes are essential for nervous system development, coming from simple precursors (left) to complex functional tissue with cell-cell interactions (right). It is assumed that DNT toxicants exert their toxicity by disturbing at least one of these processes. Therefore, disturbances of the processes depicted here in blue boxes are key events of adverse outcome pathways relevant for DNT. For a DNT *in vitro* test battery all these biological processes should be covered by one or more test methods (adapted from Bal-Price et al. 2018).

In the last decades, the field of *in vitro* testing has progressively produced a huge selection of alternative models, resembling several developmental processes in different species, cell types as well as brain regions and developmental stages (Fritsche et al. 2015, 2018a). Here, primary rat cells are the most abundant and best studied cell system, addressing developmental processes at distinct neurodevelopmental timing. Despite their usefulness for a variety of applications, the issue of inter-species extrapolation from rats to humans is still omnipresent (Fritsche et al. 2017; Terron and Bennekou Hougaard 2018; Sachana et al. 2019). Recently, six human-based cell models (hESC, hiPSC, hNPC, ReNcell CX, hUCBSC and LUHMES cells) were identified, enabling the assessment of 16 neurodevelopmental KEs *in vitro* (Fritsche 2016; Bal-Price et al. 2018). However, these KEs are not comprehensive as they fail to cover processes relevant for radial glia proliferation, glia maturation, dendritic spine formation, dendrite formation, axonal growth, neuronal maturation and neuronal network formation. That is why rodent-based models have to be considered until human-based models reach a state of readiness which is suitable for compound testing (Fritsche 2016; Bal-Price et al. 2018).

### 1.4 The 'Neurosphere Assay' as an *in vitro* model for DNT testing

One test system, which is useful for studying several neurodevelopmental KEs and part of the above described proposed *in vitro* test battery, is the 'Neurosphere Assay', a three-dimensional (3D) primary *in vitro* cell culture model based on primary neural progenitor cells (NPCs). During the last 15 years, the 'Neurosphere Assay' has been established, well characterized and standardized for regulatory use (Moors et al. 2007, 2009; Baumann et al. 2014, 2015, 2016; Barenys et al. 2017, 2019, 2021; manuscript 2.4 - Masjosthusmann et al. 2018; Nimtz et al. 2019). NPCs are gained from full brain homogenates of human fetuses of gestational week 16 to 19, or rodent and rabbit brains at comparable developmental times (Workman et al. 2013), allowing the direct comparison between species in very similar cell systems (Baumann et al. 2016; Barenys et al. 2017, 2021; Dach et al. 2017; Masjosthusmann et al. 2018; Walter et al. 2019). NPCs, cultured as free-floating 3D neurospheres, are able to mimic multiple KEs of brain development, e.g. proliferation, migration and differentiation into neural effector cells (radial glia cells, astrocytes, neurons and oligodendrocytes). A schematic overview over NPC culturing and the assay procedure is given in Figure 5.



**Figure 5: NPC culture and experimental setup of the ‘Neurosphere Assay’.** NPCs are generated from fetal human brain (purchased from Lonza, Verviers, Belgium) or postnatal day 1 (PND1) mouse, rat and rabbit brains by dissection, digestion and homogenization. NPCs are cultivated as free-floating 3D neurospheres in the presence of growth factors (EGF, FGF). Neurospheres are passaged by mechanical dissociation. After withdrawal of growth factors and contact to an extracellular matrix (ECM) consist of Poly-D-Lysine (PDL) and Laminin, cells adhere and migrate radially out of the sphere core, thereby differentiating into the main effector cells of the brain, namely astrocytes (red), neurons (magenta) and oligodendrocytes (green). Cell nuclei are stained with Hoechst 33258 (blue).

The ‘Neurosphere Assay’ consists of six individual assays: proliferation assay (NPC1a/b), migration assay (NPC2), as well as neuronal differentiation assay (NPC3), neuronal morphology assay (NPC4), oligodendrocyte differentiation assay (NPC5), and thyroid hormone (TH)-dependent oligodendrocyte maturation assay (NPC6), all measuring different endpoints under chemical exposure. For saving time and resources, the assays NPC2-5 can be multiplexed. Figure created with BioRender.com.

In suspension culture and in presence of growth factors, human epidermal growth factor (EGF) and human or rat fibroblast growth factor (FGF), isolated NPCs continue to proliferate and form 3D neurospheres (Reynolds et al. 1992; Buc-Caron 1995; Svendsen et al. 1995; Chalmers-Redman et al. 1997). 3D cultures are thought to resemble the *in vivo* situation better than 2D monolayer cultures due to their superior complexity of directional growth, cell-to-cell- and cell-to-matrix connectivity (Yamada and Cukierman 2007; Alépée 2014). Neurospheres can be passaged by

periodical mechanical dissociation, thereby enabling culture for several weeks (rodent, rabbit NPCs) or even month (human NPCs; Svendsen et al. 1997, 1998). Upon withdrawal of growth factors and plating on a PDL/laminin matrix, NPCs radially migrate out of the sphere core and start to express proteins of the main brain effector cells: glial fibrillary acidic protein (GFAP) for astrocytes, beta-III-tubulin (TUBB3) for neurons and O4 for oligodendrocytes (Piper et al. 2001; Reubinoff et al. 2001; Moors et al. 2009). Thereby, the stem/progenitor cell characteristics, evident by nestin expression, decreases with increasing migration and differentiation time (Schmuck et al. 2017; Hofrichter et al. 2017). The multicellularity of differentiating neurospheres holds the advantage of more physiological cell-cell interactions and communication compared to conventionally single cell type cell systems.

The 'Neurosphere Assay' is set up to analyze compounds' impacts on NPC development. Proliferation is assessed by measuring area size increase over time (NPC1a) and by incorporation of the thymidine analogue bromodeoxyuridine (BrdU, NPC1b), which is an indirect measure of DNA synthesis. Effects on NPC migration are determined by measuring the radial glia migration distance (NPC2a) from the sphere core. Additionally, neuronal (NPC2b) and oligodendrocyte migration (NPC2c) are defined as mean distance of all neurons/oligodendrocytes within the migration area divided by radial glia migration distance. The differentiation into neurons (NPC3) and oligodendrocytes (NPC5) is determined as number of all  $\beta$ (III)tubulin- and O4-positive cells in percent of the total number of Hoechst-positive nuclei in the migration area. Up to date, detection of astrocytes is not fully included within the standardized assay procedure. All neurons that were identified in NPC3 are analyzed for their morphology by characterizing neurite length (NPC4a) and area (NPC4a). Strikingly, all test methods except for NPC1 can be multiplexed and deliver simultaneous readouts on a variety of migration and differentiation endpoints. Another independent assay is focused on thyroid hormone (TH)-dependent oligodendrocyte maturation (NPC6). It is well documented that the terminal differentiation into myelinating oligodendrocytes is tightly regulated by THs, especially the thyroxine metabolite triiodothyronine (T3; Annunziata et al. 1983; Baas et al. 1997). By quantifying mRNA expression of myelin basic protein (*MBP*, for human NPC) or myelin oligodendrocyte glycoprotein (*Mog*, for rodent NPC) divided by the percentage of oligodendrocytes (assessed in NPC5) in the mixed-culture migration area of each neurosphere, the (TH)-dependent oligodendrocyte maturation can be examined, thereby identifying compounds acting as TH disruptors (Dach et al. 2017; manuscript 2.7 - Klose et al. 2021b). In addition, the evaluation of DNT-specificity of compound effects is investigated by comparison of specific DNT endpoints to simultaneously assessed unspecific cytotoxicity (LDH assays) and viability (Alamar Blue assay).

A high content image analysis (HCA) tool (Omnisphero) allows a fast and automated quantification of migration distance, neuronal differentiation and their morphology as well as differentiation into oligodendrocytes (Schmuck et al. 2017). Two convolutional neural networks (CNN), that are implemented in Omnisphero are able to identify neurons and oligodendrocytes, and facilitate a reliable and reproducible analysis, free of human counting bias (Förster et al. submitted 7<sup>th</sup> June 2021 to Cytometry Part A).

Altogether, all endpoints can be analyzed at least in a medium throughput set up allowing a fast and cost-efficient screening of chemicals.

The 'Neurosphere Assay' is part of a current EFSA/OECD DNT *in vitro* testing battery (DNT-IVB) that was recently assembled for regulatory purposes and challenged with 119 compounds of different compound classes (e.g. carbamates, metals, neonicotinoids, organochlorines/fluorines, and organophosphates pyrethroids; Masjosthusmann et al. 2020). Next to the NPC-based methods (NPC1-5), human induced pluripotent stem cell (hiPSC)-derived neural crest cells (NCC), human mesencephalic cells (LUHMES) and hiPSC-derived peripheral neurons were applied to study further neurodevelopmental KEs *in vitro*, like NCC migration (cMINC/UKN2) and additively neurite morphology (NeuriTox/UKN4, PeriTox/UKN5; Krug et al. 2013a; Nyffeler et al. 2017b; Delp et al. 2018). Using selected known human DNT positive and negative compounds as benchmarks, this battery performed with a sensitivity of 82.7 % and a specificity of 88.2 % (Masjosthusmann et al. 2020).

## 1.5 Exemplary compound classes with unknown DNT potential

Despite regulations like REACH (Registration, Evaluation, Authorization, and Restriction of Chemical substances), several compounds have already been marketed without having a full profile of their environmental behavior and toxicological properties. Especially, the evidence for causing DNT in humans has been substantiated only for few compounds (Grandjean and Landrigan 2014; Aschner et al. 2017), whereas the DNT potential for the majority of chemicals has not been evaluated.

In this thesis, two case studies of substance classes that in general have very little information on DNT hazard were performed. One for screening and prioritization of flame retardants (FRs) and one on hazard characterization of two Chinese Herbal Medicines (CHMs).

### 1.5.1 Flame retardants

The chemical group of FRs comprises diverse classes of compounds, applied to furniture and consumer products, like plastics and textiles, as well as to electrical devices and infant products to reduce the risk of fire. FRs reduce the risk of fire as they inhibit or delay the spread of fire by suppressing the chemical reactions in the flame or by forming a protective layer on the surface of a material.

Within the past decades FRs like polychlorinated biphenyls (PCBs) or PBDEs have been identified as threats to human health (Kimbrough 1995; Darnerud et al. 2001).

The earliest FRs used were PCBs. Due to their toxicity, PCBs were already banned in 1977 (Kimbrough and Krouskas 2003) and subsequently chlorine was substituted by bromine resulting in PBDEs. However, also PBDEs were identified as hazardous to human health, as they especially induce neurodevelopmental toxicity (Chao et al. 2007; Roze et al. 2009; Shy et al. 2011; Eskenazi et al. 2013). Consequently, they were banned in the early 2000's (Blum et al. 2019) but are still persistent in the environment, including humans (Shaw and Kannan 2009; Yogui and Sericano 2009; Ma et al. 2013; Law et al. 2014). Considering the toxicological concerns and the wide application of PBDEs, there was a clear need to replace these compounds by safe(r) and less persistent alternatives. PBDEs were first replaced by other brominated flame retardants (e.g. tetrabromobisphenol A (TBBPA)) and further substituted by organophosphorus FRs (OPFRs). Despite regulations like REACH several OPFRs have already been marketed without having a full profile of their toxicological potential. The global FR consumption has exceeded 2 million tons per year and is yet expected to increase due to international flammability standards (Ceresna 2018). Similar to PBDEs, OPFRs are not chemically bound to polymers, leading to a high potential of leakage into the environment by volatilization, abrasion and dissolution (van der Veen and de Boer 2012; Wang et al. 2015). Thus, an ubiquitous occurrence of OPFRs in various indoor environmental matrices, such as food, drinking water, indoor air and dust can be observed and humans are multiply exposed to OPFRs via ingestion, inhalation and dermal absorption (Bacaloni et al. 2007; Bergman et al. 2012; Waaijers et al. 2013; Fromme et al. 2014; Poma et al. 2018; Ma et al. 2019; Chupeau et al. 2020).

Children and especially toddlers are highly exposed towards FRs via house dust, as they frequently proximate to the floor and exercise hand-to-mouth activities. In contrast, infants, older children or adults are mainly exposed via cord blood, breast milk or food, respectively (reviewed by Sjödin et al. 2003; Frederiksen et al. 2009). In addition, the internal doses of FRs measured in children are higher compared to adults due to their higher body surface area to internal mass ratio (Mizouchi et al. 2015; Butt et al. 2016; Sugeng et al. 2017).



In contrast to the PBDEs, there is still relatively limited information regarding the toxicity of OPFRs, including their effects on brain development. However, it is a primary area of concern, as OPFRs bear some structural similarities to organophosphorus pesticides, that have been identified to disturb nervous system development (Grandjean and Landrigan 2006, 2014; Burke et al. 2017; Mie et al. 2018). Other studies have illustrated that OPFRs also act as neurotoxicants (Luttrell et al. 1993; Behl et al. 2015; Gasperini et al. 2017), and *in vitro* data based on *C. elegans* and zebrafish larval demonstrate abnormalities regarding their development upon exposure to some OPFRs (Behl et al. 2015; Alzualde et al. 2018). Concerning DNT, recent studies clearly demonstrate the DNT potential of OPFRs in rat primary spheroids (Hogberg et al. 2020) and rat cortical neurons (Behl et al. 2015). Furthermore, first epidemiological studies have reported associations between OPFR exposure and behavioural abnormalities and impaired cognitive performance in children (Hutter et al. 2013; Lipscomb et al. 2017). However, the dataset available for the DNT potential of OPFRs reveals a gap, specifically regarding their MoAs and human-based toxicity assessment.

### 1.5.2 Chinese Herbal Medicines

Traditional Chinese Medicine (TCM) has been applied for thousands of years. TCM practitioners use diverse mind and body practices, like acupuncture and Thai Chi, as well as herbal products to prevent a broad variety of health problems (Hu 2015). The multitude of CHMs are a substance class with in general has very little information on DNT hazard. For centuries, CHMs have been widely used during pregnancy to relieve symptoms like morning sickness (Flaws 2005) and treat complications, especially to prevent miscarriage during early pregnancy (Li et al. 2013). There are thousands of CHMs, amongst them more than 300 are currently administered to pregnant women in clinical practices.

Generally, CHMs are considered safe due to their natural origin and availability as teas. In contrast to pharmaceuticals or products of western medicine/chemical community and their strictly regulated approval procedures, purchasing and consuming CHMs is not restricted to any official regulations.

In the last decades, the consumption of CHMs during pregnancy has been increasing not only in Asian countries, but worldwide. Over 60 % and 45 % pregnant women in Canada (Hollyer et al. 2002) and in the United States (Glover et al. 2003), respectively, use CHMs during their pregnancy, while the consumption in European countries averages up to 20 % (Hemminki et al. 1991; Glover et al. 2003; Nordeng and Havnen 2004).

Some CHMs have been found to be contaminated with e.g. undeclared plant or animal material, drugs (warfarin, dexamethasone, diclofenac, cyproheptadine and paracetamol), heavy metals

(arsenic, lead, and cadmium) or pesticides (Coghlan et al. 2015). Strikingly, in some CHM the arsenic level was ten times higher than the recommended daily intake limit (Coghlan et al. 2015). Arsenic is already classified as neurotoxic and its potential to cause DNT was recently demonstrated as well (Grandjean and Landrigan 2006; Masjosthusmann et al. 2019). Furthermore, a large-scale reproductive and developmental toxicity study in pregnant mice identified embryotoxic potential of commonly used CHMs that are recommended during pregnancy (Wang et al. 2012).

However, the hazard overall and specifically the hazard for DNT of most CHMs has not been thoroughly investigated.

## 1.7 Aim of this thesis

A wide variety of molecular and cellular processes is known to be essential for proper human brain development, which makes the developing brain particularly vulnerable to a chemical insult. However, for the majority of chemicals that are in use the developmental neurotoxic potential is not characterized and essentially there is still a large data gap in the mechanistic understanding of chemically-induced adverse neurodevelopmental outcomes. This huge data gap is mainly due to the insufficiently sensitive triggers for requesting the currently in use *in vivo* guideline studies. In addition, these studies are highly demanding with regard to time, money and animals and thus are not suited for testing large numbers of chemicals. Further limitations include their high variability and lack of reproducibility as well as the uncertainty of extrapolation from animals to humans. Therefore, regulators, academic, and industrial scientists recently agreed on a need for a new testing strategy to assess the DNT potential of chemicals in a time- and cost-efficient, human-relevant predictive manner by using new approach methodologies. Although these methods cannot fully replace current *in vivo* testing, they allow mechanism-based hazard identification and prioritization for further testing. In this context, case studies dealing with the effects of different compound classes on the DNT-IVB are very helpful tools for elevating the acceptance of such alternative methods.

To contribute to the overall goal of elaborating an accepted alternative for DNT evaluation based on case studies, the following aims were addressed in this thesis:

1. Investigation of the DNT potential of 15 selected flame retardants by using a human DNT *in vitro* testing battery and analyzing the data in a weight-of-evidence approach to prioritize the compounds for further testing.
2. Hazard characterization of two selected Chinese Herbal Medicines by evaluating their adverse neurodevelopmental effects using the 'Neurosphere Assay' methods NPC1-5.
3. Identification of the modes-of-action of TBBPA and both CHMs to develop, apply and expand putative AOPs.
4. Expand the knowledge on neurosphere application for chemical testing to disease modeling.



## 2 Manuscripts

The present thesis consists of eight manuscripts.

The first manuscript 2.1, 'Development of the Concept for Stem Cell-Based Developmental Neurotoxicity Evaluation' (Fritsche et al. 2018b) is a review article, which points out the scientific rationales for endpoints that are currently selected for assay establishment using human stem/progenitor cells. Such assays are thought to be assembled as building blocks for a DNT testing battery covering a large variety of neurodevelopmental endpoints over time.

In the second manuscript 2.2, 'Current Availability of Stem Cell-Based *In Vitro* Methods for Developmental Neurotoxicity (DNT) Testing' (Fritsche et al. 2018a) the availability of stem cell-based *in vitro* methods for DNT evaluation that is based on the concept of neurodevelopmental process assessment is reviewed. The current state of the art on neural stem/progenitor cell-based methods including a variety of specific endpoints for the evaluation of DNT is summarized.

The third manuscript 2.3, 'The Neurosphere Assay as an *In Vitro* Method for Developmental Neurotoxicity (DNT) Evaluation' (Nimtz et al. 2019) is a book chapter describing one of the methods suitable for DNT evaluation *in vitro*, the 'Neurosphere Assay'. It is explained how the different test methods NPC1-6 are performed by given a detailed description of the individual endpoint evaluations and how some of them can be multiplexed in a time-and cost-efficient manner. While this chapter is focused on human-based NPCs, the next manuscript deals with the comparison of human and rodent generated NPCs.

The fourth manuscript 2.4, 'A transcriptome comparison of time-matched developing human, mouse and rat neural progenitor cells reveals human uniqueness' (Masjosthusmann et al. 2018) provides a molecular characterization of developing neural progenitor cells in a species comparative manner. Here, mRNA expression profiles of developing human, mouse and rat NPCs were generated and compared and key regulators of fundamental neurodevelopmental processes were identified to overall characterize the 'Neurosphere Assay' and its biological application domain.

Within the fifth manuscript 2.5, 'Rabbit neurospheres as a novel *in vitro* tool for studying neurodevelopmental effects induced by intrauterine growth restriction' (Barenys et al. 2021) a rabbit neurosphere culture was established to characterize differences in basic processes of neurogenesis induced by intrauterine growth restriction (IUGR). This manuscript clearly demonstrates the usefulness of the rabbit 'Neurosphere Assay' for testing DNT compounds as a

complementary method to the rodent based 'Neurosphere Assay'. Moreover, rabbit NPCs seemed well suited for characterizing so far unknown neurodevelopmental effects on the cellular level induced by IUGR and they might be used for a future identification of possible disease biomarkers, as well as for the evaluation and selection of specific neuroprotective therapies.

In the sixth manuscript 2.6, 'Neurodevelopmental toxicity assessment of flame retardants using a human DNT *in vitro* testing battery' (Klose et al. 2021a) the 'Neurosphere Assay' methods NPC1-5 were extended with the UKN2, UKN4 and UKN5 assays, performed in collaboration with Prof. Leist and the University of Konstanz. These assays comprise the OECD/EFSA DNT *in vitro* testing battery that was recently assembled for regulatory purposes (Masjosthusmann et al. 2020). The manuscript 2.6 investigated the neurodevelopmental hazard of selected flame retardants and analyzed the data in a weight-of-evidence approach to prioritize the compounds for further testing. Overall, this study suggests that the human cell-based DNT *in vitro* battery is a promising approach for neurodevelopmental hazard assessment and compound prioritization in risk assessment.

The seventh manuscript 2.7, 'TBBPA Targets Converging Key Events of Human Oligodendrocyte Development Resulting in Two Novel AOPs' (Klose et al. 2021b) deals with the brominated flame retardant tetrabromobisphenol A (TBBPA) and its effect on oligodendrocyte development. By combining the oligodendrocyte maturation assay, NPC6, with large-scale transcriptomics, two modes-of-action by which TBBPA interferes with the establishment of a population of mature, myelin-producing oligodendrocytes were identified. The data was used to build AOPs for a better comprehension of DNT hazards. Furthermore, comparative analyses of human and rat NPCs revealed that human oligodendrogenesis is more sensitive to endocrine disruption by TBBPA than those of rats.

The last manuscript 2.8, 'Application of the Adverse Outcome Pathway concept for investigating developmental neurotoxicity potential of Chinese Herbal Medicines by using human neural progenitor cells *in vitro*' evaluated the adverse neurodevelopmental effects of two selected Chinese herbal medicines, Lei Gong Teng and Tian Ma, by using the 'Neurosphere Assay' methods NPC1-5, which are based on human NPCs complemented by transcriptome analyses. Data generated in this study were placed in an AOP-context by applying one and expanding a second already existing putative DNT-AOP.

## 2.1 Development of the Concept for Stem Cell-Based Developmental Neurotoxicity Evaluation

Ellen Fritsche, Marta Barenys, **Jördis Klose**, Stefan Masjosthusmann, Laura Nimtz, Martin Schmuck, Saskia Wuttke and Julia Tigges

### *Toxicological Science*

Die Entwicklung des menschlichen Gehirns besteht aus einer Vielzahl komplexer, räumlicher und zeitlicher Prozesse, die durch eine chemische Exposition gestört werden und zu irreversiblen Beeinträchtigungen des Nervensystems führen können. Um solch eine chemische Beeinträchtigung in einem alternativen Assay bewerten zu können, muss das komplexe Zusammenspiel der Gehirnentwicklung in dessen einzelne neurologische Entwicklungsprozesse zerlegt werden. Eine Kombination verschiedener alternativer Assays ermöglicht es, sogenannte spezifische neurologische Entwicklungsendpunkte abzubilden. In diesem Review stellen wir eine wissenschaftliche Begründung für neurologische Entwicklungsendpunkte dar, die derzeit ausgewählt werden, um Assays basierend auf menschlichen Stamm- und Vorläuferzellen zu etablieren. Es wird angenommen, dass Assays, die diese wichtigen neurologischen Entwicklungsendpunkte abdecken, das Gerüst einer zukünftigen auf Stamm- und Vorläuferzellen beruhenden DNT Testbatterie bilden werden.

## CONTEMPORARY REVIEW

# Development of the Concept for Stem Cell-Based Developmental Neurotoxicity Evaluation

Ellen Fritsche,<sup>\*,†,1,2</sup> Marta Barenys,<sup>‡,2</sup> Jördis Klose,<sup>\*,2</sup> Stefan Masjosthusmann,<sup>\*,2</sup> Laura Nimtz,<sup>\*,2</sup> Martin Schmuck,<sup>\*,2</sup> Saskia Wuttke,<sup>\*,2</sup> and Julia Tigges<sup>\*,2</sup>

<sup>\*</sup>IUF - Leibniz Research Institute for Environmental Medicine, 40225 Düsseldorf, Germany; <sup>†</sup>Heinrich Heine University, 40225 Düsseldorf, Germany; and <sup>‡</sup>University of Barcelona, Spain

<sup>1</sup>To whom correspondence should be addressed. Fax: +49 (0) 211 3389 226; E-mail: ellen.fritsche@uni-duesseldorf.de.

<sup>2</sup>These authors contributed equally to this study.

## ABSTRACT

Human brain development consists of a series of complex spatiotemporal processes that if disturbed by chemical exposure causes irreversible impairments of the nervous system. To evaluate a chemical disturbance in an alternative assay, the concept evolved that the complex procedure of brain development can be disassembled into several neurodevelopmental endpoints which can be represented by a combination of different alternative assays. In this review article, we provide a scientific rationale for the neurodevelopmental endpoints that are currently chosen to establish assays with human stem/and progenitor cells. Assays covering these major neurodevelopmental endpoints are thought to assemble as building blocks of a DNT testing battery.

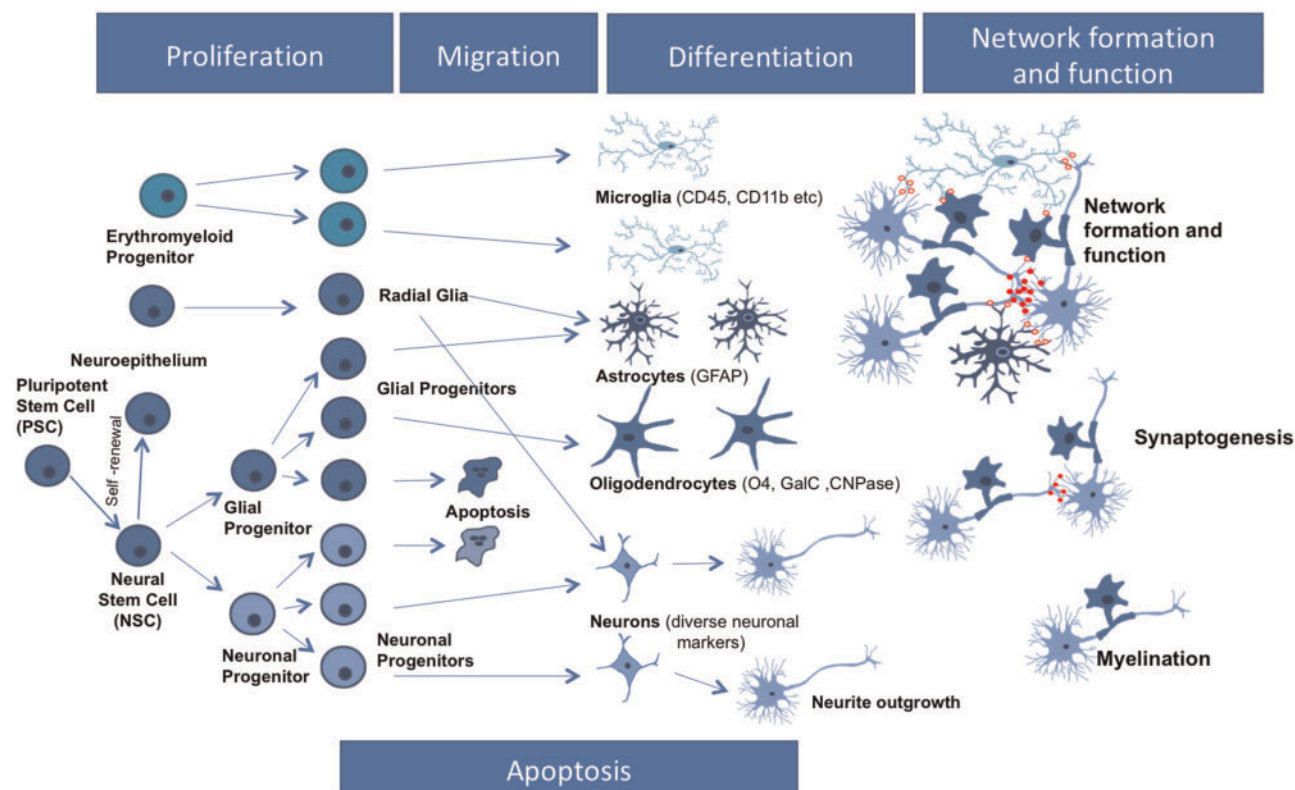
**Key words:** stem cells; ESC; cellular and molecular biology.

For almost 20 years there has been considerable concern that chemical exposure might contribute to the increasing incidence of neurodevelopmental diseases in children (Bennett *et al.*, 2016; Grandjean and Landrigan, 2006, 2014; Schettler, 2001). Despite this concern, most chemicals have not been evaluated for their neurodevelopmental toxicity (Crofton *et al.*, 2012; Goldman and Koduru, 2000). The main reason for this data gap lies in the resource-intensity of the current guideline studies: EPA 870.6300 developmental neurotoxicity (DNT) guideline (U.S. EPA, 1998) and the draft OECD 426 guideline (OECD, 2007). These guidelines demand significant time, money and animals (Crofton *et al.*, 2012; Lein *et al.*, 2005) and are therefore not suited for testing large number of chemicals. The DNT TestSmart initiative originated and led by Alan Goldberg from the John's Hopkins University in 2006, took this issue up by bringing international scientists into communication on how to test for DNT with alternative methods (Lein *et al.*, 2007). Since then,

international researchers have been developing concepts on how to use and interpret such alternative DNT methods with the final goal of regulatory application (Bal-Price *et al.*, 2012, 2015, 2018; Crofton *et al.*, 2011; Fritsche *et al.*, 2017, 2018; Lein *et al.*, 2005). The concept evolved that the complex procedure of brain development is disassembled into spatiotemporal neurodevelopmental processes that are necessary for forming a functional brain AND can be tested for adverse effects of compounds in *in vitro* assays (Bal-Price *et al.*, 2015, 2018; Fritsche, 2016; Lein *et al.*, 2007). Here, human-based systems are preferred because species differences in toxicokinetics, e.g., due to developmental timing, and/or toxicodynamics might affect responses to compounds (Dach *et al.*, 2017; Gassmann *et al.*, 2010; Gold *et al.*, 2005; Knight, 2007; Leist and Hartung, 2013; Masjosthusmann *et al.*, 2018; Seok *et al.*, 2013).

In the following paragraphs, we will provide the scientific rationales for the endpoints that are currently chosen for assay





**Figure 1.** Neurodevelopmental processes essential for nervous system development. It is assumed that DNT toxicants exert their toxicity by disturbing at least one of these processes. Therefore, disturbances of the processes depicted here in blue boxes are key events of adverse outcome pathways relevant for DNT. From Bal-Price *et al.* (2018).

establishment with human stem/progenitor cells and depicted in Figure 1. Such assays are then thought to assemble as building blocks of a DNT testing battery covering neurodevelopmental endpoints over time.

### ESC DIFFERENTIATION TO NEUROEPITHELIAL PRECURSORS/INDUCTION OF NEURONAL ROSETTES

During embryogenesis, stem cells develop into the primordium including the primordium of the central nervous system (CNS). During this neurulation, the neural plate and the neural groove form that lead to the emergence of the neural tube by fusing of the neural folds. Polarization and patterning of the neural tube ultimately develop into the 3 major vesicles of the future brain: forebrain, midbrain, and hindbrain (reviewed by Silbereis *et al.*, 2016). Neural tube and axial defects of the vertebrate embryo belong to the most common developmental malformations in man. They include neural tube defects, which are among the most prominent birth defects in the human population with a prevalence of around 35 cases of spina bifida, 20 cases of anencephaly, and 10 cases of encephalocele per 100 000 births (CDC, <http://www.cdc.gov/ncbddd/birthdefects/data.html>; last accessed July 16, 2019). In addition, disruption of axial development might cause diverse craniofacial, limb, and cardiac malformations. During evaluation of developmental effects of chemicals and pharmaceuticals with experimental animal studies, neural tube and axial defects are frequently observed findings (Knudsen *et al.*, 2009). Examples for such human teratogens are anticonvulsants (e.g. valproate and carbamazepine),

cytostatic agents (e.g. cyclophosphamide and methotrexate), and retinoids. An adverse outcome pathway framework was recently developed linking neural tube and axial defects to modulation of retinoic acid homeostasis (Tonk *et al.*, 2015). This framework was used as one of the building blocks for generation of developmental toxicity ontology (Baker *et al.*, 2018).

Human embryonic stem cells are able to differentiate into early neuroepithelial precursor (NEP) in the form of neural rosettes. These peculiar structures represent an *in vitro* primitive neural stem cell state with all the properties of neural plate cells and recapitulate the early neurulation events that bring the formation and closure of the neural tube (Elkabatz *et al.*, 2008; Lazzari *et al.*, 2006; Pankratz *et al.*, 2007). Such cells have a default anterior-dorsal pattern that is reverted by exposure to ventralizing signals such as sonic hedgehog and fibroblast growth factor 8 (Cowan *et al.*, 2004).

### NEURAL PROGENITOR CELL PROLIFERATION

The brain is a highly organized structure and its development depends on the proliferation of a variety of progenitor cell types. When compared with lissencephalic species like mice and rats, brains of gyrencephalic species, like humans and ferrets, contain a larger variety of neural progenitor cells (NPCs) involved in e.g., the formation of the 6-layered neocortex. Also duration of proliferative NPC activity correlates with brain complexity, i.e. the phase of extensive progenitor self-renewal takes 2 weeks in mouse and 3 months in human developing brains. Such proliferative activity is directly coupled to the number of produced neural cells including neurons during corticogenesis, thus determining brain size, as well as to the formation of cortical gyri

and sulci. Here, centrosome-related proteins that determine spindle orientation and centrosome biosynthesis, the primary cilium, junctional adhesion molecules, and cell cycle length, determine NPC proliferation (comprehensively reviewed in Uzquiano *et al.*, 2018). A disturbance of NPC proliferation during brain development leads to significant alterations of brain morphology like a reduction of size, weight, or volume of the entire brain (microcephaly; de Groot *et al.*, 2005) or of individual brain structures (Moore *et al.*, 2006) having detrimental effects on the neurological outcome (Lang and Gershon, 2018; Ostergaard *et al.*, 2012). Besides genetic factors (Uzquiano *et al.*, 2018), also environmental elements can cause microcephaly. One recent example is Zika virus infection causing microcephaly in children (Devakumar *et al.*, 2018; Tang *et al.*, 2016).

## NPC APOPTOSIS

Apoptosis is a crucial and strictly regulated event during brain development. Too much apoptosis can deplete the NPC pool in the developing brain. Here, loss of centrosome biogenesis in NPC, e.g., by deletion of *Cenpj* (*Sas4*), causes mitotic delay and an elimination of a subtype of NPC, apical radial glia (aRG), from the ventricular zone (VZ). This results in a thinning of upper cortical layers and microcephaly (reviewed in Uzquiano *et al.*, 2018). On the contrary, reduction in apoptosis due to inactivation of caspases or their copartners like *Apaf* can lead to morphological defects like hyperplastic brains. An apoptosis pathway involving caspases-3 and -9 is of particular importance in the developing brain. A reduction in apoptosis observed in *Casp9*<sup>-/-</sup> knockouts is thought to account for increased numbers of Bromodeoxyuridine-positive cells in the germinal zones of the brain that is consistent with an increased survival of NEP. As a consequence, both the VZ and forebrain cortical structures are expanded in these knockout mice, disrupting cortical organization and ultimately resulting in intracranial hemorrhage and death (Hakem *et al.*, 1998; Yoshida *et al.*, 1998). Apoptosis is therefore a well-balanced procedure where disturbance in either direction has detrimental outcomes.

## RADIAL GLIA PROLIFERATION

Radial glia cells play key roles during cerebral cortex development. They are not a uniform cell type but are specified into different radial glia types with different functions across species. Describing the detailed functions of radial glia types extends beyond the scope of this article, for more in-depth information the interested reader is referred to excellent review articles (Gotz and Huttner, 2005; Uzquiano *et al.*, 2018). Briefly, aRG cells comprise the predominant neuronal progenitor cell type within the developing neocortex. They are highly polarized cells, exhibiting basal processes attached to the basement membrane, and apical processes linked by adhesion with cerebrospinal fluid in the ventricles. aRGs undergo asymmetric proliferative division into postmitotic neurons and neurogenic progenitors. In gyrencephalic species including humans, the initial pool of aRGs is greater than in lissencephalic species mainly contributing to neurogenesis through the production of a variety of basally located progenitors including basal radial glia-like cells (bRG), which are mainly intermediate progenitors (IPs). In primates including humans, IPs undergo several rounds of self-renewing before terminal differentiation. This higher neuronal production in gyrencephalic species impacts cortical size and folding (Borrell and Gotz, 2014; Fish *et al.*, 2008; Uzquiano *et al.*, 2018). Besides radial glia function as primary stem and

progenitor cells that proliferate (see above) and give rise to neurons and glia, they also act as scaffolds for migrating neurons building the cerebral cortex architecture (Borrell and Gotz, 2014; Gotz and Huttner, 2005; Malatesta and Gotz, 2013). Due to the fundamental role of radial glia cells in brain development, disturbance of their biology will have detrimental results. For example, induced proliferation of the gyrencephalic ferret bRG leads to an expansion of the cortical surface area and the formation of new folds and fissures, while it increases surface area without creating new folds and fissures in the mouse (Nonaka-Kinoshita *et al.*, 2013). The instance that there are primate-human specific traits in brain ontogenesis that are targets of brain diseases and cortical malformations, like in the Miller-Dieker Syndrome, might explain why mouse models often fail to recapitulate patients' phenotypes (reviewed in Uzquiano *et al.*, 2018).

## NEURAL CREST CELL/RADIAL GLIA/NEURONAL MIGRATION

Different neural cell types need proper migration during development. During embryogenesis, neural crest cells (NCC) migrate to distinct parts of the embryo developing into e.g. sensory and enteric neurons, Schwann cells, melanocytes, craniofacial structures like bone and cartilage, and chromaffin cells of the adrenal gland. Defective NCC migration and differentiation can cause a variety of diseases like cleft palate, hearing loss, Morbus Hirschsprung or CHARGE syndrome (Dupin and Sommer, 2012; Mayor and Theveneau, 2013).

Cortex development takes place during the fetal phase of brain development involving radial glia as well as neuronal migration (Borrell and Gotz, 2014). This neuronal migration process on scaffolds generated by radial glia migration is a fundamental neurodevelopmental key event, because radial glia as well as postmitotic differentiating cells migrate and differentiate over time into the main effector cells neurons, astrocytes and oligodendrocytes thereby ensuring normal brain structure and function (Carpenter *et al.*, 1999). Developmental brain disorders such as heterotopia and lissencephaly or diseases such as schizophrenia and epilepsy have been associated with disruptions of this cortical migratory process (Barkovich *et al.*, 2005; Bozzi *et al.*, 2012; Volk *et al.*, 2012).

## ASTROCYTE DIFFERENTIATION/MATURATION

During the last decades, the view on astrocytes' physiology and their contribution to toxicity and disease has fundamentally changed. Although they were initially thought to play only a supporting and scaffolding role in brain, an increasing diversity of functions—also in a brain region-specific context—have now been appointed to this diverse cell type (reviewed in Hu *et al.*, 2016; Volterra and Meldolesi, 2005). Astrocytes create the brain environment, build up the microarchitecture of the brain parenchyma, maintain brain homeostasis, store and distribute energy substrates, control the development of neural cells, contribute to synaptogenesis, and synaptic maintenance, regulate cerebral blood flow, maintain the blood-brain barrier, and provide brain defense. Therefore, astroglia differentiation is a crucial event during brain development. Astrocytes express astroglial intermediate filament proteins like glial fibrillary acidic protein (GFAP) and vimentin, thus expression of GFAP is commonly used as a specific marker for astrocyte identification. However, it is to consider that *in situ* the levels of GFAP expression vary

quite considerably. For example, GFAP is expressed by virtually every Bergmann glial cell in the cerebellum whereas only about 15%–20% of astrocytes in the cortex of mature animals express GFAP. The same heterogeneity of astrocyte marker expression is also seen in different astrocyte *in vitro* methods (Lundin *et al.*, 2018). There is a large variety of different astrocytes present in brains probably conferring to the heterogeneity of astrocyte marker expression. For example, protoplasmic astrocytes are present in gray matter, while fibrous astrocytes are present in white matter yet with region-specific functions (Hu *et al.*, 2016). Another large class of astroglial cells are the radial glia, which are bipolar cells each with an ovoid cell body and elongated processes (described earlier Uzquiano *et al.*, 2018). After maturation, radial glia disappear from many brain regions and transform into stellate astrocytes (Adapted from Kettenmann and Verkhratsky, 2011).

Astrocytes seem to play a “yin-and-yang” role in health maintenance and disease of the brain. Their responses and roles in brain pathologies range from beneficial to adverse. Such astrocyte responses to a variety of stimuli are called reactive astrogliosis, a context-dependent process undergoing a mild, moderate or severe substantial alteration of morphology and molecular function, i.e. releasing inflammatory factors. Reactive astrocyte responses might also be involved in the pathogenesis of neurodegenerative diseases like Parkinson’s and Alzheimer’s disease as well as amyotrophic lateral sclerosis. In addition, they seem to contribute to the pathogenesis of demyelinating diseases as well as brain aging (reviewed in Hu *et al.*, 2016). Despite just astrocyte marker expression, astrocyte function is crucial when studying astrocyte development. Four key astrocytic features of importance are (Lundin *et al.*, 2018): the uptake of the neurotransmitter glutamate, essential for synapse dynamics; inflammatory response to trauma; calcium signaling response to neurotransmitters; and the secretion of apolipoprotein E, a lipid and cholesterol transporter in the brain (Bazargani and Attwell, 2016; Khakh and Sofroniew, 2015; Yu *et al.*, 2014).

## OLIGODENDROCYTE DIFFERENTIATION/MATURATION

Oligodendrogenesis is necessary for proper brain function, as oligodendrocytes form and keep myelin sheaths around axons, a necessity for nerve cell function by enabling salutatory conduction. The peak of this process starts during the late fetal period and continues until the child’s third year of age. Because myelin inhibits synaptogenesis and neuronal plasticity, this extended myelin production in humans prolongs the phase for learning capacities and memory (reviewed in Silbereis *et al.*, 2016). Several processes are involved in the generation of a sufficient number and proper functioning of oligodendrocytes. These include oligodendrocyte formation from oligodendrocyte progenitor cells (OPCs), maturation of OPCs, generation of myelin from matured oligodendrocytes and finally correct myelin sheet enclosure around axons. Disturbance of oligodendrocyte development may result in demyelination diseases that severely affect neuronal functioning and can be accompanied by impaired e.g. sensory, motor, or vegetative functions as well as memory (Baumann and Pham-Dinh, 2001; Nawaz *et al.*, 2015).

Oligodendrocyte development is linked to thyroid hormone (TH) action. Children suffering from the Allan-Herndon-Dudley Syndrome experience intrauterine brain hypothyroidism due to a mutation in the TH transporter monocarboxylate transporter 8 (MCT-8) resulting in delayed CNS myelination (Rodrigues *et al.*, 2014; Tonduti *et al.*, 2013). From the clinical data it is not clear if

this myelination delay is due to less oligodendrocyte formation or maturation or a combination of both. However, *in vitro* studies using primary human neurospheres differentiating into oligodendrocytes suggest that TH induces oligodendrocyte maturation, but not formation, while in mouse neurospheres both endpoints are TH-dependent (Dach *et al.*, 2017). Thus, the oligodendrocyte maturation assay seems to be well suited to study TH disruption in developing human and mouse NPC.

## NEUROGENESIS AND NEURONAL MATURATION

Neurogenesis in the human CNS begins shortly after the fusion of neural folds. Here, motor neurons in the ventral horn of the cervical spinal cord and neurons of certain cranial nerve nuclei in the brainstem appear first at gestational week 4 (Bayer and Altman, 2007; O’Rahilly and Muller, 2006). Prenatal neurogenesis continues throughout embryonic and fetal development mainly in the neocortex and the cerebellum. The cerebral cortex of a middle-aged male is estimated to be comprised of 16.34 billion neurons (Azevedo *et al.*, 2009), which are produced from neural stem or progenitor cells within the VZ and subventricular zone (SVZ) of the developing cerebral cortical wall. Of those, approximately 80% (13.07 billion) are estimated to be excitatory glutamatergic projection neurons (i.e. pyramidal and modified pyramidal neurons; DeFelipe *et al.*, 2002) and the rest are GABAergic inhibitory interneurons (reviewed by Silbereis *et al.*, 2016). Neurons are indispensable for life and their differentiation patterns are tightly regulated. Thus, modulation of neuronal differentiation into both directions (promotion or inhibition of neurogenesis) is considered as adverse. For example, reduced neurogenesis is thought to be involved in the pathogenesis of depressive mood disorders (Song and Wang, 2011) or the intellectual disabilities in Down Syndrome patients initiated during the fetal period (Guidi *et al.*, 2018; Stagni *et al.*, 2018).

Subsequent to neuronal differentiation, dendritic, and axonal (neurite) outgrowth followed by the formation of synapses are key cellular features associated with the functional maturation of the CNS. At midgestation, immature neocortical neurons have spread axons and instigated to expand dendrites that initiate an extended period of axon outgrowth, dendritic arborization and synaptogenesis extending into early childhood. Despite this general developmental concept, these processes vary substantially between brain layers, areas, and human neocortical neuronal subtypes (reviewed by Silbereis *et al.*, 2016).

## NEURONAL SUBTYPE DIFFERENTIATION

During brain development neural stem and progenitor cells produce a variety of neuronal subtypes, which differentiate at different stages and in different regions of the brain. For example, glutamatergic neurons are generated from the VZ and SVZ of the dorsal mesencephalon (Fode *et al.*, 2000; Guillemot, 2007), GABAergic neurons from the ventral telencephalon (Casarosa *et al.*, 1999; Hansen *et al.*, 2010, 2013; Poitras *et al.*, 2007), while dopaminergic neurons are generated from several brain regions like the mesencephalon, hypothalamus, and retinal and olfactory bulbs (Alizadeh *et al.*, 2015; Arenas *et al.*, 2015; Zhang and van den Pol, 2015). Occurrence of neuronal subtype differentiation during early neurogenesis into 80% excitatory and 20% inhibitory neurons and their interactions are essential for the neuronal function of the CNS (DeFelipe *et al.*, 2002; Hansen *et al.*, 2010, 2013; Workman *et al.*, 2013).



## SYNAPTOGENESIS/NEURONAL NETWORK FORMATION

During early neurogenesis neurons start to mature, connect, and become electrically active in the embryonic phase of neurodevelopment—between the fourth and fifth postconceptional week (Okado *et al.*, 1979; Zecevic and Antic, 1998). For the function of the CNS this neuronal maturation and the formation of synapses is crucial. The neuronal intercellular communication takes place at synaptic connections, which is associated with learning and memory through synaptic plasticity (Lundin *et al.*, 2018). When synaptogenesis is disrupted by a compound, neuronal network activity is altered (Robinette *et al.*, 2011). Here, synaptogenesis might converge on a variety of neurodevelopmental processes, i.e. key events, converging a compounds' effects on neuronal (subtype) differentiation, neurite outgrowth, axon or dendrite formation, dendritic spine development or synaptogenesis itself. Thus, this functional endpoint is a crucial readout for integration of neuronal function of the human brain.

## CONCLUSION

Taken together, these neurodevelopmental processes have been identified somewhat as a minimum requirement for a proposed DNT testing battery, covering the complexity of neurodevelopmental processes as well as timing aspects of brain development. Moreover, they are considered for a DNT testing battery because there are stem/progenitor cell methods available allowing the set up of test methods for DNT evaluation (Bal-Price *et al.*, 2018). However, the current state of the science concerning identified endpoints is probably still at an early, immature state. The key events discussed here have clear rationales for their crucial function during brain development. Other key events like astrocyte differentiation and maturation, especially with regards to astrocyte heterogeneity, astroglia function, neuronal maturation, and neuronal network formation; however, are less well characterized. Moreover, the complexity of brain region-specific neural differentiation and function is not well understood, especially in the human context. Hormonal contributions to brain development are manifold and complex and chemicals with endocrine activities are suspected to interfere with neurodevelopment (WHO-UNEP, 2012). Here, interference with estrogen, androgen, retinoid, progesterone, peroxysome proliferator-activated receptor, or endocannabinoid signaling pathways might have implications for the developing brain at specific developmental stages. Especially sex hormone-related cellular and organ function is crucial for the development of gender-specific behavior, which follows species-specific traits (Wallen and Baum, 2002). As basic scientific knowledge on these neurodevelopmental key events deepens, implications for additional toxicity testing will arise and with this an involvement of stem/progenitor cell-based methods for studying additional endpoints. However, the current state-of-knowledge is a satisfying start to put a DNT testing battery into action that covers neurodevelopmental endpoints across time.

## REFERENCES

- Alizadeh, R., Hassanzadeh, G., Soleimani, M., Joghataei, M. t., Siavashi, V., Khorgami, Z., and Hadjighassem, M. (2015). Gender and age related changes in number of dopaminergic neurons in adult human olfactory bulb. *J. Chem. Neuroanat.* **69**, 1–6.
- Arenas, E., Denham, M., and Villaescusa, J. C. (2015). How to make a midbrain dopaminergic neuron. *Development* **142**, 1918–1936.
- Azevedo, F. A. C., Carvalho, L. R. B., Grinberg, L. T., Farfel, J. M., Ferretti, R. E. L., Leite, R. E. P., Filho, W. J., Lent, R., and Herculano-Houzel, S. (2009). Equal numbers of neuronal and nonneuronal cells make the human brain an isometrically scaled-up primate brain. *J. Comp. Neurol.* **513**, 532–541.
- Baker, N., Boobis, A., Burgoon, L., Carney, E., Currie, R., Fritsche, E., Knudsen, T., Laffont, M., Piersma, A. H., Poole, A., *et al.* (2018). Building a developmental toxicity ontology. *Birth Defects Res.* **110**, 502–518.
- Bal-Price, A., Crofton, K. M., Leist, M., Allen, S., Arand, M., Buetler, T., Delrue, N., FitzGerald, R. E., Hartung, T., Heinonen, T., *et al.*, (2015). International STakeholder Network (ISTNET): Creating a developmental neurotoxicity (DNT) testing road map for regulatory purposes. *Arch. Toxicol.* **89**, 269–287.
- Bal-Price, A., Hogberg, H. T., Crofton, K. M., *et al.* (2018) Recommendation on test readiness criteria for new approach methods in toxicology: Exemplified for developmental neurotoxicity. *ALTEX* doi: 10.14573/altex.1712081
- Bal-Price, A. K., Coecke, S., Costa, L., Crofton, K. M., Fritsche, E., Goldberg, A., Grandjean, P., Lein, P. J., Li, A., Lucchini, R., *et al.* (2012). Advancing the science of developmental neurotoxicity (DNT): Testing for better safety evaluation. *ALTEX* **29**, 202–215.
- Barkovich, A. J., Kuzniecky, R. I., Jackson, G. D., Guerrini, R., and Dobyns, W. B. (2005). A developmental and genetic classification for malformations of cortical development. *Neurology* **65**, 1873–1887.
- Baumann, N., Pham-Dinh, D. (2001). Biology of Oligodendrocyte and Myelin in the Mammalian Central Nervous System. *Physiol. Rev.* **81**, 871–927.
- Bayer, S. A., and Altman, J. (2007) *Atlas of Human Central Nervous System Development*, Vol. 1–5. CRC Press, Boca Raton, Florida.
- Bazargani, N., and Attwell, D. (2016). Astrocyte calcium signaling: The third wave. *Nat. Neurosci.* **19**, 182–189.
- Bennett, D., Bellinger, D. C., Birnbaum, L. S., Bradman, A., Chen, A., Cory-Slechta, D. A., Engel, S. M., Fallin, M. D., Halladay, A., Hauser, R., *et al.* (2016). Project TENDR: Targeting environmental neuro-developmental risks the TENDR consensus Statement. *Environ. Health Perspect.* **124**, A118–A122.
- Borrell, V., and Gotz, M. (2014). Role of radial glial cells in cerebral cortex folding. *Curr. Opin. Neurobiol.* **27**, 39–46.
- Bozzi, Y., Casarosa, S., and Caleo, M. (2012). Epilepsy as a neurodevelopmental disorder. *Front. Psychiatry* **3**, 19.
- Carpenter, M. K., Cui, X., Hu, Z.-y., Jackson, J., Sherman, S., Seiger, Å., and Wahlberg, L. U. (1999). In vitro expansion of a multipotent population of human neural progenitor cells. *Exp. Neurol.* **158**, 265–278.
- Casarosa, S., Fode, C., and Guillemot, F. (1999). Mash1 regulates neurogenesis in the ventral telencephalon. *Development* **126**, 525–534.
- Cowan, C. A., Klimanskaya, I., McMahon, J., Atienza, J., Witmyer, J., Zucker, J. P., Wang, S., Morton, C. C., McMahon, A. P., Powers, D., *et al.* (2004). Derivation of embryonic stem-cell lines from human blastocysts. *N. Engl. J. Med.* **350**, 1353–1356.
- Crofton, K. M., Mundy, W. R., Lein, P. J., Bal-Price, A., Coecke, S., Seiler, A. E. M., Knaut, H., Buzanska, L., and Goldberg, A. (2011). Developmental neurotoxicity testing: Recommendations for developing alternative methods for

- the screening and prioritization of chemicals. *ALTEX* **28**, 9–15.
- Crofton, K. M., Mundy, W. R., and Shafer, T. J. (2012). Developmental neurotoxicity testing: A path forward. *Congenit. Anom.* **52**, 140–146.
- Dach, K., Bendt, F., Huebenthal, U., Giersiefer, S., Lein, P. J., Heuer, H., and Fritsche, E. (2017). BDE-99 impairs differentiation of human and mouse NPCs into the oligodendroglial lineage by species-specific modes of action. *Sci. Rep.* **7**, 44861.
- de Groot, D. M. G., Hartgring, S., van de Horst, L., Moerkens, M., Otto, M., Bos-Kuijpers, M. H. M., Kaufmann, W. S. H., Lammers, J. H. C. M., O'Callaghan, J. P., Waalkens-Berendsen, I. D. H., et al. (2005). 2D and 3D assessment of neuropathology in rat brain after prenatal exposure to methylazoxymethanol, a model for developmental neurotoxicity. *Reprod. Toxicol.* **20**, 417–432.
- DeFelipe, J., Alonso-Nanclares, L., and Arellano, J. I. (2002). Microstructure of the neocortex: Comparative aspects. *J. Neurocytol.* **31**, 299–316.
- Devakumar, D., Bamford, A., Ferreira, M. U., Broad, J., Rosch, R. E., Groce, N., Breuer, J., Cardoso, M. A., Copp, A. J., Alexandre, P., et al. (2018). Infectious causes of microcephaly: Epidemiology, pathogenesis, diagnosis, and management. *Lancet Infect. Dis.* **18**, e1–e13.
- Dupin, E., and Sommer, L. (2012). Neural crest progenitors and stem cells: From early development to adulthood. *Dev. Biol.* **366**, 83–95.
- Elkabetz, Y., Panagiotakos, G., Al Shamy, G., Socci, N. D., Tabar, V., and Studer, L. (2008). Human ES cell-derived neural rosettes reveal a functionally distinct early neural stem cell stage. *Genes Dev.* **22**, 152–165.
- Epa, U.S. (1998). Health Effects Guidelines OPPTS 870.6300. *Dev. Neurotox. Study Vol EPA* **71**, 1–2.
- Fish, J. L., Dehay, C., Kennedy, H., and Huttner, W. B. (2008). Making bigger brains—the evolution of neural-progenitor-cell division. *J. Cell Sci.* **121**, 2783–2793.
- Fode, C., Ma, Q., Casarosa, S., Ang, S. L., Anderson, D. J., and Guillemot, F. (2000). A role for neural determination genes in specifying the dorsoventral identity of telencephalic neurons. *Genes Dev.* **14**, 67–80.
- Fritsche, E. (2016) Report on integrated testing strategies for the identification and evaluation of chemical hazards associated with the developmental neurotoxicity (DNT). In Report of the OECD/EFSA workshop on developmental neurotoxicity (DNT): The use of non-animal test methods for regulatory purposes. OECD Environment, Health and Safety Publications Series on Testing and Assessment 242 ENV/JM/MONO 63. Available at: <https://http://www.efsa.europa.eu/sites/default/les/12.FRITSCHKE.pdf>
- Fritsche, E., Crofton, K. M., Hernandez, A. F., et al. (2017). OECD/EFSA workshop on developmental neurotoxicity (DNT): The use of non-animal test methods for regulatory purposes. *ALTEX* **34**, 311–315.
- Fritsche, E., Grandjean, P., Crofton, K. M., et al. (2018) Consensus statement on the need for innovation, transition and implementation of developmental neurotoxicity (DNT) testing for regulatory purposes. *Toxicol. Appl. Pharmacol.* doi: 10.1016/j.taap.2018.02.004
- Gassmann, K., Abel, J., Bothe, H., Haarmann-Stemmann, T., Merk, H. F., Quasthoff, K. N., Rockel, T. D., Schreiber, T., and Fritsche, E. (2010). Species-specific differential AhR expression protects human neural progenitor cells against developmental neurotoxicity of PAHs. *Environ. Health Perspect.* **118**, 1571–1577.
- Gold, L. S., Manley, N. B., Slone, T. H., Rohrbach, L., and Garfinkel, G. B. (2005). Supplement to the Carcinogenic Potency Database (CPDB): Results of animal bioassays published in the general literature through 1997 and by the National Toxicology Program in 1997–1998. *Toxicol. Sci.* **85**, 747–808.
- Goldman, L. R., and Koduru, S. (2000). Chemicals in the environment and developmental toxicity to children: A public health and policy perspective. *Environ. Health Perspect.* **108**(Suppl 3), 443–448.
- Gotz, M., and Huttner, W. B. (2005). The cell biology of neurogenesis. *Nat. Rev. Mol. Cell Biol.* **6**, 777–788.
- Grandjean, P., and Landrigan, P. J. (2006). Developmental neurotoxicity of industrial chemicals. *Lancet* **368**, 2167–2178.
- Grandjean, P., and Landrigan, P. J. (2014). Neurobehavioural effects of developmental toxicity. *Lancet Neurol.* **13**, 330–338.
- Guidi, S., Giacomini, A., Stagni, F., et al. (2018). Abnormal development of the inferior temporal region in fetuses with Down syndrome. *Brain Pathol.* doi: 10.1111/bpa.12605[AW: Guidi et al. (2018).]
- Guillemot, F. (2007). Cell fate specification in the mammalian telencephalon. *Prog. Neurobiol.* **83**, 37–52.
- Hakem, R., Hakem, A., Duncan, G. S., Henderson, J. T., Woo, M., Soengas, M. S., Elia, A., de la Pompa, J. L., Kagi, D., Khoo, W., et al. (1998). Differential requirement for caspase 9 in apoptotic pathways in vivo. *Cell* **94**, 339–352.
- Hansen, D. V., Lui, J. H., Flandin, P., Yoshikawa, K., Rubenstein, J. L., Alvarez-Buylla, A., and Kriegstein, A. R. (2013). Non-epithelial stem cells and cortical interneuron production in the human ganglionic eminences. *Nat. Neurosci.* **16**, 1576–1587.
- Hansen, D. V., Lui, J. H., Parker, P. R., and Kriegstein, A. R. (2010). Neurogenic radial glia in the outer subventricular zone of human neocortex. *Nature* **464**, 554–561.
- Hu, X., Yuan, Y., Wang, D., and Su, Z. (2016). Heterogeneous astrocytes: Active players in CNS. *Brain Res. Bull.* **125**, 1–18.
- Kettenmann, H., and Verkhratsky, A. (2011). Neuroglia—living nerve glue. *Fortschritte Neurol. Psychiatr.* **79**, 588–597.
- Khakh, B. S., and Sofroniew, M. V. (2015). Diversity of astrocyte functions and phenotypes in neural circuits. *Nat. Neurosci.* **18**, 942–952.
- Knight, A. (2007). Animal experiments scrutinised: Systematic reviews demonstrate poor human clinical and toxicological utility. *ALTEX* **24**, 320–325.
- Knudsen, T. B., Martin, M. T., Kavlock, R. J., Judson, R. S., Dix, D. J., and Singh, A. V. (2009). Profiling the activity of environmental chemicals in prenatal developmental toxicity studies using the U.S. EPA's ToxRefDB. *Reprod. Toxicol.* **28**, 209–219.
- Lang, P. Y., and Gershon, T. R. (2018). A new way to treat brain tumors: Targeting proteins coded by microcephaly genes? Brain tumors and microcephaly arise from opposing derangements regulating progenitor growth. Drivers of microcephaly could be attractive brain tumor targets. *Bioessays* **40**, 1700243.
- Lazzari, G., Colleoni, S., Giannelli, S. G., Brunetti, D., Colombo, E., Lagutina, I., Galli, C., and Broccoli, V. (2006). Direct derivation of neural rosettes from cloned bovine blastocysts: A model of early neurulation events and neural crest specification in vitro. *Stem Cells* **24**, 2514–2521.
- Lein, P., Locke, P., and Goldberg, A. (2007). Meeting report: Alternatives for developmental neurotoxicity testing. *Environ. Health Perspect.* **115**, 764–768.
- Lein, P., Silbergeld, E., Locke, P., and Goldberg, A. M. (2005). In vitro and other alternative approaches to developmental neurotoxicity testing (DNT). *Environ. Toxicol. Pharmacol.* **19**, 735–744.

- Leist, M., and Hartung, T. (2013). Inflammatory findings on species extrapolations: Humans are definitely no 70-kg mice. *Arch. Toxicol.* **87**, 563–567.
- Lundin, A., Delsing, L., Clausen, M., Ricchiuto, P., Sanchez, J., Sabirsh, A., Ding, M., Synnergren, J., Zetterberg, H., Brolén, G., et al. (2018). Human iPSC-derived astroglia from a stable neural precursor state show improved functionality compared with conventional astrocytic models. *Stem Cell Rep.* **10**, 1030–1045.
- Malatesta, P., and Gotz, M. (2013). Radial glia - From boring cables to stem cell stars. *Development* **140**, 483–486.
- Masjosthusmann, S., Becker, D., Petzuch, B., et al. (2018). A transcriptome comparison of time-matched developing human, mouse and rat neural progenitor cells reveals human uniqueness. *Toxicology and Applied Pharmacology* doi: 10.1016/j.taap.2018.05.009
- Mayor, R., and Theveneau, E. (2013). The neural crest. *Development* **140**, 2247–2251.
- Moore, H., Jentsch, J. D., Ghajarnia, M., Geyer, M. A., and Grace, A. A. (2006). A neurobehavioral systems analysis of adult rats exposed to methylazoxymethanol acetate on E17: Implications for the neuropathology of schizophrenia. *Biol. Psychiatry* **60**, 253–264.
- Nawaz, S., Sánchez, P., Schmitt, S., Snaidero, N., Mitkovski, M., Velte, C., Brückner, B.R., Alexopoulos, I., Czopka, T., Jung, S.Y., et al. (2015). Actin filament turnover drives leading edge growth during myelin sheath formation in the central nervous system. *Dev. Cell* **34**, 139–151.
- Nonaka-Kinoshita, M., Reillo, I., Artegiani, B., Ángeles Martínez-Martínez, M., Nelson, M., Borrell, V., and Calegari, F. (2013). Regulation of cerebral cortex size and folding by expansion of basal progenitors. *EMBO J.* **32**, 1817–1828.
- OECD, (2007). OECD TG426 - Developmental Neurotoxicity Study. OECD TG426 Dev. *Neurotox. study* 1–21.
- O’Rahilly, R., and Muller, F. (2006) *The Embryonic Human Brain: An Atlas of Developmental Stages*, 3rd ed. Wiley-Liss.
- Okado, N., Kakimi, S., and Kojima, T. (1979). Synaptogenesis in the cervical cord of the human embryo: Sequence of synapse formation in a spinal reflex pathway. *J. Compar. Neurol.* **184**, 491–518.
- Ostergaard, P., Simpson, M. A., Mendola, A., Vasudevan, P., Connell, F. C., van Impel, A., Moore, A. T., Loeys, B. L., Ghalamkarpour, A., Onoufriadis, A., et al. (2012). Mutations in KIF11 cause autosomal-dominant microcephaly variably associated with congenital lymphedema and chorioretinopathy. *Am. J. Hum. Genet.* **90**, 356–362.
- Pankratz, M. T., Li, X. J., Lavaute, T. M., Lyons, E. A., Chen, X., and Zhang, S. C. (2007). Directed neural differentiation of human embryonic stem cells via an obligated primitive anterior stage. *Stem Cells* **25**, 1511–1520.
- Poitras, L., Ghanem, N., Hatch, G., and Ekker, M. (2007). The proneural determinant MASH1 regulates forebrain *Dlx1/2* expression through the *I12b* intergenic enhancer. *Development* **134**, 1755–1765.
- Robinette, B. L., Harrill, J. A., Mundy, W. R., and Shafer, T. J. (2011). In vitro assessment of developmental neurotoxicity: Use of microelectrode arrays to measure functional changes in neuronal network ontogeny. *Front. Neuroeng.* **4**, 1.
- Rodrigues, F., Grenha, J., Ortez, C., Nascimento, A., Morte, B., M-Belinchón, M., Armstrong, J., and Colomer, J. (2014). Hypotonic male infant and MCT8 deficiency - a diagnosis to think about. *BMC Pediatrics* **14**, 252.
- Schettler, T. (2001). Toxic threats to neurologic development of children. *Environ. Health Perspect.*, **109**(Suppl 6), 813–816.
- Seok, J., Warren, H. S., Cuenca, A. G., Mindrinos, M. N., Baker, HenryV., Xu, W., Richards, D. R., McDonald-Smith, G. P., Gao, H., Hennessy, L., et al. (2013). Genomic responses in mouse models poorly mimic human inflammatory diseases. *Proc. Natl. Acad. Sci. U. S. A.* **110**, 3507–3512.
- Silbereis, J. C., Pochareddy, S., Zhu, Y., Li, M., and Sestan, N. (2016). The cellular and molecular landscapes of the developing human central nervous system. *Neuron* **89**, 248–268.
- Song, C., and Wang, H. (2011). Cytokines mediated inflammation and decreased neurogenesis in animal models of depression. *Prog. Neuro-Psychopharmacol. Biol. Psychiatry* **35**, 760–768.
- Stagni, F., Giacomini, A., Emili, M., Guidi, S., and Bartesaghi, R. (2018). Neurogenesis impairment: An early developmental defect in Down syndrome. *Free Radic. Biol. Med.* **114**, 15–32.
- Tang, H., Hammack, C., Ogden, S. C., Wen, Z., Qian, X., Li, Y., Yao, B., Shin, J., Zhang, F., Lee, E. M., et al. (2016). Zika virus infects human cortical neural progenitors and attenuates their growth. *Cell Stem Cell* **18**, 587–590.
- Tonduti, D., Vanderver, A., Berardinelli, A., Schmidt, J. L., Collins, C. D., Novara, F., Genni, A. D., Mita, A., Triulzi, F., Brunstrom-Hernandez, J. E., et al. (2013). MCT8 deficiency: Extrapyramidal symptoms and delayed myelination as prominent features. *J. Child Neurol.* **28**, 795–800.
- Tonk, E. C., Pennings, J. L., and Piersma, A. H. (2015). An adverse outcome pathway framework for neural tube and axial defects mediated by modulation of retinoic acid homeostasis. *Reprod. Toxicol.* **55**, 104.
- Uzquiano, A., Gladwyn-Ng, I., Nguyen, L., et al., (2018). Cortical progenitor biology: Key features mediating proliferation versus differentiation. *J. Neurochem.* doi: 10.1111/jnc.14338
- Volk, D. W., Matsubara, T., Li, S., Sengupta, E. J., Georgiev, D., Minabe, Y., Sampson, A., Hashimoto, T., and Lewis, D. A. (2012). Deficits in transcriptional regulators of cortical parvalbumin neurons in schizophrenia. *Am. J. Psychiatry* **169**, 1082–1091.
- Volterra, A., and Meldolesi, J. (2005). Astrocytes, from brain glue to communication elements: The revolution continues. *Nat. Rev. Neurosci.* **6**, 626–640.
- Wallen, K., and Baum, M. J. (2002) Masculinization and defeminization in altricial and precocial mammals: Comparative aspects of steroid hormone action. *Hormones, Brain and Behavior*, pp. 385–423.
- WHO-UNEP (2012) State of the Science of Endocrine Disrupting Chemicals. World Health Organization, United Nations Environment Programme.
- Workman, A. D., Charvet, C. J., Clancy, B., Darlington, R. B., and Finlay, B. L. (2013). Modeling transformations of neurodevelopmental sequences across mammalian species. *J. Neurosci.* **33**, 7368–7383.
- Yoshida, H., Kong, Y. Y., Yoshida, R., Elia, A. J., Hakem, A., Hakem, R., Penninger, J. M., and Mak, T. W. (1998). Apaf1 is required for mitochondrial pathways of apoptosis and brain development. *Cell* **94**, 739–750.
- Yu, J. T., Tan, L., and Hardy, J. (2014). Apolipoprotein E in Alzheimer’s disease: An update. *Annu. Rev. Neurosci.* **37**, 79–100.
- Zecevic, D., and Antic, S. (1998). Fast optical measurement of membrane potential changes at multiple sites on an individual nerve cell. *Histochem. J.* **30**, 197–216.
- Zhang, X., and van den Pol, A. N. (2015). Dopamine/tyrosine hydroxylase neurons of the hypothalamic arcuate nucleus release GABA, communicate with dopaminergic and other arcuate neurons, and respond to dynorphin, met-enkephalin, and oxytocin. *J. Neurosci.* **35**, 14966–14982.

---

## Development of the Concept for Stem Cell-Based Developmental Neurotoxicity Evaluation

Ellen Fritsche, Marta Barenys, **Jördis Klose**, Stefan Masjosthusmann, Laura Nimtz, Martin Schmuck, Saskia Wuttke and Julia Tigges

Journal:	Toxicological Sciences (Toxicol Sci)
Impact Factor:	4.081 (2016)
Contribution to the publication:	20 % Writing of the manuscript sections 'neural progenitor cell proliferation', 'neural crest cell/radial glia/neuronal migration' and 'Oligodendrocyte differentiation/maturation'
Type of authorship:	first authorship
Status of the publication:	Published 29 <sup>th</sup> June 2018

## 2.2 Current Availability of Stem Cell-Based *In Vitro* Methods for Developmental Neurotoxicity (DNT) Testing

Ellen Fritsche, Marta Barenys, **Jördis Klose**, Stefan Masjosthusmann, Laura Nimtz, Martin Schmuck, Saskia Wuttke, and Julia Tigges

*Toxicological Science*

Es gibt Hinweise darauf, dass die Exposition gegenüber Chemikalien während der menschlichen Entwicklung zu irreversiblen Beeinträchtigungen des Nervensystems führen kann. Daher hat das Testen von Substanzen auf ihr entwicklungsneurotoxisches Potential eine hohe Priorität für verschiedene Interessengruppen: Wissenschaft, Industrie und Aufsichtsbehörden. Aufgrund der hohen Ressourcenintensität der derzeit durchgeführten *in vivo* Richtlinien-basierten Studien für die Testung auf Entwicklungsneurotoxizität (developmental neurotoxicity; DNT), sind von den Regulierungsbehörden alternative Methoden gewünscht, die wissenschaftlich valide sind und gleichzeitig eine hohe Vorhersagbarkeit für den Menschen aufweisen. In diesem Review überprüfen wir die Verfügbarkeit von alternativen *in vitro* Methoden, welche auf Stamm- und Vorläuferzellen basieren, die neurologische Entwicklungsprozesse abbilden können und für eine DNT-Bewertung geeignet sind. Diese Methoden werden zu einer bislang noch lückenhaften DNT-*in-vitro*-Testbatterie zusammengefügt.



## CONTEMPORARY REVIEW

# Current Availability of Stem Cell-Based *In Vitro* Methods for Developmental Neurotoxicity (DNT) Testing

Ellen Fritsche,<sup>\*,1,2</sup> Marta Barenys,<sup>†,2</sup> Jördis Klose,<sup>†,2</sup> Stefan Masjosthusmann,<sup>†,2</sup> Laura Nimtz,<sup>†,2</sup> Martin Schmuck,<sup>†,2</sup> Saskia Wuttke,<sup>†,2</sup> and Julia Tigges<sup>†,2</sup>

<sup>†</sup>Heinrich Heine University, 40225, Düsseldorf, Germany; and <sup>†</sup>IUF - Leibniz Research Institute for Environmental Medicine 40225, Düsseldorf, Germany

<sup>1</sup>To whom correspondence should be addressed. Fax: +49 (0) 211 3389 226; E-mail: ellen.fritsche@uni-duesseldorf.de.

<sup>2</sup>All authors contributed equally to this study.

## ABSTRACT

There is evidence that chemical exposure during development can cause irreversible impairments of the human developing nervous system. Therefore, testing compounds for their developmentally neurotoxic potential has high priority for different stakeholders: academia, industry, and regulatory bodies. Due to the resource-intensity of current developmental neurotoxicity (DNT) *in vivo* guidelines, alternative methods that are scientifically valid and have a high predictivity for humans are especially desired by regulators. Here, we review availability of stem-/progenitor cell-based *in vitro* methods for DNT evaluation that is based on the concept of neurodevelopmental process assessment. These test methods are assembled into a DNT *in vitro* testing battery. Gaps in this testing battery addressing research needs are also pointed out.

**Key words:** developmental neurotoxicity testing; DNT; neurological damage.

There is evidence that chemical exposure during development can cause irreversible impairments of the human developing nervous system (Andersen *et al.*, 2000; Bearer, 2001; Claudio, 2001; Grandjean and Landrigan, 2006, 2014; Mendola *et al.*, 2002; Rodier, 1995; Slikker, 1994). Neurological damage ranging from subtle to severe imposes significant burdens on affected individuals, their families, and society (Goldman and Koduru, 2000; Weiss and Lambert, 2000). Therefore, testing compounds for their developmentally neurotoxic potential has high priority for different stakeholders: academia, industry, and regulatory bodies (Bal-Price *et al.*, 2015; Crofton *et al.*, 2014; Fritsche *et al.*, 2017, 2018). Due to the resource intensity of current DNT *in vivo* guidelines, alternative methods that are scientifically valid and have a high predictivity for humans are especially desired by regulators (Bal-Price *et al.*,

2012, 2015, 2018a; Crofton *et al.*, 2011; Fritsche *et al.*, 2017, 2018; Lein *et al.*, 2005).

Development of these alternative methods are based on the strategy that the complex procedure of brain development is disassembled into spatiotemporal neurodevelopmental processes that are necessary for forming a brain. According to the adverse outcome pathway concept, such are key events for DNT that can be tested for adverse effects of compounds in *in vitro* assays (Bal-Price *et al.*, 2015, 2018a). To avoid species differences in responses to compound exposure (Baumann *et al.*, 2016; Dach *et al.*, 2017; Gassmann *et al.*, 2010; Harrill *et al.*, 2011a; Masjosthusmann *et al.*, 2018), key event-related DNT evaluation is preferably using human cells, ie, neural stem/progenitor cells (NS/PC) including human-induced pluripotent stem cell (hiPSC)-derived NPC as a source

(Bal-Price *et al.*, 2018b; Singh *et al.*, 2016). In this article, we will summarize the current state of the art on NS/PC-based methods for evaluation of neurodevelopmental toxicity. DNT methods published until April 2014 were assembled in a systematic review earlier (Fritsche *et al.*, 2015).

## ESC DIFFERENTIATION TO NEUROEPITHELIAL PRECURSORS (NEP)/INDUCTION OF NEURONAL ROSETTES

Tests for studying compound effects on the early neurodevelopmental endpoint stem cell differentiation to NEP based on human embryonic stem cells (hESC) were developed (summarized in Fritsche *et al.*, 2015; Shinde *et al.*, 2015; Waldmann *et al.*, 2014). Here, rosette morphology and/or gene expression and viability are measured. In addition, a teratogenicity index was developed as a test method for distinguishing between DNT-specific and cytotoxic compound effects that promotes performing transcriptome-based DNT studies at noncytotoxic concentrations (Waldmann *et al.*, 2014). In a recent work, disturbance of neural rosette formation from hESC was studied in the context of toxicant-dependent altered DNA methylation (Du *et al.*, 2018). Similar to hESC, hiPSC also form neural rosettes that further mature to neurons when injected into mouse motorcortex (Malchenko *et al.*, 2014).

## NPC PROLIFERATION

Proliferation of neural progenitor cells determines brain size (de Groot *et al.*, 2005). Different cell systems are available to study effects on proliferation *in vitro*: hESC-generated NPC, primary hNPC, hiPSC-derived NPC, the human umbilical cord blood (hUCB)-NSC line or ReNcell CX-based systems assessing proliferation in two-dimensional (2D) cultures with the bromodeoxyuridine (BrdU) or ethynyldeoxyuridine (EdU) assay that quantifies incorporation of the thymidine analogue BrdU or EdU into the DNA via fluorescence or luminescence-labeled antibodies, or by quantifying Ki67 expression. A variety of groups used hESC-based methods for studying the effects of single (summarized in Fritsche *et al.*, 2015; Sohn *et al.*, 2017; Wang *et al.*, 2016) or multiple (Behl *et al.*, 2015; Radio *et al.*, 2015) compounds on NPC proliferation. Lately, the frequency of cell cycles per day was calculated from the number of hESC-NSC, which was counted daily using a Neubauer hemocytometer (Vichier-Guerre *et al.*, 2017). While this is a cheap and easy method, it has a high variability and needs verification by an additional established method like the BrdU assay.

Also, 3D NPC aggregates generated from primary human material (Lonza, Belgium; NPC1 Assay; Bal-Price *et al.*, 2018a) or from hiPSC (Hofrichter *et al.*, 2017) called neurospheres are used for assessing compound effects on NPC proliferation. Here, the diameter increase of individual spheres over time or BrdU incorporation are two different ways of measuring cell replication (Baumann *et al.*, 2015, 2016; Fritsche *et al.*, 2015). The increase in sphere diameter over time of single spheres plated in wells of a 96-well plate is a fast and cheap possibly first tier screening method for analyzing cell proliferation.

## NPC APOPTOSIS

Apoptosis is a well-balanced process during brain development with alterations in both directions, increase or decrease, having negative implications for organ development (Hakem *et al.*,

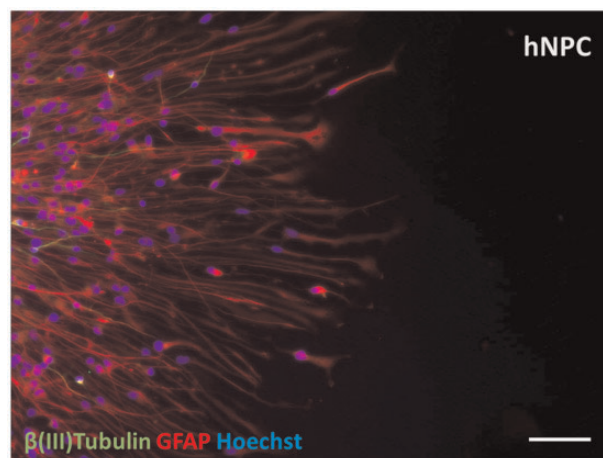


Figure 1. hNPC (Lonza, Verviers, Belgium) were plated onto poly D-lysine/laminin-coated glass slides. After 24 hours, cells were fixed with paraformaldehyde and stained with antibodies against GFAP and  $\beta$ (III)tubulin. Nuclei were stained with Hoechst. Scale bar = 50 $\mu$ m

1998; Uzquiano *et al.*, 2018). It can be measured by different methods *in vitro* ranging from early events like mitochondria calcium or cytochrome c release or annexin V presentation, intermediate processes like caspase activation or late apoptotic activities like nuclear condensation, micronucleus formation, or chromatin disintegration. Several stem cell-based cell systems are suitable for detection of xenobiotic-induced apoptosis, ie, hESC-NPC and ReNcell CX culture, primary hNPC growing as monolayers in 2D, or as neurospheres in 3D (summarized in Fritsche *et al.*, 2015). Lately, the neurosphere system was used for studying the effects of gestational age and sex on methylmercury-induced apoptosis by quantification of condensed nuclei (Edoff *et al.*, 2017). With the ReNcell CX culture, a high content imaging analysis (HCA) assay based on multiplexed activated caspase-3/-7 (apoptosis) and protease (viability) activities. This method was applied to a comparative study of mouse cortical NPC (Millipore, Temecula, CA), immortalized NPC (ReNcell CX, Millipore), hESC-derived NSC (ArunA Biomedical, Athens, GA), and hiPSC-derived pure neuronal cultures (iCell, Cellular Dynamics International, Madison, WI) using 12 positive and negative compounds impressively demonstrating different susceptibilities toward compound-induced apoptosis between species and between brain cells of different developmental stages (Druwe *et al.*, 2015). Another comparative study assessed caspase-3/-7 activation by multiple compounds in a 384-well format using primary hNPC growing as monolayers (ThermoFisher, Waltham, Massachusetts), the neuroblastoma cell line SH-SY5Y, and the immortalized fetal mesencephalic cell line LUHMES. These different cell types show different sensitivities toward compound-induced caspase-3/-7 activation (Tong *et al.*, 2017). A different commercial hNPC source are ENStem-ATM hNPCs (ArunA Biomedical, Athens, Georgia). These cells growing in monolayers were used for multiplexed imaging analyses of live/dead/apoptotic cells by calcein AM/PI stainings in 96-well plates (Kim *et al.*, 2016).

## RADIAL GLIA PROLIFERATION

The multitudes of radial glia cell types play diverse key roles during cerebral cortex development (Gotz and Huttner, 2005; Uzquiano *et al.*, 2018). Stem cell-based *in vitro* methods for studying compound effects on radial glia are sparse. Primary

hNPC (Lonza, Verviers, Belgium) growing as neurospheres is one cell system producing migrating, nestin+/GFAP+ cells that have radial glia-like morphology after 24 h in differentiation culture (Figure 1; Bal-Price et al., 2018a). These differentiated hNPC express a variety of radial glia cell markers and respond to bone morphogenetic protein (BMP)2 with increased astrocyte differentiation (Masjosthusmann et al., 2018). Radial glia can also be differentiated from rosette-forming hESC or hiPSC (Malchenko et al., 2014).

## MIGRATION OF NEURAL CREST CELLS (NCC)/RADIAL GLIA/NEURONS

Different neural cell types need proper migration during development. During embryogenesis, NCC migrate to distinct parts of the embryo developing into a variety of extracerebral cells and tissues causing diseases like cleft palate, hearing loss, Morbus Hirschsprung, or CHARGE syndrome when defective (Dupin and Sommer, 2012; Mayor and Theveneau, 2013). NCC migration can be studied with an *in vitro* assay, the “MINC Assay”, based on neural crest cells (NCC) that are differentiated from hESC (Zimmer et al., 2012). There are two different ways to perform the MINC Assay: the scratch method (Dresler et al., 2015; Pallocca et al., 2016; Zimmer et al., 2012, 2014) or the recently developed stamp method (Nyffeler et al., 2017) with the latter being more robust.

Cortex development involves radial glia migration leading to the development of a scaffold that is subsequently used by neurons to migrate along these glial fibers and reach their final cortical destination (Borrell and Gotz, 2014). One well-characterized migration assay is part of the “Neurosphere Assay” (NPC2; Bal-Price et al., 2018a). Migration distance that cells cover by radially migrating out of the plated neurosphere is analyzed either manually using programs like ImageJ (Bal-Price et al., 2018a; Barenys et al., 2017; Baumann et al., 2015, 2016; Edoff et al., 2017; Fritsche et al., 2015; Ivanov et al., 2016) or by HCA using the software “Omnisphero” (Schmuck et al., 2017). An important issue when evaluating effects of compounds on NPC migration with the ‘Neurosphere Assay’ is to distinguish between specific effects on migration and secondary migration effects due to cytotoxicity. Our recent data shows that migration distance or pattern, which determines the size of the total migration area, defines the magnitude of signal of viability assays like the Cell Titer Blue Assay (CTB Assay; Promega) because it is related to cell number. A different viability/cytotoxicity assay measuring a readout not directly dependent on cell number, like LDH leakage, indicates the specific effects of methylmercury (MeHgCl) on migration without producing cell death at two different time points (Figs. 2A and 2B). Similarly, epigallocatechin gallate (EGCG) inhibits adhesion and migration of hNPC thereby changing the migration pattern and area (Figure 2C; Bal-Price et al., 2017; Barenys et al., 2017). After 3 days of migration in the presence of EGCG, the CTB assay suggests that EGCG reduces cell viability (Figure 2D). However, FACS analyses identifying annexin V-/PI-positive cells clearly show that EGCG does not cause cell death, but diminishes the cell area with access to the CTB substrate (Figure 2E).

Migrated cells of the NPC2 assay form a 2-layered cell layer with neurons migrating on top of the glia cells (Alépée et al., 2014; Baumann et al., 2016). This enables measuring not only glia cell migration, but also the neuronal migration by assessing individual neuronal positions using the software Omnisphero

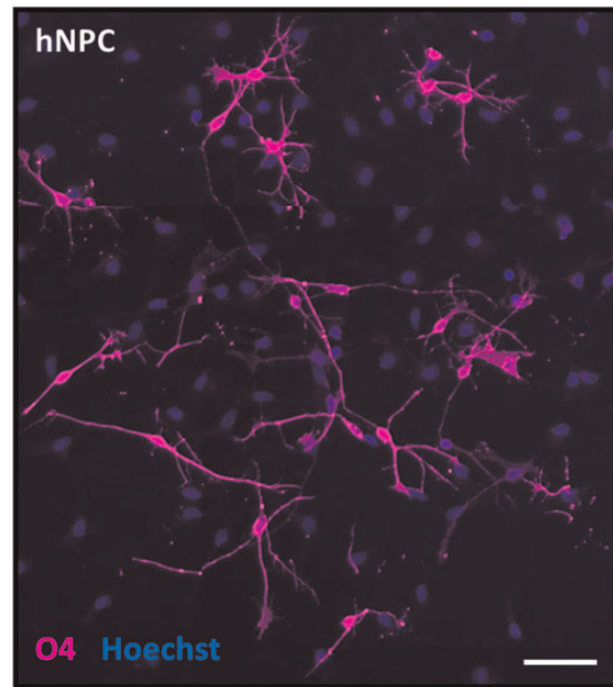


Figure 2. Oligodendrocyte differentiation of primary hNPC. Oligodendrocyte differentiation was assessed by immunocytochemical staining for the oligodendrocyte marker O4 of 5 days differentiated hNPC. Nuclei were counterstained with Hoechst. Scale bar = 50µm. The staining method was previously published in Baumann et al. (2014, 2015).

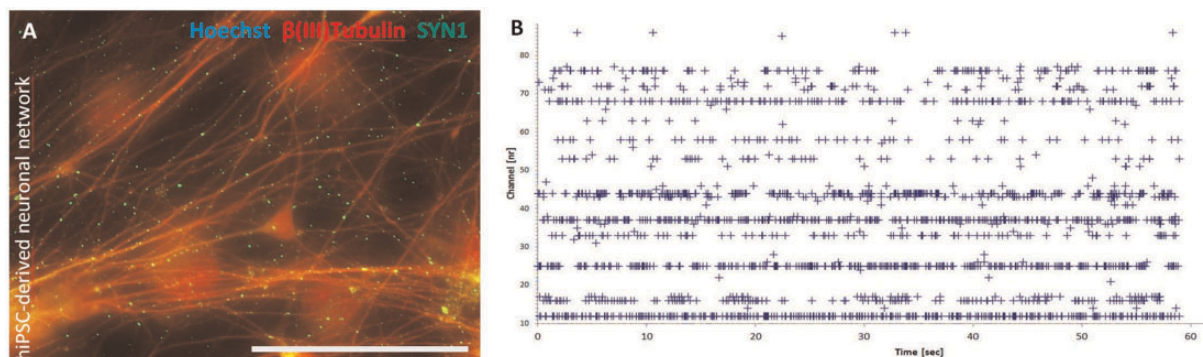
(Schmuck et al., 2017). Hence, NPC2 can be utilized to assess radial glia and neuronal migration at the same time.

Migration analyses can also be performed with hiPSC-derived NPC (hiNPC2; Hofrichter et al., 2017). Migration distance is similar between NPC2 and hiNPC. Yet, the first cells migrating from the hiNPC neurosphere are neurons and not radial glia as from the hNPC sphere.

## ASTROCYTE DIFFERENTIATION/MATURATION

Astroglia differentiation is a crucial event during brain development because astrocytes obtain a variety of central functions in brain (Kettenmann and Verkhratsky, 2011). Astrocyte differentiation can be measured in developing mixed cell cultures by counting the percentage of, eg, GFAP+ or vimentin+ cells from the total number of differentiated hESC, primary hNPC or hUCB-NSC (summarized in Fritsche et al., 2015; Edoff et al., 2017). Lately, also hiPSC differentiation into the astrocyte lineage was employed in a toxicological context either in 2D (after 28 days) or in 3D (after 56 days) by creating “brain balls” in shaking cultures (Pamies et al., 2017, 2018b; Pistollato et al., 2014). Moreover, morphogen-induced astrocyte maturation can be studied in the context of the “Neurosphere assay” (Masjosthusmann et al., 2018). Apart from toxicology, clearly more data on astrocyte differentiation is available on the basic science level, which is summarized, eg, in Chandrasekaran et al. (2016). Astrocyte function as the most relevant readout was recently compared between long-term self-renewing hiPSC-derived neuroepithelial-like stem cells (ltNES; Falk et al., 2012)-astrocytes, human primary adult astrocytes (phaAstro), an astrocytoma cell line CCF-STTG1 (CCF), and hiPSC-derived astrocytes from Cellular Dynamics International (iCellAstro). Here, ltNES-astrocytes were the only ones expressing functional, glutamate





**Figure 3.** Synapse formation and neuronal network activity of a hiPSC-derived network. A, hiPSC (IMR-90, Wicell) were neurally induced to NPCs using the NIM-protocol (Hofrichter *et al.* 2017) and differentiated on D-lysine/laminin-coated glass slides for 28 days, fixed with paraformaldehyde and stained for  $\beta$ (III)-tubulin<sup>+</sup> neurons and synapsin1<sup>+</sup> presynaptic structures, respectively. Nuclei were stained with Hoechst. Scale bar=100  $\mu$ m. B, Spikeraster plot of spontaneous electrical activity of a hiPSC-derived neuronal network cultivated for 20 days on D-lysine/laminin-coated microelectrode arrays.

transporting SLC1A3 protein, which is an assay suitable for higher throughput drug screening (Lundin *et al.*, 2018).

### OLIGODENDROCYTE DIFFERENTIATION/MATURATION

Oligodendrogenesis is necessary for proper brain functioning as oligodendrocytes form and keep myelin sheaths around axons (Baumann and Pham-Dinh, 2001). Data on chemical effects on hESC-, hNPC-, or hUCB-NSC-derived oligodendrocytes are summarized in Fritsche *et al.* (2015). Different groups have recently established further oligodendrocyte differentiation protocols using hESC/hiPSC growing feeder-free (Douvaras *et al.*, 2014; Gorris *et al.*, 2015; Madill *et al.*, 2016; Yamashita *et al.*, 2017) or in presence of feeder cells (Douvaras *et al.*, 2014; Ehrlich *et al.*, 2017; Gorris *et al.*, 2015; Madill *et al.*, 2016; Nicaise *et al.*, 2017) in a 2D format. Pamies *et al.* (2018b) used hiPSC-derived 3D “brain balls” to study differentiation of oligodendrocytes in a toxicological context. Oligodendrocytes emerge late during nervous system development and differentiation of hESC/hiPSC into the oligodendrocyte lineage following the above-mentioned protocols needs several weeks making medium-to-high throughput screening for oligodendrocyte toxicity using hESC/hiPSC a great challenge. In contrast, oligodendrocyte formation and maturation can be studied with hNPC growing as neurospheres with the NPC5/6 assay within a neurosphere differentiation time of 5 days (Figure 3; Bal-Price *et al.*, 2018a; Dach *et al.*, 2017). These assays are based on manual or automated oligodendrocyte quantification as a measure for oligodendrocyte formation (NPC5; Figure 3; Bal-Price *et al.*, 2018a; Barenys *et al.*, 2017), which is the normalization basis for subsequent thyroid hormone (TH)-dependent myelin basic protein (MBP) expression as a measure for oligodendrocyte maturation (Bal-Price *et al.*, 2018a; Dach *et al.*, 2017). Interference of a compound with the TH-induced oligodendrocyte maturation is thus an assay for identifying TH disruptors (NPC6). Oligodendrocyte precursor cells can also be enriched by isolation from gestational week 10–13 fetal human neurospheres (Lu *et al.*, 2015).

### NEUROGENESIS

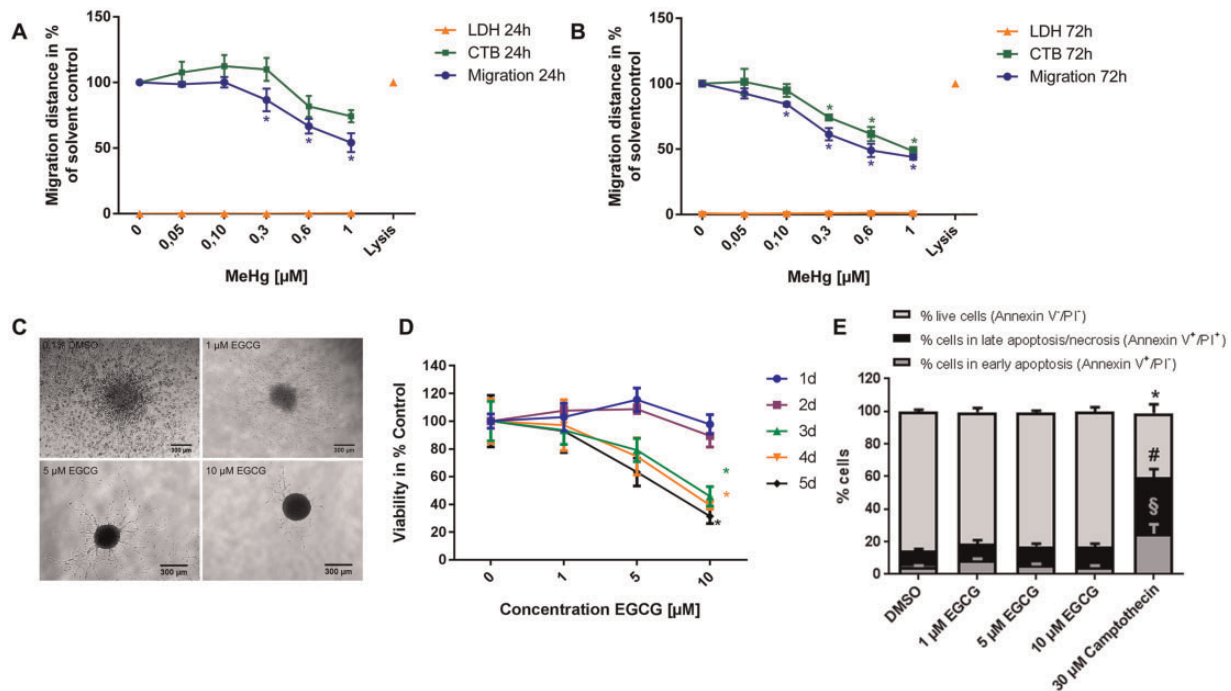
Neurogenesis is one of the most frequently studied endpoints for DNT evaluation. Compounds’ effects on neuronal differentiation have been studied in hESC- (summarized in Ehashi *et al.*, 2014; Fritsche *et al.*, 2015; Schulpen *et al.*, 2015; Sohn *et al.*, 2017;

Zeng *et al.*, 2016), hiPSC-derived (Pistolato *et al.*, 2017) mixed neuronal-glia or hUCB-NSC (summarized in Fritsche *et al.*, 2015; Kashyap *et al.*, 2015; Zychowicz *et al.*, 2014) cultures in 2D, as well as in hiPSC-derived mixed-culture “brain balls” in 3D (Pamies *et al.*, 2017) and hiPSC-generated (Hofrichter *et al.*, 2017) or primary neurospheres (summarized in Fritsche *et al.*, 2015 and Bal-Price *et al.*, 2018a; Masjosthusmann *et al.*, 2018) differentiating in “secondary 3D” structures. Within some of the above-mentioned studies, differences in sensitivity and specificity of DNT effects between neuronal cells toward methylmercury were observed. These are probably due to the large differences in stem cell cultivation and differentiation protocols concerning, eg, medium, feeder cell status, timing, differentiation through hESC-derived NPC or direct neuronal differentiation, amounts of glia present and level of quality control, just to mention some. Especially quality control and reporting standards are a large issue in current stem cell work that urgently need standardization as recently voiced by a workshop report on “Advanced good cell culture practice for human primary, stem cell-derived and organoid models” (Pamies *et al.*, 2018a).

Concerning cell-type composition, mixed neuron-glia cultures are advantageous for DNT testing as different cell types might have different susceptibilities toward compounds (Pei *et al.*, 2016), eg, astroglia might alter developmental toxicity to neurons (Wu *et al.*, 2017). In addition, the advantage of the monolayer differentiation protocols clearly lie in the more simple evaluation, eg, by high content image analyses (HCA), whereas the 3D differentiated methods are more complex to evaluate via immunostainings. Somewhat in-between are neurosphere-based methods that differentiate in so-called “secondary 3D” structures, ie, maintaining the multicellular organism aspect (Masjosthusmann *et al.*, 2018) despite plating of spheres on a 2D surface (Alépée *et al.*, 2014).

### NEURONAL MATURATION

Dendritic and axonal (neurite) outgrowth followed by the formation of synapses are key cellular features associated with the functional maturation of the CNS. Neurite morphology can be measured with a variety of methods including neurite number, length, branching, or area using HCA, a fairly reliable and suitable image-based method for higher throughput applications (Harrill *et al.*, 2010, 2011a; He *et al.*, 2012; Wilson *et al.*, 2014). Cell



**Figure 4.** hNPC growing as neurospheres in proliferation culture, were plated for migration analyses onto poly D-lysine/laminin-coated glass slides in presence and absence of MeHgCl. After (A) 24 and (B) 72 h, migration distance was measured from the outer sphere rim to the furthest migrated cells at four opposite positions. Cell titer blue (CTB) and lactate dehydrogenase (LDH) assays were performed as described previously (Baumann et al. 2014). C, Neurospheres were plated as described in (A) in presence and absence of epigallocatechin gallate (EGCG). After 24 h the migration area was analyzed visually by phase contrast microscopy and for better visualization images were subjected to a black/white filter. D, Viability analyses using the CTB assay were performed on each day up to 5 DIV. E, On day 5, FACS analyses of dissociated hNPC were performed after annexin V/PI staining. As a positive control, spheres were treated with the topoisomerase I inhibitor camptothecin. (A, B, D) \* $p \leq .05$ ; (E) §  $p \leq .05$  of annexin + /PI-cells; #  $p \leq .05$  of annexin + /PI+ cells; \* $p \leq .05$  of live cells.

material for such analyses includes hESC-derived almost pure neuronal cultures (hN2TM, Aruna Biomedical Inc., Athens, Georgia; Behl et al., 2015; Harrill et al., 2011a; Wilson et al., 2014) that were treated after neuronal specification had already taken place; hESC-derived hNP cells (hNP1<sup>TM</sup> 00001, Aruna Biomedical Inc.) treated when cells were making the transition from proliferating NPC to postmitotic neurons (Wang et al., 2016); hESC-derived hNPC (Chemicon-Millipore Norcross, Georgia; Zeng et al., 2016); 3D aggregated hESC-derived embryoid bodies (He et al., 2012); hiPSC-generated iCell neurons (Cellular Dynamics International; Ryan et al., 2016); hiPSC-derived hNPC growing as neurospheres (Hofrichter et al., 2017); primary NPC differentiating into mixed cultures (NPC4; Bal-Price et al., 2018a; Edoff et al., 2017; Schmuck et al., 2017), ie, multiple parameters of the neurosphere assay including neurite morphology can be assessed with the algorithm Omnisphero (www.omnisphero.com; last accessed July 2018; Schmuck et al., 2017); or LUHMES cells (Krug et al., 2013; Scholz et al., 2011).

## NEURONAL SUBTYPE DIFFERENTIATION

During brain development, neural stem and progenitor cells produce a variety of neuronal subtypes, which differentiate at different stages and in different regions of the brain. Compounds' effects on neuronal subtype differentiation has mostly been assessed for dopaminergic (DA) neurons using hESC (Huang et al., 2017; Stummann et al., 2009; Zeng et al., 2006), for DA as well as cholinergic neurons using hUCB-NSC (Kashyap et al., 2015) and for DA, glutamate- and GABAergic neurons employing hiPSC (Pistollato et al., 2017).

## SYNAPTOGENESIS/NEURONAL NETWORK FORMATION

During early neurogenesis neurons start to mature, become electrically active and connect via synapses (Okado et al., 1979; Zecevic and Antic, 1998). For the function of the CNS this neuronal maturation and the formation of synapses is crucial. So far, DNT testing for synaptogenesis and neuronal activity in the developing brain has mainly been performed using rat primary cells (Harrill et al., 2011b; Hogberg et al., 2011; Robinette et al., 2011) and no *in vitro* DNT study has been published using hESC or hiPSC for assessing compound effects on neuronal network activity. However, there are a number of promising systems under development that have been used for acute neurotoxicity evaluations studying either synaptogenesis and/or neuronal electrical activity including hESC (Kapucu et al., 2012; Oh et al., 2016; Sandström et al., 2017; Yla-Outinen et al., 2010) or hiPSC neuronal network differentiation methods (Figure 3; Hofrichter et al., 2017; Pellett et al., 2015; Pistollato et al., 2017; Toivonen et al., 2013). Here, the use of hiPSC-derived neuronal networks growing directly on microelectrode arrays (MEAs) seems to be a promising method for screening neurodevelopmental toxins for their adverse effects on neuronal network formation.

What are the difficulties one faces with stem cell-based active neuronal networks for DNT evaluation? Every single neuronal network differentiates into a variable amount of neurons, ie, variable neuron/glia ratio, as well as neuronal subtypes that form neuronal connections by chance. Therefore, each network exhibits its own baseline activity level with high MEA-to-MEA variability making comparison of developmentally exposed neuronal networks to control networks very difficult. In

addition, network activity is generally not very high compared with rodent networks. Developing rat networks differentiate faster and show much higher activity levels and synchronization than stem cell-based human networks. This makes analyses of the adverse effects of toxicants on human networks much more difficult. To overcome these restrictions and make neuronal human stem cell-based networks more standardized and reproducible, one can envision making use of the relatively new method of 3D bioprinting (Zhuang *et al.*, 2018). Using this method, neural cells might directly be printed in a three-dimensional hydrogel precisely on MEAs (Tedesco *et al.*, 2018).

## SUMMARY AND CONCLUSION

During the last 15 years, much effort has been put into establishment, scientific validation, and test method set up for DNT *in vitro* evaluation. In addition to primary rodent cultures, which are valuable cell methods for comparing compounds' effects *in vivo* to *in vitro*, stem/progenitor cell-based methods have become available that can now be assembled into a DNT *in vitro* testing battery (summarized in Bal-Price *et al.*, 2018a). Such a testing battery is necessary for covering the immense complexity of neurodevelopmental processes as well as timing aspects of brain development. However, the current state of the science concerning the testing battery is probably still at an early, immature state. While a variety of important key events are very well covered in the strategy, ie, neural proliferation, apoptosis, NPC migration, neuronal differentiation and neurite morphology, there are also some crucial aspects less well covered. These include glia differentiation and maturation, glia cell function, neuronal maturation, and neuronal network formation with assessment of electrical network activity. Moreover, the complexity of brain region-specific neural differentiation and function has not been addressed in DNT assays yet. However, basic science is moving down this path by creating brain region-specific organoids (Lancaster *et al.*, 2013; Qian *et al.*, 2016) that might be suited for studying region-specific effects of compounds on neurodevelopmental key events. In addition, hormone-related DNT has only been touched marginally with stem cell-based human DNT *in vitro* assays by studying interference with cellular thyroid hormone (Dach *et al.*, 2017) or glucocorticoid signaling (Moors *et al.*, 2012). Hormonal contributions to brain development are much more manifold and complex and chemicals with endocrine activities are thus suspected to interfere with neurodevelopment (WHO-UNEP, 2012). Here, interference with estrogen, androgen, retinoid, progesterone, peroxysome proliferator-activated receptor, or endocannabinoid signaling pathways might have implications for the developing brain at specific developmental stages. Especially sex hormone-related cellular and organ function is crucial for the development of gender-specific behavior, which follows species-specific traits (Wallen and Baum, 2002). Molecular aspects of the development of such human sex-specific behavior is an understudied field of research posing a challenge for *in vitro* DNT evaluation. Yet, primary human cells show some sex-specific neurodevelopmental key event response differences toward methylmercury (Edoff *et al.*, 2017) without understanding the mechanistic implications behind these observations yet. Attempts are made to tackle this issue with rodent *in vitro* methods (Keil *et al.*, 2017). In this line, the largest challenge will be the understanding of disturbance of emotional and intellectual consciousness by chemical exposure in humans. Understanding physiology behind these human traits is a

prerequisite that might enable establishment of adverse outcome pathways for these fundamental human aspects in the future.

## Funding

This work was supported by the German Ministry of Education and Research [grant number 16V0899]; the Ministry of Innovation, Science and Research of North Rhine Westphalia; and a German Academic Exchange Service (DAAD) Research Fellowship.

## REFERENCES

- Alépée, N., Bahinski, A., Daneshian, M., De Wever, B., Fritsche, E., Goldberg, A., Hansmann, J., Hartung, T., Haycock, J., and Hogberg, H. (2014). State-of-the-art of 3D cultures (organ-on-a-chip) in safety testing and pathophysiology. *Altex* **31**, 441–477.
- Andersen, H. R., Nielsen, J. B., and Grandjean, P. (2000). Toxicologic evidence of developmental neurotoxicity of environmental chemicals. *Toxicology* **144**, 121–127.
- Bal-Price, A. K., Coecke, S., Costa, L., Crofton, K. M., Fritsche, E., Goldberg, A., Grandjean, P., Lein, P. J., Li, A., Lucchini, R., *et al.* (2012). Advancing the science of developmental neurotoxicity (DNT): Testing for better safety evaluation. *Altex* **29**, 202–215.
- Bal-Price, A., Crofton, K. M., Leist, M., Allen, S., Arand, M., Buetler, T., Delrue, N., FitzGerald, R. E., Hartung, T., Heinonen, T., *et al.* (2015). International STakeholder NETwork (ISTNET): Creating a developmental neurotoxicity (DNT) testing road map for regulatory purposes. *Arch. Toxicol.* **89**, 269–287.
- Bal-Price, A., Hogberg, H. T., Crofton, K. M., *et al.* (2018a). Recommendation on test readiness criteria for new approach methods in toxicology: Exemplified for developmental neurotoxicity. *Altex*, doi: 10.14573/altex.1712081.
- Bal-Price, A., Lein, P. J., Keil, K. P., Sethi, S., Shafer, T., Barenys, M., Fritsche, E., Sachana, M., and Meek, M. E. B. (2017). Developing and applying the adverse outcome pathway concept for understanding and predicting neurotoxicity. *Neurotoxicology* **59**, 240–255.
- Bal-Price, A., Pistollato, F., Sachana, M., Bopp, S. K., Munn, S., and Worth, A. (2018b). Strategies to improve the regulatory assessment of developmental neurotoxicity (DNT) using *in vitro* methods. *Toxicol. Appl. Pharmacol.*, doi: 10.1016/j.taap.2018.02.008.
- Barenys, M., Gassmann, K., Baksmeier, C., Heinz, S., Reverte, I., Schmuck, M., Temme, T., Bendt, F., Zschauer, T. C., Rockel, T. D. (2017). Epigallocatechin gallate (EGCG) inhibits adhesion and migration of neural progenitor cells *in vitro*. *Arch. Toxicol.* **91**, 827–837.
- Baumann, N., and Pham-Dinh, D. (2001). Biology of oligodendrocyte and myelin in the mammalian central nervous system. *Physiol. Rev.* **81**, 871–927.
- Baumann, J., Barenys, M., Gassmann, K., and Fritsche, E. (2014). Comparative human and rat “neurosphere assay” for developmental neurotoxicity testing. In *Current Protocols in Toxicology* (L. G. Costa, J. C. Davila, D.A. Lawrence, D. J. Reed, Eds), Vol. **59**, pp. 12.21.1–12.21.24. John Wiley & Sons.
- Baumann, J., Dach, K., Barenys, M., Giersiefer, S., Goniwiecha, J., Lein, P. J., and Fritsche, E. (2015) *Application of the Neurosphere Assay for DNT Hazard Assessment: Challenges and Limitations*, pp. 1–29. Humana Press, Totowa, NJ.



- Baumann, J., Gassmann, K., Masjosthusmann, S., DeBoer, D., Bendt, F., Giersiefer, S., and Fritsche, E. (2016). Comparative human and rat neurospheres reveal species differences in chemical effects on neurodevelopmental key events. *Arch. Toxicol.* **90**, 1415–1427.
- Bearer, C. F. (2001). Developmental neurotoxicity. Illustration of principles. *Pediatr. Clin. N. Am.* **48**, 1199–1213. ix.
- Behl, M., Hsieh, J.-H., Shafer, T. J., Mundy, W. R., Rice, J. R., Boyd, W. A., Freedman, J. H., Hunter, E. S., Jarema, K. A., Padilla, S., et al. (2015). Use of alternative assays to identify and prioritize organophosphorus flame retardants for potential developmental and neurotoxicity. *Neurotoxicol. Teratol.* **52**, 181–193.
- Borrell, V., and Gotz, M. (2014). Role of radial glial cells in cerebral cortex folding. *Curr. Opin. Neurobiol.* **27**, 39–46.
- Chandrasekaran, A., Avci, H. X., Leist, M., Kobolak, J., and Dinnyes, A. (2016). Astrocyte differentiation of human pluripotent stem cells: New tools for neurological disorder research. *Front Cell Neurosci* **10**, 215.
- Claudio, L. (2001). NIEHS investigates links between children, the environment, and neurotoxicity. *Environ. Health Perspect.* **109**, A258–A261.
- Crofton, K., Fritsche, E., Ylikomi, T., and Bal-Price, A. (2014). International STakeholder NETwork (ISTNET) for creating a developmental neurotoxicity testing (DNT) roadmap for regulatory purposes. *Altex* **31**, 223–224.
- Crofton, K. M., Mundy, W. R., Lein, P. J., Bal-Price, A., Coecke, S., Seiler, A. E. M., Knaut, H., Buzanska, L., and Goldberg, A. (2011). Developmental neurotoxicity testing: Recommendations for developing alternative methods for the screening and prioritization of chemicals. *Altex* **28**, 9–15.
- Dach, K., Bendt, F., Huebenthal, U., Giersiefer, S., Lein, P. J., Heuer, H., and Fritsche, E. (2017). BDE-99 impairs differentiation of human and mouse NPCs into the oligodendroglial lineage by species-specific modes of action. *Sci. Rep.* **7**, 44861.
- de Groot, D. M. G., Hartgring, S., van de Horst, L., Moerkens, M., Otto, M., Bos-Kuijpers, M. H. M., Kaufmann, W. S. H., Lammers, J. H. C. M., O'Callaghan, J. P., Waalkens-Berendsen, I. D. H., et al. (2005). 2D and 3D assessment of neuropathology in rat brain after prenatal exposure to methylazoxymethanol, a model for developmental neurotoxicity. *Reprod. Toxicol.* **20**, 417–432.
- Douvaras, P., Wang, J., Zimmer, M., Hanchuk, S., O'Bara, M. A., Sadiq, S., Sim, F. J., Goldman, J., and Fossati, V. (2014). Efficient generation of myelinating oligodendrocytes from primary progressive multiple sclerosis patients by induced pluripotent stem cells. *Stem Cell Rep.* **3**, 250–259.
- Dreser, N., Zimmer, B., Dietz, C., Sügis, E., Pallocca, G., Nyffeler, J., Meisig, J., Blüthgen, N., Berthold, M. R., Waldmann, T., et al. (2015). Grouping of histone deacetylase inhibitors and other toxicants disturbing neural crest migration by transcriptional profiling. *Neurotoxicology* **50**, 56–70.
- Druwe, I., Freudenrich, T. M., Wallace, K., Shafer, T. J., and Mundy, W. R. (2015). Sensitivity of neuroprogenitor cells to chemical-induced apoptosis using a multiplexed assay suitable for high-throughput screening. *Toxicology* **333**, 14–24.
- Du, L., Sun, W., Li, X. M., Li, X. Y., Liu, W., and Chen, D. (2018). DNA methylation and copy number variation analyses of human embryonic stem cell-derived neuroprogenitors after low-dose decabromodiphenyl ether and/or bisphenol A exposure. *Hum. Exp. Toxicol.* **37**, 475–485.
- Dupin, E., and Sommer, L. (2012). Neural crest progenitors and stem cells: From early development to adulthood. *Dev. Biol.* **366**, 83–95.
- Edoff, K., Raciti, M., Moors, M., Sundstrom, E., and Ceccatelli, S. (2017). Gestational age and sex influence the susceptibility of human neural progenitor cells to low levels of MeHg. *Neurotox. Res.* **32**, 683–693.
- Ehashi, T., Suzuki, N., Ando, S., Sumida, K., and Saito, K. (2014). Effects of valproic acid on gene expression during human embryonic stem cell differentiation into neurons. *J. Toxicol. Sci.* **39**, 383–390.
- Ehrlich, M., Mozafari, S., Glatza, M., Starost, L., Velychko, S., Hallmann, A.-L., Cui, Q.-L., Schambach, A., Kim, K.-P., Bachelin, C., et al. (2017). Rapid and efficient generation of oligodendrocytes from human induced pluripotent stem cells using transcription factors. *Proc. Natl. Acad. Sci. U.S.A.* **114**, E2243–E2252.
- Falk, A., Koch, P., Kesavan, J., Takashima, Y., Ladewig, J., Alexander, M., Wiskow, O., Tailor, J., Trotter, M., Pollard, S., et al. (2012). Capture of neuroepithelial-like stem cells from pluripotent stem cells provides a versatile system for in vitro production of human neurons. *PLoS One* **7**, e29597.
- Fritsche, E., Crofton, K. M., Hernandez, A. F., Hougaard Bennekou, S., Leist, M., Bal-Price, A., Reaves, E., Wilks, M. F., Terron, A., Solecki, R. (2017). OECD/EFSA workshop on developmental neurotoxicity (DNT): The use of non-animal test methods for regulatory purposes. *Altex* **34**, 311–315.
- Fritsche, E., Alm, H., Baumann, J., Geerts, L., Hakansson, H., Masjosthusmann, S., and Witters, H. (2015) *Literature Review on in Vitro and Alternative Developmental Neurotoxicity (DNT) Testing Methods*. EFSA Supporting Publication 2015; EFSA Journal: EN-778, 186 pp.
- Fritsche, E., Grandjean, P., Crofton, K. M., Aschner, M., Goldberg, A., Heinonen, T., Hessel, E. V. S., Hogberg, H. T., Bennekou, S. H., Lein, P. J. (2018). Consensus statement on the need for innovation, transition and implementation of developmental neurotoxicity (DNT) testing for regulatory purposes. *Toxicol. Appl. Pharmacol.*, doi: 10.1016/j.taap.2018.02.004.
- Gassmann, K., Abel, J., Bothe, H., Haarmann-Stemmann, T., Merk, H. F., Quasthoff, K. N., Rockel, T. D., Schreiber, T., and Fritsche, E. (2010). Species-specific differential AhR expression protects human neural progenitor cells against developmental neurotoxicity of PAHs. *Environ. Health Perspect.* **118**, 1571–1577.
- Goldman, L. R., and Koduru, S. (2000). Chemicals in the environment and developmental toxicity to children: A public health and policy perspective. *Environ. Health Perspect.* **108(Suppl 3)**, 443–448.
- Gorris, R., Fischer, J., Erwes, K. L., Kesavan, J., Peterson, D. A., Alexander, M., Nöthen, M. M., Peitz, M., Quandt, T., Karus, M., et al. (2015). Pluripotent stem cell-derived radial glia-like cells as stable intermediate for efficient generation of human oligodendrocytes. *Glia* **63**, 2152–2167.
- Gotz, M., and Huttner, W. B. (2005). The cell biology of neurogenesis. *Nat. Rev. Mol. Cell. Biol.* **6**, 777–788.
- Grandjean, P., and Landrigan, P. J. (2006). Developmental neurotoxicity of industrial chemicals. *Lancet* **368**, 2167–2178.
- Grandjean, P., and Landrigan, P. J. (2014). Neurobehavioural effects of developmental toxicity. *Lancet Neurol.* **13**, 330–338.
- Hakem, R., Hakem, A., Duncan, G. S., Henderson, J. T., Woo, M., Soengas, M. S., Elia, A., de la Pompa, J. L., Kagi, D., Khoo, W., et al. (1998). Differential requirement for caspase 9 in apoptotic pathways in vivo. *Cell* **94**, 339–352.
- Harrill, J. A., Freudenrich, T. M., Machacek, D. W., Stice, S. L., and Mundy, W. R. (2010). Quantitative assessment of neurite outgrowth in human embryonic stem cell-derived hN2 cells

- using automated high-content image analysis. *Neurotoxicology* **31**, 277–290.
- Harrill, J. A., Freudenrich, T. M., Robinette, B. L., and Mundy, W. R. (2011). Comparative sensitivity of human and rat neural cultures to chemical-induced inhibition of neurite outgrowth. *Toxicol. Appl. Pharmacol.* **256**, 268–280.
- Harrill, J. A., Robinette, B. L., and Mundy, W. R. (2011). Use of high content image analysis to detect chemical-induced changes in synaptogenesis *in vitro*. *Toxicol. In Vitro* **25**, 368–387.
- He, X., Imanishi, S., Sone, H., Nagano, R., Qin, X.-Y., Yoshinaga, J., Akanuma, H., Yamane, J., Fujibuchi, W., Ohsako, S., et al. (2012). Effects of methylmercury exposure on neuronal differentiation of mouse and human embryonic stem cells. *Toxicol. Lett.* **212**, 1–10.
- Hofrichter, M., Nimtz, L., Tigges, J., et al. (2017) Comparative performance analysis of human iPSC-derived and primary neural progenitor cells (NPC) grown as neurospheres *in vitro*. *Stem Cell Res.* **25**, 72–82.
- Hogberg, H. T., Sobanski, T., Novellino, A., Whelan, M., Weiss, D. G., and Bal-Price, A. K. (2011). Application of micro-electrode arrays (MEAs) as an emerging technology for developmental neurotoxicity: Evaluation of domoic acid-induced effects in primary cultures of rat cortical neurons. *Neurotoxicology* **32**, 158–168.
- Huang, B., Ning, S., Zhang, Q., Chen, A., Jiang, C., Cui, Y., Hu, J., Li, H., Fan, G., Qin, L., et al. (2017). Bisphenol A represses dopaminergic neuron differentiation from human embryonic stem cells through downregulating the expression of insulin-like growth factor 1. *Mol. Neurobiol.* **54**, 3798–3812.
- Ivanov, D. P., Al-Rubai, A. J., Grabowska, A. M., and Pratten, M. K. (2016). Separating chemotherapy-related developmental neurotoxicity from cytotoxicity in monolayer and neurosphere cultures of human fetal brain cells. *Toxicol. In Vitro* **37**, 88–96.
- Kapucu, F. E., Tanskanen, J. M., Mikkonen, J. E., Yla-Outinen, L., Narkilahti, S., and Hyttinen, J. A. (2012). Burst analysis tool for developing neuronal networks exhibiting highly varying action potential dynamics. *Front. Comput. Neurosci.* **6**, 38.
- Kashyap, M. P., Kumar, V., Singh, A. K., Tripathi, V. K., Jahan, S., Pandey, A., Srivastava, R. K., Khanna, V. K., and Pant, A. B. (2015). Differentiating neurons derived from human umbilical cord blood stem cells work as a test system for developmental neurotoxicity. *Mol. Neurobiol.* **51**, 791–807.
- Keil, K. P., Sethi, S., Wilson, M. D., Chen, H., and Lein, P. J. (2017). *In vivo* and *in vitro* sex differences in the dendritic morphology of developing murine hippocampal and cortical neurons. *Sci. Rep.* **7**, 8486.
- Kettenmann, H., and Verkhratsky, A. (2011). Neuroglia–living nerve glue. *Fortschr. Neurol. Psychiatr.* **79**, 588–597.
- Kim, H. Y., Wegner, S. H., Van Ness, K. P., Park, J. J., Pacheco, S. E., Workman, T., Hong, S., Griffith, W., and Faustman, E. M. (2016). Differential epigenetic effects of chlorpyrifos and arsenic in proliferating and differentiating human neural progenitor cells. *Reprod. Toxicol.* **65**, 212–223.
- Krug, A. K., Balmer, N. V., Matt, F., Schonenberger, F., Merhof, D., and Leist, M. (2013). Evaluation of a human neurite growth assay as specific screen for developmental neurotoxicants. *Arch. Toxicol.* **87**, 2215–2231.
- Lancaster, M. A., Renner, M., Martin, C.-A., Wenzel, D., Bicknell, L. S., Hurles, M. E., Homfray, T., Penninger, J. M., Jackson, A. P., Knoblich, J. A., et al. (2013). Cerebral organoids model human brain development and microcephaly. *Nature* **501**, 373–379.
- Lein, P., Silbergeld, E., Locke, P., and Goldberg, A. M. (2005). *In vitro* and other alternative approaches to developmental neurotoxicity testing (DNT). *Environ. Toxicol. Pharmacol.* **19**, 735–744.
- Lu, Y., Yang, Y., Wang, Z., Wang, C., Du, Q., Wang, Q., and Luan, Z. (2015). Isolation and culture of human oligodendrocyte precursor cells from neurospheres. *Brain Res. Bull.* **118**, 17–24.
- Lundin, A., Delsing, L., Clausen, M., Ricchiuto, P., Sanchez, J., Sabirsh, A., Ding, M., Synnergren, J., Zetterberg, H., Brolén, G., et al. (2018). Human iPSC-derived astroglia from a stable neural precursor state show improved functionality compared with conventional astrocytic models. *Stem Cell Rep.* **10**, 1030–1045.
- Madill, M., Fitzgerald, D., O’Connell, K. E., Dev, K. K., Shen, S., and Fitz Gerald, U. (2016). *In vitro* and *ex vivo* models of multiple sclerosis. *Drug Discov. Today* **21**, 1504–1511.
- Malchenko, S., Xie, J., de Fatima Bonaldo, M., Vanin, E. F., Bhattacharyya, B. J., Belmadani, A., Xi, G., Galat, V., Goossens, W., Seftor, R. E. B., et al. (2014). Onset of rosette formation during spontaneous neural differentiation of hESC and hiPSC colonies. *Gene* **534**, 400–407.
- Masjosthusmann, S., Becker, D., Petzuch, B., et al. (2018). A transcriptome comparison of time-matched developing human, mouse and rat neural progenitor cells reveals human uniqueness. *Toxicol. Appl. Pharmacol.*, doi: 10.1016/j.taap.2018.05.009
- Mayor, R., and Theveneau, E. (2013). The neural crest. *Development* **140**, 2247–2251.
- Mendola, P., Selevan, S. G., Gutter, S., and Rice, D. (2002). Environmental factors associated with a spectrum of neurodevelopmental deficits. *Mental Retard. Dev. Disabil. Res. Rev.* **8**, 188–197.
- Moors, M., Bose, R., Johansson-Haque, K., Edoff, K., Okret, S., and Ceccatelli, S. (2012). Dickkopf 1 mediates glucocorticoid-induced changes in human neural progenitor cell proliferation and differentiation. *Toxicol. Sci.* **125**, 488–495.
- Nicaise, A. M., Banda, E., Guzzo, R. M., Russomanno, K., Castro-Borrero, W., Willis, C. M., Johnson, K. M., Lo, A. C., and Crocker, S. J. (2017). iPSC-derived neural progenitor cells from PPMS patients reveal defect in myelin injury response. *Exp. Neurol.* **288**, 114–121.
- Nyffeler, J., Karreman, C., Leisner, H., et al. (2017). Design of a high-throughput human neural crest cell migration assay to indicate potential developmental toxicants. *Altex* **34**, 75–94.
- Oh, J.-H., Son, M.-Y., Choi, M.-S., Kim, S., Choi, A.-Y., Lee, H.-A., Kim, K.-S., Kim, J., Song, C. W., Yoon, S., et al. (2016). Integrative analysis of genes and miRNA alterations in human embryonic stem cells-derived neural cells after exposure to silver nanoparticles. *Toxicol. Appl. Pharmacol.* **299**, 8–23.
- Okado, N., Kakimi, S., and Kojima, T. (1979). Synaptogenesis in the cervical cord of the human embryo: Sequence of synapse formation in a spinal reflex pathway. *J. Comp. Neurol.* **184**, 491–518.
- Pallosca, G., Grinberg, M., Henry, M., Frickey, T., Hengstler, J. G., Waldmann, T., Sachinidis, A., Rahnenführer, J., and Leist, M. (2016). Identification of transcriptome signatures and biomarkers specific for potential developmental toxicants inhibiting human neural crest cell migration. *Arch. Toxicol.* **90**, 159–180.
- Pamies, D., Barreras, P., Block, K., et al. (2017). A human brain microphysiological system derived from induced pluripotent stem cells to study neurological diseases and toxicity. *Altex* **34**, 362–376.
- Pamies, D., Bal-Price, A., Chesne, C., et al. (2018a). Advanced good cell culture practice for human primary, stem cell-derived



- and organoid models as well as microphysiological systems. *Altex*, doi: 10.14573/altex.1710081 10.14573/altex.1712221
- Pamies, D., Block, K., Lau, P., et al. (2018b). Rotenone exerts developmental neurotoxicity in a human brain spheroid model. *Toxicol. Appl. Pharmacol.*, doi: 10.1016/j.taap.2018.02.003
- Pei, Y., Peng, J., Behl, M., Sipes, N. S., Shockley, K. R., Rao, M. S., Tice, R. R., and Zeng, X. (2016). Comparative neurotoxicity screening in human iPSC-derived neural stem cells, neurons and astrocytes. *Brain Res.* **1638**, 57–73.
- Pellett, S., Schwartz, M. P., Tepp, W. H., Josephson, R., Scherf, J. M., Pier, C. L., Thomson, J. A., Murphy, W. L., and Johnson, E. A. (2015). Human induced pluripotent stem cell derived neuronal cells cultured on chemically-defined hydrogels for sensitive *in vitro* detection of botulinum neurotoxin. *Sci. Rep.* **5**, 14566.
- Pistollato, F., Canovas-Jorda, D., Zagoura, D., and Bal-Price, A. (2017). Nrf2 pathway activation upon rotenone treatment in human iPSC-derived neural stem cells undergoing differentiation towards neurons and astrocytes. *Neurochem. Int.* **108**, 457–471.
- Pistollato, F., Lousse, J., Scelfo, B., Mennecozzi, M., Accordi, B., Basso, G., Gaspar, J. A., Zagoura, D., Barilari, M., Palosaari, T., et al. (2014). Development of a pluripotent stem cell derived neuronal model to identify chemically induced pathway perturbations in relation to neurotoxicity: Effects of CREB pathway inhibition. *Toxicol. Appl. Pharmacol.* **280**, 378–388.
- Qian, X., Nguyen, H. N., Song, M. M., Hadiono, C., Ogden, S. C., Hammack, C., Yao, B., Hamersky, G. R., Jacob, F., Zhong, C., et al. (2016). Brain-region-specific organoids using mini-bioreactors for modeling ZIKV exposure. *Cell* **165**, 1238–1254.
- Radio, N. M., Breier, J. M., Reif, D. M., Judson, R. S., Martin, M., Houck, K. A., Mundy, W. R., and Shafer, T. J. (2015). Use of neural models of proliferation and neurite outgrowth to screen environmental chemicals in the toxcast phase I library. *Appl. In Vitro Toxicol.* **1**, 131–139.
- Robinette, B. L., Harrill, J. A., Mundy, W. R., and Shafer, T. J. (2011). *In vitro* assessment of developmental neurotoxicity: Use of microelectrode arrays to measure functional changes in neuronal network ontogeny. *Front. Neuroeng.* **4**, 1.
- Rodier, P. M. (1995). Developing brain as a target of toxicity. *Environ. Health Perspect.* **103(Suppl 6)**, 73–76.
- Ryan, K. R., Sirenko, O., Parham, F., Hsieh, J.-H., Cromwell, E. F., Tice, R. R., and Behl, M. (2016). Neurite outgrowth in human induced pluripotent stem cell-derived neurons as a high-throughput screen for developmental neurotoxicity or neurotoxicity. *Neurotoxicology* **53**, 271–281.
- Sandström, J., Eggermann, E., Charvet, I., Roux, A., Toni, N., Greggio, C., Broyer, A., Monnet-Tschudi, F., and Stoppini, L. (2017). Development and characterization of a human embryonic stem cell-derived 3D neural tissue model for neurotoxicity testing. *Toxicol. In Vitro* **38**, 124–135.
- Schmuck, M. R., Temme, T., Dach, K., de Boer, D., Barenys, M., Bendt, F., Mosig, A., and Fritsche, E. (2017). Omnisphero: A high-content image analysis (HCA) approach for phenotypic developmental neurotoxicity (DNT) screenings of organoid neurosphere cultures *in vitro*. *Arch. Toxicol.* **91**, 2017–2028.
- Scholz, D., Pörtl, D., Genewsky, A., Weng, M., Waldmann, T., Schildknecht, S., and Leist, M. (2011). Rapid, complete and large-scale generation of post-mitotic neurons from the human LUHMES cell line. *J. Neurochem.* **119**, 957–971.
- Schulpen, S. H., de Jong, E., de la Fonteyne, L. J., de Klerk, A., and Piersma, A. H. (2015). Distinct gene expression responses of two anticonvulsant drugs in a novel human embryonic stem cell based neural differentiation assay protocol. *Toxicol. In Vitro* **29**, 449–457.
- Shinde, V., Klima, S., Sureshkumar, P. S., et al. (2015). Human pluripotent stem cell based developmental toxicity assays for chemical safety screening and systems biology data generation. *J. Visual. Exp.* **100**, e52333.
- Singh, S., Srivastava, A., Kumar, V., Pandey, A., Kumar, D., Rajpurohit, C. S., Khanna, V. K., Yadav, S., and Pant, A. B. (2016). Stem cells in neurotoxicology/developmental neurotoxicology: Current scenario and future prospects. *Mol. Neurobiol.* **53**, 6938–6949.
- Slikker, W. Jr. (1994). Principles of developmental neurotoxicology. *Neurotoxicology* **15**, 11–16.
- Sohn, H. M., Kim, H. Y., Park, S., Han, S. H., and Kim, J. H. (2017). Isoflurane decreases proliferation and differentiation, but none of the effects persist in human embryonic stem cell-derived neural progenitor cells. *J. Anesth.* **31**, 36–43.
- Stummann, T. C., Hareng, L., and Bremer, S. (2009). Hazard assessment of methylmercury toxicity to neuronal induction in embryogenesis using human embryonic stem cells. *Toxicology* **257**, 117–126.
- Tedesco, M. T., Di Lisa, D., Massobrio, P., Colistra, N., Pesce, M., Catelani, T., Dellacasa, E., Raiteri, R., Martinoia, S., Pastorino, L., et al. (2018). Soft chitosan microbeads scaffold for 3D functional neuronal networks. *Biomaterials* **156**, 159–171.
- Toivonen, S., Ojala, M., Hyysalo, A., Ilmarinen, T., Rajala, K., Pekkanen-Mattila, M., Äänismaa, R., Lundin, K., Palgi, J., Weltner, J., et al. (2013). Comparative analysis of targeted differentiation of human induced pluripotent stem cells (hiPSCs) and human embryonic stem cells reveals variability associated with incomplete transgene silencing in retrovirally derived hiPSC lines. *Stem Cells Transl. Med.* **2**, 83–93.
- Tong, Z.-B., Hogberg, H., Kuo, D., Sakamuru, S., Xia, M., Smirnova, L., Hartung, T., and Gerhold, D. (2017). Characterization of three human cell line models for high-throughput neuronal cytotoxicity screening. *J. Appl. Toxicol.* **37**, 167–180.
- Uzquiano, A., Gladwyn-Ng, I., Nguyen, L., et al. (2018). Cortical progenitor biology: Key features mediating proliferation versus differentiation. *J. Neurochem.*, doi: 10.1111/jnc.14338.
- Vichier-Guerre, C., Parker, M., Pomerantz, Y., Finnell, R. H., and Cabrera, R. M. (2017). Impact of selective serotonin reuptake inhibitors on neural crest stem cell formation. *Toxicol. Lett.* **281**, 20–25.
- Waldmann, T., Rempel, E., Balmer, N. V., König, A., Kolde, R., Gaspar, J. A., Henry, M., Hescheler, J., Sachinidis, A., Rahnenführer, J., et al. (2014). Design principles of concentration-dependent transcriptome deviations in drug-exposed differentiating stem cells. *Chem. Res. Toxicol.* **27**, 408–420.
- Wallen, K., Baum, M. J., (2002). Masculinization and Defeminization in Altricial and Precocial Mammals: Comparative Aspects of Steroid Hormone Action. *Hormones, Brain and Behavior*. pp. 385–423.
- Wang, X., Yan, M., Zhao, L., Wu, Q., Wu, C., Chang, X., and Zhou, Z. (2016). Low-dose methylmercury-induced genes regulate mitochondrial biogenesis via miR-25 in immortalized human embryonic neural progenitor cells. *Int. J. Mol. Sci.* **17**, 2058.
- Weiss, B., and Lambert, G. (2000). Framing the research agenda of developmental neurotoxicology in children. Session VIII. Summary and research needs. *Neurotoxicology* **21**, 277–278.
- WHO-UNEP. (2012). State of the Science of Endocrine Disrupting Chemicals. World Health Organization, United Nations Environment Programme.

- Wilson, M. S., Graham, J. R., and Ball, A. J. (2014). Multiparametric high content analysis for assessment of neurotoxicity in differentiated neuronal cell lines and human embryonic stem cell-derived neurons. *Neurotoxicology* **42**, 33–48.
- Wu, X., Yang, X., Majumder, A., Swetenburg, R., Goodfellow, F. T., Bartlett, M. G., and Stice, S. L. (2017). From the cover: Astrocytes are protective against chlorpyrifos developmental neurotoxicity in human pluripotent stem cell-derived astrocyte-neuron cocultures. *Toxicol. Sci.* **157**, 410–420.
- Yamashita, T., Miyamoto, Y., Bando, Y., et al. (2017). Differentiation of oligodendrocyte progenitor cells from dissociated monolayer and feeder-free cultured pluripotent stem cells. *PLoS One* **12**, e0171947.
- Yla-Outinen, L., Heikkila, J., Skottman, H., Suuronen, R., Aanismaa, R., and Narkilahti, S. (2010). Human cell-based micro electrode array platform for studying neurotoxicity. *Front. Neuroeng.* **3**, 111.
- Zecevic, D., and Antic, S. (1998). Fast optical measurement of membrane potential changes at multiple sites on an individual nerve cell. *Histochem. J.* **30**, 197–216.
- Zeng, X., Chen, J., Deng, X., Liu, Y., Rao, M. S., Cadet, J.-L., and Freed, W. J. (2006). An *in vitro* model of human dopaminergic neurons derived from embryonic stem cells: mPP+ toxicity and GDNF neuroprotection. *Neuropsychopharmacology* **31**, 2708–2715.
- Zeng, Y., Kurokawa, Y., Win-Shwe, T.-T., Zeng, Q., Hirano, S., Zhang, Z., and Sone, H. (2016). Effects of PAMAM dendrimers with various surface functional groups and multiple generations on cytotoxicity and neuronal differentiation using human neural progenitor cells. *J. Toxicol. Sci.* **41**, 351–370.
- Zhuang, P., Sun, A. X., An, J., Chua, C. K., and Chew, S. Y. (2018). 3D neural tissue models: From spheroids to bioprinting. *Biomaterials* **154**, 113–133.
- Zimmer, B., Lee, G., Balmer, N. V., Meganathan, K., Sachinidis, A., Studer, L., and Leist, M. (2012). Evaluation of developmental toxicants and signaling pathways in a functional test based on the migration of human neural crest cells. *Environ. Health Perspect.* **120**, 1116–1122.
- Zimmer, B., Pallocca, G., Dreser, N., et al. (2014). Profiling of drugs and environmental chemicals for functional impairment of neural crest migration in a novel stem cell-based test battery. *Arch. Toxicol.* **88**, 1109–1126.
- Zychowicz, M., Dziedzicka, D., Mehn, D., Kozłowska, H., Kinsner-Ovaskainen, A., Stępień, P. P., Rossi, F., and Buzanska, L. (2014). Developmental stage dependent neural stem cells sensitivity to methylmercury chloride on different biofunctional surfaces. *Toxicol. In Vitro* **28**, 76–87.

---

## Current Availability of Stem Cell-Based *In Vitro* Methods for Developmental Neurotoxicity (DNT) Testing

Ellen Fritsche, Marta Barenys, **Jördis Klose**, Stefan Masjosthusmann, Laura Nimtz, Martin Schmuck, Saskia Wuttke and Julia Tigges

Journal:	Toxicological Sciences (Toxicol Sci)
Impact Factor:	4.081 (2016)
Contribution to the publication:	20 % Writing of the manuscript sections ‘neural progenitor cell proliferation’, ‘neural crest cell/radial glia/neuronal migration’ and ‘Oligodendrocyte differentiation/maturation’; Performance of the experiments included in Fig. 4 A and B.
Type of authorship:	first authorship
Status of the publication:	Published 5 <sup>th</sup> July 2018

## 2.3 The Neurosphere Assay as an *In Vitro* Method for Developmental Neurotoxicity (DNT) Evaluation

Laura Nimtz, **Jördis Klose**, Stefan Masjosthusmann, Marta Barenys and Ellen Fritsche

*Cell Culture Techniques, Neuromethods vol. 145, Chapter 8*

Das sich entwickelnde menschliche zentrale Nervensystem ist anfälliger für die nachteiligen Auswirkungen chemischer Wirkstoffe als das erwachsene Gehirn. Aufgrund des Mangels an verfügbaren Daten zu Substanzen, welche die humane neurologische Entwicklung stören, besteht derzeit ein dringender Bedarf, Chemikalien auf ihr entwicklungsneurotoxisches Potential hin zu untersuchen und nachfolgend zu regulieren. Alternative Teststrategien könnten diese Lücke füllen, da sie ein schnelles und ressourceneffizientes Überprüfen von chemischen Verbindungen für eine Vielzahl von Endpunkten der neurologischen Entwicklung gewährleisten. Die Komplexität des sich entwickelnden Nervensystems erfordert hierbei eine Reihe von Tests, die sowohl frühe, als auch späte Entwicklungsprozesse abdecken. Einer dieser Tests ist der "Neurosphären Assay". Hierbei handelt es sich um ein 3D *in vitro* Modell, welches auf menschlichen neuralen Progenitorzellen (NPC) basiert und für die Bewertung von Entwicklungsneurotoxizität (developmental neurotoxicity; DNT) geeignet ist. Mit diesem Assay kann man entwicklungsneurotoxisch wirkende Chemikalien identifizieren, die grundlegende neurologische Entwicklungsprozesse stören, wie z.B. NPC Proliferation, Migration, Differenzierung zu Neuronen und Oligodendrozyten, sowie Schilddrüsenhormon (TH)-abhängige Oligodendrozytenreifung. Durch die Einbeziehung von Viabilität- und Zytotoxizitätstests kann zwischen spezifischer DNT Effekten und allgemeiner Zytotoxizität unterschieden werden. In diesem Buchkapitel wird erklärt, wie die verschiedenen Testmethoden des „Neurosphären-Assays“, d.h. NPC1–6, durchgeführt und zeit- und kosteneffizient zusammengefasst werden.



## The Neurosphere Assay as an In Vitro Method for Developmental Neurotoxicity (DNT) Evaluation

Laura Nimtz, Jördis Klose, Stefan Masjosthusmann, Marta Barenys, and Ellen Fritsche

### Abstract

The human developing central nervous system is more vulnerable to the adverse effects of chemical agents than the adult brain. At present, due to the lack of available data on human neurodevelopmental toxicants, there is an urgent need for testing and subsequently regulating chemicals for their potential to interfere with nervous system development. Alternative testing strategies might fill that gap as they allow fast and resource-efficient compound screenings for a variety of neurodevelopmental endpoints. Nervous system development is complex calling for a battery of tests that cover early and late developmental stages and a variety of neurodevelopmental processes. One of such assays is the “neurosphere assay,” an in vitro 3D model for developmental neurotoxicity (DNT) evaluation based on human neural progenitor cells. With this assay, one can identify compounds that disturb basic neurodevelopmental processes, such as NPC proliferation, migration, neuronal- and oligodendrocyte differentiation, as well as thyroid hormone (TH)-dependent oligodendrocyte maturation. By including viability and cytotoxicity assays into the workflow, the assays allow the distinction of specific DNT from general cytotoxicity. This chapter explains how the different test methods of the “neurosphere assay,” i.e., NPC1–6, are performed and how some of them can be multiplexed in a time- and cost-efficient manner.

**Key words** Developmental neurotoxicity, Neural progenitor cells, In vitro, Brain development, Neurodevelopment, DNT, Human, Alternative methods, New approach method, NAM

---

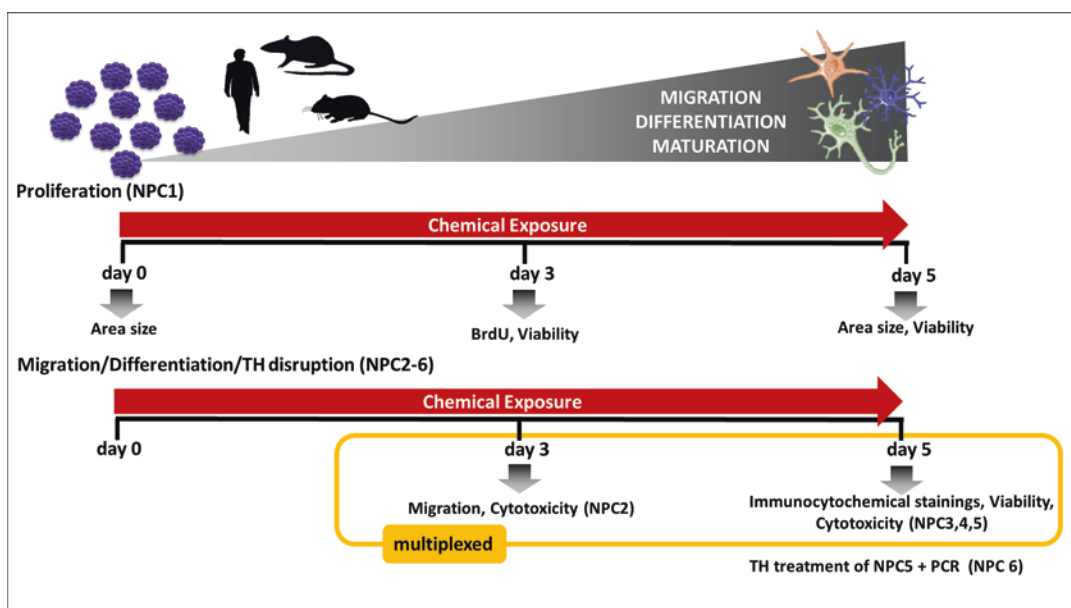
### 1 General Introduction

Within the last two decades, there has been considerable concern that exposure toward chemicals might be a contributing factor to the increasing incidence of neurodevelopmental disorders in children [1–4]. For few compounds the evidence for causing developmental neurotoxicity (DNT) is clear, whereas for the majority of chemicals this concern hampers a solid scientific basis because they have not been evaluated for their neurodevelopmental toxicity [5, 6].

---

Laura Nimtz, Jördis Klose, and Stefan Masjosthusmann are contributed equally to this manuscript.

The main reason for this data gap lies in the resource intensity of the current guideline studies: EPA 870.6300 developmental neurotoxicity (DNT) guideline [7] and the draft OECD 426 guideline [8]. These guidelines are highly demanding with regard to time, money, and animals [5, 9] and are therefore not suited for testing large number of chemicals. Therefore, international researchers have been establishing alternative methods for faster and cheaper DNT evaluation based on in vitro methods. In addition, concepts on how to use and interpret such methods with the final goal of regulatory application have been developed [9–16]. For alternative DNT evaluation, the complex procedure of brain development is disassembled into spatiotemporal neurodevelopmental processes that are necessary for forming a functional brain and can be tested for adverse effects of compounds in in vitro assays [10, 11, 16, 17]. Here, human-based systems are preferred because species differences in toxicokinetics, e.g., due to developmental timing, and/or toxicodynamics might affect responses to compounds [18–24]. In this chapter we describe one of the methods suitable for DNT evaluation, the “neurosphere assay.” This assay consists of six individual test methods (NPC1–6) measuring different endpoints, some of which can be multiplexed (Fig. 1) [11]. In the following



**Fig. 1** Experimental setup of the “neurosphere assay”. (Adapted from Masjosthusmann et al. [23]). NPC were generated from fetal human brain (Lonza, Verviers, Belgium) or postnatal day (PND)1 mouse and rat brains and cultivated as free-floating neurospheres. The “neurosphere assay” consists of six individual assays: proliferation assay (NPC1), migration assay (NPC2), as well as neuronal differentiation assay (NPC3), neuronal morphology assay (NPC4), oligodendrocyte differentiation assay (NPC5), and thyroid hormone (TH)-dependent oligodendrocyte maturation assay (NPC6) for measuring different endpoints under chemical exposure. For saving time and resources, the assays NPC2-5 can be multiplexed. Gene expression analyses in the TH disruption assay (NPC6) quantify the oligodendrocyte-specific maturation genes *MBP*, *MOBP*, and *MOG* [18]

paragraphs, a detailed description of the individual endpoint evaluations will be given. These endpoints can also be evaluated with neurospheres generated from rodents, which goes beyond the scope of this chapter [18, 19, 25, 26].

### 1.1 Cell Culture

Human neurospheres gain size by cultivation in the presence of growth factors. By mechanical passaging with a razor blade (chopping), neurospheres are cut into small cubes, which round up to smaller neurospheres of a uniform size within 1 day in proliferation medium and subsequently again continue to grow in size. By using this method, neurospheres are expanded and cultivated over several months without losing their proliferative capacity.

### 1.2 Materials

Proliferation medium:

DMEM (Gibco GlutaMAX, Life Technologies GmbH) and Hams F12 (Gibco GlutaMAX, Life Technologies GmbH) 3:1 supplemented with 2% B27 (Life Technologies GmbH). Epidermal growth factor (EGF, Life Technologies GmbH) and recombinant human fibroblast growth factor (FGF, R&D Systems) are dissolved at 10 µg/mL in sterile PBS containing 0.1% BSA and 1 mM DTT and stored at -20 °C. EGF and FGF are diluted in the medium at a final concentration of 20 ng/mL each for human neurospheres. Antibiotics (100× penicillin/streptomycin) are added to a 1× final concentration. Prepared medium containing supplements, growth factors, and antibiotics can be stored up to 2 weeks at 4 °C.

### 1.3 Methods

All steps need to be performed under sterile conditions.

#### 1.3.1 Culturing of Human Neurospheres

Feed human neurospheres every 2–3 days by replacing half of the medium with fresh proliferation medium.

#### 1.3.2 Expand the Human Neurospheres by Mechanical Chopping

1. To increase growth and survival, neurospheres are chopped the latest when they reach a diameter of 0.7 mm, alternatively once a week.
2. For chopping use a McIlwain tissue chopper, and clean it with terralin.
3. Soak a double-edged razor blade in 100% acetone, and sterilize the sliding table and the chopping arm with terralin.
4. Carefully secure the blade onto the chopping arm. Make sure the blade is parallel to the chopping surface.
5. Check and if necessary set the chopper settings (*see Note 1*).
6. Prepare 10-cm petri dishes for the newly chopped neurospheres by filling them with 20 mL proliferation medium each (*see Note 2*).

7. Transfer the neurospheres with as little medium as possible from the 10-cm petri dish into the middle of an inverted lid of a 6-cm petri dish.
8. Remove the remaining medium with a pipet in order to prevent the neurospheres from moving during the chopping process.
9. Place the dish lid on the chopper, and move the sliding table to the starting position.
10. Turn on the power, and press “reset.”
11. When all neurospheres on the lid are chopped, stop and raise the chopping arm, and reposition the table in the starting position.
12. Rotate the dish lid 90°, and repeat steps 10 and 11.
13. When the neurospheres are chopped in the second direction, remove the dish lid from the chopper, and add about 1 mL proliferation medium to the cells.
14. Resuspend the chopped neurospheres by gently pipetting them up and down, and then equally distribute the cell suspension into the prepared new petri dishes.
15. Put the cells back into the cell culture incubator (*see Note 3*).
16. After chopping is complete, clean the chopper with terralin, and eventually discard the razor blade (usually one blade can be used three times each side) (*see Note 4*).
17. Feed human neurospheres every 2–3 days by replacing half of the medium with fresh B27 proliferation medium with growth factors.
18. When the chopped neurospheres gain a sphere diameter of 0.3 mm (usually 2–3 days after chopping), they are used for experiments.

#### 1.4 Notes

Note 1: The blade force should be set straight up, and the chop distance should be set between 0.15 and 0.25 mm depending on the sphere size you wish to recover.

Note 2: Usually two to three new petri dishes are gained from one petri dish of chopped neurospheres.

Note 3: We keep the dishes in the incubator until we need them the next time, either for feeding or for plating an experiment.

Note 4: Make sure the neurospheres are well distributed in the petri dish to avoid aggregation.

---

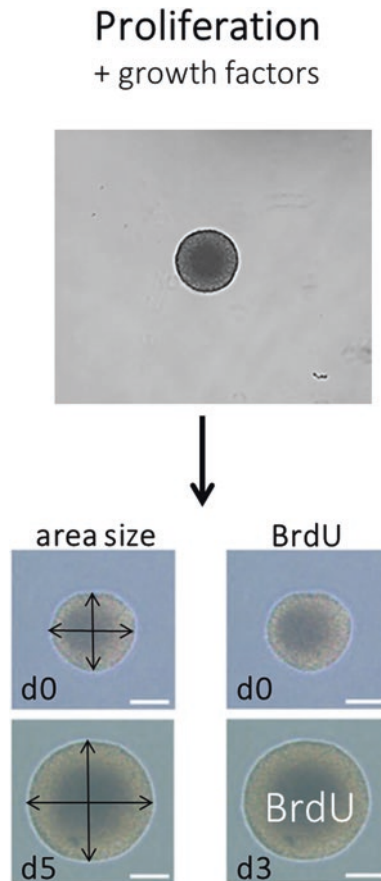
## 2 Proliferating Neurospheres

### 2.1 The Proliferation Assay (NPC1)

A fundamental neurodevelopmental key event (KE) is cell proliferation. Disturbance of proliferation during brain development can lead to smaller brains as an adverse outcome in vivo [27]. The NPC1 assay measures neural proliferation by using primary hNPC of fetal



origin (Lonza, Verviers, Belgium) grown as neurospheres in 3D. Proliferation can be studied by measuring the increase in sphere diameter (by area) over 5 days in vitro (DIV) using phase-contrast microscopy [19, 25, 28–32] and/or by measuring BrdU incorporation after 3 DIV using a luminescence-based BrdU assay (Roche) and a luminometer (Fig. 2) [25, 28]. Sphere diameter is measured with ImageJ and change in diameter monitored for each individual sphere. The same setup is used for the BrdU assay, where BrdU incorporation into the DNA of hNPC is measured by using a luminometer. The endpoint-specific control for this assay is withdrawal of growth factors significantly reducing hNPC proliferation. Because measuring the area in individual spheres is quick, easy, and inexpensive, it can be used as a first tier for a first-hit identification. Yet, the direct proliferation assay, quantifying BrdU incorporation into the DNA, is subsequently used for final assessment of disturbance of NPC proliferation by substances.



**Fig. 2** Proliferation assay (NPC1). Human neural progenitor cells (NPC) are grown as neurospheres under proliferating conditions. Proliferation is assessed by performing a BrdU Cell Proliferation ELISA (Roche©) on day3 (d3) and/or measuring the increase in sphere area size on day 5 (d5). The latter is a quick and inexpensive test that can be used as a first tier screen assay. Scale bars = 0.15 mm

---

### 3 Proliferation Assay (NPC1): Readout – Area Size

#### 3.1 Materials

Proliferation medium (*see above*)  
H<sub>2</sub>O, deionized and sterile  
U-bottom 96-well plate (clear)

#### 3.2 Methods

All steps need to be performed under sterile conditions.

##### 3.2.1 Plating Spheres for NPC1: Readout – Area Size

1. Chop spheres 1–3 days prior to the experiment (*see Note 1*).
2. Equilibrate proliferation medium with and without growth factors to 37 °C, 5% CO<sub>2</sub> for 60 min.
3. Prepare all treatment and control solutions, and add 100 µL to each well of a U-bottom 96-well plate.

##### Controls:

- (a) Media control (MC): only proliferation medium.
  - (b) Solvent control (SC): proliferation medium with respective solvent.
  - (c) Endpoint-specific control (PC): proliferation medium without growth factors.
  - (d) If combined with the lactase dehydrogenase (LDH) cytotoxicity assay and/or the CellTiter-Blue (CTB) viability assay, prepare lysis control (LC) and background control (BG) (*see Sects. 9 and/or 10*).
4. Fill all wells surrounding wells with plated cells with 100 µL deionized and sterile water.
  5. Presort the desired amount of spheres ( $0.3 \pm 0.025$  mm) out of the petri dish into a new petri dish with 3–5 mL of proliferation medium (37 °C).
  6. From the presorted spheres, transfer 1 sphere in 2,5 µL of medium into a well in a U-bottom 96-well plate. The tip has to be changed between different conditions.
  7. Incubate the cells for 5 days at 37 °C, 5% CO<sub>2</sub>.
  8. The cells have to be fed on day 2 or 3.
  9. For feeding, half of the medium (50 µL) is removed and substituted with freshly prepared control/treatment proliferation medium (pre-warmed to 37 °C).

##### 3.2.2 Taking Images of Individual Spheres

On days 0 (between 0 and 2 h after plating), 1, 2, and 5, the plate is scanned in the Cellomics ArrayScan VTI (Thermo Fisher) using the bioapplication colocalization V4 of the vHCS-Scan software (V6.6.0; build 8153). This software takes a phase-contrast image of each sphere in its individual well and directly analyzes the sphere area. Alternatively, individual phase-contrast images can be taken

with a regular microscope equipped with a camera. Images can be analyzed for sphere area size using ImageJ.

All results in fold of control are pooled from independent experiments, SD and SEM are calculated, and statistical analyses are performed. Data are analyzed with the software GraphPad Prism 6.0 using OneWay ANOVA and Bonferroni's post hoc test. Significance threshold is established at  $p < 0.05$ .

### 3.3 Notes

There are no relevant notes for this protocol.

---

## 4 Proliferation Assay (NPC1): Readout – BrdU Incorporation

### 4.1 Materials

Proliferation medium with and without growth factors (*see above*)  
H<sub>2</sub>O, deionized and sterile

Cell Proliferation ELISA, BrdU (#11669915001, Roche/Sigma, +2 to +8 °C)

1 (Red flip-up cap) BrdU labeling reagent

2 (Red) Fix Denat

3 (Blue) Anti-BrdU-POD

4 (Blue) Antibody dilution solution

5 (Green) Washing buffer

6 (Black) Substrate component A

7 (Yellow) Substrate component B

Accutase (#A1110501; Life Technologies)

U-bottom 96-well plate (clear)

Flat-bottom 96-well plate (black)

### 4.2 Methods

All steps need to be performed under sterile conditions.

Follow the instructions from NPC1 with the readout “area size” for preparing and plating of neurospheres.

#### 4.2.1 Preparation for Cell Proliferation ELISA

1. Dissolve anti-BrdU-POD (3, blue) in 1.1 mL double dist. water for 10 min and mix thoroughly. Solution can be stored at +2 to +8 °C for several months.
2. Dilute BrdU labeling reagent 1:100 in proliferation medium without growth factors (shortly before use).
3. Pre-warm an aliquot of Accutase at 37 °C for 15 min.
4. Dilute anti-BrdU-POD stock solution (3, blue) 1:100 in antibody dilution solution (4, blue) to prepare anti-BrdU working solution (shortly before use).
5. Dilute washing buffer (5, green) 1:10 in deionized water to prepare washing solution.

6. Dilute substrate component B (7, yellow) 1:100 in substrate component A (6, black) to prepare substrate solution. Prepare substrate solution before washing (see Sect. 4.2.2, *step 15*), and incubate for 5–10 min at 37 °C (protect from light).

4.2.2 Procedure  
of the Cell Proliferation  
ELISA

1. Eighteen hours before termination of the experiment, add 10  $\mu\text{L}$  of BrdU labeling dilution (see Sect. 4.2.1, 2) to each well except for the background for BrdU.
2. Incubate the spheres for additional 18 h at 37 °C, 5%  $\text{CO}_2$ .
3. After 16 h of incubation, the LDH and the CTB Assays are performed (see Sects. 9 and 10).
4. For sphere dissociation needed for BrdU evaluation, pipette 25  $\mu\text{L}$  pre-warmed Accutase to the edge of each well of a new, black 96-well plate, and incubate for 10 min at 37 °C.
5. Transfer each sphere with 10  $\mu\text{L}$  medium into the Accutase drop of the new plate. Make sure that each sphere is pipetted into the same well position of the new plate.
6. Incubate 10 min at 37 °C.
7. Singularize cells by pipetting up and down (15–20 times) with a 100  $\mu\text{L}$  tip (set the pipette to 50  $\mu\text{L}$ , and use a new set of tips for each treatment).
8. Spread the drop well across the well.
9. Heat the plate with a hairdryer until it is completely dry (there should be at least 10 cm space between the hairdryer and the plate).
10. Add 200  $\mu\text{L}$  Fix Denat solution to each well, and incubate for 45 min at room temperature.
11. Remove fixation solution by flicking off into the sink and tapping the plate on a paper towel.
12. Add 100  $\mu\text{L}$  anti-BrdU-POD working solution (see Sect. 4.2.1, *step 4*) to each well, and incubate for 1.5 h at room temperature.
13. Prepare substrate solution (see Sect. 4.2.1 *bullet 5*) and washing solution (see Sect. 4.2.1, *step 6*) 15 min before the end of the incubation period.
14. Remove solution by flicking off into the sink and tapping the plate on a paper towel.
15. Wash wells three times with 200  $\mu\text{L}$ /well washing solution (see Sect. 4.2.1, *step 6*) for 1 min, and shake the plate horizontally for 10–20 s.
16. Remove washing solution by flicking off into the sink and tapping the plate on a paper towel.

17. Add 100  $\mu$ L substrate solution (see Sect. 4.2.1, step 6) to each well, and incubate 5 min at room temperature. During this time, protect the plate from light.
18. Place the plate without lid into the plate reader for measuring luminescence.
19. Open a protocol (*see below Specification of plate reader protocol for TECAN fluorescence plate reader Infinite M200Pro*) for reading the BrdU assay.
20. Select the wells that you want to measure, and start the measurement.

#### 4.2.3 Specification of TECAN Plate Reader Protocol

Mode	Luminescence
Attenuation	NONE
Integration time	1000 ms
Settle time	0 ms
Plate	Thermo Fisher Scientific-Nunclon 96 Flat Bottom Black Polystyrene Cat. No.: 437869/437958 [NUN96fb_LumiNunc FluoroNunc.pdf]

#### 4.2.4 Data Export and Evaluation

1. Save the Excel file with raw data.
2. Copy the raw data into your evaluation sheet.
3. Calculate MEAN of all technical replicate measurements.
4. Subtract MEAN of BrdU from the MEAN of all conditions.
5. Calculate BG subtracted MEAN of each condition as percent of SC.
6. All results in fold of control are pooled from independent experiments, SD and SEM are calculated, and statistical analyses are performed. Data are analyzed with the software GraphPad Prism 6.0 using OneWay ANOVA and Bonferroni's post hoc test. Significance threshold is established at  $p < 0.05$ .

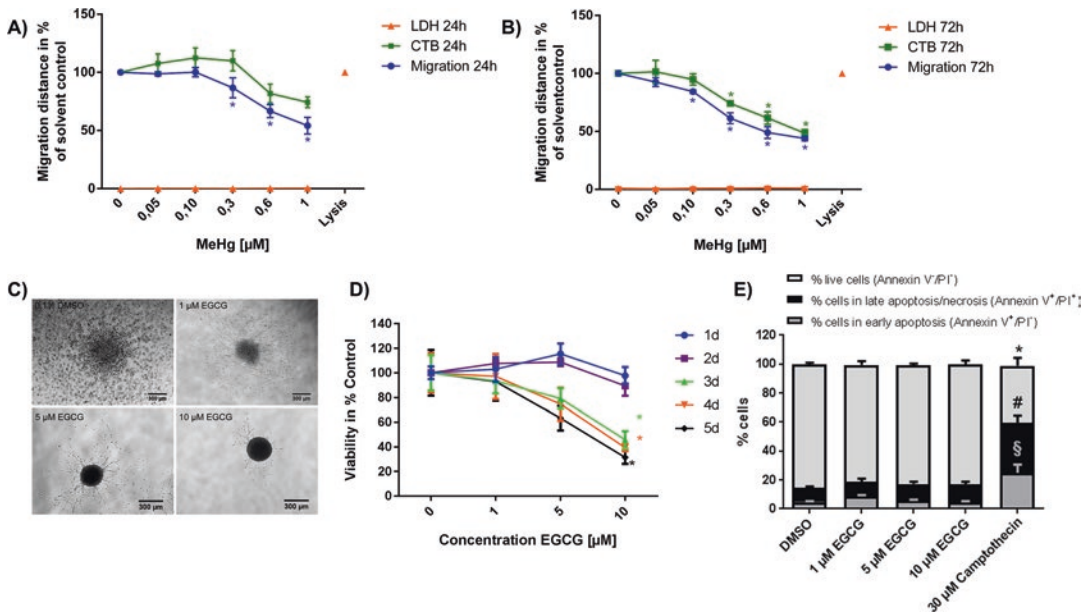
#### 4.3 Notes

There are no relevant notes for this protocol.

## 5 Differentiating Neurospheres

### 5.1 Migration Assay (NPC2)

During cortex development glial cells form a scaffold for neurons to migrate from proliferating niches to their final cortical destination. This migration is a fundamental neurodevelopmental KE since its disturbance leads to alterations in cortex formation, as it occurs, e.g., in methylmercury-exposed children [33].



**Fig. 3** Migration assay (NPC2) with exemplary migration effect of EGCG treatment. (Taken from Fritsche et al. [36] with permission of *Toxicological Science*). hNPCs, growing as neurospheres in proliferation culture, were plated for migration analyses onto poly-D-lysine/laminin-coated glass slides in presence and absence of MeHgCl. After (a) 24 h and (b) 72 h, migration distance was measured from the outer sphere rim to the furthest migrated cells at four opposite positions. CellTiter-Blue (CTB) and Lactate Dehydrogenase (LDH) Assays were performed as described previously [25]. (c), Neurospheres were plated as described in (a) in presence and absence of epigallocatechin gallate (EGCG). After 24 h the migration area was analyzed visually by phase-contrast microscopy, and for better visualization images were subjected to a black/white filter. (d), Viability analyses using the CTB Assay were performed on each day up to 5 DIV. (e), On day 5, FACS analyses of dissociated hNPC were performed after annexin V/PI staining. As a positive control, spheres were treated with the topoisomerase I inhibitor camptothecin. (a, b, d)  $p \leq 0.05$ ; (e) §  $p \leq 0.05$  of annexin<sup>+</sup>/PI<sup>-</sup> cells; #  $p \leq 0.05$  of annexin<sup>+</sup>/PI<sup>+</sup> cells; \*  $p \leq 0.05$  of live cells

Plating primary human neurospheres of fetal origin on a poly-D-lysine/laminin-coated surface in medium devoid of growth factors initiates radial NPC migration out of the sphere core, thus allowing the study of this essential KE in a plate, i.e., a 96-well plate. In this culture, first migrating cells are nestin- and SOX-2-positive and show radial glia morphology [25, 30, 34, 35]. Moreover, their migration is laminin-integrin dependent (Fig. 3) [36, 37]. In this protocol we present a method to evaluate the ability of hNPCs to migrate out of the sphere core by measuring the maximum covered distance over the coated surface after 3 days in vitro. The migration distance can also be determined at any day up to 5 days by using high-content image analyses (HCA) and the Omnisphero program [37, 38] as described in Sect. 6.2.6.

**5.2 Materials**

Proliferation medium (see Sect. 1.1)  
 Flat-bottom 96-well plates (clear)

Poly-D-lysine: Dissolve poly-D-lysine (#P0899, Sigma-Aldrich) at 0.1 mg/mL in sterile water. Store up to 1 month at  $-20^{\circ}\text{C}$ .

Sterile water

One milligram per milliliter laminin (#L2020, Sigma-Aldrich)

Phosphate-buffered saline with  $\text{Ca}^{2+}$  and  $\text{Mg}^{2+}$  (PBS; Gibco, Life Technologies GmbH), sterile

Differentiation medium: DMEM (Gibco GlutaMAX, Life Technologies GmbH), Hams F12 (Gibco GlutaMAX, Life Technologies GmbH) 3:1 supplemented with 1% of N2 (Life Technologies GmbH), and antibiotic solution (100 $\times$  penicillin/streptomycin) to 1 $\times$  final. Store for up to 2 weeks at  $4^{\circ}\text{C}$ .

PP2 (#P0042-5MG, Sigma-Aldrich)

### 5.3 Methods

All steps need to be performed under sterile conditions.

Follow the instructions in "Expand the Human Neurospheres by Mechanical Chopping" to prepare neurospheres for plating.

#### 5.3.1 Coating of 24- or 96-Well Plates

1. Fill each well with 300  $\mu\text{L}$  (24-well plate) or 50  $\mu\text{L}$  (96-well plate) poly-D-lysine (PDL), and incubate for 1 h at  $37^{\circ}\text{C}$ .
2. Wash each well with 500  $\mu\text{L}$  (24-well plate) or 100  $\mu\text{L}$  (96-well plate) sterile deionized water.
3. Afterward, fill every well with 300  $\mu\text{L}$  (24-well plate) or 50  $\mu\text{L}$  (96-well plate) laminin (1:80 dilution of laminin in sterile deionized water), and incubate for 1 h at  $37^{\circ}\text{C}$  (*see Note 1*).
4. Wash each well with 500  $\mu\text{L}$  (24-well plate) or 100  $\mu\text{L}$  (96-well plate) sterile deionized water.
5. Wash each well with 500  $\mu\text{L}$  (24-well plate) or 100  $\mu\text{L}$  (96-well plate) sterile PBS.

#### 5.3.2 Preparation of Exposure Solutions and Endpoint-Specific Controls

1. Prepare the desired dilution series of the test compound from a stock solution in differentiation medium. The final concentration of the solvent should be the same in all dilutions and not exceed 0.3% (v/v) for DMSO and 1% (v/v) for deionized water or PBS. The maximum solvent concentration for other solvents needs to be tested separately.
2. Prepare the following controls:  
*Controls:*
  - (a) Media control (MC): only differentiation medium.
  - (b) Solvent control (SC): differentiation medium with respective solvent.
  - (c) Positive control (PC): 10  $\mu\text{M}$  PP2 in differentiation medium. PP2 is a src-kinase inhibitor and therefore serves as an endpoint-specific control for cell migration [34].



- (d) If combined with LDH Assay and/or CTB Assay, prepare lysis control (LC) and background control (BG) (see Sects. 9 and/or 10) (*see Note 2*).
3. Fill the needed wells of a coated 96-well plate with 100  $\mu$ L of the exposure solutions (*see Note 3*).
4. Fill all wells surrounding cell-containing wells with 100  $\mu$ L deionized and sterile water.

### 5.3.3 Plating Neurospheres for NPC2

1. Fill a 6-cm petri dish with 5 mL differentiation medium (*see Note 4*).
2. Select neurospheres with a diameter of  $0.3 \pm 0.025$  mm with a 100- $\mu$ L tip using a binocular microscope, and transfer them into the 6-cm petri dish with N2 differentiation medium (*see Note 5*).
3. Transfer each neurosphere in 2.5  $\mu$ L medium into the middle of a well of the 96-well plate filled with the experimental solutions. The tip should be changed between different conditions (*see Note 6*).
4. Incubate neurospheres at 37 °C, 5% CO<sub>2</sub>.

### 5.3.4 Cultivation and Image Acquisition

1. After a total incubation time of 3 days at 37 °C, 5% CO<sub>2</sub>, take a picture of each sphere including the whole migration area with a phase-contrast microscope.
2. The experiment finishes with the assessment of cell viability and cytotoxicity using the CTB Assay and/or the LDH Assay (see Sects. 9 and/or 10 for description) (*see Note 2*).
3. In case you want to multiplex NPC2 with NPC3, 4, 5, or 6, you should solely perform the LDH Assay, and not the CTB Assay, because the CTB Assay might disturb the differentiation process, while the LDH Assay uses medium that can be collected during the necessary medium change on day 3 (*see descriptions of NPC3–6*).
4. When multiplexed with NPC3–6, then a second measure of migration will automatically be done when the sphere is imaged after 5 days of differentiation by analyzing positions of Hoechst-stained nuclei (*see description of NPC3–5*).

### 5.3.5 Image Analysis

1. Use ImageJ for measuring four radii of the migration area in perpendicular angles from the edge of the neurosphere to the furthest migrated cells in each phase-contrast image.
2. Calculate the mean of the four radii to obtain the mean migrated distance of each neurosphere.
3. Calculate the mean migrated distance of all neurospheres from each exposure condition.



4. In addition, Omnisphero will calculate migration distance using positions of Hoechst stained nuclei automatically across the whole migration area of each sphere (*see description of NPC3–5*).

All results in fold of control are pooled from independent experiments, SD and SEM are calculated, and statistical analyses are performed. Data are analyzed with the software GraphPad Prism 6.0 using OneWay ANOVA and a Bonferroni's post hoc test. Significance threshold is established at  $p < 0.05$ .

#### 5.4 Notes

Note 1: Plates can be stored with laminin at 4 °C for up to 7 days.

Note 2: The distinction of compound-specific effects on NPC migration with the “neurosphere assay” and secondary migration effects due to cytotoxicity is an important issue. Recent data reveal that the migration distance and/or the pattern of the migration area defines the dimension of signal of viability assays like the CellTiter-Blue Assay (CTB Assay; Promega), due to cell number relation. Specific effects of DNT compounds, e.g., methylmercury (MeHgCl), on migration without producing cell death can be measured by combining to different cytotoxicity/viability assays at a time. The combination of a cell viability assay and the additional readout of a LDH Assay, which is not directly cell number dependent, indicates compound-specific cytotoxicity effects at two different time points (Fig. 3a, b) [36].

Similarly, epigallocatechin gallate (EGCG) inhibits the migration and adhesion of hNPC on an extracellular matrix by changing the migration pattern and area (Fig. 3c) [36, 37, 39]. The migration in presence of EGCG and the CTB Assay suggests that EGCG reduces cell viability after 3 days (Fig. 8.3d) [36, 37]. However, annexin V-/PI-positive cells, identified with FACS analysis, clearly demonstrate that EGCG does not cause cell death, but reduces the cell area with access to the CTB substrate (Fig. 3e) [36].

Note 3: The plate should be equilibrated at 37 °C and 5% CO<sub>2</sub> until the neurospheres are plated.

Note 4: This step is important to wash out remaining growth factors from the proliferation medium.

Note 5: Make sure the neurospheres for the experiment are round and uniform in size.

Note 6: Make sure that the sphere is placed in the middle of the well.

## 6 Assays for Differentiation of NPC into Neurons (NPC3/4) and Oligodendrocytes (NPC5)

Differentiation of NPC into different effector cells (neurons, oligodendrocytes, and astrocytes) and the subsequent outgrowth of neurites are major processes of brain development and a prerequisite for the formation of a functional brain. In the “neurosphere assay,” the test methods NPC3, 4, and 5 represent the crucial processes of neuronal differentiation, neuronal morphology, and oligodendrocyte differentiation, respectively, and are applied to assess chemical actions on these processes. Therefore, hNPCs are plated as neurospheres on a poly-D-lysine/laminin matrix in a 96-well plate format as described under NPC2. Those cells migrate radially out of the sphere core (NPC2) and differentiate into radial glia, neurons, and oligodendrocytes [25, 26, 35, 40]. In the NPC3 assay, neuronal cells in the migration area are identified by immunocytochemical staining for  $\beta$ (III)tubulin (Fig. 4), while in the NPC4 assay, these  $\beta$ (III)tubulin<sup>+</sup> neurons are analyzed for their morphological parameters (neurite length, number of branching points, number of neurites). Oligodendrocytes are identified in the migration area by immunocytochemical stainings for O4 (Fig. 8.4) in the NPC5 assay. The test methods NPC2–5 in combination with an assessment of cell viability and cytotoxicity can be multiplexed in one experimental setup.

### 6.1 Materials

Poly-D-lysine: Dissolve poly-D-lysine (#P0899, Sigma-Aldrich) at 0.1 mg/mL in sterile water. Store up to 1 month at  $-20^{\circ}\text{C}$ .

Sterile water

One milligram per milliliter laminin (#L2020, Sigma-Aldrich)

Phosphate-buffered saline with  $\text{Ca}^{2+}$  and  $\text{Mg}^{2+}$  (PBS; Gibco, Life Technologies GmbH), Proliferation medium (see Sect. 1.1)

Differentiation medium (see Sect. 4.1)

Epidermal growth factor (EGF, Life Technologies GmbH)

Bone morphogenetic protein 7 (BMP7, provided by Prof. Pamela Lein, UC Davis; [28])

Paraformaldehyde (12%): Dissolve 12 g PFA in 100 mL phosphate-buffered saline (PBS) and add 5 drops of 1 N NaOH. Heat the solution carefully to  $70^{\circ}\text{--}80^{\circ}\text{C}$  in a fume hood, and cool to room temperature. Divide into 1-mL aliquots. Store aliquots up to 1 year at  $-80^{\circ}\text{C}$ , and use them freshly.

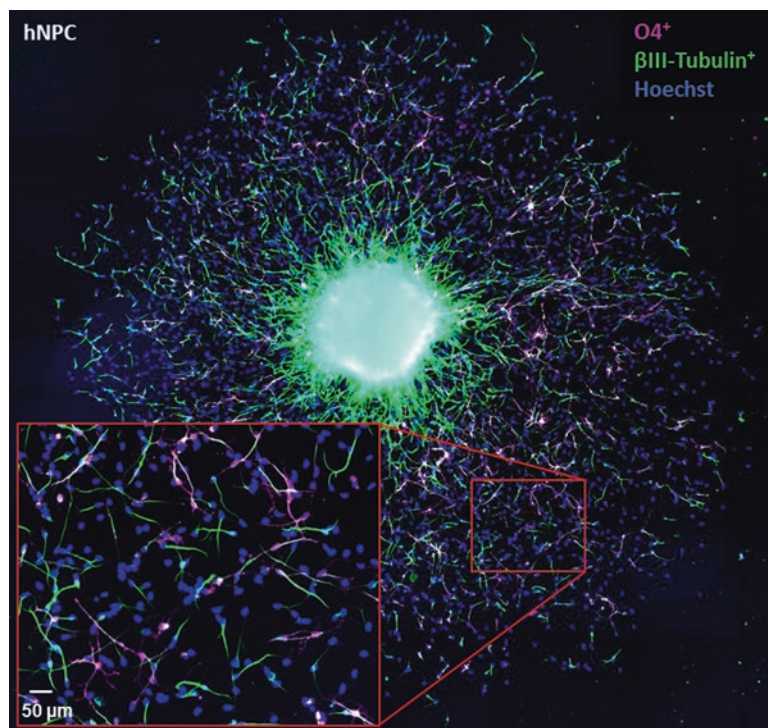
Goat Serum (#G9023, Sigma-Aldrich)

Triton X-100 (#T8787, Sigma-Aldrich)

bisBenzimide, Hoechst 33258 (#B1155, Sigma-Aldrich)

Mouse IgM anti-O4 (R&D Systems)

Rabbit IgG anti- $\beta$ (III)tubulin (#T2200, Sigma-Aldrich)



**Fig. 4** Immunocytochemical double stainings of neurons and oligodendrocytes differentiated in the migration area of hNPCs. One neurosphere was plated in each well of a 96-well plate in differentiation medium. After 5 days of differentiation, spheres were fixed, and neuronal as well as oligodendrocyte differentiation was assessed by immunocytochemical stainings of migrated and simultaneously differentiated hNPCs for the neuronal marker  $\beta$ (III)-Tubulin<sup>+</sup> (green), the oligodendrocyte marker O4<sup>+</sup> (pink), and Hoechst<sup>+</sup> (blue) for nuclei. One hundred images were taken using the Cellomics Array Scan VTI HCS Reader from Thermo Fisher Scientific to cover the whole sphere. The self-written algorithm Omnisphero ([www.omnisphero.com](http://www.omnisphero.com); [38]) assembled the 100 images into one sphere depiction. The inlay is an enlargement of the stained sphere migration area. Scale bar = 50  $\mu$ m

Alexa 546 IgG (#A11010, Invitrogen)

Alexa 488 IgM (#A11001, Invitrogen)

Flat-bottom 96-well plates (clear)

## 6.2 Methods

### 6.2.1 Preparation of Exposure Solutions

1. Prepare the desired dilution series of the test compound from a stock solution in differentiation medium.
  - (a) The final concentration of the solvent should be the same in all dilutions and not exceed 0.3% (v/v) for DMSO and 1% (v/v) for deionized water or PBS. The maximum solvent concentration for other solvents needs to be tested separately.

2. Prepare a solvent control by adding solvent to the differentiation medium in the same concentration as used for the exposure solutions.
3. For NPC3 prepare a solution of 20 ng/mL EGF in N2 differentiation medium.
  - (a) EGF inhibits the formation of neurons and therefore serves as an endpoint-specific control for neuronal differentiation.
4. For NPC5 prepare a solution of 100 ng/mL BMP-7 in N2 differentiation medium.
  - (a) BMP-7 inhibits the formation of O4<sup>+</sup> oligodendrocytes and therefore serves as an endpoint-specific control for this endpoint.
5. Fill each well of a coated 96-well plate with 100  $\mu$ L of the respective exposure solutions (*see Note 2*).

#### 6.2.2 Plating of Neurospheres

1. Fill a 6-cm petri dish with 5 mL N2 differentiation medium (*see Note 3*).
2. Select neurospheres with a diameter of  $0.3 \pm 0.025$  mm with a 100- $\mu$ L tip using a binocular microscope, and transfer them into the 6-cm petri dish with N2 differentiation medium (*see Note 4*).
3. Transfer each neurosphere in 2.5  $\mu$ L medium into the middle of a well of the 96-well plate filled with the experimental solutions (*see Note 5*).

#### 6.2.3 Cultivation and Feeding of the Experiments

1. The 96-well plates containing the plated neurospheres are incubated for 3 days at 37 °C and 5% CO<sub>2</sub>.
2. On day 3 the cells are fed by removal of 50  $\mu$ L of the exposure solution and addition of 50  $\mu$ L freshly prepared exposure solution.
  - (a) The removed solution can be used to determine cytotoxicity using the LDH Assay (*see Sect. 10*).
  - (b) The exposure solutions are prepared as described in points 1–4 (*Sect. 6.2.1*).
3. The neurospheres are incubated for another 2 days until day 5 of differentiation.
4. After a total incubation time of 5 days, the experiment is ended with the assessment of cell viability and cytotoxicity using the CTB Assay and the LDH Assay, respectively (*see Sects. 9 and/ or 10 for description*).

#### 6.2.4 Immunocyto- chemical (ICC) Stainings of Differentiated Neurospheres

1. Add 12% PFA to each well for achieving a final concentration of 4% PFA/well.
  - (a) In case you performed no viability assessment, the final volume of your experiment did not change, and you have to add 50  $\mu$ L 12% PFA to each well.

- (b) In case you performed a viability assessment using the CTB Assay (see Sect. 9 for description), the final volume of your experiment increased, so you have to add 66,6  $\mu\text{L}$  12% PFA to each well.
  - (c) In case you performed a cytotoxicity assessment using the LDH Assay (see Sect. 10 for description), the volume of the well decreased, so you have to add 25  $\mu\text{L}$  12% PFA to each well.
  - (d) In case you performed a viability and a cytotoxicity assessment, you have to add 33,3  $\mu\text{L}$  12% PFA to each well.
2. Incubate 30 min at 37 °C.
  3. Remove the PFA solution with a residual of 50  $\mu\text{L}$ /well, and discard it into the PFA waste (*see Note 6*).
  4. Wash 6  $\times$  3 min by addition and removal of 100  $\mu\text{L}$  PBS (discard to PFA waste).
    - (a) After the last washing step, remove 110  $\mu\text{L}$  with 40  $\mu\text{L}$  remaining in the well.
  5. Add 10  $\mu\text{L}$  blocking solution to each well.
    - (a) Blocking solution: PBS with 50% (v/v) GS.
  6. Incubate 15 min at 37 °C.
  7. Remove 10  $\mu\text{L}$  from each well.
  8. Add 10  $\mu\text{L}$  O4 first antibody solution to each well.
    - (a) O4 first antibody solution: 1:40 dilution of mouse IgM anti-O4 in PBS with 10% (v/v) GS.
  9. Incubate overnight at 4 °C.
  10. Wash 6  $\times$  3 min by addition and removal of 100  $\mu\text{L}$  PBS.
    - (a) After the last washing step, remove 110  $\mu\text{L}$  with 40  $\mu\text{L}$  remaining in the well.
  11. Add 10  $\mu\text{L}$  Alexa 488 2nd antibody solution to each well.
    - (a) Alexa 488 2nd antibody solution: 1:50 dilution of Alexa 488 IgM in PBS with 10% (v/v) GS and 5% (v/v) Hoechst33258.
  12. Incubate 30 min at 37 °C.
  13. Wash 6  $\times$  3 min by addition and removal of 100  $\mu\text{L}$  PBS each.
    - (a) After the last washing step, remove 116  $\mu\text{L}$  with 34  $\mu\text{L}$  remaining in the well.
  14. Repeat fixation by addition of 16  $\mu\text{L}$  12% PFA to a final concentration of 4%.
  15. Incubate 30 min at 37 °C.
  16. Wash 6  $\times$  3 min by addition and removal of 100  $\mu\text{L}$  PBS each, and discard to PFA waste.

- (a) After the last washing step, remove 110  $\mu\text{L}$  with 40  $\mu\text{L}$  remaining in the well.
17. Add 10  $\mu\text{L}$  blocking solution to each well.
  - (a) Blocking solution: PBS-T (0.5% (v/v) Triton X-100 in PBS) with 50% (v/v) GS.
18. Incubate 15 min at 37 °C.
19. Add 10  $\mu\text{L}$   $\beta$ (III)tubulin first antibody solution to each well.
  - (a)  $\beta$ (III)tubulin first antibody solution: 1:40 dilution of rabbit IgG anti- $\beta$ (III)tubulin in PBS-T (0.1% (v/v) Triton X-100 in PBS) with 10% (v/v) GS.
20. Incubate 60 min at 37 °C.
21. Wash 6  $\times$  3 min by addition and removal of 100  $\mu\text{L}$  PBS each.
  - (a) After the last washing step, remove 110  $\mu\text{L}$  with 40  $\mu\text{L}$  remaining in the well.
22. Add 10  $\mu\text{L}$  Alexa 546 2nd antibody solution to each well.
  - (a) Alexa 546 2nd antibody solution: 1:20 dilution of Alexa 546 IgG in PBS with 10% (v/v) GS and 5% (v/v) Hoechst33258.
23. Incubate 30 min at 37 °C.
24. Wash 6  $\times$  3 min by addition and removal of 100  $\mu\text{L}$  PBS each.
  - (a) After the last washing step, add 150  $\mu\text{L}$  PBS to a final volume of 200  $\mu\text{L}$  (*see Note 7*).

### 6.2.5 Image Acquisition and Analysis

1. Images of each well are acquired with the ArrayScan VTI (Thermo Fisher).
  - (a) Objective: LD Plan Neofluar 20 $\times$ /0.4 (Zeiss).
  - (b) Resolution: 552  $\times$  552 pixel (1 pixel = 0.88  $\mu\text{m}$ ).
  - (c) Channels:
    - (i) BGRFR-386-23-filter for Hoechst-stained nuclei
    - (ii) BGRFR-549-15-filter for  $\beta$ (III)tubulin-stained neurons
    - (iii) BGRFR-488-20-filter for O4-stained oligodendrocytes
  - (d) One well is imaged with a total of 100 images per channel.
2. Nuclei are quantified by rescanning all images using the Spot Detector bioapplication colocalization V4 of the vHCS-Scan software (V6.6.0; build 8153).
3. Nuclei coordinates are exported from the vHCS-View software into a comma-separated value file.
4. All images are exported as 16-bit images from the vHCS-View software.
5. High-content image analysis (HCA) is performed using the Omnisphero Platform [38].



### 6.2.6 Omnisphero

The Omnisphero platform (<https://www.omnisphero.com/>; [38]) is a freely available high-content image analysis (HCA) tool that was specifically developed for the automated analysis of immunocytochemically stained, heterogeneous cell cultures with varying cell densities as experienced in the “neurosphere assay.” Omnisphero is able to identify, count, skeletonize, and position  $\beta$ (III)tubulin<sup>+</sup> neurons and identify and quantify O4<sup>+</sup> oligodendrocytes. Thereby, Omnisphero allows an automated assessment of neuronal and oligodendrocyte numbers, cell distributions (neuronal and oligodendrocyte density distribution), and neuronal morphology (neurite length, number of branching points, number of neurites). Other novel endpoints that can be assessed with the Omnisphero software are cell type-specific migration (radial glia, neuronal, and oligodendrocyte migration) as well as migration patterning.

All results in fold of control are pooled from independent experiments, SD and SEM are calculated, and statistical analyses are performed. Data are analyzed with the software GraphPad Prism 6.0 using OneWay ANOVA and a Bonferroni's post hoc test. Significance threshold is established at  $p < 0.05$ .

### 6.3 Notes

Note 1: Plates can be stored with laminin at 4 °C for up to 7 days.

Note 2: The plate should be equilibrated at 37 °C and 5% CO<sub>2</sub> until the neurospheres are plated.

Note 3: This step is important to wash out remaining growth factors from the proliferation medium.

Note 4: Make sure the neurospheres for the experiment are round and uniform in size.

Note 5: Make sure that the sphere is placed in the middle of the well.

Note 6: To avoid washing off of cells, the neurospheres should always be covered with at least 50  $\mu$ L of liquid.

Note 7: ICC images should be taken within the next week. Store plates at 4–8 °C and protected from light.

---

## 7 The NPC Thyroid Hormone (TH) Disruption Assay (NPC6)

Maturation of oligodendrocytes plays an important role during brain development. By quantifying mRNA expression of myelin basic protein (*MBP*), myelin-associated oligodendrocytic basic *protein* (*MOBP*), or myelin oligodendrocyte glycoprotein (*MOG*) divided by the percentage of O4<sup>+</sup> cells differentiated after 5 days in the neurosphere migration area (assessed in NPC5), the maturation of O4<sup>+</sup> oligodendrocytes can be examined. This *MBP/MOBP/MOG*-oligodendrocyte ratio is defined as the oligodendrocyte maturation quotient ( $Q_M$ ). During NPC development  $Q_M$  increases

when cultures are exposed to the thyroid hormone (TH) triiodo-thyronine (T3, [18]). Cellular TH disruption of developing hNPC can be tested by assessment of  $Q_M$  with test compounds. Here, cellular TH signaling is disturbed when  $Q_M$  (TH + compound) <  $Q_M$  (TH) when  $Q_M$  is not disturbed by the compound alone in absence of TH. In case the compound affects oligodendrocyte differentiation (NPC5) without lowering  $Q_M$ , the compound is an oligodendrocyte toxin rather than a TH disruptor.

## 7.1 Materials

Flat-bottom 24-well plate (clear), precoated (coating protocol see Sect. 5.1)

Flat-bottom 96-well plate (clear), precoated (coating protocol see Sect. 5.1)

Differentiation medium (see Sect. 5.1)

H<sub>2</sub>O, deionized and sterile

Phosphate-buffered saline with CaCl<sub>2</sub> and MgCl<sub>2</sub> (PBS; Gibco, Life Technologies)

3,3',5-Triiodo-L-thyronine (T3; Sigma Aldrich, #T2877)

Ninety-six percent ethanol (EtOH)

Hydrogen chloride (HCl)

## 7.2 Methods

All steps need to be performed under sterile conditions.

### 7.2.1 Preparation for Cell Plating

1. Chop primary human neurospheres (hNPCs) 3 days before plating (chopping protocol see Sect. 1.3.2).
2. Use primary human neurospheres passage 1–3.

### 7.2.2 Plating Spheres for NPC6

1. Equilibrate differentiation media to 37 °C, 5% CO<sub>2</sub> for 60 min.
2. Prepare all treatment, co-treatment, and control solutions. Add 5 × 100 μL to each well of a pre-coated (see Sect. 5.1) flat-bottom 96-well plate (for later O4 staining) and 3 × 1 mL to each well of a pre-coated flat-bottom 24-well plate (for later polymerase chain reaction (PCR)) (see Note 1).

Controls:

- (a) Media control (MC): only differentiation media.
- (b) Solvent control (SC): differentiation media with respective solvent.

Solvent concentrations in the experiments contain % of respective chemical solvent, 0.01% EtOH/HCl and 3 nM T3. For 0.01% EtOH/HCl and T3 with a solvent concentration of 0.01% EtOH/HCl in the stock solutions the following components are required:

- 100% EtOH/HCl in differentiation medium 1:10 (10% EtOH/HCl)



- Three hundred micrometer T3 in EtOH/HCl 1:10 (30  $\mu$ M T3 in 100% EtOH/HCl)
  - Thirty micrometer T3 in differentiation medium 1:10 (3  $\mu$ M T3 in 10% EtOH/HCl) (*see Note 2*).
- (c) Positive control (PC): BMP-7100 ng/mL.
- (d) If combined with LDH Assay and/or CTB Assay, prepare lysis control (LC) and background control (BG) (*see Sects. 9 and/or 10*).
3. Fill all wells surrounding cell-containing wells with 100  $\mu$ L (96-well plate) and 1 mL (24-well plate) deionized and sterile water, respectively.
  4. Presort 0.3 mm neurospheres in differentiation medium: for each condition (treatment) 35  $\times$  0.3 mm neurospheres are plated (5  $\times$  1 sphere in a 96-well plate for O4 staining and 3  $\times$  10 spheres in a 24-well plate for PCR analysis); furthermore 10 additional neurospheres are needed for controls (BMP-7 as the endpoint-specific control for oligodendrocyte differentiation and Triton X-100 as a lysis control for the cytotoxicity assay).
  5. Take up 1 neurosphere in 2  $\mu$ L differentiation medium from the presorted spheres, and place it into the middle of a well of a 96-well plate.
  6. Take up 10 neurospheres in 20  $\mu$ L differentiation medium from the presorted spheres, and place them into a well of a 24-well plate (*see Note 3*).
  7. Incubate these differentiating spheres for 5 days at 37  $^{\circ}$ C, 5% CO<sub>2</sub>.
  8. Feed spheres on day 3.
  9. For feeding, half of the media (96-well 50  $\mu$ L, 24-well 500  $\mu$ L) is removed and substituted with freshly prepared control respective treatment solution (pre-warmed to 37  $^{\circ}$ C).

### 7.2.3 Viability Assay and Fixation

1. After 5 days of differentiation, measure viability with the CTB Assay, and afterward fix the spheres in the 96-well plates for later immunocytochemical stainings.
2. For viability/cytotoxicity assays and fixation of spheres, *see Sects. 9 and/or 10*.
3. After fixation the plate can be stored in the fridge until staining is performed (for a maximum of 1 week, *see Sect. 6*).

### 7.2.4 Immunocytochemical Staining and Counting of O4<sup>+</sup> Cells and Fluorescence Microscopy

1. For the 96-well oligodendrocyte staining with the O4 antibody, *see protocol Sect. 6.2.4*.
2. For plate scanning using fluorescence microscopy with the Cellomics ArrayScan, *see protocols Sects. 6.2.5 and 6.2.6*.

7.2.5 *Harvesting of RNA*

1. After 5 days of differentiation, remove medium from the wells of the 24-well plate.
2. Add 350  $\mu$ L RLT buffer (RNeasy Mini Kit, Qiagen).
3. Scratch the cells.
4. Pipette lysates up and down thrice, and fill them into 1.5 mL Eppendorf cups.
5. Store RNA lysates at  $-80^{\circ}\text{C}$  until you purify the RNA.
6. For RNA purification use the RNeasy Mini Kit from Qiagen according to the manufacturer's protocol.
7. The RNA can be stored at  $-80^{\circ}\text{C}$  (*see Note 4*).
8. For reverse transcription the Quantitect Reverse Transcription Kit from Qiagen is used.
9. The real time RT-PCR is carried out with QuantiFast<sup>®</sup> SYBR<sup>®</sup> Green PCR (*see Note 5*).
10. Gene product-specific copy numbers were determined as published earlier [18].

7.2.6 *Normalization of Gene Expression to the Percentage of Oligodendrocytes*

1. Perform both, O4 staining and gene expression experiments in parallel, three times independently.
2. Gene expression (copy numbers *MBP/MOBP/MOG*/10.000  $\beta$ *ACTIN*) of each treatment condition (pooled technical replicates) of each experiment is divided by its respective percentage of oligodendrocytes from the parallel immunostaining experiment.
3. Gene expression/oligodendrocytes ( $Q_M$ ) of the solvent control is set to 1 for each experiment, and the  $Q_M$  for the TH treatment as the positive control is expressed in fold of solvent control for each experiment.
4. After pooling  $Q_M$  from independent experiments, SD and SEM are calculated, and statistical analyses are performed. Data are analyzed with the software GraphPad Prism 6.0 using TwoWay ANOVA and a Tukey's post hoc test. Significance threshold is established at  $p < 0.05$ .
5. Assess the  $Q_M$  of a chemical by itself and in co-treatment with 3 nM T3. If the  $Q_M$  of the chemical by itself is not lower than that of the solvent control, but is significantly different from the T3 treatment, the compound is a TH disruptor with regard to TH-induced oligodendrocyte maturation in vitro.

7.3 *Notes*

Note 1: Plate 96-well plates for O4 staining and 24-well plates for PCR of oligodendrocyte maturation markers on the same day using the same neurosphere stock cultures. Dilution series for the 96-well and the 24-well plates are prepared at once.

Note 2: Always use 10% EtOH/HCl, T3 in 10% EtOH/HCl and the chemical 1:1000 as the highest concentration, a pre-dilution of chemical in solvent might be required.

Note 3: Shake the 24-well plate gently to distribute neurospheres within the well. They need enough space from each other to migrate correctly.

Note 4: RNA of 10 NA0.3 mm neurospheres per sample is used. The RNA content is not measured before each reverse transcription but lies between 10 and 30 ng/ $\mu$ L for ten human NPCs (depending on size and migration area).

Note 5: Primer sequences for the oligodendrocyte maturation gene *MBP/MOBP/MOG* and the housekeeping gene  $\beta$ *ACTIN* are:

Species	Gene	Forward primer 5'–3'	Reverse primer 5'–3'
Human	<i>MBP</i>	CAGAGCGTCCGACTATAAAATCG	GGTGGGTTTTTCAGCGTCTA
	<i>MOBP</i>	ACCCATCTGCCCTCAGACTTA	GCATCTGTAGTTGTTACATCAGC
	<i>MOG</i>	CAATTACCGGAGTGGAGGCA	GTGCATGTCCCCTTACTGCT
	$\beta$ <i>ACTIN</i>	CAGGAAGTCCCTTGCCATCC	ACCAAAGCCTTCATACATCTCA

## 8 Assessment of Cell Viability and Cytotoxicity

The six individual test methods (NPC1–6) described above assess the effect of a chemical on processes that are specific for brain development. The unspecific effect of a compound on general cell viability however will ultimately affect DNT-specific endpoints like NPC proliferation, migration, or differentiation. To distinguish between effects on general cell viability and specific effects on DNT endpoints, cell viability and/or cytotoxicity needs to be determined in the same assay.

Cell viability can be measured with the CTB Assay. This assay provides a fluorometric measure for viable cells as living cells reduce the indicator dye resazurin to the fluorescent metabolite resorufin thus reflecting their metabolic (cellular reductase) capacity [39]. This assay is made for determining viability in a plate reader format. As the cells are incubated with the indicator dye, the experiment needs to be terminated shortly after incubation, i.e., fixed with PFA for subsequent immunocytochemical stainings (NPC3–5).

Cytotoxicity can be assessed with the LDH Assay. This assay is a fluorescent measure of the release of lactate dehydrogenase (LDH) from cells with a damaged membrane. LDH released into the culture medium is proportional to the number of damaged/dead cells and can be measured with an enzymatic reaction that also results in the conversion of resazurin to the fluorescent resorufin [41, 42]. As the LDH Assay uses the supernatant of cultured cells,

the assay does not disturb cell cultivation and is thus the method of choice when cells need to be cultivated further like with the migration assay (NPC2) when multiplexed with the differentiation assays (NPC3–5) or the TH disruption assay (NPC6).

---

## 9 CellTiter-Blue (CTB) Assay

### 9.1 Materials

CellTiter-Blue cell viability assay kit (#G8081, Promega;  $-20\text{ }^{\circ}\text{C}$ )

CellTiter-Blue reagent (protect from light)

Triton X-100 (#T8787, Sigma-Aldrich)

Differentiation medium (see Sect. 5.1)

Proliferation medium (without growth factors; see Sect. 1.1)

Flat-bottom 96-well plate (clear)

### 9.2 Methods

For the assessment of cell viability using the CTB Assay, a lysis control (LC) and a background control (BG; culture medium without cells) are needed in addition to the endpoint-specific controls of each assay NPC1–6.

1. Culture cells for the desired period and with the desired compound exposure.
2. Thaw and equilibrate CellTiter-Blue reagent to RT for 2 h protected from light.
3. Dilute 10% (v/v) Triton X-100 solution 1:5 in each well of lysis control (2  $\mu\text{L}$  in each well; final concentration 2%).
4. Fill empty wells just with medium.
5. Preincubate 20 min at  $37\text{ }^{\circ}\text{C}$  and 5%  $\text{CO}_2$ .

#### 9.2.1 With Removal of Medium for LDH Assay in the Differentiation Assays

1. Dilute CellTiter-Blue reagent 1:7.5 in differentiation medium. For one well dilute 11  $\mu\text{L}$  of CellTiter-Blue reagent in 72  $\mu\text{L}$  of differentiation medium.
2. Add 83  $\mu\text{L}$  to each well, and incubate at  $37\text{ }^{\circ}\text{C}$  and 5%  $\text{CO}_2$  for 2 h.

#### 9.2.2 Without Removal of Medium in the Differentiation Assays

1. Dilute CellTiter-Blue reagent 1:3 in differentiation medium. For one well dilute 11  $\mu\text{L}$  of CellTiter-Blue reagent in 22  $\mu\text{L}$  of differentiation medium.
2. Add 33  $\mu\text{L}$  to each well, and incubate at  $37\text{ }^{\circ}\text{C}$  and 5%  $\text{CO}_2$  for 2 h.

#### 9.2.3 In the BrdU Assay

1. Dilute CellTiter-Blue reagent 1:3 in proliferation medium without growth factors. For one well dilute 12  $\mu\text{L}$  of CellTiter-Blue reagent in 24  $\mu\text{L}$  of proliferation medium.
2. Add 36  $\mu\text{L}$  to each well, and incubate at  $37\text{ }^{\circ}\text{C}$  and 5%  $\text{CO}_2$  for 2 h.

9.2.4 *Fluorescence Measurement and Data Evaluation*

1. Measure fluorescence at an excitation wavelength of 540 nm and emission wavelength of 590 nm.
2. Calculate the MEAN of all replicate measurements.
3. Subtract the MEAN of BG from the MEAN of all conditions.
4. Calculate BG subtracted MEAN of each condition as percent of SC.
5. All results in fold of control are pooled from independent experiments, SD and SEM are calculated, and statistical analyses are performed. Data are analyzed with the software GraphPad Prism 6.0 using OneWay ANOVA and Bonferroni's post hoc test. Significance threshold is established at  $p < 0.05$ .

9.3 *Notes*

There are no relevant notes for this protocol.

---

## 10 Lactate Dehydrogenase (LDH) Assay

10.1 *Materials*

CytoTox-ONE Homogeneous Membrane Integrity Assay Kit (#G7891, Promega;  $-20\text{ }^{\circ}\text{C}$ )

Substrate mix

Assay buffer

Triton X-100 (#T8787, Sigma-Aldrich)

Differentiation medium (see Sect. 5.1)

Proliferation medium (without growth factors; see Sect. 1.1)

Flat-bottom 96-well plate (clear)

10.2 *Methods*

For the assessment of cytotoxicity using the LDH Assay, the same controls as for the CTB Assay are needed (*see above*).

1. Culture cells for the desired period and with the desired compound exposure.
2. Prepare CytoTox-ONE Reagent as indicated in the supplier's instructions.
3. Dilute 10% (v/v) Triton X-100 solution 1:5 in each well of lysis control (2  $\mu\text{L}$  in each well; final concentration 2%).
4. Incubate 20 min at  $37\text{ }^{\circ}\text{C}$  and 5%  $\text{CO}_2$ .
5. Remove 50  $\mu\text{L}$  of medium, and transfer into a new 96-well plate.
6. Equilibrate medium in new plate to RT for 10 min.
7. Add 50  $\mu\text{L}$  of CytoTox-ONE Reagent (RT) to each well.
8. Incubate at RT for 2 h.

10.2.1 *Fluorescence Measurement and Data Evaluation*

1. Measure fluorescence at an excitation wavelength of 540 nm and emission wavelength of 590 nm.
2. Calculate the MEAN of all replicate measurements.
3. Subtract the MEAN of BG from the MEAN of all conditions.
4. Calculate BG subtracted MEAN of each condition as percent of LC.
5. All results in percent of LC are pooled from independent experiments, SD and SEM are calculated, and statistical analyses are performed. Data are analyzed with the software GraphPad Prism 6.0 using OneWay ANOVA and Bonferroni's post hoc test. Significance threshold is established at  $p < 0.05$ .

10.3 *Notes*

There are no relevant notes for this protocol.

References

1. Bennett D, Bellinger D, Health LB-E et al (2016) Project TENDR: targeting environmental neuro-developmental risks. the TENDR consensus statement. *Environ Health Perspect* 124:A118–A122
2. Grandjean P, Landrigan P (2006) Developmental neurotoxicity of industrial chemicals. *Lancet* 368:2167–2178
3. Grandjean P, Landrigan PJ (2014) Neurobehavioural effects of developmental toxicity. *Lancet Neurol* 13:330–338
4. Schettler T (2001) Toxic threats to neurologic development of children. *Environ Health Perspect* 109:813–816
5. Crofton KM, Mundy WR, Shafer TJ (2012) Developmental neurotoxicity testing: a path forward. *Congenit Anom (Kyoto)* 52:140–146
6. Goldman LR, Koduru S (2000) Chemicals in the environment and developmental toxicity to children: a public health and policy perspective. *Environ Health Perspect* 108(Suppl 3):443–448
7. US-EPA (1998) Health effects test guidelines OPPTS 870.6300. *Dev Neurotox Study EPA 712-C-98-239*
8. OECD (2007) OECD guidelines for the testing of chemicals/section 4: Health effects. Test no. 426: developmental neurotoxicity study. *Dev Neurotox study P.26*
9. Lein P, Silbergeld E, Locke P et al (2005) In vitro and other alternative approaches to developmental neurotoxicity testing (DNT). *Environ Toxicol Pharmacol* 19:735–744
10. Bal-Price A, Crofton KM, Leist M et al (2015) International Stakeholder Network (ISTNET): creating a developmental neurotoxicity (DNT) testing road map for regulatory purposes. *Arch Toxicol* 89:269–287
11. Bal-Price A, Hogberg HT, Crofton KM et al (2018) Recommendation on test readiness criteria for new approach methods in toxicology: exemplified for developmental neurotoxicity. *Altex* 35:306–352
12. Bal-Price AK, Coecke S, Costa L et al (2012) Conference report: advancing the science of developmental neurotoxicity (DNT): testing for better safety evaluation. *ALTEX* 29:202–215
13. Crofton KM, Mundy WR, Lein PJ et al (2011) Developmental neurotoxicity testing: recommendations for developing alternative methods for the screening and prioritization of chemicals. *ALTEX* 28:9–15
14. Fritsche E, Crofton KM, Hernandez AF et al (2017) OECD/EFSA workshop on developmental neurotoxicity (DNT): the use of non-animal test methods for regulatory purposes. *ALTEX* 34:311–315
15. Fritsche E, Grandjean P, Crofton KM et al (2018) Consensus statement on the need for innovation, transition and implementation of developmental neurotoxicity (DNT) testing for regulatory purposes. *Toxicol Appl Pharmacol* 354:3–6
16. Lein P, Locke P, Goldberg A (2007) Meeting report: alternatives for developmental neurotoxicity testing. *Environ Health Perspect* 115:764–768
17. Fritsche E (2016) Report on integrated testing strategies for the identification and evaluation of chemical hazards associated with the devel-

- opmental neurotoxicity (DNT). In: Report of the OECD/EFSA workshop on developmental neurotoxicity (DNT): the use of non-animal test. OECD Environ Heal Saf Publications Ser Test Assess 242
18. Dach K, Bendt F, Huebenthal U et al (2017) BDE-99 impairs differentiation of human and mouse NPCs into the oligodendroglial lineage by species-specific modes of action. *Sci Rep* 7:1–11
  19. Gassmann K, Abel J, Bothe H et al (2010) Species-specific differential AhR expression protects human neural progenitor cells against developmental neurotoxicity of PAHs. *Environ Health Perspect* 118:1571–1577
  20. Gold LS, Manley NB, Slone TH et al (2005) Supplement to the carcinogenic potency database (CPDB): results of animal bioassays published in the general literature through 1997 and by the national toxicology program in 1997–1998. *Toxicol Sci* 85:747–808
  21. Knight A (2008) Systematic reviews of animal experiments demonstrate poor contributions toward human healthcare. *Rev Recent Clin Trials* 3:89–96
  22. Leist M, Hartung T (2013) Reprint: inflammatory findings on species extrapolations: humans are definitely no 70-kg mice. *ALTEX* 30: 227–230
  23. Masjosthusmann S, Becker D, Petzuch B et al (2018) A transcriptome comparison of time-matched developing human, mouse and rat neural progenitor cells reveals human uniqueness. *Toxicol Appl Pharmacol* 354:40–55
  24. Seok J, Warren HS, Cuenca AG et al (2013) Genomic responses in mouse models poorly mimic human inflammatory diseases. *Proc Natl Acad Sci U S A* 110:3507–3512
  25. Baumann J, Barenys M, Gassmann K, Fritsche E (2014) Comparative human and rat “neurosphere assay” for developmental neurotoxicity testing. In: Costa LG, Davila JC, Lawrence DA, Reed DJ (eds) *Current protocols in toxicology*, vol 59. Wiley, pp 12.21.1–12.21.24. <https://doi.org/10.1002/0471140856.tx1221s59>
  26. Baumann J, Gassmann K, Masjosthusmann S, DeBoer D, Bendt F, Giersiefer S, Fritsche E (2016) Comparative human and rat neurospheres reveal species differences in chemical effects on neurodevelopmental key events. *Arch Toxicol* 90:1415–1427
  27. Tang H, Hammack C, Ogden SC et al (2016) Zika virus infects human cortical neural progenitors and attenuates their growth. *Cell Stem Cell* 18:587–590
  28. Baumann J, Dach K, Barenys M, Giersiefer S, Goniwiecha J, Lein PJ, Fritsche E (2015) Application of the Neurosphere assay for DNT Hazard assessment: challenges and limitations. Humana Press, Totowa, pp 1–29
  29. Gassmann K, Baumann J, Giersiefer S, Schuwald J, Schreiber T, Merk HF, Fritsche E (2012) Automated neurosphere sorting and plating by the COPAS large particle sorter is a suitable method for high-throughput 3D in vitro applications. *Toxicol In Vitro* 26:993–1000
  30. Moors M, Rockel TD, Abel J, Cline JE, Gassmann K, Schreiber T, Schuwald J, Weinmann N, Fritsche E (2009) Human neurospheres as three-dimensional cellular systems for developmental neurotoxicity testing. *Environ Health Perspect* 117:1131–1138
  31. Schreiber T, Gassmann K, Götz C et al (2010) Polybrominated diphenyl ethers induce developmental neurotoxicity in a human in vitro model: evidence for endocrine disruption. *Environ Health Perspect* 118:572–578
  32. Tofighi R, Wan Ibrahim WN, Rebellato P et al (2011) Non-dioxin-like polychlorinated biphenyls interfere with neuronal differentiation of embryonic neural stem cells. *Toxicol Sci* 124:192–201
  33. Choi BH (1989) The effects of methylmercury on the developing brain. *Prog Neurobiol* 32:447–470
  34. Moors M, Cline JE, Abel J, Fritsche E (2007) ERK-dependent and -independent pathways trigger human neural progenitor cell migration. *Toxicol Appl Pharmacol* 221:57–67
  35. Edoff K, Raciti M, Moors M et al (2017) Gestational age and sex influence the susceptibility of human neural progenitor cells to low levels of MeHg. *Neurotox Res* 32:683–693
  36. Fritsche E, Barenys M, Klose J, Masjosthusmann S, Nimtz L, Schmuck M, Wuttke S, Tigges J (2018) Current availability of stem cell-based in vitro methods for developmental neurotoxicity (DNT) testing. *Toxicol Sci* 165:21–30
  37. Barenys M, Gassmann K, Baksmeier C, Heinz S, Reverte I, Schmuck M, Temme T, Bendt F, Zschauer TC, Rockel TD (2017) Epigallocatechin gallate (EGCG) inhibits adhesion and migration of neural progenitor cells in vitro. *Arch Toxicol* 91:827–837
  38. Schmuck MR, Temme T, Dach K et al (2017) Omnisphero: a high-content image analysis (HCA) approach for phenotypic developmental neurotoxicity (DNT) screenings of organoid neurosphere cultures in vitro. *Arch Toxicol* 91:2017–2028
  39. Bal-Price A, Lein PJ, Keil KP, Sethi S, Shafer T, Barenys M, Fritsche E, Sachana M, Meek MEB (2017) Developing and applying the adverse outcome pathway concept for understanding



- and predicting neurotoxicity. *Neurotoxicology* 59:240–255
40. Moors M, Bose R, Johansson-Hague K et al (2012) Dickkopf 1 mediates glucocorticoid-induced changes in human neural progenitor cell proliferation and differentiation. *Toxicol Sci* 125:488–495
  41. TECHNICAL BULLETIN, CellTiter-Blue® cell viability assay, revised 3/16, TB317, Promega, USA
  42. TECHNICAL BULLETIN, CytoTox-ONE™ homogeneous membrane integrity assay, revised 5/09, TB306, Promega, USA



## The Neurosphere Assay as an *In Vitro* Method for Developmental Neurotoxicity (DNT) Evaluation

Laura Nimtz, **Jördis Klose**, Stefan Masjosthusmann, Marta Barenys and Ellen Fritsche

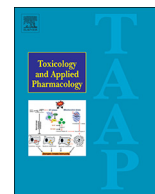
Journal:	Cell Culture Techniques, Neuromethods vol. 145, Chapter 8
Impact Factor:	not calculated for book chapters
Contribution to the publication:	20 % Writing of the manuscript sections 'Cell Culture, Materials and Methods' and 'The NPC Thyroid Hormone (TH) Disruption Assay (NPC6)'
Type of authorship:	first authorship
Status of the publication:	Published 26 <sup>th</sup> April 2019

## 2.4 A transcriptome comparison of time-matched developing human, mouse and rat neural progenitor cells reveals human uniqueness

Stefan Masjosthusmann, Daniel Becker, Barbara Petzuch, **Jördis Klose**, Clara Siebert, Rene Deenen, Marta Barenys, Jenny Baumann, Katharina Dach, Julia Tigges, Ulrike Hübenthal, Karl Köhrer, Ellen Fritsche

*Toxicology and Applied Pharmacology*

Es ist weitestgehend akzeptiert, dass die Entwicklung des menschlichen Gehirns einzigartige Merkmale aufweist, die nicht von Nagern als Modellorganismen repräsentiert werden können. Offensichtliche Gründe hierfür sind die evolutionäre Distanz sowie die unterschiedliche Physiologie. Aus diesem Grund birgt die Übertragung von tierbasierten Forschungsergebnissen auf die Situation im Menschen immer ein gewisses Sicherheitsrisiko bezüglich einer falschen Vorhersage. In dieser Studie charakterisieren wir sich entwickelnde neurale Progenitorzellen (NPC) von Mensch, Maus und Ratte anhand der Änderungen ihres Transkriptomprofils im Laufe ihrer Differenzierung von proliferierenden NPC zu differenzierten Effektorzellen. Darüber hinaus identifizierten wir wichtige Regulatoren, welche neurologische Entwicklungsprozesse, wie Migration und Differenzierung regulieren. Die Folgen der Modulation von drei dieser identifizierten Regulatoren, wurden näher in einem speziesspezifischen Kontext untersucht. Unsere Ergebnisse zeigen, dass die drei Spezies über die Differenzierungszeit sowohl qualitative als auch quantitative Unterschiede in ihrem Expressionsprofil aufweisen, jedoch die wesentlichen Prozesse der Gehirnentwicklung wie Zellmigration, Neurogenese und Gliogenese, sowie die Entwicklung multizellulärer Organismen aufweisen. Diese Studie unterstreicht die Bedeutung für das Verständnis von Speziesunterschieden und den Nutzen von menschlich basierten *in vitro* Modellen für die pharmakologische und toxikologische Forschung.



## A transcriptome comparison of time-matched developing human, mouse and rat neural progenitor cells reveals human uniqueness

Stefan Masjosthusmann<sup>a</sup>, Daniel Becker<sup>a</sup>, Barbara Petzuch<sup>a</sup>, Jördis Klose<sup>a</sup>, Clara Siebert<sup>a</sup>, Rene Deenen<sup>b</sup>, Marta Barenys<sup>a</sup>, Jenny Baumann<sup>a</sup>, Katharina Dach<sup>a,d</sup>, Julia Tigges<sup>a</sup>, Ulrike Hübenthal<sup>a</sup>, Karl Köhrer<sup>b</sup>, Ellen Fritsche<sup>a,c,\*</sup>

<sup>a</sup> IUF - Leibniz Research Institute for Environmental Medicine, Auf'm Hennekamp 50, 40225 Duesseldorf, NRW, Germany

<sup>b</sup> Biological and Medical Research Centre (BMFZ), Medical Faculty, Heinrich-Heine-University, Universitätsstraße 1, 40225 Duesseldorf, NRW, Germany

<sup>c</sup> Medical Faculty, Heinrich-Heine-University, Universitätsstraße 1, 40225 Duesseldorf, NRW, Germany

<sup>d</sup> Department of Molecular Biosciences, University of California-Davis School of Veterinary Medicine, Davis, CA 95616, United States

### ARTICLE INFO

#### Keywords:

Species differences  
DNT  
Developmental neurotoxicity  
Brain development  
Neurosphere  
Alternative method

### ABSTRACT

It is widely accepted that human brain development has unique features that cannot be represented by rodents. Obvious reasons are the evolutionary distance and divergent physiology. This might lead to false predictions when rodents are used for safety or pharmacological efficacy studies. For a better translation of animal-based research to the human situation, human in vitro systems might be useful. In this study, we characterize developing neural progenitor cells from prenatal human and time-matched rat and mouse brains by analyzing the changes in their transcriptome profile during neural differentiation. Moreover, we identify hub molecules that regulate neurodevelopmental processes like migration and differentiation. Consequences of modulation of three of those hubs on these processes were studied in a species-specific context. We found that although the gene expression profiles of the three species largely differ qualitatively and quantitatively, they cluster in similar GO terms like cell migration, gliogenesis, neurogenesis or development of multicellular organism. Pharmacological modulation of the identified hub molecules triggered species-specific cellular responses. This study underlines the importance of understanding species differences on the molecular level and advocates the use of human based in vitro models for pharmacological and toxicological research.

### 1. Introduction

Pharmacological research as well as drug safety testing have mainly been based on studies in laboratory animals. Besides ethical concerns and high resource needs with regards to time and money, laboratory animals do frequently fail to predict beneficial or adverse compound effects for humans leading to high attrition rates when moving from preclinical research to clinical drug applications (Arrowsmith and Miller, 2013; Waring et al., 2015), e.g. rodents only correctly identified 43% out of 150 pharmaceuticals known to be toxic in man (Olson et al., 2000). Also, an analysis of systematic reviews published in the “Scopus” database on the human clinical or toxicological utility of animal experiments revealed that in only 10% of the reviews animal models were significantly useful (Knight, 2007). Several reasons were identified to be responsible for this unsatisfactory translation from animals to

humans. For one, poor performance quality and reporting of animal studies impedes prediction (Hartung, 2009; Kilkenny et al., 2010; Knight, 2007; Leist and Hartung, 2013; van der Worp et al., 2010). Moreover, species differences can hamper predictive value of animal in vivo studies (Gold et al., 2005; Knight, 2007; Leist and Hartung, 2013; Seok et al., 2013). Such limited predictions might result in high attrition rates during the drug development process causing economic damage and lack of treatment (De Keyser et al., 1999; Perel et al., 2007; Seok et al., 2013; Waring et al., 2015). Incorrect information on human safety or toxicity of substances is equally severe as it might result in serious human health effects as experienced with thalidomide or TGN1412, which did not show animal toxicity in the species tested but caused serious toxicities in humans (Attarwala, 2010; Miller and Stromland, 1999). While performance quality and reporting of animal studies can be improved e.g. by introducing more stringent quality

\* Corresponding author at: IUF - Leibniz Research Institute for Environmental Medicine, Duesseldorf, NRW 40225, Germany.

E-mail addresses: [Stefan.Masjosthusmann@iuf-duesseldorf.de](mailto:Stefan.Masjosthusmann@iuf-duesseldorf.de) (S. Masjosthusmann), [barbara.petzuch@mnet-mail.de](mailto:barbara.petzuch@mnet-mail.de) (B. Petzuch), [Joerdis.Klose@IUF-Duesseldorf.de](mailto:Joerdis.Klose@IUF-Duesseldorf.de) (J. Klose), [clara@hocke-siebert.de](mailto:clara@hocke-siebert.de) (C. Siebert), [Rene.deenen@thermofisher.com](mailto:Rene.deenen@thermofisher.com) (R. Deenen), [mbarenys@ub.edu](mailto:mbarenys@ub.edu) (M. Barenys), [kdach@ucdavis.edu](mailto:kdach@ucdavis.edu) (K. Dach), [Julia.Tigges@IUF-Duesseldorf.de](mailto:Julia.Tigges@IUF-Duesseldorf.de) (J. Tigges), [Ulrike.Huebenthal@IUF-Duesseldorf.de](mailto:Ulrike.Huebenthal@IUF-Duesseldorf.de) (U. Hübenthal), [koehrer@uni-duesseldorf.de](mailto:koehrer@uni-duesseldorf.de) (K. Köhrer), [ellen.fritsche@iuf-duesseldorf.de](mailto:ellen.fritsche@iuf-duesseldorf.de), [ellen.fritsche@uni-duesseldorf.de](mailto:ellen.fritsche@uni-duesseldorf.de) (E. Fritsche).

<https://doi.org/10.1016/j.taap.2018.05.009>

Received 21 December 2017; Received in revised form 4 May 2018; Accepted 8 May 2018  
Available online 09 May 2018

0041-008X/ © 2018 Elsevier Inc. All rights reserved.

criteria (Dirnagl and Fisher, 2012), species differences in human vs. animal physiology and/or pathology cannot rapidly be overcome using *in vivo* whole animal studies.

To improve “human relevance” in safety and efficacy studies, one can make use of human cell-based *in vitro* methods. Although such methods lack pharmacokinetics of the whole organism (absorption, distribution, metabolism, excretion), they are thought to maintain their pharmacodynamics of the target cell *in vitro*. There are many examples for species-specific differences in the molecular equipment of cells that can determine compound action (Jenkins et al., 2012; Oberheim et al., 2009; Perreault et al., 2013; Seok et al., 2013; Strasser et al., 2013).

We have previously shown that such specificities in toxicodynamics across species are also maintained in primary, time-matched neurospheres from humans, mice and/or rats *in vitro* (Baumann et al., 2015; Dach et al., 2017; Gassmann et al., 2010). Three dimensional (3D) neurospheres consist of neural progenitor cells (NPC) that allow assessment of compound-specific effects on NPC proliferation, radial migration, differentiation into neurons, astrocytes and oligodendrocytes as well as neuronal migration and neurite outgrowth (Barenys et al., 2016; Baumann et al., 2015, 2014; Dach et al., 2017; Gassmann et al., 2012; Schmuck et al., 2016). Moreover, modes of action of substances can be studied with this organoid cell culture method (Barenys et al., 2016; Dach et al., 2017; Moors et al., 2007; Schreiber et al., 2010). Due to these attributes, this “Neurosphere Assay” is thought to be a valuable part of an alternative testing battery for developmental neurotoxicity (DNT) evaluation (Fritsche, 2016; Bal-Price et al., 2018).

This transcriptome-based study was designed to understand the species-specific nature of immature brain cells, analyze the pathways underlying the neurodevelopmental functions that can be studied using the “Neurosphere Assay” (Baumann et al., 2015; Bal-Price et al., 2018) and compare pathway functions between the three species: human, mouse and rat. These species were chosen due to human relevance, presence of transgenic animals and regulatory usage, respectively. Specific marker gene expression analyses identified human-specific traits in the human compared to rodent NPC. Gene Ontology (GO) term clustering (Bindea et al., 2009) and subsequent protein-protein interaction enrichment analyses (Bindea et al., 2013; Szklarczyk et al., 2015) were used to identify the functional pathways driving NPC functions computationally. These were then validated by functional studies *in vitro* using respective model compounds across the three species. The functionally validated microarray data defines the biological application domain of the “Neurosphere Assay” and identifies species specificities in signaling relevant for neurodevelopmental functions.

## 2. Material and methods

### 2.1. Chemicals

Bone morphogenetic protein 2 (BMP2) was purchased from R&D Systems (#355-BM; Wiesbaden, Germany). A stock solution (2.5 µg/mL) was prepared in B27 medium. *N*-[*N*-(3,5-Difluorophenacetyl)-*L*-alanyl]-*S*-phenylglycine *t*-butyl ester (DAPT) and Epidermal Growth factor receptor (EGFR) -inhibitor PD153035 were purchased from Sigma-Aldrich (#D5942, #SML0564; Taufkirchen, Germany). For DAPT and PD153035 stock solutions of 40 mM and 10 mM were prepared in dimethyl sulfoxide (DMSO; Carl Roth GmbH; Karlsruhe, Germany), respectively. Working solutions were prepared in N2 with 0, 0.1, 0.13 or 0.25% DMSO.

### 2.2. Cell culture

Human neural progenitor cells [hNPC, male, gestational week (GW) 16–18] isolated from whole brain were purchased from Lonza Verviers SPRL (CAT. # PT-2599; LOT NO.:0000339988 and 0000277692;

Verviers, Belgium). Rodent neural progenitor cells [post-natal day (PND)1] were prepared as described previously for rat (Baumann et al., 2014) and mouse (Dach et al., 2017). The time point for rodent sample preparation (PND1) was selected based on a comparative algorithm across species (Workman et al., 2013). According to this algorithm, brain developmental processes in GW 16–18 in human NPC are most similar to processes observed in rodent brain development at PND1 ([www.translatingtime.org](http://www.translatingtime.org)). Human and rodent NPC were cultured as neurospheres in proliferation medium consisting of DMEM (Life Technologies, Darmstadt, Germany) and Hams F12 (Life Technologies; 3:1) supplement with 2% B27 (Life Technologies), 1% penicillin and streptomycin (Pan-Biotech, Aidenbach, Germany), 20 ng/mL epidermal growth factor (EGF, Life Technologies), 20 ng/mL recombinant human fibroblast growth factor (FGF, R&D systems) for hNPC and mNPC and 10 ng/mL recombinant rat FGF (R&D systems) for rNPC. The culture was maintained at 37 °C with 5% CO<sub>2</sub>. The culture was fed every two to three days by replacing half the medium with fresh medium and passaged every week by mechanical chopping of the spheres with a tissue chopper (McIlwain Tissue Chopper, Vibratome). To initiate differentiation, NPC were plated on poly-D-lysine/laminin (Sigma Aldrich) coated 6 well plates in differentiation medium for 3 and 5 days. The differentiation medium consisted of DMEM (Life Technologies) and Ham F12 (Life Technologies; 3:1) supplement with 1% N2 (Life Technologies) and 1% penicillin and streptomycin (Pan Biotech). For differentiation of mNPC 1% fetal calf serum (FCS; Biochrome, Berlin, Germany) was added to the culture medium.

### 2.3. The “Neurosphere Assay”

To analyze pathway modulation on a functional level we quantified cell migration, as well as neuronal- and oligodendrocyte differentiation in differentiating neural progenitor cells after treatment with the pharmacological modulators BMP2, DAPT and PD153035. Therefore, spheres with a diameter of 0.3 mm were plated on poly-D-lysine/laminin (Sigma Aldrich) coated 8 chamber slides in differentiation medium for 3 and 5 days. On day 3 half the medium was replaced with freshly prepared medium. Migration was analysed 24 h and 72 h after plating. After 3 or 5 days spheres were fixed in 4% paraformaldehyde for 30 min at 37 °C and stained for neurons (βIII-tubulin positive cells) or oligodendrocytes (O4 positive cells). Cell viability was analysed with the Alamar Blue assay (CellTiter-Blue assay, Promega, Mannheim, Germany) in the same chamber/well that was used to analyze the DNT-specific endpoint (Baumann et al., 2014, 2015). Automatic counting of cell numbers in the migration area using the Omnisphero software (Schmuck et al., 2016) was an additional indicator for cell viability. For analyses of astrocyte maturation after BMP2 treatment, hNPC were also stained with an antibody against GFAP after 3 days of differentiation. Astrocyte maturation was quantified as migration distance of radial glia compared to total astrocyte migration distance because an increase in cell maturation increases the amount of mature stellate like astrocytes at the expense of radial glia (Fig. 6j). Apoptotic oligodendrocytes (O4 positive cells with condensed staining around nuclei; Fig. B. 5l) were counted and normalized to the number of nuclei.

### 2.4. Generation of RNA samples

For proliferating conditions (0d), 75 neurospheres with a diameter of 0.3 mm were collected for each replicate. For differentiation conditions (3d, 5d) neurospheres were chopped to 0.1 mm and plated at a density of 440 pieces/well in a poly-D-lysine/laminin coated 6 well plate for 3 or 5 days, respectively. RNA was isolated from a total of 54 samples, 6 replicates for each condition (0d, 3d and 5d), and species (h-, r-, and mNPC). RNA isolation was performed with the miRNeasy kit (Qiagen, Hilden, Germany) according to the manufactures protocol. Total RNA was used for microarray analysis and qRT-PCR. Quality of total RNA was analysed with the 2100 bioanalyzer (Agilent

Technologies). In parallel to the generation of RNA samples we performed the “Neurosphere Assay” to control if the cells from the same passage used for RNA analysis proliferate, differentiate and migrate according to our historical controls.

## 2.5. qRT-PCR analysis

For validation of microarray experiments we performed qRT-PCR of a set of 12–16 genes (Fig. B. 6). Therefore, RNA from the microarray samples harvested on day 0, 3, 5 was transcribed to cDNA using the QuantiTect Rev. Transcription Kit (Qiagen; Hilden, Germany) according to the manufacturer's protocol. Quantitative polymerase chain reaction (qRT-PCR) was performed using the Rotor Gene Q Cycler (Qiagen) with the QuantiFast SYBR Green PCR Kit (Qiagen) according to the manufacturer's protocol. All genes with the respective primer sequences are presented in Table A. 16. Differential expression was calculated with the ddCT method using beta actin for normalization and 0-day samples (proliferating NPC) were used as a reference set to 1.

## 2.6. Affymetrix arrays

For human NPC synthesis of cDNA and subsequent biotin labelling of cRNA was performed according to the manufacturer's protocol (3' IVT Plus Kit; Affymetrix, Inc.). Briefly, 100 ng of total RNA each were converted to cDNA, followed by in vitro transcription and biotin labelling of amplified cDNA. After fragmentation, labelled cDNA was hybridized to Affymetrix PrimeView Human Gene Expression Microarrays for 16 h at 45 °C, stained by streptavidin/phycoerythrin conjugate and scanned as described in the manufacturer's protocol.

For rodent samples synthesis of biotin labelled cDNA was performed according to the manufacturer's protocol (WT Plus Reagent Kit; Affymetrix, Inc.). Briefly, 100 ng of total RNA were converted to cDNA. After amplification by in vitro transcription and 2nd cycle synthesis, cDNA was fragmented and biotin labelled by terminal transferase. Finally, end labelled cDNA was hybridized to Affymetrix Mouse/Rat Gene 2.0 ST Gene Expression Microarrays for 16 h at 45 °C, stained by streptavidin/phycoerythrin conjugate and scanned as described in the manufacturer's protocol.

## 2.7. Data analysis and statistics

Data analyses on Affymetrix CEL files was conducted in R'. Probes within each probe set were summarized by Robust multichip average (RMA) after quantile normalization of probe level signal intensities across all samples to reduce inter-array variability. The algorithms were provided by the R packages *affy* (Gautier et al., 2004) for human samples and *oligo* (Carvalho and Irizarry, 2010) for mouse and rat samples. Differential gene expression (DEX) was statistically determined by one-way ANOVA followed by Tukey's range test (R Core Team, 2016). The significance threshold was set to  $p \leq .01$  (FDR corrected; gene expression analyses). Probes that matched this threshold for no probe set were dismissed. The Affymetrix IDs were translated into gene symbols using a translation table containing all genes matching our Affymetrix IDs. It was built using the *biomaRt* R package (Durinck et al., 2005). In a first step, a table with the gene symbols and expression data from their corresponding Affymetrix IDs was created. For genes, which matched to more than one Affymetrix ID, the mean of the differential expression per time frame was used. The  $p$ -values were combined applying Fisher's method (Fisher, 1992).

The Principal Component Analysis (PCA) is based on the significance threshold filtered expression data. Therefore, we worked with 18 data points (6 replicates per time point) per gene per species. Division by its respective median (median for one gene over 18 samples) normalized the expression data of each Affymetrix ID. We chose all genes with identical gene symbol in all species and used the *prcomp* method from the R stats package (R Core Team, 2016) to perform the

PCA. An adjacency matrix was calculated from the expression profiles of the genes over time using the *scree* package (Schwender and Fritsch, 2013). Hierarchical clustering was performed by *hclust* using unweighted pair group agglomeration method with arithmetic mean and *cutree* (R Core Team, 2016) resulting in 10 distinct clusters. These 10 clusters were manually summarized into the modules M1 – M4 according to their expression profiles over time. To allow a direct species comparison of gene expression independent of differential gene expression, we defined genes as likely to be expressed (present) or likely to be not expressed (absent) based on criteria adapted from Kang et al. (2011). A gene is called present if the median  $\log_2$  intensity value in 0-day samples is  $\geq 6$ . Genes that do not meet this criterion are defined as absent. The expression profile of single genes in heatmap (Fig. 2g) was prepared with the Multiple Experiment Viewer (MeV 4.9.0; <http://mev.tn4.org/>).

All data analyses for functional endpoints were performed using GraphPad Prism 6.00 (GraphPad Software, La Jolla California USA, [www.graphpad.com](http://www.graphpad.com)). Statistical significance analyses were performed on data normalized to solvent control (except for cell migration, here we used raw data on migration distance) from at least 3 independent experiments by one-way ANOVA followed by Dunnett's multiple comparisons test. The significance cut-off was set to  $p \leq .05$ .

## 2.8. Biological process analysis/gene ontological annotation analysis

We used the Cytoscape (version 3.4.0) plug in ClueGO/CluePedia (version 2.2.5; Bindea et al., 2013; Szklarczyk et al., 2015) for overrepresentation analyses of biological process GO clustering and network visualization. The statistical test for overrepresentation analysis was based on a two-sided hypergeometric option with a Bonferroni correction. We chose a  $p$ -value cut-off of 0.01 and a kappa score of 0.5 for GO clustering with at least two GO terms within one cluster (see parameters for analysis in Table A. 17).

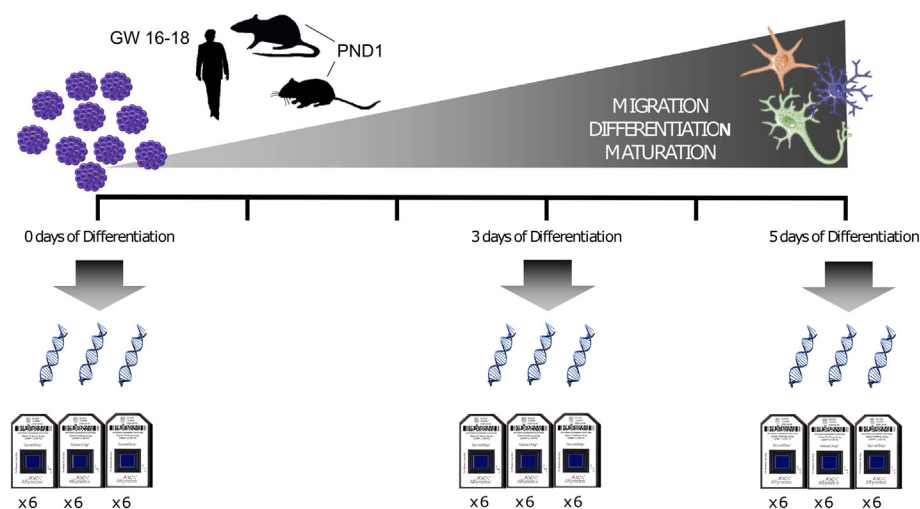
To generate gene interaction networks we used information from the STRING Protein-Protein Interaction database (Szklarczyk et al., 2015; <http://string-db.org>) within CluePedia, extracted the GO clusters cell migration, gliogenesis and neurogenesis and enriched all genes associated with the selected GO clusters with information on gene-gene or protein-protein interactions (binding, activation, expression and inhibition) with a confidence score of  $\geq 0.75$ . Highly connected genes were identified as those genes showing at least three times (migration, neurogenesis) or two times (gliogenesis) the number of connection compared to the mean number of connection per gene within the respective cluster.

## 3. Results

### 3.1. Analyses of changes in NPC mRNA expression profiles across time and species

To determine the changes in molecular equipment of NPC growing as neurospheres during the change from proliferation to differentiation (Baumann et al., 2015), we first analysed mRNA expression profiles of proliferating (0), as well as 3 and 5 days differentiating human, mouse and rat primary neural progenitor cells (hNPC, mNPC, rNPC; Fig. 1) by using microarrays (human PrimeView Array, mouse/rat Gene 2.0 ST Arrays, Affymetrix). Genes were called differentially expressed (DEX) if they were significantly ( $p \leq .01$ ) up- or downregulated by at least 2-fold between any of the three time points (0 vs. 3, 0 vs. 5, or 3 vs. 5 days). In hNPC, mNPC and rNPC a total of 1684, 1979 and 2324 genes, respectively, are DEX across all time points. The number of genes regulated in the first 3 days of differentiation (0 vs. 3) is in the same order of magnitude between the three species (1121 in hNPC, 1196, in mNPC, 1033 rNPC). With continuing NPC differentiation and maturation, more genes are DEX at day 5 (0 vs. 5) with 1531 in hNPC, 1566 in mNPC and 2159 in rNPC. Of those, 971, 849 and 927 genes (> 70%), respectively,





**Fig. 1.** Experimental set up.

NPC were generated from fetal human brain (GW16–18) or post-natal mouse and rat brain (PND1) and cultivated as floating neurospheres. RNA was isolated from proliferating (0d), as well as three and five days differentiated human, mouse and rat NPC, from 6 replicates per condition and species. Transcriptome analyses from these samples were performed using human PrimeView Array and mouse/rat Gene 2.0 ST Arrays from Affymetrix.

overlap with DEX genes at day 0 vs. 3 (Fig. 2 a-c). In rodent compared to human NPC there is a higher number of DEX genes between 3 and 5 days (43 hNPC, 362 mNPC, 732 rNPC; Fig. 2d) indicating a stronger change in cultures over 5 days in rodent compared to human NPC.

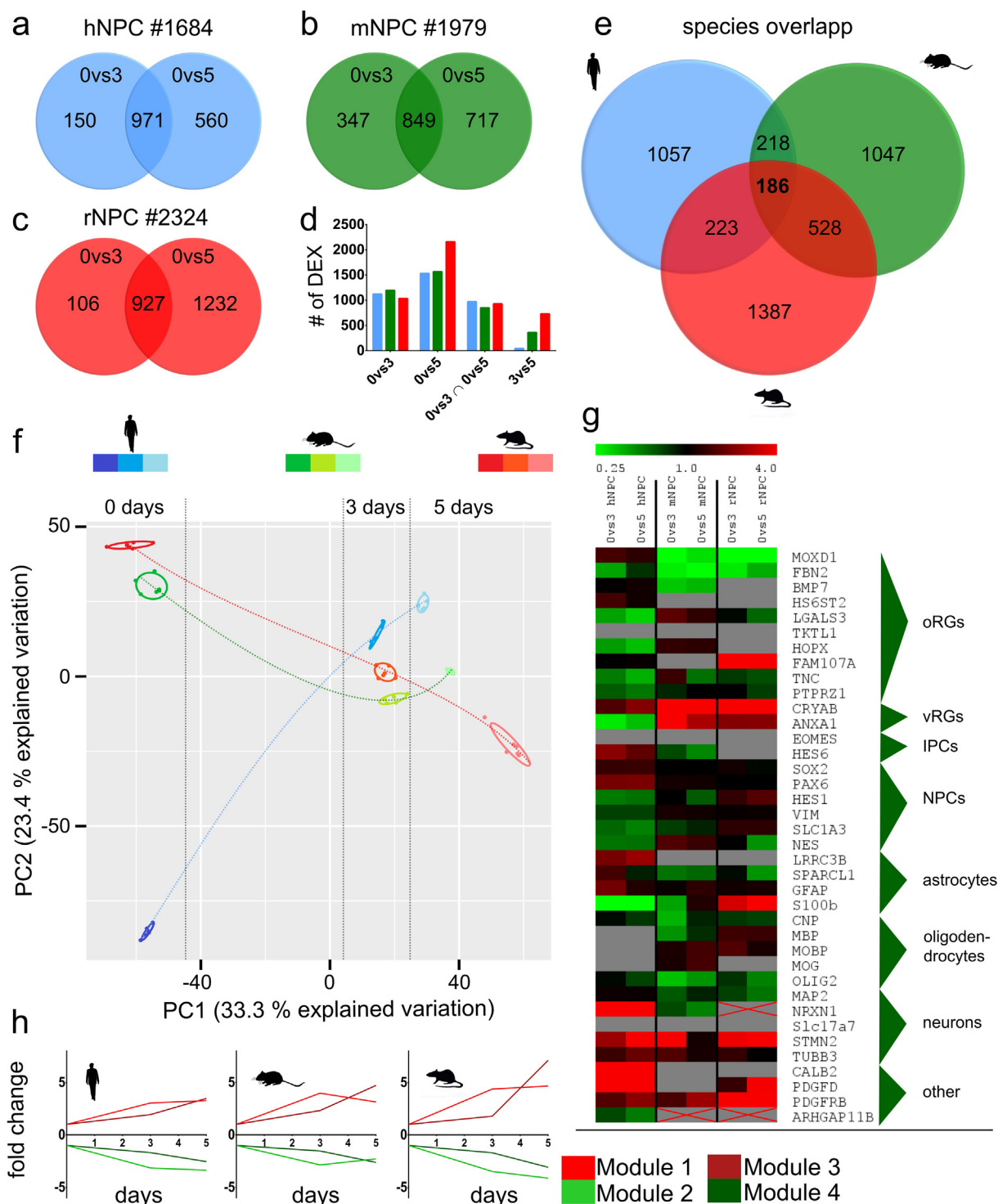
We next determined the number of commonly regulated genes between the total of 1684, 1979 and 2324 DEX genes in hNPC, mNPC and rNPC, respectively, across all time points (0vs3, 0vs5 and 3vs5 days combined). Of these, only 186 (11%) genes share the same gene symbol in all three species (Fig. 2e). This small number of overlapping DEX genes during NPC differentiation can only in part be explained by the dissimilarities of array chips, because of the 1684 DEX genes identified in hNPC 83% (1398) are present on both rodent array chips, yet are not DEX in the rodent cells (data not shown). To compare the magnitude of gene expression changes across the three species in addition to this qualitative difference of gene regulation during NPC differentiation, quantitative differences in magnitude of expression of all regulated genes ( $p \leq .01$ ; 5571) with the same gene symbols across differentiation time and between the three species were evaluated by PCA (Fig. 2f). PC1 (33% explained variation) reveals that for all species 0d samples cluster further from 3d than 3d from 5d samples, pointing towards largest gene expression changes when the cell program switches from NPC proliferation to neural differentiation compared to smaller changes during further maturation of differentiated cells from day 3 to day 5 in culture. For the species comparison, the PCA demonstrates that hNPC have a distinct differentiation dynamic compared to the rodent NPC as visible in the course of expressional changes over time (Fig. 2f, dotted lines). Differences in the differentiation dynamics are also obvious in the expressional changes of genes specific for certain cell types during brain development (Fig. 2g). Obvious examples are the neuronal marker *NRXN1* which is upregulated in hNPC (4.2 and 5.2 fold at 3 and 5 days, respectively), downregulated in mNPC (0.7 and 0.6 fold at 3 and 5 days, respectively) and not present on the microarray chip of rNPC, or the ventricular radial glia marker *ANXA1* which is downregulated in hNPC (0.3 and 0.4 fold at 3 and 5 days, respectively) and upregulated in rodent NPC (13.5 and 3.1 fold in mNPC, 2.6 and 2.6 fold in rNPC at 3 and 5 days, respectively). To allow a direct species comparison of gene expression independent of differential gene expression, we defined genes as likely to be expressed (present) or likely to be not expressed (absent) based on criteria adapted from Kang et al. (2011; only present if median  $\log_2$  intensity value in 0-day samples is  $\geq 6$ ). With this threshold we identified several genes that are likely to be only expressed in human cells (*HS6ST2*, *LRR3B*, *CALB2* or *ARHGAP11B*; Fig. 2g and Table A. 19). Taken together, the qualitative and quantitative expression data show that primary NPC from human and rodent origins obtain species-specific expression changes when differentiating to neural effector cells with only few DEX genes shared between human

and rodent NPC and with some human specific marker genes for NPC development.

For further analyses of gene function behind these expression changes, we generated expression clusters using a hierarchical cluster analysis (HCA) for all DEX genes (Fig. B. 1). We summarized these clusters according to their regulation pattern over time into 4 modules: module 1 (M1) and module 2 (M2) contain genes with the main expression changes, up and down, respectively, within the first 3 days of differentiation and no further regulation from day 3 to day 5 (Fig. 2h). These clusters contain similar numbers of genes across all species (M1: 611, 575, 504; M2: 667, 499, 404, for h-, m- and rNPC, respectively). We hypothesized that these are genes involved in the NPC program change from proliferation to neuronal and glial differentiation and the onset of cellular migration. Summarized in module 3 (M3) and module 4 (M4) are those genes, which are up- and down-regulated, respectively, mainly between day 3 and 5 in vitro. For these clusters, the numbers of genes differ between human and rodent NPC (M3: 191, 547, 887; M4: 215, 358, 428, for h-, m-, rNPC, respectively). These genes are thought to be mainly involved in processes of effector cell maturation and thus the fewer regulated genes in hNPC compared to their rodent counterparts might explain the lack in hNPC-derived neuronal maturation which seems to be enhanced in rNPC-derived neurons (Odawara et al., 2014; Ohara et al., 2015). Mean expression change of the modules M1 and M3 (Fig. 2h) corroborate the observation that mNPC and especially rNPC show stronger expression changes between 0 and 5 days than hNPC (Fig. 2d).

### 3.2. Overrepresentation analyses (ORA) of gene ontology (GO) biological processes (BP)

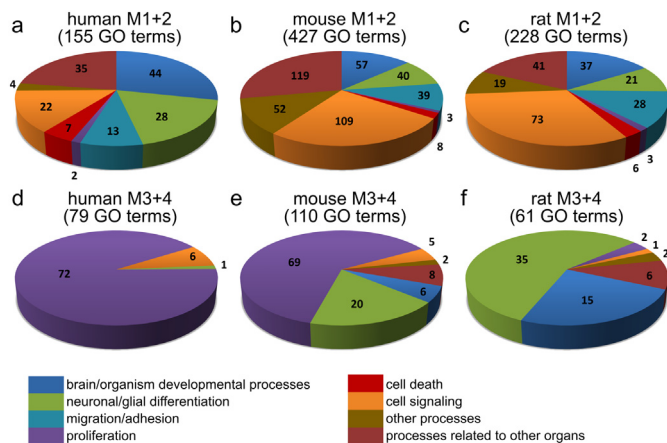
To computationally determine biological functions of genes in the temporal expression clusters, we performed ORA for the GO-terms BP using the Cytoscape plugin ClueGO (Bindea et al., 2009). We first analysed the biological functions of genes in clusters M1 and M2, where we expected the largest transcriptional changes due to the switch in cell program from proliferation to differentiation. From the 1278 DEX genes in hNPC, 1074 in mNPC and 908 in rNPC, respective 1070 (83.7%), 904 (84.2%) and 787 (86.7%) were annotated to 155 (hNPC), 427 (mNPC) and 228 (rNPC) GO terms (Table 1; Table A. 1–3). Although developing NPC from humans and rodents have only little overlap in DEX genes (11% of hNPC), 90 of the 155 (58%) GO terms enriched in hNPC were shared with rodent NPC. These GO terms are major BP involved in general organ development like anatomical structure morphogenesis (GO:0009653), organ specific developmental processes like central nervous system development (GO:0007417), or GO terms specific to some major processes of brain development that are assessed by the



**Fig. 2.** Qualitative and quantitative comparison of expression profiles across species. Differential gene expression within each species and between time points was statistically determined by one-way ANOVA followed by Tukey's range test. Genes with  $p \leq .01$  and fold change  $\geq 2$  were called differentially expressed (DEX). (a-c) Overlap of the number of DEX genes between 3 (0vs3) and 5 (0vs5) days of differentiation for human (a), mouse (b) and rat (c) NPC. (d) Comparison of the number of DEX genes for each time point (0vs3, 0vs5, overlap between 0vs3 and 0vs5 and 3vs5) between human (blue), mouse (green) and rat (red) NPC. (e) DEX genes (at any time point) that share the same gene symbol in human (blue), mouse (green), and rat (red) NPC. (f) Principal component analysis (PCA) was performed based on the expression of all significantly regulated ( $p \leq .01$ ) genes that shared the same gene symbol between species (5570) and compares the expression profile over time (0, 3 and 5 days; dark to pale) between species (human, blue; mouse, green; rat, red). (g) Expression profile of single genes associated to specific cell types during neural development and in the CNS of human, mouse and rat NPC. Genes, defined as not present are depicted in grey, genes depicted in grey with a red cross are not on the respective microarray chip. (h) Hierarchical clustering generated 10 distinct expression clusters (Table A. 1), which were further summarized into 4 modules. Data is represented as mean DEX over time of all genes within one module for human mouse and rat NPC. oRG is outer radial glia; vRG is ventricular zone radial glia; IPC is intermediate progenitor cells. (For interpretation of the references to colour in this figure legend, the reader is referred to the web version of this article.)

**Table 1**  
GO BP overrepresentation analyses.

Species	Human		Mouse		Rat	
	M1 + 2	M3 + 4	M1 + 2	M3 + 4	M1 + 2	M3 + 4
Expression cluster	M1 + 2	M3 + 4	M1 + 2	M3 + 4	M1 + 2	M3 + 4
# genes	1278	404	1074	906	908	1417
# Genes Annotated	1070	345	904	761	787	1058
# GO terms	155	79	427	110	228	61
Shared GO terms	# (% human) of GO terms					
Expression cluster	M1 + M2		M3 + M4			
Human-Mouse	122 (78)		33 (42)			
Human-Rat	98 (63)		0			
All species	90 (58)		0			
Mouse-Rat	181		45			



**Fig. 3.** Classification of GO terms into superordinate biological processes. ORA analysis was performed using the Cytoscape plugin ClueGO (Bindea et al., 2009). All overrepresented GO terms ( $p \leq .01$  based on a two-sided hypergeometric option with a Bonferroni correction) for modules 1 + 2 (a-c) and modules 3 + 4 (d-f; also see Fig. 2) were summarized into 8 superordinate processes for human (a, d), mouse (b, e) and rat (c, f) NPC based on expert judgment. Number in the pie chart represents the number of GO terms assigned to each superordinate processes.

functional “Neurosphere Assay”. Here, the processes NPC proliferation, migration, neuronal and glial differentiation as well as cell death are represented by regulation of GO terms such as cell proliferation (GO:0042127), cell motility (GO:0048870), neurogenesis (GO:0022008), axonogenesis (GO:0007409), gliogenesis (GO:0042063) or regulation of programmed cell death (GO:0043067; comprehensively shown in Table A. 4). To visualize how GO term enrichment compares in-between the three species, we summarized all GO terms into the following eight superordinate processes by expert judgment similar to Waldmann et al. (2014): (i) brain/organism developmental processes, (ii) neuronal/glial differentiation, (iii) migration/adhesion, (iv) proliferation, (v) cell death, (vi) cell signaling, (vii) other processes and (viii) processes related to other organs (Table A. 5–7). Fig. 3a-c demonstrates that from the temporal expression cluster M1 and M2, GO terms associated to ‘brain/organism developmental processes’, ‘neuronal/glial differentiation’ are the most represented and together with ‘migration/adhesion’, ‘proliferation and cell death’ make up 60% of all GO terms in hNPC, while these GO terms represent only 34% and 41% in mNPC and rNPC, respectively. GO terms associated with processes related to cell signaling correspond to 14% of all GO terms in hNPC, while this is the largest group in rodent NPC with 26% (mNPC) and 32% (rNPC) of all GO terms. In total numbers, only 31 GO terms are associated to this group in hNPC, 92 in rNPC and 164 in mNPC. Some of the processes present in rodent but not in hNPC are e.g. cell-cell signaling (GO:0007267), response to steroid hormone (GO:0048545), negative

regulation of cell communication (GO:0010648) or protein phosphorylation (GO:0006468; Table A. 4). The remaining 26% (hNPC), 40% (mNPC) and 26% (rNPC) GO terms are associated to other processes (e.g. single-organism biosynthetic process, GO: GO:0044711 or ion transport, GO:0006811) and processes in other organs. One example for the latter group is the process heart development (GO: 0007507). Although this is prima vista not related to brain development, it shares 41 of the 62 genes (66%) with the process nervous system development (GO:0007399) in hNPC (Table A. 1). This example demonstrates that GO terms of processes related to other organs might be overrepresented due to shared genes with nervous system development.

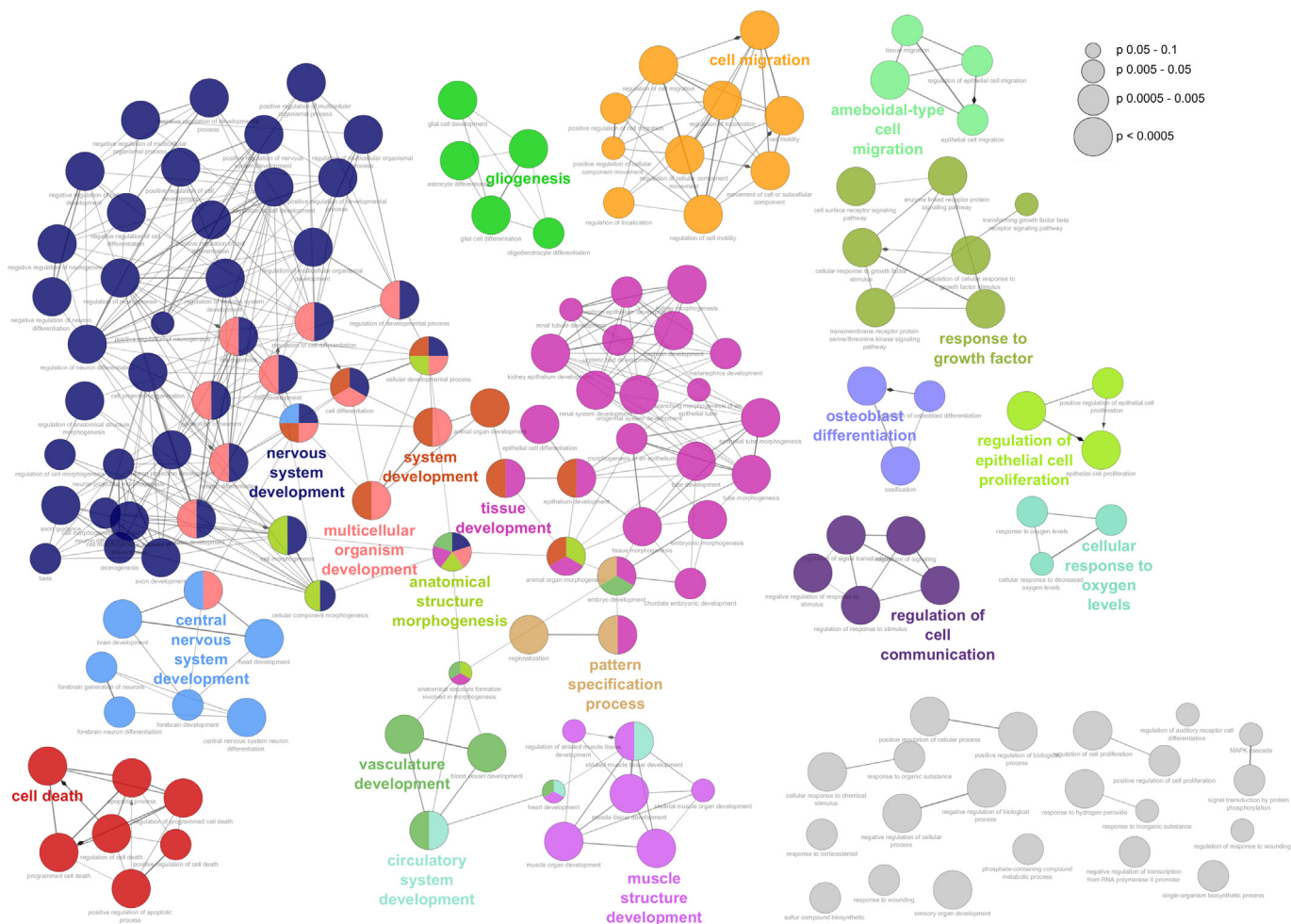
Next, we computationally analysed the biological functions of genes in clusters M3 and M4. From the 404 DEX genes in hNPC, 906 in mNPC and 1417 in rNPC, respective 345 (85.4%), 761 (84.0%) and 1058 (74.7%) were annotated to 79 (hNPC), 110 (mNPC) and 61 (rNPC) GO terms with 42% shared GO terms between hNPC and mNPC and none between hNPC and rNPC (Table 1; Table A. 8, 10–11). There are two- (mNPC) to three-fold (rNPC) more DEX genes present in rodent than in hNPC pointing to differences in culture maturation and/or species differences. This is supported by the magnitude fold change in DEX genes in rodents, mainly rat NPC, which display higher mean gene expression regulations compared to hNPC (mean regulation of M3: 3.5 fc in hNPC, 4.7 fc in mNPC, 7.1 fc in rNPC; Fig. 2h). Fig. 3d-f demonstrates that almost all GO terms in hNPC (91%) and more than half in mNPC (69%) are associated to the process of cell proliferation such as cell cycle (GO:0007049), chromosome organization (GO:0051276) or mitotic nuclear division (GO:0007067). Within these GO terms 60–100% of all associated genes are down-regulated (Table A. 8 + 10). This observation suggests that cell proliferation is still an important process during the onset of differentiation but strongly decreases between day 3 and 5 in hNPC and mNPC. Other GO terms in mNPC (18%) and more than half in rNPC (57%) are associated with the progression of cell differentiation and maturation. Here some GO clusters are cilium organization (GO:0044782) in mNPC, determination of left/right symmetry (GO:0007368) or microtubule-based process (GO:0007017) in both species and cilium morphogenesis (GO:0060271) or centriole assembly (GO:0098534) in rNPC (comprehensively shown in Table A. 10–15). Because the majority of DEX genes in M3 and M4 of hNPC were dominated by downregulated genes, we performed an ORA for upregulated genes (M3) separately. ORA of hNPC M3 shows that 16 processes involved in maturation such as axonogenesis (GO:0007409) and dendrite development (GO:0016358) are overrepresented (Table A. 9) in our data set.

Overall, the ORA of GO BP especially from M1 and M2 reflects (i) the multicellularity of the 3D neurospheres and (ii) specific neurodevelopmental processes during NPC development. These results demonstrate that molecular signatures of gene expression changes line the functional processes that are studied in the frame of the “Neurosphere Assay” in vitro over NPC differentiation. It also indicates that many of these major processes of brain development and cell organization are conserved across species, yet with distinct molecular signatures. However, there are considerable species differences in the abundance of processes related to cell signaling, proliferation or the progression of cell maturation between the in vitro systems of the three species.

### 3.3. Identification of key regulators for human neurodevelopmental processes

To identify the underlying genes and pathways of the neurodevelopmental processes studied with the “Neurosphere Assay”, we performed a clustering based on shared genes between GO terms overrepresented in modules M1 and M2 of hNPC (Fig. 4) and rodent NPC (Fig. B. 2–3). From the 19 GO clusters in hNPC we extracted those representing the major neurodevelopmental processes, i.e. cell migration, neurogenesis and gliogenesis. As the cluster neurogenesis was included in a cluster with general GO terms on (neuro)development, we





**Fig. 4.** GO clustering in hNPC.

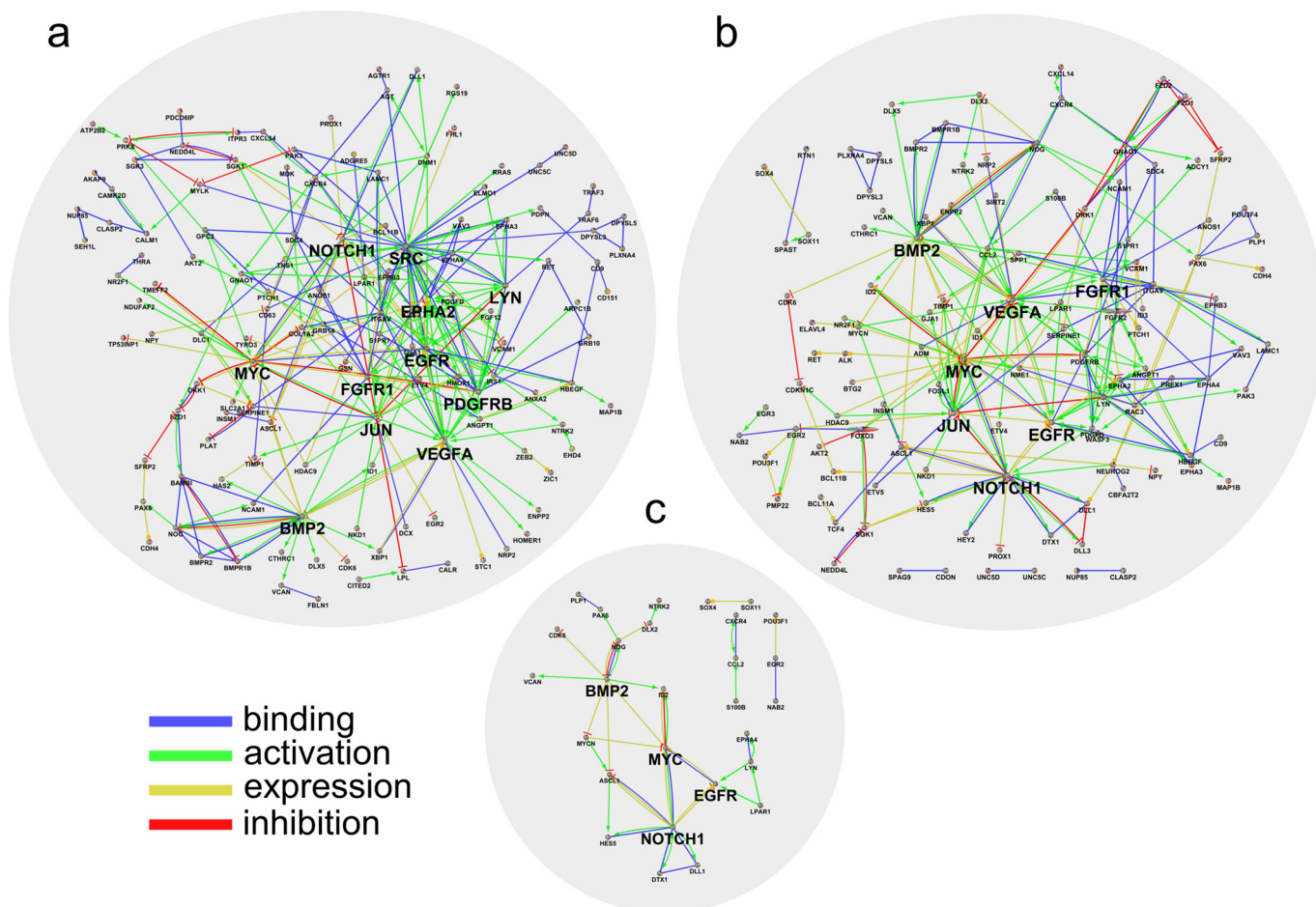
Overrepresented GO terms of modules 1 and 2 in hNPC were clustered according to gene overlap between GO terms with a kappa score threshold of 0.5 and at least three GO terms within one cluster using the Cytoscape plugin ClueGO (Bindea et al., 2009). Edge thickness represents similarity between GO terms. Node size represents significance of overrepresentation. The GO term with the highest significance determines the name of the respective GO cluster (bold; colored). Different colors represent different GO clusters. Grey nodes do not belong to a cluster. Significance thresholds of ORA were set to  $p \leq .01$  based on a two-sided hypergeometric option with a Bonferroni correction.

manually removed all GO terms, e.g. GO terms like brain development (GO:0007420), regulation of cell morphogenesis (GO:0022604) or cell development (GO:0048468) that were not directly related to neurogenesis (Fig. B. 4).

All genes within each cluster were enriched for their interaction (binding, activation, expression and inhibition) based on information from STRING protein-protein Interaction database (Szklarczyk et al., 2015); <http://string-db.org>; Fig. 5. We identified highly connected genes as key regulators (KR) or hubs for individual human neurodevelopmental processes. Genes that show at least three times (migration, neurogenesis) or two times (gliogenesis) the number of connections compared to the mean number of connections per gene within a cluster were defined to be highly connected. Thereby, we identified *BMP2*, *EGFR*, *MYC* and *NOTCH1* as KR across all three processes, *VEGFA*, *JUN* and *FGFR1* as KR for migration and neuronal differentiation and *EPHA2*, *LYN*, *PDGFRB*, *SRC* only for migration (Fig. 5; Table 2). Species comparison revealed that for mNPC and rNPC only few genes (between 7% to 14%) of the processes migration, neurogenesis and gliogenesis with interaction data are shared with hNPC. From the KR only *VEGFA* is present in the two species, a finding that could be explained by the general low number of DEX genes shared between the species. The KR for rodent NPCs are *Agt*, *Cav*, *Flt*, *Fyn*, *Itga*, *Pdgfb*, *Ptgs2* for migration in mNPC, *Cx3cr1*, *Flt1*, *Itgb4* and *Ptk2* for migration in rNPC, *Bmp4* for

neurogenesis in mNPC and *Ptk2* for neurogenesis in rNPC. For the process gliogenesis there was no KR for mNPC and the processes did not appear as a separate cluster in rNPC (Table A. 20–24; Table 2).

For functional validation of some of the KR identified in hNPC transcriptomes, we analysed the effects of their pharmacological modulation on migration, neuronal and oligodendrocyte differentiation in all three species. As KR we chose *BMP2*, *EGFR* and *NOTCH*, as they were predicted to modulate all three processes, i.e. hNPC migration, neuronal and glia differentiation (Fig. 5; Table 2). We modulated *BMP2* signaling by addition of 0.01–100 ng/mL *BMP2* during differentiation of human, mouse and rat neurospheres (Fig. 6). *BMP2* did not affect migration of human and mNPCs, but induced migration of rNPCs after 72 h ( $149.9 \pm 7.2\%$  of control at 10 ng/mL; Fig. 6a). Furthermore, *BMP2* did not affect differentiation into  $\beta$ III-tubulin positive neurons in hNPC, while it induced and reduced neuronal differentiation in mouse and rNPC, respectively ( $202.1 \pm 46.9\%$  of control at 50 ng/mL in mNPC and  $62.2 \pm 8.6\%$  of control at 5 ng/mL in rNPC; Fig. 6b). *BMP2* reduced the differentiation to O4 positive cells in all species ( $48.7 \pm 1.8\%$  and  $50.8 \pm 3.5\%$  of control at 1 ng/mL in human and rNPC, respectively and  $54.2 \pm 4.4\%$  of control at 5 ng/mL in mNPC; Fig. 6c). In addition, *BMP2* induced maturation of GFAP positive cells, as indicated by a concentration-dependent increase of mature astrocytes at the expense of radial glia cell in the migration area. This effect



**Fig. 5.** Gene-gene interaction networks of major neurodevelopmental processes overrepresented in hNPC. The cytoscape plugin GluePedia (Bindea et al., 2013) was used to enrich the GO clusters cell migration (a), neurogenesis (b) and gliogenesis (c) from the ORA of modules 1 and 2 of hNPC with information on gene-gene/protein-protein interactions (binding in blue, activation in green, expression in yellow and inhibition in red) from the STRING database (Szklarczyk et al., 2015) with a confidence score of  $\geq 0.75$ . Highly connected genes (bold) were identified as those genes showing at least three times (migration, neurogenesis) or two times (gliogenesis) the number of connections compared to the mean number of connections per gene within the respective cluster. (For interpretation of the references to colour in this figure legend, the reader is referred to the web version of this article.)

was quantified by measuring the reduction of radial glia cell migration in comparison to the total migration of GFAP positive cells (from  $82 \pm 6.2\%$  of total migration at control to  $62.4 \pm 0.9\%$  of total migration at 1 ng/mL; Fig. 6j+k). Because migrating rodent NPC did not display typical radial glia morphology in our neurosphere culture (Baumann et al., 2015), BMP2 effects on astrocyte maturation was only studied in hNPC. All effects described for BMP2 were at concentrations

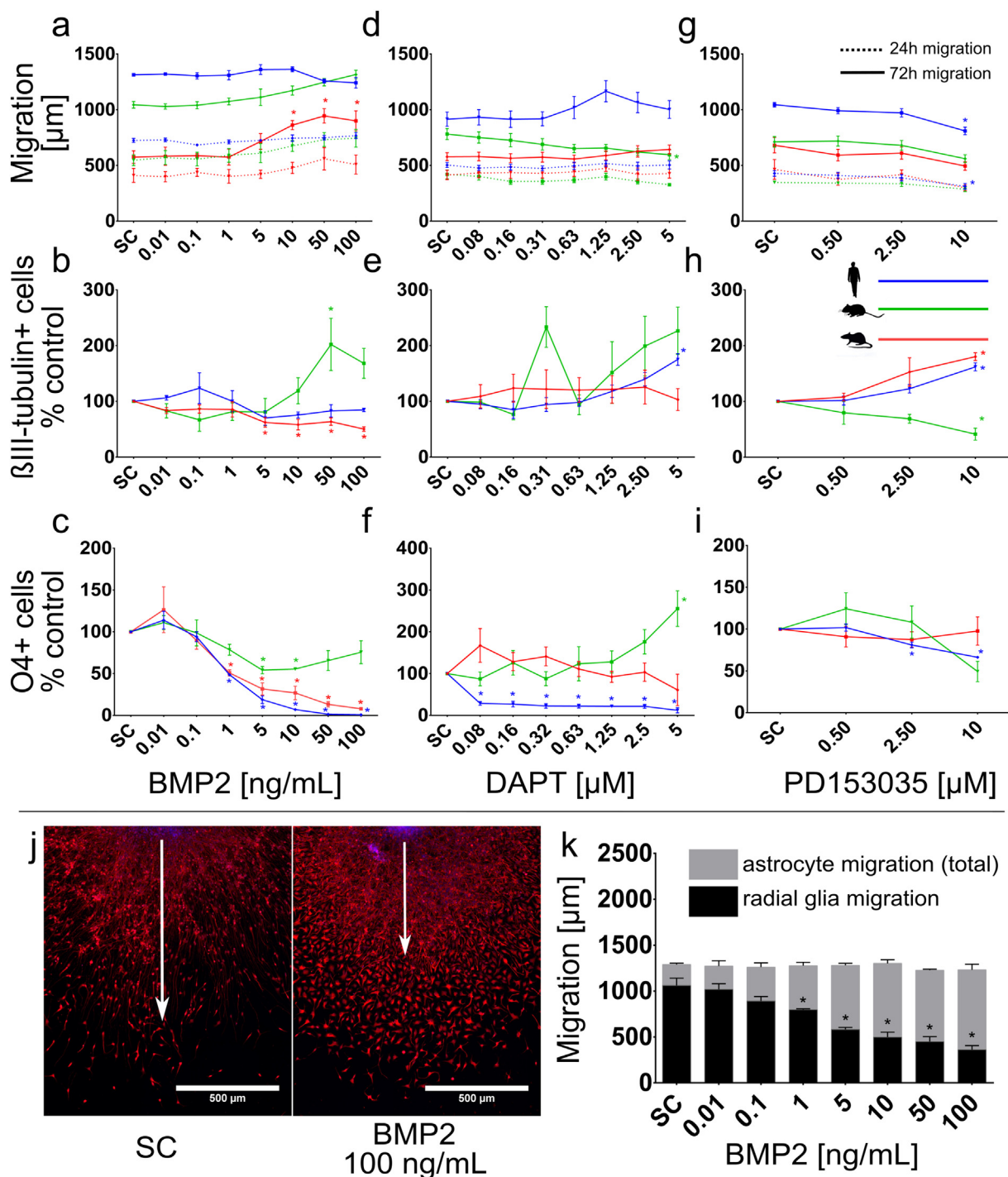
that did not affect overall cell viability measured by mitochondrial activity (Fig. B. 5a + c).

NOTCH signaling was modulated by the addition of 0.08–5  $\mu\text{M}$  of the NOTCH inhibitor DAPT. NOTCH inhibition did not affect migration of human and rNPC, but inhibited migration of mNPC after 72 h ( $76 \pm 5.7\%$  of control at 5  $\mu\text{M}$ ; Fig. 6d). Differentiation into  $\beta$ III-tubulin positive cells after 72 h was not affect by NOTCH inhibition (data

**Table 2**  
Highly connected genes as key regulator for neurodevelopmental processes.

		Migration	Neurogenesis	Gliogenesis
Human	MEAN #connections/Gene	4.3	5.7	3.4
Human	Key regulators (#connections)	BMP2*(23), EGFR*(22), EPHA2(16), FGFR1(18), JUN (20), LYN(14), MYC*(23), NOTCH1*(18), PDGFRB(18), SRC(44), VEGFA(26)	BMP2*(24) EGFR*(17), FGFR1(14), JUN (20), MYC*(25), NOTCH1*(26), VEGFA(26)	BMP2*(10), EGFR*(6), MYC*(10), NOTCH1*(14)
Mouse	MEAN #connections /Gene (overlap human in %)	4.4 (13.6%)	2.7 (14.4%)	3.3 (7.1%)
Mouse	Key regulators (#connections)	Agt(17), Cav1(20), Flt1(14), Fyn(17), Itga(17), Pdgfb (14), Ptgs2(15), Vegfa(17)	Bmp4(10)	none
Rat	MEAN #connections/Gene (overlap human in %)	2.7 (8.2%)	2.5 (7.6%)	not present
Rat	Key regulators (#connections)	Cx3cr1(10), Flt1(11), Itgb4(9), Ptk2(16)	Ptk2(9)	

\* Highly connected in all three neurodevelopmental processes.



**Fig. 6.** Pharmacological modulation of the BMP2, NOTCH and EGF pathway.

NPC from human (blue), mouse (green; differentiated in FCS) and rat (red) were treated with increasing concentrations of BMP2 (a, b, c), DAPT (NOTCH inhibitor; d, e, f) and PD1530353 (EGFR inhibitor; g, h, i) and analysed for migration (after 24 h (dotted line) and 72 h (solid line); a, d, g) neuronal differentiation (after 72 h for BMP2, EGFRi and 120 h for DAPT; b, e, h), oligodendrocyte differentiation (after 120 h; c, f, i) and astrocyte maturation (only in hNPC after BMP2 treatment; j, k). Neurons and oligodendrocytes were immunocytochemically stained with βIII-tubulin and O4, respectively, and quantified as percent of neurons/oligodendrocytes compared to Hoechst33258 counterstained nuclei. Astrocytes were stained with GFAP and maturation of radial glia cells was measured as migration of radial glia compared to total migration of GFAP positive cells. (j) Representative pictures of immunocytochemically stained astrocytes after 72 h BMP2 treatment of hNPC. Scale bar represent 500 μm, white arrow marks radial glial migration. Except for migration distance (shown as raw migration distance in μm), data was normalized to the solvent control and is displayed as concentration response relationship with mean ± SEM of at least three independent experiments. \* indicates a significant difference to solvent control based on one-way ANOVA ( $p < .05$ ) followed by Dunnett's multiple comparison test. (For interpretation of the references to colour in this figure legend, the reader is referred to the web version of this article.)

not shown). NOTCH inhibition induced neuronal differentiation only of human, not rodent NPC after 120 h ( $175.2 \pm 10.5\%$  of control at 5 μM, Fig. 6e), while after 72 h DAPT exerted no effects on neuronal

differentiation of either species. Differentiation of hNPC into O4 positive oligodendrocytes was inhibited by NOTCH inhibition ( $28.5 \pm 4.3\%$  of control at 0.16 μM DAPT), not affected in rNPC and



induced to  $255.4 \pm 42.6\%$  of control in mNPC ( $5 \mu\text{M}$  DAPT, Fig. 6f). However, these additionally formed mouse O4 positive cells did undergo apoptosis as identified in Fig. B. 5k + l, leaving non-apoptotic oligodendrocytes at the same number than the control cultures. In differentiated human or rat NPC, no apoptotic O4 positive cells were present. The highest concentrations of DAPT ( $1.25\text{--}5 \mu\text{M}$ ) reduced mitochondrial activity in all species (Fig. B. 5e). Except for rNPC at  $5 \mu\text{M}$  DAPT, this effect was not accompanied by a reduction in number of nuclei (Fig. B. 5f), which lead us to the assumption that DAPT reduces mitochondrial activity rather than affect cell viability.

Intrinsic EGF signaling was inhibited by addition of  $0.5\text{--}10 \mu\text{M}$  of the EGFR inhibitor PD1530353. Inhibition of EGFR reduced migration of hNPCs after 24 h and 72 h ( $75.0 \pm 5.9$  and  $77.5 \pm 3.2\%$  of control at  $10 \mu\text{M}$ ) and did not affect migration in m- and rNPC (Fig. 6g). Differentiation to  $\beta$ III-tubulin positive cells was induced in h- and rNPC ( $161.9 \pm 7.2\%$  and  $180.2 \pm 7.0\%$  of control at  $10 \mu\text{M}$ ) and reduced in mNPC ( $41.4 \pm 10.8\%$  of control at  $10 \mu\text{M}$ ; Fig. 6h). PD1530353 reduced the formation of O4 positive cells in hNPC ( $66.3 \pm 1.4\%$  of controls at  $10 \mu\text{M}$ ), while it did not affect the differentiation to O4 positive cells in m- and rNPC (Fig. 6i). Effects on migration in hNPC and neuronal differentiation in all species was accompanied by a reduction in number of nuclei ( $59 \pm 9.0\%$ ,  $72 \pm 5.3\%$  and  $78 \pm 6.0\%$  of control in h-, m- and rNPC, respectively). In rNPC the  $10 \mu\text{M}$  PD1530353 additionally affected viability after 72 h ( $75.6 \pm 9.0\%$  of control).

#### 4. Discussion

Within the paradigm shift of ‘Toxicology in the 21st century’ the need for in vitro assays is voiced that reliably predict human toxicity (Collins et al., 2008; NRC, 2007). One of the required toxicity endpoints with regard to chemical safety is reproductive and developmental toxicity currently assessed with the extended one-generation study (OECD, 2012). While giving valuable information for many different endpoints, this bioassay as well as the OECD TG426 specifically designed for DNT evaluation are not sufficient for identifying neurodevelopmental toxins (Fritsche et al., 2017; Tsuji and Crofton, 2012). Therefore, alternative assays predicting (neuro)developmental toxicity also for regulatory applications are urgently needed (Bal-Price et al., 2015; Fritsche et al., 2017; Bal-Price et al., 2018). For any application, a thorough understanding of the alternative test system especially on the molecular level increases confidence in the method and might allow future usage in a broader context like the ‘integrated approaches for testing and assessment’ (IATA; Judson et al., 2013; National Academy of Sciences, 2007; Roggen, 2011). This is why in this work the molecular equipment (transcriptome) of developing human NPC over time (proliferating versus 3 and 5 days differentiated cells) was assessed; they were compared to time-matched ([www.translatingtime.org](http://www.translatingtime.org); Workman et al., 2013) mouse and rat NPC transcriptomes to identify species-specificities. Pathways recognized as major regulating hubs were functionally validated for their impact on NPC migration, neuronal and oligodendrocyte differentiation across the three species (Fig. 1).

Recently it was recognized that the uniqueness of higher cognitive and emotional functions in humans is largely determined by human-specific neurodevelopmental gene expression (Dehay and Kennedy, 2009). In addition, transcriptome analyses of developing brain cells from mouse embryonic stem cells (mESC) were shown to recapitulate early neurodevelopmental stages in vitro and were thus identified as reference points for DNT testing (Abranches et al., 2009; Kuegler et al., 2010; Zimmer et al., 2011). This concept was transferred to their human correlates (hESC; van de Leemput et al., 2014) and such hESC were applied successfully in a transcriptome-based compound evaluation for the two developmental neurotoxicants methylmercury and valproic acid (Krug et al., 2013). Moreover, transcriptome analyses of neural differentiating human induced pluripotent stem cells are applied for disease modelling (Boland et al., 2017) strengthening human

relevance of such an approach.

On this basis, we studied gene expression in neurodevelopmental in vitro systems of three different species. During NPC differentiation in vitro, 1684 human, 1979 mouse and 2324 rat genes were DEX ( $> 2$ -fold up- or downregulated;  $p < .01$ ; Fig. 2a-c). In a study that analysed transcriptional changes of mouse differentiating NPC after treatment with brain derived neurotrophic factor (BDNF) or neurotrophin 4 (NT4) a total of 722 and 624 genes were differentially expressed at any of the three time points (24 h, 48 h or 96 h; van Dartel et al., 2010). The lower number of genes can be explained by the use of different microarray chips with less transcripts (13627) compared to the chips used in this study ( $> 20,000$ ). Other similar studies were performed analyzing transcriptome changes of human embryonic stem cells (ESC) differentiating to cardiomyocytes (CM; Meganathan et al., 2012). Between undifferentiated hESC and 48 h or 12 days differentiation towards the CM lineage, respective 3579 (van Dartel et al., 2010) and 3035 (Meganathan et al., 2012) transcripts were found to be differentially expressed. These are around twice as many gene changes as we found in undifferentiated compared to 3 or 5 days differentiated hNPC (Fig. 2a-c). This might be because NPC are already on their way to neural tissue, while hESC are still omnipotent and thus differ more strongly from the terminally differentiated cells.

Principle Component Analyses using all genes that are significantly changed on the arrays ( $p < .01$ ) and present in all three species (5570) revealed that the majority (56.7%) of all variance between the condition and species can be described by the first two principal components (Fig. 2f). The PCA plot clearly shows the differentiation dynamics of the NPC in vitro system and indicates that the variance within experimental groups is relatively small compared to the variance between time points and species (Fig. 2f). A similar PCA pattern was observed during hESC differentiation to CM. Here, 24 and 48 h (van Dartel et al., 2010) as well as 6 and 20 days of differentiation (Li et al., 2015) were clearly distinguishable from the stem cells of origin also pointing to highly dynamic in vitro systems with regards to differentiation capacities. Besides differences in gene expression over time within one species, we also observed well-defined distinctions in gene expression differentiation dynamics between the three species (Fig. 2f). Comparison of human and mouse ESC differentiated to embryonic bodies revealed that out of a total of 903 GO terms (biological processes), gene expression was only correlated between species in 395 and not correlated in 508 GO terms indicating substantial differences in transcriptional regulation of ESC-based embryonic body formation (Sun et al., 2007). This work supports the observed species differences in gene expression profiles during NPC development presented here.

One striking aspect of this study is that only approximately 10% of all DEX genes ( $> 2$ -fold,  $p < .01$ ; Fig. 2c) over developmental time were common in all three species (Fig. 2e). This is a very small number considering that these in vitro systems are functionally very similar, i.e. migrating and differentiating primary NPC (Baumann et al., 2015). These 186 genes cluster in 61 GO Terms (Table A. 18) that contain some specific neurodevelopmental processes, but also a large variety of non-neurodevelopmental-related biological functions. A large variety of genes in these non-specific GO Terms, however, are generally involved in tissue and organ development pointing to the fundamental biological significance of these molecules in developing cell functions. Such include MYC (present in 18 of these GO Terms), which is engaged in cellular signaling including cell proliferation (Hydbring et al., 2017), PDGFRB (present in 16 of these GO Terms), which guides a variety of developmentally-relevant signaling pathways (Demoulin and Essaghir, 2014) and FGFR2 (present in 31 of these GO Terms), that obtains multiple functions during organ development (Goetz and Mohammadi, 2013) including the brain. A comprehensive list of the commonly regulated genes and their grouping into GO Terms for biological processes can be found in Table A 18.

The DEX genes that differ between species, however, enrich in GO Terms for biological processes that were assembled into analogous

superordinate processes by expert judgment (Fig. 3). These GO terms in general reflect the neurodevelopmental processes that we study with the “Neurosphere Assay” on a functional level in vitro (Baumann et al., 2015; Moors et al., 2009) and were previously identified in the transcriptomes from developing brains in vivo (Matsuki et al., 2005). Despite the similar grouping of enriched GO terms in superordinate processes the question remains why the majority of DEX genes diverge between the species. There are three major reasons that might explain why DEX genes of human, mouse and rat NPC differ considerably over time despite qualitative similarities in GO Term clusters. The first explanation might lie in species differences in developmental timing, the second one in differences in molecular equipment and/or regulation of equivalent cells and the third one in different cell type compositions of brains from different species. It is highly likely that the results presented in this study are motivated by a mixture of all three arguments and we will now provide examples for each of them.

Timing of brain development is known to follow different temporal traits in diverse species (Rice and Barone, 2000; Semple et al., 2013; Workman et al., 2013). During human brain development, changes in the transcriptome are largest during the fetal period, i.e. 9 out of 10 genes are DEX between different developmental time points in vivo (samples taken every 2–5 post conceptual weeks (PCW) starting from PCW 4) and/or brain regions demonstrating high gene expression dynamics during pre- and early postnatal development (Kang et al., 2011). Rodent brain development underlies similar gene expression changes than ontogenesis of the human organ, yet at a more rapid pace (Chou et al., 2016; Gogolidou et al., 2013; Jaffe et al., 2014). In addition, neurodevelopmental processes that are guided by gene expression changes take place at species-specific speeds as exemplified by oligodendrogenesis, which takes 5 days in rodents, but 11–12 weeks in humans (Barateiro and Fernandes, 2014) leading to differences in oligodendrocyte-related gene expression between species also during NPC development in vitro when analyses are performed at the same time points (Baumann et al., 2015; Dach et al., 2017). Species- and cell type-specific developmental speed might also explain that human, and not rat NPC down-regulate proliferation-related genes between 3 and 5 DIV. Here, more experimental work with a higher time resolution is needed that scrutinizes proliferation of NPC and developing astrocytes in the in vitro systems. In the mouse, the situation might be different due to cell culture in FCS-containing medium as FCS strongly influences neural cells' proliferation and differentiation behavior in a concentration-dependent manner (Budhram-Mahadeo et al., 1994). FCS concentrations used in this study (1%) did not inhibit NPC differentiation. Taken all timing aspects together, it might not be surprising that gene expression profiles from identical cell types like here the primary NPC from different species gained from brains at corresponding time points (Workman et al., 2013; Fig. 1) display distinct transcriptomes in their undifferentiated state as well as during in vitro differentiation over time (Fig. 2f).

The second aspect underlying the observed species differences might be differences in molecular equipment and/or regulation of genes within cell types. A recent study revealed substantial cross-species differences between humans and mice with a dramatic shift of cortical layer-specific gene expression patterns between species indicating cross-species conservation and divergence of gene expression at anatomical and cell type levels (Zeng et al., 2012). One example from this study is *CALB2*, which is preferentially expressed in the ventricular zone/sub ventricular zone-originated interneurons and was found enriched in human compared to mouse brains (Zeng et al., 2012). Direct comparison of expression between species cannot be solely assessed by DEX genes, which describes expression changes between two time points and is a known issue when dealing with cross-species transcriptome comparisons (Lu et al., 2009). Therefore, we defined a gene as likely to be expressed (present) or likely to be not expressed (absent) based on criteria adapted from Kang et al. (2011; median log<sub>2</sub> intensity value in 0-day samples is  $\geq 6$  = present, otherwise absent). We are

aware of the technical limitations of absolute thresholds when using Affymetrix arrays intensity information, which is why the following comparisons can solely provide an indication that needs further experimental proof. With these combined methods we found that *CALB2* expression and regulation over time seems to be human NPC-specific in our data set (Fig. 2g and Table A. 19). In addition, *PDGFD* acting through *PDGFRB* regulates cell-cycle progression and progenitor cell expansion in human, but not mouse, cortex (Lui et al., 2014). This instance is also reflected in our species-overarching in vitro methods with *PDGFD* seeming to reach the “present” threshold in hNPC, but not in mouse correlates (Fig. 2g and Table A. 19). Surprisingly we observed rNPC to be similar to hNPC with regard to this marker, but to the best of our knowledge, there is no literature available to compare our findings with. Concerning genes expressed during neuro-, astroglial- and oligodendrogenesis, we also found similarities and differences in gene abundance across species. The human astrocyte-specific gene *LRR3B*, for example, seems to be exclusively present and regulated in human compared to rodent cultures, while the astrocyte maturation markers *SPARCL1*, *GFAP* and *S100b* seem to be present in NPC from all three species (Zhang et al., 2016); Fig. 2g and Table A. 19. These examples support our second notion that some of the transcriptome differences that we observe between human, mouse and rat neurospheres might be due to qualitative species-specificities.

The third explanation for the large species differences in DEX genes identified in our study might root in a different cell type composition of human compared to rodent brains. One striking macroscopic distinction of human from rodent brains is the brain surface. While human brains are gyrencephalic, rodent brains contain no gyri and sulci and are thus lissencephalic. Gyrencephaly is a result of cellular expansion of a special type of progenitor cell, the basal progenitor (BP) or outer radial glia (oRG) cell in the human enlarged outer subventricular zone (OSVZ) of the developing cortex (Borrell and Götz, 2014; Lui et al., 2011; Pollen et al., 2015; Silbereis et al., 2016; Thomsen et al., 2015). This cell type is thought to be specific for human brains and can thus be identified by human-specific molecular markers. One of these markers is the recently identified oRG cell marker *FAM107A* (synonym for *DRR1*; Lui et al., 2014; Pollen et al., 2015; Thomsen et al., 2015), which we found to be expressed in human and absent in mouse NPC, supporting the previously published data. However, we also found this marker to be present and highly regulated in rat NPC (Fig. 2g and Table A. 19). One reason for the absence of expression and regulation of *FAM107A* in developing mouse and the expression and regulation in developing rat NPC could be the neuronal expression in mouse E10.5–16.5 and rat E18.5 brains (Asano et al., 2010). While neuronal *fam107a* expression is restricted to an early embryonic timeframe and the NPC used in this study are generated from PND1 brains, mNPC do not show any expression of this gene. In rat, neuronal *fam107a* expression starts on E18.5 in vivo suggesting that our observed gene presence in developing rat NPC is due to neuronal and not radial glia cell expression, which needs further experimental confirmation. These data indicate, that a combination of developmental timing and cell type-specific expression might drive gene abundance in such mixed cell type systems.

In contrast to the oRG, ventricular zone RG (vRG) are supposedly more similar across species (Dehay and Kennedy, 2007). This seems to be reflected on the molecular level within this study as the vRG-specific *CRYAB* and *ANXA1* gene products (Thomsen et al., 2015) seem to be present in NPC of all three species (Fig. 2g and Table A. 19). Intermediate progenitor cells (IPC), however, likely seem to be absent in the culture due to absence of the IPC marker *EOMES* (*TBR2*), despite *HES6* presence in mouse and human cells (Thomsen et al., 2015; Fig. 2g). *HES6*, however, seems to have additional, *NFκB*-dependent functions in migrating neurons during cortical development (Methot et al., 2013) suggesting that *HES6* expression in those neurospheres is likely due to expression in migrating neurons and thus independent of IPC. In addition, all NPC express *HES1*, *VIM*, *SLC1A3* (*GLAST*) and *NES* (Borrell and Reillo, 2012; Lui et al., 2011; Pollen et al., 2015) supporting the

concept that also a large variety of genes are expressed in a similar fashion across species (Zeng et al., 2012). However, the here discussed data also provides evidence that some of the transcriptional species differences observed in this study are based on different cell types, i.e. oRG cells in humans (Pollen et al., 2015; Thomsen et al., 2015), which seem to be well-reflected in the neurospheres in vitro systems.

Besides the GO term grouping by expert judgment, we analysed transcriptomes from each species across differentiation time using a GO term clustering in the Cytoscape plugin ClueGO (Bindea et al., 2009; Fig. 4). The plots – and here especially the human data - illustrate that the transcriptomes mirror the in vitro functions of the 3D models, i.e. NPC proliferation, migration, differentiation into neurons and glia cells as well as apoptosis over 5 days of differentiation (Fig. 4, Fig. B 2 + 3). Comparison of the plots of the three species reveals differences in their appearance (Fig. 4, Fig. B. 2 + 3). This is probably due to two reasons. For one, attributable to the approximate 90% differences of DEX genes between species (Fig. 2C), distinct GO terms were annotated from the data sets. Secondly, existing GO term annotations for humans, mice and rats differ in quality and quantity due to the different background information available for each species (Rhee et al., 2008). As an example, the biological process “cell signaling” is defined by four times more GO terms in mouse than in human NPC-derived transcriptomes (Fig. 2). This is probably owing to the large amount of existing signaling data generated in mice compared to humans including data from the many transgenic mice that dominate biomedical research (Ormandy et al., 2009). Despite several limitations, this kind of GO analysis is still useful to point out major differences in regulated genes and the processes behind them as done in this manuscript.

For a pathway-to-function validation and species comparison we picked the three key regulators *BMP2*, *EGFR* and *NOTCH* that were computationally predicted to be involved in NPC migration, neuro- and gliogenesis in hNPC (Table 2). The data of the consequences of *BMP2*, *NOTCH* and *EGFR* pathway modulation are shown in Fig. 6.

The transforming growth factor- $\beta$  (TGF- $\beta$ ) superfamily member *BMP2* signals through BMP receptors (BMPR) Type 1 (BMPR1a/Alk3 and BMPR1b/Alk6) or Type 2 (BMPR2; Bond et al., 2012). According to the human and rodent transcriptomes, with the exception of *bmpr1b* in rat NPC, these *BMPR* are present in proliferating and differentiating cultures (Table A. 19). In contrast to the in silico prediction (Fig. 5a-c), *BMP2* only acts on glia-related endpoints in human NPC by reducing oligodendrocyte differentiation (Fig. 6c) and accelerating astroglial maturation (Fig. 6j+k). In addition to reduction of oligodendrocytes, *BMP2* induces migration and reduces neuronal differentiation of rat and induces neurogenesis in mouse NPC (Fig. 6a-c), yet *BMP2* was not predicted as a modulator of any of these endpoints in the rodent cultures (Table A. 21–24). Discrepancies of computational prediction based on GO terms and actual experimental data when using relevant cell systems might be built on the data behind GO annotations. Such data underlying GO terms are retrieved from different tissues, cell models, in vitro and in vivo analyses, species, and, in case of development, distinct developmental timing (Rhee et al., 2008). For example, in our data set gene expression of *ID1* (inhibitor of DNA binding/differentiation) strongly increases during differentiation in hNPC (9-fold at Ovs3 days). Because *BMP2* is a known transcriptional inducer of *ID1* (Katagiri et al., 2002) and both of them are annotated to the GO term cell migration (Table A. 1), this annotation contributed to the computational identification of *BMP2* as a hub gene for cell migration. Searching for the data behind this annotation, the information on *ID1* and migration is a ‘traceable author statement’ based on observations in endothelial cells (Goumans et al., 2003) and is not related to migration in the developing brain. The information that *BMP2* is related to migration is inferred from sequence or structural similarity of homolog or ortholog genes, which is a hypothesis that has no experimental proof. Consequently, data sets behind GO terms need improvement with regards to specificity of cells, tissues, species and, if applicable, developmental timing. Nevertheless, we demonstrated that *BMP2* effects on

rodent NPC are similar than previously published and showed the new information that *BMP2* induces rat NPC migration. *BMP2* induces E13.5 (mouse) and E16 (rat) NPC differentiation into  $\beta$ III-tubulin+ neurons (Liu et al., 2013; Mabie et al., 1997; Mehler et al., 2000) or reduces this process in mouse E17 NPC (Gross et al., 1996) and mouse embryonic stem cells (Gossrau et al., 2007), yet in all systems *BMP2* impedes oligodendrogenesis and in all but the mouse E13.5 *BMP2* promotes astroglial fate (summarized in Table A. 25). Thus, our data reproduces the fact that *BMP2* reduces oligodendrogenesis in rodents and adds so far unknown information that similar to *BMP7* (Baumann et al., 2015), *BMP2* reduces oligodendrocyte differentiation and induces astrocyte maturation of human NPC. The differences in the published as well as in our own data concerning *BMP2* effects on rodent neuronal differentiation (Table A. 25, Fig. 6b) are difficult to explain, but might be due to preparation and/or cultivation of cells in presence or absence of FCS (Brunner et al., 2010), brain region, origin of cells, plating in spheres or as single cells, co-treatment of *BMP2* with or without FGF2, developmental age or species.

For mammalian NOTCH signaling, a phylogenetic very well conserved signaling pathway, activation of the transmembrane NOTCH receptors 1–4 by an extracellular ligand is crucial (Imayoshi and Kageyama, 2011). According to the transcriptome data from this study, human NPC express *NOTCH1–3*, mouse NPC all four *notch* isoforms and rat NPC also *notch1–3* and all three species display expression of different isoforms of the *NOTCH* ligands *DELTA-LIKE* (*DLL*) and/or *JAGGED* (*JAG*; Table A. 19). In contrast to the in silico prediction that *NOTCH* is guiding NPC migration, neuronal and glia differentiation (Fig. 5a-c), inhibition of NOTCH signaling by the NOTCH receptor inhibitor DAPT only induces neuronal and inhibits oligodendrocyte differentiation of human NPC, while it does not affect their migration (Fig. 6d-f). Although not computationally predicted as a modulator for rodent neurodevelopmental processes in our data set, DAPT reduces mouse NPC migration and induces mouse NPC oligodendrocyte formation (Fig. 6d+f), while rat NPC were not affected by NOTCH inhibition in vitro. Effects on mNPC and neuronal differentiation in hNPC were only seen at high DAPT concentrations. However, while for monolayer cultures 1  $\mu$ M of DAPT showed maximum effects (Dovey et al., 2001), sensitivity towards signaling inhibitors using secondary 3D structures might be different (Alépée et al., 2014). Additionally, the specificity for Notch inhibition was shown by qRT-PCR experiments showing the expected down-regulation of *HES1* and up-regulation of the pro-neuronal gene *ASCL* after 2.5 and 5  $\mu$ M DAPT treatment (Fig. B. 7) that was not seen at the lower concentrations (data not shown). Activation of NOTCH signaling in neural stem cells (NSCs) has been implicated in inhibition of neuronal differentiation and terminal differentiation into the astrocyte lineage (Zhang et al., 2017) in several cell types and species including drosophila, early xenopus embryos, the developing chick retina, rat retinal progenitors and the developing mouse brain (Koch et al., 2013). Hence, the results obtained in the human neurospheres match the published data from other species, i.e. pharmacological inhibition of NOTCH with DAPT increases neuronal differentiation and inhibits oligodendrogenesis (Egawa et al., 2017; Nicolay et al., 2007; Zhang et al., 2017). Why mouse NPC acted in an opposite way than human NPC towards NOTCH inhibition could have several reasons. For one, in contrast to human and rat NPC, mNPC differentiation cultures contain FCS, which might be responsible for the different effects of DAPT on mouse compared to human NPC development (Brunner et al., 2010). Moreover, NOTCH favours the fate specification of oligodendrocytes and astrocytes in stages were cells are not yet committed to neuronal or glial fate, yet it inhibits the subsequent specification to O4<sup>+</sup> cells in favour of GFAP<sup>+</sup> cells (Grandbarbe et al., 2003; Park and Appel, 2003). Possible differences in developmental timing between human and mouse NPC culture might therefore provide an explanation for the different DAPT effects in human and mouse NPC. We also observed an increase in apoptotic O4<sup>+</sup> cells in the DAPT treated mouse cultures. This has previously been observed in vivo,



where transgenic mice with an inactive Notch1 receptor show premature oligodendrocyte differentiation at E17.5 which are eliminated by apoptotic cell death before full differentiation (Genoud et al., 2002). In addition it is striking, that rat NPC are not affected by NOTCH inhibition at all. This might be due to the low expression of NOTCH signaling pathway molecules (Table A. 19) keeping this pathway inactive in the neurosphere culture.

Epidermal Growth Factor (EGF)-dependent signaling regulates NSC proliferation, migration, and differentiation into neurons and glia cells during development (Ayuso-Sacido et al., 2010; Kuhn et al., 1997; Palazuelos et al., 2014; Sun et al., 2005a). Thereby, EGF exerts its action through the EGF-receptor (EGFR; Ayuso-Sacido et al., 2010; Palazuelos et al., 2014). The *EGFR* is expressed in NPC of the three species studied (Table A. 19). Investigating the effects of EGFR inhibition by PD153035 in absence of externally provided EGF gives insight into auto- or paracrine functions of endogenously produced EGFR ligands. Such ligands, like HB-EGF and TNF $\alpha$ , are generated through enzymatic cleavage by ADAM17/TACE (tumor necrosis factor $\alpha$  converting enzyme), e.g. guaranteeing survival, proliferation and development of cells of the oligodendrocyte lineage during development in an EGFR-dependent manner in mice (Palazuelos et al., 2014). The concentration of the EGFR inhibitor PD153035 selected in this study (up to 10  $\mu$ M) seems high, yet different cell types display different IC50 concentrations of this EGFR inhibitor (Bos et al., 1997; Fry et al., 1994; Hsu et al., 2005). In our previous work we show that a different EGFR inhibitor, AG1478, inhibits migration and ERK1/2 phosphorylation at 1  $\mu$ M (Moors et al., 2007). AG1478 and PD153035 seem equally potent in a mouse epidermal JB6 cell line (Chen et al., 2001) suggesting that effects at 10  $\mu$ M concentrations observed in this study might be due to effects of PD153035 on other cellular signaling molecules. However, specificity of small signaling pathway modulators is an on-going debate as others do find specific effects of EGFR inhibitors on e.g. EGFR-expressing cancer cells at low micro molar concentrations only when cells expressed EGFR similar to non-cancer cells (Cole et al., 2005). Therefore, these data has to be interpreted with caution. Inhibition of the human NPC EGFR produced results as expected from the in silico prediction and the scientific literature, i.e. reduced NPC migration (Moors et al., 2007) and oligodendrocyte differentiation as well as induced neuronal differentiation (Ostenfeld and Svendsen, 2004; Fig. 6g-i) showing that hNPC recapitulate physiological EGFR functions in vitro. Again, *egfr* was not identified as a hub gene in rodent NPC. Yet, as expected from the literature, PD153035 increased neuronal differentiation of rat NPC (Burrows et al., 1997), while mouse NPC responded with an inhibition of neurogenesis (Fig. 6h). This discrepancy in mNPC concerning the published literature (Ayuso-Sacido et al., 2010) is possibly be due to the usage of FCS during differentiation in this study, while the C17.2 cells used by Ayuso-Sacido et al. (2010) were differentiated in absence of FCS. Studying the effects of PD153035 on human NPC differentiation in presence of FCS substantiated this hypothesis: similar to mNPC, the EGFR inhibitor reduced hNPC neuronal differentiation in presence of FCS (Fig. B. 5m). Thus, FCS can convert cells' responses to pathway modulators implying that one has to be cautious when using FCS in cell culture medium for pathway analyses and check for human and/or in vivo relevance of data. Other than in human NPC, we did not observe inhibition of migration of rodent NPC in our study. This might be due to dissimilar EGF responses of the different glia types or maturation stages of glia in the differentiating NPC cultures of the three species (Fig. 2g; Baumann et al., 2015). Maturation and cell type-specific EGF responses due to asymmetric EGFR distribution as a mechanism for shaping brain regions or cell type diversity within brain regions was reported earlier (Sun et al., 2005b). Also in contrast to human NPC and expected from the published literature (Gonzalez-Perez et al., 2009; Hu et al., 2004; Palazuelos et al., 2014), rodent NPC oligodendrocyte differentiation is not modified by inhibition of EGFR signaling in the neurosphere cultures. Possible explanations for these discrepancies might be developmental timing and

or brain region, as rat PND0–1 hippocampal NSC's differentiation to oligodendrocytes is EGF responsive, while neuronal differentiation is not (Hu et al., 2004), which is opposite in the study presented here. Another explanation could be changing EGFR levels with developmental age (Boockvar et al., 2003) in a cell type-specific manner over time (Sun et al., 2005b). It might be suggested that faster maturation of rodent NPC in comparison to human NPC determines responses to EGF.

Taken together, our transcriptome-based data demonstrates that primary NPC from different species differ in their molecular equipment despite similar cellular functions, i.e. NPC migration, neuronal and glia differentiation. Functional pathway validation due to pharmacological modulation of pathways identified via transcriptome analyses also identified species variations. Although more species-specific functional analyses of neurodevelopmental pathways need elucidation to gain a more complete picture of the human-specific NPC connectome, this work already strongly supports the concept of human cell-based in vitro analyses for neurodevelopmental toxicity or efficacy testing. Understanding such molecular pathways underlying cellular functions in in vitro systems is fundamental for understanding the assay's application domain. In addition, comprehension of similarities and differences of pathway functions between species is of high importance for pharmacology and toxicology because a high percentage of drugs fails when translating efficacy or safety from animals to humans (Waring et al., 2015).

## Funding

This work was supported by the German Ministry of Education and Research (BMBF) [grant number 16V0899].

## Appendix A. Supplementary data

Supplementary data to this article can be found online at <https://doi.org/10.1016/j.taap.2018.05.009>.

## References

- Abranches, E., Silva, M., Pradier, L., Schulz, H., Hummel, O., Henrique, D., Bekman, E., 2009. Neural differentiation of embryonic stem cells in vitro: a road map to neurogenesis in the embryo. *PLoS One* 4, e6286. <http://dx.doi.org/10.1371/journal.pone.0006286>.
- Alépée, N., Bahinski, A., Daneshian, M., De Wever, B., Fritsche, E., Goldberg, A., Hansmann, J., Hartung, T., Haycock, J., Hogberg, H., Hoelting, L., Kelm, J.M., Kadereit, S., McVey, E., Landsiedel, R., Leist, M., Lübbert, M., Noor, F., Pellevoisin, C., Petersohn, D., Pfannenbecker, U., Reisinger, K., Ramirez, T., Rothen-Rutishauser, B., Schäfer-Korting, M., Zeilinger, K., Zurich, M.-G., 2014. State-of-the-art of 3D cultures (organs-on-a-chip) in safety testing and pathophysiology. *ALTEX* 31, 441–477. <http://dx.doi.org/10.14573/altex1406111>.
- Arrowsmith, J., Miller, P., 2013. Trial watch: phase II and phase III attrition rates 2011–2012. *Nat. Rev. Drug Discov.* 12, 569. <http://dx.doi.org/10.1038/nrd4090>.
- Asano, Y., Kishida, S., Mu, P., Sakamoto, K., Murohara, T., Kadomatsu, K., 2010. DRR1 is expressed in the developing nervous system and downregulated during neuroblastoma carcinogenesis. *Biochem. Biophys. Res. Commun.* 394, 829–835. <http://dx.doi.org/10.1016/j.bbrc.2010.03.085>.
- Attarwala, H., 2010. TGN1412: from discovery to disaster. *J. Young Pharm.* 2, 332–336. <http://dx.doi.org/10.4103/0975-1483.66810>.
- Ayuso-Sacido, A., Moliterno, J.A., Kratovac, S., Kapoor, G.S., O'Rourke, D.M., Holland, E.C., Garcia-Verdugo, J.M., Roy, N.S., Boockvar, J.A., 2010. Activated EGFR signaling increases proliferation, survival, and migration and blocks neuronal differentiation in post-natal neural stem cells. *J. Neuro-Oncol.* 97, 323–337. <http://dx.doi.org/10.1007/s11060-009-0035-x>.
- Bal-Price, A., Crofton, K.M., Leist, M., Allen, S., Arand, M., Buetler, T., Delrue, N., FitzGerald, R.E., Hartung, T., Heinonen, T., Hogberg, H., Bennekou, S.H., Lichtensteiger, W., Oggier, D., Paparella, M., Axelstad, M., Piersma, A., Rached, E., Schilter, B., Schmuck, G., Stoppini, L., Tongiorgi, E., Tiramani, M., Monnet-Tschudi, F., Wilks, M.F., Ylikomi, T., Fritsche, E., 2015. International STakeholder NETwork (ISTNET): creating a developmental neurotoxicity (DNT) testing road map for regulatory purposes. *Arch. Toxicol.* 89, 269–287. <http://dx.doi.org/10.1007/s00204-015-1464-2>.
- Bal-Price, A., Hogberg, H.T., Crofton, K.M., Daneshian, M., FitzGerald, R.E., Fritsche, E., Heinonen, T., Hougaard Bennekou, S., Klima, S., Piersma, A.H., Sachana, M., Shafer, T.J., Terron, A., Monnet-Tschudi, F., Viviani, B., Waldmann, T., Westerink, R.H.S., Wilks, M.F., Witters, H., Zurich, M.-G., Leist, M., 2018. Recommendation on test readiness criteria for new approach methods in toxicology: Exemplified for



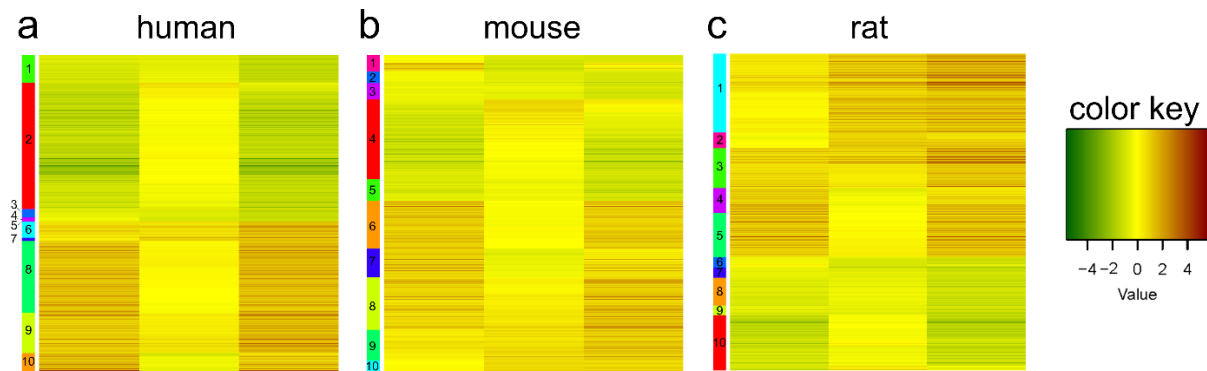
- developmental neurotoxicity. *ALTEX*. <http://dx.doi.org/10.14573/altex.1712081>.
- Barateiro, A., Fernandes, A., 2014. Temporal oligodendrocyte lineage progression: in vitro models of proliferation, differentiation and myelination. *Biochim. Biophys. Acta* 1843, 1917–1929. <http://dx.doi.org/10.1016/j.bbamcr.2014.04.018>.
- Barenys, M., Gassmann, K., Baksmeier, C., Heinz, S., Reverte, I., Schmuck, M., Temme, T., Bendt, F., Zschauer, T.C., Rockel, T.D., Unfried, K., Watjen, W., Sundaram, S.M., Heuer, H., Colomina, M.T., Fritsche, E., 2016. Epigallocatechin gallate (EGCG) inhibits adhesion and migration of neural progenitor cells in vitro. *Arch. Toxicol.* <http://dx.doi.org/10.1007/s00204-016-1709-8>.
- Baumann, J., Barenys, M., Gassmann, K., Fritsche, E., 2014. Comparative human and rat “neurosphere assay” for developmental neurotoxicity testing. *Curr. Protoc. Toxicol.* 1, 1–24. <http://dx.doi.org/10.1002/0471140856.tx1221s59>.
- Baumann, J., Dach, K., Barenys, M., Giersiefer, S., Goniwiecha, J., Lein, P.J., Fritsche, E., 2015. Application of the Neurosphere assay for DNT hazard assessment: challenges and limitations. *Methods Pharmacol. Toxicol.* 1–29. <http://dx.doi.org/10.1007/7653>.
- Bindea, G., Mlecnik, B., Hackl, H., Charoentong, P., Tosolini, M., Kirilovsky, A., Fridman, W.-H., Pagès, F., Trajanoski, Z., Galon, J., 2009. ClueGO: a Cytoscape plug-in to decipher functionally grouped gene ontology and pathway annotation networks. *Bioinformatics* 25, 1091–1093.
- Bindea, G., Galon, J., Mlecnik, B., 2013. CluePedia Cytoscape plugin: pathway insights using integrated experimental and in silico data. *Bioinformatics* 29, 661–663. <http://dx.doi.org/10.1093/bioinformatics/btt019>.
- Boland, M.J., Nazor, K.L., Tran, H.T., Szücs, A., Lynch, C.L., Paredes, R., Tassone, F., Sanna, P.P., Hagerman, R.J., Loring, J.F., 2017. Molecular analyses of neurogenic defects in a human pluripotent stem cell model of fragile X syndrome. *Brain* 140, 582–598. <http://dx.doi.org/10.1093/brain/aww357>.
- Bond, A.M., Bhalala, O.G., Kessler, J.A., 2012. The dynamic role of bone morphogenetic proteins in neural stem cell fate and maturation. *Dev. Neurobiol.* 72, 1068–1084. <http://dx.doi.org/10.1002/dneu.22022>.
- Bookvar, J.A., Kapitonov, D., Kapoor, G., Schouten, J., Counelis, G.J., Bogler, O., Snyder, E.Y., McIntosh, T.K., O'Rourke, D.M., 2003. Constitutive EGFR signaling confers a motile phenotype to neural stem cells. *Mol. Cell. Neurosci.* 24, 1116–1130.
- Borrell, V., Götz, M., 2014. Role of radial glial cells in cerebral cortex folding. *Curr. Opin. Neurobiol.* 27, 39–46. <http://dx.doi.org/10.1016/j.conb.2014.02.007>.
- Borrell, V., Reillo, I., 2012. Emerging roles of neural stem cells in cerebral cortex development and evolution. *Dev. Neurobiol.* 72, 955–971. <http://dx.doi.org/10.1002/dneu.22013>.
- Bos, M., Mendelsohn, J., Kim, Y.M., Albanell, J., Fry, D.W., Baselga, J., 1997. PD153035, a tyrosine kinase inhibitor, prevents epidermal growth factor receptor activation and inhibits growth of cancer cells in a receptor number-dependent manner. *Clin. Cancer Res.* 3, 2099–2106.
- Brunner, D., Appl, H., Pfaller, W., Gstraunthaler, G., 2010. Serum-free cell culture: the serum-free media interactive online database. *ALTEX* 27, 53–62.
- Budhram-Mahadeo, V., Lillycrop, K.A., Latchman, D.S., 1994. Cell cycle arrest and morphological differentiation can occur in the absence of apoptosis in a neuronal cell line. *Neurosci. Lett.* 165, 18–22.
- Burrows, R.C., Wancio, D., Levitt, P., Lillien, L., 1997. Response diversity and the timing of progenitor cell maturation are regulated by developmental changes in EGFR expression in the cortex. *Neuron* 19, 251–267.
- Carvalho, B.S., Irizarry, R.A., 2010. A framework for oligonucleotide microarray preprocessing. *Bioinformatics* 26, 2363–2367. <http://dx.doi.org/10.1093/bioinformatics/btq431>.
- Chen, N., Ma, W.Y., She, Q.B., Wu, E., Liu, G., Bode, A.M., Dong, Z., 2001. Transactivation of the epidermal growth factor receptor is involved in 12-O-tetradecanoylphorbol-13-acetate-induced signal transduction. *J. Biol. Chem.* 276, 46722–46728. <http://dx.doi.org/10.1074/jbc.M107156200>.
- Chou, S.-J., Wang, C., Sintupisut, N., Niou, Z.-X., Lin, C.-H., Li, K.-C., Yeang, C.-H., 2016. Analysis of spatial-temporal gene expression patterns reveals dynamics and regionalization in developing mouse brain. *Sci. Rep.* 6 (19274). <http://dx.doi.org/10.1038/srep19274>.
- Cole, G.W.J., Alleva, A.M., Reddy, R.M., Maxhimer, J.B., Zuo, J., Schrupp, D.S., Nguyen, D.M., 2005. The selective epidermal growth factor receptor tyrosine kinase inhibitor PD153035 suppresses expression of prometastasis phenotypes in malignant pleural mesothelioma cells in vitro. *J. Thorac. Cardiovasc. Surg.* 129, 1010–1017.
- Collins, F.S., Gray, G.M., Bucher, J.R., 2008. TOXICOLOGY: transforming environmental health protection. *Science* (80-) 319, 906–907. <http://dx.doi.org/10.1126/science.1154619>.
- Dach, K., Bendt, F., Huebenthal, U., Giersiefer, S., Lein, P.J., Heuer, H., Fritsche, E., 2017. BDE-99 impairs differentiation of human and mouse NPCs into the oligodendroglial lineage by species-specific modes of action. *Sci. Rep.* 7, 44861. <http://dx.doi.org/10.1038/srep44861>.
- De Keyser, J., Sulter, G., Luiten, P.G., 1999. Clinical trials with neuroprotective drugs in acute ischaemic stroke: are we doing the right thing? *Trends Neurosci.* 22, 535–540.
- Dehay, C., Kennedy, H., 2007. Cell-cycle control and cortical development. *Nat. Rev. Neurosci.* 8, 438–450. <http://dx.doi.org/10.1038/nrn2097>.
- Dehay, C., Kennedy, H., 2009. Transcriptional regulation and alternative splicing make for better brains. *Neuron*. <http://dx.doi.org/10.1016/j.neuron.2009.05.006>.
- Demoulin, J.-B., Essaghir, A., 2014. PDGF receptor signaling networks in normal and cancer cells. *Cytokine Growth Factor Rev.* 25, 273–283. <http://dx.doi.org/10.1016/j.cytogr.2014.03.003>.
- Dirnagl, U., Fisher, M., 2012. International, multicenter randomized preclinical trials in translational stroke research: It's time to act. *J. Cereb. Blood Flow Metab.* 32, 933–935. <http://dx.doi.org/10.1038/jcbfm.2012.51>.
- Durinck, S., Moreau, Y., Kasprzyk, A., Davis, S., De Moor, B., Brazza, A., Huber, W., 2005. BioMart and Bioconductor: a powerful link between biological databases and microarray data analysis. *Bioinformatics* 21, 3439–3440. <http://dx.doi.org/10.1093/bioinformatics/bti525>.
- Agawa, N., Shindo, A., Liang, A.C., Du, Y., Xing, C., Lo, E.K., Itoh, K., Kinoshita, H., Maki, T., Takahashi, R., Sudo, R., Spector, M., Lok, J., Arai, K., 2017. A novel three-dimensional culture system for oligodendrocyte precursor cells. *Stem Cells Dev.* 26, 1078–1085. <http://dx.doi.org/10.1089/scd.2016.0306>.
- Fisher, R.A., 1992. *Statistical Methods for Research Workers*. pp. 66–70. [http://dx.doi.org/10.1007/978-1-4612-4380-9\\_6](http://dx.doi.org/10.1007/978-1-4612-4380-9_6).
- Fritsche, E., 2016. Report on Integrated Testing Strategies for the Identification and Evaluation of Chemical Hazards Associated with the Developmental Neurotoxicity (DNT), to Facilitate Discussions at the Joint EFSA/OECD Workshop on DNT.
- Fritsche, E., Crofton, K.M., Hernandez, A.F., Hougaard Bennekou, S., Leist, M., Bal-Price, A., Reaves, E., Wilks, M.F., Terron, A., Solecki, R., Gourmelon, A., 2017. OECD/EFSA workshop on developmental neurotoxicity (DNT): the use of non-animal test methods for regulatory purposes. *ALTEX* 34, 311–315. <http://dx.doi.org/10.14573/altex.1701171>.
- Fry, D.W., Kraker, A.J., McMichael, A., Ambrosio, L.A., Nelson, J.M., Leopold, W.R., Connors, R.W., Bridges, A.J., 1994. A specific inhibitor of the epidermal growth factor receptor tyrosine kinase. *Science* 265, 1093–1095.
- Gassmann, K., Abel, J., Bothe, H., Haarmann-Stemmann, T., Merk, H.F., Quasthoff, K.N., Rockel, T.D., Schreiber, T., Fritsche, E., 2010. Species-specific differential ahr expression protects human neural progenitor cells against developmental neurotoxicity of PAHs. *Environ. Health Perspect.* 118, 1571–1577. <http://dx.doi.org/10.1289/ehp.0901545>.
- Gassmann, K., Baumann, J., Giersiefer, S., Schuwald, J., Schreiber, T., Merk, H.F., Fritsche, E., 2012. Automated neurosphere sorting and plating by the COPAS large particle sorter is a suitable method for high-throughput 3D in vitro applications. *Toxicol. Vitro* 26, 993–1000. <http://dx.doi.org/10.1016/j.tiv.2012.04.025>.
- Gautier, L., Cope, L., Bolstad, B.M., Irizarry, R.A., 2004. Affy - analysis of Affymetrix GeneChip data at the probe level. *Bioinformatics* 20, 307–315. <http://dx.doi.org/10.1093/bioinformatics/btg405>.
- Genoud, S., Lappe-Siefke, C., Goebels, S., Radtke, F., Aguet, M., Scherer, S.S., Suter, U., Nave, K.-A., Mantei, N., 2002. Notch1 control of oligodendrocyte differentiation in the spinal cord. *J. Cell Biol.* 158.
- Goetz, R., Mohammadi, M., 2013. Exploring mechanisms of FGF signalling through the lens of structural biology. *Nat. Rev. Mol. Cell Biol.* 14, 166–180. <http://dx.doi.org/10.1038/nrm3528>.
- Goggolidou, P., Soneji, S., Powles-Glover, N., Williams, D., Sethi, S., Baban, D., Simon, M.M., Ragoussis, I., Norris, D.P., 2013. A chronological expression profile of gene activity during embryonic mouse brain development. *Mamm. Genome* 24, 459–472. <http://dx.doi.org/10.1007/s00335-013-9486-7>.
- Gold, L.S., Manley, N.B., Slone, T.H., Rohrbach, L., Garfinkel, G.B., 2005. Supplement to the carcinogenic potency database (CPDB): results of animal bioassays published in the general literature through 1997 and by the National Toxicology Program in 1997–1998. *Toxicol. Sci.* 85, 747–808. <http://dx.doi.org/10.1093/toxsci/kfi161>.
- Gonzalez-Perez, O., Romero-Rodriguez, R., Soriano-Navarro, M., Garcia-Verdugo, J.M., Alvarez-Buylla, A., 2009. Epidermal growth factor induces the progeny of subventricular zone type B cells to migrate and differentiate into oligodendrocytes. *Stem Cells* 27, 2032–2043. <http://dx.doi.org/10.1002/stem.119>.
- Gossrau, G., Thiele, J., Konang, R., Schmandt, T., Brüstle, O., 2007. Bone morphogenetic protein-mediated modulation of lineage diversification during neural differentiation of embryonic stem cells. *Stem Cells* 25, 939–949. <http://dx.doi.org/10.1634/stemcells.2006-0299>.
- Goumans, M.-J., Lebrin, F., Valdimarsdottir, G., 2003. Controlling the angiogenic switch: a balance between two distinct TGF- $\beta$  receptor signaling pathways. *Trends Cardiovasc. Med.* 13 (7), 301.
- Grandbarbe, L., Bouissac, J., Rand, M., Hrabé de Angelis, M., Artavanis-Tsakonas, S., Mohier, E., 2003. Delta-Notch signaling controls the generation of neurons/glia from neural stem cells in a stepwise process. *Development* 130, 1391–1402.
- Gross, R.E., Mehler, M.F., Mabie, P.C., Zang, Z., Santschi, L., Kessler, J.A., 1996. Bone morphogenetic proteins promote astroglial lineage commitment by mammalian subventricular zone progenitor cells. *Neuron* 17, 595–606.
- Hartung, T., 2009. Toxicology for the twenty-first century. *Nature* 460, 208–212. <http://dx.doi.org/10.1038/460208a>.
- Hsu, C.-H., Gao, M., Chen, C.-L., Yeh, P.-Y., Cheng, A.-L., 2005. Inhibitors of epidermal growth factor receptor suppress cell growth and enhance chemosensitivity of nasopharyngeal Cancer cells in vitro. *Oncology* 68, 538–547. <http://dx.doi.org/10.1159/000086998>.
- Hu, X., Jin, L., Feng, L., 2004. Erk1/2 but not PI3K pathway is required for neurotrophin 3-induced oligodendrocyte differentiation of post-natal neural stem cells. *J. Neurochem.* 90, 1339–1347. <http://dx.doi.org/10.1111/j.1471-4159.2004.02594.x>.
- Hydbring, P., Castell, A., Larsson, L.-G., 2017. MYC modulation around the CDK2/p27/SKP2 Axis. *Genes (Basel)* 8. <http://dx.doi.org/10.3390/genes8070174>.
- Imayoshi, I., Kageyama, R., 2011. The role of notch signaling in adult neurogenesis. *Mol. Neurobiol.* 44, 7–12. <http://dx.doi.org/10.1007/s12035-011-8186-0>.
- Jaffe, A.E., Shin, J., Collado-Torres, L., Leek, J.T., Tao, R., Li, C., Gao, Y., Jia, Y., Maher, B.J., Hyde, T.M., Kleinman, J.E., Weinberger, D.R., 2014. Developmental regulation of human cortex transcription and its clinical relevance at single base resolution. *Nat. Neurosci.* 18, 154–161. <http://dx.doi.org/10.1038/nn.3898>.
- Jenkins, L., Harries, N., Lappin, J.E.J.E., MacKenzie, A.E.a.E., Neetoo-Isselee, Z., Southern, C., McIver, E.G.E.G., Nicklin, S.A.S.a., Taylor, D.L.D.L., Milligan, G., 2012. Antagonists of GPR35 display high species ortholog selectivity and varying modes of action. *J. Pharmacol. Exp. Ther.* 343, 1–3. <http://dx.doi.org/10.1124/jpet.112.198945>.
- Judson, R., Kavlock, R., Martin, M., Reif, D., Houck, K., Knudsen, T., Richard, A., Tice, R.R., Whelan, M., Xia, M., Huang, R., Austin, C., Daston, G., Hartung, T., Fowle, J.R.,

- Wooce, W., Tong, W., Dix, D., 2013. Perspectives on validation of high-throughput assays supporting 21st century toxicity testing. *ALTEX* 30, 51–56.
- Kang, H.J., Kawasawa, Y.I., Cheng, F., Zhu, Y., Xu, X., Li, M., Sousa, A.M.M., Pletikos, M., Meyer, K.A., Sedmak, G., 2011. Spatio-temporal transcriptome of the human brain. *Nature* 478, 483–489.
- Katagiri, T., Imada, M., Yanai, T., Suda, T., Takahashi, N., Kamijo, R., 2002. Identification of a BMP-responsive element in *Id1*, the gene for inhibition of myogenesis. *Genes Cells* 7, 949–960.
- Kilkenny, C., Browne, W., Cuthill, I., Emerson, M., Altman, D., 2010. Improving bioscience research reporting: the ARRIVE guidelines for reporting animal research. *J. Pharmacol. Pharmacother.* 1, 94. <http://dx.doi.org/10.4103/0976-500X.72351>.
- Knight, A., 2007. Animal experiments scrutinised: systematic reviews demonstrate poor human clinical and toxicological utility. *ALTEX* 24, 320–325.
- Koch, U., Lehal, R., Radtke, F., 2013. Stem cells living with a notch. *Development* 140, 689–704. <http://dx.doi.org/10.1242/dev.080614>.
- Krug, A.K., Kolde, R., Gaspar, J.A., Rempel, E., Balmer, N.V., Meganathan, K., Vojnits, K., Baquie, M., Waldmann, T., Ensenat-Waser, R., Jagtap, S., Evans, R.M., Julien, S., Peterson, H., Zagoura, D., Kadereit, S., Gerhard, D., Sotiriadou, I., Heke, M., Natarajan, K., Henry, M., Winkler, J., Marchan, R., Stoppini, L., Bosgra, S., Westerhout, J., Verwei, M., Vilo, J., Kortenkamp, A., Hescheler, J., Hothorn, L., Bremer, S., van Thriel, C., Krause, K.H., Hengstler, J.G., Rahnenfuhrer, J., Leist, M., Sachinidis, A., 2013. Human embryonic stem cell-derived test systems for developmental neurotoxicity: a transcriptomics approach. *Arch. Toxicol.* 87, 123–143. <http://dx.doi.org/10.1007/s00204-012-0967-3>.
- Kuegler, P.B., Zimmer, B., Waldmann, T., Baudis, B., Ilmjär, S., Hescheler, J., Gaughwin, P., Brundin, P., Mundt, W., Bal-Price, A.K., Schratzenholz, A., Krause, K.-H., van Thriel, C., Rao, M.S., Kadereit, S., Leist, M., 2010. Markers of murine embryonic and neural stem cells, neurons and astrocytes: reference points for developmental neurotoxicity testing. *ALTEX* 27, 17–42.
- Kuhn, H.G., Winkler, J., Kempermann, G., Thal, L.J., Gage, F.H., 1997. Epidermal growth factor and fibroblast growth factor-2 have different effects on neural progenitors in the adult rat brain. *J. Neurosci.* 17, 5820–5829.
- Leist, M., Hartung, T., 2013. Reprint: inflammatory findings on species extrapolations: humans are definitely no 70-kg mice. *ALTEX* 30, 227–230. <http://dx.doi.org/10.1007/s00204-013-1038-0>.
- Li, Y., Lin, B., Yang, L., 2015. Comparative transcriptomic analysis of multiple cardiovascular fates from embryonic stem cells predicts novel regulators in human Cardiogenesis. *Sci. Rep.* 5 (9758). <http://dx.doi.org/10.1038/srep09758>.
- Liu, H., Jia, D., Li, A., Chau, J., He, D., Ruan, X., Liu, F., Li, J., He, L., Li, B., 2013. p53 regulates neural stem cell proliferation and differentiation via BMP-Smad1 signaling and *Id1*. *Stem Cells Dev.* 22, 913–927. <http://dx.doi.org/10.1089/scd.2012.0370>.
- Lu, Y., Huggins, P., Bar-Joseph, Z., 2009. Cross species analysis of microarray expression data. *Bioinformatics* 25, 1476–1483. <http://dx.doi.org/10.1093/bioinformatics/btp247>.
- Lui, J.H., Hansen, D.V., Kriegstein, A.R., 2011. Development and evolution of the human neocortex. *Cell* 146, 18–36. <http://dx.doi.org/10.1016/j.cell.2011.06.030>.
- Lui, J.H., Nowakowski, T.J., Pollen, A.A., Javaherian, A., Kriegstein, A.R., Oldham, M.C., 2014. Radial glia require PDGFRβ-PDGFRβ signalling in human but not mouse neocortex. *Nature* 515, 264–268. <http://dx.doi.org/10.1038/nature13973>.
- Mabie, P.C., Mehler, M.F., Marmor, R., Papavasiliou, A., Song, Q., Kessler, J.A., 1997. Bone morphogenetic proteins induce astroglial differentiation of oligodendroglial-astroglial progenitor cells. *J. Neurosci.* 17, 4112–4120.
- Matsuki, T., Hori, G., Furuichi, T., 2005. Gene expression profiling during the embryonic development of mouse brain using an oligonucleotide-based microarray system. *Mol. Brain Res.* 136, 231–254. <http://dx.doi.org/10.1016/j.molbrainres.2005.02.008>.
- Meganathan, K., Jagtap, S., Wagh, V., Winkler, J., Gaspar, J.A., Hildebrand, D., Trusch, M., Lehmann, K., Hescheler, J., Schlueter, H., Sachinidis, A., 2012. Identification of thalidomide-specific transcriptomics and proteomics signatures during differentiation of human embryonic stem cells. *PLoS One* 7, e44228. <http://dx.doi.org/10.1371/journal.pone.0044228>.
- Mehler, M.F., Mabie, P.C., Zhu, G., Gokhan, S., Kessler, J.A., 2000. Developmental changes in progenitor cell responsiveness to bone morphogenetic proteins differentially modulate progressive CNS lineage fate. *Dev. Neurosci.* 22, 74–85. 17429.
- Method, L., Hermann, R., Tang, Y., Lo, R., Al-Jehani, H., Jhas, S., Svoboda, D., Slack, R.S., Barker, P.A., Stifani, S., 2013. Interaction and antagonistic roles of NF- $\beta$  and Hes6 in the regulation of cortical neurogenesis. *Mol. Cell. Biol.* 33, 2797–2808. <http://dx.doi.org/10.1128/MCB.01610-12>.
- Miller, M.T., Stromland, K., 1999. Teratogen update: thalidomide: a review, with a focus on ocular findings and new potential uses. *Teratology* 60, 306–321. [http://dx.doi.org/10.1002/\(SICI\)1096-9926\(199911\)60:5<306::AID-TERA11>3.0.CO;2-Y](http://dx.doi.org/10.1002/(SICI)1096-9926(199911)60:5<306::AID-TERA11>3.0.CO;2-Y).
- Moors, M., Cline, J.E., Abel, J., Fritsche, E., 2007. ERK-dependent and -independent pathways trigger human neural progenitor cell migration. *Toxicol. Appl. Pharmacol.* 221, 57–67. <http://dx.doi.org/10.1016/j.taap.2007.02.018>.
- Moors, M., Rockel, T.D., Abel, J., Cline, J.E., Gassmann, K., Schreiber, T., Shuwald, J., Weinmann, N., Fritsche, E., 2009. Human neurospheres as three-dimensional cellular systems for developmental neurotoxicity testing. *Environ. Health Perspect.* 117, 1131–1138. <http://dx.doi.org/10.1289/ehp.0800207>.
- National Academy of Sciences, 2007. Toxicity Testing in the 21st Century: A vision and a strategy. *Altoxicol. Natl. Academies Press, Washington, D.C.* <http://dx.doi.org/10.17226/11970>.
- Nicolay, D.J., Doucette, J.R., Nazari, A.J., 2007. Transcriptional control of oligodendrogenesis. *Glia* 55, 1287–1299.
- NRC, 2007. Toxicity Testing in the 21st Century: A Vision and a Strategy. The National Academies Press, Washington, DC. <http://dx.doi.org/10.17226/11970>.
- Oberheim, N.A., Takano, T., Han, X., He, W., Lin, J.H., Wang, F., Xu, Q., Wyatt, J.D., Pilcher, W., Ojemann, J.G., Ransom, B.R., Goldman, S.A., Nedergaard, M., 2009. Uniquely hominid features of adult human astrocytes. *J. Neurosci.* 29, 3276–3287. <http://dx.doi.org/10.1523/jneurosci.4707-08.2009>.
- Odawara, A., Saitoh, Y., Alhebshi, A.H., Gotoh, M., Suzuki, I., 2014. Long-term electrophysiological activity and pharmacological response of a human induced pluripotent stem cell-derived neuron and astrocyte co-culture. *Biochem. Biophys. Res. Commun.* 443, 1176–1181. <http://dx.doi.org/10.1016/j.bbrc.2013.12.142>.
- OECD, 2012. Test No. 443: extended one-generation reproductive toxicity study. In: OECD Guidelines for the Testing of Chemicals. OECD Publishing Section 4. <https://doi.org/10.1787/9789264185371-en>.
- Ohara, Y., Koganezawa, N., Yamazaki, H., Roppongi, R.T., Sato, K., Sekino, Y., Shirao, T., 2015. Early-stage development of human induced pluripotent stem cell-derived neurons. *J. Neurosci. Res.* 93, 1804–1813. <http://dx.doi.org/10.1002/jnr.23666>.
- Olson, H., Betton, G., Robinson, D., Thomas, K., Monro, A., Kolaja, G., Lilly, P., Sanders, J., Sipes, G., Bracken, W., Dorato, M., Van Deun, K., Smith, P., Berger, B., Heller, A., 2000. Concordance of the toxicity of pharmaceuticals in humans and in animals. *Regul. Toxicol. Pharmacol.* 32, 56–67. <http://dx.doi.org/10.1006/rtp.2000.1399>.
- Ormandy, E.H., Schuppli, C.A., Weary, D.M., 2009. Worldwide trends in the use of animals in research: the contribution of genetically-modified animal models. *Altern. Lab. Anim.* 37, 63–68.
- Ostenfeld, T., Svendsen, C.N., 2004. Requirement for neurogenesis to proceed through the division of neuronal progenitors following differentiation of epidermal growth factor and fibroblast growth factor-2-responsive human neural stem cells. *Stem Cells* 22, 798–811. <http://dx.doi.org/10.1634/stemcells.22-5-798>.
- Palazuelos, J., Crawford, H.C., Klingener, M., Sun, B., Karelis, J., Raines, E.W., Aguirre, A., 2014. TACE/ADAM17 is essential for oligodendrocyte development and CNS myelination. *J. Neurosci.* 34, 11884–11896. <http://dx.doi.org/10.1523/JNEUROSCI.1220-14.2014>.
- Park, H.-C., Appel, B., 2003. Delta-notch signaling regulates oligodendrocyte specification. *Development* 130, 3747–3755.
- Perel, P., Roberts, I., Sena, E., Wheble, P., Briscoe, C., Sandercock, P., Macleod, M., Mignini, L.E., Jayaram, P., Khan, K.S., 2007. Comparison of treatment effects between animal experiments and clinical trials: systematic review. *BMJ* 334, 197. <http://dx.doi.org/10.1136/bmj.39048.407928.BE>.
- Perreault, M., Feng, G., Will, S., Gareski, T., Kubasiak, D., Marquette, K., Vugmeyster, Y., Unger, T.J., Jones, J., Qadri, A., Hahm, S., Sun, Y., Rohde, C.M., Zwijnenberg, R., Paulsen, J., Gimeno, R.E., 2013. Activation of TrkB with TAM-163 results in opposite effects on body weight in rodents and non-human Primates. *PLoS One* 8. <http://dx.doi.org/10.1371/journal.pone.0062616>.
- Pollen, A.A., Nowakowski, T.J., Chen, J., Retallack, H., Sandoval-Espinosa, C., Nicholas, C.R., Shuga, J., Liu, S.J., Oldham, M.C., Diaz, A., Lim, D.A., Leyrat, A.A., West, J.A., Kriegstein, A.R., 2015. Molecular identity of human outer radial glia during cortical development. *Cell* 163, 55–67. <http://dx.doi.org/10.1016/j.cell.2015.09.004>.
- R Core Team, 2016. R: A Language and Environment for Statistical Computing. R Found. Stat. Comput. Vienna, Austria.
- Rhee, S.Y., Wood, V., Dolinski, K., Draghici, S., 2008. Use and misuse of the gene ontology annotations. *Nat. Rev. Genet.* 9, 509–515.
- Rice, D., Barone, S., 2000. Critical periods of vulnerability for the developing nervous system: evidence from humans and animal models. *Environ. Health Perspect.* 108 (Suppl. 3), 511–533. <http://dx.doi.org/10.1289/ehp.00108s3511>.
- Roggen, E.L., 2011. In vitro toxicity testing in the twenty-first century. *Front. Pharmacol.* 2 (3). <http://dx.doi.org/10.3389/fphar.2011.00003>.
- Schmuck, M.R., Temme, T., Dach, K., de Boer, D., Barenys, M., Bendt, F., Mosig, A., Fritsche, E., 2016. Omnisphero: a high-content image analysis (HCA) approach for phenotypic developmental neurotoxicity (DNT) screenings of organoid neurosphere cultures in vitro. *Arch. Toxicol.* 1–12. <http://dx.doi.org/10.1007/s00204-016-1852-2>.
- Schreiber, T., Gassmann, K., Goetz, C., Huebenthal, U., Moors, M., Krause, G., Merk, H.F., Nguyen, N.H., Scanlan, T.S., Abel, J., Rose, C.R., Fritsche, E., 2010. Polybrominated diphenyl ethers induce developmental neurotoxicity in a human in vitro model: evidence for endocrine disruption. *Environ. Health Perspect.* 118, 572–578. <http://dx.doi.org/10.1289/ehp.0901435>.
- Schwender, H., Fritsch, A., 2013. ScRime: Analysis of High-Dimensional Categorical Data such as SNP Data. (R Packag. version 1.3.3).
- Semple, B.D., Blomgren, K., Gimlin, K., Ferriero, D.M., Noble-Haesslein, L.J., 2013. Brain development in rodents and humans: identifying benchmarks of maturation and vulnerability to injury across species. *Prog. Neurobiol.* <http://dx.doi.org/10.1016/j.pneurobio.2013.04.001>.
- Seok, J., Warren, H.S., Cuenca, A.G., Mindrinos, M.N., Baker, H.V., Xu, W., Richards, D.R., McDonald-Smith, G.P., Gao, H., Hennessy, L., Finnerty, C.C., López, C.M., Honari, S., Moore, E.E., Minei, J.P., Cuschieri, J., Bankey, P.E., Johnson, J.L., Sperry, J., Nathens, A.B., Billiar, T.R., West, M.A., Jeschke, M.G., Klein, M.B., Gamelli, R.L., Gibran, N.S., Brownstein, B.H., Miller-Graziano, C., Calvano, S.E., Mason, P.H., Cobb, J.P., Rahme, L.G., Lowry, S.F., Maier, R.V., Moldawer, L.L., Herndon, D.N., Davis, R.W., Xiao, W., Tompkins, R.G., Inflammation and Host Response to Injury, L.S.C.R.P., 2013. Genomic responses in mouse models poorly mimic human inflammatory diseases. *Proc. Natl. Acad. Sci. U. S. A.* 110, 3507–3512. <http://dx.doi.org/10.1073/pnas.1222878110>.
- Silbereis, J.C., Pochareddy, S., Zhu, Y., Li, M., Sestan, N., 2016. The cellular and molecular landscapes of the developing human central nervous system. *Neuron*. <http://dx.doi.org/10.1016/j.neuron.2015.12.008>.
- Strasser, A., Wittmann, H.-J., Buschauer, A., Schneider, E.H., Seifert, R., 2013. Species-dependent activities of G-protein-coupled receptor ligands: lessons from histamine receptor orthologs. *Trends Pharmacol. Sci.* 34, 13–32. <http://dx.doi.org/10.1016/j.tips.2012.10.004>.
- Sun, Y., Goderie, S.K., Temple, S., 2005a. Asymmetric distribution of EGFR receptor during mitosis generates diverse CNS progenitor cells. *Neuron* 45, 873–886. <http://>

- [dx.doi.org/10.1016/j.neuron.2005.01.045](http://dx.doi.org/10.1016/j.neuron.2005.01.045).
- Sun, Y., Goderie, S.K., Temple, S., 2005b. Asymmetric distribution of EGFR receptor during mitosis generates diverse CNS progenitor cells. *Neuron* 45, 873–886. <http://dx.doi.org/10.1016/j.neuron.2005.01.045>.
- Sun, Y., Li, H., Liu, Y., Shin, S., Mattson, M.P., Rao, M.S., Zhan, M., 2007. Cross species transcriptional profiles establish a functional portrait of embryonic stem cells. *Neurosciences* 77, 247–265. <http://dx.doi.org/10.1016/j.ygeno.2006.09.010>.Cross.
- Szklarczyk, D., Franceschini, A., Wyder, S., Forslund, K., Heller, D., Huerta-Cepas, J., Simonovic, M., Roth, A., Santos, A., Tsafou, K.P., Kuhn, M., Bork, P., Jensen, L.J., Von Mering, C., 2015. STRING v10: protein-protein interaction networks, integrated over the tree of life. *Nucleic Acids Res.* 43, D447–D452. <http://dx.doi.org/10.1093/nar/gku1003>.
- Thomsen, E.R., Mich, J.K., Yao, Z., Hodge, R.D., Doyle, A.M., Jang, S., Shehata, S.I., Nelson, A.M., Shapovalova, N.V., Levi, B.P., Ramanathan, S., 2015. Fixed single-cell transcriptomic characterization of human radial glial diversity. *Nat Methods*. <http://dx.doi.org/10.1038/NMETH.3629>.
- Tsuji, R., Crofton, K.M., 2012. Developmental neurotoxicity guideline study: issues with methodology, evaluation and regulation. *Congenit. Anom. (Kyoto)*. 52, 122–128. <http://dx.doi.org/10.1111/j.1741-4520.2012.00374.x>.
- van Dartel, D.A.M., Pennings, J.L.A., de la Fonteyne, L.J.J., van Herwijnen, M.H., van Delft, J.H., van Schooten, F.J., Piersma, A.H., 2010. Monitoring developmental toxicity in the embryonic stem cell test using differential gene expression of differentiation-related genes. *Toxicol. Sci.* 116, 130–139. <http://dx.doi.org/10.1093/toxsci/kfq127>.
- van de Leemput, J., Boles, N.C., Kiehl, T.R., Corneo, B., Lederman, P., Menon, V., Lee, C., Martinez, R.A., Levi, B.P., Thompson, C.L., Yao, S., Kaykas, A., Temple, S., Fasano, C.A., 2014. CORTECON: a temporal transcriptome analysis of in vitro human cerebral cortex development from human embryonic stem cells. *Neuron* 83, 51–68. <http://dx.doi.org/10.1016/j.neuron.2014.05.013>.
- van der Worp, H.B., Howells, D.W., Sena, E.S., Porritt, M.J., Rewell, S., O'Collins, V., Macleod, M.R., 2010. Can animal models of disease reliably inform human studies? *PLoS Med.* 7, e1000245. <http://dx.doi.org/10.1371/journal.pmed.1000245>.
- Waldmann, T., Rempel, E., Balmer, N.V., Konig, A., Kolde, R., Gaspar, J.A., Henry, M., Hescheler, J., Sachinidis, A., Rahnenfuhrer, J., Hengstler, J.G., Leist, M., 2014. Design principles of concentration-dependent transcriptome deviations in drug-exposed differentiating stem cells. *Chem. Res. Toxicol.* 27, 408–420. <http://dx.doi.org/10.1021/tx400402j>.
- Waring, M.J., Arrowsmith, J., Leach, A.R., Leeson, P.D., Mandrell, S., Owen, R.M., Pairedeau, G., Pennie, W.D., Pickett, S.D., Wang, J., Wallace, O., Weir, A., 2015. An analysis of the attrition of drug candidates from four major pharmaceutical companies. *Nat. Rev. Drug Discov.* 14, 475–486. <http://dx.doi.org/10.1038/nrd4609>.
- Workman, A.D., Charvet, C.J., Clancy, B., Darlington, R.B., Finlay, B.L., 2013. Modeling transformations of neurodevelopmental sequences across mammalian species. *J. Neurosci.* 33, 7368–7383. <http://dx.doi.org/10.1523/JNEUROSCI.5746-12.2013>.
- Zeng, H., Shen, E.H., Hohmann, J.G., Oh, S.W., Bernard, A., Royall, J.J., Glattfelder, K.J., Sunkin, S.M., Morris, J.A., Guillozet-Bongaarts, A.L., Smith, K.A., Ebbert, A.J., Swanson, B., Kuan, L., Page, D.T., Overly, C.C., Lein, E.S., Hawrylycz, M.J., Hof, P.R., Hyde, T.M., Kleinman, J.E., Jones, A.R., 2012. Large-scale cellular-resolution gene profiling in human neocortex reveals species-specific molecular signatures. *Cell* 149, 483–496. <http://dx.doi.org/10.1016/j.cell.2012.02.052>.
- Zhang, Y., Sloan, S.A., Clarke, L.E., Caneda, C., Plaza, C.A., Blumenthal, P.D., Vogel, H., Steinberg, G.K., Edwards, M.S.B., Li, G., Duncan, J.A., Cheshier, S.H., Shuer, L.M., Chang, E.F., Grant, G.A., Gephart, M.G.H., Barres, B.A., 2016. Purification and characterization of progenitor and mature human astrocytes reveals transcriptional and functional differences with mouse. *Neuron* 89, 37–53. <http://dx.doi.org/10.1016/j.neuron.2015.11.013>.
- Zhang, R., Engler, A., Taylor, V., 2017. Notch: an interactive player in neurogenesis and disease. *Cell Tissue Res.* <http://dx.doi.org/10.1007/s00441-017-2641-9>.
- Zimmer, B., Kuegler, P.B., Baudis, B., Genewsky, A., Tanavde, V., Koh, W., Tan, B., Waldmann, T., Kadereit, S., Leist, M., 2011. Coordinated waves of gene expression during neuronal differentiation of embryonic stem cells as basis for novel approaches to developmental neurotoxicity testing. *Cell Death Differ.* 18, 383–395. <http://dx.doi.org/10.1038/cdd.2010.109>.

**Supplementary Material****A transcriptome comparison of time-matched developing human, mouse and rat neural progenitor cells reveals human uniqueness**

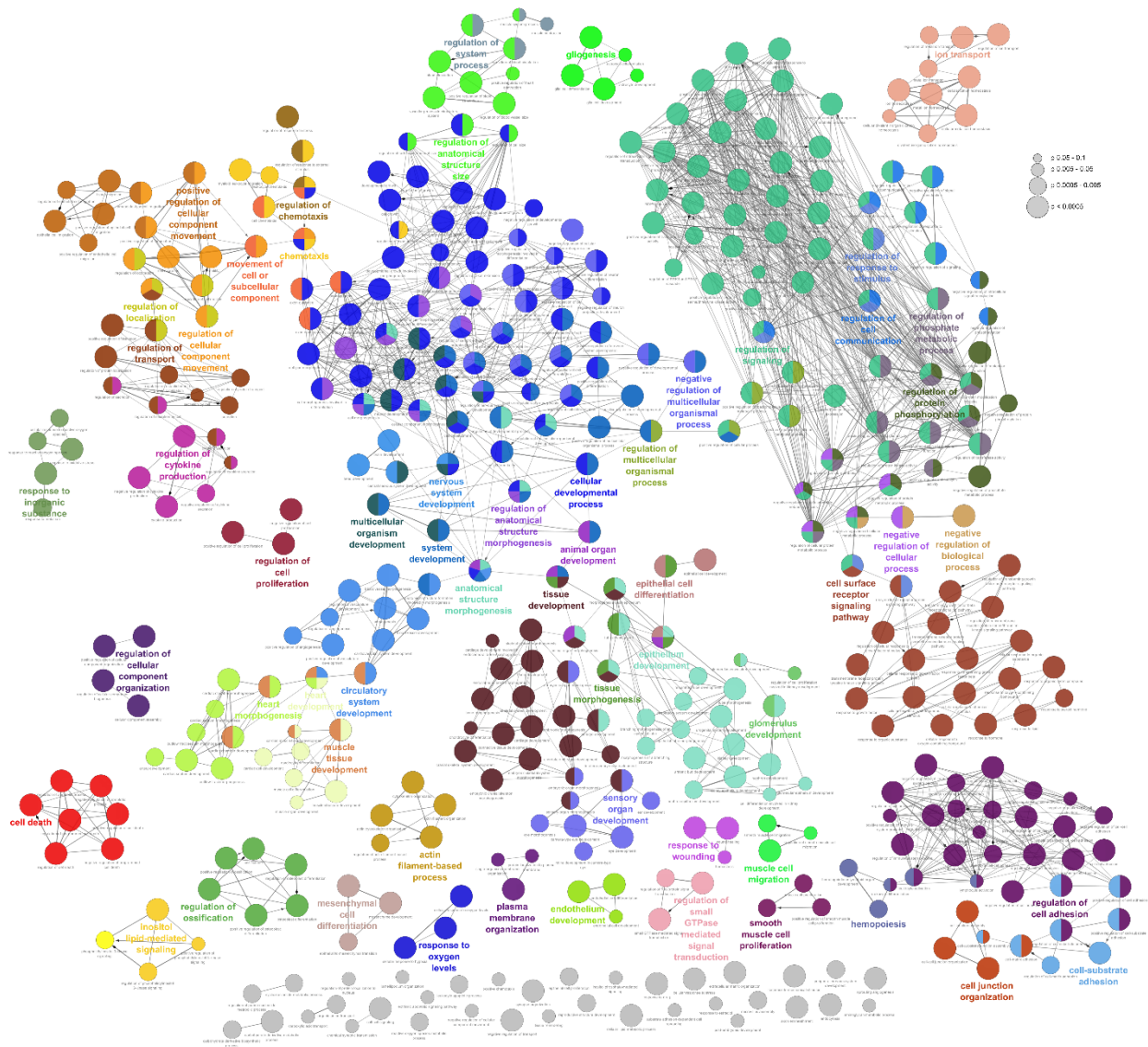
Stefan Masjosthusmann, Daniel Becker, Barbara Petzuch, **Jördis Klose**, Clara Siebert, Rene Deenen, Marta Barenys, Jenny Baumann, Katharina Dach, Julia Tigges, Ulrike Hübenthal, Karl Köhrer, Ellen Fritsche



**Fig. B. 1.** Hierarchical cluster analysis.

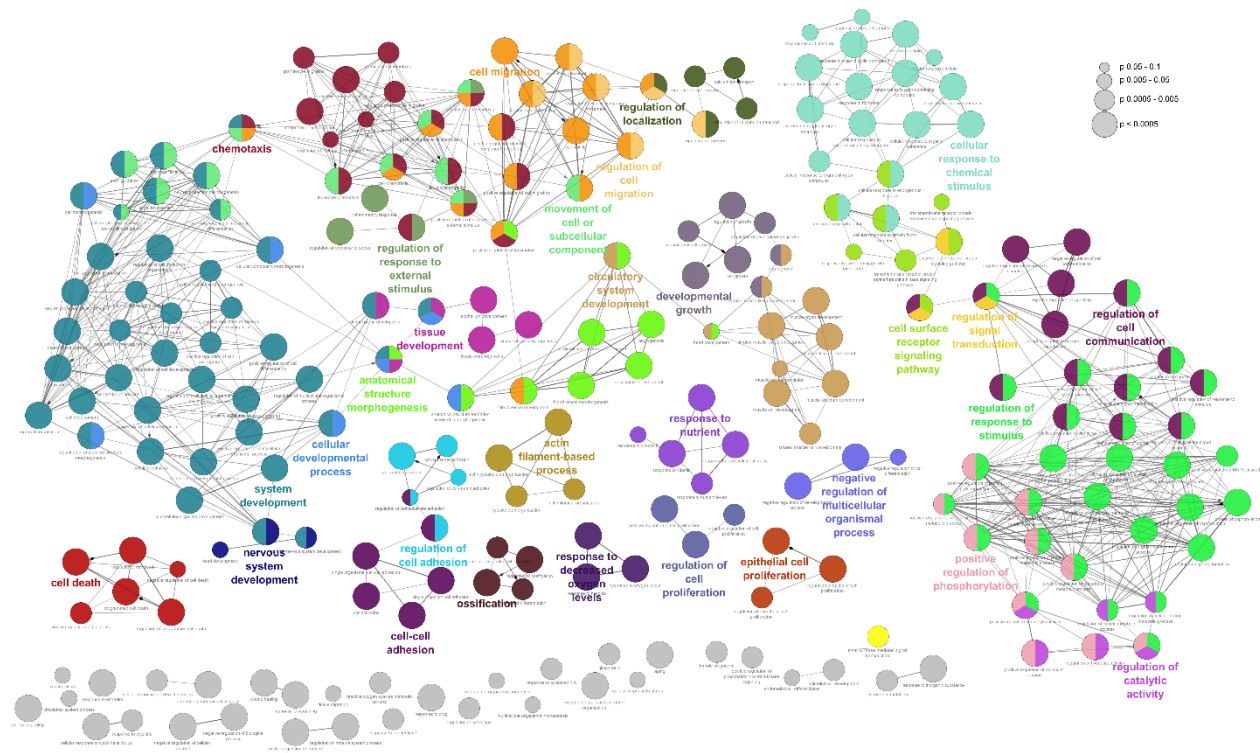
Hierarchical clustering of all genes that were differentially expressed ( $p \leq 0.01$  and fold change  $\geq 2$ ) between any two time points (0vs3, 0vs5 and 3vs5) in human (a) mouse (b) and rat (c) NPC was performed using an unweighted pair group agglomeration method with arithmetic mean and cutree, resulting in 10 distinct clusters as indicated by colored bars (random coloring) to the left of each heatmap.





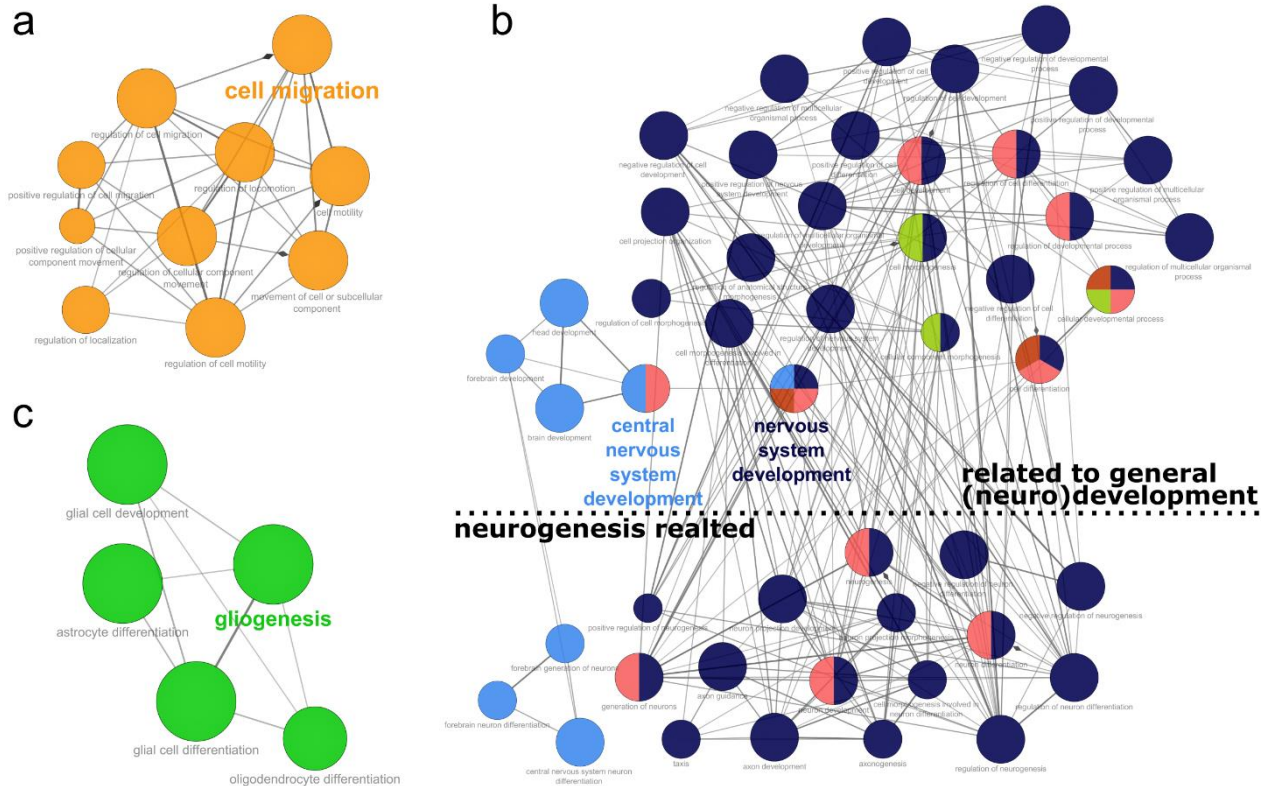
**Fig. B. 2.** GO clustering in mNPC.

Overrepresented GO terms of modules 1 and 2 (see Fig. 2h) in mNPC were clustered according to gene overlap between GO terms with a kappa score threshold of 0.5 and at least three GO terms within one cluster using the Cytoscape plugin ClueGO. Edge thickness represents similarity between GO terms. Node size represents significance of overrepresentation. The GO term with the highest significance determines the name of the respective GO cluster (bold; colored). Different colors represent different GO cluster. Grey nodes do not belong to a cluster. Significance thresholds of ORA was set to  $p \leq 0.01$  based on a two-sided hypergeometric option with a Bonferroni correction.



**Fig. B. 3.** GO clustering in rNPC.

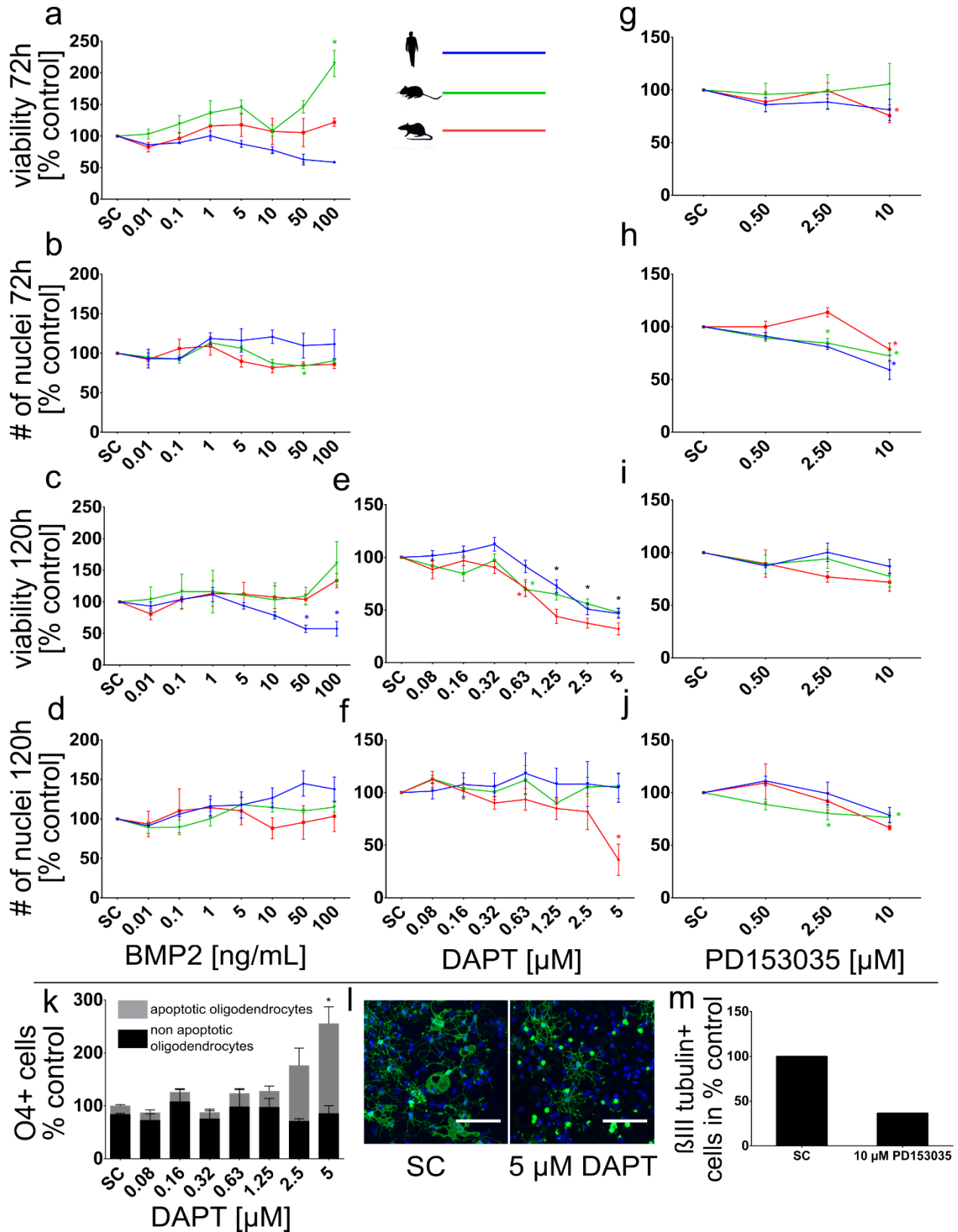
Overrepresented GO terms of modules 1 and 2 in rNPC were clustered according to gene overlap between GO terms with a kappa score threshold of 0.5 and at least three GO terms within one cluster using the Cytoscape plugin ClueGO (Bindea et al. 2009). Edge thickness represents similarity between GO terms. Node size represents significance of overrepresentation. The GO term with the highest significance determines the name of the respective GO cluster (bold; colored). Different colors represents different GO cluster. Grey nodes do not belong to a cluster. Significance thresholds of ORA was set to  $p \leq 0.01$  based on a two-sided hypergeometric option with a Bonferroni correction.



**Fig. B. 4.** Relevant GO term cluster for neurodevelopmental processes in hNPC.

GO term clusters for biological processes related to cell migration (a), neurogenesis (b) and gliogenesis (c) and extracted from GO term clustering in Fig. 4. (c) demonstrates the selection of GO terms related to neurogenesis that were extracted for enrichment with information on gene-gene/protein-protein interactions (binding, activation, expression and inhibition) based on the STRING database as presented in Fig. 5. For information on node size and related significance see Fig. 4.

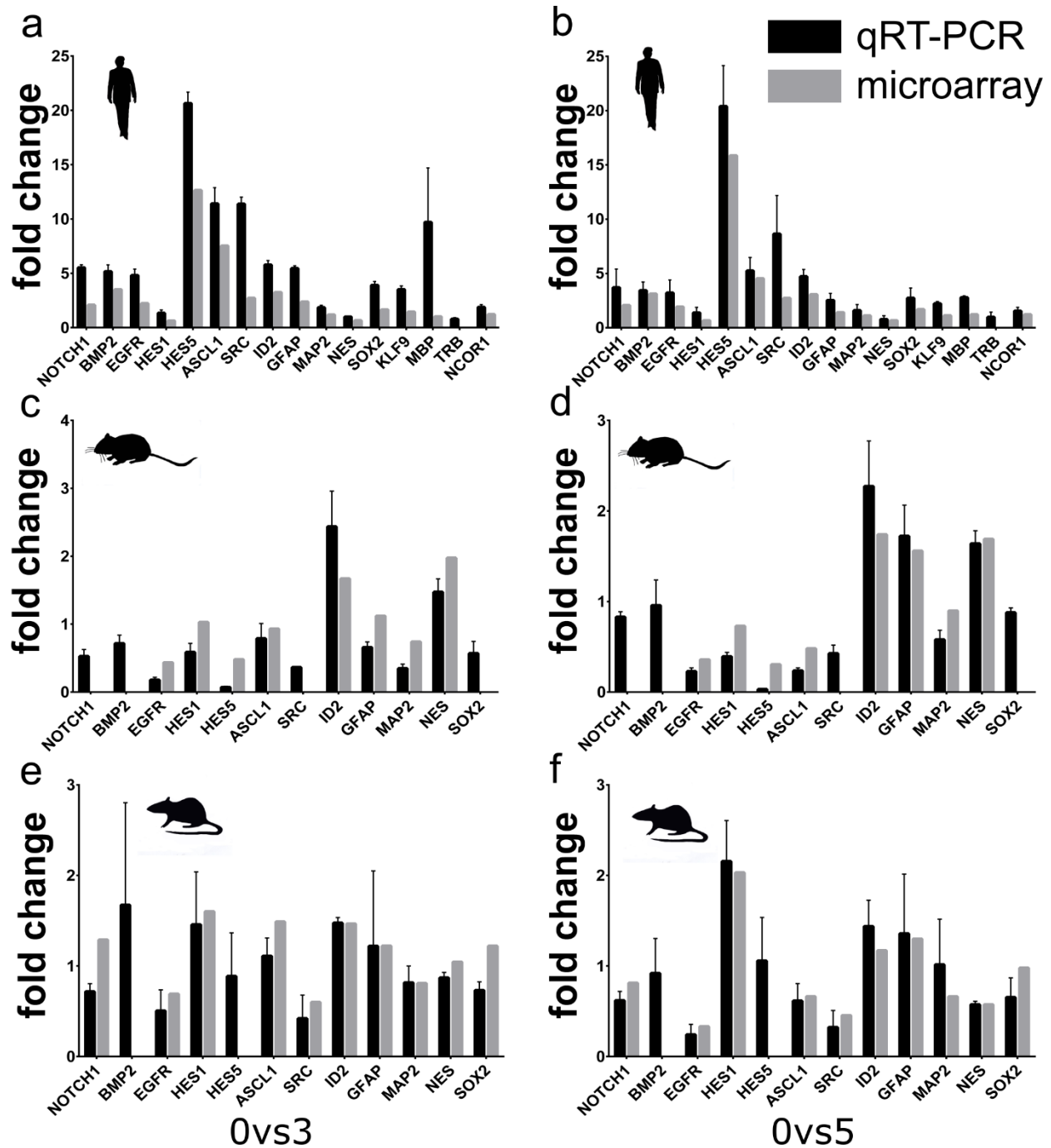




**Fig. B. 5.** Pharmacological modulation of the BMP2, NOTCH and EGF pathway.

NPC from human (blue), mouse (green) and rat (red) were treated with increasing concentrations of BMP2 (a, b, c, d), DAPT (NOTCH inhibitor; e, f) and PD153035 (EGFR inhibitor; g, h, i, j) and analyzed for viability

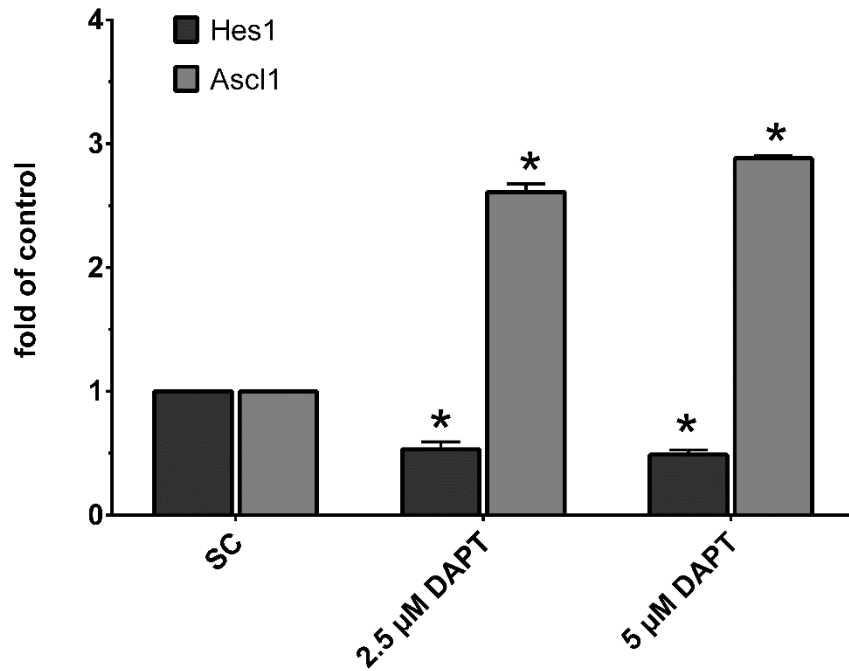
and nuclei count (after 72h and 120h). Viability was assessed as mitochondrial activity by Alamar-Blue assay. Nuclei were counterstained with Hoechst33258 and automatically quantified. (k) Percentage of apoptotic compared to non-apoptotic O4 positive cells in mNPC after 120h DAPT treatment. (l) Representative pictures of immunocytochemically stained oligodendrocytes with and without DAPT treatment. Scale bar represent 100  $\mu$ m. (m) hNPC cultured in 1% FCS during differentiation were treated with 10  $\mu$ M PD1530353 and analyzed for neuronal differentiation after 72h. Data of m represents one independent experiment normalized to the solvent control. Data of all other experiments was normalized to the solvent control and is displayed as concentration response relationship as mean  $\pm$  SEM of at least three independent experiments. \*indicates a significant difference from solvent control based on one-way ANOVA ( $p < 0.05$ ) followed by Dunnett's multiple comparison test.



**Fig. B. 6.** Validation of microarray experiments by qRT-PCR.

Gene expression of mRNA samples from human, mouse and rat NPC that were used for microarray analysis (three replicates) was analyzed by qRT-PCR and compared to results of microarray analysis.

Data is presented as fold change from qRT-PCR (black; mean  $\pm$  SD) and microarray analysis (grey) between 0 and 3 days (a, c, e) and 0 and 5 days (b, d, f) of human (a, b), mouse (c, d) and rat (e, f) NPC.



**Fig. B. 7.** Regulation of Notch dependent genes after DAPT exposure.

Gene expression of the Notch specific genes Hes1 and Ascl1 was analyzed after DAPT (2.5 and 5 μM) in human NPC. Data is presented as mean of fold change from solvent control ± SEM from three independent experiments. \*indicates a significant difference to solvent control based on one-way ANOVA ( $p < 0.05$ ).

## **A transcriptome comparison of time-matched developing human, mouse and rat neural progenitor cells reveals human uniqueness**

Stefan Masjosthusmann, Daniel Becker, Barbara Petzuch, **Jördis Klose**, Clara Siebert, Rene Deenen, Marta Barenys, Jenny Baumann, Katharina Dach, Julia Tigges, Ulrike Hübenthal, Karl Köhrer, Ellen Fritsche

Journal:	Toxicology and Applied Pharmacology (TAAP)
Impact Factor:	3.859
Contribution to the publication:	15 % Planning, performance and evaluation of experiments with bone morphogenetic protein 2 (BMP2)
Type of authorship:	co-authorship
Status of the publication:	Published 9 <sup>th</sup> May 2018


## 2.5 Rabbit neurospheres as a novel *in vitro* tool for studying neurodevelopmental effects induced by intrauterine growth restriction

Marta Barenys, Miriam Illa, Maxi Hofrichter, Carla Loreiro, Laura Pla, **Jördis Klose**, Britta Anna Kühne, Jesús Gómez-Catalán, Jan Matthias Braun, Fatima Crispi, Eduard Gratacós, Ellen Fritsche

### *Stem Cells Translational Medicine*

Das Ziel dieser Studie bestand darin, eine Kaninchen-basierte Neurosphärenkultur zu entwickeln, um Unterschiede in den grundlegenden Prozessen der Neurogenese zu charakterisieren, die durch intrauterine Wachstumsretardierung (intrauterine growth restriction; IUGR) induziert werden. Es wurde eine neuartige *in vitro* Neurosphärenkultur entwickelt, die auf der Verwendung von frisch präparierten oder eingefrorenen neuralen Vorläuferzellen basiert, welche aus neugeborenen (PND0) Kaninchengehirnen stammen. Fünf Tage nach erfolgter operativer IUGR Induzierung trächtiger Kaninchen wurden die Kaninchenföten per Kaiserschnitt entnommen, die neuralen Vorläuferzellen isoliert und entweder direkt kultiviert oder entsprechend bis zur Kultivierung bei -80°C eingefroren. Die neuralen Vorläuferzellen waren in der Lage spontan nach 7 Tagen unter Kulturbedingungen 3D Neurosphären zu bilden. Sowohl Kontrollneurosphären, als auch IUGR-Neurosphären verfügen über die Fähigkeit zu migrieren, zu proliferieren und zu Neuronen, Astrozyten oder Oligodendrozyten zu differenzieren. Die Möglichkeit, ihre Reaktionen zu modulieren, wurde durch eine Exposition gegenüber Positiv- und Negativkontrollen, bezogen auf die jeweiligen Endpunkte, getestet. Ein direkter Vergleich beider Neurosphärentypen zeigte, dass IUGR-Neurosphären eine signifikante Beeinträchtigung der Oligodendrozytenbildung aufweisen, während bei allen anderen untersuchten Endpunkten kein signifikanter Unterschied beobachtet werden konnte. Diese Beeinträchtigung der Oligodendrozytendifferenzierung konnte durch eine IUGR-Neurosphären Exposition *in vitro* gegenüber dem Schilddrüsenhormon Triiodothyronin, welches *in vivo* bei der Reifung der weißen Gehirnsubstanz eine Rolle spielt, rückgängig gemacht werden. Das neue Kaninchen-Neurosphärenmodell und die Ergebnisse dieser Studie eröffnen die Möglichkeit, mehrere Substanzen vorab *in vitro* zu testen, um neuroprotektive Kandidaten gegen IUGR induzierte neurologische Entwicklungsschäden zu identifizieren. Dies geht mit einer Reduzierung der bisher notwendigen Tierversuche und eines mechanistisch relevanteren Ansatzes auf zellulärer Ebene einher.

# Rabbit neurospheres as a novel in vitro tool for studying neurodevelopmental effects induced by intrauterine growth restriction

Marta Barenys<sup>1,2</sup>  | Miriam Illa<sup>3</sup> | Maxi Hofrichter<sup>1</sup> | Carla Loreiro<sup>3</sup> |  
 Laura Pla<sup>3</sup> | Jördis Klose<sup>1</sup> | Britta Anna Kühne<sup>2,3</sup> | Jesús Gómez-Catalán<sup>2</sup> |  
 Jan Matthias Braun<sup>1</sup> | Fatima Crispi<sup>3</sup> | Eduard Gratacós<sup>3</sup> | Ellen Fritsche<sup>1</sup>

<sup>1</sup>IUF—Leibniz Research Institute for Environmental Medicine, Düsseldorf, Germany

<sup>2</sup>GRET, INSA-UB and Toxicology Unit, Pharmacology, Toxicology and Therapeutical Chemistry Department, Faculty of Pharmacy, University of Barcelona, Barcelona, Spain

<sup>3</sup>BCNatal-Barcelona Center for Maternal-Fetal and Neonatal Medicine (Hospital Clínic and Hospital Sant Joan de Déu), Fetal i+D Fetal Medicine Research Center, IDIBAPS, University of Barcelona, Center for Biomedical Research on Rare Diseases (CIBER-ER), Barcelona, Spain

## Correspondence

Marta Barenys, PhD, GRET, INSA-UB and Toxicology Unit, Pharmacology, Toxicology and Therapeutical Chemistry Department, Faculty of Pharmacy, University of Barcelona, Av. Joan XXIII, 27-31, 08028 Barcelona, Spain. Email: mbarneys@ub.edu

## Funding information

Health Department of the Catalan Government, Grant/Award Number: SLT006/17/00325; Fundació Bosch i Gimpera, Grant/Award Number: 300155; AGAUR, Grant/Award Number: 2017 SGR n° 1531; "LaCaixa" Foundation, Grant/Award Numbers: LCF/PR/GN18/10310003, LCF/PR/GN14/10270005; European Regional Development Fund/European Social Fund; Instituto de Salud Carlos III, Grant/Award Number: PI18/01763

## Abstract

The aim of this study was to develop a rabbit neurosphere culture to characterize differences in basic processes of neurogenesis induced by intrauterine growth restriction (IUGR). A novel in vitro neurosphere culture has been established using fresh or frozen neural progenitor cells from newborn (PND0) rabbit brains. After surgical IUGR induction in pregnant rabbits and cesarean section 5 days later, neural progenitor cells from both control and IUGR groups were isolated and directly cultured or frozen at  $-80^{\circ}\text{C}$ . These neural progenitor cells spontaneously formed neurospheres after 7 days in culture. The ability of control and IUGR neurospheres to migrate, proliferate, differentiate to neurons, astrocytes, or oligodendrocytes was compared and the possibility to modulate their responses was tested by exposure to several positive and negative controls. Neurospheres obtained from IUGR brains have a significant impairment in oligodendrocyte differentiation, whereas no significant differences are observed in other basic processes of neurogenesis. This impairment can be reverted by in vitro exposure of IUGR neurospheres to thyroid hormone, which is known to play an essential role in white matter maturation in vivo. Our new rabbit neurosphere model and the results of this study open the possibility to test several substances in vitro as neuroprotective candidates against IUGR induced neurodevelopmental damage while decreasing the number of animals and resources and allowing a more mechanistic approach at a cellular functional level.

## KEYWORDS

cell culture, differentiation, experimental models, growth inhibition, nervous system, oligodendrocytes, progenitor cells

[Correction added on 14 December 2020, after first online publication: Projekt Deal funding statement has been added.]

This is an open access article under the terms of the Creative Commons Attribution-NonCommercial License, which permits use, distribution and reproduction in any medium, provided the original work is properly cited and is not used for commercial purposes.

© 2020 The Authors. STEM CELLS TRANSLATIONAL MEDICINE published by Wiley Periodicals LLC on behalf of AlphaMed Press.



## 1 | INTRODUCTION

Intrauterine growth restriction (IUGR) is defined as a significant reduction of the fetal growth rate leading to a birth weight below the 10th centile for the corresponding gestational age.<sup>1</sup> The prevalence in developing countries accounts for 5% to 10% of all pregnancies, being a global health issue that is associated to short- and long-term neurodevelopmental damage, cognitive dysfunctions and cardiovascular adverse outcomes.<sup>2,3</sup> Placental insufficiency, the primary cause of IUGR, reduces the quantity of nutrients reaching the fetus and leads to fetal development under chronic hypoxia followed by fetal acidosis. Placental insufficiency affects up to 7% of all gestations<sup>4,5</sup> and in approximately 50% of these cases it derives in clinically evident middle and long-term neurological consequences defined as subtle cognitive and behavioral disabilities.<sup>6-9</sup> Different animal models and advanced imaging techniques have been used to better understand the mechanisms underlying neuronal impairments and perinatal brain maturation alterations induced by IUGR.<sup>10</sup> However, there is still a large knowledge gap on the mechanisms underlying these alterations<sup>2</sup> and a lack of research models to better characterize the IUGR-associated brain injury (reviewed by Fleiss et al. 2019<sup>11</sup>).

In order to have a human-relevant experimental model of neurodevelopmental damage induced by IUGR, the BCNatal research group developed an IUGR model in pregnant rabbits.<sup>12</sup> This animal model reproduces the neurodevelopmental manifestations of IUGR occurring in clinical cases, including postnatal functional and structural deficits.<sup>12,13</sup> The selection of the rabbit species was based on the higher similarity to humans in terms of placentation and gestational circulatory changes,<sup>12,14</sup> as well as the resemblance regarding white matter maturation, which in both species happens during the postnatal period.<sup>13,15,16</sup> According to the model developed by Workman et al.,<sup>16</sup> to predict the “precocial score” for neurodevelopment, rabbit species presents a precocial score at birth (0.537) more similar to humans (0.654) than other species, including rats (0.445) or mice (0.408). Likewise, at the neonatal period, diffusion MRI in whole organ preparations from a rabbit model showed differences on diffusion related parameters either at gray and white matter, revealing a pattern of microstructural brain changes produced by IUGR already at birth.<sup>13</sup> Interestingly, decreased fractional anisotropy in white matter structures has been suggested to reflect oligodendrocyte injury,<sup>17,18</sup> whereas in the gray matter areas it seems to reflect changes in neuronal arborisation.<sup>19</sup> Furthermore, follow-up studies of IUGR rabbits have unraveled changes in their cerebral connections,<sup>3,20</sup> which correlate very well with the clinical observation that IUGR-affected children also present cerebral connection alterations in connectomic-studies.<sup>21</sup> Linking this clinical adverse outcome with the neurodevelopmental alterations observed in rabbits gives evidence that the rabbit IUGR model is a good model to study IUGR-induced structural changes in humans.<sup>12,22,23</sup>

However, in this *in vivo* model, it is difficult to identify the origin of the functional and structural deficits induced by IUGR, and so far, it was not possible to understand which basic cellular processes are altered during brain development under IUGR. To solve this limitation, we established an *in vitro* model based on primary rabbit neuronal progenitor cells (NPCs) allowing the investigation of the basic

### Significance statement

To the best of the authors' knowledge, this article describes for the first time a valuable method for generation of 3D rabbit neurospheres that can be differentiated to neurons, astrocytes, and oligodendrocytes. This method is applied for modeling the neurodevelopmental effects of intrauterine growth restriction (IUGR), for toxicity testing, and for efficacy testing of possible new pharmaceuticals. In this study, the authors found differences in basic processes of neurogenesis induced by IUGR, showed that neurospheres obtained from IUGR brains have a significant impairment in oligodendrocyte differentiation, and demonstrated that this impairment can be reverted by *in vitro* exposure of IUGR neurospheres to thyroid hormone.

neurodevelopmental processes affected by IUGR. In this model, rabbit NPCs obtained from control and IUGR pups are cultured as three-dimensional (3D) cell aggregates called neurospheres. Neurosphere cultures from other species have previously been established and have been utilized for mimicking basic processes of fetal brain development like NPC proliferation, migration and differentiation into neurons, oligodendrocytes and astrocytes.<sup>24-29</sup> In this study, for the very first time, a rabbit neurosphere culture was developed and characterized. In addition, we successfully developed a freezing and thawing protocol, which allows storing and prolonging the use of rabbit NPCs obtained from one litter and enables interlaboratory transfer of material. The ability to freeze and thaw rabbit neurospheres reduces the number of animals used and is thus much more time- and cost-efficient. Due to the multicellular nature of the neurosphere method and the possibility to study a variety of neurodevelopmental processes with it, neurospheres are a valuable test system for studying a plethora of cellular effects initiated by a variety of different modes of action.<sup>24,28,30-33</sup> Therefore, they seemed well suited for characterizing so far unknown neurodevelopmental effects on the cellular level induced by IUGR. With this method, we identified that rabbit NPCs derived from IUGR pups have a significant impairment in oligodendrocyte differentiation. Moreover, we discovered that exposure to thyroid hormone L-triiodothyronine (T3) can revert this significant impairment unraveling a possible future therapeutic strategy. This new methods thus opens the door to easy and cost-efficient testing of possible neuroprotective therapies for IUGR.

## 2 | MATERIALS AND METHODS

### 2.1 | Rabbit neurosphere generation

Rabbit tissue obtention for this study was approved by the Ethic Committee for Animal Experimentation of the University of Barcelona. Protocols were accepted with the license number: OB 392/19 SJD. Rabbit neural progenitor cells were isolated from nine newborn

postnatal day (PND) 0 or 1 New Zealand rabbits whole brains by dissection, mechanical dissociation, digestion (20 minutes incubation with papain 20 U/mL at 37°C), mechanical homogenization into a cell suspension, and centrifugation (5 minutes at 800 rpm). The cell pellet obtained was cultured as a cell suspension for 1 week at 37°C and 7.5% CO<sub>2</sub> in polyhydroxyethylmethacrylate (Poly-HEMA) coated dishes with "proliferation medium" [consisting in DMEM and Hams F12 3:1 supplemented with 2% B27, and 20 ng/mL epidermal growth factor (EGF) and recombinant human fibroblast growth factor (FGF), 100 U/mL penicillin and 100 µg/mL streptomycin], half volume of which was exchanged every 2 to 3 days.

## 2.2 | Neurosphere freezing and thawing protocol

During the neural progenitor cells isolation from 8 out of the 9 whole rabbit pup brains described above, half of the volume of the cell suspension obtained after resuspension in proliferation medium was centrifuged again (5 minutes at 800 rpm), the supernatant discarded and the pellet gently resuspended in freezing media instead (1:1; volume of pellet: volume of "freezing medium" [consisting in 70% (v/v) proliferation medium, 20% (v/v) fetal calf serum, and 10% (v/v) dimethyl sulfoxide (DMSO)]). Cell suspension in freezing medium was distributed in 1 mL per cryo-vial and immediately placed in a cryo-device filled with propanol to ensure a freezing rate of -1°C/min, and stored at -80°C.

Each cryo-vial was thawed approximately 1 month after freezing by brief immersion in a 37°C water bath, transference of cells to 15 mL of "proliferation medium" preconditioned at 37°C and 7.5% CO<sub>2</sub> for 2 hours, and gentle resuspension. Cell suspension was centrifuged (5 minutes, 800 rpm), supernatant discarded and cells transferred to Poly-HEMA coated dishes filled with "proliferation medium" supplemented with Rho kinase (ROCK) inhibitor Y-276322 at a final concentration of 10 µM, to enhance recovery and growth of cryopreserved cells.<sup>34</sup> Half of the volume of "proliferation medium" per petri dish was exchanged every 2 to 3 days by "proliferation medium" without ROCK inhibitor.

## 2.3 | Rabbit "Neurosphere Assay"

Fresh or thawed neurospheres formed in the "proliferation medium" culture, were mechanically passaged before starting experiments with a chopper to 0.2 mm<sup>2</sup> squares to ensure homogeneous neurosphere size, and allowed to recover spherical shape in "proliferation medium" in Poly-HEMA coated dishes. On the experiment plating day (considered experiment day 0), 0.3 mm diameter neurospheres were selected and plated in one of the following conditions depending on the assay to perform.

### 2.3.1 | Proliferation assay

One neurosphere per well was plated in 96 well-round bottom-plates coated with Poly-HEMA and filled with 100 µL of "proliferation

medium." Plate was cultured at 37°C and 7.5% CO<sub>2</sub> for 7 days. One bright-field picture per neurosphere was taken on days 0, 2, 4, 6, and 7. Every 2 days, 50 µL of "proliferation medium" per well were renewed. Neurosphere diameter was measured in each picture with ImageJ.

### 2.3.2 | Migration assays

Five neurospheres per chamber were plated in PDL/Laminin coated 8-chamber slides filled with 500 µL of "differentiation medium" [consisting in DMEM and Hams F12 3:1 supplemented with N2 (Invitrogen), penicillin and streptomycin (100 U/mL and 100 µg/mL)]. After 1 and 3 days of culture, bright-field pictures were taken to monitor migration progression by measuring the distance from the neurosphere core to the furthest migrated cells in four points per neurosphere using ImageJ.

### 2.3.3 | Neuronal differentiation assay

At day 3, after taking pictures for migration, neurospheres were fixed with paraformaldehyde (PFA) 4% (1 hour, 37°C), washed twice with phosphate-buffered saline (PBS) and stored in PBS until immunostained. For immunostaining, slides were incubated at room temperature with a blocking solution with 10% goat serum in PBS-T (PBS containing 0.1% Triton X-100) for 5 minutes. Neurospheres were incubated with a primary antibody solution containing 10% goat serum and 1:100 rabbit IgG anti-βIII-tubulin antibody in PBS-T for 1 hour at 37°C. After three washing steps with PBS, slides were incubated with secondary antibody solution containing 2% goat serum, 1:100 Hoechst 33258 and 1:200 Alexa 546 anti-rabbit IgG in PBS for 30 minutes at 37°C. After three washing steps with PBS and one with distilled water, slides were mounted with Acqua Poly/Mount (Polysciences, Inc.) and stored at 4°C until image acquisition. After immunostaining, 200× fluorescent images of two extracts of the migration area were taken per sphere in five spheres per condition in at least three independent experiments. The percentage of βIII-tubulin positive cells was quantified manually using ImageJ software<sup>34</sup> cell count tool.

### 2.3.4 | Astrocyte immunostaining

To immunostain astrocytes, the same protocol used to immunostain neurons was applied but the primary antibody solution contained 10% goat serum and 1:100 rabbit IgG anti GFAP antibody in PBS and the secondary antibody solution contained 2% goat serum, 1:100 Hoechst 33258, and 1:200 Alexa 546 anti-rabbit IgG in PBS 1:200.

### 2.3.5 | Oligodendrocyte differentiation assay

Five neurospheres per chamber were plated following the same procedure described for the migration assay. After 5 days of culture,

neurospheres were fixed (4% PFA, 1 hour, 37°C) washed twice with PBS and stored in PBS until immunostained. Slides were incubated with a primary antibody solution containing 10% goat serum, 1:200 mouse IgM anti-O4 antibody in PBS for 1 hour at 37°C. After three washing steps with PBS, slides were incubated with secondary antibody solution containing 2% goat serum, 1:100 Hoechst 33258, and 1:200 Alexa 488 anti-mouse IgM in PBS for 30 minutes at 37°C. After three washing steps with PBS and one with distilled water, slides were mounted with Acqua Poly/Mount (Polysciences, Inc.) and stored at 4°C until image acquisition. After immunostaining, 200× fluorescent images of two extracts of the migration area were taken per sphere in five spheres per condition in at least three independent experiments. The percentage of O4 positive cells was quantified manually using ImageJ software<sup>35</sup> cell count tool.

### 2.3.6 | Viability assay

At the end of migration/neuronal differentiation and oligodendrocyte differentiation assays (on days 3 and 5, respectively), and prior to fixation, a viability assay was performed by removing 200 µL medium per chamber, adding 100 µL of CellTiter-Blue Reagent (Promega) diluted 1:3 (v/v) in “differentiation medium” per chamber and incubating for 2 hours at 37°C and 7.5% CO<sub>2</sub> to measure the metabolic activity of the culture. Fluorescence of the supernatant was measured at 544/590 nm in two replicates of 100 µL per chamber transferred to two wells of a 96 well-plate and expressed as relative fluorescence units.

## 2.4 | IUGR induction in rabbits

Animal experimentation of this study was approved by the Ethic Committee for Animal Experimentation of the University of Barcelona. Protocols were accepted by the Department of Environment and Housing of the Generalitat de Catalunya with the license number: 03/17. New Zealand pregnant rabbits provided by a certified breeder were housed in separate cages with a 12/12 hours light/dark cycle, with free access to water and standard chow.

After at least 72 hours of acclimatization, IUGR was surgically induced following a previously described technique in four pregnant rabbits at 25 days of gestation.<sup>12</sup> Briefly, 40% to 50% of uteroplacental vessels that irrigate each gestational sac of one uterine horn (left or right randomly selected) were ligated obtaining the IUGR fetuses, while non-ligated gestational sacs from the contralateral horn provided normally-grown fetuses (controls). Postoperative analgesia with Buprenorphine 0.05 mg/kg was administered subcutaneously and animals were again housed with free access to water and standard chow ad libitum and were monitored daily for general health. Cesarean section was performed at 30 days of gestation. All living PND0 pups were identified and classified in control or IUGR groups depending on the uterine horn, weighted and sacrificed. Brains were immediately dissected and neural progenitor cells obtained as described in the “rabbit neurosphere generation” section.

All neural progenitor cells obtained from control and IUGR siblings were frozen at –80°C and thawed in parallel before performing any Neurosphere Assay.

## 2.5 | Inclusion criteria of IUGR PND0 rabbit pups

Strong IUGR cases are defined by a body weight lower than the 10th percentile (32.7 g; Table 1). To cover a broad range of IUGR cases, neurospheres were prepared from mild and strong IUGR pups. In this study, IUGR rabbit pups were included for neurosphere preparation if their body weight was lower than the 90th percentile (57.8 g).

## 2.6 | Statistics

Statistical analysis was performed using GraphPad Prism v6 and v7 (GraphPad Software, La Jolla, California). Concentration-dependent effects were assessed performing a one-way ANOVA analysis followed by Bonferroni post hoc test for multiple comparisons. Comparisons of two groups were performed with two-tailed t test. Significance threshold was established at  $P < .05$ .

# 3 | RESULTS

## 3.1 | Establishment of a rabbit neurosphere model

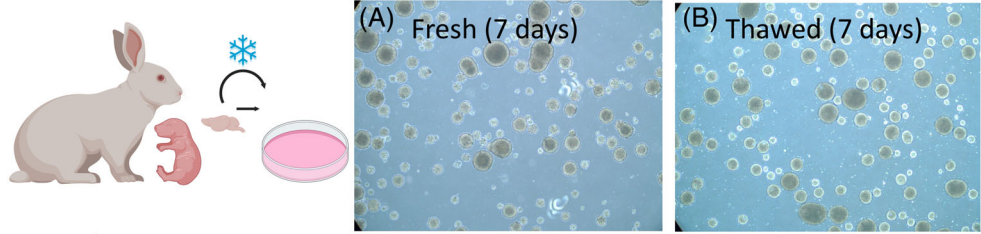
To establish a rabbit developmental neurosphere model, we first started isolating NPCs from control rabbit PND0 or PND1 brains, testing their ability to spontaneously form neurospheres and evaluating the competence of these freshly formed neurospheres to perform basic processes of neurogenesis like proliferation, migration, and differentiation. Freshly isolated rabbit NPCs spontaneously formed recognizable floating neurospheres after 4 days in culture, kept proliferating further and were big enough to be mechanically passaged (chopped) after 7 days in culture (Figure 1). Chopped neurospheres were used to start the “Neurosphere Assay” in control conditions, always compared to a positive control condition which was specific for each endpoint tested (endpoint-specific control known to alter the measured variable): the src-kinase inhibitor PP2 for migration, Epidermal Growth Factor (EGF) for neuronal differentiation and viability, bone morphogenic protein 7 (BMP7) for oligodendrocyte differentiation and withdrawal of all growth factors for proliferation. Freshly prepared rabbit NPCs growing as neurospheres migrated (mean ± SEM = 806 ± 29 µm, Figure 2) and proliferated (mean ± SEM = 18 ± 2 µm/day, Figure 2) in culture. Among cells in the migration area, we identified cells differentiating to astrocytes (GFAP<sup>+</sup> cells), to oligodendrocytes (O4<sup>+</sup> cells) and to neurons (βIII-tubulin<sup>+</sup> cells) (Figure 1). We also quantified the percentage of migrating cells differentiating to O4<sup>+</sup> cells after 5 days (mean ± SEM = 12 ± 1%, Figure 2) and to βIII-tubulin<sup>+</sup> cells after 3 days (mean ± SEM = 3 ± 1, Figure 2). For all endpoints, results

**TABLE 1** Percentile and body weight of rabbit pups on day PND0

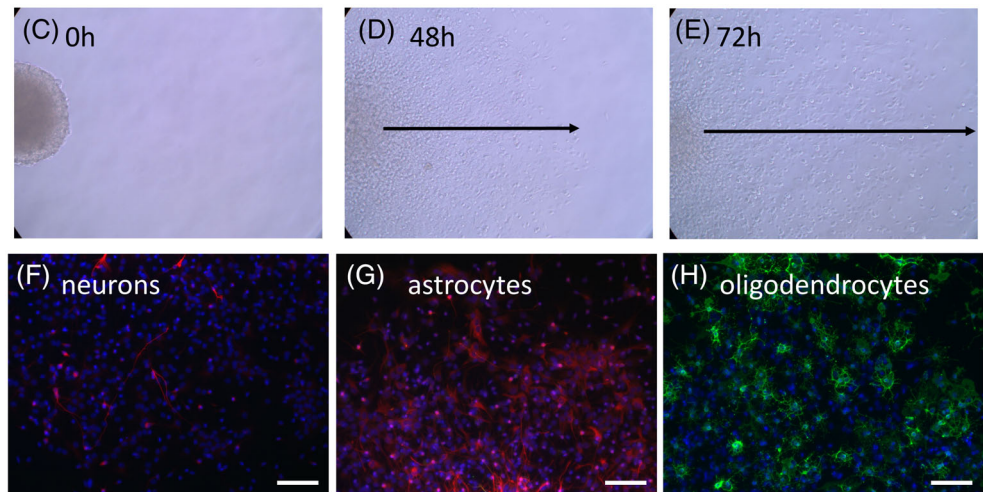
Percentile	5	10	25	50	75	90	95
PND0 body weight (g)	29.5	32.7	39.7	46.3	52.2	57.8	62.1

**FIGURE 1** Graphical summary of the rabbit “Neurosphere Assay.” Culture establishment: PND0 rabbit brains are dissected and either frozen or directly cultured until neurosphere formation (A, 7 days in culture after dissection; B, 7 days in culture after thawing). “Neurosphere Assay” starts when neurospheres of a diameter of 300  $\mu\text{m}$  are plated in 8-chamber slides and maintained under differentiating conditions to evaluate migration (C, 0 hours; D, 48 hours; E, 72 hours after plating) and differentiation into neurons (F, 72 hours after plating,  $\beta$ III-tubulin in red and Hoechst 33258 in blue), into astrocytes (G, 72 hours after plating, GFAP in red and Hoechst 33258 in blue) or into oligodendrocytes (H, 120 hours after plating, O4 in green and Hoechst 33258 in blue). Scale bars = 100  $\mu\text{m}$ . Neurospheres were also plated in 96-well plates under proliferating conditions and evaluated for diameter increase up to 7 days (I, representative image of a proliferating neurosphere from day 0 to day 7)

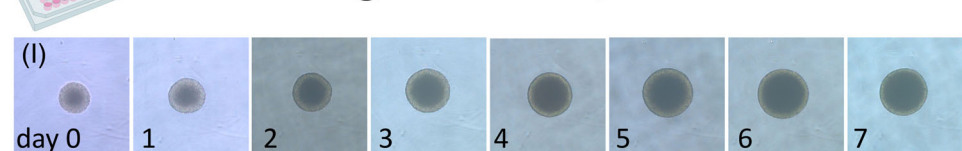
### Culture establishment:



### Differentiating conditions: migration & differentiation



### Proliferating conditions: proliferation

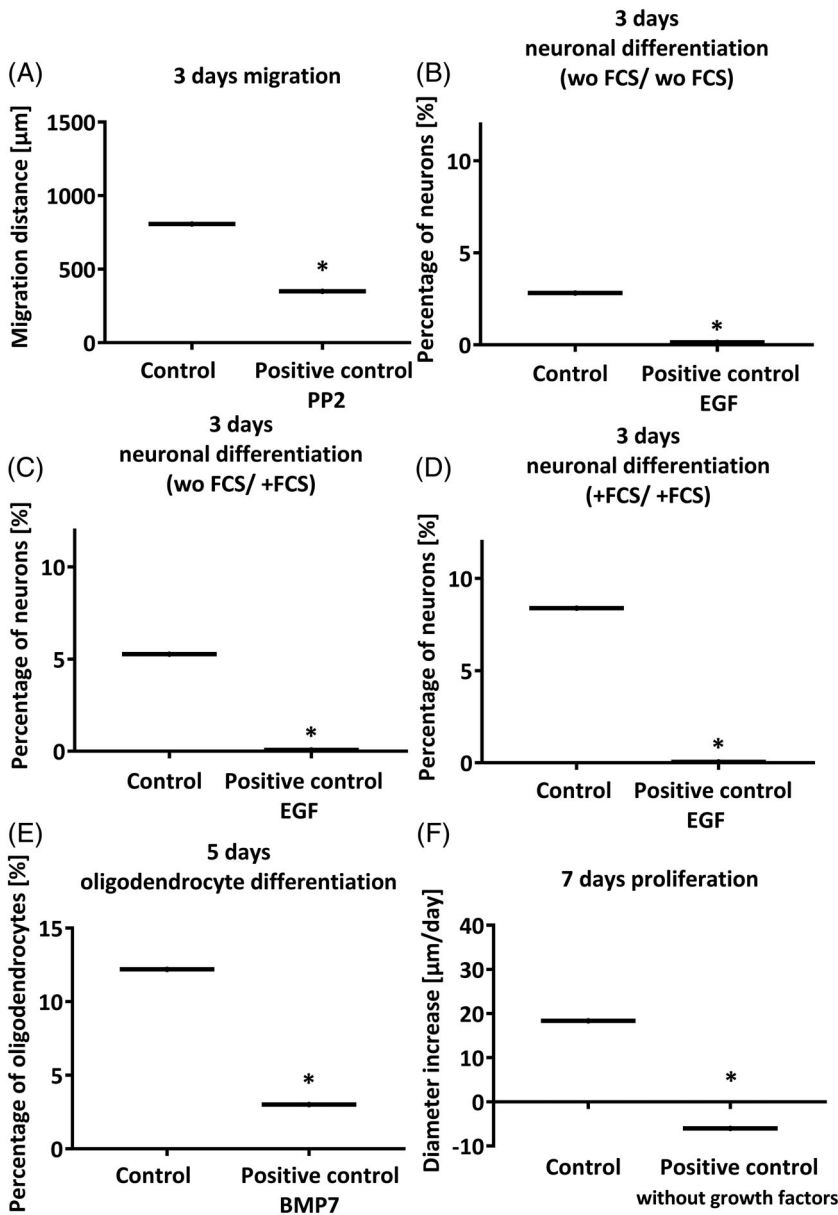


obtained with rabbit neurospheres allowed to observe alterations of the endpoint in both directions, positive and negative as recommended for the development of new alternative methods.<sup>36</sup> Besides, all positive controls included to each endpoint and tested in parallel to control, proved to be able to significantly modify the response obtained similar to human NPCs, indicating that the system is dynamic and can be influenced by known substances interfering with neurogenic processes. However, neuronal differentiation was relatively low compared to the values established for other species (human neurospheres = 5%<sup>37</sup>). Therefore, other culture conditions were tested, mainly the addition of fetal calf serum (FCS) either in differentiation medium or in both proliferation and differentiation medium (Figure 2). Both conditions led to an increased percentage of cells differentiating into neurons and exceeding 5% of differentiation. The longer the cells were exposed to FCS, the higher the percentage of neurons was (Figure 2).

After establishing all endpoints of the “Neurosphere Assay” for fresh neurospheres, a freezing protocol was tested, either after first passaging of neurospheres (passage 1) or directly after isolation of neural progenitor cells from rabbit brain (passage 0).

When the freezing protocol was applied after the first passaging of neurospheres (passage 1), NPCs lost their capabilities to develop in all endpoints of the “Neurosphere Assay” (mainly due to too low neuronal differentiation and too low proliferation; see Supporting Information Figure S1), and therefore, this option was directly discarded. Nevertheless, the application of the freezing protocol on freshly isolated NPCs, before the formation of neurospheres (passage 0), led to results in the “Neurosphere Assay” comparable to fresh neurospheres (see Material and methods section for more details about freezing and thawing protocol). Thawed NPCs spontaneously formed recognizable neurospheres after 4 days in vitro and were big enough to be chopped after 7 days in vitro (Figure 1). Results of proliferation, migration and





**FIGURE 2** Results of the “Neurosphere Assay” establishment with freshly prepared rabbit neurospheres. Rabbit neurospheres were cultured for 3, 5, or 7 days under control or specific positive control conditions for each endpoint tested (PP2 10  $\mu\text{M}$ ; EGF 10 ng/mL; BMP7 100 ng/mL). A, 3 days migration; B, 3 days neuronal differentiation without supplementary FCS in the medium (wo FCS/wo FCS); C, 3 days neuronal differentiation with addition of 1% FCS in the differentiation medium (wo FCS/+FCS); D, 3 days neuronal differentiation with addition of 1% FCS in the proliferation and differentiation medium (+FCS/+FCS); E, 5 days oligodendrocyte differentiation; F, 7 days proliferation. All endpoints were evaluated in five neurospheres/condition in at least three independent experiments. Results presented as boxes and whiskers according to Tukey method. \* $P < .05$  vs control

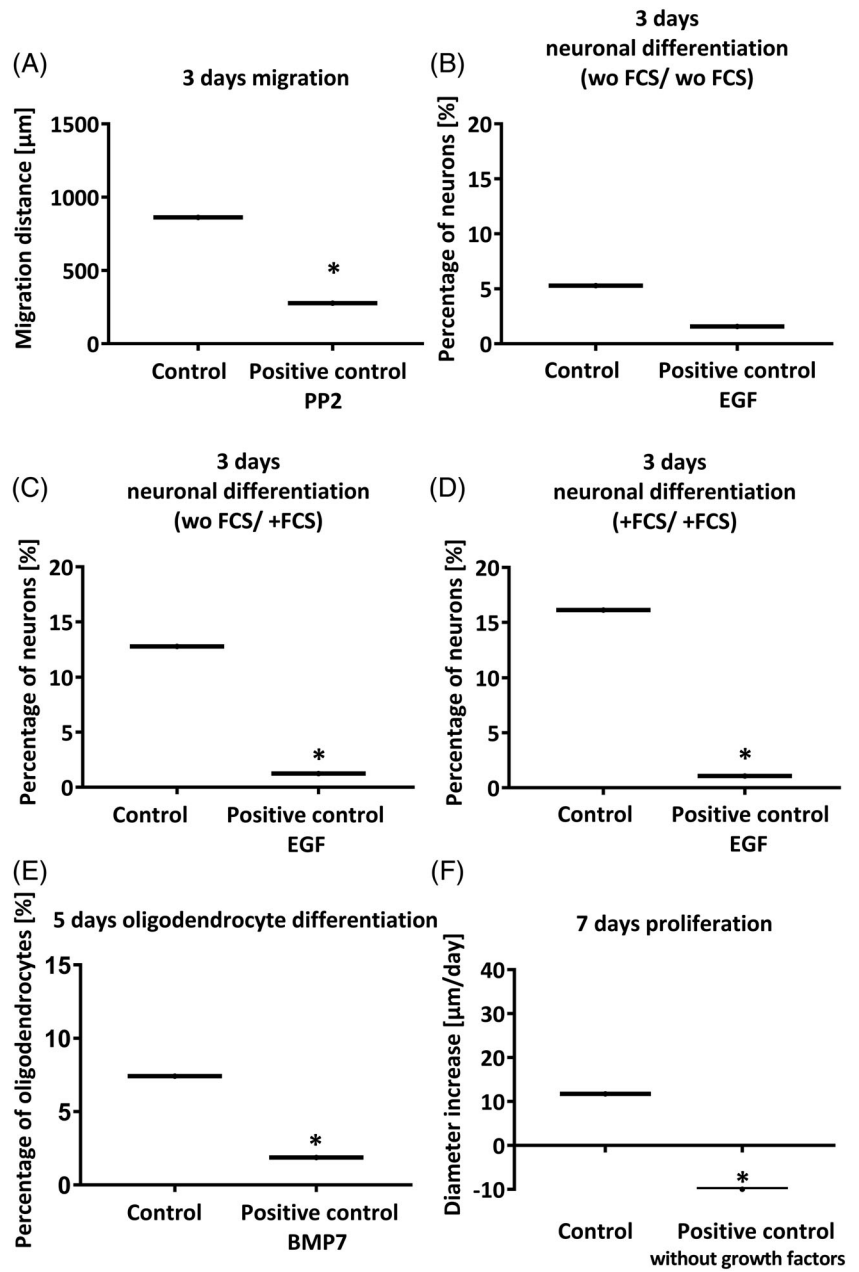
differentiation assays met quality criteria as shown in Figure 3. Interestingly, thawed neurospheres also achieved a 5% mean differentiation to neurons without adding any FCS to the differentiation or proliferation medium, probably because the freezing medium already contained FCS. Even so, as previously assayed with fresh spheres, FCS addition to differentiation and/or proliferating medium was also tested. In this case, FCS addition also induced an increase in neuronal differentiation, and as previously observed for fresh neurospheres, the longer the cells were exposed to FCS, the higher the percentage of neurons was. However, in this case, the percentage of neurons was so high in some wells (Figure 3; mean  $> 15\%$ ) that neurons were growing in clumps and overlapping one another making it very difficult to correctly quantify them. As thawed neurospheres without FCS addition in culture produced a percentage of neurons that could be precisely quantified, and also with the aim to not introduce more factors to the medium which could mask adverse effects induced by

physical or chemical agents in future tests, this culture condition (without FCS) was chosen for further experiments.

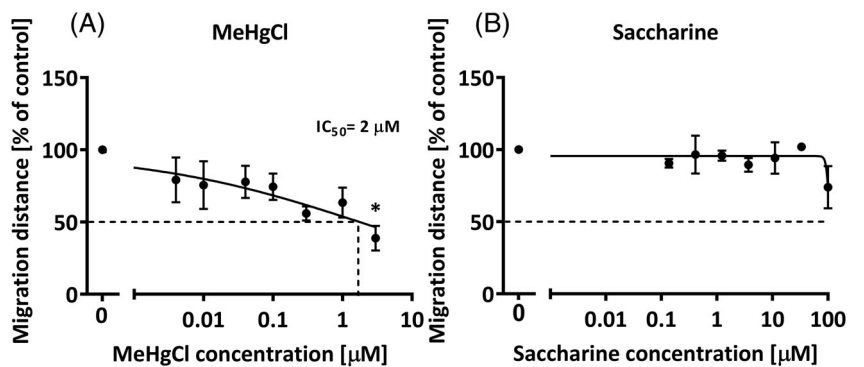
Thawed neurospheres were also tested in parallel in control and positive control conditions, using the same compounds than for fresh neurospheres. In all cases, positive controls decreased the result obtained in control conditions. In view of these results, all further experiments were performed with neurospheres submitted to the freezing protocol at passage 0.

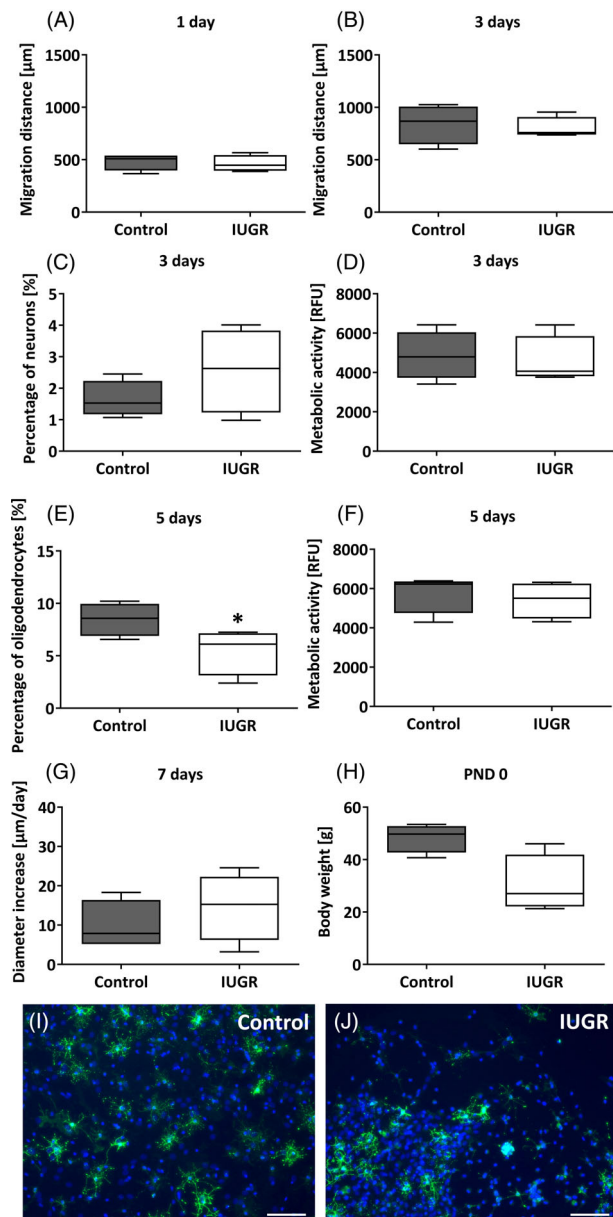
To prove that rabbit neurospheres are able to detect alterations induced during the course of neurodevelopment without being oversensitive, we exposed them to two compounds in a concentration-range mode, a positive and a negative control, following the recommendations of Crofton et al.<sup>36</sup> One is a known neurodevelopmental toxicant in humans and animals, methylmercury chloride (MeHgCl; positive control) and the other one a compound known to have no effects on neurodevelopment in humans and animals, saccharine

**FIGURE 3** Results of the “Neurosphere Assay” establishment with thawed rabbit neurospheres. Thawed rabbit neurospheres were cultured for 3, 5, or 7 days under control conditions or exposed to specific positive controls for each endpoint tested (PP2 10  $\mu$ M; EGF 10 ng/mL; BMP7 100 ng/mL). A, 3 days migration; B, 3 days neuronal differentiation without supplementary FCS in the medium (wo FCS/wo FCS); C, 3 days neuronal differentiation with addition of 1% FCS in the differentiation medium (wo FCS/+FCS); D, 3 days neuronal differentiation with addition of 1% FCS in the proliferation and differentiation medium (+FCS/+FCS); E, 5 days oligodendrocyte differentiation; F, 7 days proliferation. All endpoints were evaluated in five neurospheres/condition in at least three independent experiments. Results presented as boxes and whiskers according to Tukey’s method. \* $P < .05$  vs control



**FIGURE 4** Rabbit neurospheres sensitivity and specificity evaluation. Thawed rabbit neurospheres were cultured for 1 day with increasing concentrations of the known neurodevelopmental toxicant: MeHgCl, A, or a compound known to have no neurodevelopmental adverse effects: Saccharine, B. Results presented as mean  $\pm$  SEM of at least three independent experiments including five neurospheres/concentration and analyzed by ANOVA and Bonferroni post hoc test. \* $P < .05$  vs control





**FIGURE 5** Comparison of control and IUGR neurospheres on basic processes of neurogenesis. Thawed rabbit neurospheres obtained from control and IUGR animals were cultured for 3, 5, or 7 days and comparatively tested for each endpoint of the “Neurosphere Assay.” A, Migration distance after 1 day; or B, 3 days; C, neuronal differentiation after 3 days; D, metabolic activity after 3 days; E, oligodendrocyte differentiation after 5 days; F, metabolic activity after 5 days; G, diameter increase after 7 days; H, body weight of control and IUGR pups on PND0; I and J, representative pictures of oligodendrocyte differentiation in control and IUGR neurospheres, respectively. Scale bars = 100 μm. All endpoints (except body weight, H) were evaluated in five neurospheres/condition in at least three independent experiments. Results presented as boxes and whiskers according to Tukey method. \* $P < .05$  IUGR vs control

(negative control; reviewed by Aschner et al.<sup>38</sup>). MeHgCl induced a significant and concentration-dependent decrease in neural progenitor cell migration, with an  $IC_{50}$  of 2 μM (Figure 4), while saccharine did

not significantly decrease migration at any concentration tested (maximum concentration tested = 100 μM).

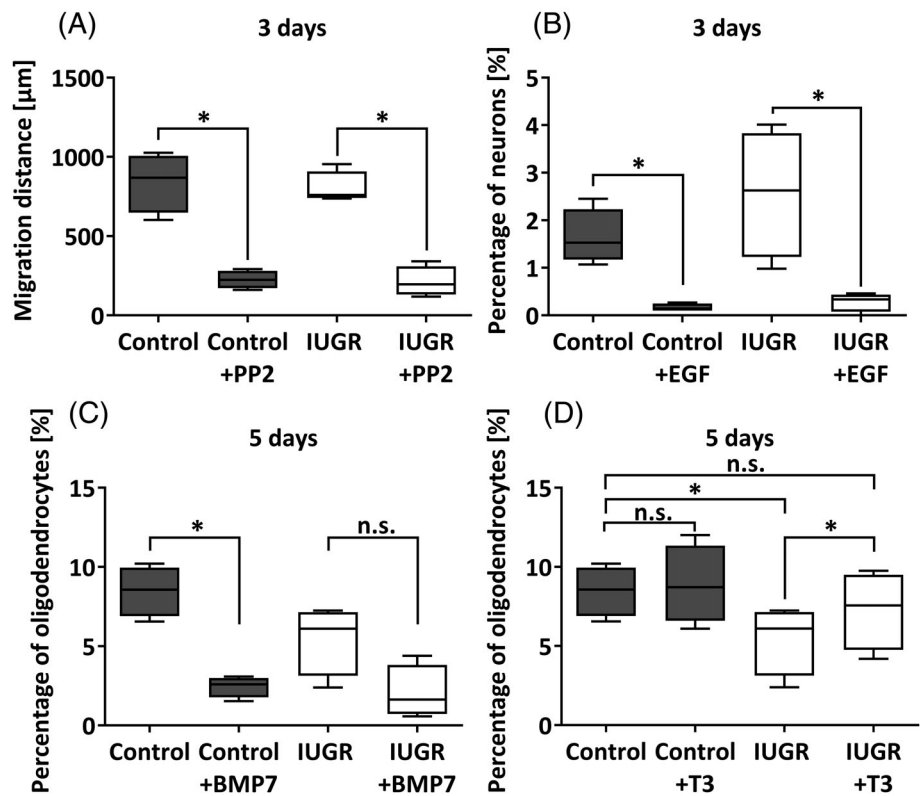
### 3.2 | Evaluation of the effects of IUGR in neurodevelopmental processes

The aim of establishing a rabbit neurosphere culture was to develop a model to study the effects of IUGR on brain development in a more time- and cost-efficient way with using fewer numbers of animals. Therefore, we used the rabbit “Neurosphere Assay” to investigate the specific consequences of IUGR induction by ligation of 40% to 50% of uteroplacental vessels irrigating the gestational sac between GD25 and GD30. Neurospheres from four control and four IUGR pups with mean birth weight  $\pm$  SEM = 48.4  $\pm$  1.4 g and 30.3  $\pm$  2.7 g respectively ( $P = .06$ ; Figure 5), and belonging to three different litters were frozen and thawed in pairs and submitted to exactly the same conditions in vitro. The neurospheres of these four pups per experimental group were used to perform all following experiments. Neurospheres from IUGR animals did not present any significant difference in NPC proliferation after 7 days in culture or in migration after 1 or 3 days in culture (Figure 5). A non-significant increase in neuronal differentiation was observed in IUGR neurospheres (Figures 5), while oligodendrocyte differentiation was significantly decreased in IUGR neurospheres compared to control spheres (Figures 5). Viability of these NPCs, measured by their metabolic activity, was not altered in any of these cases (3 or 5 days in culture; Figure 5), indicating that the decreased number of differentiated oligodendrocytes is a specific effect not induced by general cytotoxicity. By contrast, there were no differences between control and IUGR neurospheres proliferating capabilities (Figure 5). In summary, the results of the “Neurosphere Assay” indicated that IUGR impairs NPCs’ differentiation ability into oligodendrocytes, while their proliferation and migration potential is not affected. To contextualize these in vitro results, it is important to remark that both, mild and strong IUGR cases were included (Figure 5) in the preparation of neurospheres for these tests and therefore, the total body weight of IUGR pups was not significantly reduced compared to the controls ( $P = .06$ ). This approach was chosen to cover the broad range of cases that IUGR can display, and to exclude the possibility of detecting effects that are only present in the most severe IUGR cases.

Furthermore, the response of control and IUGR neurospheres to positive controls known to modulate the response of each endpoint was also compared (Figure 6). As previously shown in Figure 3, positive controls significantly reduce the respective readouts of all endpoints in control spheres. However, in IUGR spheres, the exposure to BMP7 did not significantly reduce oligodendrocyte differentiation, probably because in IUGR neurospheres oligodendrocyte differentiation was already reduced per se (Figure 6). Even if the effect of BMP7 was not significant, it reduced the mean oligodendrocyte differentiation in IUGR neurospheres. These data show that the process is also dynamic in IUGR neurospheres as compounds in vitro can still modulate the impairment of oligodendrocyte differentiation. In the next step, we tested if this decreased differentiation can also be modulated



**FIGURE 6** Comparison of the response of IUGR and control neurospheres to known modulators of basic neurogenesis processes. Thawed rabbit neurospheres obtained from control and IUGR animals were cultured for 3 or 5 days and comparatively tested for each endpoint. Neuronal differentiation was analyzed after 3 days under control conditions or exposed to either PP2 10  $\mu$ M, A, or EGF 20 ng/mL, B, oligodendrocyte differentiation was analyzed after 5 days under control conditions or exposed to either BMP7 100 ng/mL, C, or T3 3 nM, D. All endpoints were evaluated in five neurospheres/condition in at least three independent experiments. Results presented as boxes and whiskers according to Tukey method. \* $P < .05$  vs control condition; n.s.: not significant



in the opposite direction to increase the percentage of oligodendrocytes and revert the observed adverse effect. Thyroid hormone (TH) plays an essential role in white matter maturation and myelin formation.<sup>39-42</sup> For this reason, we exposed control and IUGR neurospheres to L-triiodothyronine (T3; CAS: 55-06-1; Sigma-Aldrich), the active form of TH, at a concentration similar to the total T3 concentration in human serum, 3 nM.<sup>43-46</sup> T3 exposure significantly induced the percentage of oligodendrocyte differentiation of IUGR neurospheres to control levels, while it did not affect the percentage of differentiation in control neurospheres (Figure 6). Hence, although the cellular damage was set while cells were still in the in vivo context, in vitro exposure of ex vivo NPCs to T3 can revert the deleterious effect of IUGR in oligodendrocyte differentiation.

## 4 | DISCUSSION

The neurosphere model based on NPCs is a valuable tool to study the progress of basic neurodevelopmental processes.<sup>47</sup> Therefore, we have previously established “Neurosphere Assays” based on rat, mouse or human NPCs as methods to evaluate the adverse effects of chemical or physical agents on neurodevelopment.<sup>24-28,30,37,48</sup> Due to its nature as a primary cell culture, the neurosphere model retains the original characteristics of the neuro- and gliogenic populations of the brain, and reflects their physiological and physiopathological characteristics. To evaluate the effects of IUGR in neurodevelopment, the ideal situation would be to use a human NPC based “Neurosphere Assay” to avoid species translation limitations.<sup>49</sup> Yet commercially

available hNPCs are derived from healthy individuals, and hNPCs from IUGR individuals are such an extremely scarce material that they are unviable to establish a permanent research model for mechanistic investigations. Therefore, and considering that the rabbit in vivo model previously developed in BCNatal mimics the neurodevelopmental features of human IUGR individuals better than other rat in vivo models, and that rabbits are perinatal brain developers<sup>50</sup> similar to humans and unlike rodents,<sup>51</sup> we decided to establish a rabbit neurosphere culture for the first time. The combination of a 3D in vitro neurodevelopmental testing strategy, with the clinically relevant IUGR experimental animal model allowed us to study IUGR neurodevelopmental consequences by decomposing them into basic neurodevelopmental processes, which are evaluated separately. This methodology offers a research approach that allows studying a complex clinical problem on the cellular, and eventually also molecular level. By employing this newly established in vitro model we identified that rabbit NPCs from IUGR individuals have a significantly reduced ability to form oligodendrocytes. Moreover, we were able to revert this damage by T3 in vitro exposure.

In the present study, we established the in vitro rabbit neurosphere model with cells obtained from freshly dissected rabbit brains (Figure 2) and we tested different freezing protocols, choosing the best one (based on PO cells) for the use of NPCs in the “Neurosphere Assay” (Figure 3). Neurospheres obtained from both protocols (from fresh and frozen cells) spontaneously formed after 7 days in culture and were able to perform all basic neurodevelopmental processes (proliferation, migration, and differentiation) similar to neurospheres from other species, for example, rats, mice and humans.<sup>24-28,30,37,48</sup> Among the

differentiated cells, glial cells outnumbered neuronal cells, according to the situation described in vivo for other species indicating that a massive number of glial cells is generated during postnatal neurodevelopment.<sup>52</sup> Specific data in vivo for rabbits during the postnatal period could not be found, but the glia neuron ratio described in adult rabbits also shows that in all brain areas except in the cerebellum, glial cells outnumber neurons.<sup>53</sup> According to the 3R principle of Russel and Burch (1959) for the reduction, replacement and refinement of animal experimentation the established freezing and thawing protocol for rabbit NPCs constitutes a durable technique to reduce and refine the use of animals. Neurospheres obtained from both protocols are dynamic systems since their ability to proliferate, migrate or differentiate was modified by exposure to known positive control compounds (PP2, EGF, BMP7, or growth factor removal in Figures 2 and 3). With respect to the modulation of the performance of these neurospheres, we also proved that a known developmental neurotoxic compound, MeHgCl, induces a significant decrease in cell migration (Figure 4), showing that this rabbit neurosphere model is sensitive to known noxious agents. The IC<sub>50</sub> concentration detected by the model is in line with previously detected IC<sub>50</sub> concentrations in human primary or human iPSC-derived neurosphere models for migration disturbance<sup>26,30,54</sup> and correlates well with concentrations achieved in vivo after the administration of MeHgCl doses affecting neurodevelopment.<sup>55</sup> Understanding the sensitivity of a model is a key step for its establishment, that is, it is also essential to ensure that the system is not over-reactive to any stimulus, which means that known innocuous compounds for neurodevelopment should not alter the response of neurospheres in the assay. For this purpose, saccharine was chosen as negative control, because it was already selected as a harmless compound for neurodevelopment by a panel of experts.<sup>38</sup> When saccharine was added to the neurosphere culture in concentrations up to 100 μM no adverse effect in migration was observed, indicating the specificity of the assay. This tiered approach for the establishment of the rabbit neurosphere culture, besides being a necessary preliminary group of steps for our subsequent study of IUGR effects, is an essential procedure for the establishment of the method as an alternative model for developmental neurotoxicity detection and the screening and prioritization of chemicals (following the recommendations from Crofton et al.<sup>36</sup>). Current neurodevelopmental studies on the effects of exposure to substances during the pre- and early postnatal period are based on the in vivo OECD guidelines 426 (OECD, 2007), 414 (OECD, 2018), and FDA guideline S5 (R3) (FDA 2017) which define rat as the preferred rodent and rabbit as the preferred nonrodent animal. A rat neurosphere model for compound evaluation has already been available since 2014,<sup>37</sup> and now the addition of the neurosphere model of the preferred nonrodent animal opens the door to combine these two models for in vitro DNT evaluation in case the use of human material is not possible or for understanding species differences in response to exogenous insults.

After performing all establishment steps with control neurospheres: establishment of the (a) fresh culture, (b) freezing and thawing protocol, and analyzing the system's, (c) dynamism, (d) sensitivity, and (e) specificity, we compared the performance of control and IUGR NPCs in the "Neurosphere Assay." Here, we identified a significant reduction in oligodendrocyte formation in IUGR

NPCs. This observation in vitro leads to the possible correlation with a poor myelination in vivo as a cause of neurological damage secondary to IUGR. Our finding is in line with previous studies in vivo reporting that IUGR leads to white matter injury with a deficiency of mature oligodendrocytes<sup>56,57</sup> and adversely affected myelination processes in brain histology studies.<sup>13</sup> It is important to remark that the adverse effect on oligodendrogenesis in this study was detected in neurospheres obtained both from severe and mild IUGR cases, and therefore the effect was not only observed in the most severe IUGR cases. These findings are in line with clinical and neuroimaging data supporting the existence of fetal abnormal neurodevelopment across all stages of severity in IUGR. In comparison of control and IUGR neurospheres, we also observed an increase in neuronal differentiation after 3 days in culture but this effect was not significant. Future investigations should focus on the prolongation of the period in culture to obtain more stable results (decrease deviation of IUGR results) and to clarify if this incipient increase is significant after 5, 7, 14, or more days in culture and it is consequently another alteration underlying IUGR neural damage. Besides, after a longer culture period, further neurodevelopmental endpoints could also be added to the assay, like neurite outgrowth, neurite branching, synaptogenesis and probably neuronal network activity. In future work it would also be of high interest to assess alterations in astrocyte differentiation, using the protocol established here.

We finally tested a possible future neurotherapy for IUGR: in vitro exposure to 3 nM of T3 completely reverted the damage induced by IUGR by inducing oligodendrocyte differentiation, while it did not increase the percentage of oligodendrocytes in control neurospheres (Figure 6). This TH effect in rabbit control NPCs is similar to the one observed in human neurospheres in vitro, where 3 nM T3 exposure does not induce an increase in the percentage of oligodendrocytes in control neurospheres, but induces oligodendrocyte maturation.<sup>32</sup> If T3 also induces rabbit oligodendrocyte maturation in vitro will be subject to future studies. The transferability of this possible therapy to the clinical field, needs to be carefully assessed for this particular condition, but in support of its transferability it is important to mention that preclinical studies and clinical studies using Tetrac, the TH analog 3,5,3',5'-tetraiodothyroacetic acid, have already been conducted or are conducted at the moment with the goal of supplementing hypothyroid developing brains with TH (ClinicalTrials.gov identifier: NCT04143295). Preclinical studies in mice show that postnatal administration of this potent TH receptor agonist offers the opportunity to reduce the neurological damage associated to the lack of MCT8, a transporter playing a critical role in the uptake of thyroid hormones.<sup>58</sup> The results of the clinical trials conducted in MCT8 deficiency patients (also known as Allan-Herndon-Dudley syndrome) will be of high importance to evaluate the future transferability of the proposed therapeutic strategy in IUGR cases.

In summary, we established an in vitro model for the study of IUGR-induced neural damage which is faster, more economic and more ethical than the current in vivo approaches in rabbits. Using our new model we detected that oligodendrogenesis is reduced in IUGR brains and that this effect is reversed by exposure to T3. This work opens the door to the use of the rabbit "Neurosphere Assay" (a) for

testing developmental neurotoxic compounds as a complementary method to the rat “Neurosphere Assay,” (b) for studying IUGR-induced neural damage on the cellular and molecular level, (c) for a future identification of possible disease biomarkers, and (d) for the evaluation and selection of specific neuroprotective therapies.

## ACKNOWLEDGMENTS

We thank Dr. Catrin Albrecht for her logistical support and valuable advice. Graphical abstract and Figure 1 were created with BioRender.com. This study has been funded by Instituto de Salud Carlos III through the project “PI18/01763” (co-funded by European Regional Development Fund/European Social Fund, “Investing in your future”), from “LaCaixa” Foundation under grant agreements LCF/PR/GN14/10270005 and LCF/PR/GN18/10310003, and from AGAUR under grant 2017 SGR n° 1531. B.A.K. received a scholarship from Fundació Bosch i Gimpera (project number: 300155) and C.L. received the support the Health Department of the Catalan Government (grant n° SLT006/17/00325). Open access funding enabled and organized by Projekt DEAL.

## CONFLICT OF INTEREST

The authors declared no potential conflicts of interest.

## AUTHOR CONTRIBUTIONS

M.B.: conception and design, collection and assembly of data, data analysis and interpretation, manuscript writing; M.I.: conception and design, provision of study material, data analysis and interpretation, manuscript critical revision; M.H.: collection and assembly of data, data analysis and interpretation; C.L., L.P., J.K.: collection and assembly of data; B.A.K.: data analysis and interpretation, manuscript writing; J.G.-C.: provision of study material, manuscript critical revision; J. M.B.: administrative support, provision of study material; F.C.: conception and design, data analysis and interpretation, financial support; E.G.: conception and design, financial support, manuscript critical revision; E.F.: conception and design, data analysis and interpretation, manuscript critical revision. All authors have read and approved the final manuscript.

## DATA AVAILABILITY STATEMENT

The data that support the findings of this study are available from the corresponding author upon reasonable request.

## ORCID

Marta Barenys  <https://orcid.org/0000-0001-5046-9796>

## REFERENCES

- Sharma D, Shastri S, Sharma P. Intrauterine growth restriction: antenatal and postnatal aspects. *Clin Med Insights Pediatr*. 2016;10: CMPed.S40070. <https://doi.org/10.4137/CMPed.S40070>.
- Eixarch E, Muñoz-Moreno E, Bargallo N, Batalle D, Gratacos E. Motor and cortico-striatal-thalamic connectivity alterations in intrauterine growth restriction. *Am J Obstet Gynecol*. 2016;214(6):725.e1-725.e9. <https://doi.org/10.1016/j.ajog.2015.12.028>.
- Batalle D, Muñoz-Moreno E, Arbat-Plana A, et al. Long-term reorganization of structural brain networks in a rabbit model of intrauterine growth restriction. *Neuroimage*. 2014;100:24-38. <https://doi.org/10.1016/j.neuroimage.2014.05.065>.
- Kady SM, Gardosi J. Perinatal mortality and fetal growth restriction. *Best Pract Res Clin Obstet Gynaecol*. 2004;18(3):397-410. <https://doi.org/10.1016/j.bpobgyn.2004.02.009>.
- Marsal K. Intrauterine growth restriction. *Curr Opin Obstet Gynecol*. 2002;14(2):127-135.
- Geva R, Eshel R, Leitner Y, Valevski AF, Harel S. Neuropsychological outcome of children with intrauterine growth restriction: a 9-year prospective study. *Pediatrics*. 2006;118(1):91-100. <https://doi.org/10.1542/peds.2005-2343>.
- Morsing E, Åsard M, Ley D, Stjernqvist K, Maršál K. Cognitive function after intrauterine growth restriction and very preterm birth. *Pediatrics*. 2011;127(4):e874-e882. <https://doi.org/10.1542/peds.2010-1821>.
- Tideman E, Maršál K, Ley D. Cognitive function in young adults following intrauterine growth restriction with abnormal fetal aortic blood flow. *Ultrasound Obstet Gynecol*. 2007;29(6):614-618. <https://doi.org/10.1002/uog.4042>.
- Geva R, Eshel R, Leitner Y, Fattal-Valevski A, Harel S. Memory functions of children born with asymmetric intrauterine growth restriction. *Brain Res*. 2006;1117(1):186-194. <https://doi.org/10.1016/j.brainres.2006.08.004>.
- Rees S, Harding R, Walker D. The biological basis of injury and neuroprotection in the fetal and neonatal brain. *Int J Dev Neurosci*. 2011;29(6):551-563. <https://doi.org/10.1016/j.ijdevneu.2011.04.004>.
- Fleiss B, Wong F, Brownfoot F, et al. Knowledge gaps and emerging research areas in intrauterine growth restriction-associated brain injury. *Front Endocrinol (Lausanne)*. 2019;10:1-24. <https://doi.org/10.3389/fendo.2019.00188>.
- Eixarch E, Figueras F, Hernández-Andrade E, et al. An experimental model of fetal growth restriction based on selective ligation of uteroplacental vessels in the pregnant rabbit. *Fetal Diagn Ther*. 2009;26(4):203-211. <https://doi.org/10.1159/000264063>.
- Eixarch E, Batalle D, Illa M, et al. Neonatal neurobehavior and diffusion MRI changes in brain reorganization due to intrauterine growth restriction in a rabbit model. *PLoS One*. 2012;7(2):1-12. <https://doi.org/10.1371/journal.pone.0031497>.
- Carter AM. Animal models of human placentation—a review. *Placenta*. 2007;28(Suppl):S41-S47. <https://doi.org/10.1016/j.placenta.2006.11.002>.
- Derrick M, Luo NL, Bregman JC, et al. Preterm fetal hypoxia-ischemia causes hypertonia and motor deficits in the neonatal rabbit: a model for human cerebral palsy? *J Neurosci*. 2004;24(1):24-34. <https://doi.org/10.1523/JNEUROSCI.2816-03.2004>.
- Workman AD, Charvet CJ, Clancy B, Darlington RB, Finlay BL. Modeling transformations of neurodevelopmental sequences across mammalian species. *J Neurosci*. 2013;33(17):7368-7383. <https://doi.org/10.1523/JNEUROSCI.5746-12.2013>.
- Drobyshevsky A, Derrick M, Wyrwicz AM, et al. White matter injury correlates with hypertonia in an animal model of cerebral palsy. *J Cereb Blood Flow Metabol* 2007;27:270-281. <https://doi.org/10.1038/sj.jcbfm.9600333>
- van de Looij Y, Lodygensky GA, Dean J, et al. High-field diffusion tensor imaging characterization of cerebral white matter injury in lipopolysaccharide-exposed fetal sheep. *Pediatr Res*. 2012;72(3):285-292. <https://doi.org/10.1038/pr.2012.72>.
- McKinstry RC, Mathur A, Miller JH, et al. Radial organization of developing preterm human cerebral cortex revealed by non-invasive water diffusion anisotropy MRI. *Cereb Cortex*. 2002;12(12):1237-1243. <https://doi.org/10.1093/cercor/12.12.1237>.

20. Illa M, Eixarch E, Bataille D, et al. Long-term functional outcomes and correlation with regional brain connectivity by MRI diffusion tractography metrics in a near-term rabbit model of intrauterine growth restriction. *PLoS One*. 2013;8(10):e76453. <https://doi.org/10.1371/journal.pone.0076453>.
21. Bataille D, Eixarch E, Figueras F, et al. Altered small-world topology of structural brain networks in infants with intrauterine growth restriction and its association with later neurodevelopmental outcome. *Neuroimage*. 2012;60(2):1352-1366. <https://doi.org/10.1016/j.neuroimage.2012.01.059>.
22. Bassan H, Leider Trejo L, Kariv N, et al. Experimental intrauterine growth retardation alters renal development. *Pediatr Nephrol*. 2000; 15(3-4):192-195. <https://doi.org/10.1007/s004670000457>.
23. Eixarch E, Hernandez-Andrade E, Crispi F, et al. Impact on fetal mortality and cardiovascular Doppler of selective ligation of uteroplacental vessels compared with undernutrition in a rabbit model of intrauterine growth restriction. *Placenta*. 2011;32(4):304-309. <https://doi.org/10.1016/j.placenta.2011.01.014>.
24. Barenys M, Gassmann K, Baksmeier C, et al. Epigallocatechin gallate (EGCG) inhibits adhesion and migration of neural progenitor cells in vitro. *Arch Toxicol*. 2017;91:827-837. <https://doi.org/10.1007/s00204-016-1709-8>.
25. Moors M, Cline JE, Abel J, Fritsche E. ERK-dependent and -independent pathways trigger human neural progenitor cell migration. *Toxicol Appl Pharmacol*. 2007;221(1):57-67. <https://doi.org/10.1016/j.taap.2007.02.018>.
26. Moors M, Rockel TD, Abel J, et al. Human neurospheres as three-dimensional cellular systems for developmental neurotoxicity testing. *Environ Health Perspect*. 2009;117(7):1131-1138. <https://doi.org/10.1289/ehp.0800207>.
27. Breier JM, Gassmann K, Kayser R, et al. Neural progenitor cells as models for high-throughput screens of developmental neurotoxicity: state of the science. *Neurotoxicol Teratol*. 2010;32(1):4-15. <https://doi.org/10.1016/j.ntt.2009.06.005>.
28. Gassmann K, Abel J, Bothe H, et al. Species-specific differential AhR expression protects human neural progenitor cells against developmental neurotoxicity of PAHs. *Environ Health Perspect*. 2010;118(11):1571-1577.
29. Schreiber T, Gassmann K, Götz C, et al. Polybrominated diphenyl ethers induce developmental neurotoxicity in a human in vitro model: evidence for endocrine disruption. *Environ Health Perspect*. 2010;118(4):572-578. <https://doi.org/10.1289/ehp.0901435>.
30. Baumann J, Gassmann K, Masjosthusmann S, et al. Comparative human and rat neurospheres reveal species differences in chemical effects on neurodevelopmental key events. *Arch Toxicol*. 2016;90(6):1415-1427. <https://doi.org/10.1007/s00204-015-1568-8>.
31. Gassmann K, Schreiber T, Dingemans MML, et al. BDE-47 and 6-OH-BDE-47 modulate calcium homeostasis in primary fetal human neural progenitor cells via ryanodine receptor-independent mechanisms. *Arch Toxicol*. 2014;88(8):1537-1548. <https://doi.org/10.1007/s00204-014-1217-7>.
32. Dach K, Bendt F, Huebenthal U, et al. BDE-99 impairs differentiation of human and mouse NPCs into the oligodendroglial lineage by species-specific modes of action. *Sci Rep*. 2017;7(March):1-11. <https://doi.org/10.1038/srep44861>.
33. Masjosthusmann S, Siebert C, Huebenthal U, Bendt F, Baumann J, Fritsche E. Arsenite interrupts neurodevelopmental processes of human and rat neural progenitor cells: the role of reactive oxygen species and species-specific antioxidative defense. *Chemosphere*. 2019;235:447-456. <https://doi.org/10.1016/j.chemosphere.2019.06.123>.
34. Claassen DA, Desler MM, Rizzino A. ROCK inhibition enhances the recovery and growth of cryopreserved human embryonic stem cells and human induced pluripotent stem cells. *Mol Reprod Dev*. 2009;76(8):722-732. <https://doi.org/10.1002/mrd.21021>.
35. Schneider CA, Rasband WS, Eliceiri KW. NIH Image to ImageJ: 25 years of image analysis. *Nat Methods*. 2012;9(7):671-675. <https://doi.org/10.1038/nmeth.2089>.
36. Crofton KM, Mundy WR, Lein PJ, et al. Developmental neurotoxicity testing: recommendations for developing alternative methods for the screening and prioritization of chemicals. *ALTEX*. 2011;28(1):9-15. <https://doi.org/10.14573/altex.2011.1.009>.
37. Baumann J, Barenys M, Gassmann K, Fritsche E. Comparative human and rat "neurosphere assay" for developmental neurotoxicity testing. *Curr Protoc Toxicol*. 2014;1(SUPPL.59):1-24. <https://doi.org/10.1002/0471140856.tx1221s59>.
38. Aschner M, Ceccatelli S, Daneshian M, et al. Reference compounds for alternative test methods to indicate developmental neurotoxicity (DNT) potential of chemicals: example lists and criteria for their selection and use. *ALTEX*. 2017;34(1):49-74. <https://doi.org/10.14573/altex.1604201>.
39. Namba N, Etani Y, Kitaoka T, et al. Clinical phenotype and endocrinological investigations in a patient with a mutation in the MCT8 thyroid hormone transporter. *Eur J Pediatr*. 2008;167(7):785-791. <https://doi.org/10.1007/s00431-007-0589-6>.
40. Rodrigues F, Grenha J, Ortez C, et al. Hypotonic male infant and MCT8 deficiency—a diagnosis to think about. *BMC Pediatr*. 2014;14(38 cm):252. <https://doi.org/10.1186/1471-2431-14-252>.
41. Marta CB, Adamo AM, Soto EF, Pasquini JM. Sustained neonatal hyperthyroidism in the rat affects myelination in the central nervous system. *J Neurosci Res*. 1998;53(2):251-259. [https://doi.org/10.1002/\(SICI\)1097-4547\(19980715\)53:2<251::AID-JNR14>3.0.CO;2-9](https://doi.org/10.1002/(SICI)1097-4547(19980715)53:2<251::AID-JNR14>3.0.CO;2-9).
42. Rodriguez-Pena A, Ibarrola N, Iniguez MA, Munoz A, Bernal J. Neonatal hypothyroidism affects the timely expression of myelin-associated glycoprotein in the rat brain. *J Clin Invest*. 1993;91(3):812-818. <https://doi.org/10.1172/JCI116301>.
43. Anckarsäter R, Zetterberg H, Blennow K, Anckarsäter H. Association between thyroid hormone levels and monoaminergic neurotransmission during surgery. *Psychoneuroendocrinology*. 2007;32(8-10):1138-1143. <https://doi.org/10.1016/j.psyneuen.2007.07.007>.
44. Johansson P, Almqvist EG, Johansson J-O, et al. Reduced cerebrospinal fluid level of thyroxine in patients with Alzheimer's disease. *Psychoneuroendocrinology*. 2013;38(7):1058-1066. <https://doi.org/10.1016/j.psyneuen.2012.10.012>.
45. Hagen GA, Elliott WJ. Transport of thyroid hormones in serum and cerebrospinal fluid. *J Clin Endocrinol Metab*. 1973;37(3):415-422. <https://doi.org/10.1210/jcem-37-3-415>.
46. Nishikawa M, Inada M, Naito K, et al. 3,3',5'-Triiodothyronine (reverse T3) in human cerebrospinal fluid. *J Clin Endocrinol Metab*. 1981;53(5):1030-1035. <https://doi.org/10.1210/jcem-53-5-1030>.
47. Svendsen CN, ter Borg MG, Armstrong RJ, et al. A new method for the rapid and long term growth of human neural precursor cells. *J Neurosci Methods*. 1998;85(2):141-152. [https://doi.org/10.1016/S0165-0270\(98\)00126-5](https://doi.org/10.1016/S0165-0270(98)00126-5).
48. Fritsche E, Cline JE, Nguyen N-H, Scanlan TS, Abel J. Polychlorinated biphenyls disturb differentiation of normal human neural progenitor cells: clue for involvement of thyroid hormone receptors. *Environ Health Perspect*. 2005;113(7):871-876.
49. Leist M, Hartung T. Inflammatory findings on species extrapolations: humans are definitely no 70-kg mice. *Arch Toxicol*. 2013;87(4):563-567.
50. Harel S, Shapira Y, Tomer A, Donahue MJ, Quilligan E. Vascular-induced intrauterine growth retardation: relations between birth weight and the development of biochemical parameters in young rabbits. *Isr J Med Sci*. 1985;21(10):829-832.
51. Drobyshevsky A, Jiang R, Derrick M, Luo K, Tan S. Functional correlates of central white matter maturation in perinatal period in rabbits. *Exp Neurol*. 2014;261:76-86. <https://doi.org/10.1016/j.expneurol.2014.06.021>.

52. Herculano-Houzel S. The glia/neuron ratio: how it varies uniformly across brain structures and species and what that means for brain physiology and evolution. *Glia*. 2014;62(9):1377-1391. <https://doi.org/10.1002/glia.22683>.
53. Herculano-Houzel S, Ribeiro P, Campos L, et al. Updated neuronal scaling rules for the brains of Glires (rodents/lagomorphs). *Brain Behav Evol*. 2011;78(4):302-314. <https://doi.org/10.1159/000330825>.
54. Hofrichter M, Nimtz L, Tigges J, et al. Comparative performance analysis of human iPSC-derived and primary neural progenitor cells (NPC) grown as neurospheres in vitro. *Stem Cell Res*. 2017;25:72-82. <https://doi.org/10.1016/j.scr.2017.10.013>.
55. Lewandowski TA, Ponce RA, Charleston JS, Hong S, Faustman EM. Effect of methylmercury on midbrain cell proliferation during organogenesis: potential cross-species differences and implications for risk assessment. *Toxicol Sci*. 2003;75(1):124-133.
56. Tolcos M, Petratos S, Hirst JJ, et al. Blocked, delayed, or obstructed: what causes poor white matter development in intrauterine growth restricted infants? *Prog Neurobiol*. 2017;154:62-77. <https://doi.org/10.1016/j.pneurobio.2017.03.009>.
57. Reid MV, Murray KA, Marsh ED, Golden JA, Simmons RA, Grinspan JB. Delayed myelination in an intrauterine growth

retardation model is mediated by oxidative stress upregulating bone morphogenetic protein 4. *J Neuropathol Exp Neurol*. 2012;71(7):640-653. <https://doi.org/10.1097/NEN.0b013e31825cfa81>.

58. Horn S, Kersseboom S, Mayerl S, et al. Tetrac can replace thyroid hormone during brain development in mouse mutants deficient in the thyroid hormone transporter Mct8. *Endocrinology*. 2013;154(2):968-979. <https://doi.org/10.1210/en.2012-1628>.

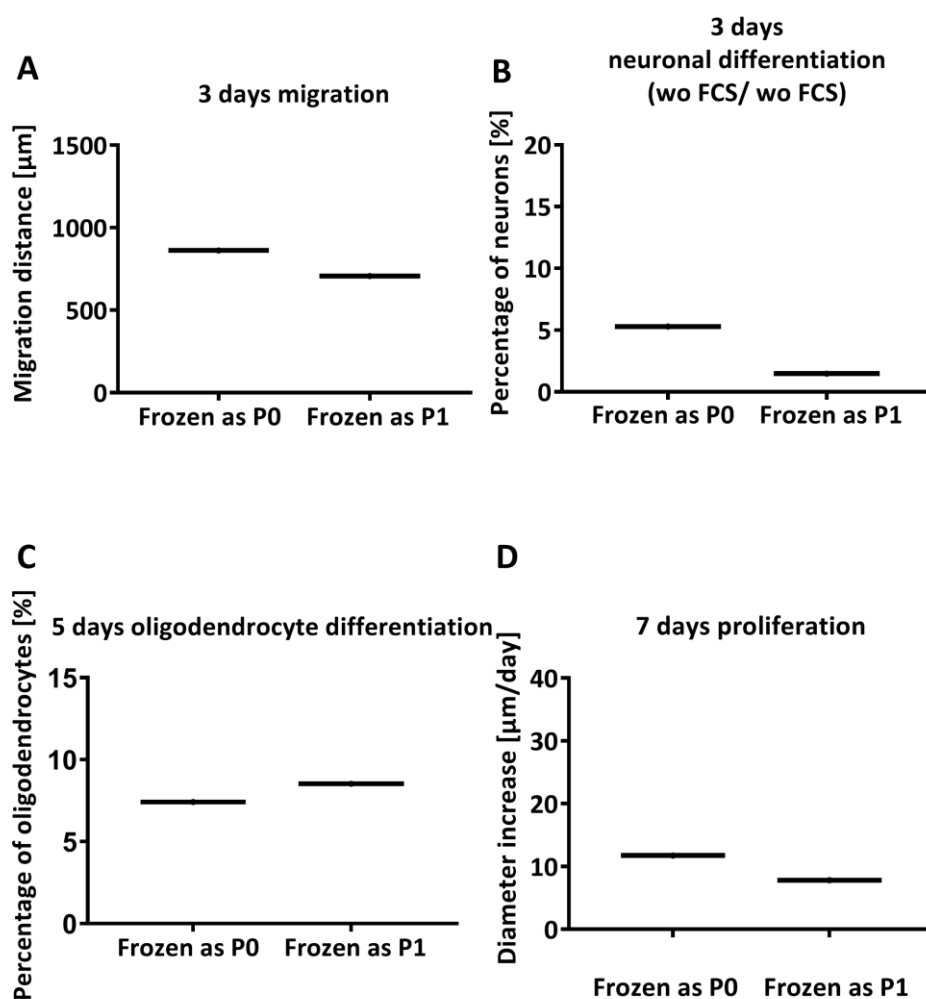
#### SUPPORTING INFORMATION

Additional supporting information may be found online in the Supporting Information section at the end of this article.

**How to cite this article:** Barenys M, Illa M, Hofrichter M, et al. Rabbit neurospheres as a novel in vitro tool for studying neurodevelopmental effects induced by intrauterine growth restriction. *STEM CELLS Transl Med*. 2021;10:209-221. <https://doi.org/10.1002/sctm.20-0223>

**Supplementary Material****Rabbit neurospheres as a novel *in vitro* tool for studying neurodevelopmental effects induced by intrauterine growth restriction**

Marta Barenys, Miriam Illa, Maxi Hofrichter, Carla Loreiro, Laura Pla, **Jördis Klose**, Britta Anna Kühne, Jesús Gómez-Catalán, Jan Matthias Braun, Fatima Crispi, Eduard Gratacós, Ellen Fritsche



**Figure S1:** Comparison of results of neurospheres which were frozen at passage 0 (P0) or at passage 1 (P1). Results of passage 0 are the same results presented in Figure 3 as control group.



**Rabbit neurospheres as a novel *in vitro* tool for studying neurodevelopmental effects induced by intrauterine growth restriction**

Marta Barenys, Miriam Illa, Maxi Hofrichter, Carla Loreiro, Laura Pla, **Jördis Klose**, Britta Anna Kühne, Jesús Gómez-Catalán, Jan Matthias Braun, Fatima Crispi, Eduard Gratacós, Ellen Fritsche

Journal: Stem Cells Translational Medicine

Impact Factor: 6.429 (2019-2020)

Contribution to the publication: 5 %

Some rabbit NPC preparation and cell culture,  
Performance of most of the migration experiments with  
control neurospheres

Type of authorship: co-authorship

Status of the publication: Published 9<sup>th</sup> October 2020



## 2.6 Neurodevelopmental toxicity assessment of flame retardants using a human DNT *in vitro* testing battery

**Jördis Klose**, Melanie Pahl, Kristina Bartmann, Farina Bendt, Jonathan Blum, Xenia Dolde, Anna-Katharina Holzer, Ulrike Hübenthal, Hagen Eike Keßel, Katharina Koch, Stefan Masjosthusmann, Sabine Schneider, Lynn-Christin Stürzl, Selina Woeste, Andrea Rossi, Adrian Covaci, Mamta Behl, Marcel Leist, Julia Tigges, Ellen Fritsche

### *Cell Biology and Toxicology*

Aufgrund ihrer neurologischen Entwicklungstoxizität sind Flammschutzmittel (flame retardants; FRs) wie z.B. polybromierte Diphenylether verboten und durch alternative FRs wie z.B. Organophosphate ersetzt worden, deren toxikologisches Profil jedoch meistens unbekannt ist. Um ihre neurologische Entwicklungstoxizität einzuschätzen, haben wir diesbezüglich das Gefährdungspotential mehrerer FRs untersucht. Das verwendete Testset umfasste hierbei ausgemusterte polybromierte FRs und Organophosphate: 2,2'4,4'-Tetrabromdiphenylether (BDE-47), 2,2'4,4',5-Pentabromdiphenylether (BDE-99), Tetrabromobisphenol A, Triphenylphosphat, Tris(2-butoxyethyl)phosphat und dessen Metabolit Bis-(2-butoxyethyl)phosphat, Isodecyl diphenyl phosphat, Isopropyliertes Triphenylphosphat, Trikresylphosphat, Tris(1,3-Dichlor-2-propyl)phosphat, Tert-Butylphenyl diphenyl phosphat, 2-Ethylhexyldiphenylphosphat, Tris(1-chlorisopropyl)phosphat und Tris(2-chlorethyl)phosphat. Hierfür verwendeten wir eine humanbasierte DNT *in vitro* Testbatterie, die eine Vielzahl von Endpunkten der neurologischen Entwicklung abdeckt. Die Potenz gemäß der jeweils empfindlichsten Benchmark-Konzentration (BMC) über die Batterie hinweg lag im Bereich von  $< 1 \mu\text{M}$  (5 FRs),  $1 < 10 \mu\text{M}$  (7 FRs) bis zum Bereich von  $> 10 \mu\text{M}$  (3 FRs). Die Datenauswertung zur Priorisierung mit dem ToxPi-Tool ergab eine andere Rangfolge a) als mit den BMC Werten und b) im Vergleich zu den ToxCast-Daten, was darauf hindeutet, dass die DNT-Gefahr dieser FRs durch ToxCast-Assays nicht gut vorhergesagt wird. Die Extrapolation der BMC Werte ausgehend von der DNT *in vitro* Batterie auf die FR-Exposition des Menschen lediglich über die Muttermilch deutet auf ein eher geringes Risiko für einzelne Verbindungen hin. In Anbetracht der Tatsache, dass der Mensch jedoch Gemischen ausgesetzt ist, kann dies dennoch zu einem Risiko führen, insbesondere wenn verschiedene Chemikalien durch unterschiedliche Wirkmechanismen an gemeinsamen Endpunkten wie der Oligodendrozytendifferenzierung konvergieren. Diese FRs Fallstudie legt nahe, dass eine auf menschlichen Zellen basierende DNT *in vitro* Batterie ein vielversprechender Ansatz für die entwicklungsneurologische Gefahreinschätzung und die Priorisierung von Verbindungen bei der Risikobewertung darstellt.



# Neurodevelopmental toxicity assessment of flame retardants using a human DNT in vitro testing battery

Jördis Klose · Melanie Pahl · Kristina Bartmann · Farina Bendt · Jonathan Blum · Xenia Dolde · Nils Förster · Anna-Katharina Holzer · Ulrike Hübenthal · Hagen Eike Keßel · Katharina Koch · Stefan Masjosthusmann · Sabine Schneider · Lynn-Christin Stürzl · Selina Woeste · Andrea Rossi · Adrian Covaci · Mamta Behl · Marcel Leist · Julia Tigges · Ellen Fritsche

Received: 16 November 2020 / Accepted: 11 March 2021  
© The Author(s) 2021

**Abstract** Due to their neurodevelopmental toxicity, flame retardants (FRs) like polybrominated diphenyl ethers are banned from the market and replaced by alternative FRs, like organophosphorus FRs, that have mostly unknown toxicological profiles. To study their neurodevelopmental toxicity, we evaluated the hazard of several FRs including phased-out polybrominated FRs and organophosphorus FRs: 2,2',4,4'-tetrabromodiphenylether

(BDE-47), 2,2',4,4',5-pentabromodiphenylether (BDE-99), tetrabromobisphenol A, triphenyl phosphate, tris(2-butoxyethyl) phosphate and its metabolite bis-(2-butoxyethyl) phosphate, isodecyl diphenyl phosphate, triphenyl isopropylated phosphate, tricresyl phosphate, tris(1,3-dichloro-2-propyl) phosphate, tert-butylphenyl diphenyl phosphate, 2-ethylhexyl diphenyl phosphate, tris(1-chloroisopropyl) phosphate, and tris(2-chloroethyl)

## Highlights

- A human DNT in vitro testing battery was applied for assessing hazards of phased-out and alternative flame retardants (FR) for prioritization.
- Oligodendrocyte development was identified as a common key event for FR-induced DNT in vitro.
- Multiple modes-of-action seem to contribute to oligodendrocyte toxicity.
- Prioritization of FRs according to the DNT in vitro battery differs from FRs ranking using ToxCast assays.

J. Klose · M. Pahl · K. Bartmann · F. Bendt · U. Hübenthal · H. E. Keßel · K. Koch · S. Masjosthusmann · S. Schneider · L.-C. Stürzl · S. Woeste · A. Rossi · J. Tigges · E. Fritsche  
IUF-Leibniz Research Institute for Environmental Medicine, Auf'm Hennekamp 50, 40225 Duesseldorf, NRW, Germany

J. Blum · X. Dolde · A.-K. Holzer · M. Leist  
Department of Biology, University of Konstanz, Universitätsstraße 10, 78464 Konstanz, BW, Germany

N. Förster  
Faculty for Biology and Biotechnology, Bioinformatics Group, RUB – Ruhr University Bochum, Bochum, Germany

A. Covaci  
Toxicological Centre, Department of Pharmaceutical Sciences, University of Antwerp, Universiteitsplein 1, 2610 Wilrijk, Belgium

M. Behl  
Division of the National Toxicology Program, National Institute of Environmental Health Sciences, Research Triangle Park, Durham, North Carolina 27709, USA

E. Fritsche (✉)  
Medical Faculty, Heinrich-Heine-University, Universitätsstraße 1, 40225 Duesseldorf, NRW, Germany  
e-mail: ellen.fritsche@uni-duesseldorf.de

phosphate. Therefore, we used a human cell-based developmental neurotoxicity (DNT) *in vitro* battery covering a large variety of neurodevelopmental endpoints. Potency according to the respective most sensitive benchmark concentration (BMC) across the battery ranked from  $<1 \mu\text{M}$  (5 FRs),  $1<10 \mu\text{M}$  (7 FRs) to the  $>10 \mu\text{M}$  range (3 FRs). Evaluation of the data with the ToxPi tool revealed a distinct ranking (a) than with the BMC and (b) compared to the ToxCast data, suggesting that DNT hazard of these FRs is not well predicted by ToxCast assays. Extrapolating the DNT *in vitro* battery BMCs to human FR exposure via breast milk suggests low risk for individual compounds. However, it raises a potential concern for real-life mixture exposure, especially when different compounds converge through diverse modes-of-action on common endpoints, like oligodendrocyte differentiation in this study. This case study using FRs suggests that human cell-based DNT *in vitro* battery is a promising approach for neurodevelopmental hazard assessment and compound prioritization in risk assessment.

**Keywords** Developmental neurotoxicity · Flame retardants · Human cell-based testing battery · 3D *in vitro* model · New approach methodologies · Hazard assessment

## Introduction

Flame retardants (FRs) inhibit or delay the spread of fire by suppressing chemical reactions in the flame or by forming a protective layer on the material surface (Darnerud et al. 2001). They are used in commercial products, such as electronics, furniture, and textiles. Since the 1970s, polybrominated diphenyl ether (PBDEs) had been in use as FRs. However, due to their accumulation in environmental samples, house dust, food, animal and human tissues (Darnerud et al. 2001; De Wit 2002; Law et al. 2014) and their adversity for human health, particularly neurodevelopment (Chao et al. 2007; Roze et al. 2009; Shy et al. 2011; Eskenazi et al. 2013), the European Commission and the U.S. Environmental Protection Agency (US EPA) caused a phase out of PBDEs in 2004 (Blum et al. 2019). Despite their market ban, they are still present in the environment (Yogui and Sericano 2009; Ma et al. 2013; Law et al. 2014). With the phasing out, PBDEs were replaced by presumably safer and less persistent alternative FRs (aFRs), including organophosphorus FRs (OPFRs). Several aFRs were released onto the market,

although their kinetics and toxicities, specifically their neurodevelopmental hazards, have not been sufficiently investigated. Available data on the physico-chemical properties, environmental persistence, bioaccumulation, and toxicity of a subset of aFRs recently displayed large data gaps (van der Veen and de Boer 2012; Bergman et al. 2012; Waaijers et al. 2013). Similar to PBDEs, there has been growing evidence of widespread exposure to aFRs, as they were found in house dust, furniture foam, and baby articles (Stapleton et al. 2009; Sugeng et al. 2017), as well as in hand wipes and urine samples of children (Stapleton et al. 2014; Mizouchi et al. 2015; He et al. 2018a, b; Bastiaensen et al. 2019a). In general, children and especially toddlers are highly exposed towards FRs as they frequently spend their time close to the floor and exercise children-specific mouthing behavior (Fischer et al. 2006; Toms et al. 2009; Sugeng et al. 2017). Due to this high exposure and the fact that the developmental nervous system is a sensitive target organ for many FRs and organophosphorus pesticides (Muñoz-Quezada et al. 2013), which are structurally similar to OPFRs, it is essential to assess the developmental neurotoxicity (DNT) potential of aFRs (Hirsch et al. 2017).

Current DNT testing follows the *in vivo* guideline studies OECD 426 (OECD 2007) or EPA 870.6300 (EPA 1998) performed with rats. These studies are highly demanding with regard to time, money, and animals (Lein et al. 2005; Crofton et al. 2012) and are not suited for large scale DNT testing. Further limitations include their high variability and lack of reproducibility, as well as the uncertainty of extrapolation from animals to humans (Tsuji and Crofton 2012; Terron and Bennekou Hougaard 2018; Sachana et al. 2019). Therefore, regulators, academic, and industrial scientists recently agreed on a need for a new testing strategy to assess the DNT potential of chemicals (Crofton et al. 2014; Bal-Price et al. 2015; Fritsche et al. 2018b). A mechanistically informed, fit-for-purpose, human-relevant *in vitro* DNT test battery was suggested that covers different neurodevelopmental processes and stages (Andersen 2003; Bal-Price et al. 2018) and allows a faster and cheaper evaluation of substances for their DNT potential (EFSA 2013; Bal-Price et al. 2015, 2018; Fritsche et al. 2015, 2017, 2018a).

In this study, human-induced pluripotent stem cell (hiPSC)-derived neural crest cells (NCC), human mesencephalic cells (LUHMES), 3D human primary neural progenitor cell (NPC)-based neurospheres, as well as hiPSC-derived peripheral neurons were applied to study distinct neurodevelopmental key events (KEs)

in vitro. These KEs include NPC proliferation (NPC1), NCC (cMINC/UKN2), radial glia (NPC2a), neuronal (NPC2b) and oligodendrocyte (NPC2c) migration, differentiation into neurons (NPC3), neurite morphology (NPC4, NeuriTox/UKN4, PeriTox/UKN5), and oligodendrocyte differentiation (NPC5; Baumann et al. 2016; Barenys et al. 2017; Schmidt et al. 2017; Fritsche et al. 2018a; Masjosthusmann et al. 2018; Nimtz et al. 2019; Krebs et al. 2020b). These assays comprise a current DNT in vitro testing battery that was recently assembled to test 119 compounds (e.g., carbamates, metals, neonicotinoids, organochlorines/fluorines, and organophosphates pyrethroids) for regulatory purposes. Using selected known human DNT positive and negative compounds as benchmark, this battery performed with a sensitivity of 100% and a specificity of 88% (Masjosthusmann et al. 2020).

To study the neurodevelopmental hazard of FRs, we analyzed their adverse effects on the endpoints of this battery of human neurodevelopmental assays. FRs used include a set of phased-out and currently in use compounds. The phased-out FRs are PBDEs 2,2',4,4'-tetrabromodiphenylether (BDE-47) and 2,2',4,4',5-pentabromodiphenylether (BDE-99), while the current-use FRs include the organophosphorus FRs (OPFRs), such as triphenyl phosphate (TPHP), tris (2-butoxyethyl) phosphate (TBOEP) and its metabolite bis-(2-butoxyethyl) phosphate (BBOEP), isodecyl diphenyl phosphate (IDDPHP), triphenyl isopropylated phosphate (IPPHP), tricresyl phosphate (TCP), tris (1,3-dichloro-isopropyl) phosphate (TDCIPP), tert-butylphenyl diphenyl phosphate (t-BPDPHP), tri-O-cresyl phosphate (TOCP), 2-ethylhexyl diphenyl phosphate (EHDPHP), tris (1-chloro-isopropyl) phosphate (TCIPP), and tris (2-chloroethyl) phosphate (TCEP), as well as the brominated FR Tetrabromobisphenol A (TBBPA) (Table S1). The in vitro data were related to hazardous doses by toxicokinetic considerations. Moreover, such data were compared to potential exposure situations. Relating the phenomics of the in vitro methods to molecular signatures, we performed RNA sequencing analyses. This approach represents a case study for a new risk assessment paradigm for DNT by using phenotypic readouts of human cell-based assays that cover a variety of neurodevelopmental endpoints and studying their molecular signatures in response to different FRs.

## Material and methods

### Chemicals

TBBPA, BDE-99, TCEP, TPHP, TOCP, and TBOEP (for NPC assays) were purchased from Sigma-Aldrich and were dissolved as 50 mM and 20 mM stocks in dimethyl sulfoxide (DMSO; Carl Roth GmbH). The metabolite BBOEP (1500 ng/ $\mu$ L in Methanol) was custom synthesized by Dr. Vladimir Belov (Max Planck Institute, Göttingen, Germany) with a purity > 98% as measured by MS and NMR techniques. The FRs TCIPP, t-BPDPHP, and EHDPHP were obtained from ToxCast and are diluted in DMSO with stock concentration of 20 mM. All other flame retardants IDDPHP, IPPHP, TCP, TDCIPP, BDE-47 (for NPC assays) as well as TBBPA, BDE-47, BDE-99, TCEP, TPHP, IDDPHP, IPPHP, EHDPHP, t-BPDPHP, and TCP (for UKN assays) were provided by M. Behl from the National Toxicology Program, and stock solutions of 20 mM in DMSO were prepared. Solvent concentrations were 0.1% DMSO and 0.4% MeOH for BBOEP in dose-response experiments.

### Cell culture

Human NPCs (hNPCs) from three different individuals (gestational week 16-19) were purchased from Lonza Verviers SPRL, Belgium. They were thawed and isolated as previously described (Baumann et al. 2016). hNPCs were cultured as free floating neurospheres in proliferation medium consisting of DMEM (Life Technologies) and Hams F12 (Life Technologies) (3:1) supplemented with 2% B27 (Life Technologies), 20 ng/mL EGF (Thermo Fisher), FGF (R&D Systems), and 1% penicillin and streptomycin (Pan-Biotech). Neurospheres were cultivated at 37 °C with 5% CO<sub>2</sub>, passaged mechanically with a tissue chopper (McIlwain) once a week and thrice a week half of the medium was replaced.

For the cMINC assay (UKN2), NCCs are differentiated from the hiPSC line IMR90\_clone #4 (WiCell, Wisconsin) by plating cells on Matrigel-coated 6-well plates (Falcon) at a density of 50000 cells/cm<sup>2</sup>. One day prior differentiation, cells are cultivated in essential 8 (E8) medium (DMEM/F12 supplemented with 15 mM Hepes, 16 mg/mL L-ascorbic-acid, 0.7 mg/mL sodium selenite, 20  $\mu$ g/mL insulin, 10  $\mu$ g/mL holo-transferrin, 100 ng/mL bFGF, 1.74 ng/mL TGF $\beta$ ) containing



10  $\mu\text{M}$  Rock inhibitor. Until 11 days in vitro (DIV), cells receive KSR medium (knock out DMEM, 15% knock out serum replacement, 1% GlutaMax, 1% MEM NEAA solution, 50  $\mu\text{M}$  2-mercaptoethanol) which is gradually replaced by 25% increments of N2-S medium (DMEM/F12, 1.55 mg/mL glucose, 1% GlutaMax, 0.1 mg/mL apotransferrin, 25  $\mu\text{g}/\text{mL}$  insulin, 20 nM progesterone, 100  $\mu\text{M}$  putrescine, 30 nM selenium). From -1 DIV to 11 DIV, cells are cultured at 37 °C with 5%  $\text{CO}_2$  and a daily medium change was performed. From 0 DIV to 2 DIV, medium is supplemented with 20 ng/mL Noggin. From 0 DIV to 3 DIV, it is supplemented with 10  $\mu\text{M}$  SB431542 and from 2 DIV to 11 DIV with 3  $\mu\text{M}$  CHIR 99021. After 11 DIV, cells are detached and resuspended in N2-S medium supplemented with 20 ng/mL EGF and 20 ng/mL FGF2 and seeded as droplets (10  $\mu\text{L}$ ) on poly-L-ornithine (PLO)/laminin/fibronectin-coated 10-cm dishes. Until 39 DIV, cells are expanded by weekly splitting in N2-S medium supplied with EGF and FGF2 and a medium change is performed every other day. On 39 DIV, cells are detached, resuspended in freeze medium (FBS with 10% DMSO), and frozen at a concentration of  $4 \times 10^6$  cells per mL at -80 °C overnight. After 24 h, cells are stored in liquid nitrogen until further use.

For the NeuroTox assay (UKN4), LUHMES cells are cultured and handled as described before (Lotharius et al. 2005; Scholz et al. 2011; Krug et al. 2013a). They are maintained in proliferation medium (PMed; AdvDMEM/F12 supplemented with 2 mM glutamine,  $1 \times \text{N2}$  supplement and 40 ng/mL FGF) at 37 °C with 5%  $\text{CO}_2$ . Cells are passaged every second or third day when reaching approximately 80% confluency. For pre-differentiation,  $8 \times 10^6$  (45000 cells/ $\text{cm}^2$ ) cells are seeded one day before in PMed. Differentiation is started by switching to differentiation medium (DMed; AdvDMEM/F12 supplemented with 2 mM glutamine,  $1 \times \text{N2}$  supplement, 2.25  $\mu\text{M}$  tetracycline, 1 mM dibutyryl cAMP and 2 ng/mL GDNF).

For the PeriTox assay (UKN5), sensory neurons are differentiated from the hiPSC line SBAD2, which was derived and characterized at the University of Newcastle from Lonza fibroblasts CC-2511, Lot 293971 with the tissue acquisition number 24245 (Baud et al. 2017). Culturing, handling, and differentiation are performed according to standard protocols (Thomson et al. 1998; Chambers et al. 2013; Hoelting et al. 2016). Generation of sensory neurons is started on -2 DIV by resuspending hiPSCs in E8 medium containing 10  $\mu\text{M}$

Rock inhibitor Y-27632. After replating cells at a density of 55000 cells/ $\text{cm}^2$  on Matrigel coated 6-well plates (Falcon), a daily medium change is performed from -1 DIV until 10 DIV. E8 medium supplemented with rock inhibitor (10  $\mu\text{M}$ ) is refreshed on -1 DIV. On 0 DIV, neural differentiation is initiated and until 10 DIV cells receive KSR medium which is, from 4 DIV onward, gradually replaced by 25% increments of N2-S medium. Until 4 DIV medium is supplied with 35 ng/mL Noggin, 600 nM dorsomorphin and 10  $\mu\text{M}$  SB431542 to initiate neutralization via dual-SMAD inhibition. From 2 DIV to 10 DIV, three further pathway inhibitors are added (1.5  $\mu\text{M}$  CHIR99021, 5  $\mu\text{M}$  SU5402, and 5  $\mu\text{M}$  DAPT). On 10 DIV, cells are detached, resuspended in freeze medium (FBS with 10% DMSO) and frozen at a concentration of  $8 \times 10^6$  cells per mL at -80 °C overnight. After 24 h, cells are stored in liquid nitrogen until further use.

#### The “neurosphere assay”—NPC1-5

hNPCs were chopped to 0.2 mm 2–3 days before plating to reach a defined size of 0.3 mm. Each compound was tested in serial dilution (1:3) with 7 concentrations and a solvent control (SC) plated in five replicate wells per condition in 96-well plates (proliferation U-bottom, Falcon; differentiation flat bottom, Greiner). Each well contained one sphere in 100  $\mu\text{L}$  of the respective medium and FR/solvent(s) (proliferation medium (description in “Cell culture”); differentiation medium consisting of DMEM (Life Technologies), Hams F12 (Life Technologies) 3:1 supplemented with 1% of N2 (Life Technologies) and 1% penicillin and streptomycin (Pan-Biotech)). The 1:3 solution series and plate filling, LDH, CTB, and feeding step were performed automatically by STARlet 8 ML pipette robot system (MICROLAB STAR® M; Hamilton).

#### Proliferation

The proliferation by area (NPC1a) was assessed as slope of the increase in sphere size up to 3 DIV (0 h, 24 h, 48 h, and 72 h) measured by brightfield microscopy and using high content imaging (Cellomics Scan software, Version 6.6.0; Thermo Fisher Scientific). Proliferation by bromodeoxyuridine (BrdU; NPC1b) was analyzed after 3 DIV via a luminescence-based BrdU Assay (Roche) as previously published in Nimtz et al. (2019).

### *Immunocytochemical stainings*

By plating neurospheres into 100  $\mu\text{L}$  differentiation medium on a poly-D-lysine (0.1 mg/mL, Sigma-Aldrich) and laminin (12.5  $\mu\text{g}/\text{mL}$ , Sigma-Aldrich)-coated 96-well plate (flat bottom, Greiner), spheres settle down and NPCs migrate radially out of the sphere core concurrently differentiating, into radial glia, neurons, and oligodendrocytes. After 5 days of migration and differentiation, human neurospheres were fixed with 4% paraformaldehyde (PFA, Merck) for 30 min at 37 °C and directly afterwards washed three times for 3 min with 250  $\mu\text{L}$  PBS (Biochrom) before stored at 4 °C until staining. Cells were always covered with 40  $\mu\text{L}$  PBS, and for staining, 10  $\mu\text{L}$  blocking solution (PBS, 50% Goat Serum (GS, Sigma-Aldrich) and 5% Bovines Serum Albumin (BSA, Serva Electrophoresis)) per well was added and incubated for 15 min at 37 °C. After removal of 10  $\mu\text{L}$ , cells were stained overnight at 4 °C with 10  $\mu\text{L}$  mouse IgM oligodendrocyte O4 antibody solution 1:400 (in PBS with 10% GS and 1% BSA; R&D System) followed by three 3-min washing steps by addition and removal of 250  $\mu\text{L}$  PBS. After the last washing step, 260  $\mu\text{L}$  was removed and 10  $\mu\text{L}$  secondary antibody solution in PBS (1:400 Alexa Fluor 488 anti-mouse IgM (Life Technologies), 10% GS, 5% BSA) was added for 30 min at 37 °C. After washing steps as previously described, cells were fixed a second time for 30 min at 37 °C in 4% PFA, followed by three 3-min washing steps and permeabilization in 0.5% PBS-T for 5 min at room temperature. Afterwards, cells were blocked for 15 min at 37 °C with 10  $\mu\text{L}$  PBS, 50% Rabbit Serum (RS, Sigma-Aldrich), and 5% BSA. For neuronal staining, neurospheres were incubated for 1 h at 37 °C with 10  $\mu\text{L}$  conjugated rabbit TUBB3 674 antibody (Abcam) 1:400 (in PBS with 10% RS, 1% BSA, and 5% Hoechst 33258 (Sigma-Aldrich)). After three additional 3-min washing steps, 250  $\mu\text{L}$  PBS was added to each well and the plates were stored in the dark at 4 °C. Images of immunocytochemical stainings of three channels (386 nm for Hoechst stained nuclei, 647 nm for  $\beta$ (III)tubulin stained neurons, 488 nm for O4 stained oligodendrocytes) were acquired with a 200-fold magnification and a resolution of 552 $\times$ 552 pixel using the HCS Studio Cellomics software (version 6.6.0; Thermo Fisher Scientific).

### *Migration and differentiation*

Radial glia migration distance (72 h, NPC2a) was analyzed by manual measurement of the radial migration

from the sphere core on brightfield images as number of pixels which is converted to micrometers. After 120 h, it is assessed by automatically identifying (Schmuck et al. 2016) the migration area of each sphere of Hoechst stained nuclei on fluorescence images. The migration distance of neurons (NPC2b) and oligodendrocytes (NPC2c) is defined as mean distance of all neurons/oligodendrocytes within the migration area divided by radial glia migration distance after 120 h. The differentiation into neurons (NPC3) and oligodendrocytes (NPC5) is determined as number of all  $\beta$ (III)tubulin and O4-positive cells in percent of the total amount of Hoechst-positive nuclei in the migration area and is performed automatically using two convolutional neural networks (CNN) based on the Keras architecture implemented in Python 3, which were trained to identify both cell types. All neurons that were identified in NPC3 are analyzed for their morphology (NPC4) by characterizing the neurite length (in  $\mu\text{m}$ ) and area (amount of pixel). Detection of migration (120 h, NPC2) and morphological analysis (NPC4) is calculated automatically by high-content image analysis (HCA) tool Omnisphero (Schmuck et al. 2016). Migrating/differentiating neurospheres were exposed to FRs/solvent(s) for 5 days. On day 3, half of the exposure/solvent medium was exchanged and the supernatant was used to detect cytotoxicity by measuring lactate dehydrogenase (LDH) leakage.

### “cMINC assay” UKN2

NCCs were thawed and seeded into 96-well plates in N2-S medium containing FGF2 and EGF according to the previously published protocol (Nyffeler et al. 2017). Cells were seeded around stoppers to create a circular cell-free area and after 24 h stoppers were removed to allow cell migration. One day later, cells were exposed to FRs/solvent(s) for 24 h. The number of migrated cells into the cell free zone was quantified 48 h after stopper removal and 24 h after treatment. Cells were stained with Calcein-AM and Hoechst-33342 (H-33342), and high content imaging was performed. Four images for migration were taken to cover the region of interest (ROI) using a high content imaging microscope (Cellomics ArrayScanVTI), and Calcein and H-33342 double-positive cell numbers were determined by an automated algorithm (RingAssay software; <http://invitro-tox.uni-konstanz.de>). For viability, four fields close to the well borders, i.e., outside the ROI,

were imaged. Viable cells were defined by double-positivity for H-33342 and calcein and determined by an automated algorithm as described before (Nyffeler et al. 2017). TBBPA, BDE-47, BDE-99, IDDPHP, TCP, t-BPDPHP, and EHDPHP were tested in serial dilution (1:2) with 6 concentrations and SC, while TPHP and IPPHP were tested with 5 concentrations (Nyffeler et al. 2017). TCEP, TDCIPP, and TCIPP were negative within a 20- $\mu$ M pre-screening and therefore not tested further (data not shown). TBOEP, BBOEP, and TOCP were tested 1:3 with 6 concentrations and SC based on the method described in this study. Each compound concentration was plated in 4 replicate wells per condition.

#### “NeuriTox assay” UKN4

After 2 days of differentiation, 30000 LUHMES cells were reseeded into each well of a 96-well plate in DMed containing only tetracycline. After cells' attachment for 1 h, they were exposed to FRs/solvent(s) for 24 h. One hour before read-out, cells were stained with Calcein-AM and H-33342 and imaged via a high-content imaging microscope (Cellomics ArrayScanVTI, Thermo Fisher Scientific) to assess neurite area. For neurite area determination, an automated algorithm was used, which calculates the area of the cell soma and subtracts this area from all calcein-positive pixels imaged (Stiegler et al. 2011; Krug et al. 2013a). To assess viability, all stained nuclei (H-33342 positive) are used to determine total cell number and H-33342 and calcein double-positive cells are defined as viable cells (Stiegler et al. 2011; Krug et al. 2013a). Each compound was tested in serial dilutions (1:3) with 10 concentrations starting at 20  $\mu$ M and SC plated in three replica wells per condition. Effects of TBBPA, BDE-47, BDE-99, IDDPHP, TCP, t-BPDPHP, EHDPHP, TPHP, and IPPHP were assessed in a previous screening (Delp et al. 2018). TDCIPP, TOCP, and TCIPP were negative in a pre-screening at 20  $\mu$ M and therefore not tested any further (data not shown).

#### “PeriTox assay” UKN5

Differentiated sensory neurons were thawed and seeded in 25% KSR/75% N2-S medium supplemented with 1.5  $\mu$ M CHIR99021, 5  $\mu$ M SU5402, and 5  $\mu$ M DAPT into 96-well plates at a density of 100000 cells per  $\text{cm}^2$ . After cells' attachment for 1 h, they were exposed to

FRs/solvent(s) for 24 h. Assessments of neurite area and viability of the cells were performed as described above for the UKN4 assay. Each compound concentration was tested in three wells per plate (technical replicates) in a serial dilution (1:3) with 6 concentrations starting at 20  $\mu$ M and SC. Effects of TBBPA, BDE-47, BDE-99, IDDPHP, TCP, t-BPDPHP, EHDPHP, TPHP, and IPPHP were assessed in a previous screening (Delp et al. 2018). TDCIPP, TOCP, and TCIPP were negative in a pre-screening at 20  $\mu$ M and therefore not tested any further (data not shown).

#### Viability and cytotoxicity

To distinguish compound effects from secondary effects due to loss of viability and cytotoxicity, respective assays were performed in parallel. Thereby, all viability and cytotoxicity assays are multiplexed within the respective assay. hNPC viability was assessed as mitochondrial activity by using an Alamar blue assay (CellTiter-Blue Assay (CTB); Promega) in the last 2 h of the respective compound treatment period (NPC1 at 3 DIV; NPC2-5 at 5 DIV). Cytotoxicity of treated hNPCs was detected by measuring LDH (CytoTox-ONE membrane integrity Assay; Promega) after 3 (NPC1; NPC2-5) and 5 (NPC2-5) DIV. It is of note that a reduced radial glia migration area causes a reduction in the CTB readout due to a diminished cell number without necessarily affecting cell viability (Fritsche et al. 2018a). Thus, when radial glia migration is inhibited by a compound, the LDH assay is solely the reference for DNT specificity of NPC2-5. Assessment of viability within the UKN assays was performed as described above.

#### RNA sequencing and RT-qPCR

For RNA sequencing (RNASeq) experiments, 1000 neurospheres per well with a defined size of 0.1 mm were plated onto PDL/laminin-coated 6-well plates and cultivated for 60 h in the presence and absence of selected FRs. The RNA isolation was performed using the RNeasy Mini Kit (Qiagen) according to the manufacturer's protocol. Total RNA was analyzed for high quality using the Agilent High Sensitivity RNA ScreenTape System for Agilent 4150 TapeStation Bioanalyzer (Agilent Technologies) for human samples with an RNA integrity number (RIN)  $\geq$  8. All samples in this study showed high-quality RINs  $\geq$  8.5. For RNASeq,

1.0 µg total RNA was used for library preparation using the TruSeq RNA Sample Prep Kit v2 according to the manufacturer's protocol (Illumina). All steps of the protocol were performed as described in the Illumina kit. DNA library templates were quantified using the Qubit™ 4 Fluorometer and the Qubit 1× dsDNA HS Assay Kit (Thermo Fisher Scientific). Quality control and fragment size analysis were performed on Agilent 4150 TapeStation System and the Agilent D1000 Screen Tape System (Agilent Technologies). Sequencing was performed on a MiSeq instrument (Illumina) using v3 chemistry, resulting in an average of 50 million reads per library with 1×76 bp paired end setup.

Raw data were uploaded on BaseSpace Sequence Hub (Illumina) for FastQ generation. RNAseq analysis was performed using the Illumina pipeline (Illumina Annotation Engine 2.0.10.0). The resulting raw reads were assessed for quality, adapter content and duplication rates with the Illumina FASTQ file generation pipeline. Trimmed and filtered reads were aligned versus the *Homo sapiens* reference genome (UCSC hg19) using STAR Aligner (STAR\_2.6.1a). Total number of reads was quantified using both TopHat2 and Salmon Quantification (0.11.2). Strelka Variant Caller (2.9.9) was used to detect somatic single nucleotide variants (SNVs).

Quantitative real-time polymerase chain reaction (RT-qPCR) was performed with the QuantiFast SYBR Green PCR Kit (Qiagen) within the Rotor Gene Q Cycler (Qiagen). Therefore, 250 ng RNA was transcribed into cDNA using the QuantiTect Reverse Transcription Kit (Qiagen) according to manufacturer's instructions. Analysis was performed using the software Rotor-Gene Q Series version 2.3.4 (Qiagen). Copy numbers (CN) of the genes of interest were calculated by using gene-specific copy number standards as described previously in detail (Walter et al. 2019) and normalized to the housekeeping gene *beta-actin*. Gene CN of solvent control and FR treated differentiated spheres were normalized to proliferative spheres, which are thought to express very low numbers of oligodendrocyte-specific mRNA. Here, the solvent control visualizes oligodendrocyte-related gene expression as a function of normal NPC development that can directly be compared to sphere development in presence of FRs.

### Toxicological Priority Index

For relative toxicological ranking and hierarchical clustering, the BMC values of the tested FRs were integrated

and visualized by using the Toxicological Priority Index Graphical User Interface (ToxPi GUI) version 2.3 (Gangwal et al. 2012). In ToxPi, the BMC values across the data set of each endpoint were scaled with the formula  $-\log_{10}(x)+6$  from 0 to 1, while 1 represents the lowest BMC and therefore the most potent compound. If BMC was not reached, a concentration of  $10^6$  was applied before, which became 0 upon scaling. Data are visualized in a pie chart, where every slice represents one DNT endpoint (Fig. 7). The farther the slice extends from its origin, the more potent the compound in this endpoint. In comparison, ToxCast data was used to give an initial idea on the general toxicity of these FRs across a variety of assays. Regarding ToxCast AC<sub>50</sub> (half-maximal activity concentration), values below a given cytotoxicity limit were used and scaled as described above. Each slide was assigned as one intended target family and contains several assays for respective endpoints.

### Data analysis and statistics

All neurosphere experiments were performed with at least two different individuals. Experiments were defined as independent if they were generated with NPCs from different individuals or from a different passage of cells. For cMINC, NeuroTox, and PeriTox assays, biological replicates represent an independent experiment on another day with a different batch of NCCs, LUHMES cells, or 10 DIV sensory neurons thawed. If not otherwise indicated, results are presented as mean ± SEM. For dose-response curves, a sigmoidal (variable slope) or bell-shaped curve fit was applied using GraphPad Prism 8.2.1. Statistical significance was calculated using the same software and one-way ANOVA with Bonferroni's post hoc tests ( $p \leq 0.05$  was termed significant).

BMC as well as upper and lower confidence intervals (CI) were calculated with GraphPad Prism 8.2.1. Based on overlap of confidence intervals of the BMCs calculated for the DNT-specific endpoints and the endpoints related to cytotoxicity/viability, NPC endpoints were classified as DNT-specific (no CI overlap), unspecific (CI overlap  $\geq 10\%$ ), or borderline ( $0 > CI < 10\%$ ; Masjosthusmann et al. 2020). The classification model applied for UKN assays is based on a ratio cutoff for the ratio between the BMC for cell viability and the specific endpoints (ratio BMC<sub>10</sub> viability/BMC<sub>25</sub> migration  $\geq 1.3$  in UKN2 assay; ratio BMC<sub>25</sub> viability/BMC<sub>25</sub>



neurite area  $\geq 4$  in UKN4 assay or  $\geq 3$  in UKN5 assay). This is in line with the respective classification models suggested in previous publications (Krug et al. 2013b; Hoelting et al. 2016; Nyffeler et al. 2017).

## Results

### Experimental design of the human DNT testing battery

We assessed the neurodevelopmental hazard of 15 FRs (Table S1) and analyzed their adverse effects using a battery of human-based neurodevelopmental in vitro assays (Fig. 1). Within NPC assays, proliferation (NPC1), migration (NPC2), and differentiation into the main effector cells of the human brain, i.e., radial glia, neurons (NPC3), and oligodendrocytes (NPC5), were evaluated. NPC3 was multiplexed with NPC4, which quantifies neurite morphology by analyzing their length and area. The cMINC (UKN2) assay measures neural crest cell (NCC) migration and viability, while NeuriTox (UKN4) and PeriTox (UKN5) assays assess neurite morphology and viability of LUHMES cells and hiPSC-derived peripheral neurons, respectively. Finally, cytotoxicity was assessed after 3 (NPC1) and 5 (NPC2-5) DIV and cell viability was detected at the end of each assay. Additionally, RNA sequencing analyses provide further insight into the modes-of-action of FR toxicity.

Three out of the 15 analyzed FRs (BBOEP, TCIPP, and TCEP) did not produce significant effects in any of the tested endpoints up to a concentration of 20  $\mu\text{M}$ . Therefore, the respective graphs are shown in supplementary Figs. S1–3.

### hNPC proliferation is exclusively disturbed by alternative flame retardants

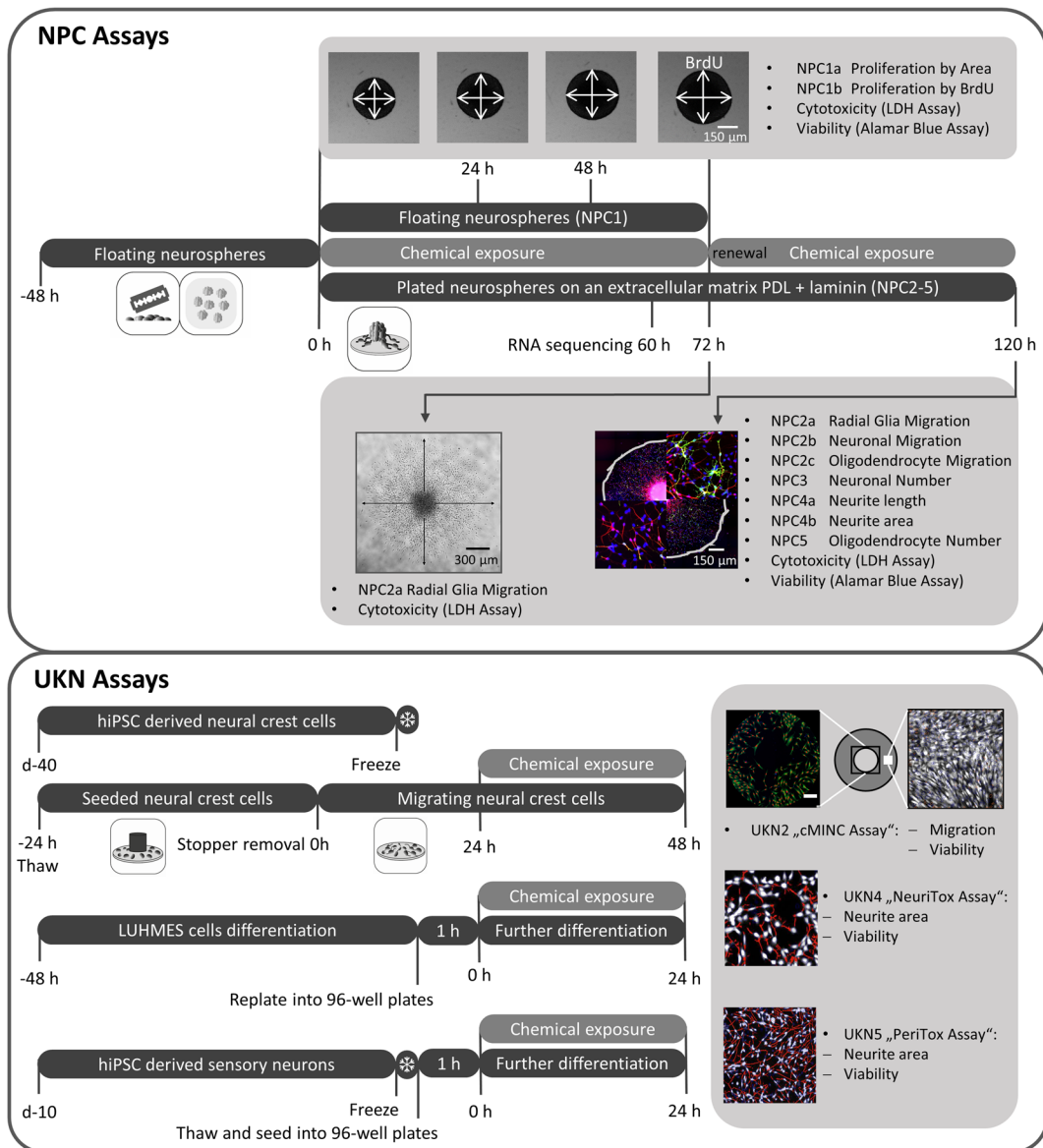
A fundamental neurodevelopmental KE is NPC proliferation. The analyzed PBDEs and aFRs did not affect sphere area increase over time (NPC1a; Fig. 2(a)). BrdU incorporation (NPC1b), however, as a direct measure of DNA synthesis has a higher sensitivity than NPC1a and EHDPHP and TCP reduced BrdU incorporation significantly (Fig. 2(b)) with EHDPHP being the more potent one with significant diminution of proliferation at 0.25  $\mu\text{M}$  and 20  $\mu\text{M}$  to  $70.5 \pm 4.3\%$  and  $37.4 \pm 2.7\%$  of the controls, respectively. TCP inhibited proliferation to  $65.9 \pm 8.3\%$  and  $58.5 \pm 6.8\%$  of controls at 6.6  $\mu\text{M}$  and 20  $\mu\text{M}$ ,

respectively. Neither viability nor cytotoxicity were altered by any of the analyzed FRs at the employed concentration levels, with the exception of IPPHP, which induced the mitochondrial activity at the highest concentration up to  $121.1 \pm 4.9\%$  of control. The endpoint-specific control for NPC1 was hNPC cultivation in absence of growth factors causing significantly reduced proliferation (Suppl. Fig. 4(a, b)).

### FRs affect migration in a cell type-specific manner

Next, we analyzed NCC (UKN2), radial glia (NPC2a), neuronal (NPC2b), and oligodendrocyte (NPC2c) migration in the presence and absence of FRs. NCC migration was affected by PBDEs, as well as organophosphorus aFRs and was significantly inhibited by 9 out of the 15 FRs tested (Fig. 3(a)). TBBPA reduced NCC migration to  $52.6 \pm 9.2\%$  and  $31.3 \pm 3.5\%$  of control at 2.5  $\mu\text{M}$  and 5  $\mu\text{M}$ , respectively (Fig. 3(a, c)). BDE-47, t-BDPHP, and TCP ( $\geq 5 \mu\text{M}$ ) significantly reduced the number of migrating NCCs to  $37.1 \pm 9.6\%$ ,  $53.5 \pm 4.8\%$ , and  $56.6 \pm 4.4\%$  of controls, respectively. TOCP (6.67  $\mu\text{M}$ ) and BDE-99 (10  $\mu\text{M}$ ) significantly inhibited NCC migration to  $43.2 \pm 7.6\%$  and  $69.5 \pm 6.7\%$  of controls, respectively, while EHDPHP, IDDPHP, and TPHP disturbed NCC migration at the highest concentration to  $31.8 \pm 23.1\%$ ,  $52.7 \pm 10.6\%$ , and  $65.3 \pm 10.2\%$  of respective controls. NCC viability was significantly affected by 5  $\mu\text{M}$  TBBPA ( $81.1 \pm 1.7\%$ ); by  $\geq 10 \mu\text{M}$  EHDPHP ( $\leq 93.8 \pm 2.7\%$ ), TCP ( $\leq 90.9 \pm 1.0\%$ ), and IPPHP ( $\leq 93.1 \pm 1.2\%$ ); and by 20  $\mu\text{M}$  BDE-47 ( $86.6 \pm 5.5\%$ ) and TOCP ( $63.3 \pm 10.2\%$ ; Fig. 3(b)). Cytochalasin D (200 nM) served as an endpoint specific control for UKN2 (data not shown). Similar to NCC migration, TBBPA is the most potent FR for hNPC migration inhibition, significantly disturbing radial glia (NPC2a), neuron (NPC2b), and oligodendrocyte (NPC2c) migration at concentrations  $\geq 2.2 \mu\text{M}$  (Fig. 3(d, g)). Consequently, TBBPA decreased respective CTB values at concentrations  $\geq 2.2 \mu\text{M}$  to  $\leq 64.8 \pm 2.7\%$  of controls. However, also cytotoxicity was induced to  $25.1 \pm 3.3\%$  (72 h) and  $25.4 \pm 2.0\%$  (120 h) of the lysis control at concentrations  $\geq 2.2 \mu\text{M}$  TBBPA (Fig. 3(e)).

The phased-out PBDEs did not affect migration behavior of differentiating hNPCs, while some OPFRs (TPHP, TDCIPP, IPPHP, and t-BDPHP) disturbed radial glia and oligodendrocyte migration selectively at the highest concentration of 20  $\mu\text{M}$ . After 72 h, TPHP and TDCIPP inhibited radial glia migration to  $86.3 \pm$



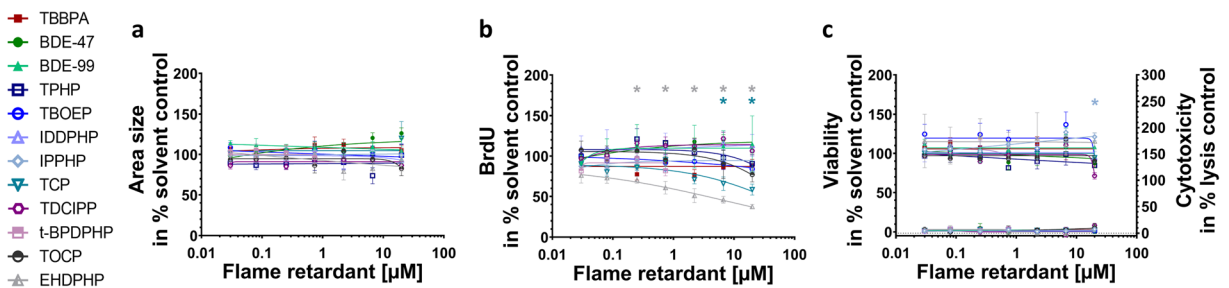
**Fig. 1** Schematic overview of the battery of human-based neurodevelopmental in vitro assays. Experimental procedures for single assays are depicted schematically. Single endpoints

investigated by the battery assays are listed in gray boxes with their respective readout approach. PDL, poly-D-lysine; BrdU, bromodeoxyuridine; LDH, lactate dehydrogenase

2.9% and  $90.5 \pm 2.5\%$  of controls, respectively (Fig. 3(f)). After 120 h, the influence of TPHP was reversed demonstrating the adaptive capabilities of the system. IPPHP, TDCIPP, and t-BPDHP inhibited radial glia migration (120 h) decreasing the distance to  $85.6 \pm 8.1\%$ ,  $82.2 \pm 3.8\%$ , and  $71.5 \pm 14.0\%$  of respective controls (Fig. 3(h)). None of the tested FRs altered neuronal migration distance (Fig. 3(i)), while oligodendrocyte migration was significantly shortened at  $20 \mu\text{M}$  of EHDHP, IPPHP, and t-BPDHP to  $83.6 \pm 3.5\%$ ,

$83.0 \pm 7.2\%$ , and  $73.1 \pm 8.3\%$  of respective controls (Fig. 3(j)). Both phased-out PBDEs and OPFRs did not impact cell viability/cytotoxicity at the conditions tested, except for TDCIPP ( $20 \mu\text{M}$ ) reducing mitochondrial activity (Fig. 3(k)). Strikingly,  $6.6 \mu\text{M}$  and  $20 \mu\text{M}$  IDDPHP increased cell viability to  $133.2 \pm 4.9\%$  and  $151.4 \pm 13.0\%$  of control, respectively, without affecting migration distance. The same effect was caused by  $20 \mu\text{M}$  EHDHP (Fig. 3(h, k)). The endpoint-specific control for NPC2 was the src-kinase inhibitor PP2





**Fig. 2.** Influence of FRs on proliferative hNPCs (NPC1). Spheres were plated in 96-well U-bottom plates and exposed to increasing FRs concentration over 72 h. Proliferation was studied by measuring the increase of sphere area (NPC1a) (a) and by quantifying BrdU incorporation (NPC1b) (b) into the DNA. In parallel, viability and cytotoxicity (c) were assessed by performing Alamar Blue Assay and LDH Assay. Data are represented as means  $\pm$

SEM (except EHDPPH in NPC1a and CTB  $n=2$  mean  $\pm$  SD). Highest concentrations ( $\geq 2.2$   $\mu\text{M}$ ) of t-BPDPPH are not shown as spheres attached and differentiated. Statistical significance was calculated using one-way ANOVA followed by Bonferroni's post hoc tests ( $p \leq 0.05$  was considered significant). BrdU, bromodeoxyuridine

significantly reducing migration to  $36.9 \pm 29.9\%$  of control (Suppl. Fig. 4(c)).

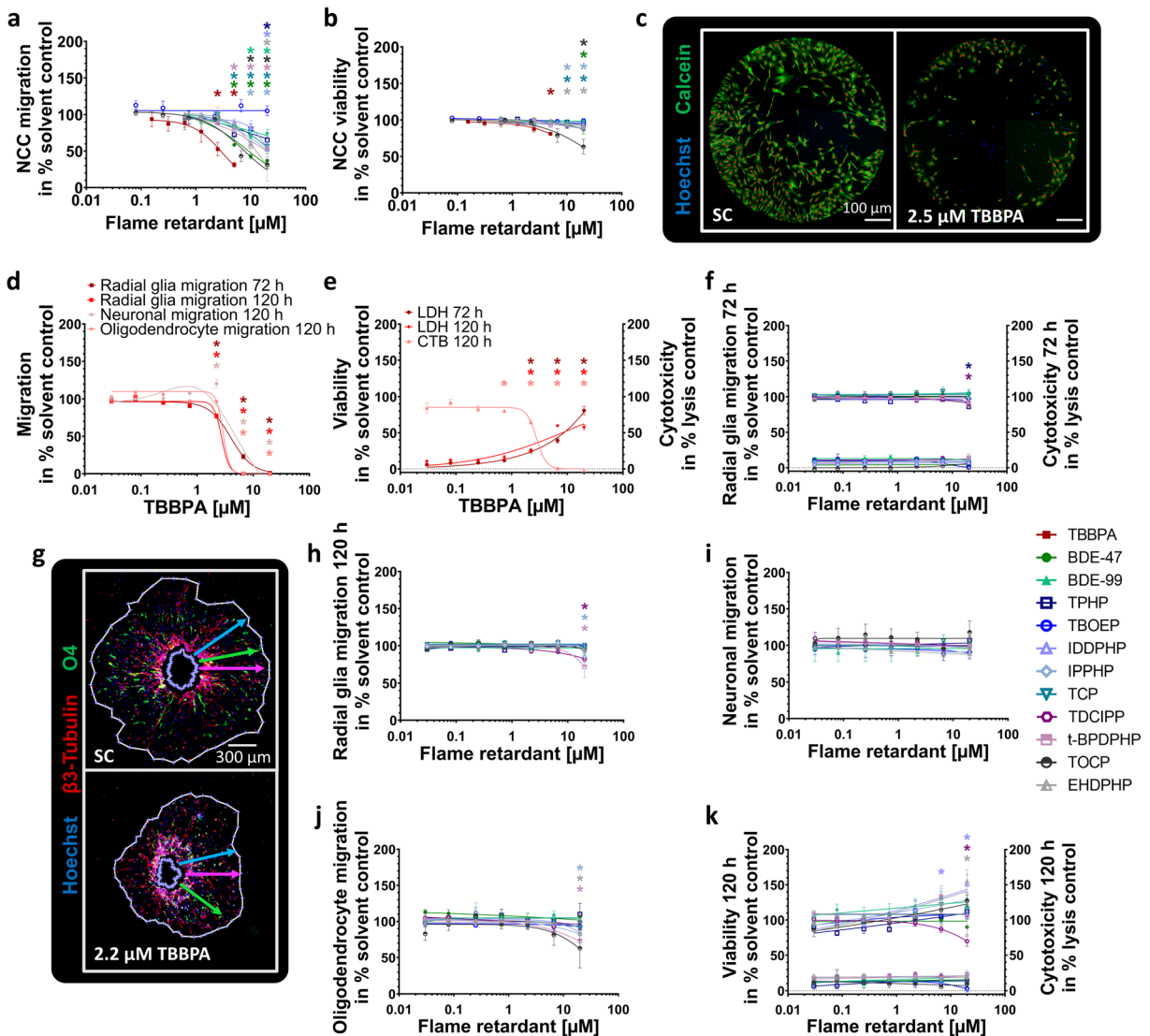
Phased-out PBDEs and OPFRs do not interfere with neuronal differentiation and hardly affect neurite morphology

Within the migration area, hNPCs differentiate into different effector cells. In this study, 9.8% of the cells differentiated into neurons (Suppl. Fig. 4d). To analyze the influences of FRs on hNPC neuronal differentiation and neuronal morphology, NPC3 and NPC4 were performed. TBBPA (2.2  $\mu\text{M}$ ) reduced the total number of nuclei significantly to  $60.8 \pm 7.0\%$  of control (Fig. 4(a, e)), which agrees with inhibition of radial glia migration (Fig. 3(d)). At higher TBBPA concentrations (6.6  $\mu\text{M}$  and 20  $\mu\text{M}$ ), no nuclei and neurons were present (Fig. 4(a)) because migration was completely inhibited (Fig. 3(d)). The organophosphate-based IDDPHP (6.6  $\mu\text{M}$  and 20  $\mu\text{M}$ ) increased the number of nuclei to  $122.7 \pm 7.9\%$  and  $133.4 \pm 6.2\%$  of controls, respectively (Fig. 4(c, e)) explaining the increased cell viability measures (Fig. 3(k)). All other FRs tested did not influence neuronal differentiation at concentrations up to 20  $\mu\text{M}$  (Fig. 4(b, e)). For NPC3, the endpoint-specific control EGF significantly inhibited the total number of neurons to  $1.0 \pm 0.2\%$  of total cell number (Suppl. Fig. 4(d)). The neurite length (NPC4) was significantly inhibited to  $30.4 \pm 13.8\%$  of control by 20  $\mu\text{M}$  TOCP only (Fig. 4(d)), while neurite area was not affected by any FR analyzed (Suppl. Fig. 3(f)). Additionally, LUHMES cells (UKN4) and hiPSC-derived peripheral neurons (UKN5) were used to analyze neurite morphology based

on two different cell types. Neurite outgrowth of both neuronal cell types (Fig. 4(f-h)) as well as their corresponding viability measures (Suppl. Fig. 3(i-j)) were not affected significantly by any of the FRs tested. As an endpoint-specific control for UKN4/5, cells were treated with 50 nM narciclasine which significantly reduced neurite outgrowth (data not shown).

Alteration of oligodendrocyte differentiation by all FR classes

Under differentiating conditions, 4.4% of the cells within the migration area differentiated into oligodendrocytes in this study (Suppl. Fig. 5c). Under the influence of TBBPA, differentiation into oligodendrocytes was specifically and significantly reduced starting from a concentration of 0.25  $\mu\text{M}$  (to  $66.2 \pm 8.9\%$  of control; Fig. 5(a, e)), as it was below the induction of cytotoxicity (Fig. 3(e)). BDE-47 significantly increased oligodendrocyte differentiation at low concentrations (0.03  $\mu\text{M}$  to  $147.4 \pm 4.1\%$ ; 0.08  $\mu\text{M}$  to  $172.5 \pm 6.4\%$  of control), whereas the highest concentration (20  $\mu\text{M}$ ) reduced their number to  $10.9 \pm 5.9\%$  of control (Fig. 5(b, e)). Also, BDE-99 disturbed oligodendrocyte differentiation significantly at 2.5  $\mu\text{M}$  to  $35.2 \pm 11.7\%$ , at 5  $\mu\text{M}$  to  $10.4 \pm 7.1\%$ , and at 10  $\mu\text{M}$  to  $0.4 \pm 0.2\%$  (data taken from (Dach et al. 2017); Fig. 5(c, e)). The OPFR TDCIPP reduced the number of oligodendrocytes at 2.2  $\mu\text{M}$  to  $52.5 \pm 5.6\%$  of control (Fig. 5(d, e)). IDDPHP, TPHP, IPPHP, TOCP, and t-BPDPPH produced similar results as they significantly affected oligodendrocyte differentiation at the two highest concentrations of 6.6  $\mu\text{M}$  and 20  $\mu\text{M}$  (Fig. 5(f, g, h, i, j, k, o)).

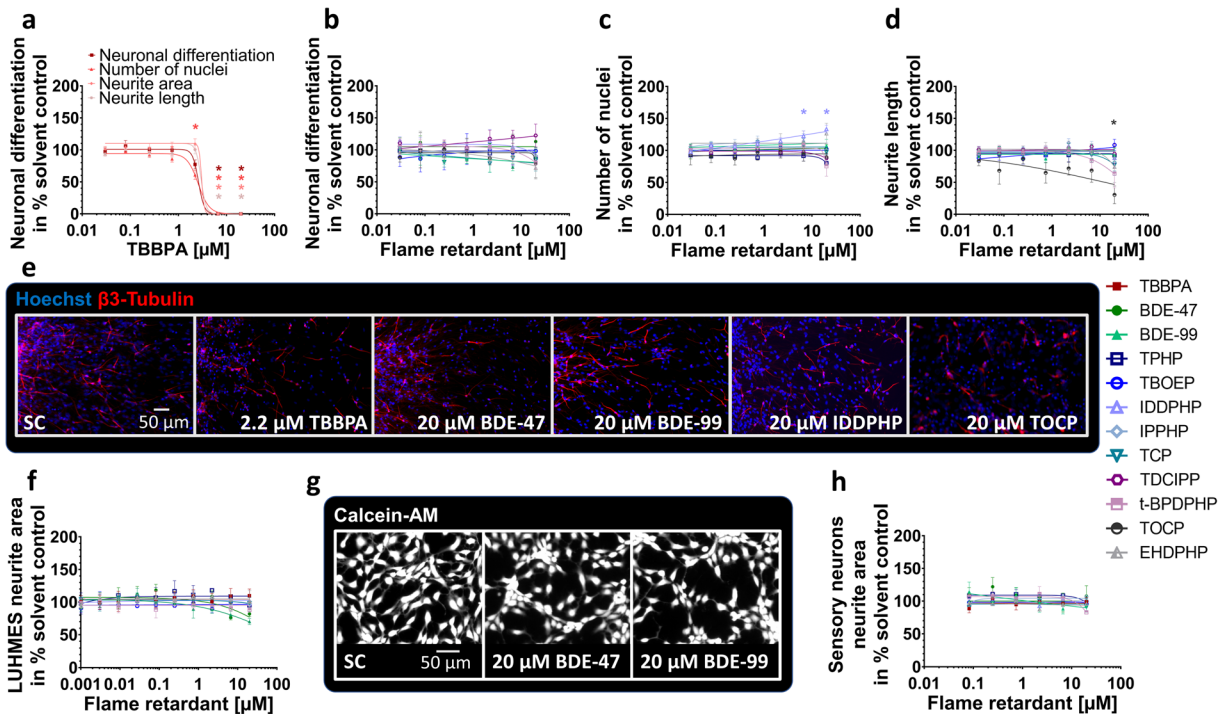


**Fig. 3** Effects of FRs on different migration endpoints (NPC2, UKN2). NCCs were seeded around a stopper into 96-well plates. After stopper removal cells begin to migrate and were exposed to FRs/solvent(s) for 24 h. Cells were stained with Calcein-AM and H-33342, and the number of migrated cells (a) into the cell free zone was quantified using Cellomics ArrayScanVTI. Double-positive cell numbers were determined by an automated algorithm (marked with red dots, c). Viability was defined as the number of double-positive cells outside the ROI (b). Spheres were plated for hNPC migration analyses onto poly-D-lysine/laminin-coated 96-well plates in presence and absence of FRs for 120 h. Radial glia

migration (72 h) was determined by manually measuring the radial migration from the sphere core (d; f). After 120 h, the radial glia (d; h), neuronal (d; i), and oligodendrocyte migration (d; j) were assessed by automatically identifying (Omnisphero) the migration area of Hoechst stained nuclei,  $\beta$ (III)tubulin-stained neurons, and O4<sup>+</sup> oligodendrocytes (g). In parallel, viability and cytotoxicity (e; f; k) were assessed by the Alamar Blue and the LDH Assay. Data are represented as means  $\pm$  SEM (except BDE-99 NPC2b; TOCP LDH 120 h,  $n=2$ , means  $\pm$  SD). Statistical significance was calculated using one-way ANOVA followed by Bonferroni's post hoc tests ( $p \leq 0.05$  was considered significant). ROI, region of interest

Despite the fact that IDDPHP caused an increase in the number of nuclei (Fig. 4(c)), there were still less oligodendrocytes differentiated (Fig. 5(f, j)). EHDPHP, TCP, and TBOEP significantly reduced oligodendrocyte differentiation only at 20  $\mu$ M to

$36.5 \pm 8.3\%$ ,  $31.1 \pm 7.4\%$ , and  $24.8 \pm 9.0\%$  of controls, respectively (Fig. 5(l, m, n, o)). The endpoint-specific control BMP7 significantly reduced total number of oligodendrocytes to  $0.4 \pm 0.1\%$  (Suppl. Fig. 4(e)).



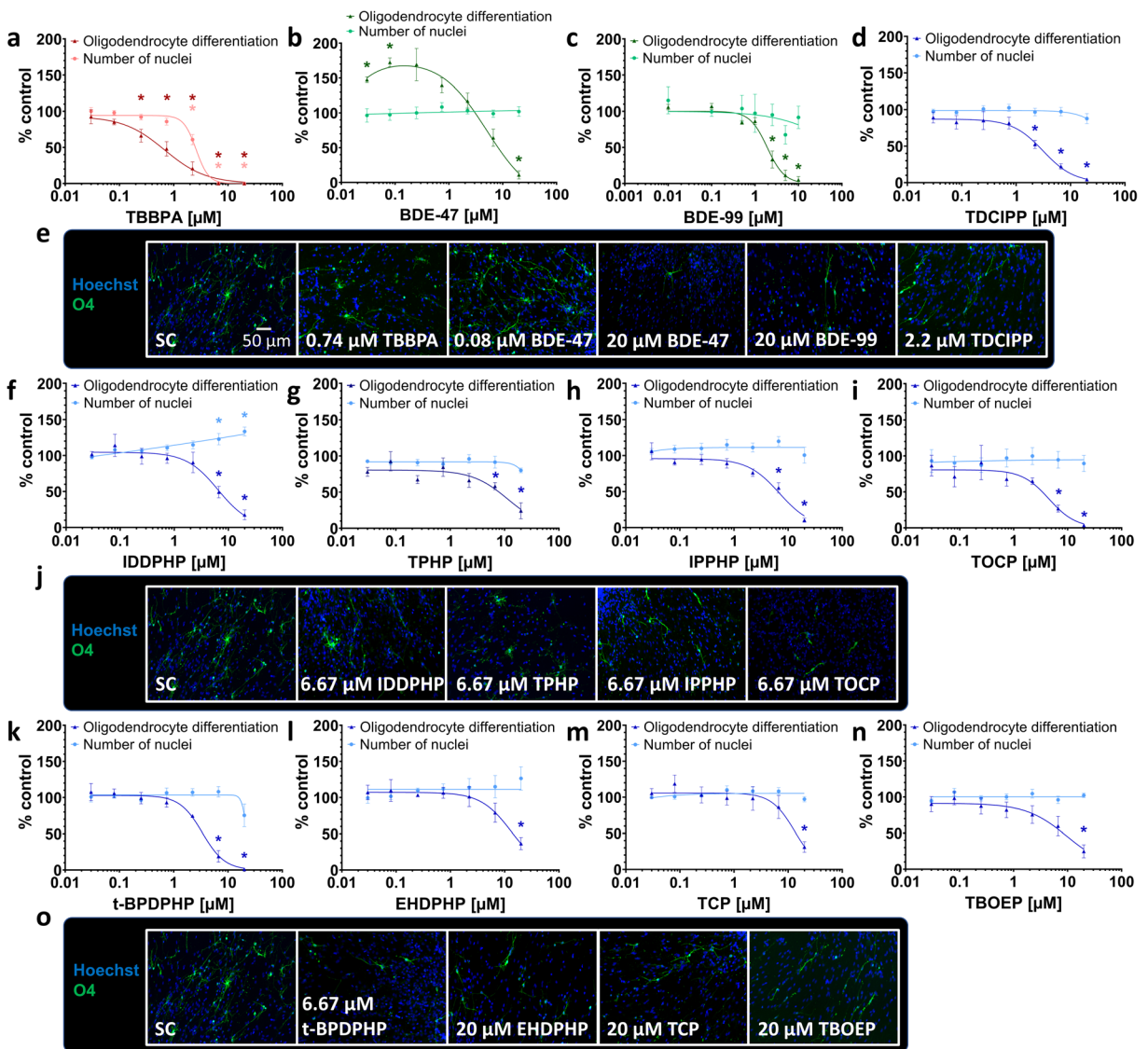
**Fig. 4** Neuronal differentiation and morphology (NPC3, NPC4, UKN4, UKN5) in the presence and absence of FRs. Spheres were plated onto poly-D-lysine/laminin-coated 96-well plates in the presence and absence of FRs. Differentiation into neurons (**a**, **b**) was determined automatically by using a convolutional neural network (CNN) running on Keras implemented in Python 3. The number of all  $\beta$ (III)tubulin-positive cells (red) in percent of Hoechst positive nuclei (blue) in the migration area after 120 h of differentiation was calculated (**c**, **e**). Morphology (**d**) was determined automatically by using the software Omnisphero.

LUHMES cells and hiPSC derived sensory neurons were treated for 24 h in presence or absence of FRs and stained with Calcein-AM and H-33342 (**g**, LUHMES cells). An automated algorithm calculates the neurite area via subtraction of a calculated soma area from all calcein positive pixels (**f**, **h**). Data are represented as means  $\pm$  SEM (except BDE-99 NPC3,  $n=2$ , means  $\pm$  SD). Statistical significance was calculated using one-way ANOVA followed by Bonferroni's post hoc tests ( $p < 0.05$  was considered significant)

### Transcriptome changes in hNPCs

Since we identified 12 out of 15 FRs as disruptors of oligodendrocyte differentiation and for most of these compounds this endpoint was the only neurodevelopmental process disturbed in differentiating NPCs at these concentrations, we performed RNASeq analyses of neurospheres exposed to BMC<sub>50</sub> concentrations of selected FRs for 60 h. FR selection was based on DNTPi clustering choosing at least one FR from each DNTPi cluster (Fig. 7). For BDE-47, which produced a bell-shaped concentration-response curve, the highest significant concentration for the oligodendrocyte inducing effect was studied in addition. These experiments aimed at gaining understanding about similar or different modes-of-actions (MoA) underlying the observed endophenotype. The PCA analysis was based on 18941 genes and indicates the differences of individual FRs to the controls (Fig. 6(a)). The plot shows the highest

transcriptional variation in cells treated with EHDPHP compared to the controls. Both phased-out PBDEs (higher concentration for BDE-47), TOCP and IDDPHP, and t-BDPDHP, TDCIPP, and TBBPA clearly separated from the controls, while the low BDE-47 concentration did not lead to a separation from the controls. A hierarchical clustering of FRs based on their different gene expression levels was generated with Minkowski distance analyses (Fig. 6(b)). Similar to the PCA plot, EHDPHP was the most distanced FR to control and IDDPHP, TOCP, as well as BDE-99 and the higher concentration of BDE-47 form two clusters in an independent manner to the control. BDE-47 (0.08  $\mu\text{M}$ ), TDCIPP, TBBPA, and t-BDPDHP also form a cluster away from the controls, yet with less distance than the other compounds. This clustering is also reflected in the heatmap shown in Fig. 6(c). Here, the Z-score of up- and downregulated genes visually demonstrates that the pattern of BDE-47 (low), TDCIPP,



**Fig. 5** Differentiation into oligodendrocytes (NPC5) in the presence and absence of FRs. Spheres were plated onto poly-D-lysine/laminin-coated 96-well plates in the presence and absence of FRs. Differentiation into oligodendrocytes was determined automatically based on immunocytochemical stainings (e, j, o) and by using a convolutional neural network (CNN) running on Keras

implemented in Python 3. The number of all O4-positive cells (green) in percent of Hoechst positive nuclei (blue) in the migration area after 120 h of differentiation was calculated (a, b, c, d, f, g, h, i, k, l, m, n). Data are represented as means ± SEM. Statistical significance was calculated using one-way ANOVA followed by Bonferroni's post hoc tests ( $p < 0.05$  was considered significant)

TBBPA, and t-BDPDHP is similar to the pattern of controls. Equally to the PCA variance and Minkowski cluster, the patterns of IDDPHP and TOCP, as well as of both phased-out PBDEs, are visually similar to each other. Again, EHDHP was clearly different from the controls and the other FRs.

To understand qualitative changes in gene expression related to FR effects on oligodendrocytes, we analyzed genes involved in selected pathways that relate to

toxicity of the oligodendrocyte lineage (Simons and Trajkovic 2006; Káradóttir et al. 2008; Volpe et al. 2011; Marinelli et al. 2016) listed in Fig. 6(d) and visualized those in respective heatmaps (Suppl. Fig. 6). Heatmap hierarchical clusters were used for classification into several levels. Level 1 (dark blue) describes the most distanced cluster from control, while the separation between samples and controls decreases in hierarchy up to > level 4 (white). In all pathways analyzed except for



NOTCH1 signaling (level 3), EHDPHP reached level 1 suggesting that EHDPHP interfered with a wide variety of oligodendrocyte-relevant cell signaling. Similarly, the phased-out PBDEs affected a broad variety of genes belonging to these pathway gene clusters. Here it is of interest that BDE-99 did not affect genes involved in cholesterol biosynthesis or mitochondrial calcium transport. TOCP and IDDPHP, which clustered in the previous analyses (Fig. 6(a, b)), also displayed a similar pattern in the pathway analyses. Both most strongly influenced NOTCH1 signaling and at a lower level affected almost all other pathways except for ROS detoxification. TDCIPP and t-BPDPHP both exerted the least effects on the pathways as they disturb multiple pathways at level 4 without pathway overlap.

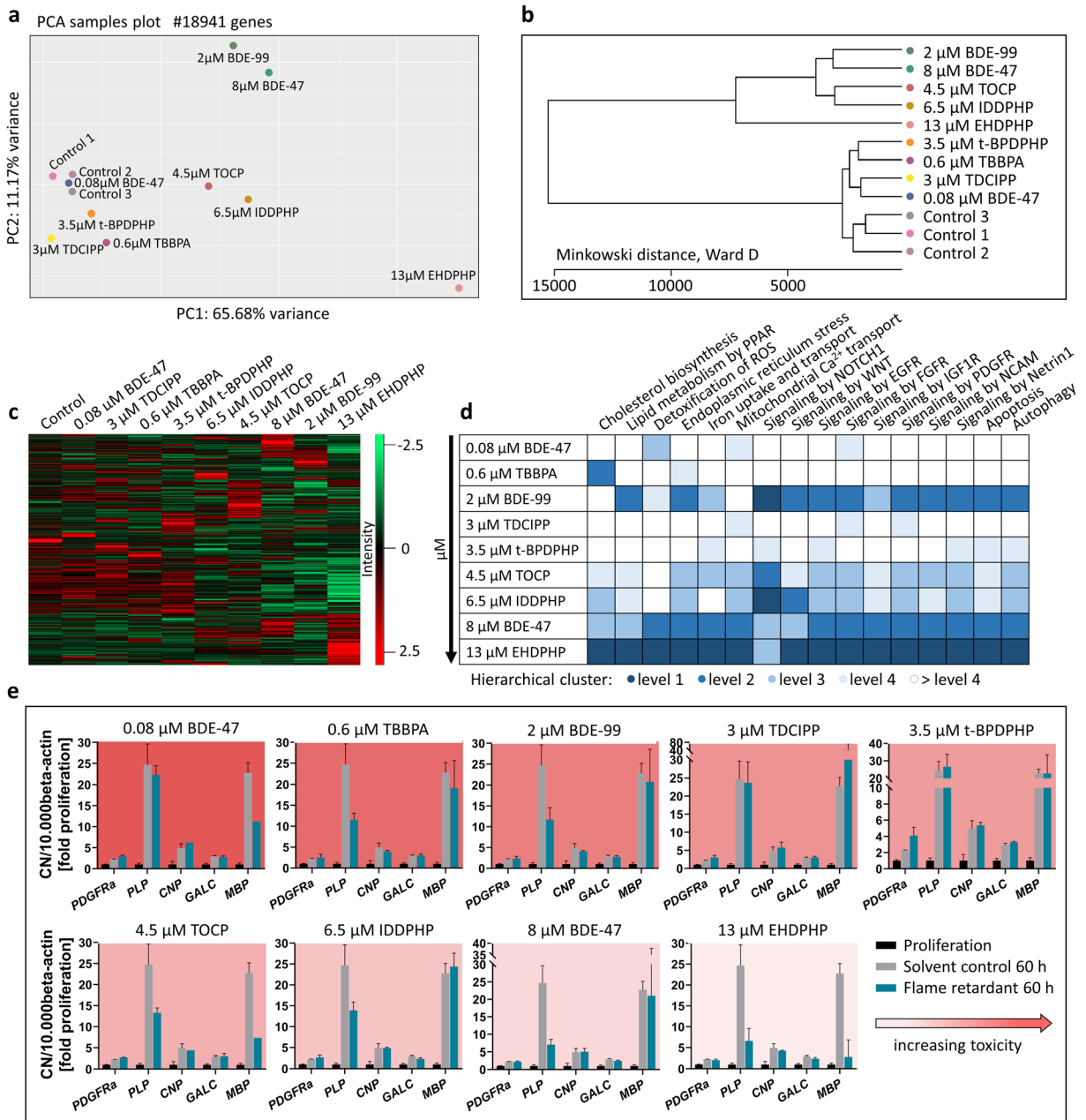
A special case in MoA seems to be TBBPA as it strongly and selectively affected cholesterol biosynthesis at level 2 and endoplasmic reticulum stress at level 4, while all other pathways are unaffected. These RNASeq data confirm previous Affymetrix microarray data identifying altered cholesterol metabolism as the predominant non-endocrine pathway affected by TBBPA in differentiating neurospheres (Klose et al. 2020). These data indicate that the studied FRs disturb a variety of pathways that influence amongst others oligodendrocyte differentiation. As this is a mixed culture, we cannot exclude that the signals produced by FRs are also derived from the other cell types in differentiated neurospheres, i.e., radial glia and neurons. It is to note that these RNASeq results are based on an  $n=1$  each that give an orientation on similar or distinct MoA of the individual FR but need to be substantiated by more in-depth work in the future.

Due to the low percentage of oligodendrocytes (4.4%) within the migration area, the depth of RNASeq was not sufficient to detect transcription of oligodendrocyte-related genes in detail. Therefore, we performed RT-qPCR analyses of five oligodendrocyte-specific transcripts representing their different maturation stages (Fig. 6(e)). Gene expression data of the solvent control of differentiated spheres normalized to proliferating spheres reveal “normal” neurosphere development over a time course of 60 h (gray bars). These can be directly compared to the FR-treated samples (blue bars). Gene products chosen are representative for increasing oligodendrocyte maturation stages ( $PDGFR\alpha < PLP < CNP < GALC < MBP$ ; Baumann and Pham-Dinh 2001; Kuhn et al. 2019), although these are onsets of expression and the markers show considerable overlaps. All gene products were expressed at least twofold higher in differentiating versus

proliferating spheres supporting oligodendrocyte formation in the neurosphere system (Dach et al. 2017). FR exposure altered developmental gene expression changes from proliferating to 60 h differentiating neurospheres. Only t-BPDPHP induced a twofold expression induction of  $PDGFR\alpha$  mRNA, a gene expressed in oligodendrocyte progenitor cells (OPCs) and pre-oligodendrocytes (pre-OLs), but not in immature and mature oligodendrocytes (OLs), suggesting a delay in oligodendrocyte maturation.  $PLP$  is expressed in OPCs, pre-OLs, and OLs and was strongly reduced by TBBPA, BDE-99, TOCP, IDDPHP, BDE-47, and EHDPHP mirroring general reduction of OLs across maturation stages. In contrast,  $CNP$  and  $GALC$  mRNA, which are expressed in all oligodendrocyte stages but the OPCs, were not affected by any of the compounds.  $MBP$  gene expression, one of the latest oligodendrocyte maturation markers, was reduced by BDE-47 (low concentration), TOCP, and EHDPHP (Fig. 6(e)). Interestingly, BDE-47 induced oligodendrocyte formation. These data demonstrate that despite the common phenotypical result of reduction in oligodendrocyte differentiation (besides BDE-47 low concentration), FRs’ molecular effects on oligodendrocyte marker expression patterns are compound-specific.

#### Compound classification based on BMC calculation

In order to provide a common metric of comparison across the different assays and substances, the benchmark dose (BMD) approach, which is recommended by the EFSA Scientific Committee (Hardy et al. 2017), was used. For in vitro toxicity testing, benchmark concentration (BMC) is comparable to the BMD (Krebs et al. 2020a) and derived from concentration-response information. The benchmark response (BMR) value was defined based on the variability of the respective endpoints (NPC1-5, Suppl. Fig. 4; UKN, Masjosthusmann et al. 2020). All BMCs calculated from all data points of the fitted concentration-response curves are listed in Table 1, with the respective upper and lower confidence intervals given in supplementary Table 2. From the FRs, which achieved BMCs, several questions can be drawn: (i) Are the observed effects DNT-specific or unspecific hits according to the classification models (Masjosthusmann et al. 2020)? (ii) What is the most sensitive endpoint (MSE) for each FR? And (iii) what is the potency ranking of the FRs? Most compound effects assessed by the battery are DNT-specific (Table 1), yet BBOEP, TCEP, and TCIPP did not reach DNT-specificity according to the



**Fig. 6** RNA sequencing and RT-qPCR. Human NPCs differentiated for 60 h in the presence of 0.6  $\mu$ M TBBPA, 2  $\mu$ M BDE-99, 3  $\mu$ M TDCIPP, 3.5  $\mu$ M t-BPDPPH, 4.5  $\mu$ M TOCP, 6.5  $\mu$ M IDDPHP, 8  $\mu$ M BDE-47, and 13  $\mu$ M EHDHPH. These concentrations represent the BMC<sub>50</sub> values of oligodendrocyte differentiation inhibition. 0.08  $\mu$ M BDE-47 induced oligodendrocyte differentiation. Controls 1–3 represent spheres plated in solvent control 0.1% DMSO. PCA (a) and Minkowski distance plot (b) analyses were performed using the PCAGO online software (<https://pcago.bioinf.uni-jena.de/>) as previously described (Gerst and Hölzer 2019). Both plots were generated by normalizing the total number of reads of different samples to the Transcript per Kilobase Million (TPM) count. The heatmap (c) was generated using Perseus Version 1.6.2.2 (<https://www.maxquant.org/perseus/>).

Therefore, the Z-scores of TPM values were used with a cut-off of one valid value per condition. Classification of impact on oligodendrocyte differentiation-relevant pathways (d) was performed by expert judgment based on hierarchical clustering of pathway-related genes (Suppl. Fig. 6) and was categorized into four levels (level 1 as most and level 4 as least distanced to one merged control). Gene expression (e) of *platelet-derived growth factor receptor A* (*PDGFR $\alpha$* ), *proteolipid protein* (*PLP*), *cyclic-nucleotide-phosphodiesterase* (*CNP*), *galactosylceramidase* (*GALC*) and *myelin basic protein* (*MBP*) was assessed via RT-qPCR and normalized to the housekeeping gene beta actin (*ACTB*). In addition to solvent control (gray bars), proliferative spheres (black bars) were used as an internal control. Data are represented as mean  $\pm$  SD from 1 to 3 biological replicates



**Table 1** Summary of BMCs across the DNT in vitro testing battery. Specific hits are highlighted bold and borderline hits are marked *curative*. Red colored specifies most sensitive endpoints(MSEs). \*Induced effects. Numbers are given in  $\mu\text{M}$ . No value assumes BMCs > 20  $\mu\text{M}$ 

		Brominated (BFRs)			Organophosphates (OPFRs)											
		TBBPA	BDE-47	BDE-99	TPHP	TBOEP	IDDPHP	IPPHP	TCP	TDCPP	t-BPDPPH	TOCP	EHDPPH	BBOEP	TCEP	TCIPP
<i>Proliferation by area</i>	BMC <sub>20</sub>	-	-	-	-	-	-	-	-	-	-	-	-	-	-	-
<i>Proliferation by BrdU</i>		-	-	-	-	-	-	-	<b>0.86</b>	-	-	17.2	<b>0.02</b>	-	18.9	-
<i>Proliferation CTB</i>		-	-	-	-	-	-	9.62*	-	19.2	-	-	-	19.9	-	-
<i>Proliferation LDH</i>		-	-	-	-	-	-	-	-	-	-	-	-	-	-	-
<i>Radial glia migr. 72 h</i>	BMC <sub>20</sub>	1.93	-	-	-	-	-	-	-	-	-	-	-	-	-	-
<i>Radial glia migr. 120 h</i>		2.15	-	-	-	-	-	-	-	-	15.73	-	-	-	-	-
<i>Neuronal migration</i>		2.60	-	-	-	-	-	-	-	-	-	-	-	-	-	-
<i>Oligo. migration</i>		2.23	-	-	-	-	-	-	-	-	12.54	8.12	-	-	-	-
<i>LDH 72 h</i>		1.75*	-	-	-	-	-	-	-	-	-	-	-	-	-	-
<i>LDH 120 h</i>		0.63*	-	-	-	-	-	-	-	-	-	-	-	-	-	-
<i>CTB 120 h</i>		1.38	-	3.56*	-	-	1.79*	5.50*	-	11.2	-	12.9*	5.88*	-	-	-
<i>Neurite length</i>		2.31	-	-	-	-	-	-	-	-	9.55	0.12	17.9	-	-	-
<i>Neurite area</i>		2.49	-	-	-	-	-	-	-	-	15.8	0.51	19.8	-	-	-
<i>Number of nuclei</i>		1.49	-	-	-	-	3.10	-	-	-	19.8	-	8.72	-	-	-
<i>Number of neurons</i>		2.18	-	-	-	-	-	-	-	12.8*	-	18.8	10.3	-	-	-
<i>Number of oligodendrocytes</i>		BMC <sub>50</sub>	-	<b>0.03*</b>	-	-	-	-	-	-	-	-	-	-	-	-
<i>NCC migration</i>	BMC <sub>25</sub>	<b>0.55</b>	<b>8.00</b>	<b>1.91</b>	<b>6.39</b>	<b>7.62</b>	<b>6.45</b>	<b>6.88</b>	<b>13.2</b>	<b>3.13</b>	<b>3.37</b>	<b>4.49</b>	<b>13.1</b>	-	-	
<i>NCC viability</i>	BMC <sub>10</sub>	2.78	14.2	-	-	-	-	-	16.9	-	14.0	3.44	11.4	-	-	
<i>LUHMES neurite area</i>	BMC <sub>25</sub>	-	-	12.3	-	-	-	-	-	-	-	-	-	-	-	
<i>LUHMES viability</i>		-	13.5	15.0	-	-	-	-	-	-	-	-	-	-	-	
<i>Sensory N. neurite area</i>		-	-	-	-	-	-	-	-	-	-	-	-	-	-	
<i>Sensory N. viability</i>		-	-	-	-	-	-	-	-	-	-	-	-	-	-	

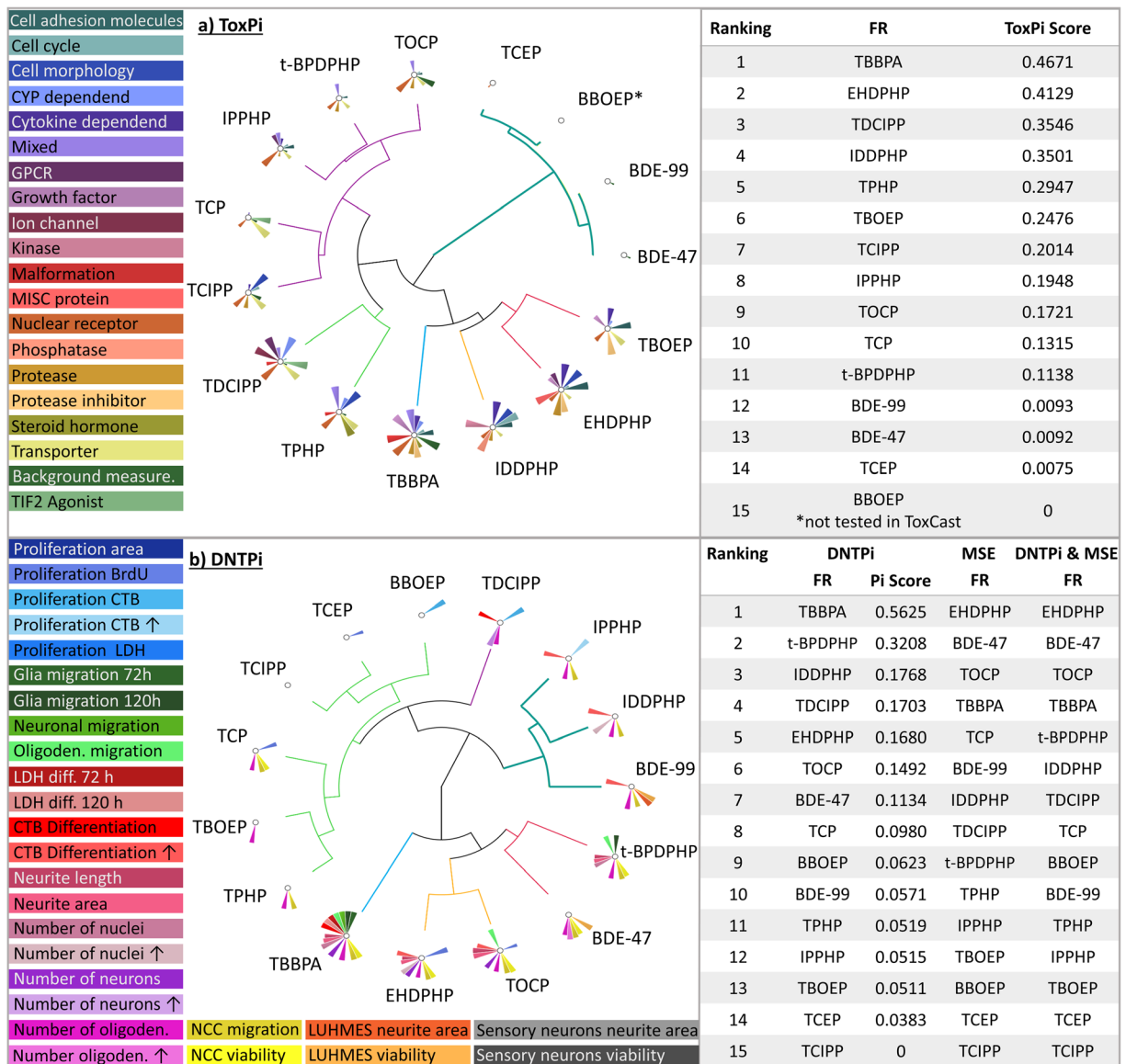
classification models. For TBBPA, most endpoints were affected at concentrations also inducing cytotoxicity. Based on specific DNT hits, the MSE for each compound across the DNT battery was assessed. In most cases (7/12), it was oligodendrocyte differentiation (NPC5), followed by NCC migration (UKN2; 2/12), NPC proliferation (NPC1; 2/12), and neurite morphology (NPC4; 1/12). The other assays did not provide MSE. Potency ranking was as follows: EHDPPH > BDE-47 > TOCP > TBBPA > TCP > BDE-99 > IDDPHP > TDCCP > t-BPDPPH > TPHP > IPPHP > TBOEP (Fig. 7).

#### Compound prioritization: ToxPi vs. DNTPi

Another currently propagated compound prioritization instrument is the Toxicological Prioritization Index (ToxPi) tool introduced by the US EPA (Reif et al. 2010; Marvel et al. 2018). Using this tool, FR testing results were visualized and prioritized according to their DNT profiles generated in this study by producing DNTpis (Fig. 7(b)), which are then compared to their toxicological profiles of the existing ToxCast data (ToxPis; Fig. 7(a); <https://www.epa.gov/chemical-research/toxicity-forecasting>). Here, the whole toxicological profiles are taken into account, i.e., also FR

effects on cell viability, and specific and non-specific hits are not distinguished. In general, the size of the Pi pieces does not reflect the actual BMC values but relates the BMCs for the studied compound to the BMCs of this endpoint across the highest and lowest values of the whole endpoint data set across all compounds irrespective of the values by distributing them between 0 and 1. Hence, it is a relative, not an absolute value. The ToxPi tool then hierarchically clusters the FRs within the ToxPis and the DNTpis according to their potency and assay hit patterns. Producing ToxPi information on compound clustering and ranking of a compound class for “general” (ToxPis) and “specific” toxicity, here DNT (DNTpis) gives information on the specificity of the compound effects.

Our ToxPi evaluation of the compound class of FRs clearly indicates that the Pi clustering is very different between the ToxPis and the DNTpis. For example, the two phased-out PBDEs are almost negative in the ToxCast assays and cluster collectively, while they evoke multiple responses in the DNT assays resulting in separate clusters. Similarly, e.g., TCIPP gives alerts in the ToxPi, while there is no effect in the DNTpis. Additionally, the program creates toxicity rankings and, in both rankings, TBBPA was classified as the most potent one. However, the overall ranking differs from each other, for example, t-



**Fig. 7** Visualization and prioritization of FRs generated with ToxPi. ToxPis for general (a) and DNT-specific (b) toxicities using the ToxCast data and the results of the DNT in vitro battery, respectively. Graphs were produced with the Toxicological Prioritization Index (ToxPi) and Graphical User Interface (GUI) tool version 2.3. Size of pie slices represents relative strength of effect

on respective endpoint. For DNTPi and MSE ranking, first priority was given to MSE (Table 1); in the second line, ToxPi ranking was considered, e.g., for compounds with similar MSEs (starting from number 4 in the MSE analysis (Table 1; Suppl. Fig. 5a), due to overlapping 3-fold ranges for the MSE). \*BBOEP was not tested in ToxCast

BPDPPH ranks on number 2 in the DNTPi and on number 11 in the ToxPis. Similarly, TCIPP ranks on number 15 in the DNTPi and on number 7 in the ToxPis suggesting that general toxicity is not a good predictor for DNT. As the ToxPi tool does not distinguish between DNT-specific and non-DNT-specific effects and the ranking takes rather the number of modified endpoints than the effective concentrations, which relate to potency, into

account, we next combined the MSE-based (Table 1; Fig. 7; Suppl. Fig. 5(a)) with the ToxPi (Fig. 7) ranking. Therefore, the MSE with DNT-specific hits (Table 1; Suppl. Fig. 5(a)) was set to the first priority and, in the second line, DNTPi ranking was considered, e.g., for compounds with similar MSEs (starting from number 4 in the MSE analysis (Table 1; Suppl. Fig. 5(a)) due to overlapping 3-fold ranges for the MSE (Masjosthusmann

et al. 2020). Merging the two ranking strategies changes some of the FR ranking, yet not the four most potent compounds EHDPHP, BDE-47, TOCP, and TBBPA and results in the final ranking of FRs due to the data of this study (DNTPi and MSE; Fig. 7).

## Discussion

In this study, we applied a human-based DNT in vitro battery of tests as a first case study for screening and prioritization of 15 data-poor compounds belonging to the class of FRs including phased out and alternative FRs. By using the BMC concept, specific DNT hits and most sensitive endpoints were identified across the endpoints of the battery. These scatter across the broad variety of neurodevelopmental processes investigated in this study.

### TCP and EHDPHP

Two FRs, TCP, and EHDPHP inhibited NPC proliferation (NPC1) as the MSE at fairly low concentrations ( $BMC_{20}$  0.86 and 0.02  $\mu\text{M}$ , respectively). Proliferation is a fundamental neurodevelopmental KE that, when altered, might cause microcephaly (Tang et al. 2016). This is the first time that the specific impact of TCP and EHDPHP on cell proliferation was shown in human cells. Previous work demonstrated neurodevelopmental behavioral adversities in a zebrafish model of these compounds at concentrations of 4 and 5  $\mu\text{M}$  lowest nominal effect levels, respectively (Alzualde et al. 2018). This model is well suited for informing on adverse outcomes but does not provide mechanistic information. A strong DNT potential for TCP was also identified in a recent study using a rat primary cell-based spheroid model. Concentrations as low as 0.1  $\mu\text{M}$  decreased the neurotransmitter content and affected genes related to neurotransmitter production after an exposure period of 14 days (Hogberg et al. 2020).

### TOCP

TOCP was the only FR altering neurite length of young, primary fetal neurons as the MSE ( $BMC_{20}$  0.12  $\mu\text{M}$ ). Neurotoxicity of TOCP was previously observed in ferret (Stumpf et al. 1989) and in the hen sciatic nerve accompanied by a reduction in nerve calcium (Luttrell et al. 1993). Interference with neuronal calcium levels

could hint to a potential TOCP developmental MoA as calcium signaling is crucial for neurite outgrowth via regulating growth cone motility (Gasperini et al. 2017). TOCP was also identified as a neurotoxicant, as it disturbed the neural network activity in rat cortical neurons (Behl et al. 2015). Yet, these studies did not investigate neurodevelopment, but adult neurotoxicity.

### IDDPHP

Interestingly, the OPFR IDDPHP induced the number of nuclei in the migration area as the MSE, probably due to excessive migration or proliferation of radial glia cells, the major and still proliferative cell type in the migration area. As IDDPHP did not alter radial glia migration distance, the action of IDDPHP on their proliferation seems to be the more probable explanation. However, this has to be substantiated by further experiments in the future. When it comes to radial glia, species specificities become crucial, as this cell type regulates evolutionary specificities of cortex formation (Zilles et al. 2013). Their proliferation and migration are tightly regulated processes orchestrating species-specific development of the cortex, with a special role in its folding in gyrencephalic species, like humans (Borrell and Götz 2014). Hence, interference with radial glia neural progenitors underlie a number of cortical malformations and cause mental retardation in genetic and infectious diseases (Guerrini and Dobyns 2014; Hu et al. 2014; Juric-Sekhar and Hevner 2019). In a recent study, IDDPHP triggered an increase of *nestin* expression, and this was interpreted as evidence of reactive astrogliosis (Hogberg et al. 2020). However, there may be alternative explanations, as changes in *nestin* may also point to effects on the radial glia and neural stem cell compartments. Zebrafish behavior was also affected by IDDPHP, yet at fairly high nominal lowest effect levels (40  $\mu\text{M}$ ) with no knowledge on the underlying mechanisms (Alzualde et al. 2018).

### IPPHP and t-BPDPHP

NCC migration was the most sensitive endpoint (together with oligodendrocyte differentiation) upon IPPHP ( $BMC_{20}$  6.66  $\mu\text{M}$ ) and t-BPDPHP ( $BMC_{20}$  4.05) exposure. Disturbance of NCC migration causes, e.g., cleft palate or loss of functional hearing (Mayor and Theveneau 2013). Our data from human cells are in good agreement with model systems from other species:

micromolar concentrations of IPPHP and t-BPDPHP were also toxic for zebrafish (Behl et al. 2015; Alzualde et al. 2018), *Caenorhabditis elegans* (Behl et al. 2015; Boyd et al. 2016), rat cortical neurons (Behl et al. 2015), and 3D rat brain spheres (Hogberg et al. 2020). t-BPDPHP specifically inhibits neurite outgrowth of rat cortical neurons at 14.9  $\mu\text{M}$  (Behl et al. 2015), an effect that we observe at similar concentrations in the NPC4, but not in the UKN4/5 assays. Similarly, IPPHP solely inhibits NCC, but not radial glia, neuronal or oligodendrocyte migration, while t-BPDPHP does alter other cell type migration at higher concentrations. Why different migration or neurite outgrowth assays yield different hits and are thus complementary to each other is probably due to different cell types, species, and neurodevelopmental timing represented in the assays. Hence, toxicity patterns across the battery reflect compounds different MoA by specifically altering certain targets.

#### Oligodendrocyte differentiation

Oligodendrocyte differentiation was the endpoint most frequently altered as the MSE upon cellular FR exposure with the following compound potency ranking: BDE-47 (low) > TBBPA > BDE-99 > TDCCP > t-BPDPHP > TPHP > IPPHP > TBOEP. Oligodendrocytes are necessary for proper brain functioning as they form and keep myelin sheaths around axons, thereby allowing rapid saltatory conduction of neuronal action potentials (Baumann and Pham-Dinh 2001; Kuhn et al. 2019). Hence, impaired oligodendrogenesis and resulting hypomyelination due to genetic disorders or severe brain injury contribute to functional adverse outcomes manifesting in neurological disorders such as the Alan-Herndon-Dudley Syndrome (López-Espindola et al. 2014; Tonduti et al. 2014) or periventricular leukomalacia (Back et al. 2001). Developing oligodendrocytes also exert a high susceptibility to stressors like reactive oxygen species and are sensitive to excitotoxicity and endoplasmic reticulum stress. They have a high energy and iron demand, are dependent on functional lipid metabolism, and their development and function are highly regulated by different hormones and growth factors (Bradl and Lassmann 2010; Volpe et al. 2011; Marinelli et al. 2016). Hence, developing oligodendrocytes can be concerned by a large variety of substances through a broad spectrum of MoA.

#### BDE-47 and oligodendrocyte differentiation

Since deviation from normal development into both directions, i.e., increase or decrease of a neurodevelopmental process, is considered adverse (Foti et al. 2013), the increase in oligodendrocyte differentiation by BDE-47 in the low nanomolar range needs attention. Consequences of increased oligodendrocyte differentiation are hypermyelination, an outcome observed for example in individuals with autism spectrum disorder (Ben Bashat et al. 2007; Wolff et al. 2013; Razek et al. 2014). So far, BDE-47 was found to reduce mouse and human oligodendrocyte differentiation similar to the effects observed in this study at higher concentrations (Schreiber et al. 2010; Li et al. 2013). Li et al. (2013) did not test with BDE-47 concentrations that induced oligodendrocytes here (< 0.3  $\mu\text{M}$ ), whereas Schreiber et al. (2010) used concentrations as low as 0.1  $\mu\text{M}$ . Here, inter-individual differences could explain the missing inducing oligodendrocyte effect as neurospheres used were generated from a different donor. Thus, it is increasing confidence that the data produced in this paper represents data from three different individuals. In addition, Schreiber et al. (2010) quantified oligodendrocytes by manual counting, while cells in this work here were identified using a convolutional neuronal network (CNN), which is more reliable, reproducible, and free of human counting bias. The induction mechanism of oligodendrocyte differentiation by BDE-47 is so far unknown. The performed RNASeq analyses did not reach a sufficient depth for such a cell type-specific molecular clarification. Interestingly, oligodendrocyte toxicity pathways are already triggered at 80 nM BDE-47 (Fig. 6(d)), probably resulting in loss of MBP-expressing more mature oligodendrocytes that is overridden by an unknown, oligodendrocyte-inducing trigger. In rat brain spheres, BDE-47 (0.1–5  $\mu\text{M}$ ) did not appear to affect *mbp* gene expression, but it caused a transient increase in myelin-associated glycoprotein (*mag*) transcript at 5  $\mu\text{M}$  (Hogberg et al. 2020). Our previous species comparison of in vitro oligodendrogenesis found significant differences in timing, regulation of gene expression and response to toxicants between human and mouse oligodendrocytes (Dach et al. 2017; Klose et al. 2020). On the basis of these observations, it is likely that human neurospheres (as used here) will show differences to rat spheres. The difference in exposure schemes and readouts further complicates direct comparisons. A striking difference is for instance that none of the 15 FRs had any effect on human neuronal differentiation, while all 5 FRs tested in rat spheres reduced

neurofilament and other specifically neuronal markers (Hogberg et al. 2020).

#### TBBPA and oligodendrocyte differentiation

Similarly, TBBPA reduces oligodendrocyte differentiation. From the toxicity pathways analyzed by RNASeq, mainly genes relating to cholesterol biosynthesis were deregulated by TBBPA. This MoA was previously described as a putative adverse outcome pathway (Klose et al. 2020). TBBPA did not affect the number of corpus callosum CNP<sup>+</sup> oligodendrocytes (Saegusa et al. 2009) or Ret<sup>+</sup> oligodendrocytes (Fujimoto et al. 2013) in developmental rat studies. This might be due to the markers used in the in vivo study, as e.g., *CNP* expression did not, but only *PLP* expression changed upon TBBPA treatment in this study. Also, species (Dach et al. 2017) or brain regions with heterogeneous oligodendrocyte populations (Hayashi and Suzuki 2019) might have affected the results.

#### RNASeq analyses

In the Minkowski distance cluster and gene heatmap (Fig. 6(b, c)), the low concentration BDE-47, TBBPA, TDCIPP, and t-BPDPHP clustered together close to the controls. Different from TBBPA, the latter two change gene expression in variable oligodendrocyte toxicity pathways. These data suggest that either one specific pathway, like cholesterol metabolism for TBBPA, or multiple hits across distinct converging pathways like in the case of TDCIPP or t-BPDPHP, can summit in the same endophenotype. Minkowski cluster further demonstrates that TOCP, IDDPHP, PBDEs, and EHDPHP differ most from the controls and they strongly affect a large variety of oligodendrocyte toxicity pathways. Because oligodendrocytes provide just around 4% of the cells in the migration area, it is highly unlikely that these strong alterations in mRNA expression profiles can be attributed to oligodendrocytes only, but probably also derive from radial glia and/or neurons in the migration area. Because all other phenotypic endpoints of the neurosphere assay were not affected, these data clearly show the high susceptibility of oligodendrocytes towards alterations of these pathways and thus supports the notion of “just being an oligodendrocyte seems enough to put these cells at greater risk of damage” (Bradl and Lassmann 2010).

#### Compound prioritization

Such DNT in vitro battery data can be used for compound prioritization. Here, different methods are at hand. For one, BMC values with CI allow distinguishing between DNT-specific and DNT-unspecific hits (Masjosthusmann et al. 2020) giving objective potency ranking measures. However, this method takes only the MSE and not, e.g., the number of affected endpoints into consideration. To account for both, we merged the MSE method with the ToxPi approach by prioritizing for BMCs first and secondly adding the ToxPi ranking when BMCs of MSE of different compounds were located within their 3-fold ranges. In our opinion, prioritization for DNT only by ToxPi might include high uncertainty, because altering only one DNT endpoint can have detrimental effects on neurodevelopment, especially when it happens at low concentrations. Using this merged approach, our study revealed that BDE-47 and BDE-99, which are already banned due to their neurodevelopmental toxicity, rank as 2nd and 10th out of the 15 FRs investigated. Of the currently used aFRs, only TCIPP did not produce a hit in the battery according to the BMCs. However, also TCEP and BBOEP did not yield statistically significant hits, but just reached their BMC<sub>20</sub> values. Therefore, these three aFRs are rated as the least toxic with the DNT in vitro battery, while EHDPHP together with BDE-47 summit at the top as the most hazardous FR. These data indicate that the DNT in vitro battery is a useful tool for prioritizing compounds for their DNT hazard potential. It has to be noted that the battery applied here still has known gaps that need to be closed in the future. These include test methods for neuronal network formation (Frank et al. 2017; Shafer et al. 2019; Nimtzt et al. 2020) including synaptogenesis (Pistollato et al. 2020), astrocyte, and microglia performance.

One question that arises is if such a DNT in vitro battery is at all necessary or if DNT might as well be predicted by the general ToxCast assays. To answer this question, FR DNT in vitro battery is compared to ToxCast data by ToxPi versus DNTPi assessment. The results demonstrate the uniqueness of the DNT in vitro battery for DNT hazard assessment. Such an approach has never been executed before and was shown here to be very helpful for assays' specificity analyses.



## Moving from hazard to risk

When moving from hazard characterization to risk assessment, exposure data is crucial. Biomonitoring data for parent compounds currently available (Table 2; Cariou et al. 2008; Sundkvist et al. 2010; Kim et al. 2014; Tang and Zhai 2017; Beser et al. 2019; Ma et al. 2019; Chupeau et al. 2020) reveal a gap on human FR exposure data, especially for OPFRs. While phased-out PBDEs and TBPPA can be measured in human samples, most OPFRs metabolize fast and parent compounds cannot be detected, e.g., in cord blood or breast milk. Therefore, the occurrence of OPFR metabolites is measured in urinary samples of adults (Bastiaensen et al. 2019b; Gibson et al. 2019; Chupeau et al. 2020; Li et al. 2020) and children (He et al. 2018a, b; Bastiaensen et al. 2019a; Gibson et al. 2019; Chupeau et al. 2020) or in

hair (Kucharska et al. 2015; Chupeau et al. 2020). These studies clearly demonstrate the existence of OPFR metabolites in human samples, especially in children.

For relating such biomonitoring data to the studied in vitro hazards, we converted the internal FR concentrations from cord blood or breast milk given in nanograms per gram of fat to molarity by using a fat content of 5.8 g/L for serum (Akins et al. 1989; Phillips et al. 1989; Covaci et al. 2006; Rylander et al. 2006) and 33 g/L for breast milk (Kent et al. 2006; Prentice et al. 2016). Such in vitro–in vivo comparisons are very crude and do not account for in vitro kinetics or for actual fetal brain concentrations in vivo.

Hence, advanced kinetic modelling would be eventually needed to perform proper in vitro to in vivo extrapolation (IVIVE). Nevertheless, our crude evaluations revealed cord blood values for BDE-99, BDE-47, and TBBPA of

**Table 2** Exposure data collected from published FR measurements in human breast milk and cord blood samples (Cariou et al. 2008; Sundkvist et al. 2010; Kim et al. 2014; Tang and Zhai 2017; Beser et al. 2019; Ma et al. 2019; Chupeau et al. 2020)

	Breast milk						Cord blood					
	BDE-99		BDE-47		TBBPA		BDE-99		BDE-47		TBBPA	
	ng/g lw	μM	ng/g lw	μM	ng/g lw	μM	ng/g lw	μM	ng/g lw	μM	ng/g lw	μM
<i>Korea</i>	54.0	0.0316	31.0	0.0211	-	-	19.0	0.0020	36.0	0.0044	-	-
<i>China</i>	10.8	0.0063	27.5	0.0187	-	-	3.45	0.0004	8.49	0.0010	-	-
<i>Japan</i>	3.20	0.0019	4.90	0.0033	-	-	-	-	0.12	0.00001	-	-
<i>Philippines</i>	0.82	0.0005	3.60	0.0024	-	-	-	-	-	-	-	-
<i>Vietnam</i>	0.38	0.0002	0.40	0.0003	-	-	-	-	-	-	-	-
<i>USA</i>	6.40	0.0037	29.7	0.0202	-	-	23.3	0.0024	4.60	0.0006	-	-
<i>France</i>	0.53	0.0003	1.15	0.0008	4.1	0.0025	7.43	0.0008	-	-	103	0.0111
<i>Germany</i>	0.18	0.0001	0.45	0.0003	-	-	-	-	-	-	-	-
<i>UK</i>	0.80	0.0005	2.70	0.0018	-	-	-	-	-	-	-	-
<i>Sweden</i>	0.48	0.0003	2.28	0.0015	-	-	0.22	0.00002	3.4	0.0004	-	-
<i>Spain</i>	0.51	0.0003	0.54	0.0004	-	-	4.3	0.0004	3.3	0.0004	-	-
	Breast milk											
	TPHP		TBOEP		TCEP		TCIPP		EHDPHP		TCP	
	ng/g lw	μM	ng/g lw	μM	ng/g lw	μM	ng/g lw	μM	ng/g lw	μM	ng/g lw	μM
<i>Japan</i>	1.40	0.0014	0.24	0.0002	0.14	0.0002	-	-	-	-	-	-
<i>Philippines</i>	19.0	0.0192	22.0	0.0182	42.0	0.0554	-	-	-	-	2.30	0.0021
<i>Vietnam</i>	4.90	0.0050	-	-	-	-	-	-	-	-	0.28	0.0003
<i>Sweden</i>	8.50	0.0086	4.70	0.0039	4.90	0.0065	45.0	0.0453	6.50	0.0059	0.80	0.0007
<i>Spain</i>	9.90	0.0100	14.8	0.0123	-	-	12.5	0.0126	-	-	19.0	0.0170
	TPHP		TBOEP		TCEP		TCIPP		EHDPHP		IDDPHP	
	ng/mL	μM	ng/mL	μM	ng/mL	μM	ng/mL	μM	ng/mL	μM	ng/mL	μM
<i>USA</i>	0.15	0.0005	1.44	0.0036	0.04	0.0001	0.22	0.0005	0.02	0.00006	0.01	0.00003



0.002, 0.004, and 0.011  $\mu\text{M}$  in a Korean (PBDEs) and French (TBBPA) cohort, respectively (Table 2). Breast milk concentrations calculated to 0.032 and 0.021  $\mu\text{M}$  for BDE-99 and BDE-47 in Korea and 0.003 for TBBPA in France. OPFRs in breast milk occur with the highest measured values across all FRs with TCEP 0.055  $\mu\text{M}$ , TPHP 0.019  $\mu\text{M}$ , and TBOEP 0.018  $\mu\text{M}$  (Philippines) and TCIPP 0.045  $\mu\text{M}$  (Sweden). Assuming a breast milk intake of 1 L/day, exposure to these FRs approximates to 32 nmol/day BDE-99, 21 nmol/day BDE-47, 3 nmol/day TBBPA, 55 nmol/day TCEP, 19 nmol/day TPHP, 18 nmol/day TBOEP, and 45 nmol/day TCIPP. While the BMCs calculated for DNT in vitro hazard for BDE-99 and OPFRs are more than one order of magnitude lower than the estimated daily intake and cord blood concentrations, the BDE-47 BMC for the MSE is just one order of magnitude higher than the estimated exposure (suggesting a bioavailability of 100%, slow/no liver metabolism, perfect blood-brain-barrier (BBB) passage (1:1), and protein binding according to logP prediction model).

However, humans are generally exposed to compound mixtures including FRs, pesticides, pharmaceuticals, toxic metals, and other environmental contaminants. Therefore, individual compound exposure easily adds up to mixtures at relevant concentrations that might exert additive, synergistic, or antagonistic effects, especially when the same converging endpoint is affected. This is likely the case for oligodendrocytes because they seem to be the most susceptible cell type of the brain. Mixture experiments as well as sophisticated IVIVE are needed to substantiate these concerns.

## Summary and conclusion

In summary, we tested 15 FRs including phased-out PBDEs, TBBPA and OPFRs for their neurodevelopmental toxicity in a human cell-based DNT in vitro battery. FR hazards across different neurodevelopmental endpoints were used for calculating BMC and CI leading to a potency ranking. Evaluation of the data with the ToxPi tool revealed a distinct ranking that we combined with the BMC ordering for final prioritization. In addition, comparison of DNT hazard ranking according to the ToxPi tool with the ToxCast data revealed DNT-specific hazard for this group of FRs that is not well predicted by ToxCast assays. Extrapolating DNT battery BMC to human FR exposure via breast milk suggests low risk for individual compounds but raises concern for mixture exposure, which

is the real-life situation. This is especially of apprehension when different compounds converge through diverse MoA on common endpoints like oligodendrocyte differentiation in this study.

This case study using FRs contextualized with the performance characteristics of the battery using diverse compound classes (Masjosthusmann et al. 2020) suggests that using a human cell-based DNT in vitro battery for hazard assessment for compound prioritization is a promising approach for future risk assessment procedures.

**Supplementary Information** The online version contains supplementary material available at <https://doi.org/10.1007/s10565-021-09603-2>.

**Author contribution** All authors read, commented, and approved the manuscript. Jödis Klose: study conception, investigation, data collection and analysis, figure design, writing. Melanie Pahl: investigation, data collection and analysis. Kristina Bartmann: investigation. Farina Bendt: investigation. Jonathan Blum: study conception, investigation, data collection and analysis. Xenia Dolde: study conception, investigation, data collection and analysis. Nils Förster: software. Anna-Katharina Holzer: study conception, investigation, data collection and analysis. Ulrike Hübenthal: investigation. Hagen Eike Keßel: software. Katharina Koch: study conception. Stefan Masjosthusmann: study conception and data analysis. Sabine Schneider: data analysis. Selina Woeste: investigation. Andrea Rossi: data analysis. Adrian Covaci: resources. Mamta Behl: resources. Marcel Leist: study conception, funding acquisition for all experiments performed with NCCs, LUHMES cells, and hiPSC-derived neurons; writing. Julia Tigges: study conception, supervision, project administration and writing. Ellen Fritsche: study conception, supervision, funding acquisition for all experiments performed with hNPCs, project administration, and writing.

**Funding** Open Access funding enabled and organized by Projekt DEAL. This work was supported by the FOKO (Forschungskommision of the medical faculty of the Heinrich-Heine-University) (2016-53), the EFSA (European Food Safety Authority) (OC/EFSA/PRAS/2017/01), CERST (Center for Alternatives to Animal Testing) of the Ministry for Culture and Science of the State of North-Rhine Westphalia, Germany) (file number 233-1.08.03.03-121972/131—1.08.03.03—121972), and the DFG Ursula M. Händel Tierschutzpreis to EF (DFG FR 1392/6-1). It has received funding from the European Union's Horizon 2020 research and innovation program under grant agreement No. 681002 (EU-ToxRisk) and No. 825759 (ENDpoiNTs).

## Declarations

**Ethics approval** hNPCs were purchased from Lonza Verviers SPRL, Belgium, and work was approved by the ethics committee of the Heinrich-Heine University Duesseldorf.

**Conflict of interest** The authors declare that they have no conflicts of interest.

## References

- Akins JR, Waldrep K, Bernert JT. The estimation of total serum lipids by a complete enzymatic 'summation' method. *Clin Chim Acta*. 1989;184:219–26.
- Alzualde A, Behl M, Sipes NS, Hsieh JH, Alday A, Tice RR, et al. Toxicity profiling of flame retardants in zebrafish embryos using a battery of assays for developmental toxicity, neurotoxicity, cardiotoxicity and hepatotoxicity toward human relevance. *Neurotoxicol Teratol*. 2018;70:40–50. <https://doi.org/10.1016/j.ntt.2018.10.002>.
- Andersen SL. Trajectories of brain development: point of vulnerability or window of opportunity? *Neurosci Biobehav Rev*. 2003;27:3–18. [https://doi.org/10.1016/S0149-7634\(03\)00005-8](https://doi.org/10.1016/S0149-7634(03)00005-8).
- Back SA, Luo NL, Borenstein NS, Levine JM, Volpe JJ, Kinney HC. Late oligodendrocyte progenitors coincide with the developmental window of vulnerability for human perinatal white matter injury. *J Neurosci*. 2001;21:1302–12. <https://doi.org/10.1523/jneurosci.21-04-01302.2001>.
- Bal-Price A, Crofton KM, Leist M, Allen S, Arand M, Buetler T, et al. International STakeholder NETwork (ISTNET): creating a developmental neurotoxicity (DNT) testing road map for regulatory purposes. *Arch Toxicol*. 2015;89:269–87. <https://doi.org/10.1007/s00204-015-1464-2>.
- Bal-Price A, Hogberg HT, Crofton KM, et al. Recommendation on test readiness criteria for new approach methods in toxicology: exemplified for developmental neurotoxicity. *ALTEX*. 2018;35:306–52. <https://doi.org/10.14573/altex.1712081>.
- Barenys M, Gassmann K, Baksmeier C, Heinz S, Reverte I, Schmuck M, et al. Epigallocatechin gallate (EGCG) inhibits adhesion and migration of neural progenitor cells in vitro. *Arch Toxicol*. 2017;91:827–37. <https://doi.org/10.1007/s00204-016-1709-8>.
- Bastiaensen M, Ait Bamai Y, Araki A, van den Eede N, Kawai T, Tsuboi T, et al. Biomonitoring of organophosphate flame retardants and plasticizers in children: associations with house dust and housing characteristics in Japan. *Environ Res*. 2019a;172:543–51. <https://doi.org/10.1016/j.envres.2019.02.045>.
- Bastiaensen M, Malarvannan G, Been F, Yin S, Yao Y, Huygh J, et al. Metabolites of phosphate flame retardants and alternative plasticizers in urine from intensive care patients. *Chemosphere*. 2019b;233:590–6. <https://doi.org/10.1016/j.chemosphere.2019.05.280>.
- Baud A, Wessely F, Mazzacuva F, McCormick J, Camuzeaux S, Heywood WE, et al. A multiplex high-throughput targeted proteomic assay to identify induced pluripotent stem cells. *Anal Chem*. 2017;89:2440–8. <https://doi.org/10.1021/acs.analchem.6b04368>.
- Baumann N, Pham-Dinh D. Biology of oligodendrocyte and myelin in the mammalian central nervous system. *Physiol Rev*. 2001;81:871–927. <https://doi.org/10.1152/physrev.2001.81.2.871>.
- Baumann J, Dach K, Barenys M, et al. Application of the neurosphere assay for DNT hazard assessment: challenges and limitations. *Methods Pharmacol Toxicol*. 2016;49:1–29. [https://doi.org/10.1007/7653\\_2015\\_49](https://doi.org/10.1007/7653_2015_49).
- Behl M, Hsieh JH, Shafer TJ, Mundy WR, Rice JR, Boyd WA, et al. Use of alternative assays to identify and prioritize organophosphorus flame retardants for potential developmental and neurotoxicity. *Neurotoxicol Teratol*. 2015;52:181–93. <https://doi.org/10.1016/j.ntt.2015.09.003>.
- Ben Bashat D, Kronfeld-Duenias V, Zachor DA, Ekstein PM, Hendler T, Tarrasch R, et al. Accelerated maturation of white matter in young children with autism: a high b value DWI study. *Neuroimage*. 2007;37:40–7. <https://doi.org/10.1016/j.neuroimage.2007.04.060>.
- Bergman Å, Rydén A, Law RJ, de Boer J, Covaci A, Alae M, et al. A novel abbreviation standard for organobromine, organochlorine and organophosphorus flame retardants and some characteristics of the chemicals. *Environ Int*. 2012;49:57–82.
- Beser MI, Pardo O, Beltrán J, Yusà V. Determination of 21 perfluoroalkyl substances and organophosphorus compounds in breast milk by liquid chromatography coupled to orbitrap high-resolution mass spectrometry. *Anal Chim Acta*. 2019;1049:123–32. <https://doi.org/10.1016/j.aca.2018.10.033>.
- Blum A, Behl M, Birnbaum LS, Diamond ML, Phillips A, Singla V, et al. Organophosphate ester flame retardants: are they a regrettable substitution for polybrominated diphenyl ethers? *Environ Sci Technol Lett*. 2019;6:638–49. <https://doi.org/10.1021/acs.estlett.9b00582>.
- Borrell V, Götz M. Role of radial glial cells in cerebral cortex folding. *Curr Opin Neurobiol*. 2014;27:39–46. <https://doi.org/10.1016/j.conb.2014.02.007>.
- Boyd WA, Smith MV, Co CA, Pirone JR, Rice JR, Shockley KR, et al. Developmental effects of the ToxCast™ phase I and phase II chemicals in *Caenorhabditis elegans* and corresponding responses in zebrafish, rats, and rabbits. *Environ Health Perspect*. 2016;124:586–93. <https://doi.org/10.1289/ehp.1409645>.
- Bradl M, Lassmann H. Oligodendrocytes: biology and pathology. *Acta Neuropathol*. 2010;119:37–53. <https://doi.org/10.1007/s00401-009-0601-5>.
- Cariou R, Antignac J-P, Zalko D, Berrebi A, Cravedi JP, Maume D, et al. Exposure assessment of French women and their newborns to tetrabromobisphenol-A: occurrence measurements in maternal adipose tissue, serum, breast milk and cord serum. *Chemosphere*. 2008;73:1036–41. <https://doi.org/10.1016/j.chemosphere.2008.07.084>.
- Chambers SM, Qi Y, Mica Y, Lee G, Zhang XJ, Niu L, et al. Combined small molecule inhibition accelerates developmental timing and converts human pluripotent stem cells into nociceptors. *Nat Biotechnol*. 2013;30:715–20. <https://doi.org/10.1038/nbt.2249>.
- Chao HR, Wang SL, Lee WJ, Wang YF, Pöpke O. Levels of polybrominated diphenyl ethers (PBDEs) in breast milk from central Taiwan and their relation to infant birth outcome and maternal menstruation effects. *Environ Int*. 2007;33:239–45. <https://doi.org/10.1016/j.envint.2006.09.013>.

- Chuveau Z, Bonvallot N, Mercier F, le Bot B, Chevrier C, Glouennec P. Organophosphorus flame retardants: a global review of indoor contamination and human exposure in Europe and epidemiological evidence. *Int J Environ Res Public Health*. 2020;17:1–24. <https://doi.org/10.3390/ijerph17186713>.
- Covaci A, Voorspoels S, Thomsen C, van Bavel B, Neels H. Evaluation of total lipids using enzymatic methods for the normalization of persistent organic pollutant levels in serum. *Sci Total Environ*. 2006;366:361–6. <https://doi.org/10.1016/j.scitotenv.2006.03.006>.
- Crofton KM, Mundy WR, Shafer TJ. Developmental neurotoxicity testing: a path forward. *Congenit Anom (Kyoto)*. 2012;52:140–6. <https://doi.org/10.1111/j.1741-4520.2012.00377.x>.
- Crofton K, Fritsche E, Ylikomi T, Bal-Price A. International STakeholder NETwork (ISTNET) for creating a Developmental Neurotoxicity Testing (DNT) roadmap for regulatory purposes. *ALTEX*. 2014;31:223–4. <https://doi.org/10.14573/altex.1402121>.
- Dach K, Bendt F, Huebenthal U, Giersiefer S, Lein PJ, Heuer H, et al. BDE-99 impairs differentiation of human and mouse NPCs into the oligodendroglial lineage by species-specific modes of action. *Sci Rep*. 2017;7:1–11. <https://doi.org/10.1038/srep44861>.
- Damerud PO, Eriksen GS, Jóhannesson T, Larsen PB, Viluksela M. Polybrominated diphenyl ethers: occurrence, dietary exposure, and toxicology. *Environ Health Perspect*. 2001;109:49–68. <https://doi.org/10.1289/ehp.01109s149>.
- De Wit CA. An overview of brominated flame retardants in the environment. *Chemosphere*. 2002;46:583–624. [https://doi.org/10.1016/S0045-6535\(01\)00225-9](https://doi.org/10.1016/S0045-6535(01)00225-9).
- Delp J, Gutbier S, Klima S, et al. A high-throughput approach to identify specific neurotoxicants/developmental toxicants in human neuronal cell function assays. *ALTEX*. 2018;35:235–53. <https://doi.org/10.14573/altex.1712182>.
- EFSA. Scientific Opinion on the developmental neurotoxicity potential of acetamiprid and imidacloprid. *EFSA J*. 2013;11:1–47. <https://doi.org/10.2903/j.efsa.2013.3471>.
- EPA 1998. EPA test guidelines for pesticides and toxic substances. Health effects test guidelines: OPPTS 870.6300 developmental neurotoxicity study. <https://www.epa.gov>
- Eskenazi B, Chevrier J, Rauch SA, Kogut K, Harley KG, Johnson C, et al. In utero and childhood polybrominated diphenyl ether (PBDE) exposures and neurodevelopment in the CHAMACOS study. *Environ Health Perspect*. 2013;121:257–62.
- Fischer D, Hooper K, Athanasiadou M, Athanassiadis I, Bergman Å. Children show highest levels of polybrominated diphenyl ethers in a California family of four: a case study. *Environ Health Perspect*. 2006;114:1581–4. <https://doi.org/10.1289/ehp.8554>.
- Foti F, Menghini D, Mandolesi L, Federico F, Vicari S, Petrosini L. Learning by observation: insights from Williams syndrome. *PLoS One*. 2013;8:1–10. <https://doi.org/10.1371/journal.pone.0053782>.
- Frank CL, Brown JP, Wallace K, Mundy WR, Shafer TJ. Developmental neurotoxicants disrupt activity in cortical networks on microelectrode arrays: results of screening 86 compounds during neural network formation. *Toxicol Sci*. 2017;160:121–35. <https://doi.org/10.1093/toxsci/kfx169>.
- Fritsche E, Alm H, Baumann J, Geerts L, Håkansson H, Masjosthusmann S, et al. Literature review on in vitro and alternative developmental neurotoxicity (DNT) testing methods. *EFSA Support Publ*. 2015;12:1–186. <https://doi.org/10.2903/sp.efsa.2015.en-778>.
- Fritsche E, Crofton KM, Hernandez AF, et al. OECD/EFSA workshop on developmental neurotoxicity (DNT): the use of non-animal test methods for regulatory purposes. *ALTEX*. 2017;34:311–5. <https://doi.org/10.14573/altex.1701171s>.
- Fritsche E, Barenys M, Klose J, Masjosthusmann S, Nimtz L, Schmuck M, et al. Current availability of stem cell-based in vitro methods for developmental neurotoxicity (DNT) testing. *Toxicol Sci*. 2018a;165:21–30. <https://doi.org/10.1093/toxsci/kfy178>.
- Fritsche E, Grandjean P, Crofton KM, Aschner M, Goldberg A, Heinonen T, et al. Consensus statement on the need for innovation, transition and implementation of developmental neurotoxicity (DNT) testing for regulatory purposes. *Toxicol Appl Pharmacol*. 2018b;354:3–6. <https://doi.org/10.1016/j.taap.2018.02.004>.
- Fujimoto H, Woo G-H, Morita R, et al. Increased cellular distribution of vimentin and ret in the cingulum of rat offspring after developmental exposure to decabromodiphenyl ether or 1,2,5,6,9,10-hexabromocyclododecane. *J Toxicol Pathol*. 2013;26:119–29. <https://doi.org/10.1293/tox.26.119>.
- Gangwal S, Reif DM, Mosher S, Egeghy PP, Wambaugh JF, Judson RS, et al. Incorporating exposure information into the toxicological prioritization index decision support framework. *Sci Total Environ*. 2012;435–436:316–25. <https://doi.org/10.1016/j.scitotenv.2012.06.086>.
- Gasparini RJ, Pavez M, Thompson AC, Mitchell CB, Hardy H, Young KM, et al. How does calcium interact with the cytoskeleton to regulate growth cone motility during axon path-finding? *Mol Cell Neurosci*. 2017;84:29–35. <https://doi.org/10.1016/j.mcn.2017.07.006>.
- Gerst R, Hölzer M (2019) PCAGO: an interactive web service to analyze RNA-Seq data with principal component analysis. *bioRxiv*. <https://doi.org/10.1101/433078>
- Gibson EA, Stapleton HM, Calero L, Holmes D, Burke K, Martinez R, et al. Differential exposure to organophosphate flame retardants in mother-child pairs. *Chemosphere*. 2019;219:567–73. <https://doi.org/10.1016/j.chemosphere.2018.12.008>.
- Guerrini R, Dobyns WB. Malformations of cortical development: clinical features and genetic causes. *Lancet Neurol*. 2014;13:710–26. [https://doi.org/10.1016/S1474-4422\(14\)70040-7](https://doi.org/10.1016/S1474-4422(14)70040-7).
- Hardy A, Benford D, Halldorsson T, et al. Update: use of the benchmark dose approach in risk assessment. *EFSA J*. 2017;15:1–41. <https://doi.org/10.2903/j.efsa.2017.4658>.
- Hayashi C, Suzuki N. Heterogeneity of Oligodendrocytes and Their Precursor Cells. *Adv Exp Med Biol*. 2019;1190:53–62. [https://doi.org/10.1007/978-981-32-9636-7\\_5](https://doi.org/10.1007/978-981-32-9636-7_5)
- He C, English K, Baduel C, Thai P, Jagals P, Ware RS, et al. Concentrations of organophosphate flame retardants and plasticizers in urine from young children in Queensland, Australia and associations with environmental and behavioural factors. *Environ Res*. 2018a;164:262–70. <https://doi.org/10.1016/j.envres.2018.02.040>.
- He C, Toms L-ML, Thai P, van den Eede N, Wang X, Li Y, et al. Urinary metabolites of organophosphate esters: concentrations and age trends in Australian children. *Environ Int*.

- 2018b;111:124–30. <https://doi.org/10.1016/j.envint.2017.11.019>.
- Hirsch C, Striegl B, Mathes S, Adlhart C, Edelmann M, Bono E, et al. Multiparameter toxicity assessment of novel DOPO-derived organophosphorus flame retardants. *Arch Toxicol*. 2017;91:407–25. <https://doi.org/10.1007/s00204-016-1680-4>.
- Hoelting L, Klima S, Karreman C, Grinberg M, Meisig J, Henry M, et al. Stem cell-derived immature human dorsal root ganglia neurons to identify peripheral neurotoxicants. *Stem Cells Transl Med*. 2016;5:476–87. <https://doi.org/10.5966/sctm.2015-0108>.
- Hogberg HT, de Cássia da Silveira E, Sá R, Kleensang A, et al. Organophosphorus flame retardants are developmental neurotoxicants in a rat primary brainsphere in vitro model. *Arch Toxicol*. 2020;95:207–28. <https://doi.org/10.1007/s00204-020-02903-2>.
- Hu WF, Chahrour MH, Walsh CA. The diverse genetic landscape of neurodevelopmental disorders. *Annu Rev Genomics Hum Genet*. 2014;15:195–213. <https://doi.org/10.1146/annurev-genom-090413-025600>.
- Juric-Sekhar G, Hevner RF. Malformations of cerebral cortex development: molecules and mechanisms. *Annu Rev Pathol Mech Dis*. 2019;14:293–318. <https://doi.org/10.1146/annurev-pathmechdis-012418-012927>.
- Káradóttir R, Hamilton NB, Bakiri Y, Attwell D. Spiking and nonspiking classes of oligodendrocyte precursor glia in CNS white matter. *Nat Neurosci*. 2008;11:450–6. <https://doi.org/10.1038/nn2060>.
- Kent JC, Mitoulas LR, Cregan MD, Ramsay DT, Doherty DA, Hartmann PE. Volume and frequency of breastfeedings and fat content of breast milk throughout the day. *Pediatrics*. 2006;117:387–95. <https://doi.org/10.1542/peds.2005-1417>.
- Kim JW, Isobe T, Muto M, Tue NM, Katsura K, Malarvannan G, et al. Organophosphorus flame retardants (PFRs) in human breast milk from several Asian countries. *Chemosphere*. 2014;116:91–7. <https://doi.org/10.1016/j.chemosphere.2014.02.033>.
- Klose J, Tigges J, Masjosthusmann S, et al. TBBPA targets converging key events of human oligodendrocyte development resulting in two novel AOPs. *ALTEX Prepr*. 2020;38:1–18. <https://doi.org/10.14573/altex.2007201>.
- Krebs A, Nyffeler J, Karreman C, et al. Determination of benchmark concentrations and their statistical uncertainty for cytotoxicity test data and functional in vitro assays. *ALTEX*. 2020a;37:155–63. <https://doi.org/10.14573/altex.1912021>.
- Krebs A, van Vugt-Lussenburg BMA, Waldmann T, Albrecht W, Boei J, ter Braak B, et al. The EU-ToxRisk method documentation, data processing and chemical testing pipeline for the regulatory use of new approach methods. *Arch Toxicol*. 2020b;94:2435–61. <https://doi.org/10.1007/s00204-020-02802-6>.
- Krug AK, Balmer NV, Matt F, Schönenberger F, Merhof D, Leist M. Evaluation of a human neurite growth assay as specific screen for developmental neurotoxicants. *Arch Toxicol*. 2013a;87:2215–31. <https://doi.org/10.1007/s00204-013-1072-y>.
- Krug AK, Kolde R, Gaspar JA, Rempel E, Balmer NV, Meganathan K, et al. Human embryonic stem cell-derived test systems for developmental neurotoxicity: a transcriptomics approach. *Arch Toxicol*. 2013b;87:123–43. <https://doi.org/10.1007/s00204-012-0967-3>.
- Kucharska A, Cequier E, Thomsen C, Becher G, Covaci A, Voorspoels S. Assessment of human hair as an indicator of exposure to organophosphate flame retardants. Case study on a Norwegian mother-child cohort. *Environ Int*. 2015;83:50–7. <https://doi.org/10.1016/j.envint.2015.05.015>.
- Kuhn S, Gritti L, Crooks D, Dombrowski Y. Oligodendrocytes in development, myelin generation and beyond. *cells* 2019;1424:1–23. <https://doi.org/10.3390/cells811424>
- Law RJ, Covaci A, Harrad S, Herzke D, Abdallah MAE, Fernie K, et al. Levels and trends of PBDEs and HBCDs in the global environment: status at the end of 2012. *Environ Int*. 2014;65:147–58. <https://doi.org/10.1016/j.envint.2014.01.006>.
- Lein P, Silbergeld E, Locke P, Goldberg AM. In vitro and other alternative approaches to developmental neurotoxicity testing (DNT). *Environ Toxicol Pharmacol*. 2005;19:735–44. <https://doi.org/10.1016/j.etap.2004.12.035>.
- Li T, Wang W, Pan YW, Xu L, Xia Z. A hydroxylated metabolite of flame-retardant PBDE-47 decreases the survival, proliferation, and neuronal differentiation of primary cultured adult neural stem cells and interferes with signaling of ERK5 map kinase and neurotrophin 3. *Toxicol Sci*. 2013;134:111–24. <https://doi.org/10.1093/toxsci/kft083>.
- Li M, Yao Y, Wang Y, Bastiaensen M, Covaci A, Sun H. Organophosphate ester flame retardants and plasticizers in a Chinese population: significance of hydroxylated metabolites and implication for human exposure. *Environ Pollut*. 2020;257:257. <https://doi.org/10.1016/j.envpol.2019.113633>.
- López-Espíndola D, Morales-Bastos C, Grijota-Martínez C, Liao XH, Lev D, Sugo E, et al. Mutations of the thyroid hormone transporter MCT8 cause prenatal brain damage and persistent hypomyelination. *J Clin Endocrinol Metab*. 2014;99:E2799–804. <https://doi.org/10.1210/jc.2014-2162>.
- Lotharius J, Falsig J, Van Beek J, et al. Progressive degeneration of human mesencephalic neuron-derived cells triggered by dopamine-dependent oxidative stress is dependent on the mixed-lineage kinase pathway. *J Neurosci*. 2005;25:6329–42. <https://doi.org/10.1523/JNEUROSCI.1746-05.2005>.
- Luttrell WE, Olajos EJ, Pleban PA. Change in hen sciatic nerve calcium after a single oral dose of tri-O-tolyl phosphate. *Environ Res*. 1993;60:290–4.
- Ma Y, Salamova A, Venier M, Hites RA. Has the phase-out of PBDEs affected their atmospheric levels? Trends of PBDEs and their replacements in the great lakes atmosphere. *Environ Sci Technol*. 2013;47:11457–64. [dx.doi.org https://doi.org/10.1021/es403029m](https://doi.org/10.1021/es403029m).
- Ma J, Zhu H, Kannan K. Organophosphorus flame retardants and plasticizers in breast milk from the United States. *Environ Sci Technol Lett*. 2019;6:525–31. <https://doi.org/10.1021/acs.estlett.9b00394>.
- Marinelli C, Bertalot T, Zusso M, Skaper SD, Giusti P. Systematic review of pharmacological properties of the oligodendrocyte lineage. *Front Cell Neurosci*. 2016;10:1–27. <https://doi.org/10.3389/fncel.2016.00027>.
- Marvel SW, To K, Grimm FA, et al. ToxPi Graphical User Interface 2.0: dynamic exploration, visualization, and sharing of integrated data models. *BMC Bioinformatics*. 2018;19:1–7. <https://doi.org/10.1186/s12859-018-2089-2>.



- Masjosthusmann S, Becker D, Petzuch B, Klose J, Siebert C, Deenen R, et al. A transcriptome comparison of time-matched developing human, mouse and rat neural progenitor cells reveals human uniqueness. *Toxicol Appl Pharmacol.* 2018;354:40–55. <https://doi.org/10.1016/j.taap.2018.05.009>.
- Masjosthusmann S, Blum J, Bartmann K, et al. Establishment of an a priori protocol for the implementation and interpretation of an in-vitro testing battery for the assessment of developmental neurotoxicity. *EFSA J.* 2020;17:1938e. <https://doi.org/10.2903/sp.efsa.2020.EN-1938>.
- Mayor R, Theveneau E. The neural crest. *Dev Glance.* 2013;140:2247–51. <https://doi.org/10.1242/dev.091751>.
- Mizouchi S, Ichiba M, Takigami H, Kajiwara N, Takamuku T, Miyajima T, et al. Exposure assessment of organophosphorus and organobromine flame retardants via indoor dust from elementary schools and domestic houses. *Chemosphere.* 2015;123:17–25. <https://doi.org/10.1016/j.chemosphere.2014.11.028>.
- Muñoz-Quezada MT, Lucero BA, Barr DB, Steenland K, Levy K, Ryan PB, et al. Neurodevelopmental effects in children associated with exposure to organophosphate pesticides: a systematic review. *Neurotoxicology.* 2013;39:158–68. <https://doi.org/10.1016/j.neuro.2013.09.003>.
- Nimtz L, Klose J, Masjosthusmann S, et al. The neurosphere assay as an in vitro method for developmental neurotoxicity (DNT) evaluation. *Cell Cult Tech Neuromethods.* 2019;145:141–68. <https://doi.org/10.1007/978-1-4939-9228-7>.
- Nimtz L, Hartmann J, Tigges J, Masjosthusmann S, Schmuck M, Keßel E, et al. Characterization and application of electrically active neuronal networks established from human induced pluripotent stem cell-derived neural progenitor cells for neurotoxicity evaluation. *Stem Cell Res.* 2020;45:101761. <https://doi.org/10.1016/j.scr.2020.101761>.
- Nyffeler J, Dolde X, Krebs A, Pinto-Gil K, Pastor M, Behl M, et al. Combination of multiple neural crest migration assays to identify environmental toxicants from a proof-of-concept chemical library. *Arch Toxicol.* 2017;91:3613–32. <https://doi.org/10.1007/s00204-017-1977-y>.
- OECD 2007. OECD guideline for the testing of chemicals: health effects. Test No. 426: developmental neurotoxicity study. <http://www.oecd.org/dataoecd/20/52/37622194.pdf>
- Phillips DL, Pirkle JL, Burse VW, Bemert JT Jr, Henderson LO, Needham LL. Chlorinated hydrocarbon levels in human serum: effects of fasting and feeding. *Arch Environ Contam Toxicol.* 1989;18:495–500. <https://doi.org/10.1007/BF01055015>.
- Pistolato F, De Gyves EM, Carpi D, et al. Assessment of developmental neurotoxicity induced by chemical mixtures using an adverse outcome pathway concept. *Environ Heal A Glob Access Sci Source.* 2020;19:1–26. <https://doi.org/10.1186/s12940-020-00578-x>.
- Prentice P, Ong KK, Schoemaker MH, Tol EAF, Vervoort J, Hughes IA, et al. Breast milk nutrient content and infancy growth. *Acta Paediatr Int J Paediatr.* 2016;105:641–7. <https://doi.org/10.1111/apa.13362>.
- Razek AA, Mazroa J, Baz H. Assessment of white matter integrity of autistic preschool children with diffusion weighted MR imaging. *Brain and Development.* 2014;36:28–34. <https://doi.org/10.1016/j.braindev.2013.01.003>.
- Reif DM, Martin MT, Tan SW, Houck KA, Judson RS, Richard AM, et al. Endocrine profiling and prioritization of environmental chemicals using toxcast data. *Environ Health Perspect.* 2010;118:1714–20. <https://doi.org/10.1289/ehp.1002180>.
- Roze E, Meijer L, Bakker A, van Braeckel KNJA, Sauer PJJ, Bos AF. Prenatal exposure to organohalogenes, including brominated flame retardants, influences motor, cognitive, and behavioral performance at school age. *Environ Health Perspect.* 2009;117:1953–8. <https://doi.org/10.1289/ehp.0901015>.
- Rylander L, Nilsson-Ehle P, Hagmar L. A simplified precise method for adjusting serum levels of persistent organohalogen pollutants to total serum lipids. *Chemosphere.* 2006;62:333–6. <https://doi.org/10.1016/j.chemosphere.2005.04.107>.
- Sachana M, Bal-Price A, Crofton KM, Bennekou SH, Shafer TJ, Behl M, et al. International regulatory and scientific effort for improved developmental neurotoxicity testing. *Toxicol Sci.* 2019;167:45–57. <https://doi.org/10.1093/toxsci/kfy211>.
- Saegusa Y, Fujimoto H, Woo G-H, Inoue K, Takahashi M, Mitsumori K, et al. Developmental toxicity of brominated flame retardants, tetrabromobisphenol A and 1,2,5,6,9,10-hexabromocyclododecane, in rat offspring after maternal exposure from mid-gestation through lactation. *Reprod Toxicol.* 2009;28:456–67. <https://doi.org/10.1016/j.reprotox.2009.06.011>.
- Schmidt BZ, Lehmann M, Gutbier S, Nembo E, Noel S, Smirnova L, et al. In vitro acute and developmental neurotoxicity screening: an overview of cellular platforms and high-throughput technical possibilities. *Arch Toxicol.* 2017;91:1–33. <https://doi.org/10.1007/s00204-016-1805-9>.
- Schmuck MR, Temme T, Dach K, et al. Omnisphero: a high-content image analysis (HCA) approach for phenotypic developmental neurotoxicity (DNT) screenings of organoid neurosphere cultures in vitro. *Arch Toxicol.* 2016:1–12. <https://doi.org/10.1007/s00204-016-1852-2>.
- Scholz D, Pörtl D, Genewsky A, Weng M, Waldmann T, Schildknecht S, et al. Rapid, complete and large-scale generation of post-mitotic neurons from the human LUHMES cell line. *J Neurochem.* 2011;119:957–71. <https://doi.org/10.1111/j.1471-4159.2011.07255.x>.
- Schreiber T, Gassmann K, Götz C, Hübenthal U, Moors M, Krause G, et al. Polybrominated diphenyl ethers induce developmental neurotoxicity in a human in vitro model: evidence for endocrine disruption. *Environ Health Perspect.* 2010;118:572–8. <https://doi.org/10.1289/ehp.0901435>.
- Shafer TJ, Brown JP, Lynch B, Davila-Montero S, Wallace K, Friedman KP. Evaluation of chemical effects on network formation in cortical neurons grown on microelectrode arrays. *Toxicol Sci.* 2019;169:436–55. <https://doi.org/10.1093/toxsci/kfz052>.
- Shy C-G, Huang H-L, Chang-Chien G-P, Chao HR, Tsou TC. Neurodevelopment of infants with prenatal exposure to polybrominated diphenyl ethers. *Bull Environ Contam Toxicol.* 2011;87:643–8. <https://doi.org/10.1007/s00128-011-0422-9>.
- Simons M, Trajkovic K. Neuron-glia communication in the control of oligodendrocyte function and myelin biogenesis. *J Cell Sci.* 2006;119:4381–9. <https://doi.org/10.1242/jcs.03242>.
- Stapleton HM, Klosterhaus S, Eagle S, Fuh J, Meeker JD, Blum A, et al. Detection of organophosphate flame retardants in furniture foam and U.S. house dust. *Environ Sci Technol.* 2009;43:7490–5. <https://doi.org/10.1021/es9014019>.

- Stapleton HM, Misenheimer J, Hoffman K, Webster TF. Flame retardant associations between children's handwipes and house dust. *Chemosphere*. 2014;116:54–60. <https://doi.org/10.1016/j.chemosphere.2013.12.100>.
- Stiegler NV, Krug AK, Matt F, Leist M. Assessment of chemical-induced impairment of human neurite outgrowth by multiparametric live cell imaging in high-density cultures. *Toxicol Sci*. 2011;121:73–87. <https://doi.org/10.1093/toxsci/kfr034>.
- Stumpf AM, Tanaka D, Aulerich RJ, Bursian SJ. Delayed neurotoxic effects of tri-*o*-tolyl phosphate in the european ferret. *J Toxicol Environ Health*. 1989;26:61–73. <https://doi.org/10.1080/15287398909531233>.
- Sugeng EJ, Leonards PEG, van de Bor M. Brominated and organophosphorus flame retardants in body wipes and house dust, and an estimation of house dust hand-loadings in Dutch toddlers. *Environ Res*. 2017;158:789–97. <https://doi.org/10.1016/j.envres.2017.07.035>.
- Sundkvist AM, Olofsson U, Haglund P. Organophosphorus flame retardants and plasticizers in marine and fresh water biota and in human milk. *J Environ Monit*. 2010;12:943–51. <https://doi.org/10.1039/b921910b>.
- Tang J, Zhai JX. Distribution of polybrominated diphenyl ethers in breast milk, cordblood and placentas: a systematic review. *Environ Sci Pollut Res*. 2017;24:21548–73. <https://doi.org/10.1007/s11356-017-9821-8>.
- Tang H, Hammack C, Ogden SC, Wen Z, Qian X, Li Y, et al. Zika virus infects human cortical neural progenitors and attenuates their growth. *Cell Stem Cell*. 2016;18:587–90. <https://doi.org/10.1016/j.stem.2016.02.016>.
- Terron A, Bennekou Hougaard S. Towards a regulatory use of alternative developmental neurotoxicity testing (DNT). *Toxicol Appl Pharmacol*. 2018;354:19–23. <https://doi.org/10.1016/j.taap.2018.02.002>.
- Thomson JA, Itskovitz-Eldor J, Shapiro SS, et al. Embryonic stem cell lines derived from human blastocysts. *Science*. 1998;282(80):1145–7. <https://doi.org/10.1126/science.282.5391.1145>.
- Toms L-ML, Sjödin A, Harden F, Hobson P, Jones R, Edenfield E, et al. Serum polybrominated diphenyl ether (PBDE) levels are higher in children (2-5 years of age) than in infants and adults. *Environ Health Perspect*. 2009;117:1461–5. <https://doi.org/10.1289/ehp.0900596>.
- Tonduti D, Vanderver A, Berardinelli A, et al. MCT8 deficiency: extrapyramidal symptoms and delayed myelination as prominent features. *Child Neurol Psychiatry*. 2014;28:795–800. <https://doi.org/10.1177/0883073812450944.MCT8>.
- Tsuji R, Crofton KM. Developmental neurotoxicity guideline study: issues with methodology, evaluation and regulation. *Congenit Anom (Kyoto)*. 2012;52:122–8. <https://doi.org/10.1111/j.1741-4520.2012.00374.x>.
- van der Veen I, de Boer J. Phosphorus flame retardants: properties, production, environmental occurrence, toxicity and analysis. *Chemosphere*. 2012;88:1119–53. <https://doi.org/10.1016/j.chemosphere.2012.03.067>.
- Volpe JJ, Kinney HC, Jensen FE, Rosenberg PA. The developing oligodendrocyte: key cellular target in brain injury in the premature infant. *Int J Dev Neurosci*. 2011;29:423–40. <https://doi.org/10.1016/j.ijdevneu.2011.02.012>.
- Waaaijers SL, Kong D, Hendriks HS, et al. Persistence, Bioaccumulation, and Toxicity of Halogen-Free Flame Retardants. *Rev Environ Contam Toxicol*. 2013;222:1–71. <https://doi.org/10.1007/978-1-4614-6470-9>.
- Walter KM, Dach K, Hayakawa K, et al. Ontogenetic expression of thyroid hormone signaling genes: An in vitro and in vivo species comparison. *PLoS One*. 2019;14:1–26. <https://doi.org/10.1371/journal.pone.0221230>.
- Wolff JJ, Ph D, Gu H, et al. Differences in white matter fiber tract development present from 6 to 24 months in infants with autism. *Am J Psychiatry*. 2013;169:589–600. <https://doi.org/10.1176/appi.ajp.2011.11091447.Differences>.
- Yogui GT, Sericano JL. Polybrominated diphenyl ether flame retardants in the U.S. marine environment: a review. *Environ Int*. 2009;35:655–66. <https://doi.org/10.1016/j.envint.2008.11.001>.
- Zilles K, Palomero-Gallagher N, Amunts K. Development of cortical folding during evolution and ontogeny. *Trends Neurosci*. 2013;36:275–84. <https://doi.org/10.1016/j.tins.2013.01.006>.

**Publisher's note** Springer Nature remains neutral with regard to jurisdictional claims in published maps and institutional affiliations.



## **Supplemental Information**

### **Neurodevelopmental toxicity assessment of flame retardants using a human DNT *in vitro* testing battery**

Klose J<sup>1</sup>, Pahl M<sup>1</sup>, Bartmann K<sup>1</sup>, Bendt F<sup>1</sup>, Blum J<sup>2</sup>, Dolde X<sup>2</sup>, Förster N<sup>3</sup>, Holzer A-K<sup>2</sup>, Hübenthal U<sup>1</sup>, Keßel HE<sup>1</sup>, Koch K<sup>1</sup>, Masjosthusmann S<sup>1</sup>, Schneider S<sup>1</sup>, Stürzl L<sup>1</sup>, Woeste S<sup>1</sup>, Rossi A<sup>1</sup>, Covaci A<sup>4</sup>, Behl M<sup>5</sup>, Leist M<sup>2</sup>, Tigges J<sup>1</sup>, Fritsche E<sup>1,6</sup>

<sup>1</sup> IUF-Leibniz Research Institute for Environmental Medicine, Auf'm Hennekamp 50, 40225 Duesseldorf, NRW, Germany

<sup>2</sup> Department of Biology, University of Konstanz, Universitätsstraße 10, 78464 Konstanz, BW, Germany

<sup>3</sup> RUB – Ruhr University Bochum, Faculty for Biology and Biotechnology, Bioinformatics Group, Bochum, Germany

<sup>4</sup> Toxicological Centre, Department of Pharmaceutical Sciences, University of Antwerp, Universiteitsplein 1, 2610 Wilrijk, Belgium

<sup>5</sup> Division of the National Toxicology Program, National Institute of Environmental Health Sciences, Research Triangle Park, Durham, North Carolina, 27709

<sup>6</sup> Medical Faculty, Heinrich-Heine-University, Universitätsstraße 1, 40225 Duesseldorf, NRW, Germany

Correspondence: Prof. Dr. Ellen Fritsche  
Phone: +49 (0) 211 3389 217  
E-Mail: [ellen.fritsche@uni-duesseldorf.de](mailto:ellen.fritsche@uni-duesseldorf.de)

**Supplementary Table S1:** CAS numbers, chemical names, IDs and structures of the 15 analyzed FRs of this case study.

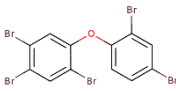
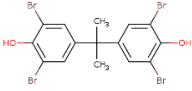
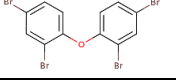
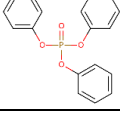

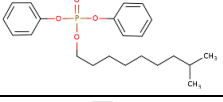
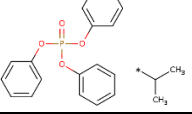
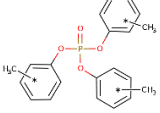
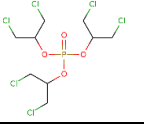
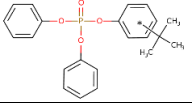
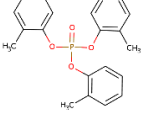
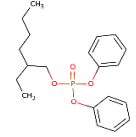
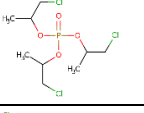
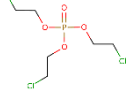
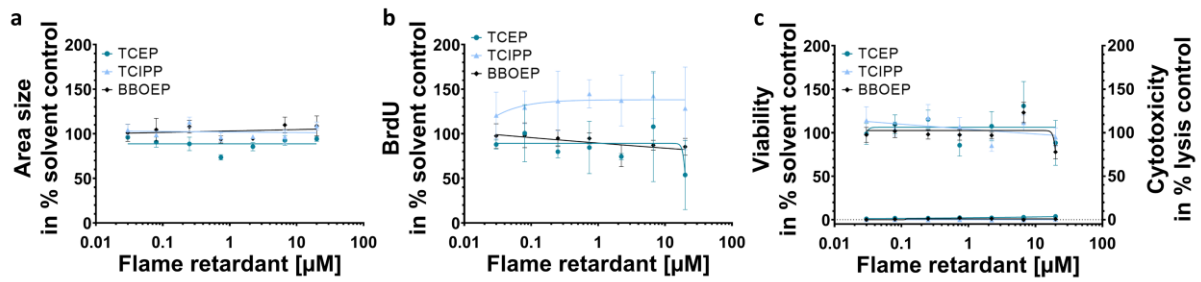
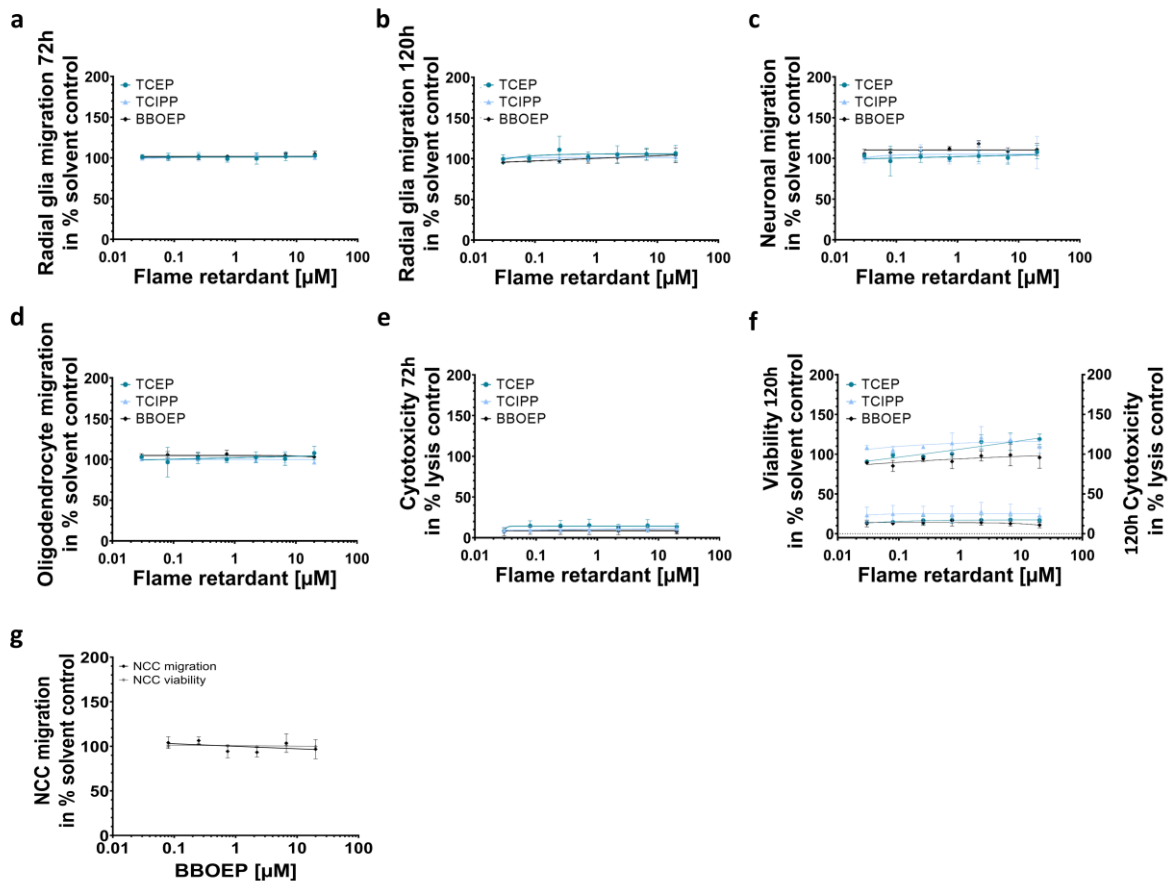
CAS number	Chemical name	ID	Structure
60348-60-9	2,2',4,4',5-Pentabromodiphenylether	BDE-99	
79-94-7	Tetrabromobisphenol A	TBBPA	
5436-43-1	2,2',4,4'-Tetrabromodiphenylether	BDE-47	
115-86-6	Triphenyl phosphate	TPHP	
78-51-3 Metabolite	Tris (2-butoxyethyl) phosphate Bis (2-butoxyethyl) phosphate	TBOEP BBOEP	
29761-21-5	Isodecyl diphenyl phosphate	IDDPHP	
68937-41-7	Isopropylated phenyl phosphate (3:1)	IPPHP	
1330-78-5	Tricresyl phosphate	TCP	
13674-87-8	Tris (1,3-dichloroisopropyl) phosphate	TDCIPP	
56803-37-3	Tert-butylphenyl diphenyl phosphate	t-BDPHP	
78-30-8	Tri-O-cresyl phosphate	TOCP	
1241-94-7	2-Ethylhexyl diphenyl phosphate	EHDPPH	
13674-84-5	Tris (1-chloroisopropyl) phosphate	TCIPP	
115-96-8	Tris (2-chloroethyl) phosphate	TCEP	

Figure S1



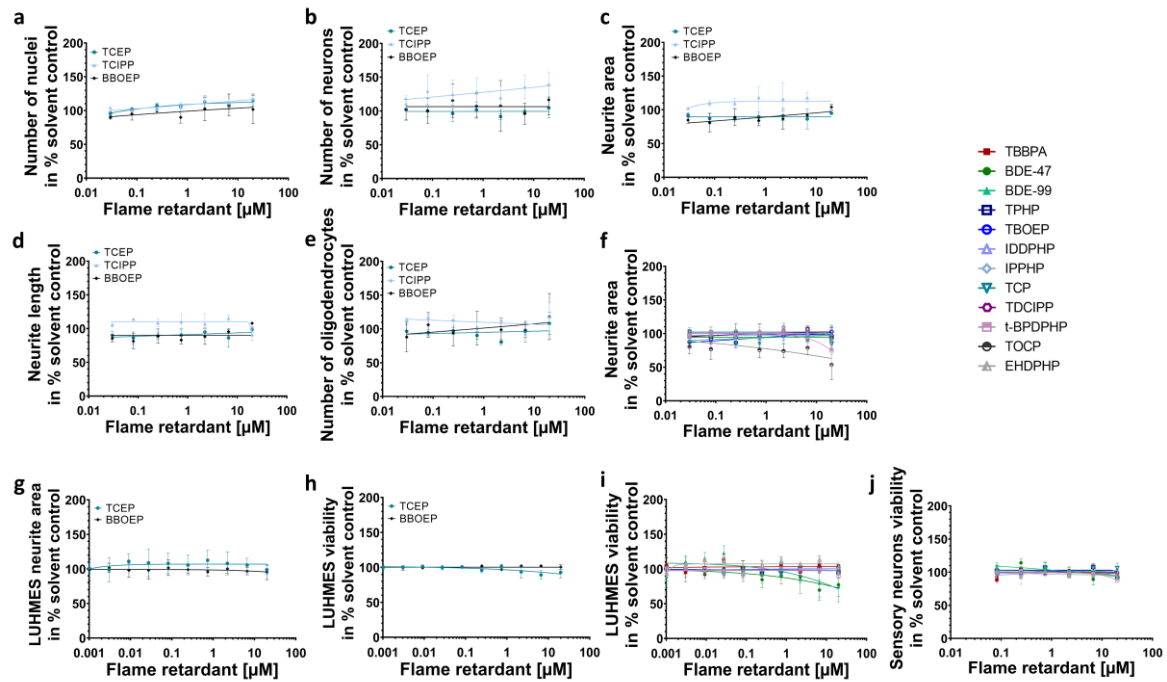
**Figure S1: Influence of residual FRs on hNPCs proliferation (NPC1) that are not shown in Figure 2.** Spheres were plated in 96-well U-bottom plates and exposed to increasing FR concentration over 72 h. Proliferation was studied by measuring the increase of sphere area (a) and by quantifying BrdU incorporation (b) into the DNA. In parallel, viability and cytotoxicity (c) were assessed by performing the Alamar Blue Assay and the LDH Assay. Data are represented as means  $\pm$  SEM. BrdU, bromodeoxyuridine

Figure S2



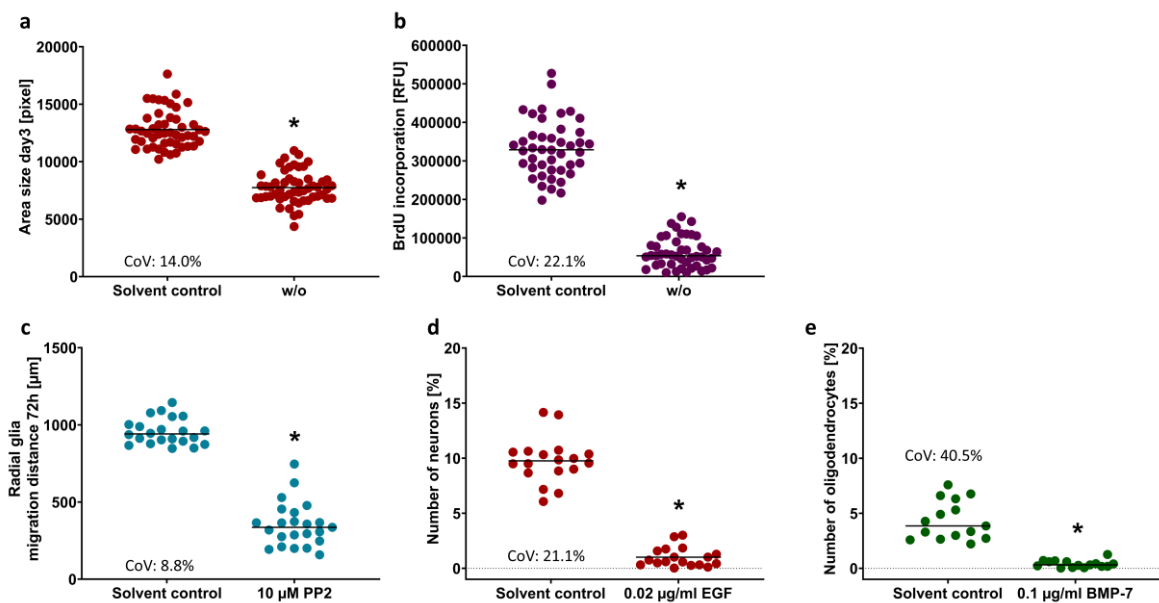
**Figure S2: Effects of residual FRs on different migration endpoints (NPC2, UKN2) that are not shown in Figure 3.** Spheres were plated for hNPC migration analyses onto poly-D-lysine/laminin-coated 96-well plates in the presence and absence of FRs for 120 h. Radial glia migration (72 h) was determined by manually measuring the radial migration from the sphere core (a). After 120 h the radial glia (b), neuronal (c) and oligodendrocyte migration (d) were assessed by automatically identifying (Omnisphero) the migration area of Hoechst stained nuclei,  $\beta$ (III)tubulin stained neurons and O4<sup>+</sup> oligodendrocytes. In parallel, viability and cytotoxicity (e; g) were assessed by the Alamar Blue and the LDH Assay. NCCs (f) were seeded around a stopper into 96-well plates. After stopper removal cells begin to migrate and were exposed to FRs for 24 h. Cells were stained with Calcein-AM and H-33342 and the number of migrated cells into the cell free zone was quantified using the Cellomics ArrayScanVTI. Viability is quantified by counting the number of double-positive cells. Data are represented as means  $\pm$  SEM.

Figure S3



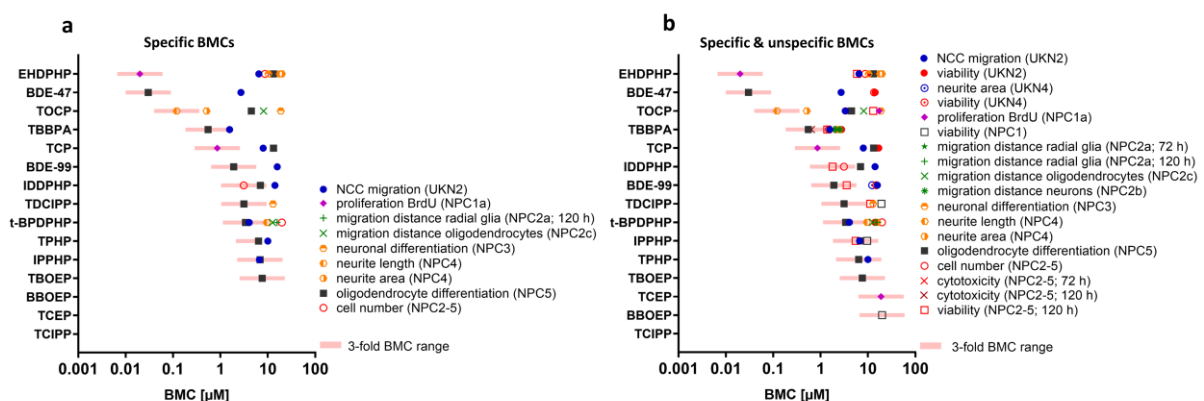
**Figure S3: Differentiation (neurons and oligodendrocytes) and neurite morphology (NPC3, NPC4, NPC5, UKN4, UKN5) in the presence and absence of residual FRs not shown in Figures 4 & 5.** Spheres were plated onto poly-D-lysine/laminin-coated 96-well plates in the presence and absence of FRs. Number of nuclei (a), neuronal differentiation (b) and morphology (c, d, f), as well as oligodendrocyte differentiation (e) was determined automatically (Omnisphero) as number of all  $\beta$ (III)tubulin, O4 positive cells in percent of Hoechst positive nuclei in the migration area after 120 h of differentiation. LUHMES cells (g) and hiPSC derived sensory neurons were treated for 24 h in presence or absence of FRs, stained with Calcein-AM and H-33342 and an automated algorithm calculates the neurite area via subtraction of a calculated soma area from all calcein positive pixels. Viability is quantified by counting the number of double-positive cells (h, i, j). Data are represented as means  $\pm$  SEM (except BBOEP and TBOEP UKN4/5 n=2 means  $\pm$  SD).

Figure S4



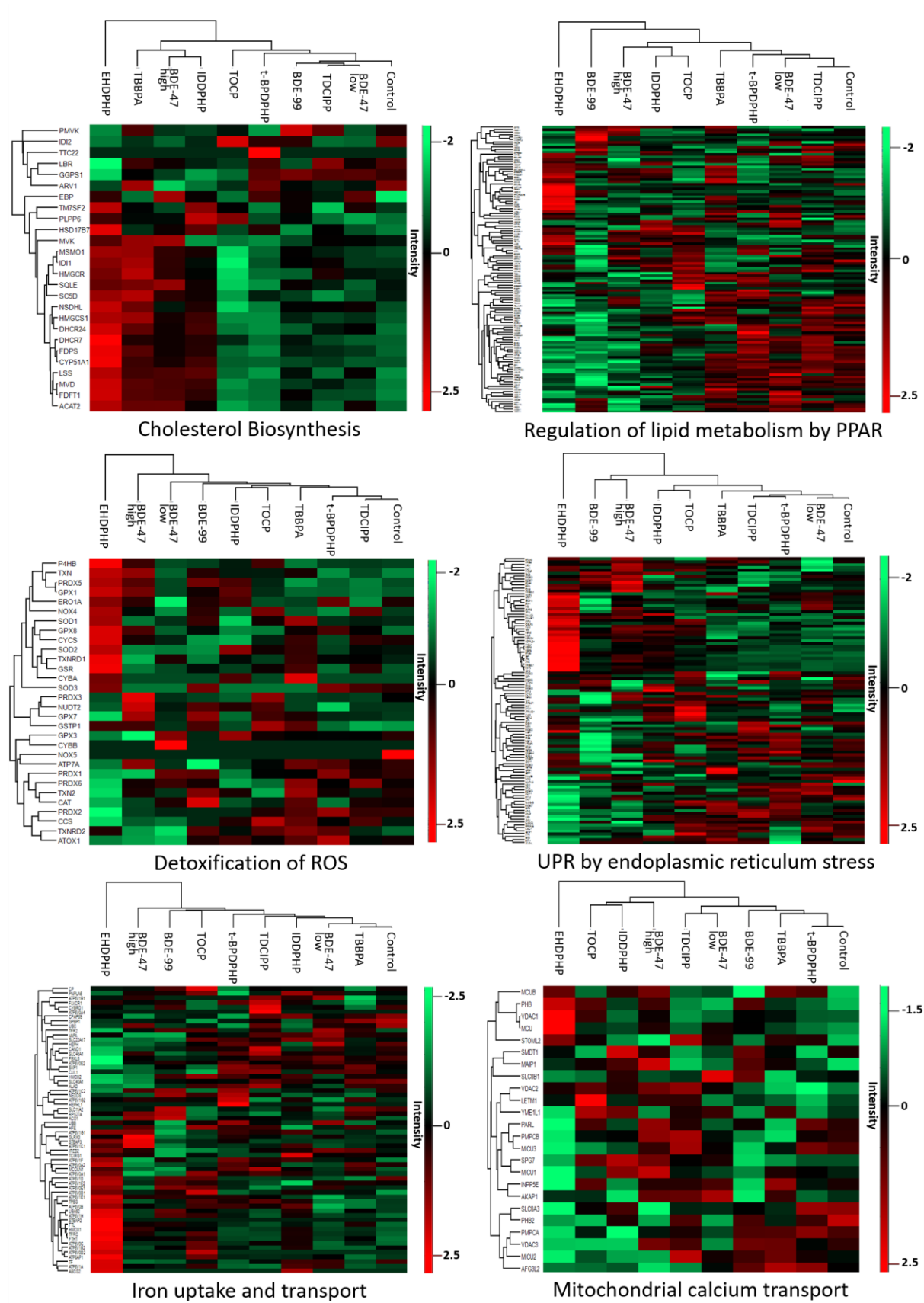
**Figure S4: Variability of solvent and endpoint specific control for NPC1, NPC2, NPC3 and NPC5. Related to Figures 2, 3, 4 and 5.** Spheres are plated in 96-well U-bottom plates and exposed to 0.1% DMSO (solvent) and Proliferation medium without growth factors (w/o) over 72 h. Proliferation was studied by measuring the sphere area (a) and by quantifying BrdU incorporation (b) into the DNA. Spheres were plated onto poly-D-lysine/laminin-coated 96 well plates and exposed to 0.1% DMSO (solvent), 10 µM PP2, 0.02 µg/ml EGF or 0.1 µg/ml BMP-7. Radial glia migration (72 h) was determined by manually measuring the radial migration from the sphere core (c). Neuronal differentiation (d) and oligodendrocyte differentiation (e) was determined automatically (Omnisphero) as number of all  $\beta$ (III)tubulin and O4 positive cells in percent of Hoechst positive nuclei in the migration area after 120 h of differentiation. Data are represented as raw values (dots) and means (black bar). Statistical significance was calculated using OneWay ANOVA and Bonferroni's post-hoc tests ( $p < 0.05$  was considered significant). The percentage indicates the coefficient of variation (CoV) of the respective endpoint. BrdU, bromodeoxyuridine

Figure S5

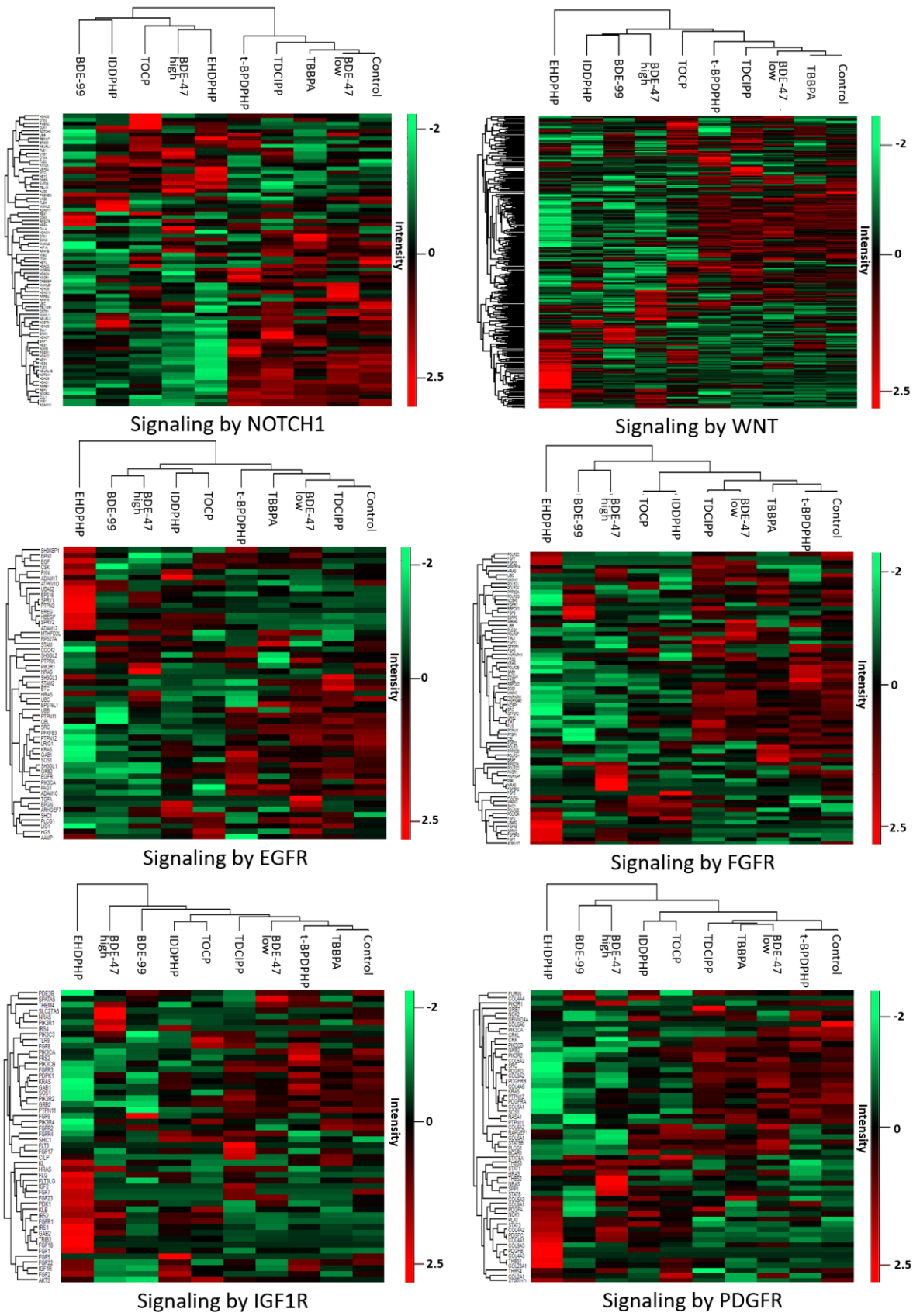


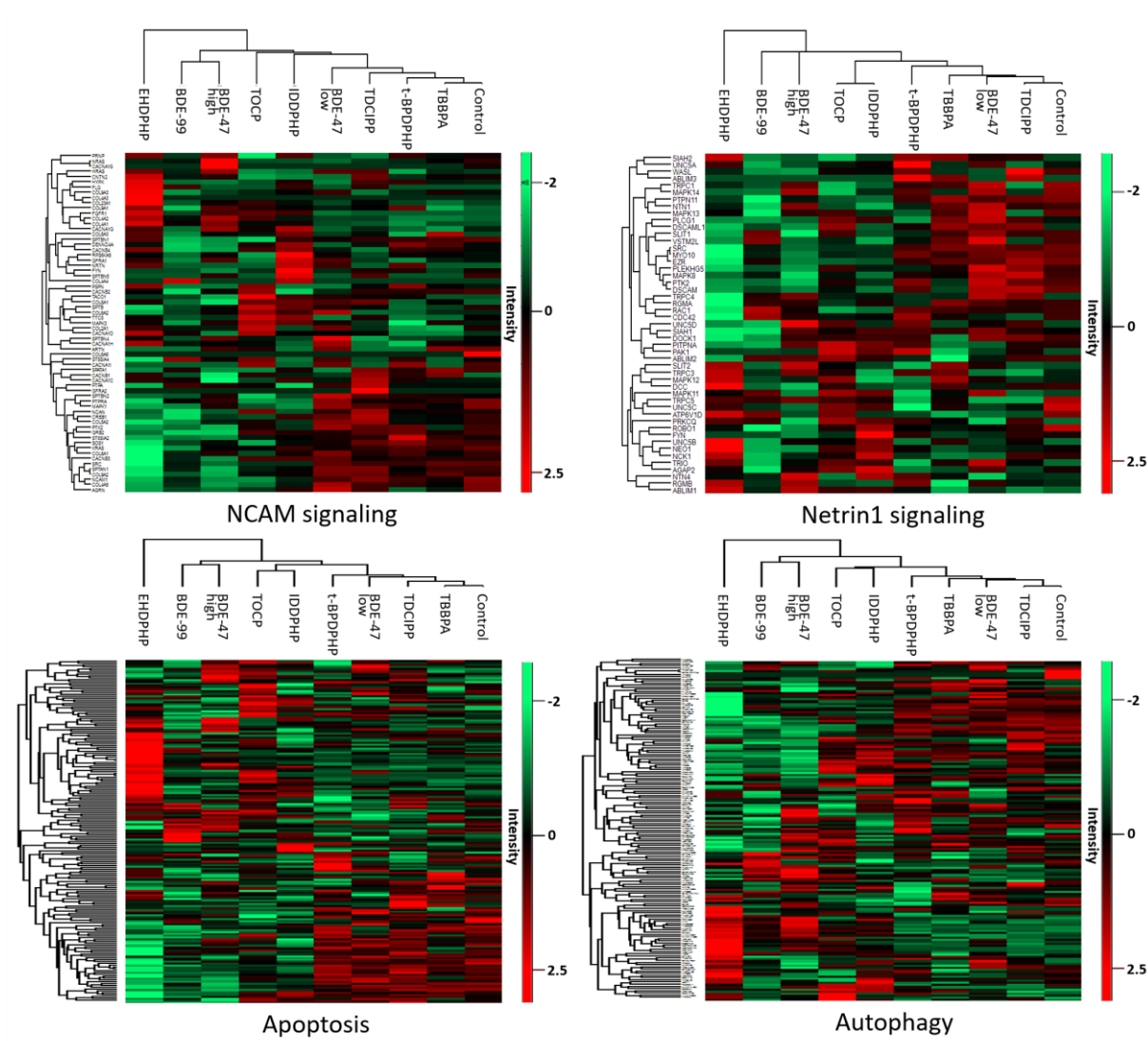
**Figure S5: BMC and 3-fold BMC range of most sensitive endpoints (MSE) across the whole data set. Related to Fig. 7.** Visualization of FRs MSE including the respective 3-fold MSE range. (a) MSEs for DNT-specific hits (no overlap of confidence intervals of the BMCs calculated for the respective endpoint and the cytotoxicity/viability). (b) MSEs for DNT-specific and – unspecific hits (confidence interval overlap  $\geq 10\%$ ), i.e. including effects on viability.

Figure S6









**Figure S6: Influence of FRs on pathways relevant for oligodendrocyte toxicity. Related to Figure 6.** Heatmaps are generated based on RNASeq experiments. The total number of reads of different samples were normalized to the Transcript per Kilobase Million (TPM) count. Heatmaps were generated by using Perseus Version 1.6.2.2 (<https://www.maxquant.org/perseus/>). Therefore, the z-score of TPM values was used with a cut-off of one valid value per conditions.

**Supplementary Table S2:** Summary of BMCs + [CI] across the DNT *in vitro* testing battery. Specific hits are highlighted **bold** and borderline hits are marked *curative*. Red colored specifies most sensitive endpoints (MSEs). \*indicates induced effects. Numbers are given in µM. No value assumes BMCs > 20 µM.

		Brominated (BFRs)			Organophosphates (OPFRs)			
		TBBPA	BDE-47	BDE-99	TPHP	TBOEP	IDDPHP	IPPHP
<i>Proliferation by area</i>	BMC <sub>20</sub>	-	-	-	-	-	-	-
<i>Proliferation by BrdU</i>		-	-	-	-	-	-	-
<i>Proliferation CTB</i>		-	-	-	-	-	-	9.62* [2.93 to 31.57]
<i>Proliferation LDH</i>		-	-	-	-	-	-	-
<i>Radial glia migr. 72 h</i>	BMC <sub>20</sub>	1.93 [1.66 to 2.24]	-	-	-	-	-	-
<i>Radial glia migr. 120 h</i>		2.15 [1.98 to 2.35]	-	-	-	-	-	-
<i>Neuronal migration</i>		2.6 [0.14 to 48.53]	-	-	-	-	-	-
<i>Oligo. migration</i>		2.23 [1.91 to 2.61]	-	-	-	-	-	-
<i>LDH 72 h</i>		1.75* [1.224 to 2.506]	-	-	-	-	-	-
<i>LDH 120 h</i>		0.63* [0.358 to 1.133]	-	-	-	-	-	-
<i>CTB 120 h</i>		1.38 [0.95 to 2.01]	-	3.56* [0.30 to 41.89]	-	-	1.79* [0.94 to 3.39]	5.50* [2.12 to 21.35]
<i>Neurite length</i>		2.31 [1.80 to 2.97]	-	-	-	-	-	-
<i>Neurite area</i>		2.49 [0.58 to 10.72]	-	-	-	-	-	-

<i>Number of nuclei</i>		1.49 [1.17 to 1.90]	-	-	-	-	<b>3.10*</b> <b>[0.12 to 75.97]</b>	-
<i>Number of neurons</i>		2.18 [1.13 to 4.20]	-	-	-	-	-	-
<i>Number of oligodendrocytes</i>	BMC <sub>50</sub>	-	<b>0.03*</b>	-	-	-	-	-
		<b>0.55</b> <b>[0.38 to 0.79]</b>	<b>8.00</b> <b>[3.06 to 22.32]</b>	<b>1.91</b> <b>[1.56 to 2.34]</b>	<b>6.39</b> <b>[2.09 to 19.59]</b>	<b>7.62</b> <b>[3.75 to 15.5]</b>	<b>6.45</b> <b>[4.69 to 10.36]</b>	<b>6.88</b> <b>[4.85 to 9.74]</b>
<i>NCC migration</i>	BMC <sub>25</sub>	<b>1.56</b>	<b>2.71</b>	<b>15.8</b>	<b>10.0</b>	-	<b>14.1</b>	<b>6.66</b>
<i>NCC viability</i>	BMC <sub>10</sub>	2.78	14.2	-	-	-	-	-
<i>LUHMES neurite area</i>	BMC <sub>25</sub>	-	-	12.3	-	-	-	-
<i>LUHMES viability</i>		-	13.5	15.0	-	-	-	-
<i>Sensory N. neurite area</i>		-	-	-	-	-	-	-
<i>Sensory N. viability</i>		-	-	-	-	-	-	-
<b>Organophosphates (OPFRs)</b>								
		TCP	TDCIPP	t-BPDPHP	TOCP	EHDPHP	BBOEP	TCEP
<i>Proliferation by area</i>	BMC <sub>20</sub>	-	-	-	-	-	-	-
<i>Proliferation by BrdU</i>		<b>0.86</b> <b>[0.21 to 3.64]</b>	-	-	17.2 [8.38 to 35.47]	<b>0.02</b> <b>[0.004 to 0.11]</b>	-	18.9 [0.083 to 149.5]
<i>Proliferation CTB</i>		-	19.2 [8.68 to 118.9]	-	-	-	19.9 [14.87 to 110.6]	-
<i>Proliferation LDH</i>		-	-	-	-	-	-	-
<i>Radial glia migr. 72 h</i>	BMC <sub>20</sub>	-	-	-	-	-	-	-
<i>Radial glia migr. 120 h</i>		-	-	<b>15.73</b> <b>[11.2 to 22.03]</b>	-	-	-	-
<i>Neuronal migration</i>		-	-	-	-	-	-	-
<i>Oligo. migration</i>		-	-	<b>12.54</b> <b>[8.61 to 18.29]</b>	<b>8.12</b> <b>[2.65 to 24.91]</b>	-	-	-
<i>LDH 72 h</i>		-	-	-	-	-	-	-
<i>LDH 120 h</i>	-	-	-	-	-	-	-	

<i>CTB 120 h</i>		-	11.2 [7.60 to 16.57]	-	12.9* [6.34 to 26.31]	5.88* [3.35 to 10.30]	-	-
<i>Neurite length</i>		-	-	<b>9.55</b> [4.41 to 20.70]	<b>0.12</b> [0.005 to 2.85]	<b>17.9</b> [9.27 to 34.62]	-	-
<i>Neurite area</i>		-	-	15.8 [6.86 to 36.18]	<b>0.51</b> [0.02 to 14.36]	<b>19.8</b> [0.62 to 329.1]	-	-
<i>Number of nuclei</i>		-	-	<b>19.8</b> [19.23 to 20.4]	-	<b>8.72*</b> [1.32 to 57.79]	-	-
<i>Number of neurons</i>		-	<b>12.8*</b> [0.09 to 1860]	-	<b>18.8</b> [3.59 to 50.21]	<b>10.3</b> [1.79 to 59.53]	-	-
<i>Number of oligodendrocytes</i>	BMC <sub>50</sub>	-	-	-	-	-	-	-
		<b>13.2</b> [8.50 to 20.5]	<b>3.13</b> [2.09 to 4.696]	<b>3.37</b> [2.58 to 4.39]	<b>4.49</b> [2.272 to 8.88]	<b>13.1</b> [8.42 to 20.28]	-	-
<i>NCC migration</i>	BMC <sub>25</sub>	<b>7.99</b>	-	<b>4.05</b>	3.32	<b>6.46</b>	-	-
<i>NCC viability</i>	BMC <sub>10</sub>	16.9	-	14.0	3.44	11.4	-	-
<i>LUHMES neurite area</i>	BMC <sub>25</sub>	-	-	-	-	-	-	-
<i>LUHMES viability</i>		-	-	-	-	-	-	-
<i>Sensory N. neurite area</i>		-	-	-	-	-	-	-
<i>Sensory N. viability</i>		-	-	-	-	-	-	-





---

## **Neurodevelopmental toxicity assessment of flame retardants using a human DNT *in vitro* testing battery**

**Jördis Klose**, Melanie Pahl, Kristina Bartmann, Farina Bendt, Jonathan Blum, Xenia Dolde, Anna-Katharina Holzer, Ulrike Hübenthal, Hagen Eike Keßel, Katharina Koch, Stefan Masjosthusmann, Sabine Schneider, Lynn-Christin Stürzl, Selina Woeste, Andrea Rossi, Adrian Covaci, Mamta Behl, Marcel Leist, Julia Tigges, Ellen Fritsche

Journal:	Cell Biology and Toxicology
Impact Factor:	6.284 (2019)
Contribution to the publication:	80 % Planning and evaluation of all hNPC experiments, performance of one-third of the hNPC experiments, writing of the manuscript
Type of authorship:	first-authorship
Status of the publication:	Accepted 11 <sup>th</sup> March 2021

## 2.7 TBBPA Targets Converging Key Events of Human Oligodendrocyte Development Resulting in Two Novel AOPs

**Jördis Kloese**, Julia Tigges, Stefan Masjosthusmann, Katharina Schmuck, Farina Bendt, Ulrike Hübenthal, Patrick Petzsch, Karl Köhrer, Katharina Koch and Ellen Fritsche

### *ALTEX – Alternatives to Animal Experimentation*

Während der Entwicklung der weißen Hirnsubstanz etablieren myelinisierende Oligodendrozyten (OLs) eine schnelle saltatorische Erregungsleitung. Eine Störung der Oligodendrogenese, z.B. durch eine gestörte Myelinisierung führt daher zu einem adversen Effekt bezogen auf die Gehirnleistung des jeweiligen Kindes. Ein komplexes Netzwerk aus hormonellen, transkriptionellen und biosynthetischen Prozessen reguliert die OL-Entwicklung, was gleichzeitig verschiedene Angriffspunkte für Umweltgifte schafft. Das bromierte Flammenschutzmittel Tetrabrombisphenol A (TBBPA) wird derzeit als endokriner Disruptor, speziell für das Schilddrüsenhormonsystems (TH) diskutiert. In dieser Studie identifizierten wir, wie TBBPA die Etablierung reifender OLs durch zwei unabhängige Wirkmechanismen (modes-of-action; MoA), abhängig und unabhängig vom TH-Signalweg beeinflusst. Durch die Kombination des zuvor veröffentlichten Oligodendrozyten Reifungsassays (NPC6) mit Transkriptomanalysen ist es uns *in vitro* gelungen, TBBPA als einen TH-Disruptor zu identifizieren, indem es Oligodendrogenese-assoziierte Gene (z.B. *MBP*, *KLF9* und *EGR1*) dereguliert und somit die menschliche OL-Reifung beeinträchtigt. Darüber hinaus stört TBBPA ein Genexpressionsnetzwerk, das die Cholesterinhomöostase reguliert und somit die OL Anzahl unabhängig vom TH-Signalweg reduziert. Diese beiden MoA konvergieren in einem AOP Netzwerk bei dem Schlüsselereignis der Hypomyelinisierung. Vergleichende Analysen von neuronalen Vorläuferzellen (NPCs) von Mensch und Ratte ergaben, dass die Oligodendrogenese beim Menschen empfindlicher gegenüber einer durch TBBPA ausgelösten endokrinen Störung ist. Daher sind ethisch unbedenkliche, kosteneffiziente und speziesübergreifende *in vitro* Methoden für die entwicklungsneurotoxische Beurteilung des Gefährdungspotentials erforderlich. Durch den Einbau von Transkriptomanalysen haben wir den NPC6-Assay auf ein höheres Leistungslevel für zukünftige regulatorische Anwendungen gebracht. Die Kombination von phänotypischen und transkriptomischen Analysen hilft dabei, MoA zu untersuchen, die letztendlich zur Erstellung von AOPs führen und mit einem besseren Verständnis der Entwicklungsneurotoxizität einher gehen.



## Research Article

# TBBPA Targets Converging Key Events of Human Oligodendrocyte Development Resulting in Two Novel AOPs

Jördis Klose<sup>1</sup>, Julia Tigges<sup>1</sup>, Stefan Masjosthusmann<sup>1</sup>, Katharina Schmuck<sup>1</sup>, Farina Bendt<sup>1</sup>, Ulrike Hübenthal<sup>1</sup>, Patrick Petzsch<sup>2</sup>, Karl Köhrer<sup>2</sup>, Katharina Koch<sup>1#</sup> and Ellen Fritsche<sup>1,3#</sup>

<sup>1</sup>IUF – Leibniz Research Institute for Environmental Medicine, Duesseldorf, Germany; <sup>2</sup>Biological and Medical Research Centre (BMFZ), Medical Faculty, Heinrich-Heine-University, Duesseldorf, Germany; <sup>3</sup>Medical Faculty, Heinrich-Heine-University, Duesseldorf, Germany

### Abstract

Myelinating oligodendrocytes (OLs) establish saltatory nerve conduction during white matter development. Thus, interference with oligodendrogenesis leads to an adverse outcome on brain performance in the child due to aberrant myelination. An intertwined network of hormonal, transcriptional and biosynthetic processes regulates OL development, thereby simultaneously creating various routes of interference for environmental toxicants. The flame retardant tetrabromobisphenol A (TBBPA) is debated as an endocrine disruptor, especially of the thyroid hormone (TH) system. We identified how TBBPA interferes with the establishment of a population of maturing OLs by two independent modes-of-action (MoA), dependent and independent of TH signaling. Combining the previously published oligodendrocyte maturation assay (NPC6) with large-scale transcriptomics, we describe TBBPA as a TH disruptor, impairing human OL maturation *in vitro* by dysregulation of oligodendrogenesis-associated genes (i.e., *MBP*, *KLF9* and *EGR1*). Furthermore, TBBPA disrupts a gene expression network regulating cholesterol homeostasis, reducing OL numbers independently of TH signaling. These two MoA converge in a novel putative adverse outcome pathway (AOP) network on the key event (KE) hypomyelination. Comparative analyses of human and rat neural progenitor cells (NPCs) revealed that human oligodendrogenesis is more sensitive to endocrine disruption by TBBPA. Therefore, ethical, cost-efficient and species-overarching *in vitro* assays are needed for developmental neurotoxicity hazard assessment. By incorporation of large-scale transcriptomic analyses, we brought the NPC6 assay to a higher readiness level for future applications in a regulatory context. The combination of phenotypic and transcriptomic analyses helps to study MoA to eventually build AOPs for a better understanding of neurodevelopmental toxicity.

## 1 Introduction

Oligodendrocytes (OLs) are responsible for axon myelination, thereby facilitating rapid saltatory conduction of action potentials within the central nervous system. During development, multipotent neural stem/progenitor cells (NSPCs) give rise to committed oligodendrocyte precursor cells (OPCs) that proliferate and migrate to the final site of myelination (Emery, 2010; van Tilborg et al., 2018). Subsequent terminal differentiation of OPCs into pre-myelinating OLs (pre-OLs), and finally myelin-producing mature OLs, involves a fine-tuned interplay of hormonal signaling, transcriptional regulation and biosynthetic processes.

The myelin membrane contains 73% lipids, of which cholesterol makes up around 30%. Almost all brain cholesterol is synthesized *de novo*, predominantly by OLs. Strikingly, OLs synthesize more than 3-fold their own weight of myelin per day (Norton and Poduslo, 1973), making a balanced cholesterol homeostasis a necessity for oligodendrocyte maturation and axon ensheathment (Mathews and Appel, 2016; Mathews et al., 2014). Accordingly, accumulation of cholesterol due to impaired transport and export causes lipotoxicity, leading to cell death of OLs (Haq et al., 2003; Bezine et al., 2017). Genetic mouse models with impaired expression of proteins regulating cholesterol clearance, such as the cholesterol exporters ABCA1 and NPC1, show reduced OPC

# contributed equally

Received July 20, 2020; Accepted October 19, 2020;  
Epub October 23, 2020; © The Authors, 2021.

ALTEX 38(2), 215-234. doi:10.14573/altex.2007201

Correspondence: Ellen Fritsche, PhD  
IUF – Leibniz Research Institute for Environmental Medicine  
Auf'm Hennekamp 50, 40225, Duesseldorf, Germany  
(ellen.fritsche@iuf-duesseldorf.de)

This is an Open Access article distributed under the terms of the Creative Commons Attribution 4.0 International license (<http://creativecommons.org/licenses/by/4.0/>), which permits unrestricted use, distribution and reproduction in any medium, provided the original work is appropriately cited.



maturation, hypomyelination, and developmental delays (Wang et al., 2018; Takikita et al., 2004; Caporali et al., 2016). Consistent with that, treatment of aberrant cholesterol storage with cyclodextrin effectively restored myelination and reduced neurodegeneration in murine models of Niemann-Pick disease type C (Saher and Stumpf, 2015). In addition to a surplus of cholesterol, also the lack of cholesterol due to impaired biosynthesis causes hypomyelination in the brain. In line with this, dietary cholesterol effectively restores myelination in mouse models of myelin disorders such as Pelizaeus-Merzbacher disease (Saher et al., 2012) and multiple sclerosis (Berghoff et al., 2017) by reestablishing OL numbers.

OL maturation is further dependent on hormonal signaling. Especially thyroid hormones (TH) are crucial for the development of white matter tracts in humans (Annunziata et al., 1983). It is well documented that the terminal differentiation into myelinating OLs is tightly regulated by the thyroxine metabolite triiodothyronine (T3) (Baas et al., 1997; Murray and Dubois-Dalcq, 1997). Binding of T3 to nuclear thyroid hormone receptors (THRs) causes transcriptional regulation of genes under control of TH response elements (TREs) (reviewed by Lee and Petratos, 2016). The importance of TH signaling for OL maturation is dramatically illustrated by pathological conditions causing hypomyelination due to TH disruption in the developing brain, such as congenital hypothyroidism (Gupta et al., 1995), maternal hypothyroidism (Wei et al., 2015) or the Allan-Herndon-Dudley syndrome (AHDS) (Gika et al., 2010; La Piana et al., 2015). Scarce TH levels during pregnancy and after birth are correlated with clinical presentations ranging from mild cognitive deficits to severe mental retardation (Rovet and Daneman, 2003; Haddow et al., 1999; Sarret et al., 1993). Importantly, TH replacement therapy has been successfully implemented in children suffering from congenital hypothyroidism (Bauer and Wassner, 2019; Gruters and Krude, 2011) and is under investigation in children with AHDS (Groeneweg et al., 2019). In accordance with the clinical observations, studies on hypothyroid rats revealed impaired expression of the myelin-associated genes myelin basic protein (*MBP*) and myelin proteolipid protein (*PLP1*) as well as reduced numbers of mature OLs (Ibarrola and Rodriguez-Pena, 1997; Schoonover et al., 2004). This is at least in part dependent on TREs present within genes associated with OL maturation such as *MBP* and Krüppel-like factor 9 (*KLF9*) (Farsetti et al., 1992; Denver and Williamson, 2009).

Given the relevance of TH disruption for oligodendrocyte development, it is necessary to consider environmental exposure of the developing brain to chemicals with thyroid-disrupting potential. As a consequence, a range of environmental chemicals

has been identified as TH disruptors. Modes-of-action (MoA) include the inhibition of iodine uptake, interference with TH metabolizing enzymes, displacement of THs from transport proteins, and antagonistic or agonistic effects at the THR level (reviewed by Zoeller, 2007).

Since differences in OL development and turnover have been described between rodents and humans, the direct translation of rodent studies into the human system is challenging (Yeung et al., 2014; Dach et al., 2017). Therefore, human cell-based *in vitro* models with a higher testing throughput than *in vivo* animal studies are needed to study the effects of chemical exposure on OL development. Our group successfully implemented the oligodendrocyte maturation assay (NPC6), which comparatively identifies disruptors of TH-dependent OL maturation in differentiating human and mouse NPC cultures (Dach et al., 2017; Bal-Price et al., 2018). Strikingly, vast species differences in OL development and resulting compound MoA were identified, emphasizing the necessity for human cell-based test systems to guarantee high predictivity for humans.

In the present study, we analyzed the effects of the brominated flame retardant (BFR) tetrabromobisphenol A (TBBPA) on OL development. TBBPA is commonly used in the manufacturing of household items and electronics to reduce flammability, making it a substance of high toxicological relevance in humans. Accordingly, several studies have reported bioaccumulation of TBBPA in serum, cord blood, and breast milk of pregnant and nursing women (Cariou et al., 2008; Kim and Oh, 2014). Moreover, since TBBPA has a reported half-life in humans of about two days, bioaccumulation indicates chronic exposure of mothers in their daily life (Sjodin et al., 2003). Of note, increased TBBPA concentrations were found in infants compared to their mothers, highlighting the impact of TBBPA exposure during human development.

## 2 Materials and methods

### Reagents

Thyroid hormone L-3,3',5 triiodothyronine (T3, #T2877), perfluorooctanoic acid (PFOA, #171468) and 3,3',5,5' tetrabromobisphenol A (TBBPA, #330396) were purchased from Merck. The following stock solutions were prepared, aliquoted, and stored at the indicated temperatures: 300  $\mu$ M T3 in a 1:1 (v/v) dilution of 96% ethanol and 1 M HCl (EtOH/HCl; both Carl Roth) stored at -20°C; 2 mM PFOA in dimethyl sulfoxide (DMSO) stored at -20°C; and 250 mM TBBPA in DMSO stored at -20°C. The THR antagonist NH-375 (NH-3) (Nguyen et al., 2002; Singh et al.,

### Abbreviations

ABCA1, ATP-binding cassette (ABC) subfamily-A transporter 1; AHDS, Allan-Herndon-Dudley syndrome; AOP, adverse outcome pathway; BFR, brominated flame retardant; BMC, benchmark concentration; CHD3, chromodomain helicase DNA binding protein 3; CRYM, crystallin Mu; DHCR7, 7-dehydrocholesterol reductase; DIO3, iodothyronine deiodinase 3; DMSO, dimethyl sulfoxide; DNT, developmental neurotoxicity; EGR1, early growth response 1; FC, fold change; FDFT1, farnesyl-diphosphate farnesyl-transferase 1; FDPS, farnesyl diphosphate synthase; HMGCR, 3-hydroxy-3-methylglutaryl-CoA reductase; HMGCS1, hydroxymethylglutaryl-CoA synthase; hNPCs, human neural progenitor cells; HR, HR lysine demethylase and nuclear receptor corepressor; IGFBP4, insulin like growth factor binding protein 4; IL33, interleukin 33; KE, key event; KLF9, Krüppel-like factor 9; MBP, myelin basic protein; MIE, molecular initiating event; MoA, mode-of-action; NH-3, THR antagonist NH-375; NMB, neuromedin B; NPCs, neural progenitor cells; NSPCs, neural stem/progenitor cells; OL, oligodendrocytes; OPCs, oligodendrocyte precursor cells; PCA, principle component analysis; PFOA, perfluorooctanoic acid; PLP1, proteolipid protein; pre-OLs, pre-myelinating OLs; PVL, periventricular leukomalacia; QM, maturation quotient; qRT-PCR, quantitative real-time polymerase chain reaction; rNPCs, rat neural progenitor cells; SERPINE2, serpin family E member 2; TBBPA, tetrabromobisphenol A; T3, triiodothyronine; TH, thyroid hormone; THR, thyroid hormone receptor; TRE, TH response element; TSHR, thyroid stimulating hormone receptor; TXNIP, thioredoxin interacting protein

2016) was diluted in DMSO, and a 1 mM stock was prepared and stored at  $-80^{\circ}\text{C}$ . The final solvent concentrations within the experiments were 0.01% EtOH/HCl and 0.1% DMSO.

#### *Neurosphere cell culture*

Human neural progenitor cells (hNPCs) derived from whole-brain homogenates of male gestational week 16-19 fetuses were purchased from Lonza (#PT-2599). Time-matched rat neural progenitor cells (rNPCs) were prepared as previously described (Baumann et al., 2014). In brief, pregnant rats (Wistar) were obtained from Charles River and rNPCs were isolated from post-natal day one pups by dissecting, digesting and homogenizing whole brains to obtain a cell suspension. Brain homogenates of all pups (male and female) were pooled prior to rNPC culture. The preparation of the rat pups agrees with the “Landesamt für Natur, Umwelt und Verbraucherschutz” (81-02.05.50.18.001) and is in accordance with §4 Abs. 3 *Tierschutzgesetz* (TierSchG). Both hNPCs and rNPCs were cultured as 3D free-floating neurospheres in the following proliferation medium: Dulbecco’s modified Eagle’s medium (DMEM, Thermo Fisher, #31966021) and Ham’s F12 (Thermo Fisher, #31765027) were mixed 3:1 (v/v) and supplemented with B27 (Thermo Fisher, #17504044), 100 U/mL penicillin and 100  $\mu\text{g}/\text{mL}$  streptomycin (PAN Biotech, #P06-07100), 20 ng/mL human epidermal growth factor (EGF, Thermo Fisher, #PHG0315), and either 20 ng/mL (hNPCs) recombinant human fibroblast growth factor (FGF, R&D Systems, #233-FB) or 10 ng/mL (rNPCs) recombinant rat FGF (R&D Systems, #3339-FB-025). Both NPCs were cultured under standard cell culture conditions in a humidified incubator at  $37^{\circ}\text{C}$  and 5%  $\text{CO}_2$  in cell culture dishes coated with poly-2-hydroxyethyl methacrylate (poly-HEMA, Merck, #P3932). Once a week, the neurospheres were passaged mechanically to 0.2 mm size with a McIlwain tissue chopper (model TC752), and 50% of the medium was replaced every second day. All cultures were tested for the absence of mycoplasma and used only up to passage 3 (hNPCs) or exclusively in passage 1 (rNPCs) to guarantee high reproducibility of the test methods.

#### *Differentiation of human and rat NPCs*

In order to study the extent of oligodendrocyte maturation in response to compound exposure, human and rat NPCs were differentiated into neurons, oligodendrocytes and astrocytes (Moors et al., 2009; Breier et al., 2010). Two days prior to plating, human and rat NPCs were chopped to a size of 0.2 mm in the respective proliferation media. On the plating day, 0.3 mm diameter neurospheres were sorted and washed in the following differentiation medium: DMEM (Thermo Fisher, #31966021) and Ham’s F12 (Thermo Fisher, #31765027) mixed 3:1 (v/v) and supplemented with 1% N2 (Thermo Fisher, #17502-048) and 100 U/mL penicillin and 100  $\mu\text{g}/\text{mL}$  streptomycin (PAN Biotech, #P06-07100).

For the immunocytochemical staining and quantification of  $\text{O4}^+$  cells, 8-chamber glass cover slides (LMS Consult) were coated with 0.1 mg/mL poly-D-lysine (PDL, Merck, #P0899) and 12.5  $\mu\text{g}/\text{mL}$  laminin (Merck, #L2020). Five 0.3 mm neurospheres were plated per well in 500  $\mu\text{L}$  differentiation medium containing the respective exposure(s) or solvent control(s). The

neurospheres were differentiated for 5 days during which cells radially migrated out of the sphere core (migration area). On day 3 of the experiment, 250  $\mu\text{L}$  medium was replaced with fresh exposure/solvent medium.

For the assessment of *MBP* and *Mog* gene expression, 0.3 mm neurospheres were differentiated for 5 days in PDL/laminin-coated 24-well plates (Sarstedt). Ten neurospheres per well were plated in 1 mL differentiation medium containing the respective exposure(s) and solvent control(s). On day 3 of the experiment, 500  $\mu\text{L}$  medium was replaced with fresh exposure/solvent medium.

#### *Assessment of cell viability*

Cell viability was measured after 5 days of differentiation using the CellTiter-Blue (CTB) assay according to the manufacturer’s instructions (Promega). Briefly, the CTB reagent was diluted 1:3 in differentiation medium and subsequently added in a ratio of 1:4 (v/v) to the 8-chamber slides. Following 2 h of incubation under standard cell culture conditions, 2-times 100  $\mu\text{L}$  supernatant per well were transferred into a 96-well plate to detect the fluorescence with a Tecan infinite M200 Pro reader (ex: 540 nm; em: 590 nm). The relative fluorescence unit (RFU) values of the replicates were averaged, and medium without cells was used to correct for background fluorescence.

#### *Immunocytochemistry*

After the viability measurement, a solution of 12% paraformaldehyde (PFA, Merck) was added to the 8-chamber slides 1:2 (v/v) to yield a final concentration of 4% PFA. The slides were incubated at  $37^{\circ}\text{C}$  for 45 min to fix the spheres and migrated cells. Until the immunocytochemical staining for  $\text{O4}$ , fixed slides were stored in phosphate-buffered saline (PBS, Biochrom) at  $4^{\circ}\text{C}$ . After 3 washing steps with PBS for 5 min, 30  $\mu\text{L}$  anti- $\text{O4}$  antibody dilution (1:200 mouse anti- $\text{O4}$  (R&D Systems #MAB1326), 10% goat serum (Merck #G9023) in PBS) were added per chamber and incubated overnight at  $4^{\circ}\text{C}$ . After 3 additional washing steps with PBS for 5 min, 30  $\mu\text{L}$  secondary antibody solution (1:250 goat anti-mouse Alexa Fluor 488 (Thermo Fisher, #A-21042), 2% Hoechst 33258 (Merck, #B1155), 1% goat serum in PBS) were added per chamber and incubated for 30 min at  $37^{\circ}\text{C}$ . The slides were washed three times with PBS, once with distilled water, and finally sealed with glass coverslips using Aqua-Poly/Mount (Polysciences, #18606).

#### *Image acquisition and quantification of $\text{O4}^+$ cells*

Imaging of stained slides was performed by high-content imaging analysis (HCA) using an automated fluorescence microscope (Cellomics ArrayScan VTI, Thermo Fisher Scientific).

Parameters were adjusted to detect nuclei (Hoechst, ex: 359 nm; em: 461 nm) and  $\text{O4}$  surface expression (Alexa-488, ex: 495 nm; em: 519 nm). The image analysis was carried out with the software Omnisphero (Schmuck et al., 2017). In brief, for 2 defined areas (1098 mm x 823 mm size; once placed above and once below the sphere core) per migration area, the number of  $\text{O4}^+$  cells were normalized to the total number of nuclei. The resulting percentages of the 2 areas from the same sphere were averaged, and the mean and standard deviation were calculated for



**Tab. 1: Primers used for quantitative real-time PCR**

Name	Primer
<i>ACTB</i> human_fw	5'-CAGGAAGTCCCTTGCCATCC-3'
<i>ACTB</i> human_rev	5'-ACCAAAAGCCTTCATACATCTCA-3'
<i>ACTB</i> rat_fw	5'-CCTCTATGCCAACACAGT-3'
<i>ACTB</i> rat_rev	5'-AGCCACCAATCCACACAG-3'
<i>MBP</i> human_fw	5'-CAGAGCGTCCGACTATAAATCG-3'
<i>MBP</i> human_rev	5'-GGTGGGTTTTTCAGCGTCTA-3'
<i>Mog</i> rat_fw	5'-TCCATCGGACTTTTGATCCTCA-3'
<i>Mog</i> rat_rev	5'-CGCTCCAGGAAGACACAACC-3'

the 5 neurospheres of every treatment condition.

#### Quantitative real-time PCR

The total RNA of neurospheres differentiated for 5 days was isolated, and 150 ng RNA were transcribed into cDNA using the RNeasy Mini Kit (Qiagen #74106) and the Quantitect Reverse Transcription Kit (Qiagen, #205313) according to the manufacturer's instructions. Quantitative real-time polymerase chain reaction (qRT-PCR) was performed with the QuantiFast SYBR Green PCR Kit (Qiagen, #204054) within the Rotor Gene Q Cycler (Qiagen) using the primers listed in Table 1. Analysis was performed with the copy number method, and *MBP/Mog* expression was normalized to 10,000 *ACTB* copy numbers to correct for differences in the amount of cDNA within the samples (Dach et al., 2017).

#### Calculation of the maturation quotient ( $Q_M$ )

As first described in Dach et al. (2017), mature oligodendrocytes are characterized by increased *MBP* (human) or *Mog* (rat) gene expression. However, assessment of the gene expression alone is not valid, since an increase in the oligodendrocyte percentage within the NPC culture would *per se* lead to higher *MBP/Mog* levels without giving information about the maturity of the cells. Thus, we calculated the maturation quotient ( $Q_M$ ), which describes the extent of *MBP/Mog* expression within the oligodendrocyte population. Thereby, the oligodendrocyte population is defined as the percentage of O4<sup>+</sup> cells within the differentiated

NPC culture. Only an increase in the  $Q_M$  represents an increase in oligodendrocyte maturation. Table 2 describes three possible scenarios when comparing the  $Q_M$  of exposed cells to the relevant controls.

#### Microarray assays

RNA isolation was performed using the RNeasy Mini Kit (Qiagen #74106) according to the manufacturer's protocol. 1,000 neurospheres with a defined size of 0.1 mm were plated per well of PDL/laminin-coated 6-well plates and cultivated for 4, 24, and 60 h for TBBPA single treatment alone and 96 h for TBBPA/T3 co-treatment. Total RNA was quantified (Qubit RNA HS Assay, Thermo Fisher Scientific), and the quality was measured by capillary electrophoresis on a fragment analyzer using the "Total RNA Standard Sensitivity Assay" (Agilent Technologies, Inc. Santa Clara, USA). All samples in this study showed high-quality RNA integrity numbers (RQN; mean = 9.9).

cDNA synthesis, *in vitro* transcription of cRNA, synthesis and subsequent biotin labeling of cDNA was performed according to the manufacturer's protocol (GeneChip® WT PLUS Reagent Kit 703174 23, January 2017; ThermoFisher scientific). In brief, 100ng total RNA were converted to cDNA, followed by *in vitro* transcription into cRNA, synthesis and biotin labeling of cDNA. After fragmentation, labeled cDNA was hybridized to Applied Biosystems™ Clariom™ S Human Gene Expression Microarray chips for 16 h at 45°C, stained with a streptavidin/phycoerythrin conjugate, and scanned as described in the manufacturer's protocol.

For validation of microarray analyses, qRT-PCR of a set of 10 genes was performed (Fig. S2<sup>1</sup>). Briefly, 500 ng RNA from microarray samples were transcribed into cDNA. RNA isolation, cDNA synthesis, and qRT-PCR were performed as described in the above section "Quantitative real-time PCR".

#### Statistics

Experiments were performed in at least 3 biological replicates for each species. All data are represented as mean ± standard error of the mean (SEM). Statistical significance was calculated with two-way ANOVA and Bonferroni's post-hoc tests using GraphPad Prism 8.2.1 software. Results with p-values below 0.05 were termed significant. Benchmark concentration (BMC<sub>50</sub> and BMC<sub>30</sub>) calculation was performed using GraphPad Prism 8.2.1 with sigmoidal curve fitting methods with the therein contained BMC model. The BMC values were defined based on the variability of the respective endpoints. Therefore, in the case of oligoden-

**Tab. 2: Evaluation of  $Q_M$  values**

Oligodendrocyte maturation quotient ( $Q_M$ )	% O4 <sup>+</sup> cells	<i>MBP/Mog</i> expression	
$Q_M$ (exposure) > $Q_M$ (control)	no effect	↑	increased maturation
$Q_M$ (exposure) > $Q_M$ (control)	↑	↑↑	increased maturation
$Q_M$ (exposure) = $Q_M$ (control)	↑	↑	no effect on maturation

<sup>1</sup> doi:10.14573/altex.2007201s



drocyte number (Fig. 3A), we choose  $BMC_{50}$  instead of  $BMC_{30}$  due to higher variations between replicates compared to the oligodendrocyte maturation assay.

#### Microarray statistical analysis

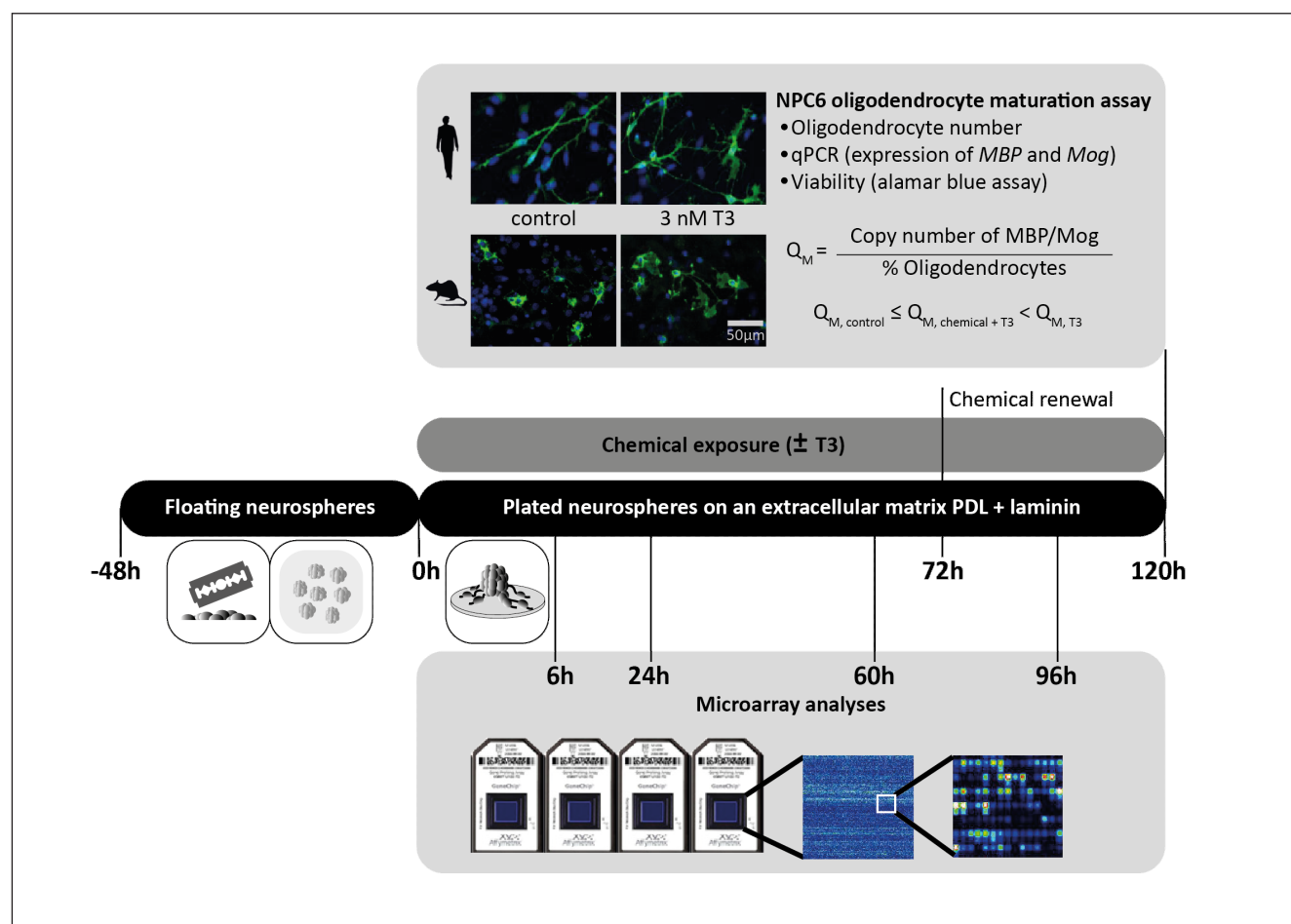
Data analyses of Affymetrix CEL files was conducted with GeneSpring GX software (Vers. 14.9.1; Agilent Technologies). To avoid inter-array variability, probes were pooled by GeneSpring's ExonRMA16 algorithm after quantile normalization of probe-level signal intensities across all samples (Bolstad et al., 2003). Input data preprocessing was concluded by baseline transformation to the median of all samples. After grouping of samples (4 biological replicates each) according to their respective experimental condition, a given probe set had to be expressed above background (i.e., fluorescence signal of that probe set was detected within the 20<sup>th</sup> and 100<sup>th</sup> percentiles of the raw signal distribution of a given array) in all 4 replicates in at least one of the conditions to be further analyzed in pairwise or ANOVA comparisons. Statistical significance was calculated with moderated t tests or

one-way ANOVA. A p-value below 0.05 was considered significant. The GO terms enrichment analysis was performed using the online tool DAVID Bioinformatics Resources 6.8.

### 3 Results

#### 3.1 Experimental setup for the identification of TH-dependent and -independent disruption of oligodendrocyte development

In this study, we combined the assessment of TBBPA's MoA for the development of OLS in a pre-established test method (NPC6) (Bal-Price et al., 2018; Dach et al., 2017) with large-scale gene expression analyses. Figure 1 is a schematic overview illustrating the applied test procedure. Two days prior to the assay, human (hNPCs) and rat (rNPCs) NPCs growing as neurospheres are mechanically passaged to a size of 0.2 mm diameter to ensure equal sphere sizes on the plating day and increase reproducibility. Differentiation is initiated by transfer of 0.3 mm spheres into differ-



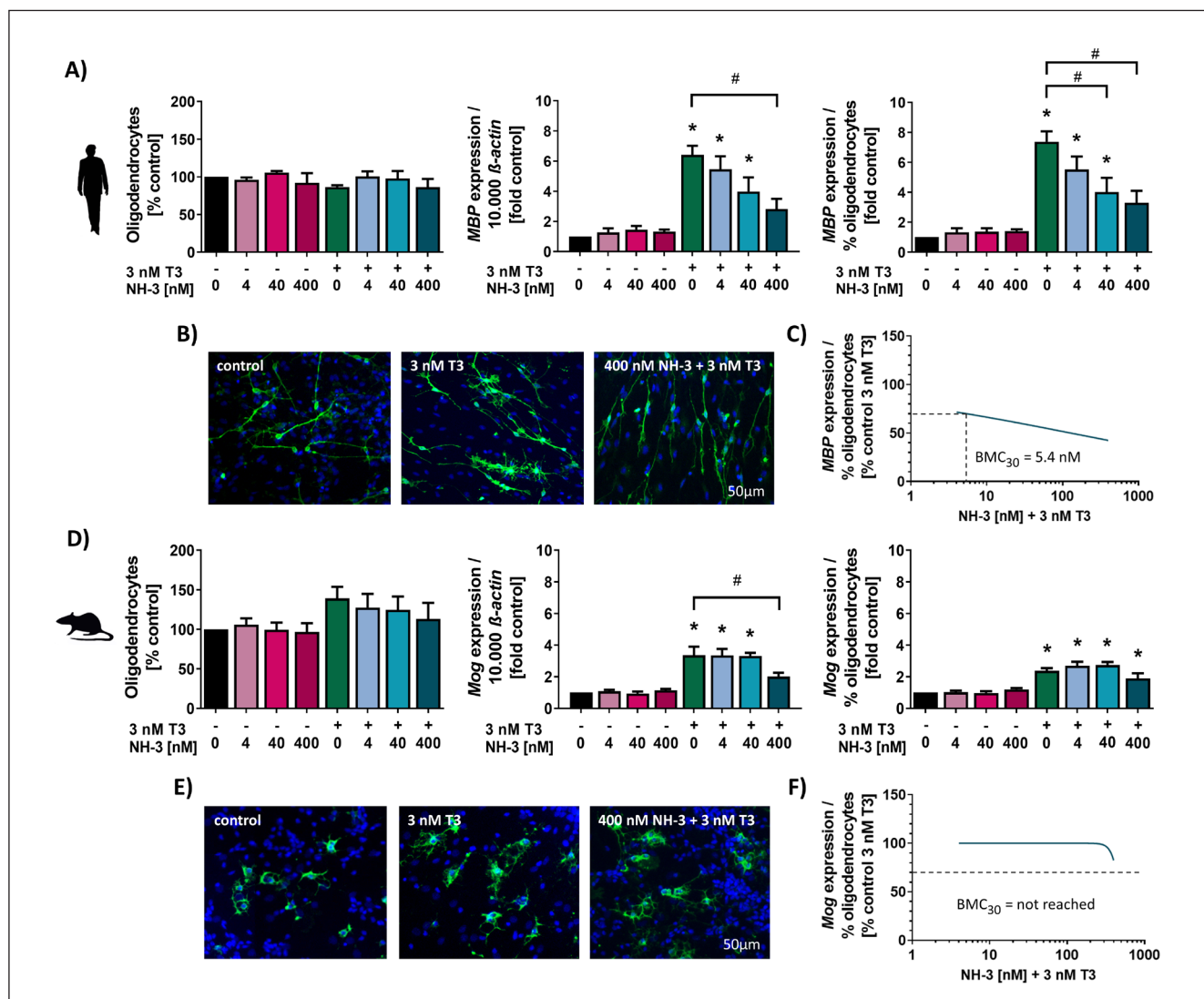
**Fig. 1: Experimental setup of the oligodendrocyte maturation (NPC6) assay**

*MBP*, myelin basic protein; *Mog*, myelin oligodendrocyte glycoprotein; PDL, poly-D-lysine;  $Q_M$ , maturation quotient; qPCR, quantitative real-time PCR; T3, triiodothyronine



entiating medium containing T3 and/or the putative TH disruptor or solvent control. Over the following five days, approximately 5% of NPCs differentiate into O4-positive pre-myelinating OLs (pre-OLs) (Barenys et al., 2017; Schmuck et al., 2017), thereby increasing the expression of *MBP* (hNPCs) or *Mog* (rNPCs). On the fifth day of differentiation, cell viability is measured to exclude that the observed effects on pre-OL numbers or gene

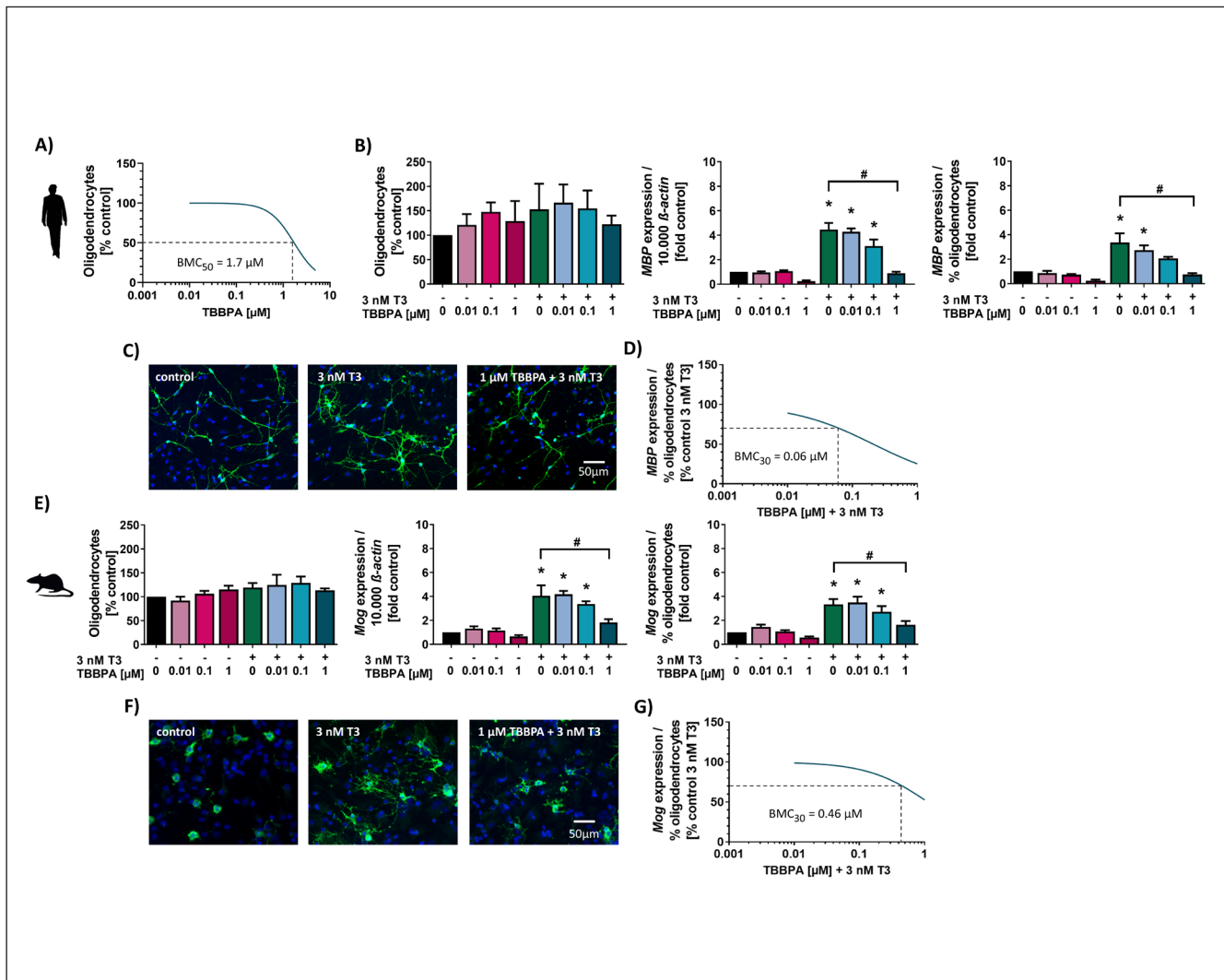
expression have unspecific causes. Furthermore, surface expression of O4 is detected by immunocytochemical staining, and the number of O4<sup>+</sup> cells within the differentiated NPC culture is calculated with automated high-content imaging analysis (HCA) (Schmuck et al., 2017). In parallel, gene expression of *MBP* (hNPCs) or *Mog* (rNPCs) is assessed with quantitative real-time PCR (qRT-PCR). The key feature of the NPC6 assay is



**Fig. 2: Human NPCs are especially sensitive to TH-dependent disruption of OL maturation by the synthetic THR antagonist NH-3** Differentiating hNPCs (A) and rNPCs (D) were treated for 5 days with solvent (DMSO), NH-3 (4, 40, 400 nM), T3 (3 nM), or T3 in combination with increasing NH-3 concentrations. The OL number was defined as the percentage of O4-positive cells within the differentiated culture. *MBP* (hNPCs, A) and *Mog* (rNPCs, D) mRNA expression was assessed via qRT-PCR and normalized to the housekeeping gene *ACTB*. The maturation quotient was defined as *MBP* (hNPCs, A) and *Mog* (rNPCs, D) mRNA expression per percentage OL. #, significant compared to T3 single-treatment. \*, significant compared to the solvent control. Representative pictures of differentiated hNPCs (B) and rNPCs (E) stained for O4 to visualize OLs. The concentration-response relationship of the TH-disruption effects of NH-3 in co-treatment with 3nM T3 was statistically evaluated in hNPCs (C) and rNPCs (F).  $BMC_{30}$  were calculated with the sigmoidal curve fitting and  $BMC_{30}$  calculation model of GraphPad Prism 8. At least three independent experiments (hNPCs  $n = 3$ ; rNPCs  $n = 4$ ) with 5 technical replicates were performed and are represented as mean  $\pm$  SEM. Statistical significance was calculated using two-way ANOVA and Bonferroni's post-hoc tests ( $p < 0.05$  was termed significant). DMSO, dimethyl sulfoxide; *MBP*, myelin basic protein; *Mog*, myelin oligodendrocyte glycoprotein; T3, triiodothyronine

the maturation quotient ( $Q_M$ ), which is defined as the *MBP* (hNPCs) or *Mog* (rNPCs) expression in gene copy numbers per percentage of pre-OLs within the differentiated NPC culture. The  $Q_M$  is a measure for the maturation state of the pre-OLs. T3 exposure increases the  $Q_M$  compared to the solvent control, whereas co-treatment with a TH-disruptor modulates the T3 effect and alters the  $Q_M$  (see Tab. 2).

The NPC6 assay was previously established in human and mouse NPCs (Dach et al., 2017). Here, the protocol was extended to rat neurospheres (Barenys et al., 2017; Baumann et al., 2016; Masjosthusmann et al., 2018, 2019), now enabling the comparison of compound potency between primary human and rat NPCs in the NPC6 assay. Furthermore, transcriptional alterations coinciding with TH-dependent and -independent effects of chemical ex-



**Fig. 3: TBBPA is a disruptor of TH-dependent OL maturation with higher potency in human NPCs**

(A) Concentration-response relationship between the OL number and TBBPA exposure.  $BMC_{50}$  was calculated with the sigmoidal curve fitting model of GraphPad Prism 8. Differentiating hNPCs (B) and rNPCs (E) were treated for 5 days with solvent (DMSO), TBBPA (0.01, 0.1, 1  $\mu$ M), T3 (3 nM), or T3 in combination with increasing TBBPA concentrations. The OL number was defined as the percentage of O4<sup>+</sup> cells within the differentiated culture. *MBP* (hNPCs, B) and *Mog* (rNPCs, E) mRNA expression was assessed via qRT-PCR and normalized to the housekeeping gene *ACTB*. The maturation quotient was defined as *MBP* (hNPCs, B) and *Mog* (rNPCs, E) mRNA expression per percentage of OLs. #, significant compared to the T3 single-treatment. \*, significant compared to solvent control. Representative pictures of differentiated hNPCs (C) and rNPCs (F) stained for O4 to visualize OLs. The concentration-response relationship of the TH-disruption effects of TBBPA in the co-treatment with 3nM T3 was statistically evaluated in hNPCs (D) and rNPCs (G).  $BMC_{30}$  were calculated with the sigmoidal curve fitting model of GraphPad Prism 8. Three independent experiments with 5 technical replicates were performed and represented as mean  $\pm$  SEM. Statistical significance was calculated using two-way ANOVA and Bonferroni's post-hoc tests ( $p < 0.05$  was termed significant). DMSO, dimethyl sulfoxide; *MBP*, myelin basic protein; *Mog*, myelin oligodendrocyte glycoprotein; TBBPA, tetrabromobisphenol A; T3, triiodothyronine



posure were characterized using microarray analyses of NPCs differentiating in the presence of the test compound alone (6 h, 24 h and 60 h) or in combination with 3nM T3 (96 h).

### 3.2 Human NPCs exhibit higher sensitivity to TH-disruption than rat NPCs

To test the performance of the NPC6 assay and study possible species-dependent effects on sensitivity to TH-disruption, a comparative analysis of OL maturation was performed with both human and rat NPCs. NPCs were differentiated for five days in the presence of 3 nM T3, increasing concentrations of the synthetic THR antagonist NH-3, which inhibits TH-dependent OL maturation (Nguyen et al., 2002; Singh et al., 2016), or a combination of both substances (Fig. 2). Cell viability was affected neither by T3, NH-3, nor the combination of both substances (Fig. S1<sup>1</sup>).

In both species, single NH-3 treatment (magenta bars) affected neither the pre-OL number nor the *MBP/Mog* expression or  $Q_M$  values. On the contrary, single T3 treatment (green bars) significantly increased *MBP/Mog* expression and  $Q_M$  values without affecting pre-OL numbers, confirming that T3-mediated THR signaling promotes OL maturation. T3 treatment was further accompanied by a more mature phenotype, since we observed increased branching and O4-expression, as assessed by immunocytochemistry (Fig. 2B,E). When directly comparing  $Q_M$  values of the two species, OL maturation in response to T3 was thrice as pronounced in hNPCs (fold-change = 7.37) compared to rNPCs (fold-change = 2.38; Fig. 2A,D). Co-treatment of 3 nM T3 with increasing NH-3 concentrations decreased the  $Q_M$  value in human but not in rat NPCs in a concentration-dependent manner.

To further quantify the effectiveness of NH-3 as a disruptor of oligodendrocyte maturation in hNPCs and rNPCs, we calculated the  $BMC_{30}$ . An NH-3 concentration of 5.4 nM reduced the  $Q_M$  by 30% in human NPCs, whereas the  $BMC_{30}$  was not yet reached at NH-3 concentrations of 400 nM in rat NPCs (Fig. 2C,F). This observation demonstrates the higher sensitivity of human OLs to TH signaling and disruption.

### 3.3 The flame retardant TBBPA is a potent disruptor of TH-dependent oligodendrocyte maturation

Exposure to the flame retardant TBBPA was previously correlated with altered TH levels in rodents (Cope et al., 2015; Van der Ven et al., 2008) and thyroid dysfunction in humans (Mughal et al., 2018; Coperchini et al., 2017). Therefore, we studied whether TBBPA is a disruptor of TH-dependent OL maturation. Concentration-finding studies revealed that after 5 days, 1.7  $\mu$ M TBBPA specifically reduced the number of O4<sup>+</sup> pre-OLs by 50% (Fig. 3A) without affecting cell viability (Fig. S1A<sup>1</sup>). Therefore, we limited TBBPA exposure in the NPC6 assay to concentrations not significantly affecting pre-OL numbers.

In accordance with our hypothesis, TBBPA concentration-dependently reduced T3-induced OL maturation with significant effects at concentrations of 1  $\mu$ M in both human and rat NPCs (Fig. 3). Similar to NH-3, TBBPA decreased the  $Q_M$  (Fig. 3B,E), the branching, and O4-staining intensity (Fig. 3C,F) of pre-OLs without affecting their numbers. However, we observed significant species differences when calculating the  $BMC_{30}$  of

TBBPA in co-treatment with T3. The  $BMC_{30}$  was almost 8-fold lower in hNPCs (0.06  $\mu$ M) compared to rNPCs (0.46  $\mu$ M), again emphasizing the greater sensitivity of human OLs to TH-disruption (Fig. 3D,G).

We further identified the surfactant perfluorooctanoic acid (PFOA) as a negative substance in the NPC6 assay. PFOA exposure is associated with thyroid dysfunction in humans, but without alterations in TH levels (Lin et al., 2013; Xiao et al., 2020). In accordance with our hypothesis that the NPC6 assay detects TH-disruption at the level of THR-mediated transcription, PFOA exposure had no effect on TH-dependent OL maturation. We observed neither alterations in the  $Q_M$  values (Fig. 4A,D) nor effects on the pre-OL morphology (Fig. 4B,E) in human or rat NPCs treated with PFOA in addition to 3 nM T3. Therefore, no  $BMC_{30}$  was calculable (Fig. 4C,F). Neither TBBPA nor PFOA significantly altered NPC viability (Fig. S1B,C<sup>1</sup>).

We identified TBBPA, but not PFOA, as a disruptor of TH-dependent oligodendrocyte maturation with a higher potency in human cells. Furthermore, the results corroborate our hypothesis that the NPC6 assay is specific in identifying TH disruption based on impaired THR-mediated transcriptional regulation.

### 3.4 TBBPA disrupts TH-dependent oligodendrocyte maturation by interfering with the transcription of THR-regulated genes

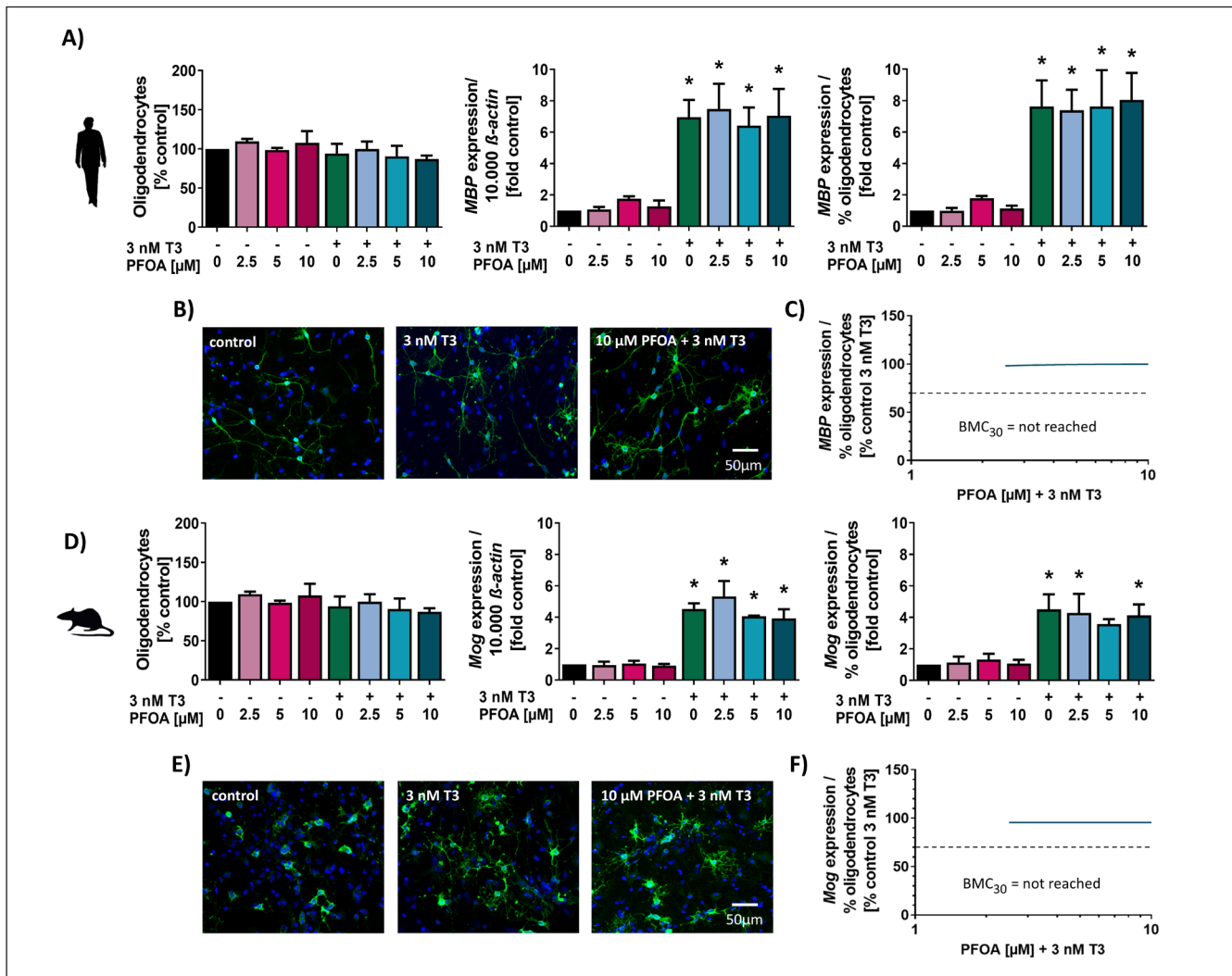
Since we identified TBBPA as an endocrine disruptor in the NPC6 assay, we hypothesized that altered transcription of TH-responsive genes evokes the impaired OL maturation. Microarray analysis of human NPCs differentiated for 96 h in the presence of 3 nM T3, 0.1  $\mu$ M or 1  $\mu$ M TBBPA, or a combination of T3 and TBBPA should reveal the most strongly regulated genes responsible for the phenotypic oligodendrocyte outcome.

Principle component analysis (PCA) indicated the highest transcriptional variation in cells treated with 3 nM T3 compared to the solvent control (dark green, Fig. 5A). Smaller variations were caused by 1  $\mu$ M TBBPA single treatment (purple). Co-treatment with 3 nM T3 and 1  $\mu$ M TBBPA (yellow) partially reversed the transcriptional changes induced by T3. Consistent with the phenotypic findings (Fig. 3), single and co-exposure with 0.1  $\mu$ M TBBPA changed the transcriptomes only marginally. Comparing the PCA plot with the numbers of differentially regulated genes (fold change (FC)  $\pm$  1.4,  $p \leq 0.05$ ; Fig. 5B), 1  $\mu$ M TBBPA (#1831) regulates more genes than 3 nM T3 (#555). However, the PCA shows that the degree of gene regulation is much higher in T3- than in TBBPA-treated hNPCs.

Looking at T3-regulated transcripts affected by TBBPA (increased cut-off stringency of  $FC \pm 2.0$ ,  $p \leq 0.05$ ), we identified 31 gene products as significantly deregulated (Fig. 5C). Additionally, we added the expression analysis of iodothyronine deiodinase 3 (*DIO3*) and Krüppel like factor 9 (*KLF9*), since we previously identified both genes to be strongly T3-dependent (Dach et al., 2017). Of these 33 genes, 23% are related to glia and oligodendrocyte development and 13% are reported to be TH-responsive genes.

Differentiation of hNPCs under T3 exposure induced expression of the TH-responsive genes chromodomain helicase DNA



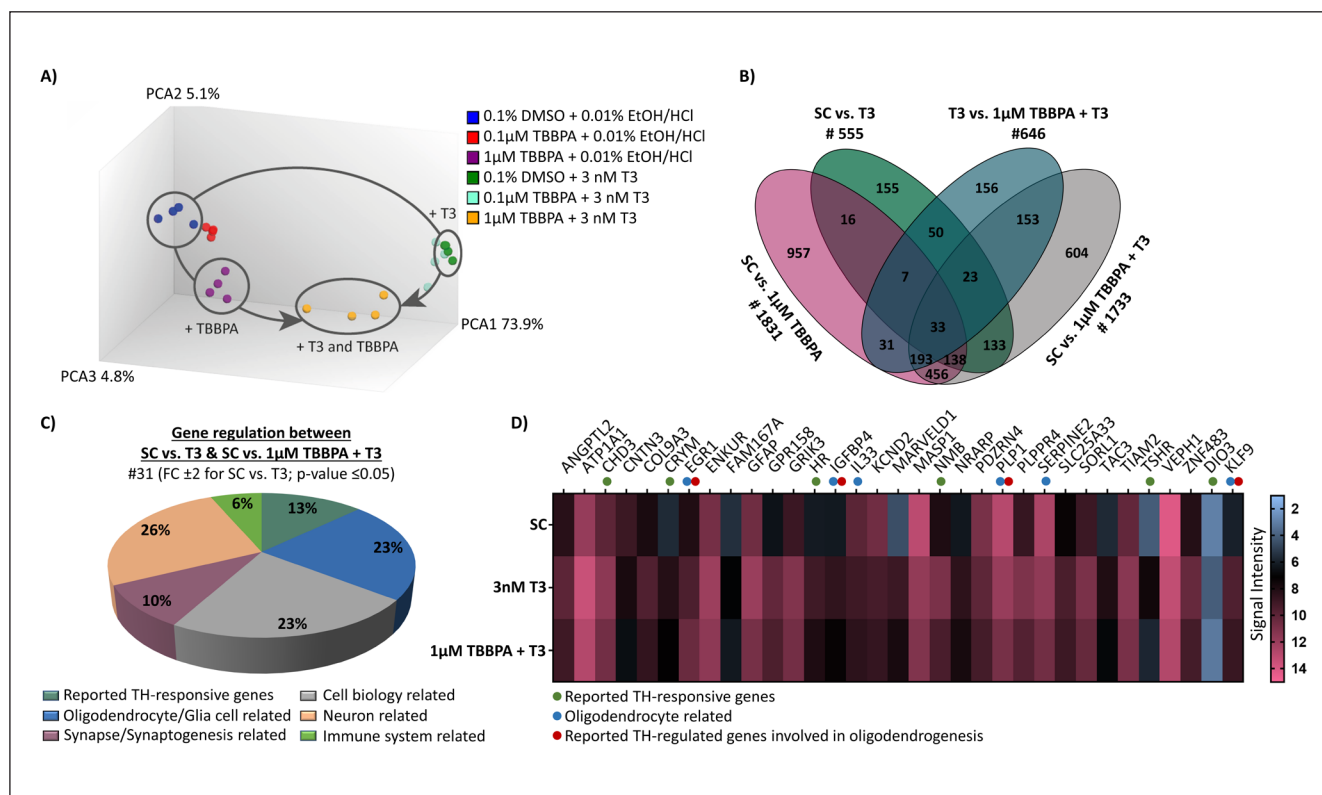


**Fig. 4: PFOA is not a disruptor of TH-dependent OL maturation**

Differentiating hNPCs (A) and rNPCs (D) were treated for 5 days with solvent (DMSO), PFOA (2.5, 5, 10  $\mu$ M), T3 (3 nM), or T3 in combination with increasing PFOA concentrations. The oligodendrocyte (OL) number was defined as the percentage of O4<sup>+</sup> cells within the differentiated culture. *MBP* (hNPCs, A) and *Mog* (rNPCs, D) mRNA expression was assessed via qRT-PCR and normalized to the housekeeping gene *ACTB*. The maturation quotient was defined as *MBP* (hNPCs, A) and *Mog* (rNPCs, D) mRNA expression per percentage of OLs. #, significant compared to T3 single-treatment. \*, significant compared to solvent control. Representative pictures of differentiated hNPCs (B) and rNPCs (E) stained for O4 to visualize OLs. The concentration-response relationship of the TH-disruption effects of PFOA in the co-treatment with 3nM T3 was statistically evaluated in hNPCs (C) and rNPCs (F). BMC<sub>30</sub> were calculated with the sigmoidal curve fitting model of GraphPad Prism 8. Three independent experiments with 5 technical replicates were performed and are represented as mean  $\pm$  SEM. Statistical significance was calculated using two-way ANOVA and Bonferroni's post-hoc tests ( $p < 0.05$  was termed significant). DMSO, dimethyl sulfoxide; *MBP*, myelin basic protein; *Mog*, myelin oligodendrocyte glycoprotein; PFOA, perfluorooctanoic acid; T3, triiodothyronine

binding protein 3 (*CHD3*), crystallin Mu (*CRYM*), HR lysine demethylase and nuclear receptor corepressor (*HR*), neuromedin B (*NMB*), thyroid stimulating hormone receptor (*TSHR*), *KLF9*, and *DIO3*, emphasizing the successful induction of THR signaling by T3 (Fig. 5D). As expected from a THR antagonist, 1  $\mu$ M TBBPA co-exposure reduced transcription of all mentioned TH-responsive genes. Furthermore, TBBPA co-exposure altered

the T3-regulated expression of six genes reportedly involved in oligodendrocyte development (early growth response 1 (*EGRI*), insulin like growth factor binding protein 4 (*IGFBP4*), interleukin 33 (*IL33*), proteolipid protein 1 (*PLP1*), serpin family E member 2 (*SERPINE2*), and *KLF9*). *EGRI/Krox-24* is expressed in OPCs, however, down-regulation is critical for maturation and inversely correlated with *MBP* expression (Sock et al., 1997; To-



**Fig. 5: Transcriptomic profiling of differentiated hNPCs reveals large-scale dysregulation of TH-responsive genes by TBBPA**  
 Differential gene expression between hNPCs exposed to solvent (DMSO), TBBPA (0.1, 1  $\mu$ M), T3 (3 nM), or TBBPA in combination with T3 was statistically determined using one-way ANOVA analyses followed by Tukey's range tests. Genes with  $p \leq 0.05$  and fold change  $\geq 1.4$  were termed differentially expressed (DEX). (A) Principal component analysis (PCA) was performed based on the expression of significantly regulated ( $p \leq 0.05$ ) genes that shared the same gene symbol between the above-mentioned exposure conditions. (B) Overlap of the number of DEX genes regulated by TBBPA (SC vs. 1  $\mu$ M TBBPA, #1831), by T3 (SC vs. T3, #555), regulated T3-dependently by TBBPA (T3 vs. 1  $\mu$ M TBBPA + T3, #646), and regulated by co-exposure with TBBPA and T3 (SC vs. 1  $\mu$ M TBBPA + T3, #1733). (C) Genes differentially regulated between SC vs. T3 and SC vs. T3 + 1  $\mu$ M TBBPA with an increased cut-off stringency of FC  $\pm$  2.0 and  $p \leq 0.05$  (#31). The numbers in the pie chart represent the percentage of genes assigned to each superordinate process. (D) Expression profile of T3-responsive genes (FC  $\pm$  2.0 and  $p \leq 0.05$ ) significantly regulated by co-exposure with TBBPA and T3. The absolute signal intensity of the 31 genes identified in (C), plus *DIO3* and *KLF9* as reportedly T3-responsive genes (Dach et al., 2017), was compared between hNPCs exposed to SC, T3 alone, and T3 in combination with 1  $\mu$ M TBBPA. Genes are highlighted as reportedly regulated by T3 (green dots), related to oligodendrogenesis (blue dots), or associated with TH-dependent regulation of oligodendrogenesis (red dots). DMSO, dimethyl sulfoxide; SC, solvent control; TBBPA, tetrabromobisphenol A; T3, triiodothyronine

pilko et al., 1997). *EGR1* expression was increased almost 2-fold in the co-treatment compared to the T3 single treatment, indicating that increased *EGR1* expression might prevent OPC maturation. We further detected that TBBPA co-exposure decreases expression of OL markers *IGFBP4* (Mewar and McMorris, 1997), *IL33* (Sung et al., 2019), *PLP1*, *SERPINE2/Nexin-1* (Blasi et al., 2002), and *KLF9* (Denver and Williamson, 2009) compared to single T3 treatment, suggesting that TBBPA disturbs the transcriptome profile necessary for proper OL development. For *EGR1*, *IGFBP4*, *PLP1*, and *KLF9*, TH-dependent transcription has already been reported, while *IL33* and *SERPINE2* were newly identified in this study.

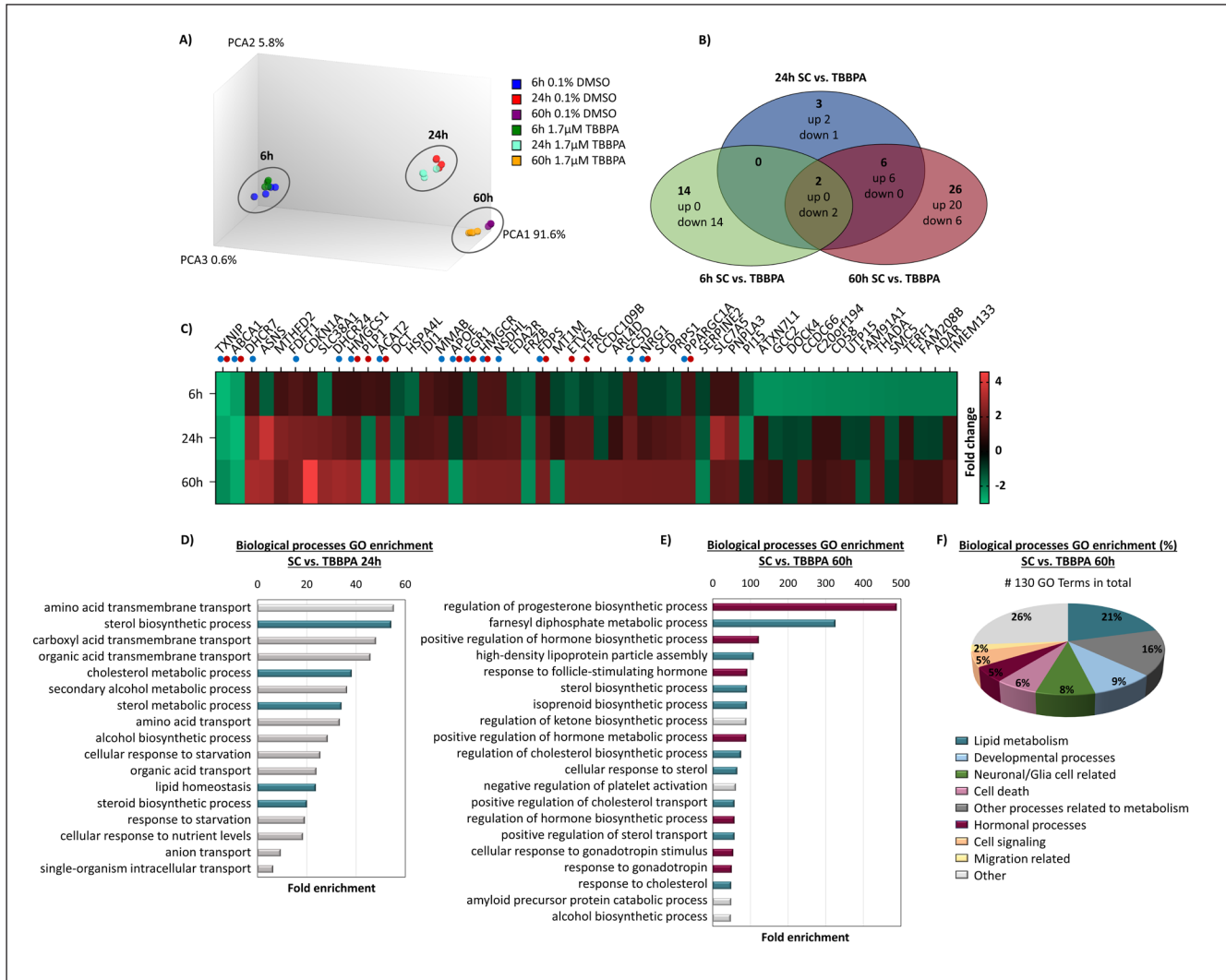
These data indicate that TBBPA disrupts OPC maturation by interfering with the transcription of TH-regulated genes.

### 3.5 TBBPA exposure disrupts oligodendrogenesis by interfering with cholesterol metabolism

Single exposure to TBBPA also affected oligodendrogenesis (BMC<sub>50</sub> 1.7  $\mu$ M TBBPA), yet with a TH-independent MoA, as no TH was present in the cultures during the differentiation process (Fig. 3A). To further characterize the underlying mechanisms, we performed microarray analyses of hNPCs differentiated for 6, 24, or 60 h under exposure to either 1.7  $\mu$ M TBBPA or vehicle (DMSO).

Similar to observations in our previous study (Masjosthusmann et al., 2018), the PCA revealed that the highest variability in gene expression (PC1, 91.6% variation) is found over the time course of differentiation (Fig. 6A). More precisely, the 6 h samples cluster further from the 24 h samples than the 24 h from the 60 h sam-





**Fig. 6: TBBPA deregulates a gene cluster involved in cholesterol metabolism independently of TH-signaling**

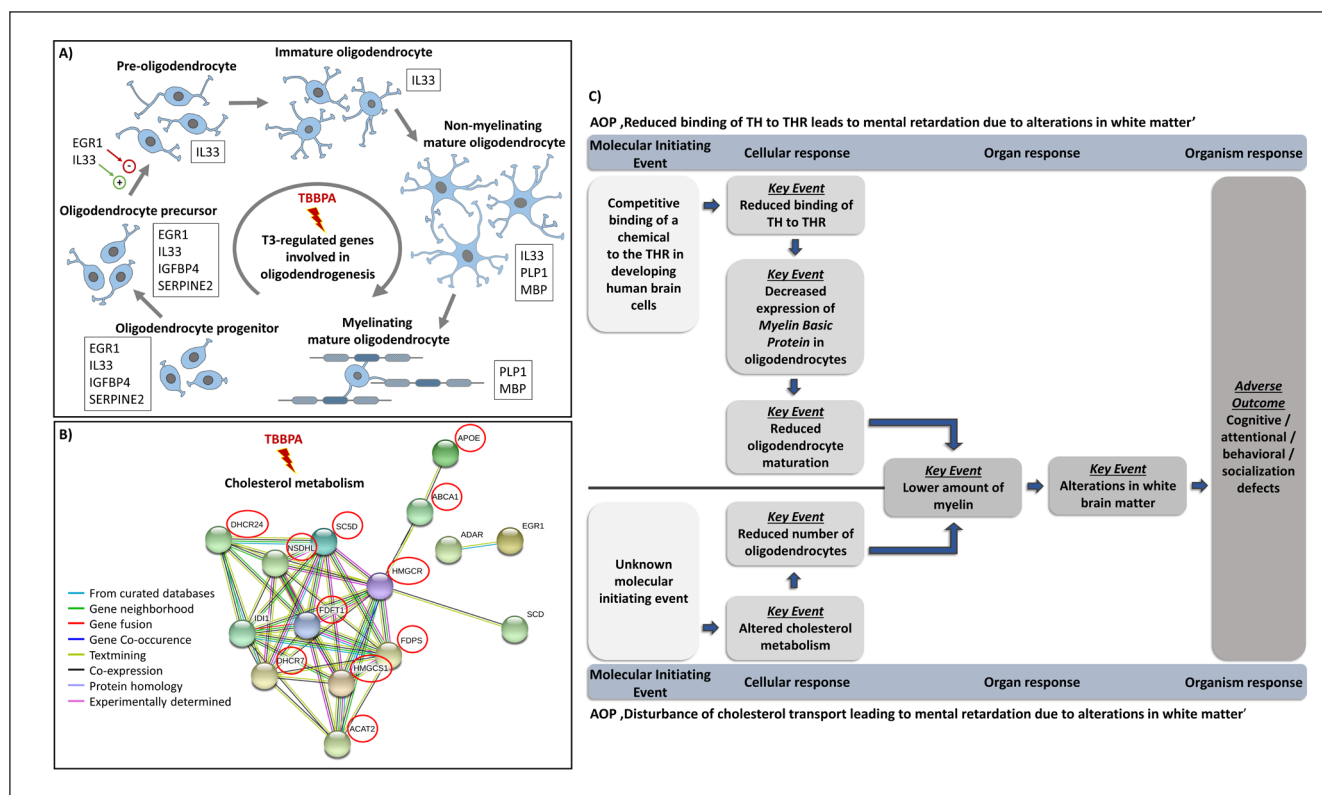
Differential gene expression between hNPCs exposed to solvent (DMSO) or TBBPA (0.1, 1  $\mu$ M) over the time course (6, 24, and 60 h) of differentiation was statistically determined using one-way ANOVA followed by Tukey's range tests. Genes with  $p \leq 0.01$  and fold change  $\geq 2$  were termed differentially expressed (DEX). (A) PCA was performed based on the expression of significantly regulated ( $p \leq 0.01$ ) genes between the above-mentioned exposure conditions. (B) Overlap of the number of DEX genes regulated by 1  $\mu$ M TBBPA over the time course of 6 h (6 h SC vs. 1  $\mu$ M TBBPA, #16), 24 h (24 h SC vs. 1  $\mu$ M TBBPA, #11), and 60 h (60 h SC vs. 1  $\mu$ M TBBPA, #34) of hNPC differentiation. (C) Expression profile of differentially regulated genes (fold-change) between SC and 1  $\mu$ M TBBPA over the time course (6, 24, and 60 h) of hNPC differentiation. (D+E) Overrepresented gene ontology (GO) terms for 24 h (D) and 60 h (E) differentiation of hNPC under 1  $\mu$ M TBBPA exposure. GO enrichment analysis was performed using the online tool DAVID Bioinformatics Resources 6.8. (F) All overrepresented GO terms were sorted by their fold enrichment; GO terms with highest fold-enrichment are displayed. The GO terms after 60 h of differentiation were further assigned to 9 superordinate processes based on expert judgment. Numbers in the pie chart represent the percentage of GO terms assigned to each superordinate process. DMSO, dimethyl sulfoxide; SC, solvent control; TBBPA, tetrabromobisphenol A; T3, triiodothyronine

ples, indicating that the majority of transcriptomic changes takes place within the first day of differentiation compared to smaller changes during later maturation processes.

The PCA further shows that less variation was caused by TBBPA exposure, however, with progressing differentiation, time differences between DMSO and 1.7  $\mu$ M TBBPA samples in-

creased. To be exact, TBBPA exposure significantly ( $p \leq 0.01$ , fold-change  $\geq 2$ ) regulated gene expression after 6 h (16 genes), 24 h (11 genes), and 60 h (34 genes) of NPC differentiation (Fig. 6B).

Only two genes were regulated by TBBPA throughout the whole differentiation process: Expression of *TXNIP* (thioredoxin interacting protein) and the cholesterol exporter *ABCA1*



**Fig. 7: Putative schematic AOPs for the converging key events in OL development disrupted by TBBPA**

(A) Genes reportedly involved in oligodendrogenesis that are TH-dependently regulated by  $1 \mu\text{M}$  TBBPA. (B) Gene-gene interaction network analysis of the genes regulated TH-independently by  $1.7 \mu\text{M}$  TBBPA shows involvement of cholesterol metabolism. (C) The putative “Thyroid Hormone Disruption AOP” includes the TH-dependent disruption of OL maturation as a central key event. The “Altered Cholesterol Metabolism AOP” comprises reduced OL numbers due to TH-independent dysregulation of cholesterol metabolism as a key event. Both AOPs converge in the common key event “lower amount of myelin” resulting in white matter alterations and adverse outcomes in the developing brain.

(ATP-binding cassette (ABC) subfamily-A transporter 1) were reduced by TBBPA exposure after 6 h, 24 h, and 60 h of differentiation (Fig. 6C). Yet, of the 51 differentially expressed genes, we identified 16 (31%) to be involved in cholesterol metabolism (blue dot, Fig. 6C). For 10 of these genes, a correlation with OL differentiation or myelination has already been described (blue and red dots, Fig. 6C).

In accordance with that, gene ontology enrichment analysis revealed a high proportion of GO terms involved in cholesterol metabolism (blue) after 24 h (Fig. 6D) and 60 h (Fig. 6E,F) TBBPA exposure. Therefore, we postulate that interference of TBBPA with cholesterol metabolism is a second, TH-independent MoA for disruption of oligodendrogenesis. How TBBPA interferes with genes involved in cholesterol metabolism, i.e., the molecular initiating event (MIE), remains elusive.

### 3.6 Two putative AOPs for the disruption of OL development converge in hypomyelination

Combining the NPC6 assay with microarray analysis, we identified two putative MoA by which TBBPA interferes with OL development. The first involves TH disruption, most likely via dis-

placing T3 from the THR and dysregulation of THR-dependent transcription (Fig. 7A). Here we hypothesize that dysregulation of genes necessary for OL maturation, such as *EGR1/Krox-24*, *IL-33*, and *KLF-9*, cause the less mature state we observed in pre-OLs differentiated in the presence of  $1 \mu\text{M}$  TBBPA. The second MoA involves the dysregulation of a whole gene expression network involved in cholesterol metabolism (Fig. 7B). Since effective cholesterol synthesis and clearance is a prerequisite for OPC survival, TBBPA exposure might reduce pre-OL numbers by interfering with early stages of OL development.

These observations lead us to the drafting of two converging putative adverse outcome pathways (AOPs) depicted in Figure 7C. The “Thyroid Hormone Disruption AOP” starts with the competitive binding of a chemical to the THR (MIE), which deregulates genes necessary for OL maturation and thus reduces the maturation state of the pre-OLs. The “Altered Cholesterol Metabolism AOP” starts with an, until now, unknown MIE, which leads to the dysregulation of genes involved in cholesterol metabolism. The disturbed cholesterol homeostasis impairs the survival of OPCs, thereby reducing the number of pre-OLs. Finally, both AOPs converge in a key event (KE) during brain develop-

ment where fewer myelin-producing OLs are present. This causes alterations in the white matter, leading to adverse outcomes such as cognitive, attentional, behavioral, and social deficits in the developing child.

#### 4 Discussion

Oligodendrocytes are indispensable for normal brain development and function (Barateiro et al., 2016). Hence, disturbed oligodendrogenesis and resulting hypomyelination cause a functional adverse outcome on brain performance, manifesting in neurological disorders such as AHDS (Sarret et al., 1993) and periventricular leukomalacia (PVL) (Back et al., 2001). Since the oligodendrocyte population established in childhood remains remarkably stable in humans, neurodevelopmental interference in oligodendrogenesis is especially problematic (Yeung et al., 2014). Oligodendrogenesis is regulated through a variety of hormonal, transcriptional and biosynthetic processes, creating various routes of interference for environmental toxicants. Since OL development begins during fetal development and continues throughout the first two years of life, exposure of pregnant women and children to compounds interfering with OL development has a high potential for causing an adverse outcome for brain development.

In the present study, we identified the flame retardant TBBPA as a potent disruptor of oligodendrogenesis. TBBPA is intensively used in the manufacturing of consumer products and therefore reported as a ubiquitous environmental and indoor contaminant (Matsukami et al., 2015; Ni and Zeng, 2013; Yang et al., 2012). It was detected with high frequency in maternal serum, cord blood serum, and breast milk samples (Abdallah and Harrad, 2011; Cariou et al., 2008; Kim and Oh, 2014) with average contamination levels in breast milk increasing steadily over the years (Shi et al., 2017). In adults, the bioavailability of TBBPA is relatively low since it is efficiently metabolized and excreted (Schauer et al., 2006). Measurements in cord blood, however, show its presence in the fetal circulation. Since the gastrointestinal tract and the metabolic capacity of fetal and infant liver are not fully developed (Veereman-Wauters, 1996; Coughtrie et al., 1988), TBBPA exposure results in bioaccumulation in the developing child *in utero* (Cariou et al., 2008; Kim and Oh, 2014).

TBBPA has frequently been discussed concerning its potency as an endocrine disruptor, especially of the TH system (Mughal et al., 2018; Coperchini et al., 2017). TBBPA impeded the binding of T3 to the THR (Kitamura et al., 2002, 2005) and enhanced the proliferation of the rat pituitary reporter cell line GH-3 *in vitro* (Kitamura et al., 2002; Hamers et al., 2006). Since thyroid hormones are indispensable for fetal development (Patel et al., 2011; de Escobar et al., 2004), TBBPA-mediated TH disruption has been studied under a developmental context. *In vivo* studies in *Danio rerio* (zebrafish) (Zhu et al., 2018; Parsons et al., 2019) and *Xenopus laevis* (Wang et al., 2017; Zhang et al., 2014) showed that developmental exposure to TBBPA reduced expression of THR-regulated genes (*THRB* and *DIO3*) and inhibited T3-induced morphological changes in the nanomolar range. Moreover,

reproductive toxicity studies in rats revealed altered serum T3 concentrations (Saegusa et al., 2009; Van der Ven et al., 2008) and decreased circulating T4 (Cope et al., 2015; Van der Ven et al., 2008) after developmental exposure of the offspring. Yet, so far, the adverse effects of TBBPA on human TH-dependent neurodevelopment have been enigmatic. Here we report for the first time that TBBPA effectively disturbs T3-mediated THR signaling in developing primary human NPCs by i) altering their TH-dependent gene expression and ii) by antagonizing TH-mediated OL maturation.

T3 exposure regulated several genes during hNPC development in our study. These included genes that were previously reported to be TH-regulated and to contribute to oligodendrogenesis, i.e., *KLF9*, *PLP1*, *IGFBP4* and *EGR1*, as well as genes that were newly identified as T3-regulated here (*IL33* and *SERPINE2*). The transcription factor *KLF9*, for example, is induced in the mouse hippocampus and cerebellum (Denver and Williamson, 2009), rat cortex, and the zebrafish embryo (Walter et al., 2019) during development. In addition, T3 induces *KLF9* expression in rat OPCs *in vitro* (Dugas et al., 2012), suggesting a role in oligodendrogenesis and/or myelin production. This is supported by *in vivo* studies reporting that *KLF9* is necessary for T3-induced zebrafish OL maturation and *MBP/Mog* expression (Dugas et al., 2012). In contrast, *KLF9*<sup>-/-</sup> mice do not show delayed OL differentiation but delayed myelin regeneration in the cortex and the corpus callosum (Dugas et al., 2012). However, since TH-dependent OL differentiation and maturation are regulated in a species-specific way (Dach et al., 2017), this is not surprising. Here we show that co-exposure of developing human NPC with T3/TBBPA antagonizes T3-induced *KLF9* expression, supporting the phenotypic observation that TBBPA decreases T3-dependent human OL maturation. Whether the TBBPA-antagonized T3-dependent *MBP* expression in hNPCs happens directly or is mediated through *KLF9* is not yet known.

Besides impaired *KLF9* signaling, the increased *EGR1/Krox-24* expression we detected upon T3/TBBPA co-exposure might also contribute to the disturbed OL maturation since down-regulation of *EGR1* is critical for OPC differentiation into a mature myelinating state (Sock et al., 1997; Topilko et al., 1997) and coincides with increased *MBP* expression during OL development in rats (Sock et al., 1997).

In contrast to the negative regulation of *EGR1*, up-regulation of *IL33* is necessary for OL lineage progression (Sung et al., 2019). In this study, *IL33* expression is reduced by T3 and further down-regulated upon T3/TBBPA co-exposure, indicating its involvement in decelerated OL maturation. Of note, mice lacking *IL33* exhibit several behavioral deficits (Dohi et al., 2017). Besides markers regulating OL lineage progression, co-exposure with TBBPA further reduced the expression of T3-impaired *PLP1*, the main component of myelin produced by mature OLs.

Consistent with our observations, transcriptomic analyses of TBBPA-exposed zebrafish embryos identified oligodendrocyte development as the most sensitive GO term (Chen et al., 2016) and confirmed suppression of *MBP* (Zhu et al., 2018). Of note, TREs are present within the promoters of *KLF9* (Denver and Williamson, 2009), *EGR1* (Ghorbel et al., 1999), and *MBP* (Far-



setti et al., 1992), suggesting that the observed TBBPA-effect is at least to some extent dependent on TH disruption on the receptor level.

While most studies report TBBPA as a strong T3-antagonist, also agonistic effects were previously reported in *in vitro* studies (Hamers et al., 2006; Kitamura et al., 2002). Why TBBPA in this study produces TH-antagonistic and -mimetic effects on TH-regulated genes in the same cell system remains puzzling. In summary, these data strongly support the notion that TBBPA interferes with TH signaling of primary human NPC.

On a cellular level, we demonstrate that TBBPA acts as a THR antagonist by reducing the T3-dependent maturation of human OL *in vitro*. Disruption of THR signaling has been reported to impair oligodendrogenesis, leading to adverse outcomes in brain development (Baas et al., 1997; Billon et al., 2002). In accordance, OL dysfunction causes diverse behavioral and cognitive deficits (Kawamura et al., 2020; Back et al., 2001).

That TBBPA exposure impairs normal brain function through interference with neurodevelopmental processes was reported in *in vivo* studies earlier. Developmental TBBPA exposure of rodents increased anxiety-related behavior (Rock et al., 2019), reduced the sociability (Kim et al., 2015) and impaired the auditory response (Lilienthal et al., 2008). Moreover, TBBPA concentrations in the nanomolar range caused hypoactivity in zebrafish embryos both dependent on (Zhu et al., 2018) and independent of (Noyes et al., 2015) TH-signaling. We therefore hypothesize that TBBPA causes behavioral and cognitive defects at least in part via disruption of TH-dependent OL maturation.

By comparative testing in human and rat NPCs, we elucidated species differences in sensitivity to TH-disruption. Human NPCs were more sensitive to T3-dependent disruption of OL maturation both by the synthetic THR antagonist NH-3 ( $BMC_{30} = 5.4$  nM in hNPCs, not reached in rNPCs) and the flame retardant TBBPA (7.7-fold lower in hNPCs). This clearly illustrates the need for test systems based on human cells in order to achieve adequate predictivity of hazard for humans.

TBBPA accumulated in the mouse striatum at acute exposure doses as low as 0.1 mg/kg/d to measured brain concentrations of 0.1 nM, which caused anxiety-related behavioral effects (Nakajima et al., 2009). Moreover, behavioral studies in zebrafish detected hypoactivity after developmental exposure to 6.4 nM TBBPA (Noyes et al., 2015), and studies in xenopus revealed efficient disruption of TH-induced morphological changes after exposure of tadpoles to 10 nM TBBPA (Zhang et al., 2014; Wang et al., 2017). These *in vivo* doses are below the range of the TH-disrupting effect of TBBPA observed in this study. However, it is difficult to compare a compound's tissue levels with nominal medium concentrations. For a direct comparison of *in vivo* with *in vitro* potency, IVIVE (*in vitro-in vivo* extrapolation) has to be performed (Wetmore et al., 2012; Bell et al., 2017).

Human exposure studies measured TBBPA concentrations of up to 3.02 nM in breast milk, leading to an estimated daily intake of up to 1.314  $\mu$ g TBBPA by breast feeding alone. Additionally, the combined exposure of the infant to TBBPA via breast milk and house dust has to be considered (Malliari and Kalantzi, 2017). Amongst the highest reported TBBPA exposure levels are house

dust samples from Japanese homes with 490-520 ng TBBPA per gram dust (Takigami et al., 2009). Furthermore, the frequent exposure to mixtures of several persistent organic pollutants may potentiate adverse effects (Lenters et al., 2019; Braun et al., 2020).

In conclusion, the increased sensitivity of human compared to rodent neurodevelopment, together with the developmental adverse effects upon nanomolar exposure observed in *in vivo* studies, indicate a potential hazard of TBBPA in the neurodevelopmental context. Kinetic evaluation including IVIVE, physiologically-based toxicokinetic (PBTK) modeling, and biokinetics of intracellular TBBPA distribution within the culture systems are needed for a more precise risk characterization. Since the sex evidently affects oligodendrocyte development (Yasuda et al., 2020) and the exposure response to TH disrupting chemicals (Leonetti et al., 2016; Przybyla et al., 2018), the use of exclusively male hNPCs is a limitation of this study. By integrating female hNPCs into the NPC6 assay in the future, we will be able to detect both sex- and species-specific effects.

Besides its action as an endocrine disruptor, we observed that TBBPA reduces the number of pre-OLs independent of TH-disruption at similar concentrations. Upon single TBBPA exposure, we observed several gene products for enzymes of cholesterol biosynthesis (7-dehydrocholesterol reductase (*DHCR7*), 24-dehydrocholesterol reductase (*DHCR24*), 3-hydroxy-3-methylglutaryl-CoA reductase (*HMGCR*), farnesyl-diphosphate farnesyltransferase 1 (*FDFT1*), farnesyl diphosphate synthase (*FDPS*)) being upregulated (Fig. 6), including the mRNA for the rate-limiting enzyme hydroxymethylglutaryl-CoA synthase (*HMGCS1*).

The high rate of cholesterol utilization in myelin-producing OLs (Norton and Poduslo, 1973) emphasizes the necessity to tightly regulate cholesterol homeostasis, since both insufficient and excessive cholesterol levels are associated with brain pathologies. Under physiological conditions, excessive intracellular cholesterol is bound by the main cholesterol transport protein apoE and exported out of the cell by ABCA1. However, TBBPA significantly reduced the gene expression of apoE (*APOE*) and *ABCA1* in differentiating hNPCs (Fig. 6). This suggests that cholesterol is less efficiently transported by apoE and ABCA1, causing a positive feedback to cholesterol biosynthesis with subsequent accumulation in the developing OLs.

The importance of cholesterol clearance is elucidated by studies on ABCA1- and apoE-knockout mice. Disturbed cholesterol export in ABCA1<sup>-/-</sup> mice reduced the proliferation and survival of OPCs and impaired myelination in the corpus callosum (Wang et al., 2018), whereas increased apoptosis of OLs was detected in apoE<sup>-/-</sup> mice (Cheng et al., 2018). Moreover, knockdown of apoE in neural stem cells (NSCs) dramatically decreased the number of O4<sup>+</sup> OLs, a phenotype that was efficiently rescued by apoE protein administration (Gan et al., 2011). The importance of cholesterol transport and export for OL survival is further elucidated by several studies reporting that induced expression or administration of ABCA1 and apoE increases OPC numbers (Cui et al., 2017; Safina et al., 2016; Wang et al., 2018), improves myelination (Zhou et al., 2019; Stoll et al., 1989), and enhances cholesterol efflux (Nelissen et al., 2012). Furthermore, apoE<sup>-/-</sup> mice



fed with a high-cholesterol diet exhibit lipotoxicity as a result of impaired cholesterol clearance (Aung et al., 2016). Lipotoxicity was also correlated with accumulation of biosynthetic precursors and break-down products in oligodendrocytes (Haq et al., 2003; Bezine et al., 2017). Hence, we propose that TBBPA, independent of TH-disruption, decreases the number of pre-OLs by interfering with cholesterol homeostasis. Further studies are needed to elucidate how exactly TBBPA deregulates THR-independent gene expression.

Since OLs represent only approximately 5% of the total differentiated hNPC culture, possible effects of TBBPA on the other cell types (NSCs, radial glia, astrocytes, and neurons) cannot be neglected. Therefore, as part of a comprehensive study on 15 widely used flame retardants (Klose et al., manuscript in preparation) we screened TBBPA in our established hNPC-based developmental neurotoxicity (DNT) battery with NPC proliferation and viability, radial glia migration, oligodendrocyte differentiation and migration, as well as neuronal differentiation and migration as phenotypical readouts (Nimtzt et al., 2019). Strikingly, we identified impaired OL differentiation/number as the most sensitive DNT effect caused by TBBPA exposure across all studied endpoints. TBBPA impairs rat neural stem cell ( $> 25 \mu\text{M}$ ; Cho et al., 2020) and human embryonic stem cell-derived neural stem cell ( $> 100 \mu\text{M}$ ; Liang et al., 2019) survival at concentrations we did not test (Klose et al., manuscript in preparation) as they are most likely not relevant for human exposure. Proper regulation of cholesterol homeostasis is crucial for neurons and astrocytes (Pfrieger and Ungerer, 2011), and disturbances are associated with disease (Valenza et al., 2015). Neither neuronal differentiation nor migration were specifically affected by up to  $20 \mu\text{M}$  TBBPA treatment (Klose et al., manuscript in preparation), indicating that these processes are less sensitive towards cholesterol homeostasis disturbances than cells of the OL lineage.

However, transcriptional changes displayed by the microarray analyses of the mixed culture could originate from other cell types besides OLs. For example, *KLF9* and *EGR1*, are crucial for neuronal maturation and synaptic plasticity, respectively (Scobie et al., 2009; Duclot and Kabbaj, 2017). These endpoints are not reflected in this neurosphere *in vitro* system due to their later stage nature, supporting the concept that it is crucial that not only the different cell types but also a variety of neurodevelopmental processes reflecting distinct developmental timing are reflected in DNT *in vitro* assessment. Concerning astrocytes, we cannot exclude effects on this cell type since they are not yet covered by the hNPC DNT battery.

Interruption of cholesterol biosynthesis in a DNT context was recently studied in a ToxCast™ chemical library screening effort using mouse neuroblastoma Neuro-2a cells with subsequent validation in human induced pluripotent stem cell (hiPSC)-derived NPCs (Wages et al., 2020). TBBPA did not present itself as one of the lead-hits, possibly due to cell type-specific effects, since OLs were not included in the ToxCast™ study, yet seem to be the most sensitive cells in the neurosphere mixed culture for this MoA (data not shown). Studying the lead-hits for disturbance of cholesterol synthesis identified by Wages et al. (2020) in NPC assays (Bal-Price et al., 2018) might shed light on the cell

types most sensitive for this MoA. This instance demonstrates that DNT MoA can be cell type-specific. When *in vitro* assays are used for DNT hazard assessment, a broad variety of brain cell types and neurodevelopmental processes should be used to identify the largest variety of MoA and reduce uncertainty, especially of negative results.

These two identified MoA for disturbance of oligodendrocyte development, i.e., TH-disruption and disturbance of cholesterol transport, converge in an AOP network on the KE myelin production (Fig. 7). The AOP “Reduced binding of TH to THR in developing brain cells leads to mental retardation due to alterations in white matter” was already submitted to the OECD based on our previous work (Dach et al., 2017). It converges with the recently published AOP network for chemically-induced thyroid activity (Noyes et al., 2019) at the level of the MIE “THR $\alpha$  binding” in developing brain cells. That THR $\alpha$ , and not THR $\beta$ , is involved in this AOP was hypothesized earlier and at this point builds on data from mice and on the approximately 30-fold higher THR $\alpha$  than THR $\beta$  mRNA expression in developing hNPC (Dach et al., 2017). In contrast, the so far unpublished AOP “Disturbance of cholesterol transport leading to mental retardation due to alterations in white matter” is based on the current novel observation that TBBPA deregulates gene expression of a gene cluster concerning cholesterol biosynthesis and transport coinciding with OL toxicity.

More compounds acting via these MoA as well as rescue experiments are needed to strengthen these two hypothetical AOPs by experimentally establishing KE relationships. Increasing the number of and converging KE for DNT will eventually lead to a large AOP network facilitating the interpretation of *in vitro* assays for the multiple applications within a risk assessment framework for DNT (Bal-Price et al., 2015). Due to the complexity of gene regulation, we cannot exclude that some TH-responsive genes are additionally regulated TH-independently by TBBPA. However, the strong antagonistic effect of TBBPA on the TH-dependent expression of known TH-responsive genes involved in OL maturation such as *KLF9* highlights its efficacy as a TH signaling disrupter during oligodendrogenesis.

In summary, we identified two MoA by which TBBPA interferes with the establishment of a population of mature, myelin-producing OLs necessary for white matter development. Since our comparative analyses revealed a higher sensitivity of human compared to rat NPC, we argue that ethical and cost-efficient *in vitro* assays based on human cells are needed to identify chemicals with the potential to disrupt oligodendrogenesis. In this study, we brought the previously published oligodendrocyte maturation assay (NPC6) (Bal-Price et al., 2018; Dach et al., 2017) to a higher readiness level for future applications in a regulatory context.

This study demonstrates that species-overarching neurosphere assays are well-suited for hazard assessment of DNT and that phenotypic combined with transcriptome analyses are powerful tools for understanding MoA and eventually building AOPs for a better comprehension of DNT hazards. Especially the multi-cellularity of the neurosphere assay, presenting NPCs, radial glia, neurons, astrocytes and oligodendrocytes makes this test meth-



od an effective instrument for multiple MoA discovery that is urgently needed for a broader and more in-depth understanding of neurodevelopmental toxicity.

## References

- Abdallah, M. A. and Harrad, S. (2011). Tetrabromobisphenol-A, hexabromocyclododecane and its degradation products in UK human milk: Relationship to external exposure. *Environ Int* 37, 443-448. doi:10.1016/j.envint.2010.11.008
- Annunziata, P., Federico, A., D'Amore, I. et al. (1983). Impairment of human brain development: Glycoconjugate and lipid changes in congenital athyroidism. *Early Hum Dev* 8, 269-278. doi:10.1016/0378-3782(83)90009-9
- Aung, H. H., Altman, R., Nyunt, T. et al. (2016). Lipotoxic brain microvascular injury is mediated by activating transcription factor 3-dependent inflammatory and oxidative stress pathways. *J Lipid Res* 57, 955-968. doi:10.1194/jlr.M061853
- Baas, D., Bourbeau, D., Sarlieve, L. L. et al. (1997). Oligodendrocyte maturation and progenitor cell proliferation are independently regulated by thyroid hormone. *Glia* 19, 324-332. doi:10.1002/(sici)1098-1136(199704)19:4<324::aid-glia5>3.0.co;2-x
- Back, S. A., Luo, N. L., Borenstein, N. S. et al. (2001). Late oligodendrocyte progenitors coincide with the developmental window of vulnerability for human perinatal white matter injury. *J Neurosci* 21, 1302-1312.
- Bal-Price, A., Crofton, K. M., Leist, M. et al. (2015). International stakeholder network (ISTNET): Creating a developmental neurotoxicity (DNT) testing road map for regulatory purposes. *Arch Toxicol* 89, 269-287. doi:10.1007/s00204-015-1464-2
- Bal-Price, A., Hogberg, H. T., Crofton, K. M. et al. (2018). Recommendation on test readiness criteria for new approach methods in toxicology: Exemplified for developmental neurotoxicity. *ALTEX* 35, 306-352. doi:10.14573/altex.1712081
- Barateiro, A., Brites, D. and Fernandes, A. (2016). Oligodendrocyte development and myelination in neurodevelopment: Molecular mechanisms in health and disease. *Curr Pharm Des* 22, 656-679. doi:10.2174/1381612822666151204000636
- Barenys, M., Gassmann, K., Baksmeier, C. et al. (2017). Epigallocatechin gallate (EGCG) inhibits adhesion and migration of neural progenitor cells in vitro. *Arch Toxicol* 91, 827-837. doi:10.1007/s00204-016-1709-8
- Bauer, A. J. and Wassner, A. J. (2019). Thyroid hormone therapy in congenital hypothyroidism and pediatric hypothyroidism. *Endocrine* 66, 51-62. doi:10.1007/s12020-019-02024-6
- Baumann, J., Barenys, M., Gassmann, K. et al. (2014). Comparative human and rat "neurosphere assay" for developmental neurotoxicity testing. *Curr Protoc Toxicol* 59, 12.21.11-24. doi:10.1002/0471140856.tx1221s59
- Baumann, J., Gassmann, K., Masjosthusmann, S. et al. (2016). Comparative human and rat neurospheres reveal species differences in chemical effects on neurodevelopmental key events. *Arch Toxicol* 90, 1415-1427. doi:10.1007/s00204-015-1568-8
- Bell, S. M., Phillips, J., Sedykh, A. et al. (2017). An integrated chemical environment to support 21<sup>st</sup>-century toxicology. *Environ Health Perspect* 125, 054501. doi:10.1289/EHP1759
- Berghoff, S. A., Gerndt, N., Winchenbach, J. et al. (2017). Dietary cholesterol promotes repair of demyelinated lesions in the adult brain. *Nat Commun* 8, 14241. doi:10.1038/ncomms14241
- Bezine, M., Debbabi, M., Nury, T. et al. (2017). Evidence of K<sup>+</sup> homeostasis disruption in cellular dysfunction triggered by 7-ketocholesterol, 24S-hydroxycholesterol, and tetracosanoic acid (C24:0) in 158N murine oligodendrocytes. *Chem Phys Lipids* 207, 135-150. doi:10.1016/j.chemphyslip.2017.03.006
- Billon, N., Jolicoeur, C., Tokumoto, Y. et al. (2002). Normal timing of oligodendrocyte development depends on thyroid hormone receptor alpha 1 (TRalpha1). *EMBO J* 21, 6452-6460. doi:10.1093/emboj/cdf662
- Blasi, F., Ciarrocchi, A., Luddi, A. et al. (2002). Stage-specific gene expression in early differentiating oligodendrocytes. *Glia* 39, 114-123. doi:10.1002/glia.10092
- Bolstad, B. M., Irizarry, R. A., Astrand, M. et al. (2003). A comparison of normalization methods for high density oligonucleotide array data based on variance and bias. *Bioinformatics* 19, 185-193. doi:10.1093/bioinformatics/19.2.185
- Braun, J. M., Buckley, J. P., Cecil, K. M. et al. (2020). Adolescent follow-up in the health outcomes and measures of the environment (home) study: Cohort profile. *BMJ Open* 10, e034838. doi:10.1136/bmjopen-2019-034838
- Breier, J. M., Gassmann, K., Kayser, R. et al. (2010). Neural progenitor cells as models for high-throughput screens of developmental neurotoxicity: State of the science. *Neurotoxicol Teratol* 32, 4-15. doi:10.1016/j.ntt.2009.06.005
- Caporali, P., Bruno, F., Palladino, G. et al. (2016). Developmental delay in motor skill acquisition in Niemann-Pick C1 mice reveals abnormal cerebellar morphogenesis. *Acta Neuropathol Commun* 4, 94. doi:10.1186/s40478-016-0370-z
- Cariou, R., Antignac, J. P., Zalko, D. et al. (2008). Exposure assessment of French women and their newborns to tetrabromobisphenol-A: Occurrence measurements in maternal adipose tissue, serum, breast milk and cord serum. *Chemosphere* 73, 1036-1041. doi:10.1016/j.chemosphere.2008.07.084
- Chen, J., Tanguay, R. L., Xiao, Y. et al. (2016). TBBPA exposure during a sensitive developmental window produces neurobehavioral changes in larval zebrafish. *Environ Pollut* 216, 53-63. doi:10.1016/j.envpol.2016.05.059
- Cheng, X., Zheng, Y., Bu, P. et al. (2018). Apolipoprotein E as a novel therapeutic neuroprotection target after traumatic spinal cord injury. *Exp Neurol* 299, 97-108. doi:10.1016/j.expneurol.2017.10.014
- Cho, J. H., Lee, S., Jeon, H. et al. (2020). Tetrabromobisphenol A-induced apoptosis in neural stem cells through oxidative stress and mitochondrial dysfunction. *Neurotox Res* 38, 74-85. doi:10.1007/s12640-020-00179-z
- Cope, R. B., Kacew, S. and Dourson, M. (2015). A reproductive, developmental and neurobehavioral study following oral exposure of tetrabromobisphenol A on Sprague-Dawley rats. *Toxicology* 329, 49-59. doi:10.1016/j.tox.2014.12.013
- Coperchini, F., Awwad, O., Rotondi, M. et al. (2017). Thyroid disruption by perfluorooctane sulfonate (PFOS) and perfluoro-



- rooctanoate (PFOA). *J Endocrinol Invest* 40, 105-121. doi:10.1007/s40618-016-0572-z
- Coughtrie, M. W., Burchell, B., Leakey, J. E. et al. (1988). The inadequacy of perinatal glucuronidation: Immunoblot analysis of the developmental expression of individual UDP-glucuronosyltransferase isoenzymes in rat and human liver microsomes. *Mol Pharmacol* 34, 729-735.
- Cui, X., Chopp, M., Zhang, Z. et al. (2017). ABCA1/ApoE/HDL pathway mediates GW3965-induced neurorestoration after stroke. *Stroke* 48, 459-467. doi:10.1161/STROKEAHA.116.015592
- Dach, K., Bendt, F., Huebenthal, U. et al. (2017). BDE-99 imF pairs differentiation of human and mouse NPCs into the oligodendroglial lineage by species-specific modes of action. *Sci Rep* 7, 44861. doi:10.1038/srep44861
- de Escobar, G. M., Obregon, M. J. and del Rey, F. E. (2004). Maternal thyroid hormones early in pregnancy and fetal brain development. *Best Pract Res Clin Endocrinol Metab* 18, 225-248. doi:10.1016/j.beem.2004.03.012
- Denver, R. J. and Williamson, K. E. (2009). Identification of a thyroid hormone response element in the mouse Kruppel-like factor 9 gene to explain its postnatal expression in the brain. *Endocrinology* 150, 3935-3943. doi:10.1210/en.2009-0050
- Dohi, E., Choi, E. Y., Rose, I. V. L. et al. (2017). Behavioral changes in mice lacking interleukin-33. *eNeuro* 4, e0147. doi:10.1523/ENEURO.0147-17.2017
- Duclot, F. and Kabbaj, M. (2017). The role of early growth response 1 (EGR1) in brain plasticity and neuropsychiatric disorders. *Front Behav Neurosci* 11, 35. doi:10.3389/fnbeh.2017.00035
- Dugas, J. C., Ibrahim, A. and Barres, B. A. (2012). The T3-induced gene KLF9 regulates oligodendrocyte differentiation and myelin regeneration. *Mol Cell Neurosci* 50, 45-57. doi:10.1016/j.mcn.2012.03.007
- Emery, B. (2010). Regulation of oligodendrocyte differentiation and myelination. *Science* 330, 779-782. doi:10.1126/science.1190927
- Farsetti, A., Desvergne, B., Hallenbeck, P. et al. (1992). Characterization of myelin basic protein thyroid hormone response element and its function in the context of native and heterologous promoter. *J Biol Chem* 267, 15784-15788.
- Gan, H. T., Tham, M., Hariharan, S. et al. (2011). Identification of ApoE as an autocrine/paracrine factor that stimulates neural stem cell survival via MAPK/ERK signaling pathway. *J Neurochem* 117, 565-578. doi:10.1111/j.1471-4159.2011.07227.x
- Ghorbel, M. T., Seugnet, I., Hadj-Sahraoui, N. et al. (1999). Thyroid hormone effects on Krox-24 transcription in the post-natal mouse brain are developmentally regulated but are not correlated with mitosis. *Oncogene* 18, 917-924. doi:10.1038/sj.onc.1202378
- Gika, A. D., Siddiqui, A., Hulse, A. J. et al. (2010). White matter abnormalities and dystonic motor disorder associated with mutations in the SLC16A2 gene. *Dev Med Child Neurol* 52, 475-482. doi:10.1111/j.1469-8749.2009.03471.x
- Groeneweg, S., Peeters, R. P., Moran, C. et al. (2019). Effectiveness and safety of the tri-iodothyronine analogue triac in children and adults with MCT8 deficiency: An international, single-arm, open-label, phase 2 trial. *Lancet Diabetes Endocrinol* 7, 695-706. doi:10.1016/S2213-8587(19)30155-X
- Gruters, A. and Krude, H. (2011). Detection and treatment of congenital hypothyroidism. *Nat Rev Endocrinol* 8, 104-113. doi:10.1038/nrendo.2011.160
- Gupta, R. K., Bhatia, V., Poptani, H. et al. (1995). Brain metabolite changes on in vivo proton magnetic resonance spectroscopy in children with congenital hypothyroidism. *J Pediatr* 126, 389-392. doi:10.1016/s0022-3476(95)70454-x
- Haddow, J. E., Palomaki, G. E., Allan, W. C. et al. (1999). Maternal thyroid deficiency during pregnancy and subsequent neuropsychological development of the child. *N Engl J Med* 341, 549-555. doi:10.1056/NEJM199908193410801
- Hamers, T., Kamstra, J. H., Sonneveld, E. et al. (2006). In vitro profiling of the endocrine-disrupting potency of brominated flame retardants. *Toxicol Sci* 92, 157-173. doi:10.1093/toxsci/kfj187
- Haq, E., Giri, S., Singh, I. et al. (2003). Molecular mechanism of psychosine-induced cell death in human oligodendrocyte cell line. *J Neurochem* 86, 1428-1440. doi:10.1046/j.1471-4159.2003.01941.x
- Ibarrola, N. and Rodriguez-Pena, A. (1997). Hypothyroidism coordinately and transiently affects myelin protein gene expression in most rat brain regions during postnatal development. *Brain Res* 752, 285-293. doi:10.1016/s0006-8993(96)01480-1
- Kawamura, A., Katayama, Y., Nishiyama, M. et al. (2020). Oligodendrocyte dysfunction due to Chd8 mutation gives rise to behavioral deficits in mice. *Hum Mol Genet* 29, 1274-1291. doi:10.1093/hmg/ddaa036
- Kim, B., Colon, E., Chawla, S. et al. (2015). Endocrine disruptors alter social behaviors and indirectly influence social hierarchies via changes in body weight. *Environ Health* 14, 64. doi:10.1186/s12940-015-0051-6
- Kim, U. J. and Oh, J. E. (2014). Tetrabromobisphenol A and hexabromocyclododecane flame retardants in infant-mother paired serum samples, and their relationships with thyroid hormones and environmental factors. *Environ Pollut* 184, 193-200. doi:10.1016/j.envpol.2013.08.034
- Kitamura, S., Jinno, N., Ohta, S. et al. (2002). Thyroid hormonal activity of the flame retardants tetrabromobisphenol A and tetrachlorobisphenol A. *Biochem Biophys Res Commun* 293, 554-559. doi:10.1016/S0006-291X(02)00262-0
- Kitamura, S., Kato, T., Iida, M. et al. (2005). Anti-thyroid hormonal activity of tetrabromobisphenol A, a flame retardant, and related compounds: Affinity to the mammalian thyroid hormone receptor, and effect on tadpole metamorphosis. *Life Sci* 76, 1589-1601. doi:10.1016/j.lfs.2004.08.030
- La Piana, R., Vanasse, M., Brais, B. et al. (2015). Myelination delay and Allan-Herndon-Dudley syndrome caused by a novel mutation in the SLC16A2 gene. *J Child Neurol* 30, 1371-1374. doi:10.1177/0883073814555189
- Lee, J. Y. and Petratos, S. (2016). Thyroid hormone signaling in oligodendrocytes: From extracellular transport to intracellular signal. *Mol Neurobiol* 53, 6568-6583. doi:10.1007/s12035-016-0013-1



- Lenters, V., Iszatt, N., Forns, J. et al. (2019). Early-life exposure to persistent organic pollutants (OCPs, PBDEs, PCBs, PFASs) and attention-deficit/hyperactivity disorder: A multi-pollutant analysis of a Norwegian birth cohort. *Environ Int* 125, 33-42. doi:10.1016/j.envint.2019.01.020
- Leonetti, C., Butt, C. M., Hoffman, K. et al. (2016). Brominated flame retardants in placental tissues: Associations with infant sex and thyroid hormone endpoints. *Environ Health* 15, 113. doi:10.1186/s12940-016-0199-8
- Liang, S., Liang, S., Zhou, H. et al. (2019). Typical halogenated flame retardants affect human neural stem cell gene expression during proliferation and differentiation via glycogen synthase kinase 3 beta and T3 signaling. *Ecotoxicol Environ Saf* 183, 109498. doi:10.1016/j.ecoenv.2019.109498
- Lilienthal, H., Verwer, C. M., van der Ven, L. T. et al. (2008). Exposure to tetrabromobisphenol a (TBBPA) in Wistar rats: Neurobehavioral effects in offspring from a one-generation reproduction study. *Toxicology* 246, 45-54. doi:10.1016/j.tox.2008.01.007
- Lin, C. Y., Wen, L. L., Lin, L. Y. et al. (2013). The associations between serum perfluorinated chemicals and thyroid function in adolescents and young adults. *J Hazard Mater* 244-245, 637-644. doi:10.1016/j.jhazmat.2012.10.049
- Malliari, E. and Kalantzi, O. I. (2017). Children's exposure to brominated flame retardants in indoor environments – A review. *Environ Int* 108, 146-169. doi:10.1016/j.envint.2017.08.011
- Masjosthusmann, S., Becker, D., Petzuch, B. et al. (2018). A transcriptome comparison of time-matched developing human, mouse and rat neural progenitor cells reveals human uniqueness. *Toxicol Appl Pharmacol* 354, 40-55. doi:10.1016/j.taap.2018.05.009
- Masjosthusmann, S., Siebert, C., Hubenthal, U. et al. (2019). Arsenite interrupts neurodevelopmental processes of human and rat neural progenitor cells: The role of reactive oxygen species and species-specific antioxidative defense. *Chemosphere* 235, 447-456. doi:10.1016/j.chemosphere.2019.06.123
- Mathews, E. S., Mawdsley, D. J., Walker, M. et al. (2014). Mutation of 3-hydroxy-3-methylglutaryl CoA synthase I reveals requirements for isoprenoid and cholesterol synthesis in oligodendrocyte migration arrest, axon wrapping, and myelin gene expression. *J Neurosci* 34, 3402-3412. doi:10.1523/JNEUROSCI.4587-13.2014
- Mathews, E. S. and Appel, B. (2016). Cholesterol biosynthesis supports myelin gene expression and axon ensheathment through modulation of P13K/Akt/mTOR signaling. *J Neurosci* 36, 7628-7639. doi:10.1523/JNEUROSCI.0726-16.2016
- Matsukami, H., Tue, N. M., Suzuki, G. et al. (2015). Flame retardant emission from e-waste recycling operation in northern vietnam: Environmental occurrence of emerging organophosphorus esters used as alternatives for PBDEs. *Sci Total Environ* 514, 492-499. doi:10.1016/j.scitotenv.2015.02.008
- Mewar, R. and McMorris, F. A. (1997). Expression of insulin-like growth factor-binding protein messenger RNAs in developing rat oligodendrocytes and astrocytes. *J Neurosci Res* 50, 721-728. doi:10.1002/(SICI)1097-4547(19971201)50:5<721::AID-JNR9>3.0.CO;2-J
- Moors, M., Rockel, T. D., Abel, J. et al. (2009). Human neurospheres as three-dimensional cellular systems for developmental neurotoxicity testing. *Environ Health Perspect* 117, 1131-1138. doi:10.1289/ehp.0800207
- Mughal, B. B., Fini, J. B. and Demeneix, B. A. (2018). Thyroid-disrupting chemicals and brain development: An update. *Endocr Connect* 7, R160-R186. doi:10.1530/EC-18-0029
- Murray, K. and Dubois-Dalcq, M. (1997). Emergence of oligodendrocytes from human neural spheres. *J Neurosci Res* 50, 146-156. doi:10.1002/(SICI)1097-4547(19971015)50:2<146::AID-JNR4>3.0.CO;2-F
- Nakajima, A., Saigusa, D., Tetsu, N. et al. (2009). Neurobehavioral effects of tetrabromobisphenol A, a brominated flame retardant, in mice. *Toxicol Lett* 189, 78-83. doi:10.1016/j.toxlet.2009.05.003
- Nelissen, K., Mulder, M., Smets, I. et al. (2012). Liver X receptors regulate cholesterol homeostasis in oligodendrocytes. *J Neurosci Res* 90, 60-71. doi:10.1002/jnr.22743
- Nguyen, N. H., Apriletti, J. W., Cunha Lima, S. T. et al. (2002). Rational design and synthesis of a novel thyroid hormone antagonist that blocks coactivator recruitment. *J Med Chem* 45, 3310-3320. doi:10.1021/jm0201013
- Ni, H. G. and Zeng, H. (2013). HBCD and TBBPA in particulate phase of indoor air in Shenzhen, China. *Sci Total Environ* 458-460, 15-19. doi:10.1016/j.scitotenv.2013.04.003
- Nimt, L., Klose, J., Masjosthusmann, S. et al. (2019). The neurosphere assay as an in vitro method for developmental neurotoxicity (DNT) evaluation. In M. Aschner and L. Costa (eds.), *Cell Culture Techniques* (141-168). *Neuromethods*. Vol. 145. New York, NY, USA: Humana. doi:10.1007/978-1-4939-9228-7\_8
- Norton, W. T. and Poduslo, S. E. (1973). Myelination in rat brain: Changes in myelin composition during brain maturation. *J Neurochem* 21, 759-773. doi:10.1111/j.1471-4159.1973.tb07520.x
- Noyes, P. D., Haggard, D. E., Gonnerman, G. D. et al. (2015). Advanced morphological – Behavioral test platform reveals neurodevelopmental defects in embryonic zebrafish exposed to comprehensive suite of halogenated and organophosphate flame retardants. *Toxicol Sci* 145, 177-195. doi:10.1093/toxsci/kfv044
- Noyes, P. D., Friedman, K. P., Browne, P. et al. (2019). Evaluating chemicals for thyroid disruption: Opportunities and challenges with in vitro testing and adverse outcome pathway approaches. *Environ Health Perspect* 127, 95001. doi:10.1289/EHP5297
- Parsons, A., Lange, A., Hutchinson, T. H. et al. (2019). Molecular mechanisms and tissue targets of brominated flame retardants, BDE-47 and TBBPA, in embryo-larval life stages of zebrafish (*Danio rerio*). *Aquat Toxicol* 209, 99-112. doi:10.1016/j.aquatox.2019.01.022
- Patel, J., Landers, K., Li, H. et al. (2011). Thyroid hormones and fetal neurological development. *J Endocrinol* 209, 1-8. doi:10.1530/JOE-10-0444
- Pfriege, F. W. and Ungerer, N. (2011). Cholesterol metabolism in neurons and astrocytes. *Prog Lipid Res* 50, 357-371.

- doi:10.1016/j.plipres.2011.06.002
- Przybyla, J., Geldhof, G. J., Smit, E. et al. (2018). A cross sectional study of urinary phthalates, phenols and perchlorate on thyroid hormones in us adults using structural equation models (NHANES 2007-2008). *Environ Res* 163, 26-35. doi:10.1016/j.envres.2018.01.039
- Rock, K. D., Gillera, S. E. A., Devarasetty, P. et al. (2019). Sex-specific behavioral effects following developmental exposure to tetrabromobisphenol A (TBBPA) in Wistar rats. *Neurotoxicology* 75, 136-147. doi:10.1016/j.neuro.2019.09.003
- Rovet, J. and Daneman, D. (2003). Congenital hypothyroidism: A review of current diagnostic and treatment practices in relation to neuropsychologic outcome. *Paediatr Drugs* 5, 141-149. doi:10.2165/00128072-200305030-00001
- Saegusa, Y., Fujimoto, H., Woo, G. H. et al. (2009). Developmental toxicity of brominated flame retardants, tetrabromobisphenol A and 1,2,5,6,9,10-hexabromocyclododecane, in rat offspring after maternal exposure from mid-gestation through lactation. *Reprod Toxicol* 28, 456-467. doi:10.1016/j.reprotox.2009.06.011
- Safina, D., Schlitt, F., Romeo, R. et al. (2016). Low-density lipoprotein receptor-related protein 1 is a novel modulator of radial glia stem cell proliferation, survival, and differentiation. *Glia* 64, 1363-1380. doi:10.1002/glia.23009
- Saher, G., Rudolphi, F., Corthals, K. et al. (2012). Therapy of Pelizaeus-Merzbacher disease in mice by feeding a cholesterol-enriched diet. *Nat Med* 18, 1130-1135. doi:10.1038/nm.2833
- Saher, G. and Stumpf, S. K. (2015). Cholesterol in myelin biogenesis and hypomyelinating disorders. *Biochim Biophys Acta* 1851, 1083-1094. doi:10.1016/j.bbalip.2015.02.010
- Sarret, C., Oliver Petit, I. and Tonduti, D. (1993). Allan-Herndon-Dudley syndrome. In M. P. Adam, H. H. Ardinger, R. A. Pagon et al. (eds.), *GeneReviews*<sup>®</sup>. Seattle, WA, USA: University of Washington, Seattle. <https://www.ncbi.nlm.nih.gov/pubmed/20301789>
- Schauer, U. M., Volkel, W. and Dekant, W. (2006). Toxicokinetics of tetrabromobisphenol a in humans and rats after oral administration. *Toxicol Sci* 91, 49-58. doi:10.1093/toxsci/kfj132
- Schmuck, M. R., Temme, T., Dach, K. et al. (2017). Omnisphere: A high-content image analysis (HCA) approach for phenotypic developmental neurotoxicity (DNT) screenings of organoid neurosphere cultures in vitro. *Arch Toxicol* 91, 2017-2028. doi:10.1007/s00204-016-1852-2
- Schoonover, C. M., Seibel, M. M., Jolson, D. M. et al. (2004). Thyroid hormone regulates oligodendrocyte accumulation in developing rat brain white matter tracts. *Endocrinology* 145, 5013-5020. doi:10.1210/en.2004-0065
- Scobie, K. N., Hall, B. J., Wilke, S. A. et al. (2009). Kruppel-like factor 9 is necessary for late-phase neuronal maturation in the developing dentate gyrus and during adult hippocampal neurogenesis. *J Neurosci* 29, 9875-9887. doi:10.1523/JNEUROSCI.2260-09.2009
- Shi, Z., Zhang, L., Zhao, Y. et al. (2017). A national survey of tetrabromobisphenol-A, hexabromocyclododecane and decabrominated diphenyl ether in human milk from China: Occurrence and exposure assessment. *Sci Total Environ* 599-600, 237-245. doi:10.1016/j.scitotenv.2017.04.237
- Singh, L., Pressly, B., Mengeling, B. J. et al. (2016). Chasing the elusive benzofuran impurity of the THR antagonist NH-3: Synthesis, isotope labeling, and biological activity. *J Org Chem* 81, 1870-1876. doi:10.1021/acs.joc.5b02665
- Sjodin, A., Patterson, D. G., Jr. and Bergman, A. (2003). A review on human exposure to brominated flame retardants – Particularly polybrominated diphenyl ethers. *Environ Int* 29, 829-839. doi:10.1016/S0160-4120(03)00108-9
- Sock, E., Leger, H., Kuhlbrodt, K. et al. (1997). Expression of Krox proteins during differentiation of the O-2A progenitor cell line CG-4. *J Neurochem* 68, 1911-1919. doi:10.1046/j.1471-4159.1997.68051911.x
- Stoll, G., Mueller, H. W., Trapp, B. D. et al. (1989). Oligodendrocytes but not astrocytes express apolipoprotein E after injury of rat optic nerve. *Glia* 2, 170-176. doi:10.1002/glia.440020306
- Sung, H. Y., Chen, W. Y., Huang, H. T. et al. (2019). Down-regulation of interleukin-33 expression in oligodendrocyte precursor cells impairs oligodendrocyte lineage progression. *J Neurochem* 150, 691-708. doi:10.1111/jnc.14788
- Takigami, H., Suzuki, G., Hirai, Y. et al. (2009). Brominated flame retardants and other polyhalogenated compounds in indoor air and dust from two houses in Japan. *Chemosphere* 76, 270-277. doi:10.1016/j.chemosphere.2009.03.006
- Takikita, S., Fukuda, T., Mohri, I. et al. (2004). Perturbed myelination process of premyelinating oligodendrocyte in Niemann-Pick type C mouse. *J Neuropathol Exp Neurol* 63, 660-673. doi:10.1093/jnen/63.6.660
- Topilko, P., Levi, G., Merlo, G. et al. (1997). Differential regulation of the zinc finger genes Krox-20 and Krox-24 (Egr-1) suggests antagonistic roles in Schwann cells. *J Neurosci Res* 50, 702-712. doi:10.1002/(SICI)1097-4547(19971201)50:5<702::AID-JNR7>3.0.CO;2-L
- Valenza, M., Marullo, M., Di Paolo, E. et al. (2015). Disruption of astrocyte-neuron cholesterol cross talk affects neuronal function in Huntington's disease. *Cell Death Differ* 22, 690-702. doi:10.1038/cdd.2014.162
- Van der Ven, L. T., Van de Kuil, T., Verhoef, A. et al. (2008). Endocrine effects of tetrabromobisphenol-A (TBBPA) in Wistar rats as tested in a one-generation reproduction study and a subacute toxicity study. *Toxicology* 245, 76-89. doi:10.1016/j.tox.2007.12.009
- van Tilborg, E., de Theije, C. G. M., van Hal, M. et al. (2018). Origin and dynamics of oligodendrocytes in the developing brain: Implications for perinatal white matter injury. *Glia* 66, 221-238. doi:10.1002/glia.23256
- Veereman-Wauters, G. (1996). Neonatal gut development and postnatal adaptation. *Eur J Pediatr* 155, 627-632. doi:10.1007/BF01957141
- Wages, P. A., Joshi, P., Tallman, K. A. et al. (2020). Screening toxcast for chemicals that affect cholesterol biosynthesis: Studies in cell culture and human induced pluripotent stem cell-derived neuroprogenitors. *Environ Health Perspect* 128, 17014. doi:10.1289/EHP5053
- Walter, K. M., Dach, K., Hayakawa, K. et al. (2019). Ontogenetic expression of thyroid hormone signaling genes: An in vit-



- ro and in vivo species comparison. *PLoS One* 14, e0221230. doi:10.1371/journal.pone.0221230
- Wang, X., Li, R., Zacharek, A. et al. (2018). Administration of downstream ApoE attenuates the adverse effect of brain ABCA1 deficiency on stroke. *Int J Mol Sci* 19, doi:10.3390/ijms19113368
- Wang, Y., Li, Y., Qin, Z. et al. (2017). Re-evaluation of thyroid hormone signaling antagonism of tetrabromobisphenol A for validating the T3-induced *Xenopus* metamorphosis assay. *J Environ Sci (China)* 52, 325-332. doi:10.1016/j.jes.2016.09.021
- Wei, W., Wang, Y., Dong, J. et al. (2015). Hypothyroxinemia induced by maternal mild iodine deficiency impairs hippocampal myelinated growth in lactational rats. *Environ Toxicol* 30, 1264-1274. doi:10.1002/tox.21997
- Wetmore, B. A., Wambaugh, J. F., Ferguson, S. S. et al. (2012). Integration of dosimetry, exposure, and high-throughput screening data in chemical toxicity assessment. *Toxicol Sci* 125, 157-174. doi:10.1093/toxsci/kfr254
- Xiao, C., Grandjean, P., Valvi, D. et al. (2020). Associations of exposure to perfluoroalkyl substances with thyroid hormone concentrations and birth size. *J Clin Endocrinol Metab* 105, doi:10.1210/clinem/dgz147
- Yang, S., Wang, S., Liu, H. et al. (2012). Tetrabromobisphenol A: Tissue distribution in fish, and seasonal variation in water and sediment of Lake Chaohu, China. *Environ Sci Pollut Res Int* 19, 4090-4096. doi:10.1007/s11356-012-1023-9
- Yasuda, K., Maki, T., Kinoshita, H. et al. (2020). Sex-specific differences in transcriptomic profiles and cellular characteristics of oligodendrocyte precursor cells. *Stem Cell Res* 46, 101866. doi:10.1016/j.scr.2020.101866
- Yeung, M. S., Zdunek, S., Bergmann, O. et al. (2014). Dynamics of oligodendrocyte generation and myelination in the human brain. *Cell* 159, 766-774. doi:10.1016/j.cell.2014.10.011
- Zhang, Y. F., Xu, W., Lou, Q. Q. et al. (2014). Tetrabromobisphenol A disrupts vertebrate development via thyroid hormone signaling pathway in a developmental stage-dependent manner. *Environ Sci Technol* 48, 8227-8234. doi:10.1021/es502366g
- Zhou, Y., Bazick, H., Miles, J. R. et al. (2019). A neutral lipid-enriched diet improves myelination and alleviates peripheral nerve pathology in neuropathic mice. *Exp Neurol* 321, 113031. doi:10.1016/j.expneurol.2019.113031
- Zhu, B., Zhao, G., Yang, L. et al. (2018). Tetrabromobisphenol A caused neurodevelopmental toxicity via disrupting thyroid hormones in zebrafish larvae. *Chemosphere* 197, 353-361. doi:10.1016/j.chemosphere.2018.01.080
- Zoeller, R. T. (2007). Environmental chemicals impacting the thyroid: Targets and consequences. *Thyroid* 17, 811-817. doi:10.1089/thy.2007.0107

#### Conflict of interest

The authors declare no conflicts of interest.

#### Funding

This work was supported by the project CERST (Center for Alternatives to Animal Testing) of the Ministry for Culture and Science of the State of North-Rhine Westphalia, Germany [file number 233-1.08.03.03-121972/131 – 1.08.03.03 – 121972], the US-EPA STAR grant [R835550], the FOKO of the Heinrich-Heine-University of Duesseldorf [2016-53], the German Research Council Ursula M. Händel-Tierschutzpreis [DFG FR 1392/6-1:], and the European Union's Horizon 2020 Research and Innovation Program, under grant agreement number: 825759 of the ENDpoiNTs project.

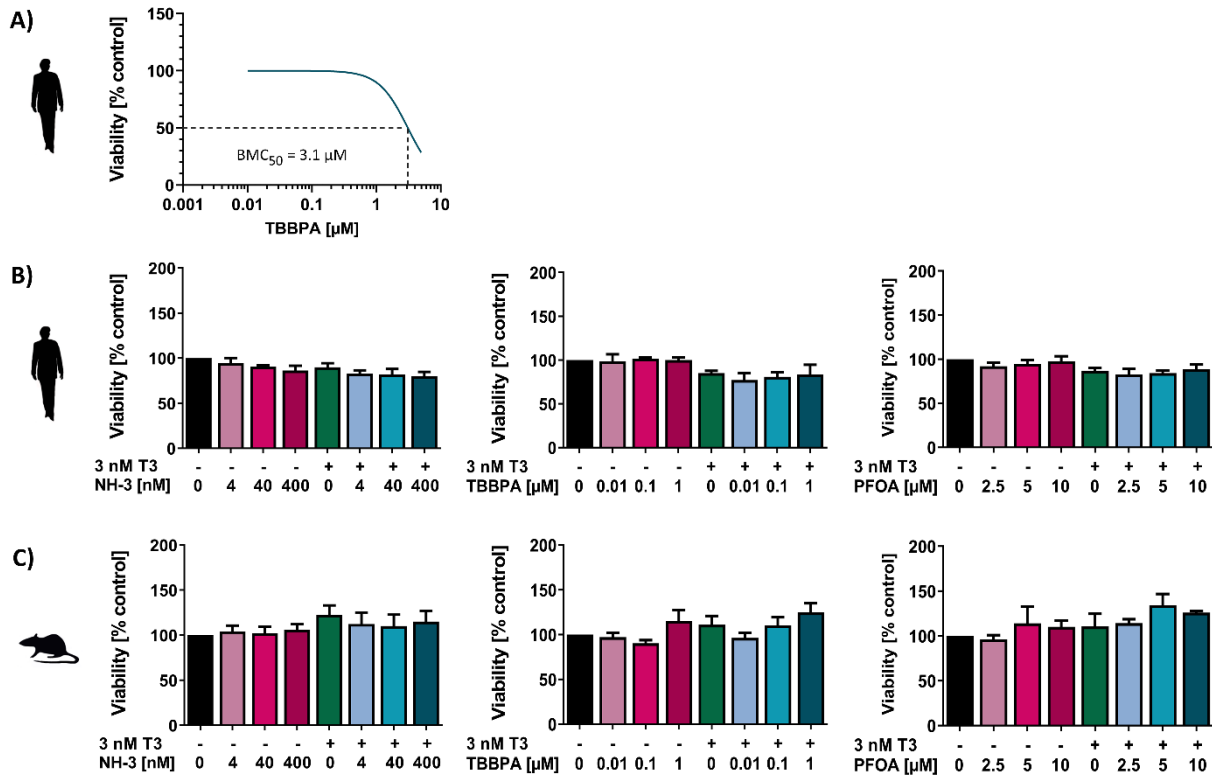
#### Acknowledgements

The authors thank Julia Kapr for assistance with the figure design.



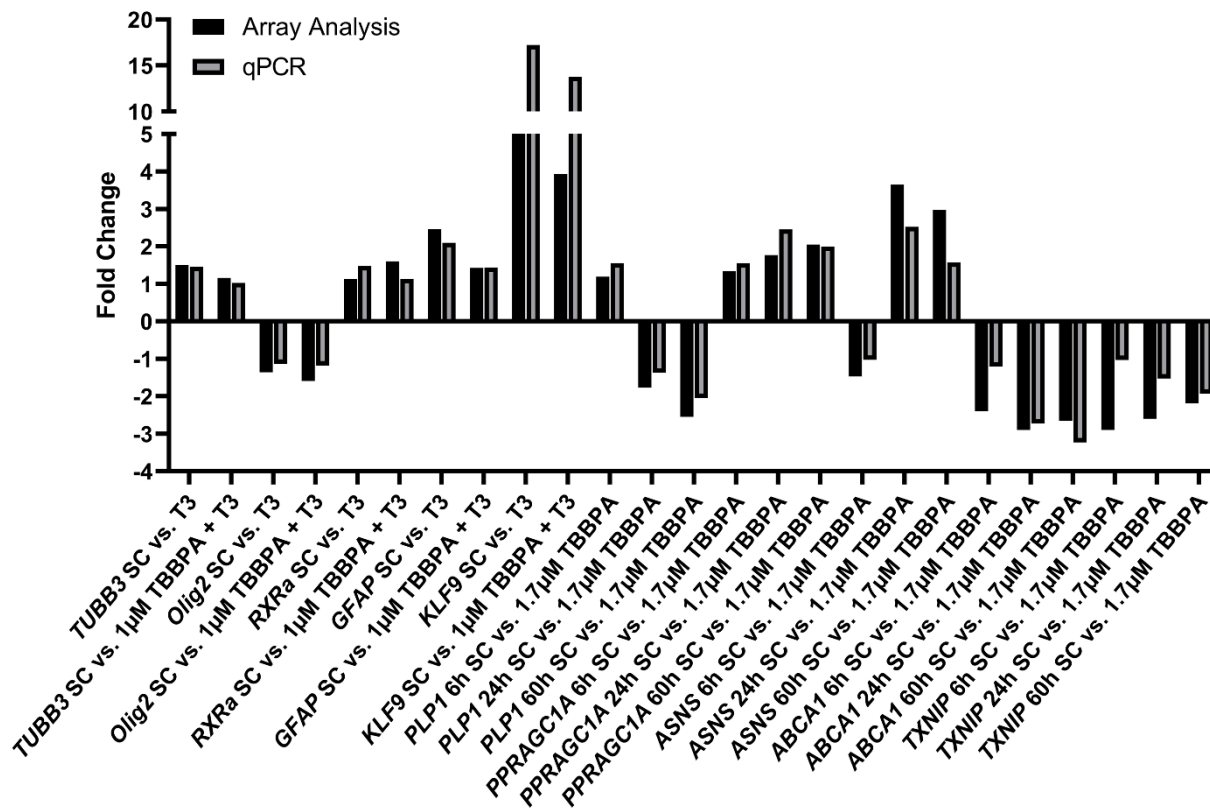
# TBBPA Targets Converging Key Events of Human Oligodendrocyte Development Resulting in Two Novel AOPs

## Supplementary Data



**Fig. S1: Viability assessment of NPCs treated with NH-3, TBBPA and PFOA alone or in combination with T3**

(A) Concentration-response of human NPCs treated with TBBPA. BMC<sub>50</sub> was calculated with GraphPad Prism 8 using the sigmoidal curve fitting and BMC<sub>50</sub> calculation models. (B,C) Human and rat NPCs were treated with increasing concentrations of NH-3, TBBPA and PFOA alone or in combination with 3 nM T3. Viability was assessed as mitochondrial activity by Alamar Blue assay after 120 h of treatment. At least 3 independent experiments with 5 technical replicates were performed in hNPCs (n = 6 for NH-3, n = 3 for TBBPA and n = 5 for PFOA) and rNPCs (n = 8 for NH-3, n = 4 for TBBPA and n = 5 for PFOA). The data are represented as mean ± SEM. Statistical significance was calculated using two-way ANOVA and Bonferroni's post-hoc tests (p < 0.05 was termed significant). TBBPA, tetrabromobisphenol A; PFOA, perfluorooctanoic acid; T3, triiodothyronine



**Fig. S2: Quantitative RT PCR validation of array analysis**

Validation of microarray data was performed with qRT PCR analysis of a set of ten genes. The fold changes were compared to the fold changes of the array analysis. A total of 500 ng RNA from microarray samples were transcribed into cDNA. cDNA, complementary DNA; qRT PCR, quantitative real-time PCR; SC, solvent control; TBBPA, tetrabromobisphenol A; T3, triiodothyronine



---

## **TBBPA Targets Converging Key Events of Human Oligodendrocyte Development Resulting in Two Novel AOPs**

**Jördis Klose**, Julia Tigges, Stefan Masjosthusmann, Katharina Schmuck, Farina Bendt, Ulrike Hübenthal, Patrick Petzsch, Karl Köhrer, Katharina Koch and Ellen Fritsche

Journal:	Alternatives to Animal Experimentation (ALTEX)
Impact Factor:	5.787 (2019)
Contribution to the publication:	65 % Planning and evaluation of all experiments, performance of most of the experiments, writing of the manuscript section 'Material and Methods'
Type of authorship:	first-authorship
Status of the publication:	Published 23 <sup>th</sup> October 2020

## 2.8 Application of the Adverse Outcome Pathway concept for investigating developmental neurotoxicity potential of Chinese Herbal Medicines by using human neural progenitor cells *in vitro*

**Jördis Klose**, Lu Li, Farina Bendt, Ulrike Hübenthal, Christian Jüngst, Patrick Petzsch, Astrid Schauss, Karl Köhrer, Ping Chung Leung, Chi Chiu Wang, Katharina Koch, Julia Tigges, Xiaohui Fan, Ellen Fritsche

*Archives of Toxicology*

Adverse Outcome Pathways (AOPs) sind organisierte Sequenzen von Schlüsselereignissen (KEs), die durch ein Xenobiotikum-induziertes molekulares Initiationsereignis (MIE) ausgelöst werden und zu einem adversen Effekt (AO) im menschlichen Organismus oder einer ökologischen Population führen. Dabei verbindet das AOP-Rahmenwerk kausal toxikologische mechanistische Informationen mit apikalen Endpunkten für regulatorische Anwendungen. AOPs sind sehr nützlich, um endophänotypische zelluläre Endpunkte, die aus In-vitro-Systemen stammen, mit gesundheitsschädlichen Auswirkungen in Beziehung zu setzen. Um die Entwicklungsneurotoxizität (developmental neurotoxicity; DNT) *in vitro* zu untersuchen, können solche zellulären Endpunkte beispielsweise mit dem humanen „Neurosphere Assay“ abgebildet werden, welcher verschiedene Endophänotypen für eine Vielzahl von entwicklungsneurologischen KEs bietet. Durch die Kombination dieses Modells mit groß angelegten Transkriptomanalysen bewerteten wir das DNT-Gefährungspotential zweier traditioneller chinesischer pflanzlicher Arzneimittel (CHMs), Lei Gong Teng (LGT) und Tian Ma (TM), und gaben weitere Einblicke in ihre Wirkungsweisen (MoA). LGT störte die hNPC-Migration, was einen außergewöhnlichen Migrationsphänotyp hervorrief. Zeitraffermikroskopie und Interventionsstudien zeigten, dass LGT die lamininabhängige Zelladhäsion stört. TM beeinträchtigte die Differenzierung zu Oligodendrozyten von humanen, jedoch nicht von Ratten NPCs und aktivierte ein Genexpressionsnetzwerk, das mit oxidativem Stress in Verbindung steht. Die LGT-Ergebnisse unterstützten ein zuvor veröffentlichtes AOP zur Adhäsion radialer Gliazellen aufgrund einer Störung der Integrin-Laminin-Bindung, während die Ergebnisse der TM-Exposition den Aufbau eines neuen mutmaßlichen Stressor-basierten AOPs hervorbrachten. Diese Studie zeigt, dass die Kombination aus phänotypischen Endpunkten mit Transkriptomanalysen einen leistungsstarken Ansatz bietet, um die MoA von Verbindungen aufzuklären und die Ergebnisse in neue oder bereits existierende AOPs zu integrieren und welcher dabei hilft die DNT-Gefahr in einem regulatorischen Kontext besser wahrzunehmen.

# Archives of Toxicology

## Application of the Adverse Outcome Pathway concept for investigating developmental neurotoxicity potential of Chinese Herbal Medicines by using human neural progenitor cells in vitro

--Manuscript Draft--

<b>Manuscript Number:</b>							
<b>Full Title:</b>	Application of the Adverse Outcome Pathway concept for investigating developmental neurotoxicity potential of Chinese Herbal Medicines by using human neural progenitor cells in vitro						
<b>Article Type:</b>	Original Article						
<b>Corresponding Author:</b>	Jördis Klose Leibniz Institute for Environmental Medical Research at the Heinrich Heine University Düsseldorf: IUF - Leibniz-Institut für umwelt- medizinische Forschung gGmbH Düsseldorf, NRW GERMANY						
<b>Corresponding Author Secondary Information:</b>							
<b>Corresponding Author's Institution:</b>	Leibniz Institute for Environmental Medical Research at the Heinrich Heine University Düsseldorf: IUF - Leibniz-Institut für umwelt- medizinische Forschung gGmbH						
<b>Corresponding Author's Secondary Institution:</b>							
<b>First Author:</b>	Jördis Klose						
<b>First Author Secondary Information:</b>							
<b>Order of Authors:</b>	Jördis Klose Lu Li Farina Bendt Ulrike Hübenthal Christian Jüngst Patrick Petzsch Astrid Schauss Karl Köhrer Ping Chung Leung Chi Chiu Wang Koch Katharina Julia Tigges Xiaohui Fan Ellen Fritsche						
<b>Order of Authors Secondary Information:</b>							
<b>Funding Information:</b>	<table border="1"> <tr> <td>Forschungskommission of the medical faculty of the Heinrich-Heine-University Dusseldorf (2016-53)</td> <td>Not applicable</td> </tr> <tr> <td>European Food Safety Authority (OC/EFSA/PRAS/2017/01)</td> <td>Not applicable</td> </tr> <tr> <td>Center for Alternatives to Animal Testing, Ministry for Culture and Science of the State of North-Rhine Westphalia (233-1.08.03.03-121972/131 – 1.08.03.03)</td> <td>Not applicable</td> </tr> </table>	Forschungskommission of the medical faculty of the Heinrich-Heine-University Dusseldorf (2016-53)	Not applicable	European Food Safety Authority (OC/EFSA/PRAS/2017/01)	Not applicable	Center for Alternatives to Animal Testing, Ministry for Culture and Science of the State of North-Rhine Westphalia (233-1.08.03.03-121972/131 – 1.08.03.03)	Not applicable
Forschungskommission of the medical faculty of the Heinrich-Heine-University Dusseldorf (2016-53)	Not applicable						
European Food Safety Authority (OC/EFSA/PRAS/2017/01)	Not applicable						
Center for Alternatives to Animal Testing, Ministry for Culture and Science of the State of North-Rhine Westphalia (233-1.08.03.03-121972/131 – 1.08.03.03)	Not applicable						

	- 121972)	
	Ursula M. Händel Tierschutzpreis DFG (DFG FR 1392/6-1)	Mrs. Ellen Fritsche
	Natural Science Foundation of Zhejiang Province (LY20H180004)	Not applicable
<b>Abstract:</b>	<p>Adverse outcome pathways (AOPs) are organized sequences of key events (KEs) that are triggered by a xenobiotic-induced molecular initiating event (MIE) and summit in an adverse outcome (AO) relevant to human or ecological health. The AOP framework causally connects toxicological mechanistic information with apical endpoints for application in regulatory sciences. AOPs are very useful to link endophenotypic, cellular endpoints in vitro to adverse health effects in vivo. In the field of in vitro developmental neurotoxicity (DNT), such cellular endpoints can be assessed using the human 'Neurosphere Assay', which depicts different endophenotypes for a broad variety of neurodevelopmental KEs. Combining this model with large-scale transcriptomics, we evaluated DNT hazards of two selected Chinese Herbal Medicines (CHMs) Lei Gong Teng (LGT) and Tian Ma (TM), and provided further insight into their modes-of-action (MoA). LGT disrupted hNPC migration eliciting an exceptional migration endophenotype. Time-lapse microscopy and intervention studies indicated that LGT disturbs laminin-dependent cell adhesion. TM impaired oligodendrocyte differentiation in human but not rat NPCs and activated a gene expression network related to oxidative stress. The LGT results supported a previously published AOP on radial glia cell adhesion due to interference with integrin-laminin binding, while the results of TM exposure were incorporated into a novel putative, stressor-based AOP. This study demonstrates that the combination of phenotypic and transcriptomic analyses is a powerful tool to elucidate compounds' MoA and incorporate the results into novel or existing AOPs for a better perception of the DNT hazard in a regulatory context.</p>	
<b>Suggested Reviewers:</b>	<p>Francesca Pistollato francesca.pistollato@ec.europa.eu Alternative method developer for developmental neurotoxicity at the EURL-ECVAM</p> <p>Horst Spielmann horst.spielmann@fu-berlin.de Specialist in Drug/Chinese Herbal Medicine toxicity</p> <p>Magdalini Sachana magdalini.sachana@oecd.org Specialist in AOP application to increase regulatory uptake of developmental neurotoxicity in vitro assays</p> <p>Christopher McPherson mcpfers1@niehs.nih.gov Neurotoxicology group and member of the National Toxicology Program, NIEHS</p>	

[Click here to view linked References](#)

1           **Application of the Adverse Outcome Pathway concept for investigating**  
2           **developmental neurotoxicity potential of Chinese Herbal Medicines by using**  
3           **human neural progenitor cells *in vitro***

4  
5  
6  
7           Jördis Klose<sup>1\*</sup>, Lu Li<sup>2,3,4,9\*</sup>, Farina Bendt<sup>1</sup>, Ulrike Hübenthal<sup>1</sup>, Christian Jüngst<sup>5</sup>, Patrick Petzsch<sup>6</sup>,  
8  
9           Astrid Schauss<sup>5</sup>, Karl Köhrer<sup>6</sup>, Ping Chung Leung<sup>4</sup>, Chi Chiu Wang<sup>3,7</sup>, Katharina Koch<sup>1</sup>, Julia  
10  
11           Tigges<sup>1</sup>, Xiaohui Fan<sup>2,9†</sup>, Ellen Fritsche<sup>1,7,8†</sup>

12  
13           <sup>1</sup> IUF-Leibniz Research Institute for Environmental Medicine, Auf'm Hennekamp 50, 40225 Duesseldorf, NRW,  
14  
15           Germany

16  
17           <sup>2</sup> College of Pharmaceutical Sciences, Zhejiang University, Hangzhou, China

18  
19           <sup>3</sup> Department of Obstetrics & Gynaecology; Li Ka Shing Institute of Health Sciences; School of Biomedical Sciences,  
20  
21           The Chinese University of Hong Kong, Shatin, N.T., Hong Kong

22  
23           <sup>4</sup> Institute of Chinese Medicine, The Chinese University of Hong Kong, Shatin, N.T., Hong Kong

24  
25           <sup>5</sup> CECAD Imaging Facility, CECAD Forschungszentrum Cologne, Joseph-Stelzmann-Str. 26, 50931 Cologne, NRW,  
26  
27           Germany

28  
29           <sup>6</sup> Biological and Medical Research Centre (BMFZ), Medical Faculty, Heinrich-Heine-University, Universitätsstraße  
30  
31           1, 40225 Duesseldorf, NRW, Germany

32  
33           <sup>7</sup> College of Basic Medical Sciences, Zhejiang Chinese Medical University, Hangzhou, China

34  
35           <sup>8</sup> Medical Faculty, Heinrich-Heine-University, Universitätsstraße 1, 40225 Duesseldorf, NRW, Germany

36  
37           <sup>9</sup> Innovation Center in Zhejiang University, State Key Laboratory of Component-Based Chinese Medicine,  
38  
39           Hangzhou, China

40  
41  
42           22  
43  
44  
45           Correspondence: Prof. Dr. Ellen Fritsche  
46           Phone: +49 (0) 211 3389 217  
47           E-Mail: [ellen.fritsche@uni-duesseldorf.de](mailto:ellen.fritsche@uni-duesseldorf.de)

48  
49           \* † authors contributed equally

50  
51  
52           28  
53           29  
54           30           **Abstract**

55           31  
56           32           Adverse outcome pathways (AOPs) are organized sequences of key events (KEs) that are triggered by  
57           33           a xenobiotic-induced molecular initiating event (MIE) and summit in an adverse outcome (AO) relevant  
58           34           to human or ecological health. The AOP framework causally connects toxicological mechanistic

35 information with apical endpoints for application in regulatory sciences. AOPs are very useful to link  
36 endophenotypic, cellular endpoints *in vitro* to adverse health effects *in vivo*. In the field of *in vitro*  
37 developmental neurotoxicity (DNT), such cellular endpoints can be assessed using the human  
38 ‘Neurosphere Assay’, which depicts different endophenotypes for a broad variety of  
39 neurodevelopmental KEs. Combining this model with large-scale transcriptomics, we evaluated DNT  
40 hazards of two selected Chinese Herbal Medicines (CHMs) Lei Gong Teng (LGT) and Tian Ma (TM), and  
41 provided further insight into their modes-of-action (MoA). LGT disrupted hNPC migration eliciting an  
42 exceptional migration endophenotype. Time-lapse microscopy and intervention studies indicated that  
43 LGT disturbs laminin-dependent cell adhesion. TM impaired oligodendrocyte differentiation in human  
44 but not rat NPCs and activated a gene expression network related to oxidative stress. The LGT results  
45 supported a previously published AOP on radial glia cell adhesion due to interference with integrin-  
46 laminin binding, while the results of TM exposure were incorporated into a novel putative, stressor-  
47 based AOP. This study demonstrates that the combination of phenotypic and transcriptomic analyses  
48 is a powerful tool to elucidate compounds’ MoA and incorporate the results into novel or existing AOPs  
49 for a better perception of the DNT hazard in a regulatory context.

## 51 Introduction

52  
53 New approach methodologies (NAMs) are non-animal-based methods, including *in vitro* approaches,  
54 which provide toxicodynamic information on chemical hazards, thereby supporting the proposed  
55 paradigm shift in toxicology - moving from the sole use of apical endpoints generated in animals  
56 towards a mechanistic understanding and more human-relevant approaches for regulatory  
57 applications (NRC 2007; Collins et al. 2008). NAMs are no stand-alone methodologies, yet need  
58 embedding into larger frameworks, i.e. integrated approaches for testing and assessment (IATAs). The  
59 IATA concept has been proposed by the Organization for Economic Cooperation and Development  
60 (OECD) member countries to embed alternative testing strategies into weight of evidence assessment  
61 for decision-making using data from various information sources (OECD 2020). IATA information on  
62 toxicodynamics might arise from Adverse Outcome Pathways (AOP), which are structured  
63 organizations of causally related biological events leading to adverse effects and provide mechanistic  
64 information on the molecular initiating event (MIE), molecular, cellular, structural and functional key  
65 events (KE) and associated key event relationships (KER; Ankley et al. 2010; OECD 2016). Thereby, AOPs  
66 serve as a knowledge assembly and communication tool between research and regulatory  
67 communities involved e.g. in regulatory and systems toxicology, biomedical challenges, in safety  
68 evaluations associated with drug development and clinical trial simulations (Carusi et al. 2018), thus  
69 covering a broad biomedical application domain. An essential platform for AOP documentation, that



70 is currently most developed, is the AOP-Wiki (<https://aopwiki.org/>), which provides a formalized,  
71 transparent, and quality-controlled data documentation and hence facilitates knowledge exchange  
72 between different stakeholders (Kandel et al. 2000; Vinken et al. 2017).

73 Spatiotemporal orchestration of molecular and cellular processes is essential for proper human brain  
74 development and contributes to the formation of a functional central nervous system (Silbereis et al.  
75 2016). This complex interplay of highly dynamic neurodevelopmental processes causes a higher  
76 vulnerability towards adverse chemical effects of the developing compared to the adult brain (Rodier  
77 1994; Rice et al. 2000). Due to the manifold KEs that happen in a time- and brain region-specific  
78 manner, creation of AOPs for developmental neurotoxicity (DNT) that cover the DNT toxicological  
79 space will be a continuous effort that is far from being completed at the moment. To date, seven AOPs  
80 are endorsed by the OECD, eleven were submitted to the AOP Wiki (<https://aopwiki.org/>) and some  
81 were published in the scientific literature (Bal-Price and Meek 2017; Barenys et al. 2019; Li et al. 2019a;  
82 Spinu et al. 2019; Chen et al. 2020; Klose et al. 2021b). Due to this low abundance of DNT-AOPs,  
83 compound hazard characterization for DNT solely on the basis of AOPs using NAMs is very difficult.  
84 DNT NAMs, in contrast, have been contributing to AOP building (Bal-Price et al. 2016; Masjosthusmann  
85 et al. 2020; EFSA 2021; Klose et al. 2021b) creating an interesting ongoing interplay in the DNT-AOP  
86 arena.

87 The multitude of Chinese Herbal Medicines (CHMs) are insufficiently characterized concerning their  
88 potential to cause DNT. For centuries, CHMs have been widely used during pregnancy to relieve  
89 symptoms like morning sickness (Flaws 2005) and treat pregnancy complications, especially to prevent  
90 miscarriage during early gestation (Li et al. 2013). Generally, CHMs are considered safe by the  
91 consumers due to their natural origin and availability as teas (Terzioglu Bebitoglu 2020). Yet it cannot  
92 be excluded that CHMs may pose adverse effects to the developing child. We recently reported on the  
93 plant-derived substance class of flavonoids as compounds with suspected developmental toxicity  
94 where – similar to CHMs – the neurodevelopmental potential is so far understudied (Barenys et al.  
95 2017b). We also identified a DNT hazard mode-of-action (MoA) for the green tea catechin  
96 epigallocatechin gallate (EGCG; Barenys et al. 2017a).

97 In the present study, we performed a case study with two selected CHMs, Lei Gong Teng (LGT; *Radix*  
98 *Et Rhizoma Tripterygii Wilfordii*, Common Threewingnut Root) and Tian Ma (TM; *Gastrodia elata*  
99 *Blume*, Tall Gastrodia Tuber) by evaluating their adverse neurodevelopmental effects with the test  
100 methods NPC1-5, which are based on developing human neural progenitor cells (hNPCs) in the  
101 ‘Neurosphere Assay’, that is part of a current OECD/EFSA (European Food Safety Authority) DNT-*in*  
102 *vitro* battery (IVB; Masjosthusmann et al. 2020, EFSA 2021). Data generated in this study are placed in  
103 an AOP-context by applying one and expanding a second already existing putative AOP for DNT.

## 105 **Materials and methods**

### 106 **Chemicals**

107  
108  
109 LGT and TM were purchased, quality-controlled, prepared and extracted from crude herbs into  
110 powders by an authorized lab within the Institute of Chinese Medicine at the Chinese University of  
111 Hong Kong. The chemical authentication was conducted by thin-layer chromatography (TLC) or high-  
112 performance liquid chromatography (HPLC) according to guidelines of the Chinese Pharmacopoeia  
113 (Chinese Pharmacopoeia Commission 2020). This confirmed the quality and quantity of chemical  
114 components in LGT and TM, also excluding any pesticide, mineral and other biological contamination.  
115 The preparation process of the crude herbs included cleaning, washing, cutting, grinding, and  
116 homogenization into fragments. In the extraction process, LGT and TM were decocted with the same  
117 amount of boiling distilled water for 2 h. The decoction was filtered and dried into powdered form  
118 using a spray-dryer and kept in a desiccator prior to use. Each extraction was prepared in one batch,  
119 and the yield rate was 6.55 % and 65.44 % for LGT and TM, respectively. The ingredients included in  
120 the two crude CHMs are listed in supplementary Table S2, and are based on records in the Chinese  
121 Pharmacopoeia and/or reports in literatures (Chinese Pharmacopoeia Commission 2020).  
122 Both powders were diluted directly in cell culture medium and 1 mg/mL stock solutions were prepared  
123 and stored at 4°C for a maximum of two days. Epigallocatechin gallate (EGCG; > 98 %) was purchased  
124 from TransMIT PlantMetaChem (Giessen, Germany). A stock solution of 10 mM in DMSO was prepared  
125 and stored at -20°C. The final solvent concentration for EGCG was 0.1 % DMSO in microarray  
126 experiments.

### 127 128 **Neurosphere cell culture**

129  
130 hNPCs derived from whole-brain homogenates of three different male individuals (gestational week  
131 16-19) were purchased from Lonza (Verviers SPRL, Belgium (#PT-2599)). They were thawed and  
132 cultured as previously described (Baumann et al. 2016; Nimtz et al. 2019). Time-matched rat NPCs  
133 (rNPCs) were isolated from postnatal day one (PND 1) pups by dissecting, digesting and homogenizing  
134 whole brains to obtain a cell suspension that spontaneously formed free-floating neurospheres  
135 (Baumann et al. 2014). The preparation of the rat pups was approved by the “Landesamt für Natur,  
136 Umwelt und Verbraucherschutz” (LANUV; 81-02.05.50.18.001) and performed according to law on  
137 animal welfare §4 Abs. 3 Tierschutzgesetz (TierSchG). NPCs were cultured as 3D free-floating  
138 neurospheres in proliferation medium consisting of DMEM (Thermo Fisher, #31966021) and Hams F12  
139 (Thermo Fisher, #31765027) (3:1) supplemented with 2 % B27 (Thermo Fisher, #17504044), 1 %  
140 penicillin and streptomycin (Pan-Biotech, #P06-07100), 20 ng/mL EGF (Thermo Fisher, #PHG0315) and  
141 either 20 ng/mL FGF (R&D Systems, #233-FB) for hNPCs or 10 ng/mL FGF (R&D Systems, #3339-FB-

142 025) for rNPCs. Neurospheres were cultivated under standard culture conditions at 37 °C with 5 % CO<sub>2</sub>  
143 in cell culture dishes coated with Poly (2-hydroxyethyl methacrylate) (poly-HEMA; Merck, #P3932).  
144 Once a week, neurospheres were passaged mechanically to 0.2 mm size using a McIlwain tissue  
145 chopper (model TC752) and thrice a week half of the medium was replaced.

#### 147 Assay conditions and chemical exposure

148  
149 Neurospheres were chopped to 0.2 mm 3 days before plating to reach a defined size of 0.3 mm.  
150 Spheres were plated in five technical replicate wells/condition in 96-well plates (flat bottom, Greiner,  
151 # 655180) with one sphere/well plated in 100 µL of differentiation medium containing 7 concentrations  
152 of CHMs serial dilutions (1:10) starting at 1 mg/ml. The differentiation medium composition was  
153 DMEM (Thermo Fisher, #31966021), Hams F12 (Thermo Fisher, #31765027) 3:1 supplemented with  
154 1 % of N2 (Thermo Fisher, #17502-048) and 1 % penicillin and streptomycin (Pan-Biotech, #P06-07100).  
155 Neurospheres were exposed for 3 (for migration/adhesion endpoints) or 5 (for differentiation  
156 endpoints) days. For the latter, on day 3, half of the exposure/solvent medium was exchanged and the  
157 supernatant was used to detect cytotoxicity by measuring lactate dehydrogenase (LDH) leakage.

#### 159 Migration, adhesion and differentiation of NPCs

160  
161 By removal of growth factors and plating neurospheres on a poly-D-lysine (PDL, 0.1 mg/mL, Merck,  
162 #P0899) and laminin (12.5 µg/mL, Merck, #L2020)-coated 96-well plate in differentiation medium,  
163 spheres settle down and NPCs migrate radially out of the sphere core and thereby differentiate into  
164 radial glia, neurons, astrocytes and oligodendrocytes.

#### 165 *Migration and adhesion*

166 Radial glia migration distance was assessed after 72 h by taking brightfield images and manual  
167 measurement of the distance between the sphere core and the furthest migrated cells as number of  
168 pixels which is converted to µm. The endpoint-specific control for NPC2 was the src-kinase inhibitor  
169 PP2 (Moors et al. 2007; Baumann et al. 2015) significantly reducing migration (data not shown). As cell  
170 migration requires cell adhesion and motility, time-lapse microscopy using a widefield system (EVOS  
171 FL Auto2, Thermo Fisher Scientific) was performed to record hNPC movement. For the time lapse  
172 experiment a 10x air objective was used and images were recorded every 5 min over a time course of  
173 24 h. Finally, videos were produced with the integrated software FL Auto2.

176 *Immunocytochemical stainings*

1  
2 177 After 3 (for migration/adhesion endpoints) or 5 (for differentiation endpoints) days of migration, NPCs  
3  
4 178 were fixed with a final concentration of 4 % paraformaldehyde (PFA; Merck). The 96-well plates were  
5  
6 179 incubated for 30 min at 37 °C and directly afterwards washed three times for 3 min with 250 µL PBS (-  
7  
8 180 /-; Biochrom) and stored in PBS at 4 °C until immunostaining was performed. Cells had to be always  
9  
10 181 covered with at least 40 µL PBS to prevent cell detachment. A blocking solution (PBS, 10 % Goat Serum  
11  
12 182 (GS; Sigma Aldrich, #G9023))/well was added and incubated for 15 min at 37 °C. After removal of  
13  
14 183 blocking solution, cells were stained as follows:

15 184 Neurospheres (migrated for 3 days) were incubated overnight at 4 °C with a rabbit IgG anti-GFAP  
16  
17 185 antibody solution (1:100, Sigma Aldrich, #G9269; in PBS-T (PBS containing 0.1 % Triton X-100) and 10 %  
18  
19 186 GS), followed by three 3 min washing steps by addition and removal of 250 µL PBS. After removal of  
20  
21 187 PBS, a secondary antibody solution in PBS (1:200 Alexa Fluor 546 anti-rabbit IgG (Invitrogen, #A11010),  
22  
23 188 2 % GS and 1 % Hoechst 33258 (Sigma Aldrich, #B1155)) was added for 30 min at 37 °C. After washing  
24  
25 189 steps as previously described, plates were stored in the dark at 4°C until further analysis.

26  
27 190 Neurospheres (migrated for 5 days) were incubated overnight at 4°C with a mouse IgM  
28  
29 191 oligodendrocyte O4 antibody solution (1:400 in PBS with 10 % GS; R&D System, #MAB1326). After 1<sup>st</sup>  
30  
31 192 antibody incubation, cells were washed three times with 250 µL PBS for 3 min and a secondary  
32  
33 193 antibody solution in PBS (1:400 Alexa Fluor 488 anti-mouse IgM (Thermo Fisher, #A-21042) and 2 % GS  
34  
35 194 was added for 30 min at 37 °C followed by washing steps and a second fixation with 4 % PFA for 30  
36  
37 195 min at 37 °C. After three additional washing steps, cells were permeabilized in 0.1 % PBS-T for 5 min at  
38  
39 196 room temperature, followed by a blocking step for 15 min at 37 °C with PBS and 10 % Rabbit Serum  
40  
41 197 (RS; Thermo Fisher, #10510). For neuronal co-staining, neurospheres were incubated for 1 h at 37 °C  
42  
43 198 with a conjugated rabbit TUBB3 674 antibody (Abcam, #190575) 1:400 (in PBS with 2 % RS and 1 %  
44  
45 199 Hoechst 33258). After washing steps, 250 µL PBS were added to each well and the plates were stored  
46  
47 200 in the dark at 4 °C.

48  
49 201 Imaging of immunochemical stainings was performed by high content imaging analysis (HCA) using an  
50  
51 202 automated fluorescence microscope (Cellomics ArrayScan VTI, Thermo Fisher Scientific). Respective  
52  
53 203 channels (386 nm for Hoechst stained nuclei, 546 nm for GFAP stained radial glia cells and astrocytes,  
54  
55 204 647 nm for  $\beta$ (III)-Tubulin stained neurons, 488 nm for O4 stained oligodendrocytes) were acquired with  
56  
57 205 a 200-fold magnification and a resolution of 552x552 pixel. The image analysis was performed with the  
58  
59 206 HCA tool Omnisphero (Schmuck et al. 2016).

56  
57 207 *Differentiation*

58  
59 208 Differentiation into neurons and oligodendrocytes was determined as the number of all  $\beta$ (III)-Tubulin  
60  
61 209 and O4 positive cells in percent of the total count of Hoechst positive nuclei. Therefore, for two defined

210 areas (1098mm x 823mm size; placed on opposite sides of the sphere core)/migration area, the  
211 number of  $\beta$ (III)-Tubulin and O4 positive cells were counted manually and then normalized to the total  
212 number of nuclei. The resulting percentages of the two areas from the same sphere were pooled and  
213 the mean was calculated for the five neurospheres of each treatment. The growth factor EGF, and  
214 bone morphogenetic protein 7 (BMP7) were used as endpoint-specific controls (Baumann et al. 2015)  
215 as they significantly reduced the total number of neurons and oligodendrocytes, respectively (data not  
216 shown).

217

### 218 Viability and cytotoxicity

219

220 Viability and cytotoxicity assays were multiplexed within the experiment to distinguish specific  
221 compound effects from secondary effects due to loss of mitochondrial reductase activity and  
222 cytotoxicity. Mitochondrial reductase activity was assessed by an alamar blue assay (CellTiter-Blue  
223 assay (CTB); Promega) in the last two hours of the compound treatment period. Cytotoxicity of treated  
224 NPCs was detected by measuring LDH (CytoTox-ONE membrane integrity assay; Promega) after 3 and  
225 5 days of migration/differentiation. Both assays were performed according to the manufacturer's  
226 instructions and as published previously (Nimtz et al. 2019). The relative fluorescence unit (RFU) values  
227 of the replicates were averaged and medium without cells was used to correct for background  
228 fluorescence. A reduction in radial glia migration decreases the CTB signal due to a diminished cell  
229 number in the migration area without necessarily affecting cell viability (Fritsche et al. 2018a). Thus, it  
230 is to note, when radial glia migration is inhibited by a compound, the LDH assay is the sole cell death  
231 reference assay for DNT specificity.

232

### 233 Microarray analysis

234

235 For microarrays analysis, 1.000 neurospheres with a defined size of 0.1 mm were plated per well of a  
236 PDL/laminin-coated 6-well-plate and treated for 6 and 24 h with LGT and EGCG, and 60 h with TM. The  
237 RNA isolation was performed using the RNeasy Mini Kit (Qiagen, #74106) according to the  
238 manufacturer's protocol. Afterwards, the total RNA was quantified (Qubit RNA HS assay, Thermo Fisher  
239 Scientific) and the quality was measured by capillary electrophoresis on a fragment analyzer using the  
240 'Total RNA Standard Sensitivity Assay' (Agilent Technologies, Inc. Santa Clara, USA). All samples had  
241 high RNA Quality Numbers (RQN; mean = 9.9).

242 cDNA synthesis, complementary RNA (cRNA conversion) synthesis and subsequent biotin labeling of  
243 cRNA was performed according to the manufacturer's protocol (GeneChip® WT PLUS Reagent Kit  
244 703174 23. January 2017; Thermo Fisher). Briefly, 100 ng of total RNA were converted to cDNA. After

245 *in vitro* transcription into cRNA and 2<sup>nd</sup> cycle synthesis, cDNA was fragmented and biotin labelled.  
246 Finally, end labelled cDNA was hybridized to Applied Biosystems™ Clariom™ S Human Gene Expression  
247 Microarray chips for 16 hours at 45°C, stained with a streptavidin/phycoerythrin conjugate, and  
248 scanned as described in the manufacturer's protocol.

249 For validation of microarray experiments, quantitative real-time polymerase chain reactions (qRT-PCR)  
250 of a set of 10 genes were performed (Suppl. Fig. S2) with the QuantiFast SYBR Green PCR Kit (Qiagen,  
251 # 204054) using a Rotor Gene Q Cycler (Qiagen). Therefore, 500 ng RNA from microarray samples were  
252 transcribed into cDNA using the RNeasy Mini Kit (Qiagen, #74106) and the Quantitect Reverse  
253 Transcription Kit (Qiagen, #205313) according to the manufacturer's instructions. Analysis was  
254 performed using the software Rotor-Gene Q Series version 2.3.4 (Qiagen). Accordingly, copy numbers  
255 (CN) of the genes of interest were calculated by using gene-specific copy number standards as  
256 described previously in detail (Walter et al. 2019) and normalized to the housekeeping gene *BETA-*  
257 *ACTIN*. Selected genes and respective primer sequences are given in supplementary Table S3.

#### 258 DCFDA ROS assay

259 Accumulation of reactive oxygen species (ROS) was measured using 2',7'-dichlorofluorescein diacetate  
260 (DCFDA; Sigma Aldrich, #D6883). Therefore, 35 neurospheres with a defined size of 0.1 mm were  
261 plated per well of black/clear bottom PDL/laminin-coated 96-well plates (Thermo Fisher, #165305) and  
262 treated with TM for 60 h. As a positive control, cells were incubated with 0.01 mM H<sub>2</sub>O<sub>2</sub> for 45 min at  
263 37 °C an 5 % CO<sub>2</sub>. After treatments, hNPCs were washed with 100 µL prewarmed PBS and cultured in  
264 100 µL differentiation medium containing 50 µM DCFDA for 30 min at 37 °C and 5 % CO<sub>2</sub>. Afterwards,  
265 hNPCs were washed on ice using 100 µL refrigerated PBS and fluorescence was determined at  
266 493em/522ex on a Tecan Infinite M200 Pro reader.

#### 269 Proliferation

270 A detailed description of the methods used to evaluate proliferation is given in the supplementary  
271 Material and Method section.

#### 274 Data analysis and statistics

275 All results are presented as mean ± standard error of the mean (SEM) from a minimum of at least three  
276 independent biological replicates. Independence is defined as experiments performed with NPCs from  
277 different individuals or from a different passage of cells. For concentration-response curves a sigmoidal  
278 (variable slope) curve fit was applied using GraphPad Prism 8.2.1. Statistical significance was calculated



281 with OneWay ANOVA and Bonferroni's post-hoc tests using the same software and results with p-  
282 values below 0.05 were termed significant.  
283 Data analyses of Microarray CEL files was conducted with GeneSpring GX software (Vers. 14.9.1;  
284 Agilent Technologies). Probes within each probe set were pooled by the GeneSprints' ExonRMA16  
285 algorithm after quantile normalization of probe-level signal intensities across all samples, leading to a  
286 reduction of inter-array variability (Bolstad et al. 2003). The process of data input was concluded by  
287 baseline transformation to the median of all samples. After grouping of samples (4 biological replicates  
288 each) according to their respective experimental condition, a given probe set had to be expressed  
289 above background (i.e., fluorescence signal of that probe set was detected within the 20<sup>th</sup> and 100<sup>th</sup>  
290 percentiles of the raw signal distribution of a given array) in all 4 replicates in at least one of the  
291 conditions to be further analyzed in pairwise or ANOVA comparisons. Statistical significance was  
292 calculated with moderate t-tests or OneWay ANOVA ( $p \leq 0.05$  was termed significant) followed by  
293 Benjamini-Hochberg tests. The overrepresented gene ontology (GO) enrichment analysis was  
294 performed using the online tool DAVID Bioinformatics Resources 6.8 (DAVID). Therefore, genes with  
295  $p \leq 0.05$  and fold change  $\geq 1.5$  (LGT and EGCG),  $\geq 2$  (TM) were termed differentially expressed (DEX).

## 296 297 **Results and discussion**

298  
299 In the last decades, the consumption of CHMs during pregnancy has been increasing not only in Asian  
300 countries, but worldwide. There are over 60 % and 45 % pregnant women in Canada (Hollyer et al.  
301 2002) and in the United States (Glover et al. 2003), respectively, using CHMs during their pregnancy,  
302 while the consumption in European countries averages to up to 20 % (Hemminki et al. 1991; Glover et  
303 al. 2003; Nordeng and Havnen 2004). However, the hazard of most CHMs has not been thoroughly  
304 investigated, since safety evaluations are commonly performed in *in vivo* studies (Li et al. 2019b).  
305 Especially DNT *in vivo* hazard assessments are extremely resource-intensive, require high amounts of  
306 animals, time and money and are thus insufficient for large scale testing (Lein et al. 2005; Crofton et  
307 al. 2012). This is one of the reasons why they are not mandatory for safety assessment of compounds  
308 in general, including CHMs. In addition, there are some uncertainties in their methodology, evaluation,  
309 and regulation and they bear the issue of species extrapolation (Tsuji and Crofton 2012; Terron and  
310 Bennekou Hougaard 2018; Sachana et al. 2019). To cover the need for DNT testing for regulatory  
311 purposes, the OECD is currently supporting the delivery of a guidance document that will facilitate the  
312 use of DNT-NAMs within a DNT-IVB in an IATA context (Sachana et al. 2021). This guidance document  
313 is supported by case studies including mechanistic evaluation of different compound classes in the  
314 DNT-IVB in a regulatory context (Sachana et al. 2021). The present study extends the OECD case studies  
315 by investigating the DNT effects of two CHMs, which belong to a totally different compound class, in

316 test methods of the current DNT-IVB set up to assess the DNT effects of two CHMs on the  
1 317 neurodevelopmental KEs NPC proliferation, NPC migration and adhesion, as well as differentiation into  
2 318 neurons and oligodendrocytes in a 3D neurosphere-based *in vitro* model consisting of human and rat  
3 319 NPCs (Baumann et al. 2016; Barenys et al. 2017a; Masjosthusmann et al. 2018; Nimtz et al. 2019;  
4 320 Masjosthusmann et al. 2020; Klose et al. 2021a; Sachana et al. 2021). This case study exemplifies the  
5 321 need for hazard characterization of substances not considered hazardous during pregnancy, like the  
6 322 two selected CHMs, TM and LGT.

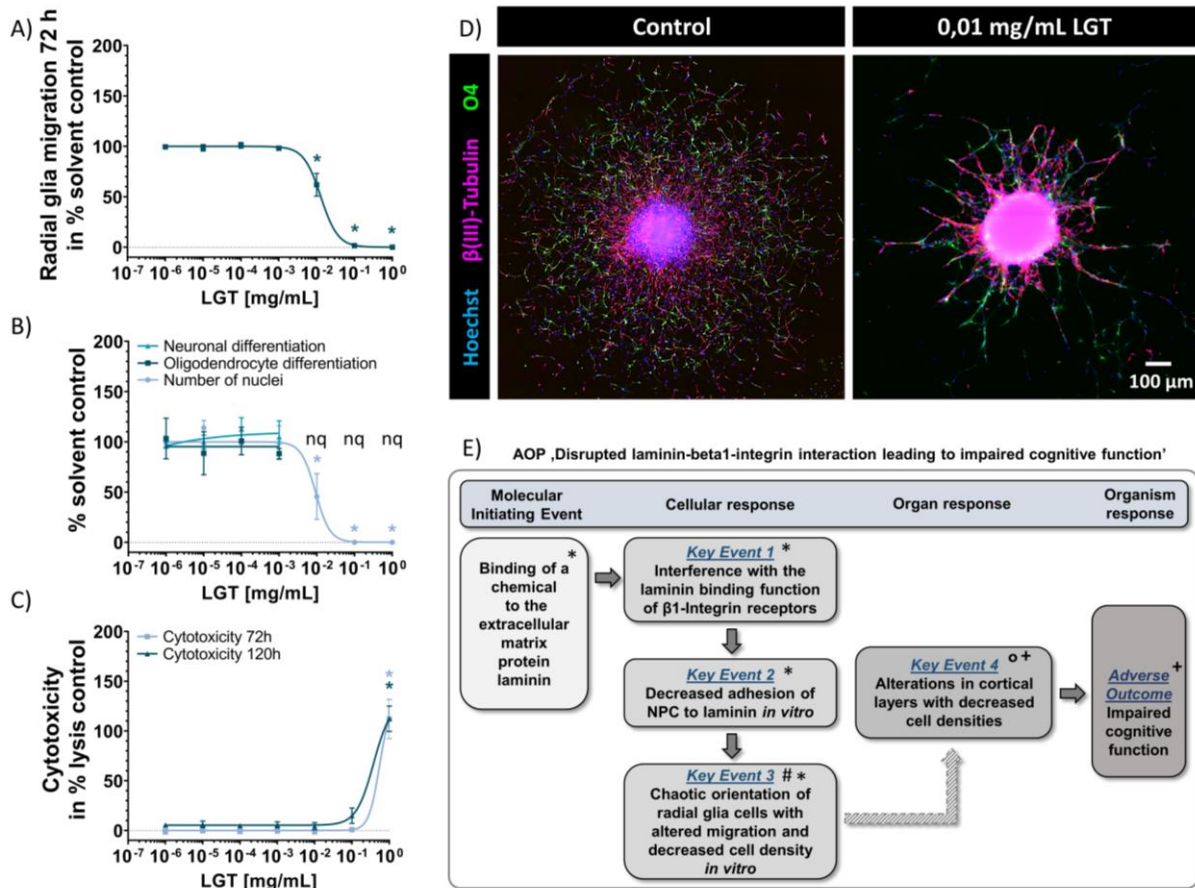
12 323 As recorded in Chinese Pharmacopoeia (Chinese Pharmacopoeia Commission 2020) LGT is classified as  
13 324 a toxic herb, as it is known to be toxic to humans, dogs, pigs and insects, but non-toxic to sheep, rabbits,  
14 325 cats and fish (Chinese Pharmacopoeia Commission 2020). Toxicity was reported for the gastrointestinal  
15 326 system (Liu et al. 2018a), the central nervous system (hypothalamus, midbrain, medulla, cerebellum  
16 327 and spinal cord; Wang et al. 2016) and the cardiovascular system (Wang et al. 2020), while bleeding  
17 328 and necrosis of the liver was also recorded (Li et al. 2020b). LGT is mainly used as a treatment for  
18 329 leprosy, rheumatoid arthritis, tuberculosis and other chronic lung disorders (Chen 2001; Wang et al.  
19 330 2018; Song et al. 2020a). Contrary, TM is classified as a non-toxic herb, as *in vivo* studies showed its  
20 331 safety in acute and sub-acute toxicity tests (Yuan et al. 2013; Zhan et al. 2016). It has a wide clinical  
21 332 application including headaches, dizziness, neurasthenia, facial cramps, limb numbness, hemiplegia,  
22 333 epilepsy, hypertension and tetanus (Dai et al. 2017; Liu et al. 2018b; Chen et al. 2019). Furthermore,  
23 334 TM is associated with insomnia relief, heart protection, memory enhancement, neuronal system  
24 335 protection and improvement of synaptic plasticity (Manavalan et al. 2012; Wang et al. 2014; Zhan et  
25 336 al. 2016; Lin et al. 2017; Huang et al. 2018). A detailed list of LD<sub>50</sub> values for both compounds can be  
26 337 found in the supplementary material (Suppl. Table S1). Both TM and LGT are commercially available  
27 338 and usually dissolved in a cup of hot water, hence orally consumed.

28 339

#### 29 340 *LGT disturbs fundamental KEs of human NPC development in vitro*

30 341 Proliferation of NPCs determines brain size (De Groot et al. 2005), illustrating an essential  
31 342 neurodevelopmental KE. In order to assess the impact of LGT on hNPC proliferation, we found  
32 343 that 0.1 mg/mL LGT significantly reduced hNPC proliferation measured by sphere size increase as well  
33 344 as BrdU incorporation into the DNA to 65.8 % ± 5.2 % and 30.4 % ± 2.9 % of untreated controls,  
34 345 respectively, without reducing viability or triggering cytotoxicity (Suppl. Fig. S1). The highest  
35 346 concentration of LGT tested (1 mg/mL) lead to a total inhibition of both hNPC proliferation  
36 347 measurements. However, also viability and cytotoxicity were significantly affected at this  
37 348 concentration (Suppl. Fig. S1).

349 Another fundamental neurodevelopmental KE is NPC migration. Cortex development takes place  
1 during the fetal phase of brain development and involves radial glia migration leading to the formation  
2 350 of a scaffold that is especially used by neurons to migrate and build the cortical layers ensuring normal  
3 351 brain structure and function (Borrell and Götz 2014). LGT exposure disturbed hNPC migration as the  
4 352 most sensitive endpoint (MSE; Fig. 1A, D) across the battery of test methods, since LGT significantly  
5 353 reduced radial glia migration distance (72 h) to  $61.9 \pm 11.3 \%$  and  $1.5 \pm 0.2 \%$  of control at  
6 354 concentrations of 0.01 mg/mL and 0.1 mg/mL, respectively (Fig. 1A), without inducing cytotoxicity (Fig.  
7 355 1C). 1 mg/mL LGT completely inhibited hNPC migration due to cytotoxicity ( $112.0 \pm 19.7 \%$  (72 h) and  
8 356  $112.3 \pm 12.7 \%$  (120 h) of the lysis control; Fig. 1C). Similar to the migration distance measurement  
9 357 shown in Fig. 1A, LGT significantly reduced the number of migrated Hoechst positive nuclei to  $45.5 \pm$   
10 358  $22.8 \%$  of control at 0.01 mg/mL with a complete loss of nuclei due to absence of migration at 0.1  
11 359 mg/mL and 1 mg/mL LGT. The decreased number of nuclei serves as a second readout for the disturbed  
12 360 cell migration. Within the migration area, hNPCs differentiate into different effector cells of the human  
13 361 brain, e.g. neurons and oligodendrocytes. To analyze the influence of LGT on hNPC neuronal and  
14 362 oligodendrocyte differentiation, all  $\beta$ (III)-Tubulin and O4 positive cells in percent of Hoechst positive  
15 363 nuclei in the migration area after 120 h of differentiation were quantified (Fig. 1B). Under influence of  
16 364 LGT ( $\leq 0.001$  mg/mL), differentiation into neurons and oligodendrocytes was not affected. Neurons  
17 365 and oligodendrocytes were not quantifiable after exposure to  $\geq 0.01$  mg/mL LGT due to the altered  
18 366 phenotype of the migration area (Fig. 1D) displaying an irregular migration pattern containing gaps  
19 367 and arborized structures with cells seeming to adhere to each other.  
20 368



**Fig. 1: Effects of LGT on hNPC migration and differentiation supporting the AOP 'Disrupted laminin-beta1-integrin interaction leading to impaired cognitive function'.** Spheres with a defined size of 0.3 mm were plated for hNPC migration analyses onto poly-D-lysine/laminin-coated 96-well plates in presence and absence of LGT for 120 h. Radial glia migration (72 h) was determined by manually measuring the radial migration from the sphere core (A). Differentiation into neurons and oligodendrocytes was determined by performing immunocytochemical stainings and using the software Omnisphero (Schmuck et al. 2016). The number of all β(III)-Tubulin positive (red) and O4 positive (green) cells in the migration area after 120 h of differentiation were counted manually and their percent of Hoechst positive nuclei (blue) was calculated (B, D). In parallel, cytotoxicity (C) was assessed by the LDH assay. At least three independent experiments with 5 technical replicates were performed and presented as mean ± SEM. Statistical significance was calculated using OneWay ANOVA followed by Bonferroni's post-hoc tests ( $p \leq 0.05$  was considered significant). The schematic AOP 'Disrupted laminin-beta1-integrin interaction leading to impaired cognitive function' includes the laminin-dependent decreased adhesion of NPCs as a central key event resulting in cortical layers alterations and adverse outcomes in the developing brain. This AOP is based on published results: \*Barenys et al. 2017 and Kühne et al. 2019; #Graus-Porta et al. 2001; °Belvindrah et al. 2007; +Amin and Borrell 2020, Fernández et al. 2016, and Long and Huttner 2019. nq = not quantifiable.

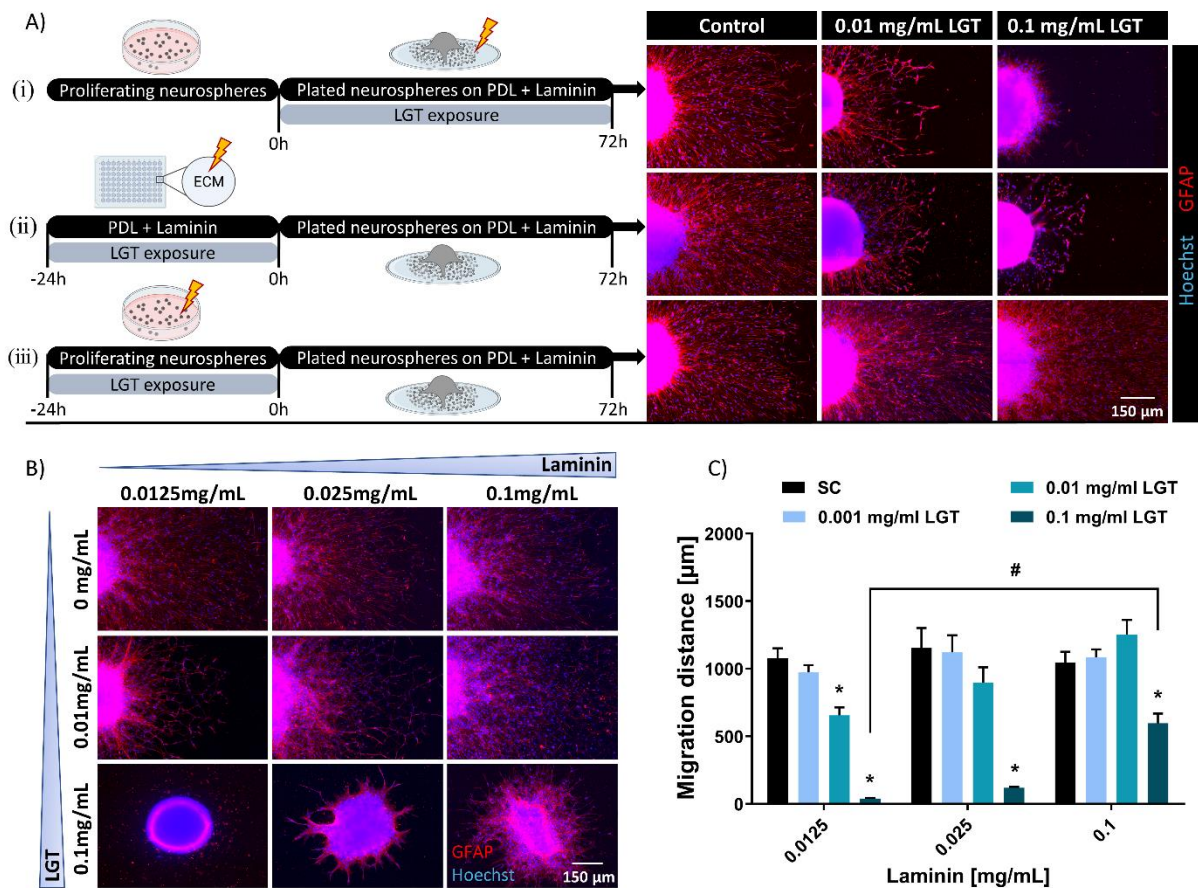
Cell migration requires cell adhesion as well as cell motility. In order to investigate whether LGT affects hNPC movement or adhesion, we next performed time-lapse microscopy of plated neurospheres over a time course of 24 h (Online Resource). The videos clearly demonstrate that 0.01 and 0.1 mg/mL LGT did not affect hNPC motility but their adhesion, since cells try to attach to the extracellular matrix (ECM) and upon unsuccessful attachment migrate back into the sphere. This impaired adhesion causes an irregular migration pattern with gaps and arborizations similar to Fig. 1D.

391 This specific neurosphere ‘gap and arborization’ endophenotype was previously observed upon  
1 392 neurosphere treatment with the flavonoid EGCG (Barenys et al. 2017a), the most abundant catechin  
2  
3 393 in green tea (Rothwell et al. 2013).

4  
5 394 Based on these data in human and rat NPCs (Barenys et al. 2017a), we generated the putative AOP  
6  
7 395 ‘Disrupted laminin- $\beta$ 1-integrin interaction leading to impaired cognitive function’ (Bal-Price et al. 2016;  
8  
9 396 Fig. 1E), which was submitted to the OECD in 2019. The MIE identified in this AOP is the interference  
10  
11 397 of a compound with the ECM protein laminin, thereby disturbing binding of NPCs via their  $\beta$ 1-integrin  
12  
13 398 receptors to laminin. Laminin is a major component of the brain’s extracellular matrix and is essential  
14  
15 399 for normal brain development and function (Chen et al. 2009). The *in vivo* relevance of  $\beta$ 1-integrin  
16  
17 400 function for cortical development was demonstrated in conditional  $\beta$ 1-integrin deficient (CNS-(nestin-  
18  
19 401 Cre)- $\beta$ 1-integrin-deficient) mice. These animals display defects in the organized laminar  
20  
21 402 cytoarchitecture of cortical structures due to defective anchoring of glial endfeet (Graus-Porta et al.  
22  
23 403 2001). *In vitro*, nestin-Cre- $\beta$ 1-integrin-deficient glia cells from these mice do not develop cell processes  
24  
25 404 with their typical radial glia fibers (Belvindrah et al. 2007), suggesting that the transmembrane  $\beta$ 1-  
26  
27 405 integrin complex regulates glial process outgrowth and endfeet anchorage, a prerequisite for neuronal  
28  
29 406 migration and positioning. Lately, the significant modulating effect of the ECM including laminin and  
30  
31 407 integrins for cortex morphogenesis, especially for gyrencephalic species like humans, has been  
32  
33 408 appreciated (Long and Huttner 2019; Amin and Borrell 2020). Hence, the AO of this AOP is ‘Impaired  
34  
35 409 cognitive function’ as a result of disturbed cortical radial glia adhesion and migration, which are  
36  
37 410 pathognomonic for disturbed cortical architecture with impaired cortical folding during development  
38  
39 411 that lead to severe intellectual disability when caused by gene mutations (Fernández et al. 2016).  
40  
41 412 Induction of this phenotype was recently used for prioritization of EGCG analogues for possible clinical  
42  
43 413 application (Kühne et al. 2019).

41  
42 414  
43 415 *LGT disturbs radial glia adhesion of human NPCs in vitro by interacting with the extracellular matrix*  
44  
45 416 *glycoprotein laminin*

46  
47 417 To elucidate if also LGT produces – similar to EGCG (Barenys et al. 2017a) – the migration  
48  
49 418 endophenotype of ‘gap and arborization’ by binding to laminin and thereby disrupting laminin-integrin  
50  
51 419 binding, we performed experiments with three different LGT exposure scenarios: (i) Spheres and ECM  
52  
53 420 were exposed to LGT during the whole migration period of 72 h, (ii) the ECM was pre-exposed to LGT  
54  
55 421 for 24 h prior to plating LGT-unexposed spheres, and (iii) proliferating spheres were pre-exposed to  
56  
57 422 LGT for 24 h and plated in absence of LGT on an unexposed laminin matrix (Fig. 2A).



**Fig. 2: LGT disturbs migration by interacting with laminin.** Spheres with a defined size of 0.3 mm were plated onto an extracellular matrix (ECM) consisting of poly-D-lysine (PDL) and Laminin, and cultured for 72 h in presence and absence of LGT under following conditions: Spheres and ECM were exposed to LGT for 72 h during the whole migration period; ECM was pre-exposed to LGT for 24 h and used to culture spheres without LGT; spheres were pre-exposed to LGT for 24 h and cultured without LGT on a non-treated ECM (A). To visualize the migration area and radial glia orientation, immunocytochemical stainings of GFAP positive cells (red) and Hoechst positive nuclei (blue) were performed. Representative immunocytochemical stainings (B) and measurement of the migration distance in  $\mu\text{m}$  (C) of hNPCs exposure to increasing LGT and laminin concentrations. Data shown in (C) are derived from at least three independent experiments with 5 technical replicates and presented as mean  $\pm$  SEM. Statistical significance was calculated using OneWay ANOVA followed by Bonferroni's post-hoc tests (\*  $p \leq 0.05$  was considered significant) and Two-way ANOVA followed by Tukey's multiple comparison test (#  $p \leq 0.05$  was considered significant). \* significant compared to respective solvent control; # significant compared to the 0.1 mg/mL LGT treatment plated on 0.0125 mg/mL laminin. Schematic experimental setup (A) was created with BioRender.com.

For visualization of the migration pattern as well as the radial glia orientation, we performed immunocytochemical stainings of GFAP<sup>+</sup> cells. The alterations in the migration phenotype are only observed when the ECM was exposed or pre-exposed to LGT (Fig. 2A, conditions ii+iii) and not when the spheres were pre-exposed to the compound and plated onto an unexposed ECM (Fig. 2A, condition i). These results suggest that LGT binds to laminin, thereby prohibiting laminin-cell surface receptor interaction, leading to a disturbed cell adhesion. To confirm this hypothesis, we performed LGT/laminin co-exposure experiments (Fig. 2B, C). Increasing the assay's laminin concentration in the 'Neurosphere Assay' from 0.0125 mg/mL to 0.025 mg/mL and 0.1 mg/mL antagonized the LGT-induced migratory endophenotype (Fig. 2B) and the decreased migration distance (Fig. 2C) in a concentration-dependent manner. 0.1 mg/mL laminin rescued the strong, LGT-induced reduced migration distance

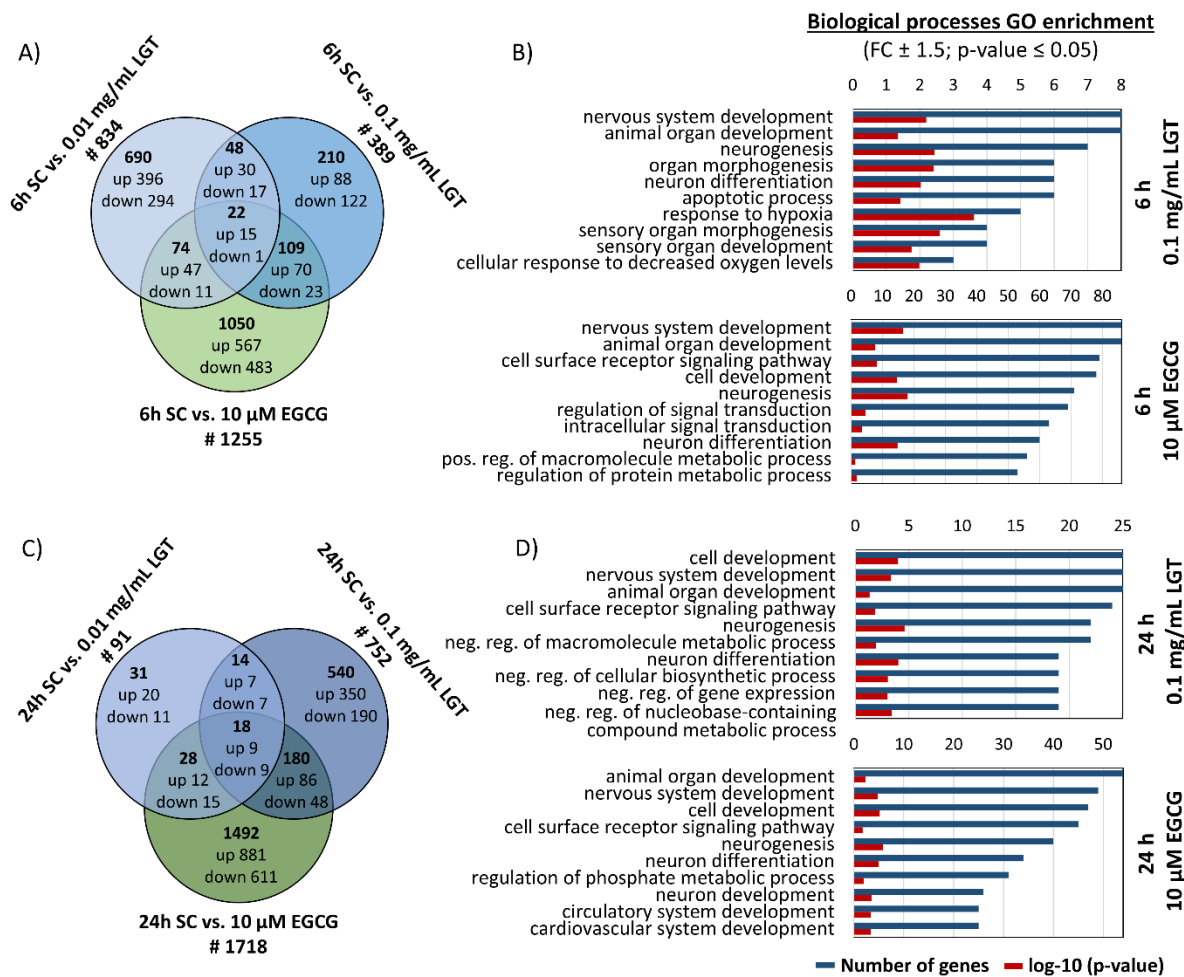


446 (39.4 ± 5.0 μm) to 597.0 ± 71.4 μm, yet did not completely compensate the adverse effect, while 0.025  
1 447 mg/ml laminin completely antagonized the migration inhibition caused by 0.01 mg/ml LGT.  
2  
3 448 Cell adhesion to the ECM protein laminin primarily depends on integrins, which are composed of a  
4  
5 449 family of α/β heterodimeric transmembrane receptors which are responsible for the cell adherence to  
6  
7 450 the ECM and take part in specialized cell-cell interactions (Hynes 2002). Integrin dimers containing β1-  
8  
9 451 and β4 subunits are known to be responsible for laminin binding, with the β1-subunit playing the major  
10  
11 452 part (Humphries et al. 2006; Barczyk et al. 2010). Chemicals that have a binding affinity to the ECM  
12  
13 453 protein laminin mask the laminin-β1 and/or β4-integrin receptor and are therefore suggested to affect  
14  
15 454 important cellular key aspects of neurodevelopment including cell adhesion, cell orientation and cell  
16  
17 455 migration thus disturbing cortical development (Graus-Porta et al. 2001; Belvindrah et al. 2007; Tzu  
18  
19 456 and Marinkovich 2008; Warren et al. 2012; Lubbers et al. 2014; Barenys et al. 2017a).  
20  
21 457 That hNPC adhesion is also mainly dependent on β1-containing receptors, was shown earlier by  
22  
23 458 Barenys et al. (2017a). In this study, RT-PCR analyses revealed mRNA expression of β1- and β4-integrin  
24  
25 459 subunits in migrating hNPCs. By using functional blocking antibodies against β1-integrin we observed  
26  
27 460 a decrease in hNPC migration and an irregular migration pattern, while a functional blockage of β4-  
28  
29 461 integrin did not result in altered hNPC migration (Barenys et al. 2017a). This migration endophenotype  
30  
31 462 of ‘gaps and arborization’ seems to be specific for disturbed hNPC adhesion, because compounds  
32  
33 463 inhibiting migration due to alterations of intracellular signaling like methylmercury chloride (MeHgCl)  
34  
35 464 or the src kinase inhibitor PP2 decrease hNPC migration without causing gap formation in the migration  
36  
37 465 area (Moors et al. 2007; Fritsche et al. 2018a; Masjosthusmann et al. 2018). Due to the striking  
38  
39 466 similarity with the endophenotype observed after EGCG treatment, we suggest that also the LGT-  
40  
41 467 induced migration phenotype is caused by interference of the compound with binding of the β1-  
42  
43 468 integrin subunit to laminin. The relevance of the previously described AOP (Bal-Price et al. 2016; Fig.  
44  
45 469 1E) for the LGT MoA is supported by experimental data, i.e. antagonization of LGT effects by laminin  
46  
47 470 (Fig. 2C) and observation of the chaotic orientation of GFAP<sup>+</sup> radial glia cells (Fig. 2A, B).

471

#### 472 *Transcriptome analyses of migrating hNPCs exposed to LGT and EGCG*

473 To further elucidate the mechanism(s) underlying the LGT or EGCG-induced migratory phenotype, we  
474 performed microarray analyses of hNPCs differentiated for 6 h and 24 h in presence of 0.01 mg/mL  
475 and 0.1 mg/mL LGT or 10 μM EGCG and their respective solvents (N2 Medium for LGT; 0.1 % DMSO for  
476 EGCG; Fig.3).



**Fig. 3: Transcriptome profiling of migrated and differentiated hNPCs treated with LGT and EGCG.** Differential gene expression between hNPCs exposed to solvent (N2 Medium for LGT; DMSO for EGCG), LGT (0.01, 0.1 mg/mL) and EGCG (10  $\mu$ M) over the time course (6 and 24 h) of differentiation was statistically determined using one-way ANOVA followed by Benjamini-Hochberg tests. Genes with  $p \leq 0.05$  and fold change  $\geq 1.5$  were termed differentially expressed (DEX). Overlap of the number of DEX genes regulated by LGT and EGCG over the time course of 6 h (A; SC vs. 0.01 mg/mL LGT, #834; SC vs. 0.1 mg/mL LGT, #389; SC vs. 10  $\mu$ M EGCG, #1255) and 24 h (C; SC vs. 0.01 mg/mL LGT, #91; SC vs. 0.1 mg/mL LGT, #752; SC vs. 10  $\mu$ M EGCG, #1718) of hNPC differentiation. Overrepresented gene ontology (GO) terms for 6 h (B) and 24 h (D) of differentiated hNPCs under influence of LGT and EGCG. GO enrichment analysis was performed using the online tool DAVID Bioinformatics Resources 6.8 (DAVID). All overrepresented GO terms were sorted by their number of genes involved (blue bars). Additionally, the p-value of each GO term is given (red bars). GO terms with highest number of genes involved are displayed. SC = solvent control.

The Venn-diagrams illustrate the total number of gene changes (Fig. 3A, C). Both concentrations of LGT (0.01 mg/mL and 0.1 mg/mL) as well as 10  $\mu$ M EGCG significantly ( $p \leq 0.01$ , fold-change  $\geq 1.5$ ) regulated the expression of 834, 389 and 1255 genes, respectively, already after 6 h (Fig. 3A), indicating that transcriptome changes take place within the first hours of migration. After 24 h of migration the number of significantly regulated genes increased to 752 and 1718 in 0.1 mg/mL LGT- and EGCG-treated spheres, respectively, while 0.01 mg/mL LGT regulated with 91 genes less than after 6h (Fig. 3C). In general, EGCG regulates more genes than LGT after both timepoints measured. Both compounds commonly regulated only 22 and 18 genes after 6 h and 24 h, respectively (Suppl. Tab. S4).

498 Strikingly, just one gene (cell-adhesion molecule-related/down-regulated by Oncogenes; *CDON*) within  
1 499 the 22 genes regulated after 6 h is directly associated with cell migration and/or adhesion, while after  
2  
3 500 24 hours none of the overlap genes is directly related to migration and/or adhesion processes. *CDON*  
4  
5 501 has been identified as a Sonic hedgehog (Shh) receptor with affiliations to the neural cell adhesion  
6  
7 502 molecule (N-CAM) family (Tenzen et al. 2006; Zhang et al. 2006). Specifically, *CDON* plays an important  
8  
9 503 role during neuronal differentiation as it binds to N-cadherin, a cell-adhesion molecule, thereby  
10  
11 504 inducing p28/MAPK signaling to direct cell differentiation (Lu and Krauss 2010). Contrary to *CDON*  
12  
13 505 upregulation caused by LGT (0.01 mg/mL FC 1.8; 0.1 mg/mL FC 2.0) and EGCG (FC 5.6), knockdown of  
14  
15 506 *CDON* in zebrafish neural crest cells (NCCs) resulted in aberrant migration, as NCCs are still able to  
16  
17 507 migrate out of the neural tube but delay directly after the initiation of migration (Powell et al. 2015).  
18  
19 508 Furthermore, this study illustrates via live cell imaging a reduced directedness of migration, increased  
20  
21 509 velocity and mispositioned cell protrusions, indicating that any disturbance in this gene results in an  
22  
23 510 adverse migratory phenotype. In our case here, it can be speculated that *CDON* expression might be a  
24  
25 511 compensatory mechanism for the aberrant migration produced by compound exposure. This has to be  
26  
27 512 more thoroughly studied in the future.

26 513 In accordance with these observations, gene ontology (GO) enrichment analyses and the ten highest  
27  
28 514 overrepresented biological processes sorted by their number of genes involved, revealed no enriched  
29  
30 515 migration and/or adhesion process after 6 h and 24 h 0.1 mg/mL LGT and 10  $\mu$ M EGCG hNPC (Fig.  
31  
32 516 3B, D). However, three of the enriched processes are directly brain-related ('nervous system  
33  
34 517 development', 'neurogenesis' and 'neuron differentiation') and overrepresented in all conditions. In  
35  
36 518 addition, the GO term 'neuron development' is present after 24 h of hNPC treatment with 10  $\mu$ M EGCG  
37  
38 519 (Fig. 3D). With the exception of 6 h 0.1 mg/mL LGT, there is one process 'cell surface receptor signaling  
39  
40 520 pathway' overrepresented in all conditions, which needs further attention regarding our findings of  
41  
42 521 altered cell-adhesion to the ECM. Here, EGCG had a greater impact since 79 (6 h) and 45 genes (24 h)  
43  
44 522 are involved, while LGT led to a deregulation of 24 genes relevant for this GO enrichment. Precisely,  
45  
46 523 only nine genes in total (Receptor-type tyrosine-protein phosphatase T, *PTPRT*; Semaphorin 3E,  
47  
48 524 *SEMA3E*; Integrin beta-5, *ITGB5*; Cadherin-6, *CADH6*; Membrane-associated guanylate kinase, *MAGI2*;  
49  
50 525 Adhesion G protein-coupled receptors (GPCRs) latrophilin 2 and 3, *ADGRL2*, *ADGRL3*; Contactin-1,  
51  
52 526 *CNTN1*; *CDON*) are directly associated with cell-adhesion. This lack of transcriptome data contributing  
53  
54 527 to the knowledge on the MoA of LGT and EGCG is not surprising, considering that the common MIE  
55  
56 528 'binding of a chemical to the extracellular matrix protein laminin' up to the KE2 'decreased adhesion  
57  
58 529 of NPC to laminin *in vitro*', ultimately leading to the observed migratory endophenotype, are  
59  
60 530 orchestrated without genomic involvement. Therefore, we interpret the observed minor  
61  
62 531 transcriptomic changes as a secondary effect and compensatory response of the cell to the defective  
63  
64 532 cell-matrix adhesion/interaction and subsequently migration.

533

1 534 *Clinical observations concerning LGT*

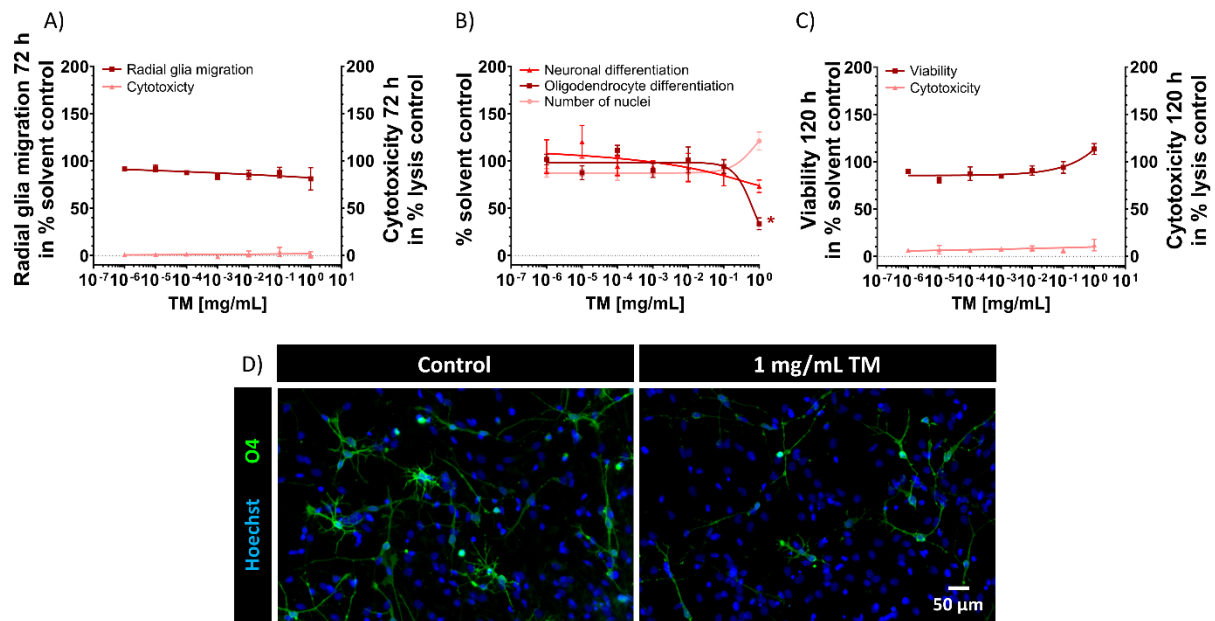
2  
3  
4 535 Strikingly, general toxicity of LGT exhibits enormous species differences *in vivo*, as it is toxic to humans,  
5  
6 536 dogs, pigs and insects, but non-toxic to sheep, rabbits, cats and fish (Chinese Pharmacopoeia  
7  
8 537 Commission 2020). Species differences might be caused by species-specificities in toxicodynamics or  
9  
10 538 toxicokinetics (Dragunow 2020). As we did not observe species differences in EGCG potency on adverse  
11  
12 539 human and rat NPC migration (Barenys et al. 2017a), it is highly likely that the adversity on NPC  
13  
14 540 adhesion/migration observed in this study is species-overarching and independent of the general  
15  
16 541 toxicity observed in earlier *in vivo* studies.

17 542 This is the first time that the specific impact of the whole LGT extract on cell adhesion was shown in  
18  
19 543 human cells *in vitro*, as most studies deal with single components and/or specific target-related *in vivo*  
20  
21 544 models trying to evaluate single MoA. Previous work from Kong *et al.* (2013) demonstrated for  
22  
23 545 triptolide, a diterpenoid triepoxide LGT constituent, matrigel-induced cell adhesion adversities in  
24  
25 546 human fibroblast-like synoviocytes of rheumatoid arthritis and human umbilical vein endothelial cells.  
26  
27 547 If the LGT-induced altered adhesion of hNPCs to laminin is also caused by triptolide is not known,  
28  
29 548 however, it can be assumed since triptolide represents one of the main active component of LGT (He  
30  
31 549 et al. 2013). To get a deeper understanding of prenatal LGT toxicity, further studies are needed,  
32  
33 550 especially to identify and quantify the adhesion-disturbing component(s) in the LGT extract mixture  
34  
35 551 we used. Moreover, single component experiments and a better understanding of the *in vitro* and *in*  
36  
37 552 *vivo* pharmacokinetics of the substance(s) are warranted. The latter will allow moving from hazard  
38  
39 553 characterization to risk assessment.

40 554

41  
42 555 *TM exposure disrupts oligodendrogenesis by producing oxidative stress*

43  
44 556 Next, we analyzed the impact of the second CHM, TM, on hNPC proliferation, radial glia migration and  
45  
46 557 differentiation into neurons as well as oligodendrocytes (Fig. 4). The proliferation of hNPCs, measured  
47  
48 558 by the increase of sphere size and by BrdU incorporation into the DNA was not significantly altered by  
49  
50 559 TM concentrations up to 1mg/mL over 72 h (Suppl. Fig. S1), nor did TM affect migration (Fig. 4A) or  
51  
52 560 neuronal differentiation (Fig. 4B) at the concentration tested. However, 1 mg/mL TM significantly  
53  
54 561 reduced the differentiation into oligodendrocytes to  $27.6 \pm 9.5$  % of control (Fig. 4B, D), without  
55  
56 562 significantly affecting the number of nuclei (Fig. 4B), viability (Fig. 4C) or inducing cytotoxicity (Fig.  
57  
58 563 4A, C).



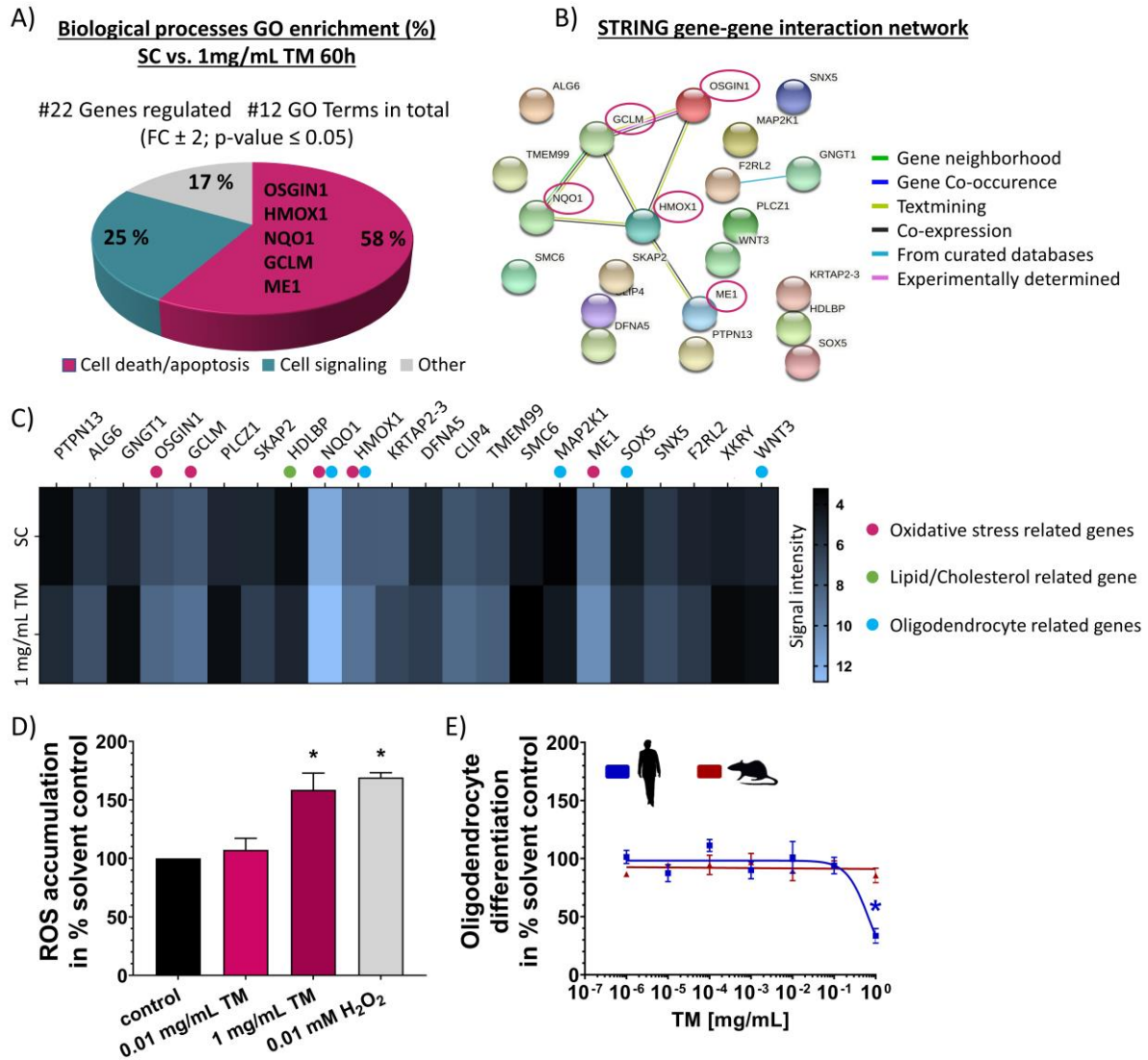
**Fig. 4: Effects of TM on hNPC migration and differentiation.** Spheres with a defined size of 0.3 mm were plated onto poly-D-lysine/laminin-coated 96-well plates and exposed to increasing TM concentrations over 120 h. Radial glia migration (72 h) was determined by manually measuring the radial migration from the sphere core (A). Differentiation into neurons and oligodendrocytes was determined by performing immunocytochemical stainings and using the software Omnisphero (Schmuck et al. 2016). The number of all  $\beta$ (III)-Tubulin positive cells (B) and O4 positive cells (B, D; green) in percent of Hoechst positive nuclei (blue) in the migration area after 120 h of differentiation was calculated manually. In parallel, viability and cytotoxicity (A, C) were assessed by the Alamar Blue and the LDH assay. At least three independent experiments with 5 technical replicates were performed and depicted as mean  $\pm$  SEM. Statistical significance was calculated using OneWay ANOVA followed by Bonferroni's post-hoc tests ( $p \leq 0.05$  was considered significant).

Since oligodendrocyte differentiation was the only analyzed neurodevelopmental endpoint affected by TM, we performed microarray analyses of hNPCs differentiated for 60 h under exposure to either 1 mg/mL TM or vehicle (differentiation medium without TM; Fig. 5) to help identify the underlying MoA.

Exposure to 1 mg/mL TM during the 60 h of neurosphere differentiation significantly ( $p \leq 0.05$ , fold change  $\geq 2$ ) regulated the expression of 22 genes compared to the respective controls (Fig. 5A, C). A gene set enrichment analysis revealed only 12 GO terms, of which more than half (58 %) were associated with cell death/apoptosis, while 25 % and 17 % were related to cell signaling and other biological processes, respectively (Fig. 5A). Looking at the GO terms associated with cell death, a set of 5 genes (oxidative stress induced growth inhibitor 1, *OSGIN1*; heme oxygenase 1, *HMOX1*; NAD(P)H dehydrogenase quinone 1, *NQO1*; glutamate-cystein ligase modifier subunit, *GCLM*; malic enzyme 1; *ME1*) related to oxidative stress were overrepresented. In accordance with that, STRING gene-gene interaction network analysis based on the 22 significantly regulated genes revealed a high correlation of the 5 genes involved in oxidative stress response (Fig. 5B). In addition to the 5 differentially expressed genes related to oxidative stress (red dots, Fig 5C), we identified 1 gene (high density lipoprotein (HDL) binding protein, *HDLBP*) to be involved in lipid/cholesterol metabolism (green dot,

591 Fig 5C), a process necessary for myelination and thereby for proper oligodendrogenesis (Berghoff et  
1 592 al. 2016). *HDLBP* binds HDL, such as cholesterol, thereby regulating excess cholesterol levels in cells.  
2  
3 593 An *HDLBP* up-regulation (FC 2.3) caused by TM may lead to excessive HDL binding, thus reducing the  
4  
5 594 availability of HDL for myelin formation, which in turn disturbs oligodendrogenesis (Li et al. 2020a).  
6  
7 595 Next to *NQO1* and *HMOX1*, 3 additional DEX genes (mitogen-activated protein kinase kinase 1,  
8  
9 596 *MAP2K1*; SRY-Box transcription factor 5, *SOX5*; Wnt family member 3, *WNT3*) are associated with  
10  
11 597 oligodendrogenesis (blue dots, Fig 5C). Downregulation of Wnt signaling, Sox5 transcriptional activity  
12  
13 598 and *MAP2K1*-dependend ERK1/2 activation are necessary for oligodendrocyte precursor (OPC)  
14  
15 599 proliferation and differentiation (Shimizu et al. 2005; Langseth et al. 2010), the maintenance of OPCs  
16  
17 600 in an undifferentiated state (Baroti et al. 2016), and the synthesis of myelin or remyelination (Jeffries  
18  
19 601 et al. 2016), respectively. In case of *SOX5*, the observed up-regulation (FC 2.1) might lead to a  
20  
21 602 continuous sojourn of OPCs in the immature state (Baroti et al. 2016), thereby decelerating  
22  
23 603 oligodendrogenesis and decreasing oligodendrocyte numbers. Since we observed *WNT3* to be down-  
24  
25 604 regulated (FC 2.0) and *MAP2K1* to be up-regulated (FC 2.1) upon TM treatment, we hypothesize a  
26  
27 605 compensatory mechanism in response to the reduced oligodendrocyte differentiation. These  
28  
29 606 observations have to be more intensively examined in the future.  
30  
31 607 Altogether, based on these transcriptomic findings, we hypothesize that oxidative stress plays a  
32  
33 608 significant role in the oligodendrocyte reduction observed after treatment with TM.  
34  
35  
36  
37  
38  
39  
40  
41  
42  
43  
44  
45  
46  
47  
48  
49  
50  
51  
52  
53  
54  
55  
56  
57  
58  
59  
60  
61  
62  
63  
64  
65





**Fig. 5: Transcriptomic profiling of differentiated hNPCs treated with TM.** Differential gene expression between hNPCs exposed to 1 mg/mL TM and untreated hNPCs over 60 h of differentiation was statistically determined using moderated t-Test followed by Benjamini-Hochberg tests. Genes (#22) with  $p \leq 0.05$  and fold change  $\geq 2$  were termed differentially expressed (DEX). Overrepresented gene ontology (GO) terms for hNPCs differentiated under the influence of 1 mg/mL TM for 60 h (A). GO enrichment analysis was performed using the online tool DAVID Bioinformatics Resources 6.8 (DAVID). The significantly regulated GO terms (#12) after 60 h of differentiation were further assigned to 3 superordinate processes based on expert judgment. Numbers in the pie chart represent the percentage of GO terms assigned to each superordinate process. Gene-gene interaction network analysis of the genes regulated by 1 mg/mL TM shows involvement of oxidative stress (B). Expression profile (absolute signal intensity) of the 22 differentially regulated genes identified in (A) between SC and 1 mg/mL (C). Genes are highlighted as reportedly regulated by oxidative stress (red dots), involved in lipid/cholesterol metabolism (green dot) or associated with oligodendrogenesis (blue dots). ROS accumulation (D) was measured via DCFDA oxidation over 60 h in hNPCs treated with 0.01 and 1 mg/mL TM. Exposure to 0.01 mM  $H_2O_2$  was used as a positive control. Human and rat spheres with a defined size of 0.3 mm were plated onto poly-D-lysine/laminin-coated 96-well plates and exposed to increasing TM concentrations over 120 h. The differentiation into oligodendrocytes was determined as number of all O4 positive cells in percent of the total amount of Hoechst positive nuclei in the migration area (E). At least three independent experiments with 5 technical replicates were performed and presented as mean  $\pm$  SEM (in (D) TM treatment  $n=4$ ;  $H_2O_2$   $n=3$ ). Statistical significance was calculated using OneWay ANOVA followed by Bonferroni's post-hoc tests and unpaired t-test for  $H_2O_2$  ( $p \leq 0.05$  was considered significant). SC = solvent control (N2-medium); OSGIN1 = oxidative stress induced growth inhibitor 1, HMOX1 = heme oxygenase 1, NQO1 = NAD(P)H dehydrogenase quinone 1, GCLM = glutamate-cystein ligase modifier subunit, ME1 = malic enzyme 1, HDLBP = high density lipoprotein binding protein,  $H_2O_2$  = hydrogen peroxide.

631 Oxidative stress is defined as an imbalance between the production of reactive oxygen species (ROS)  
632 and the antioxidant capacity of the cell. Measurements of ROS accumulation in differentiated hNPCs  
633 exposed to 1 mg/mL TM (60 h) revealed significantly induced ROS levels up to  $158.5 \pm 14.4$  % of  
634 untreated controls (Fig. 5D). As expected, the phenotypically unobtrusive concentration of  
635 0.01 mg/mL TM did not cause oxidative stress (Fig. 5D). Hence, the ROS measurements support the  
636 transcriptomic data and the endophenotypic observation of decreased hNPC oligodendrocyte  
637 differentiation. However, at this point we cannot exclude that our findings on the transcriptomic level  
638 and the ROS induction can be attributed to other cells but oligodendrocytes in our mixed culture  
639 system. However, concerning TM exposure, oligodendrocytes are the most sensitive cell type (Fig. 4B).  
640 Our hypothesis of ROS-induced oligodendrocyte toxicity is supported by previous clinical and cell  
641 biological investigations. Specifically developing human oligodendrocytes, i.e. pre-oligodendrocytes  
642 (Volpe et al. 2011; van Tilborg et al. 2016), exert a high susceptibility towards ROS. The pathognomonic  
643 relevance of ROS for impaired oligodendrogenesis is expressed in white matter injuries (WMI)  
644 occurring in premature infants. Here, free radical attack on pre-oligodendrocytes was identified as one  
645 of the major pathomechanisms responsible for the disease causing either oligodendrocyte death or  
646 oligodendrocytes with impaired cellular functions, e.g. reduced differentiation or myelination (Volpe  
647 et al. 2011). The ROS-sensitivity of pre-oligodendrocytes has multiple causes. On the one hand, it is  
648 due to their low glutathione (GSH)- and superoxide dismutase-dependent antioxidative defense, their  
649 increased expression of ROS-producing 12/15 lipoxygenase (Folkerth et al. 2004; Haynes and Van  
650 Leyen 2013) and their enormous intracellular stores of iron, which is the largest in the brain (Juurlink  
651 1997; Back et al. 1998; Marinelli et al. 2016). Iron ions in presence of hydrogen peroxide and  
652 superoxide anions catalyses formation of the highly reactive hydroxyl radical by the Haber-Weiss-  
653 reaction (Haber and Weiss 1934). Furthermore, oligodendrocytes synthesize more than 3-fold their  
654 own weight of myelin (Norton and Poduslo 1973) and facilitate membrane production of up to 100x  
655 the weight of their cell bodies per day (Ludwin 1997; McTigue and Tripathi 2008; Bradl and Lassmann  
656 2010). The myelin sheath is characterized by a high content of lipids (70 % - 85 %; Williams and Deber  
657 1993; Poitelon et al. 2020) illustrating the high vulnerability of oligodendrocytes towards ROS-initiated  
658 lipid peroxidation leading to cell death or malfunction of oligodendrocytes (Haq et al. 2003; Bezine et  
659 al. 2017).

660 In general, TM was suggested to possess antioxidative and neuroprotective properties (reviewed in  
661 Zhan et al. 2016 and Heese 2020; Xian et al. 2016). However, most studies deal with single TM  
662 components and/or are based on *in vivo* studies in adult animals (Shuchang et al. 2008; Park et al.  
663 2015; Liu et al. 2018b, 2020; Jiang et al. 2020). So far, only a few human cell-based studies reported  
664 altered ROS responses after exposure to gastrodin, one of the main components of TM. Here, gastrodin  
665 acted as an antioxidant on human retinal endothelial cells (Zhang et al. 2018), while it induced ROS-

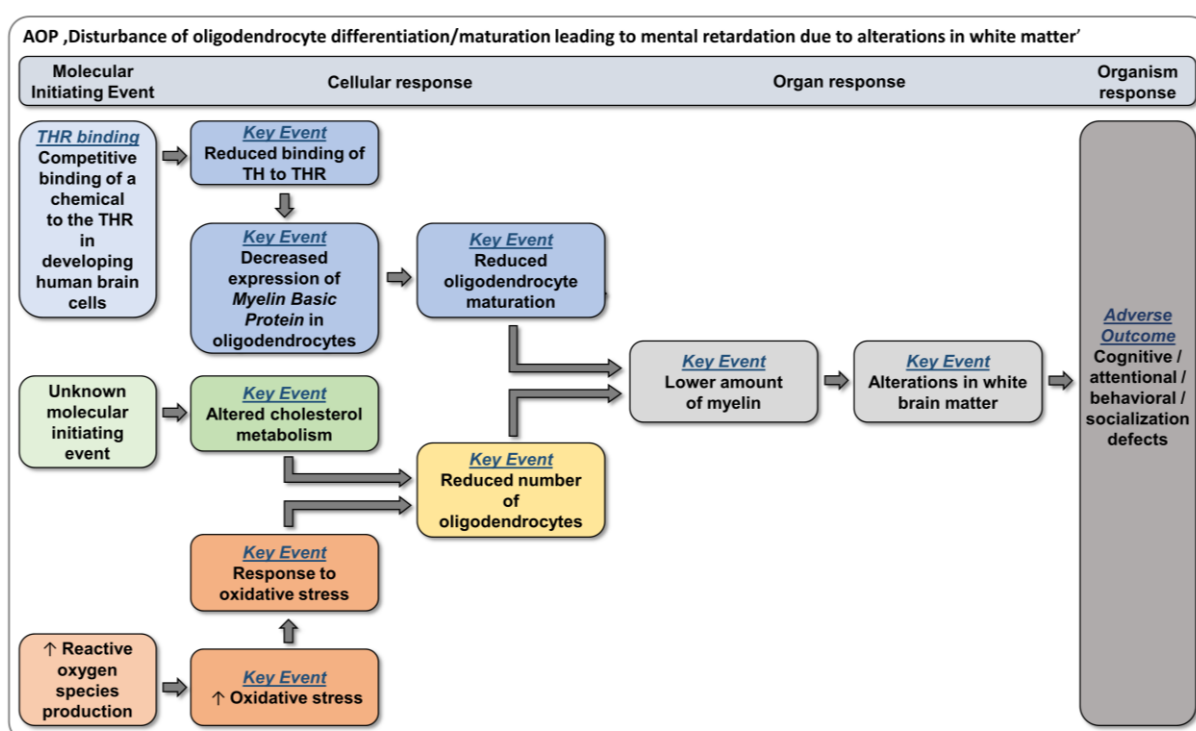
666 associated cytotoxicity in human glioblastoma cells (Liang et al. 2017). *In vivo*, TM exerted no obvious  
1 667 adverse effects, e.g. malformations, on prenatally treated rat fetuses (Yuan et al. 2013). However,  
2 668 WMI, especially more subtle forms like diffuse WMI or punctate white matter lesions (van Tilborg et  
3 669 al. 2016), were not investigated in these studies. Hence, *in vivo* effects cannot be excluded by the  
4 670 currently available data. Another possibility is that due to species differences between rodents and  
5 671 humans, an animal experiment could deliver a false-negative result. Including time-matched rat  
6 672 neurospheres into our studies (Workman et al. 2013; Baumann et al. 2014), we observed no TM-  
7 673 induced oligodendrocyte toxicity in differentiating rat NPCs, which is in strong contrast to the TM-  
8 674 induced disturbance of oligodendrocyte differentiation we detected in hNPCs (Fig. 5E). We previously  
9 675 demonstrated that human NPCs are more sensitive towards arsenite-induced oxidative stress than rat  
10 676 NPCs due to their approximately three times lower basal expression of GSH-dependent and –  
11 677 independent antioxidative defense-related genes and their lower GSH content (Masjosthusmann et al.  
12 678 2019). Regarding oxidative stress, higher protection against ROS-mediated toxicity in rodents  
13 679 compared to humans was reported for arsenite-exposed embryonic mouse brains (Allan et al. 2015),  
14 680 thalidomide-mediated toxicity in rat and rabbit whole embryo cultures (Hansen et al. 1999), embryonic  
15 681 fibroblasts *in vitro*, and adult heart tissue *in vivo* (Janssen et al. 1993; Knobloch et al. 2008). It is  
16 682 increasingly recognized that the physiology of laboratory animals often differs from human physiology  
17 683 (Knight 2007; Leist and Hartung 2013). For example, Olson et al. (2000) demonstrated that rodents  
18 684 identified only 43 % of 150 pharmaceuticals known to be toxic in humans. This is especially true for  
19 685 cellular aspects concerning the brain as central nervous system (CNS) drug development has been  
20 686 plagued by a failure to translate effective therapies from the lab to the clinic (Dragunow 2020).

37 687

#### 38 688 *Putative AOP for the disruption of oligodendrocyte development*

41 689 Combining the endophenotype of the ‘Neurosphere Assay’ with microarray analysis, we identified one  
42 690 putative MoA how TM might interfere with oligodendrocyte development. This MoA involves the  
43 691 dysregulation of a gene expression network involved in oxidative stress. Since especially pre-  
44 692 oligodendrocytes are highly susceptible towards oxidative stress, TM exposure might reduce the  
45 693 number of differentiated oligodendrocytes from hNPC by increasing intracellular ROS levels. This  
46 694 observation leads us to the implementation of a further stressor-dependent AOP with the MIE  
47 695 ‘increased reactive oxygen species production’ along with KEs connected to oxidative stress into our  
48 696 recently published stressor-based AOP network (Klose et al. 2021b; Fig. 6). Increased ROS production  
49 697 (KE257; <https://aopwiki.org/>) as a MIE was previously observed in response to oxidative stressors (e.g.  
50 698 radiation, metals and organics) and is currently under development within the AOP wiki (Song et al.  
51 699 2020b; <https://aopwiki.org/>; #238, #299, #311, #327-330, #386-387). One AOP (#17;  
52 700 <http://aopwiki.org>) already in the AOP wiki describes a linkage between oxidative stress and

701 impairment in learning and memory, yet independent of oligodendrocytes. The AOP network around  
 702 the reduced number of oligodendrocytes will therefore link to AOP #17 via the KE 'Oxidative stress'.  
 703 Moreover, both the KE 'Altered cholesterol metabolism' and KE 'Response to oxidative stress' in our  
 704 AOP network impair oligodendrocyte differentiation, thus reducing their numbers and potentially  
 705 impairing myelin production. In addition, also effects on oligodendrocyte maturation (KE 'Reduced  
 706 oligodendrocyte maturation') can in the end result in reduced brain myelin. Lower myelin causes  
 707 alterations in the white matter leading to adverse outcomes such as cognitive, attentional, behavioral,  
 708 and/or social deficits (Back et al. 2001; Gika et al. 2010; La Piana et al. 2015; Berghoff et al. 2017).  
 709 Obviously, more compounds acting via these MoA need to be identified in order to strengthen this  
 710 hypothetical AOP. In addition, KE relationships have to be experimentally established.



711  
 712 **Fig. 6: Putative AOP network for impaired oligodendrocyte development.** The previously established oligodendrocyte  
 713 development AOP network (Klose et al. 2021b) is enlarged by the MIE 'increased reactive oxygen species production' and KEs  
 714 regarding oxidative stress. ↑ = increased effects.

## 715 716 717 **Summary and conclusions**

718  
 719 In summary, we tested two selected CHMs, LGT and TM, for their potential to induce  
 720 neurodevelopmental toxicity by application of the human cell-based *in vitro* 'Neurosphere Assay',  
 721 which is part of the EFSA DNT-*in vitro* battery (Masjosthusmann et al. 2020). Both CHM caused  
 722 previously observed DNT endophenotypes, i.e. disturbed radial glia migration and impaired  
 723 oligodendrocyte differentiation. Transcriptome analyses added molecular data to the cellular

724 phenotypic observations. The LGT-induced migration endophenotype could be successfully correlated  
725 to disturbances in cell adhesion to laminin, thus mapping our new observations to an already published  
726 AOP on ‘Disrupted laminin-beta1-integrin interaction leading to developmental neurotoxicity’ (Bal-  
727 Price et al. 2016; Barenys et al. 2017a). The molecular data on TM exposure unraveled a novel stressor-  
728 dependent AOP on disturbed oligodendrocyte differentiation upon ROS accumulation along with  
729 oxidative stress that was added to the previously published AOP network on impaired oligodendrocyte  
730 development (Klose et al. 2021b). Hence, CHM are a valuable example for compounds in broad public  
731 use with insufficient hazard characterization concerning DNT. By testing whole CHM extractions,  
732 thereby covering mixtures of natural substances instead of pure compounds, we addressed a relevant  
733 “real-life” exposure scenario.

734 This study demonstrates the power of combining phenotypic with transcriptomic analyses for better  
735 understanding MoA and applying or building AOPs for DNT. Especially the multi-cellularity of the  
736 ‘Neurosphere Assay’, comprising NPCs, radial glia, neurons, astrocytes and oligodendrocytes, makes  
737 this test method an effective instrument for multiple MoA discovery due to its broad applicability  
738 domain (Masjosthusmann et al. 2020). Increasing the number of test methods to cover more KEs, such  
739 as neuronal network formation, synaptogenesis and radial-/astro-/microglia formation/function or  
740 activation, will eventually lead to larger DNT-AOP networks. Besides CHM, for most substances in our  
741 direct environment we lack information concerning their effects on neurodevelopmental endpoints  
742 (Tsuji and Crofton 2012; Fritsche et al. 2018b; Sachana et al. 2019). This concerns single compounds as  
743 well as mixtures. In the future, *in vitro* and *in vivo* toxicokinetics need to be considered for moving  
744 from hazard to risk assessment for a broad variety of substance classes to best protect the brains of  
745 our future generations.

746

## 747 References

- 748  
749 Allan AM, Hafez AK, Labrecque MT, et al (2015) Sex-dependent effects of developmental arsenic exposure on  
750 methylation capacity and methylation regulation of the glucocorticoid receptor system in the embryonic  
751 mouse brain. *Toxicol Reports* 2:1376–1390. <https://doi.org/10.1016/j.toxrep.2015.10.003>  
752 Amin S, Borrell V (2020) The Extracellular Matrix in the Evolution of Cortical Development and Folding. *Front*  
753 *Cell Dev Biol* 8:. <https://doi.org/10.3389/fcell.2020.604448>  
754 Ankley GT, Bennett RS, Erickson RJ, et al (2010) Adverse outcome pathways: A conceptual framework to  
755 support ecotoxicology research and risk assessment. *Environ Toxicol Chem* 29:730–741.  
756 <https://doi.org/10.1002/etc.34>  
757 Back SA, Gan X, Li Y, et al (1998) Maturation-dependent vulnerability of oligodendrocytes to oxidative stress-  
758 induced death caused by glutathione depletion. *J Neurosci* 18:6241–53  
759 Back SA, Luo NL, Borenstein NS, et al (2001) Late oligodendrocyte progenitors coincide with the developmental  
760 window of vulnerability for human perinatal white matter injury. *J Neurosci* 21:1302–1312.  
761 <https://doi.org/10.1523/jneurosci.21-04-01302.2001>  
762 Bal-Price A, Lein PJ, Keil KP, et al (2016) Developing and applying the adverse outcome pathway concept for  
763 understanding and predicting neurotoxicity. *Neurotoxicology*  
764 Bal-Price A, Meek ME (2017) Adverse outcome pathways: Application to enhance mechanistic understanding of  
765 neurotoxicity. *Pharmacol Ther* 179:84–95. <https://doi.org/10.1016/j.pharmthera.2017.05.006>

766 Barczyk M, Carracedo S, Gullberg D (2010) Integrins. *Cell Tissue Res* 339:269–280.  
 1 767 <https://doi.org/10.1007/s00441-009-0834-6>

2 768 Barenys M, Gassmann K, Baksmeier C, et al (2017a) Epigallocatechin gallate (EGCG) inhibits adhesion and  
 3 769 migration of neural progenitor cells in vitro. *Arch Toxicol* 91:827–837. [https://doi.org/10.1007/s00204-](https://doi.org/10.1007/s00204-016-1709-8)  
 4 770 [016-1709-8](https://doi.org/10.1007/s00204-016-1709-8)

5 771 Barenys M, Masjosthusmann S, Fritsche E (2017b) Is Intake of Flavonoid-Based Food Supplements During  
 6 772 Pregnancy Safe for the Developing Child? A Literature Review. *Curr Drug Targets* 18:196–231.  
 7 773 <https://doi.org/10.2174/1389450116666150804110049>

8 774 Barenys M, Reverte I, Masjosthusmann S, et al (2019) Developmental neurotoxicity of MDMA. A systematic  
 9 775 literature review summarized in a putative adverse outcome pathway. *Neurotoxicology* 78:209–241.  
 10 776 <https://doi.org/10.1016/j.neuro.2019.12.007>

11 777 Baroti T, Zimmermann Y, Schillinger A, et al (2016) Transcription factors Sox5 and Sox6 exert direct and indirect  
 12 778 influences on oligodendroglial migration in spinal cord and forebrain. *Glia* 64:122–138.  
 13 779 <https://doi.org/10.1002/glia.22919>

14 780 Baumann J, Barenys M, Gassmann K, Fritsche E (2014) Comparative human and rat “neurosphere assay” for  
 15 781 developmental neurotoxicity testing. *Curr Protoc Toxicol* 1:1–24.  
 16 782 <https://doi.org/10.1002/0471140856.tx1221s59>

17 783 Baumann J, Dach K, Barenys M, et al (2016) Application of the Neurosphere Assay for DNT Hazard Assessment:  
 18 784 Challenges and Limitations. *Methods Pharmacol Toxicol* 49:1–29. [https://doi.org/10.1007/7653\\_2015\\_49](https://doi.org/10.1007/7653_2015_49)

19 785 Baumann J, Dach K, Barenys M, et al (2015) Application of the Neurosphere Assay for DNT Hazard Assessment :  
 20 786 Challenges and Limitations. <https://doi.org/10.1007/7653>

21 787 Belvindrah R, Graus-Porta D, Goebbels S, et al (2007) B1 Integrins in Radial Glia But Not in Migrating Neurons  
 22 788 Are Essential for the Formation of Cell Layers in the Cerebral Cortex. *J Neurosci* 27:13854–13865.  
 23 789 <https://doi.org/10.1523/JNEUROSCI.4494-07.2007>

24 790 Berghoff SA, Gerndt N, Winchenbach J, et al (2016) Dietary cholesterol promotes repair of demyelinated lesions  
 25 791 in the adult brain. *Nat Commun* 8:. <https://doi.org/10.1038/ncomms14241>

26 792 Berghoff SA, Gerndt N, Winchenbach J, et al (2017) Dietary cholesterol promotes repair of demyelinated lesions  
 27 793 in the adult brain. *Nat Commun* 8:. <https://doi.org/10.1038/ncomms14241>

28 794 Bezine M, Debbabi M, Nury T, et al (2017) Evidence of K<sup>+</sup> homeostasis disruption in cellular dysfunction  
 29 795 triggered by 7-ketocholesterol, 24S-hydroxycholesterol, and tetracosanoic acid (C24:0) in 158N murine  
 30 796 oligodendrocytes. *Chem Phys Lipids* 207:135–150. <https://doi.org/10.1016/j.chemphyslip.2017.03.006>

31 797 Bolstad BM, Irizarry RA, Åstrand M, Speed TP (2003) A comparison of normalization methods for high density  
 32 798 oligonucleotide array data based on variance and bias. *Bioinformatics* 19:185–193.  
 33 799 <https://doi.org/10.1093/bioinformatics/19.2.185>

34 800 Borrell V, Götz M (2014) Role of radial glial cells in cerebral cortex folding. *Curr Opin Neurobiol* 27:39–46.  
 35 801 <https://doi.org/10.1016/j.conb.2014.02.007>

36 802 Bradl M, Lassmann H (2010) Oligodendrocytes: Biology and pathology. *Acta Neuropathol* 119:37–53.  
 37 803 <https://doi.org/10.1007/s00401-009-0601-5>

38 804 Carusi A, Davies MR, De Grandis G, et al (2018) Harvesting the promise of AOPs: An assessment and  
 39 805 recommendations. *Sci Total Environ* 628–629:1542–1556.  
 40 806 <https://doi.org/10.1016/j.scitotenv.2018.02.015>

41 807 Chen BJ (2001) Triptolide, a novel immunosuppressive and anti-inflammatory agent purified from a Chinese  
 42 808 herb *Tripterygium Wilfordii* Hook F. *Leuk Lymphoma* 42:253–265.  
 43 809 <https://doi.org/10.3109/10428190109064582>

44 810 Chen C, Fu YH, Li MH, et al (2019) Nuclear magnetic resonance-based metabolomics approach to evaluate  
 45 811 preventive and therapeutic effects of *Gastrodia elata* Blume on chronic atrophic gastritis. *J Pharm Biomed*  
 46 812 *Anal* 164:231–240. <https://doi.org/10.1016/j.jpba.2018.10.035>

47 813 Chen H, Chidboy MA, Robinson JF (2020) Retinoids and developmental neurotoxicity: Utilizing toxicogenomics  
 48 814 to enhance adverse outcome pathways and testing strategies. *Reprod Toxicol* 96:102–113.  
 49 815 <https://doi.org/10.1016/j.reprotox.2020.06.007>

50 816 Chen Z-L, Haegeli V, Yu H, Strickland S (2009) Cortical deficiency of laminin  $\gamma$ 1 impairs the AKT/GSK-3 $\beta$  signaling  
 51 817 pathway and leads to defects in neurite outgrowth and neuronal migration. *Dev Biol* 327:158–168.  
 52 818 <https://doi.org/10.1016/j.ydbio.2008.12.006>

53 819 Chinese Pharmacopoeia Commission (2020) Pharmacopoeia of the People’s Republic of China

54 820 Collins FS, Gray GM, Bucher JR (2008) Transforming environmental health protection. *Science* (80- ) 319:906–  
 55 821 907. <https://doi.org/10.1126/science.1154619>

56 822 Crofton KM, Mundy WR, Shafer TJ (2012) Developmental neurotoxicity testing: a path forward. *Congenit Anom*  
 57 823 (Kyoto) 52:140–146. <https://doi.org/10.1111/j.1741-4520.2012.00377.x>



824 Dai R, Wang T, Si X, et al (2017) Vasodilatory effects and underlying mechanisms of the ethyl acetate extracts  
1 825 from *Gastrodia elata*. *Can J Physiol Pharmacol* 95:564–571. <https://doi.org/10.1139/cjpp-2016-0407>  
2 826 DAVID online tool DAVID Bioinformatics Resources 6.8. <https://david.ncicrf.gov/home.jsp>  
3 827 De Groot DMG, Hartgring S, Van De Horst L, et al (2005) 2D and 3D assessment of neuropathology in rat brain  
4 828 after prenatal exposure to methylazoxymethanol, a model for developmental neurotoxicity. *Reprod*  
5 829 *Toxicol* 20:417–432. <https://doi.org/10.1016/j.reprotox.2005.04.006>  
6 830 Dragunow M (2020) Human Brain Neuropharmacology: A Platform for Translational Neuroscience. *Trends*  
7 831 *Pharmacol Sci* 41:777–792. <https://doi.org/10.1016/j.tips.2020.09.002>  
8 832 EFSA (2021) Development of Integrated Approaches to Testing and Assessment ( IATA ) on developmental  
9 833 neurotoxicity ( DNT ) risk assessment EFSA PPR Panel.  
10 834 <https://doi.org/10.2903/j.efsa.201Y.xxxx10.2903/j.efsa.201Y.xxxx>  
11 835 Fernández V, Llinares-Benadero C, Borrell V (2016) Cerebral cortex expansion and folding: what have we  
12 836 learned? *EMBO J* 35:1021–1044. <https://doi.org/10.15252/embj.201593701>  
13 837 Flaws B (2005) Chinese Medical Obstetrics, First Edit. Blue Poopy Press, Boulder, CO  
14 838 Folkerth RD, Haynes RL, Borenstein NS, et al (2004) Developmental lag in superoxide dismutases relative to  
15 839 other antioxidant enzymes in premyelinated human telencephalic white matter. *J Neuropathol Exp*  
16 840 *Neurol* 63:990–999. <https://doi.org/10.1093/jnen/63.9.990>  
17 841 Fritsche E, Barenys M, Klose J, et al (2018a) Current availability of stem cell-Based in vitro methods for  
18 842 developmental neurotoxicity (DNT) testing. *Toxicol Sci* 165:21–30. <https://doi.org/10.1093/toxsci/kfy178>  
19 843 Fritsche E, Grandjean P, Crofton KM, et al (2018b) Consensus statement on the need for innovation, transition  
20 844 and implementation of developmental neurotoxicity (DNT) testing for regulatory purposes. *Toxicol Appl*  
21 845 *Pharmacol* 354:3–6. <https://doi.org/10.1016/j.taap.2018.02.004>  
22 846 Gika AD, Siddiqui A, Hulse AJ, et al (2010) White matter abnormalities and dystonic motor disorder associated  
23 847 with mutations in the SLC16A2 gene. *Dev Med Child Neurol* 52:475–482. <https://doi.org/10.1111/j.1469-8749.2009.03471.x>  
24 848  
25 849 Glover DD, Amonkar M, Rybeck BF, Tracy TS (2003) Prescription, over-the-counter, and herbal medicine use in  
26 850 a rural, obstetric population. *Am J Obstet Gynecol* 188:1039–1045.  
27 851 <https://doi.org/10.1067/mob.2003.223>  
28 852 Graus-Porta D, Blaess S, Senften M, et al (2001)  $\beta$ 1-Class integrins regulate the development of laminae and  
29 853 folia in the cerebral and cerebellar cortex. *Neuron* 31:367–379. [https://doi.org/10.1016/S0896-6273\(01\)00374-9](https://doi.org/10.1016/S0896-6273(01)00374-9)  
30 854  
31 855 Haber F, Weiss J (1934) The Catalytic Decom position o f Hydrogen Peroxide by Iron Salts \*. 332–351  
32 856 Hansen JM, Carney EW, Harris C (1999) Differential alteration by thalidomide of the glutathione content of rat  
33 857 vs. rabbit conceptuses in vitro. *Reprod Toxicol* 13:547–554. [https://doi.org/10.1016/S0890-6238\(99\)00053-2](https://doi.org/10.1016/S0890-6238(99)00053-2)  
34 858  
35 859 Haq E, Giri S, Singh I, Singh AK (2003) Molecular mechanism of psychosine-induced cell death in human  
36 860 oligodendrocyte cell line. *J Neurochem* 86:1428–1440. <https://doi.org/10.1046/j.1471-4159.2003.01941.x>  
37 861  
38 862 Haynes RL, Van Leyen K (2013) 12/15-Lipoxygenase Expression Is Increased in Oligodendrocytes and Microglia  
39 863 of Periventricular Leukomalacia. *Dev Neurosci* 35:140–154. <https://doi.org/10.1159/000350230>  
40 864 He Y, Shi S, Zhang R, et al (2013) Determination of main effective components in tripterygium glycosides.  
41 865 Original in Chinese: 何昱,石森林,张茹萍,钱家健,范永升.雷公藤多苷主要有效成分的含量研究[J].药物  
42 866 分析杂志. *Chinese J Pharm Anal* 33:197-200(4)  
43 867 Heese K (2020) *Gastrodia elata* Blume (Tianma): Hope for Brain Aging and Dementia. *Evidence-based*  
44 868 *Complement Altern Med* 2020:. <https://doi.org/10.1155/2020/8870148>  
45 869 Hemminki E, Mantyranta T, Maili M, Paivikki K (1991) A survey on the use of alternative drugs during  
46 870 pregnancy. *J Mich Dent Assoc* 66:63–67  
47 871 Hollyer T, Boon H, Georgousis A, et al (2002) The use of CAM by women suffering from nausea and vomiting  
48 872 during pregnancy. *BMC Complement Altern Med* 2:1–6. <https://doi.org/10.1186/1472-6882-2-5>  
49 873 <https://aopwiki.org/> <https://aopwiki.org/>  
50 874 Huang CL, Wang KC, Yang YC, et al (2018) *Gastrodia elata* alleviates mutant huntingtin aggregation through  
51 875 mitochondrial function and biogenesis mediation. *Phytomedicine* 39:75–84.  
52 876 <https://doi.org/10.1016/j.phymed.2017.12.017>  
53 877 Huang J (1985) A preliminary study on the pharmacological effects of *Gastrodia* injection and *Gastroside*.  
54 878 Original in Chinese: 黄俊华. 天麻注射液及天麻甙药理作用的初步研究[J]. 中国医学科学院学报. *Acta*  
55 879 *Acad Med Sin* 005:  
56 880 Humphries JD, Byron A, Humphries MJ (2006) Integrin ligands at a glance. *J Cell Sci* 119:3901–3903.

- 881 <https://doi.org/10.1242/jcs.03098>.INTEGRIN
- 1 882 Hynes RO (2002) Integrins: Bidirectional, allosteric signaling machines. *Cell* 110:673–687.
- 2 883 [https://doi.org/10.1016/S0092-8674\(02\)00971-6](https://doi.org/10.1016/S0092-8674(02)00971-6)
- 3 884 Janssen M, Van Der Meer P, De Jong JW (1993) Antioxidant defences in rat, pig, Guinea pig, and human hearts:
- 4 885 Comparison with xanthine oxidoreductase activity. *Cardiovasc Res* 27:2052–2057.
- 5 886 <https://doi.org/10.1093/cvr/27.11.2052>
- 6 887 Jeffries MA, Urbanek K, Torres L, et al (2016) ERK1/2 activation in preexisting oligodendrocytes of adult mice
- 7 888 drives new myelin synthesis and enhanced CNS function. *J Neurosci* 36:9186–9200.
- 8 889 <https://doi.org/10.1523/JNEUROSCI.1444-16.2016>
- 9 890 Jiang T, Cheng H, Su J, et al (2020) Gastrodin protects against glutamate-induced ferroptosis in HT-22 cells
- 10 891 through Nrf2/HO-1 signaling pathway. *Toxicol Vitro* 62:104715. <https://doi.org/10.1016/j.tiv.2019.104715>
- 11 892 Juurlink BH (1997) Response of glial cells to ischemia: roles of reactive oxygen species and glutathione.
- 12 893 *Neurosci Biobehav Rev* 21:151–66
- 13 894 Kandel ER, Schwartz JH, Jessell TM (2000) Principles of neural science 4th edition, 4th edn. McGraw-Hill, New
- 14 895 York
- 15 896 Klose J, Pahl M, Bartmann K, et al (2021a) Neurodevelopmental toxicity assessment of flame retardants using a
- 16 897 human DNT in vitro testing battery. *Cell Biol Toxicol* 1–27. <https://doi.org/10.1007/s10565-021-09603-2>
- 17 898 Klose J, Tigges J, Masjosthusmann S, et al (2021b) TBBPA targets converging key events of human
- 18 899 oligodendrocyte development resulting in two novel AOPs. *ALTEX* 38:215–234.
- 19 900 <https://doi.org/10.14573/altex.2007201>
- 20 901 Knight A (2007) Animal experiments scrutinised: Systematic reviews demonstrate poor human clinical and
- 21 902 toxicological utility. *ALTEX* 24:320–325. <https://doi.org/10.14573/altex.2007.4.320>
- 22 903 Knobloch J, Reimann K, Klotz LO, Rütger U (2008) Thalidomide resistance is based on the capacity of the
- 23 904 glutathione- dependent antioxidant defense. *Mol Pharm* 5:1138–1144.
- 24 905 <https://doi.org/10.1021/mp8001232>
- 25 906 Kong X, Zhang Y, Liu C, et al (2013) Anti-Angiogenic Effect of Triptolide in Rheumatoid Arthritis by Targeting
- 26 907 Angiogenic Cascade. *PLoS One* 8:1–10. <https://doi.org/10.1371/journal.pone.0077513>
- 27 908 Kühne BA, Puig T, Ruiz-Martínez S, et al (2019) Comparison of migration disturbance potency of
- 28 909 epigallocatechin gallate (EGCG) synthetic analogs and EGCG PEGylated PLGA nanoparticles in rat
- 29 910 neurospheres. *Food Chem Toxicol* 123:195–204. <https://doi.org/10.1016/j.fct.2018.10.055>
- 30 911 La Piana R, Vanasse M, Brais B, Bernard G (2015) Myelination Delay and Allan-Herndon-Dudley Syndrome
- 31 912 Caused by a Novel Mutation in the SLC16A2 Gene. *J Child Neurol* 30:1371–1374.
- 32 913 <https://doi.org/10.1177/0883073814555189>
- 33 914 Langseth AJ, Munji RN, Choe Y, et al (2010) Wnts influence the timing and efficiency of oligodendrocyte
- 34 915 precursor cell generation in the telencephalon. *J Neurosci* 30:13367–13372.
- 35 916 <https://doi.org/10.1523/JNEUROSCI.1934-10.2010>
- 36 917 Lein P, Silbergeld E, Locke P, Goldberg AM (2005) In vitro and other alternative approaches to developmental
- 37 918 neurotoxicity testing (DNT). *Environ Toxicololology Pharmacol* 19:735–744.
- 38 919 <https://doi.org/10.1016/j.etap.2004.12.035>
- 39 920 Leist M, Hartung T (2013) Inflammatory findings on species extrapolations: Humans are definitely no 70-kg
- 40 921 mice. *Arch Toxicol* 87:563–567. <https://doi.org/10.1007/s00204-013-1038-0>
- 41 922 Li J, Settivari R, LeBaron MJ, Marty MS (2019a) An industry perspective: A streamlined screening strategy using
- 42 923 alternative models for chemical assessment of developmental neurotoxicity. *Neurotoxicology* 73:17–30.
- 43 924 <https://doi.org/10.1016/j.neuro.2019.02.010>
- 44 925 Li L, Leung PC, Chung TKH, Wang CC (2013) Systematic review of Chinese Medicine for miscarriage during early
- 45 926 pregnancy. *Evidence-based Complement Altern Med* 2014:. <https://doi.org/10.1155/2014/753856>
- 46 927 Li L, Li R, Zacharek A, et al (2020a) ABCA1 / ApoE / HDL Signaling Pathway Facilitates Myelination and
- 47 928 Oligodendrogenesis after Stroke. *Int J Mol Sci* 21:1–18. <https://doi.org/doi:10.3390/ijms21124369>
- 48 929 Li L, Yin Tang L, Liang B, et al (2019b) Evaluation of in vitro embryotoxicity tests for Chinese herbal medicines.
- 49 930 *Reprod Toxicol* 89:45–53. <https://doi.org/10.1016/j.reprotox.2019.06.001>
- 50 931 Li M, Wang J, Fu L, et al (2020b) Network pharmacology-based prediction and verification of qingluo tongbi
- 51 932 formula to reduce liver toxicity of tripterygium wilfordii via UGT2B7 in endoplasmic reticulum. *Med Sci*
- 52 933 *Monit* 26:1–11. <https://doi.org/10.12659/MSM.920376>
- 53 934 Liang WZ, Jan CR, Hsu SS (2017) Cytotoxic effects of gastrodin extracted from the rhizome of *Gastrodia elata*
- 54 935 Blume in glioblastoma cells, but not in normal astrocytes, via the induction of oxidative stress-associated
- 55 936 apoptosis that involved cell cycle arrest and p53 activation. *Food Chem Toxicol* 107:280–292.
- 56 937 <https://doi.org/10.1016/j.fct.2017.07.013>
- 57 938 Lin YE, Chou ST, Lin SH, et al (2017) Antidepressant-like effects of water extract of *Gastrodia elata* Blume on

- 939 neurotrophic regulation in a chronic social defeat stress model. *J Ethnopharmacol* 215:132–139.  
1 940 <https://doi.org/10.1016/j.jep.2017.12.044>
- 2 941 Liu G, Dai D, Rao J, et al (1974) Neuropharmacological study of vanillin from *gastrodia elata*. Original in Chinese:  
3 942 刘国卿, 戴德哉, 饶经玲, 蔡鸿生, 徐赪本. 天麻成分香荚兰醇的神经药理研究. *Chinese Tradit Herb*  
4 943 *Drugs* 5:
- 5 944 Liu L, Zhao H, Sun X, et al (2018a) Efficacy and safety of *Tripterygium wilfordii hook F* for chronic urticaria: A  
6 945 systematic review and meta-analysis. *BMC Complement Altern Med* 18:. [https://doi.org/10.1186/s12906-](https://doi.org/10.1186/s12906-018-2305-7)  
7 946 [018-2305-7](https://doi.org/10.1186/s12906-018-2305-7)
- 8 947 Liu X chang, Wu C zhu, Hu X fei, et al (2020) *Gastrodin* Attenuates Neuronal Apoptosis and Neurological Deficits  
9 948 after Experimental Intracerebral Hemorrhage. *J Stroke Cerebrovasc Dis* 29:104483.  
10 949 <https://doi.org/10.1016/j.jstrokecerebrovasdis.2019.104483>
- 11 950 Liu Y, Gao J, Peng M, et al (2018b) A review on central nervous system effects of *gastrodin*. *Front Pharmacol* 9:.  
12 951 <https://doi.org/10.3389/fphar.2018.00024>
- 13 952 Long KR, Huttner WB (2019) How the extracellular matrix shapes neural development. *Open Biol* 9:.  
14 953 <https://doi.org/10.1098/rsob.180216>
- 15 954 Lu M, Krauss RS (2010) N-cadherin ligation, but not Sonic hedgehog binding, initiates Cdo-dependent p38 $\alpha$ / $\beta$   
16 955 MAPK signaling in skeletal myoblasts. *Proc Natl Acad Sci U S A* 107:4212–4217.  
17 956 <https://doi.org/10.1073/pnas.0908883107>
- 18 957 Lubbers BR, Smit AB, Spijker S, van den Oever MC (2014) *Neural ECM in addiction, schizophrenia, and mood*  
19 958 *disorder*, 1st edn. Elsevier B.V.
- 20 959 Ludwin SK (1997) The Pathobiology of the Oligodendrocyte. *J Neuropathol Exp Neurol* 56:111–124.  
21 960 <https://doi.org/10.1097/00005072-199702000-00001>
- 22 961 Manavalan A, Ramachandran U, Sundaramurthi H, Mishra M (2012) *Gastrodia elata* Blume (tianma) mobilizes  
23 962 neuro-protective capacities. 3:219–241
- 24 963 Marinelli C, Bertalot T, Zusso M, et al (2016) Systematic Review of Pharmacological Properties of the  
25 964 Oligodendrocyte Lineage. *Front Cell Neurosci* 10:1–27. <https://doi.org/10.3389/fncel.2016.00027>
- 26 965 Masjosthusmann S, Becker D, Petzuch B, et al (2018) A transcriptome comparison of time-matched developing  
27 966 human, mouse and rat neural progenitor cells reveals human uniqueness. *Toxicol Appl Pharmacol*  
28 967 354:40–55. <https://doi.org/10.1016/j.taap.2018.05.009>
- 29 968 Masjosthusmann S, Blum J, Bartmann K, et al (2020) Establishment of an a priori protocol for the  
30 969 implementation and interpretation of an in-vitro testing battery for the assessment of developmental  
31 970 neurotoxicity. *EFSA Support Publ* 17:1–142. <https://doi.org/10.2903/sp.efsa.2020.en-1938>
- 32 971 Masjosthusmann S, Siebert C, Hübenthal U, et al (2019) Arsenite interrupts neurodevelopmental processes of  
33 972 human and rat neural progenitor cells: The role of reactive oxygen species and species-specific  
34 973 antioxidative defense. *Chemosphere* 235:447–456. <https://doi.org/10.1016/j.chemosphere.2019.06.123>
- 35 974 McTigue DM, Tripathi RB (2008) The life, death, and replacement of oligodendrocytes in the adult CNS. *J*  
36 975 *Neurochem* 107:1–19. <https://doi.org/10.1111/j.1471-4159.2008.05570.x>
- 37 976 Moors M, Cline JE, Abel J, Fritsche E (2007) ERK-dependent and -independent pathways trigger human neural  
38 977 progenitor cell migration. *Toxicol Appl Pharmacol* 221:57–67. <https://doi.org/10.1016/j.taap.2007.02.018>
- 39 978 Nimtz L, Kloese J, Masjosthusmann S, et al (2019) The Neurosphere Assay as an In Vitro Method for  
40 979 Developmental Neurotoxicity (DNT) Evaluation. In: *Cell Culture Techniques, Neuromethods*. pp 141–168
- 41 980 Nordeng H, Havnen GC (2004) Use of herbal drugs in pregnancy: A survey among 400 Norwegian women.  
42 981 *Pharmacoepidemiol Drug Saf* 13:371–380. <https://doi.org/10.1002/pds.945>
- 43 982 Norton WT, Poduslo SE (1973) Myelination in Rat Brain: Changes in Myelin Composition During Brain  
44 983 Maturation. *J Neurochem* 21:759–773. <https://doi.org/10.1111/j.1471-4159.1973.tb07520.x>
- 45 984 NRC (2007) *Toxicity Testing in the 21st Century: A Vision and a Strategy*
- 46 985 OECD (2020) *Overview of Concepts and Available Guidance related to Integrated Approaches to Testing and*  
47 986 *Assessment (IATA)*, Series on Testing and Assessment No. 329. *Environ Heal Safety, Environ Dir OECD*
- 48 987 *OECD (2016) Guidance Document for the Use of Adverse Outcome Pathways in Developing Integrated*  
49 988 *Approaches to Testing and Assessment (IATA)*, Series on Testing & Assessment No. 260. *OECD Guidel Test*  
50 989 *Chem*
- 51 990 Olson H, Betton G, Robinson D, et al (2000) Concordance of the toxicity of pharmaceuticals in humans and in  
52 991 animals. *Regul Toxicol Pharmacol* 32:56–67. <https://doi.org/10.1006/rtph.2000.1399>
- 53 992 Park Y-M, Lee B-G, Park S-H, et al (2015) Prolonged oral administration of *Gastrodia elata* extract improves  
54 993 spatial learning and memory of scopolamine-treated rats . *Lab Anim Res* 31:69.  
55 994 <https://doi.org/10.5625/lar.2015.31.2.69>
- 56 995 Poitelon Y, Kopec AM, Belin S (2020) Myelin Fat Facts: An Overview of Lipids and Fatty Acid Metabolism. *Cells*  
57 996 9:812. <https://doi.org/10.3390/cells9040812>

- 997 Powell DR, Williams JS, Hernandez-Lagunas L, et al (2015) Cdon promotes neural crest migration by regulating  
1 998 N-cadherin localization. *Dev Biol* 407:289–299. <https://doi.org/10.1016/j.ydbio.2015.07.025>
- 2 999 Rice D, Barone S, Perspectives EH, et al (2000) Critical Periods of Vulnerability for the Developing Nervous  
3 1000 System : Evidence from Humans and Animal Models Critical Periods of Vulnerability for the Developing  
4 1001 Nervous System : Evidence from Humans and Animal Models Development of the Brain in Utero.  
5 1002 108:511–533. <https://doi.org/10.1289/ehp.00108s3511>
- 6 1003 Rodier PM (1994) Vulnerable periods and processes during central nervous system development. *Environ*  
7 1004 *Health Perspect* 102:121–124. <https://doi.org/10.1289/ehp.94102121>
- 8 1005 Rothwell JA, Perez-Jimenez J, Neveu V, et al (2013) Phenol-Explorer 3.0: A major update of the Phenol-Explorer  
9 1006 database to incorporate data on the effects of food processing on polyphenol content. *Database* 2013:1–  
10 1007 8. <https://doi.org/10.1093/database/bat070>
- 11 1008 Sachana M, Bal-Price A, Crofton KM, et al (2019) International regulatory and scientific effort for improved  
12 1009 developmental neurotoxicity testing. *Toxicol Sci* 167:45–57. <https://doi.org/10.1093/toxsci/kfy211>
- 13 1010 Sachana M, Shafer TJ, Terron A (2021) Toward a better testing paradigm for developmental neurotoxicity: Oecd  
14 1011 efforts and regulatory considerations. *Biology (Basel)* 10:1–11. <https://doi.org/10.3390/biology10020086>
- 15 1012 Schmuck MR, Temme T, Dach K, et al (2016) Omnisphero: a high-content image analysis (HCA) approach for  
16 1013 phenotypic developmental neurotoxicity (DNT) screenings of organoid neurosphere cultures in vitro. *Arch*  
17 1014 *Toxicol* 1–12. <https://doi.org/10.1007/s00204-016-1852-2>
- 18 1015 Shen D-H, Chang H-W (1963) The Anticonvulsant and Analgesic Activities of Tian-Ma (*Gastrodia Elata* Blume)  
19 1016 Original in Chinese: 沈道修, 张效文. 天麻的抗惊与镇痛作用[J]. *药学学报*. *Acta Pharm Sin* 10:  
20 1017 Shimizu T, Kagawa T, Wada T, et al (2005) Wnt signaling controls the timing of oligodendrocyte development in  
21 1018 the spinal cord. *Dev Biol* 282:397–410. <https://doi.org/10.1016/j.ydbio.2005.03.020>
- 22 1019 Shuchang H, Qiao N, Piye N, et al (2008) Protective effects of *gastrodia elata* on aluminium-chloride- induced  
23 1020 learning impairments and alterations of amino acid neurotransmitter release in adult rats. *Restor Neurol*  
24 1021 *Neurosci* 26:467–473
- 25 1022 Silbereis JC, Pochareddy S, Zhu Y, et al (2016) The Cellular and Molecular Landscapes of the Developing Human  
26 1023 Central Nervous System. *Neuron* 89:248. <https://doi.org/10.1016/j.neuron.2015.12.008>
- 27 1024 Song X, Zhang Y, Dai E (2020a) Therapeutic targets of thunder god vine (*Tripterygium wilfordii* hook) in  
28 1025 rheumatoid arthritis. *Mol Med Rep* 21:2303–2310. <https://doi.org/10.3892/mmr.2020.11052>
- 29 1026 Song Y, Xie L, Lee YK, et al (2020b) Integrative assessment of low-dose gamma radiation effects on *Daphnia*  
30 1027 *magna* reproduction: Toxicity pathway assembly and AOP development. *Sci Total Environ* 705:135912.  
31 1028 <https://doi.org/10.1016/j.scitotenv.2019.135912>
- 32 1029 Spinu N, Bal-Price A, Cronin MTD, et al (2019) Development and analysis of an adverse outcome pathway  
33 1030 network for human neurotoxicity. *Arch Toxicol* 93:2759–2772. <https://doi.org/10.1007/s00204-019-02551-1>
- 34 1031 Tenzen T, Allen BL, Cole F, et al (2006) The Cell Surface Membrane Proteins Cdo and Boc Are Components and  
35 1032 Targets of the Hedgehog Signaling Pathway and Feedback Network in Mice. *Dev Cell* 10:647–656.  
36 1033 <https://doi.org/10.1016/j.devcel.2006.04.004>
- 37 1034 Terron A, Bennekou Hougaard S (2018) Towards a regulatory use of alternative developmental neurotoxicity  
38 1035 testing (DNT). *Toxicol Appl Pharmacol* 354:19–23. <https://doi.org/10.1016/j.taap.2018.02.002>
- 39 1036 Terzioglu Bebitoglu B (2020) Frequently used herbal teas during pregnancy - Short update. *Medeni Med J*  
40 1037 35:55–61. <https://doi.org/10.5222/MMJ.2020.69851>
- 41 1038 Tsuji R, Crofton KM (2012) Developmental neurotoxicity guideline study: Issues with methodology, evaluation  
42 1039 and regulation. *Congenit Anom (Kyoto)* 52:122–128. <https://doi.org/10.1111/j.1741-4520.2012.00374.x>
- 43 1040 Tzu J, Marinkovich PM (2008) Bridging structure with function: Structural, regulatory, and developmental role  
44 1041 of laminins. *Int J Biochem Cell Biol* 40:199–214. <https://doi.org/10.1016/j.biocel.2007.07.015>. BRIDGING
- 45 1042 van Tilborg E, Heijnen CJ, Benders MJ, et al (2016) Impaired oligodendrocyte maturation in preterm infants:  
46 1043 Potential therapeutic targets. *Prog Neurobiol* 136:28–49.  
47 1044 <https://doi.org/10.1016/j.pneurobio.2015.11.002>
- 48 1045 Vinken M, Knapen D, Vergauwen L, et al (2017) Adverse outcome pathways: a concise introduction for  
49 1046 toxicologists. *Arch Toxicol* 91:3697–3707. <https://doi.org/10.1007/s00204-017-2020-z>
- 50 1047 Volpe JJ, Kinney HC, Jensen FE, Rosenberg PA (2011) The developing oligodendrocyte: Key cellular target in  
51 1048 brain injury in the premature infant. *Int J Dev Neurosci* 29:423–440.  
52 1049 <https://doi.org/10.1016/j.ijdevneu.2011.02.012>
- 53 1050 Walter KM, Dach K, Hayakawa K, et al (2019) Ontogenetic expression of thyroid hormone signaling genes: An in  
54 1051 vitro and in vivo species comparison. *PLoS One* 14:1–26. <https://doi.org/10.1371/journal.pone.0221230>
- 55 1052 Wang H, Zhang R, Qiao Y, et al (2014) *Gastrodin* ameliorates depression-like behaviors and up-regulates  
56 1053 proliferation of hippocampal-derived neural stem cells in rats: Involvement of its anti-inflammatory  
57 1054

1055 action. *Behav Brain Res* 266:153–160. <https://doi.org/10.1016/j.bbr.2014.02.046>

11056 Wang J, Chen N, Fang L, et al (2018) A Systematic Review about the Efficacy and Safety of *Tripterygium wilfordii*

11057 Hook.f. Preparations Used for the Management of Rheumatoid Arthritis. *Evidence-Based Complement*

11058 *Altern Med* 2018:. <https://doi.org/10.1155/2018/1567463>

11059 Wang Q, Meng J, Dong A, et al (2016) The pharmacological effects and mechanism of *tripterygium wilfordii*

11060 Hook F in central nervous system autoimmunity. *J Altern Complement Med* 22:496–502.

11061 <https://doi.org/10.1089/acm.2016.0004>

11062 Wang Y, Wang B, Yang X (2020) The Study of Cellular Mechanism of Triptolide in the Treatment of Cancer, Bone

11063 Loss and Cardiovascular Disease and Triptolide's Toxicity. *Curr Stem Cell Res Ther* 15:18–23.

11064 <https://doi.org/10.2174/1574888X14666190301155810>

11065 Warren M, Bradley WD, Gourley SL, et al (2012) Integrin  $\beta 1$  signals through Arg to regulate postnatal dendritic

11066 arborization, synapse density, and behavior. *J Neurosci* 32:2824–2834.

11067 <https://doi.org/10.1523/JNEUROSCI.3942-11.2012>

11068 Williams KA, Deber CM (1993) The Structure and Function of Central Nervous System Myelin. *Clin Lab Sci*

11069 30:29–64

11070 Workman AD, Charvet CJ, Clancy B, et al (2013) Modeling transformations of neurodevelopmental sequences

11071 across mammalian species. *J Neurosci* 33:7368–7383. <https://doi.org/10.1523/JNEUROSCI.5746-12.2013>

11072 Xian JW, Choi AYT, Lau CBS, et al (2016) *Gastrodia* and *Uncaria* (*tianma gouteng*) water extract exerts

11073 antioxidative and antiapoptotic effects against cerebral ischemia in vitro and in vivo. *Chinese Med*

11074 (United Kingdom) 11:1–12. <https://doi.org/10.1186/S13020-016-0097-6>

11075 Yuan F, Feng Y, Li Y, et al (2013) Embryotoxicity study of Tian Ma powder in SD rats. Original in Chinese: 袁芳,

11076 冯玉茹, 李勇, 曹倩倩, 何夏萍. 天麻药材粉对SD大鼠的胚胎发育毒性. *Chin J Pharmacol Toxicol*

11077 27:604–605

11078 Zhan HD, Zhou HY, Sui YP, et al (2016) The rhizome of *Gastrodia elata* Blume – An ethnopharmacological

11079 review. *J Ethnopharmacol* 189:361–385. <https://doi.org/10.1016/j.jep.2016.06.057>

11080 Zhang Q, Chen Z, Lin C (1980) Study on Antitumor, Toxicity and Immune Function of *Hexaganthes* Chinese.

11081 Original in Chinese: 张覃沐, 陈正玉, 林晨. 六方藤的抗肿瘤、毒性及其对免疫功能影响的研究. *J*

11082 *Pharm* 15:46–46

11083 Zhang TH, Huang CM, Gao X, et al (2018) *Gastrodin* inhibits high glucose-induced human retinal endothelial cell

11084 apoptosis by regulating the SIRT1/TLR4/NF- $\kappa$ Bp65 signaling pathway. *Mol Med Rep* 17:7774–7780.

11085 <https://doi.org/10.3892/mmr.2018.8841>

11086 Zhang W, Kang JS, Cole F, et al (2006) Cdo Functions at Multiple Points in the Sonic Hedgehog Pathway, and

11087 Cdo-Deficient Mice Accurately Model Human Holoprosencephaly. *Dev Cell* 10:657–665.

11088 <https://doi.org/10.1016/j.devcel.2006.04.005>

11089 Zhang Y, Huang G, Xing S (1983) Experimental pathological study on rats poisoned by *tripterygium wilfordii*.

11090 Original in Chinese: 张益鹤, 黄光照, 邢素兰. 雷公藤中毒的大鼠实验病理研究. *J Integr Med* 6:360–362

11091 Zhen J (1983) Study on Toxicity of Total Glycosides of *Tripterygium Wilfordii* (T II). Original in Chinese: 郑家润.

11092 雷公藤总甙(T II)的毒性研究. *Acta Acad Med Sin* 002:

11093 Zhen Y, Lin J, Lin C (1994) Anti-inflammatory effect of triptolide. Original in Chinese: 郑幼兰, 林建峰, 林承才, 徐

11094 娅. 雷公藤内酯的抗炎作用. *Acta Pharmacol Sin* 06:62–65

11095 Zhen Y, Ye J, Lin D, Chen W (1982) Anti-inflammatory effect of *Tripterygium wilfordii*. Original in Chinese: 郑幼

11096 兰, 叶聚荣, 林大杰, 陈文雄. 雷公藤的抗炎作用. *Fujian Med J* 1:36–37

1103           **Declarations**

1  
2  
3  
4  
5  
6  
7  
8  
9  
10  
11  
12  
13  
14  
15  
16  
17  
18  
19  
20  
21  
22  
23  
24  
25  
26  
27  
28  
29  
30  
31  
32  
33  
34  
35  
36  
37  
38  
39  
40  
41  
42  
43  
44  
45  
46  
47  
48  
49  
50  
51  
52  
53  
54  
55  
56  
57  
58  
59  
60  
61  
62  
63  
64  
65

**Funding:** This work was supported by the FOKO (“Forschungskommission” of the medical faculty of the Heinrich-Heine-University) [2016-53], EFSA (European Food Safety Authority) [OC/EFSA/PRAS/2017/01], CERST (Center for Alternatives to Animal Testing) of the Ministry for Culture and Science of the State of North-Rhine Westphalia, Germany) [file number 233-1.08.03.03-121972/131 – 1.08.03.03 – 121972], DFG “Ursula M. Händel Tierschutzpreis” to Prof. Ellen Fritsche [DFG FR 1392/6-1] and the Zhejiang Provincial Natural Science Foundation of China [LY20H180004].

**Conflict of interest:** The authors declare no conflicts of interest.

**Ethics approval:** hNPCs were purchased from Lonza Verviers SPRL, Belgium and work was approved by the ethics committee of the Heinrich-Heine University Duesseldorf. The preparation of rat brains was approved by the “Landesamt für Natur, Umwelt und Verbraucherschutz” (81-02.05.50.18.001) and performed according to the law on animal welfare §4 Abs. 3 Tierschutzgesetz (TierSchG).



1 **Supplementary Material**

2

3 **Application of the Adverse Outcome Pathway concept for investigating**  
4 **developmental neurotoxicity potential of Chinese Herbal Medicines by using**  
5 **human neural progenitor cells *in vitro***  
6

7 Jördis Klose<sup>1\*</sup>, Lu Li<sup>2,3,4,9\*</sup>, Farina Bendt<sup>1</sup>, Ulrike Hübenthal<sup>1</sup>, Christian Jüngst<sup>5</sup>, Patrick Petzsch<sup>6</sup>,  
8 Astrid Schauss<sup>5</sup>, Karl Köhrer<sup>6</sup>, Ping Chung Leung<sup>4</sup>, Chi Chiu Wang<sup>3,7</sup>, Katharina Koch<sup>1</sup>, Julia  
9 Tigges<sup>1</sup>, Xiaohui Fan<sup>2,9†</sup>, Ellen Fritsche<sup>1,7,8†</sup>

10

11 <sup>1</sup> IUF-Leibniz Research Institute for Environmental Medicine, Auf'm Hennekamp 50, 40225 Duesseldorf, NRW,  
12 Germany

13 <sup>2</sup> College of Pharmaceutical Sciences, Zhejiang University, Hangzhou, China

14 <sup>3</sup> Department of Obstetrics & Gynaecology; Li Ka Shing Institute of Health Sciences; School of Biomedical Sciences,  
15 The Chinese University of Hong Kong, Shatin, N.T., Hong Kong

16 <sup>4</sup> Institute of Chinese Medicine, The Chinese University of Hong Kong, Shatin, N.T., Hong Kong

17 <sup>5</sup> CECAD Imaging Facility, CECAD Forschungszentrum Cologne, Joseph-Stelzmann-Str. 26, 50931 Cologne, NRW,  
18 Germany

19 <sup>6</sup> Biological and Medical Research Centre (BMFZ), Medical Faculty, Heinrich-Heine-University, Universitätsstraße  
20 1, 40225 Duesseldorf, NRW, Germany

21 <sup>7</sup> College of Basic Medical Sciences, Zhejiang Chinese Medical University, Hangzhou, China

22 <sup>8</sup> Medical Faculty, Heinrich-Heine-University, Universitätsstraße 1, 40225 Duesseldorf, NRW, Germany

23 <sup>9</sup> Innovation Center in Zhejiang University, State Key Laboratory of Component-Based Chinese Medicine,  
24 Hangzhou, China

25

26 Correspondence: Prof. Dr. Ellen Fritsche  
27 Phone: +49 (0) 211 3389 217  
28 E-Mail: [ellen.fritsche@uni-duesseldorf.de](mailto:ellen.fritsche@uni-duesseldorf.de)  
29

30 \* † authors contributed equally

31

32

33

34 **Supplementary Table S1:** LD<sub>50</sub> values of the Tian Ma and Lei Gong Teng extracts as well as of single components.

CHM extract / components	Administration	Species	LD <sub>50</sub>	Reference
TM (whole extract)	intraperitoneally	mouse (male)	61.4 g/kg	(Shen and Chang 1963)
	intraperitoneally	mouse (female)	51.4 g/kg	
	intravenously	mouse	39.8 g/kg	(Huang 1985)
Vanillic alcohol	intraperitoneally	mouse	891.3 mg/kg	(Liu et al. 1974)
Vanillin	intraperitoneally	mouse	946.0 mg/kg	
LGT (whole extract)	<i>intra</i> gastrically	mouse	112.0 g/kg	(Zhen et al. 1982)
	intraperitoneally	mouse	50.5 g/kg	
Total glycoside	<i>intra</i> gastrically	mouse	159.7 mg/kg	(Zhen 1983)
	intraperitoneally	mouse	93.9 mg/kg	
Root bark decoction	<i>intra</i> gastrically	rat (female)	21.6 g/kg	(Zhang et al. 1983)
Triptolide	intraperitoneally	mouse	1.41 mg/kg	(Zhang et al. 1980)
	intravenously	mouse	0.80 mg/kg	(Zhen et al. 1994)
	intraperitoneally	mouse	0.90 mg/kg	
	intravenously	dog	160.0 µg/kg	

35

36

37 **Supplementary Table S2:** Ingredients included in extractions of Lei Gong Teng and Tian Ma. Research was based on records  
38 in Chinese Pharmacopoeia and/or literatures. Divided in respective parts of the plant.

CHM	Part of plant	Main components/compounds
Tian Ma ( <i>Gastrodia elata</i> Blume)	Rhizoma	Gastrodin
		Gastrodioside
		p-hydroxybenzyl alcohol
		p-hydroxybenzaldehyd
		4-hydroxybenzyl methyl ether
		4- (4'-hydroxybenzyloxy)- benzyl methyl ether
		Bis-(4-hydroxybenzyloxy) ether
		Vanillyl alcohol
		Citric acid
		Methyl citrate
		Succinic acid
		Palmitic acid
		β-sitosterol
		Daucosterol
		Sucrose
	Stem/root /rootstock	Gastrodia antifungal protein
		Chitinase
		β-1,3-glucanase
		Gastrodia elata polysaccharide
		Trace elements: Fe / F / Mn / Zn / Sr / I / Cu
	Fresh plant	Gastrodin
		p-hydroxybenzyl alcohol
		p-hydroxybenzaldehyd
		3,4-dihydroxybenzyloxybenzaldehyde
		4,4-dihydroxydiphenyl methane
		p-hydroxybenzyl ethyl ether
		4,4-dihydroxydibenzyl ether
		4-ethoxymethylphenyl-4'-hydroxybenzyl ether
		Tris-[4-(β-D-glucopyranosyloxy)-benzyl] citrate, Parishin
		4-ethoxymethylphenol

CHM	Part of plant	Main components/compounds	
Lei Gong Teng (Common Threewingnut Root)	Root	Wilfordine	Celacinnine
		Wilforine	Celafurine
		Wilforgine	Wilforlide A, B
		Wilfortrine	Triptonoterpenol
		Wilfordine	16-hydroxytriptolide
		Wifornine, Euonine	Triptolide
		Wilforzine	Epitriptriolide
		Neowilforine	Tripterifordine
		1-desacetyl wilfordine	Antriptolactone
		1-desacetyl wilfortrine	Tripterygic acid
		2-debenzoyl-2-nicotinoyl wilforine	Orthosphenic acid
		Isowilfordine	$\beta$ -sitosterol
		Wilforcidine	Daucosterol
		Celagbenzine	
	Xylem of root	Triptoterpenoid lactone A	2 $\alpha$ ,3 $\alpha$ ,24-trihydroxy-12-ursene-28-oic acid
		Wilforlide A, B	Tripterygone
		Celastrol or Tripterine	Tripchlorolide
		3 $\beta$ -22 $\alpha$ -dihydroxy-12-oleanen-29-oic acid	Triptriolide
		3,24-dioxo-friedelan-29-oic acid	Linolenic acid
		3-epikatonic acid	8,9-octadecadienoic acid
		Salaspermic acid	Oleic acid
		Triptotriterpenic acid A, B, C	9-hexadecenoic acid
		Orthosphenic acid	Palmitic acid
	3 $\beta$ ,22 $\beta$ -dihydroxy-12-oleanen-29-oic acid	Stearic acid	
	Skin of root	Wilfordine	Triptonoterpene methyl ether
		Wilforine	Triptolidenol
		Wilforgine	Hypolide
		Wifornine, Euonine	Hypolide methylether
		Wifornine	Isonotriptophenolide
		Wilforjing	Triptriolide
		Wilfortrine	Triptotetraolid
		Triptonolide	Isotriptetraolide
		Triptonide	Wilforonide
		Triptolide	Wilforlide A
		Triptiolide	Glut-5-en-3 $\beta$ , 28-diol
		Trip-tophenolide	Ursan-3 $\beta$ , 5 $\alpha$ -diol
		Triptophenolide methyl ether	Polpunonic acid, Populnic acid, Maytenonic acid
		Neotriptophenolide	Triptodihydroxy acid methyl ester
		Triptonoterpene, 14-hydroxy-abieta-8, 11, 13-trien-3-one	

39

40

41

42

43

44 Supplementary Material and Method

45 *Proliferation*

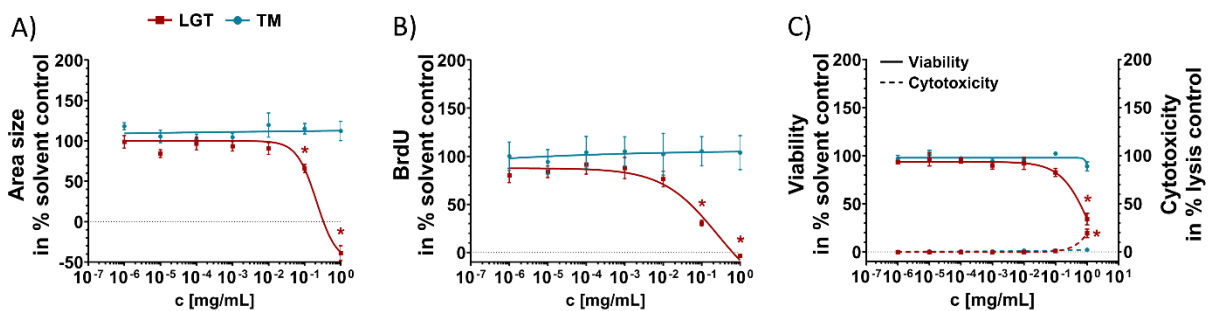
46 To evaluate the impact of LGT and TM on hNPC proliferation, both CHMs were tested in serial dilutions  
47 (1:3) with 7 concentrations as well as respective solvent (proliferation medium) and plated in five  
48 replicate wells per condition in a 96-well U-bottom plate. Per well, one sphere with a defined size of  
49 0.3 mm was plated in 100  $\mu$ L of proliferation medium containing the respective CHM concentration  
50 and incubated for 72 h. The proliferation by area was assessed as slope of the increase in sphere size  
51 up to 3 days (0 h, 24 h, 48 h and 72 h) measured by brightfield microscopy and using high content  
52 imaging (Cellomics Scan software, Version 6.6.0; Thermo Fisher Scientific). Proliferation by  
53 Bromodesoxyuridin (BrdU) was analyzed after 72 h of exposure via a luminescence-based BrdU assay  
54 (Roche) as previously published in Nimtz et al. (2019).

55 In parallel, viability and cytotoxicity assays were performed. Therefore, hNPC viability was assessed as  
56 mitochondrial activity by using an Alamar blue assay (CellTiter-Blue assay (CTB); Promega) in the last  
57 two hours of the 72 h exposure. Cytotoxicity of treated hNPCs was detected by measuring LDH in the  
58 supernatant, which was removed before the CTB assay was started by using the CytoTox-ONE  
59 membrane integrity assay (Promega).

60

61 Supplementary Figure S1

62



63

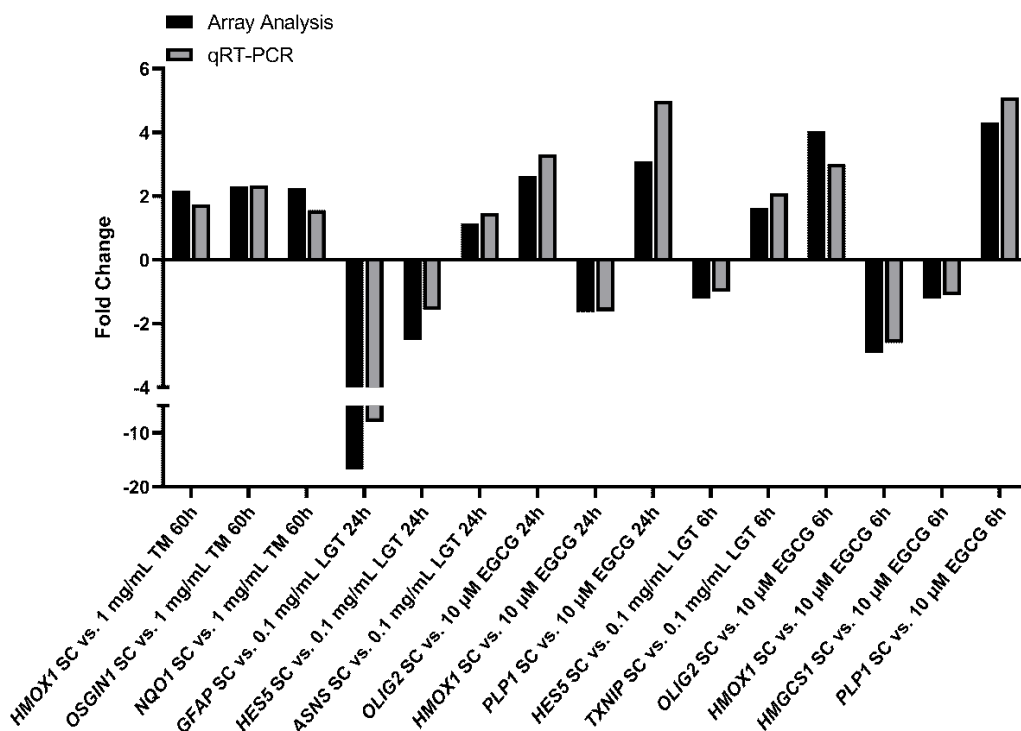
64 **Fig. S1: Influence of LGT and TM on proliferating hNPCs.** Spheres with a defined size of 0.3 mm were plated in 96-well U-  
65 bottom plates and exposed to increasing CHM concentrations over 72 h. Proliferation was studied by measuring the increase  
66 of sphere area (A) and by quantifying BrdU incorporation into the DNA (B). In parallel, viability and cytotoxicity (C)  
67 were assessed by performing Alamar Blue (viability) and LDH assay (cytotoxicity). Data are presented as mean  $\pm$  SEM. Statistical  
68 significance was calculated using OneWay ANOVA followed by Bonferroni's post-hoc tests ( $p \leq 0.05$  was considered  
69 significant). BrdU = bromodeoxyuridine.

70

71

72

73



75

76 **Fig. S2: Quantitative RT PCR validation of array analysis.** Validation of microarray data was performed with quantitative real-time polymerase chain reactions (qRT-PCR) analysis of a set of ten genes. The fold changes of qRT-PCR (grey bars) were compared to the fold changes of the array analysis (black bars). A total of 500 ng RNA from microarray samples were transcribed into cDNA (complementary DNA). qRT-PCR was performed using the QuantiFast SYBR Green PCR Kit and a Rotor Gene Q Cycler (Qiagen). Analysis was performed using the software Rotor-Gene Q Series version 2.3.4. SC = solvent control; *HMOX1* = heme oxygenase 1; *OSGIN1* = oxidative stress induced growth inhibitor 1; *NQO1* = NAD(P)H dehydrogenase quinone 1; *GFAP* = Glial fibrillary acidic protein; *HES5* = Hes Family BHLH Transcription Factor 5; *ASNS* = Asparagine Synthetase; *OLIG2* = Oligodendrocyte Transcription Factor 2; *PLP1* = Proteolipid Protein 1; *TXNIP* = *Thioredoxin Interacting Protein*; *HMGC1* = Hydroxymethylglutaryl-CoA synthase 1.

85

86

87 **Supplementary Table S3:** Set of 10 genes used for microarray validation. Forward and reverse primer sequences are listed in 5'-3'. *HMOX1* = heme oxygenase 1; *OSGIN1* = oxidative stress induced growth inhibitor 1; *NQO1* = NAD(P)H dehydrogenase quinone 1; *GFAP* = Glial fibrillary acidic protein; *HES5* = Hes Family BHLH Transcription Factor 5; *ASNS* = Asparagine Synthetase; *OLIG2* = Oligodendrocyte Transcription Factor 2; *PLP1* = Proteolipid Protein 1; *TXNIP* = *Thioredoxin Interacting Protein*; *HMGC1* = Hydroxymethylglutaryl-CoA synthase 1.

91

Primer	Forward sequence	Reverse sequence
<i>BETA-ACTIN</i>	5'-CAGGAAGTCCCTTGCCATCC-3'	5'-ACCAAAAGCCTTCATACATCTCA-3'
<i>HMOX1</i>	5'-GCCATGAACTTTGTCCGGTG-3'	5'-GGATGTGCTTTTCGTTGGGG-3'
<i>OSGIN</i>	5'-TCATCATTGTGGGTAACGGC-3'	5'-CTTCGTGTAGGGTGTGTAGC-3'
<i>NQO1</i>	5'-TATCCTGCCGAGTCTGTTCT-3'	5'-TGCAGGGGAACTGGAATA-3'
<i>GFAP</i>	5'-CACTGTGAGGCAGAAGCTC-3'	5'-CCTCCAGCGACTCAATCTTC-3'
<i>HES5</i>	5'-TCCCTGCCGTTTTAGGACAA-3'	5'-TACGGCCCTGAAGAAAGTC-3'
<i>ASNS</i>	5'-CTGCACGCCCTCTATGACA-3'	5'-TAAAAGGCAGCCAATCCTTCT-3'
<i>OLIG2</i>	5'-CCGATGACCTTTTCTGCCG-3'	5'-CCACTGCCTCCTAGCTTGTC-3'
<i>PLP1</i>	5'-TTGGCGACTACAAGACCACC-3'	5'-GGGAAGGCAATAGACTGGCA-3'
<i>TXNIP</i>	5'-CCTGAAAAGGTGTACGGCAG-3'	5'-TCTCATTCTCACCTGTTGGC-3'
<i>HMGC1</i>	5'-TATTCCAAGCCCTGCCAAGA-3'	5'-TCCAAGTTCCTCCATACCCC-3'

92

93 **Supplementary Table S4:** Gene regulation of migrating neurospheres exposed to 0.01, 0.1 mg/mL Lei Gong Teng (LGT) and  
 94 10  $\mu$ M Epigallocatechin gallate (EGCG) for 6 h (#22) and 24 h (#18). The fold changes of genes regulated by both compounds  
 95 were identified by array analysis. Upregulated genes are shown as positive values and downregulated genes are shown as  
 96 negative fold changes (-).

Timepoint	Gene	regulated by 0.01 LGT	regulated by 0.1 LGT	regulated by 10 $\mu$ M EGCG
6 hours	FAXDC2	1.5	1.9	1.9
	ACSS3	1.6	2.1	-2.4
	MT1H	-1.9	1.7	-2.0
	MT1G	-2.1	1.6	-2.4
	ZNF567	1.6	1.8	1.5
	HIST1H2BM	-2.0	-1.5	2.0
	ST7	2.2	2.0	1.8
	THOC1	2.0	2.0	1.6
	NIN	2.0	1.8	1.9
	TLR3	1.9	2.2	2.1
	THAP2	1.8	1.8	1.7
	KIAA1715	1.6	1.9	1.5
	SESN3	1.6	2.0	2.3
	GLCCI1	1.6	1.9	5.4
	CDK19	1.6	1.7	1.6
	ZIK1	1.6	1.6	1.6
	NBR1	1.6	1.8	1.5
	RASGEF1B	1.5	1.8	2.8
	HIST3H2BB	-1.5	-1.5	1.6
	SPRY4	-1.6	-2.0	-1.7
CDON	1.8	2.0	5.6	
TCP11L2	1.6	1.7	1.5	
24 hours	SNRPD3	1.6	1.7	1.5
	MT1H	-1.9	-2.1	-4.0
	MT1X	-1.6	-2.8	-4.6
	MT1B MT1CP	-1.9	-2.3	-4.2
	PLEC	-1.7	-2.8	-2.1
	OSTM1	1.5	2.0	1.5
	ICE2	1.6	1.7	1.7
	ATAD2B	1.6	1.6	1.5
	LGALS1	-1.6	-2.1	-1.9
	IFITM3	-1.6	-1.8	-12.8
	SNAP29	1.6	1.6	1.5
	RBM48	1.5	1.5	1.8
	MT1A	-1.7	-2.3	-3.3
	MT2A	-1.7	-2.4	-3.1
	MT1L	-1.6	-2.1	-4.0
	MAPK14	1.5	1.5	1.7
	PAPOLG	1.7	1.7	1.7
	RGCC	1.6	1.5	2.4



**Application of the Adverse Outcome Pathway concept for investigating developmental neurotoxicity potential of Chinese Herbal Medicines by using human neural progenitor cells *in vitro***

**Jördis Klose**, Lu Li, Farina Bendt, Ulrike Hübenthal, Christian Jüngst, Patrick Petzsch, Astrid Schauss, Karl Köhrer, Ping Chung Leung, Chi Chiu Wang, Katharina Koch, Julia Tigges, Xiaohui Fan, Ellen Fritsche

Journal:	Archives of Toxicology
Impact Factor:	5.059 (2019)
Contribution to the publication:	85 % Planning, performance and evaluation of all experiments (except evaluation of adhesion movies), writing of the manuscript
Type of authorship:	first-authorship
Status of the publication:	Submitted on 9 <sup>th</sup> June 2021



### 3 Discussion

Humans are exposed to a multitude of chemicals from many sources, including everyday-products and releases into the environment from agriculture and industrial plants (Egeghy et al. 2016). During the last decades, there has been considerable concern that exposure towards chemicals might be a contributing factor to the increasing incidence of neurodevelopmental disorders in children (Schettler 2001; Grandjean and Landrigan 2006, 2014; Bennett et al. 2016). Besides prenatal exposure when pregnant women are exposed towards chemicals, e.g. with properties to pass placental barrier, postnatal exposure can emerge as well either indirectly through breastfeeding or via direct contact to the chemical. In general, compared to adults, the internal doses of infants' or children are higher due to their immense hand-to-mouth activities and higher body surface area to internal mass ratio (Mizouchi et al. 2015; Butt et al. 2016; Sugeng et al. 2017).

Human brain development is constituted of a series of unique and complex processes, which have to take place in a correct spatiotemporal order. This precise neurodevelopmental clockwork offers manifold possibilities for chemical interactions and thus explains the high vulnerability of the developing brain towards chemicals. These fundamental neurodevelopmental processes include progenitor cell proliferation, differentiation into neuronal and glial cells, migration, apoptosis, axonal and dendritic outgrowth, myelination, synapse formation and formation of functional neural networks (Fig. 4). Importantly, an adverse chemical action during brain development, if not compensated, will manifest in cognitive or behavioral changes. However, in many cases it is challenging to identify associations between early-life chemical exposure and adverse neurodevelopmental effects. These associations still remain to be clearly demonstrated and it is expected that ongoing efforts worldwide, e.g. the 'Neurosome' or the 'Japan Environment and Children's Study' (<https://www.neurosome.eu/>, <https://www.env.go.jp/chemi/ceh/en/index.html>), as well as new research advancements (Cheroni et al. 2020) will help to identify possible causal associations.

Historically, screening and testing of chemicals for DNT is performed according to EPA or OECD *in vivo* Test Guidelines (EPA 1998; OECD 2007), which are based on animals models, preferably rats, to investigate alterations in neuroanatomical, neurophysiological, neurochemical and neurobehavioral parameters, by following perinatal chemical exposure (Makris et al. 2009; Tsuji and Crofton 2012; Tohyama 2016). Testing for DNT for regulatory purposes is currently not a standard requirement within the EU (Pistollato et al. 2021), and only mandatory when triggered based on structure-activity relationships, required for substances that cause neurotoxicity or

endocrine disruption and specifically for pesticides in the US (Schmidt et al. 2016; Pistollato et al. 2021). Beside this fact, these guidelines are highly resource intensive (animals, cost and time) and bear the issues of test complexity, difficulty in interpreting data as well as ethical reservations, leading to a limited use of the *in vivo* DNT test guidelines (Lein et al. 2005; Tsuji and Crofton 2012; Leist and Hartung 2013; Terron and Bennekou Hougaard 2018). All these issues lead to a huge gap regarding DNT hazard information for most of the existing chemicals worldwide. To date, data on DNT potential is estimated to be available only for 110-140 compounds (Grandjean and Landrigan 2006; Makris et al. 2009; Paparella et al. 2020). The limited DNT *in vivo* testing, coupled with the recent paradigm shift in toxicity testing, triggered the interest of the regulatory and research community to develop more efficient, cost-effective and human relevant alternative methods for assessing DNT exposure, hazard and risk (EFSA 2013; Crofton et al. 2014; Bal-Price et al. 2015a, 2018; Fritsche et al. 2015, 2017, 2018c, a).

### 3.1 The 'Neurosphere Assay' as part of a DNT *in vitro* testing battery (DNT-IVB)

The OECD/EFSA workshop (Fritsche et al. 2017) proposed the systematic testing of chemicals in a battery of validated and established *in vitro* assays, covering neurodevelopmental endpoints in a temporal context. A test battery instead of a single DNT assay is needed, since a single *in vitro* test system cannot fully mimic the enormous complexity of the human brain development and its maturation.

It is to note, that such a DNT-IVB is not envisioned to be a direct replacement of the *in vivo* guideline tests, especially for derivation of hazard-based decisions. However, there are some regulatory relevant scenarios for which data from the *in vitro* testing strategy could be applied to inform decision-making (Sachana et al. 2021a). Therefore, the DNT-IVB can contribute to screening of a large number of chemicals for first indications of their DNT potential and prioritization for further testing. This specifically applies to chemicals with limited data on their DNT potential. In addition, the battery can be used to screen a small number of structure/class specific chemicals to prioritize replacements for these compound classes (Manuscript 2.6 - Klose et al. 2021a). Moreover, a DNT-IVB can serve as a follow-up screening for positive chemicals identified via QSAR, read-across or other predictive computational models of DNT. In the case of single chemical hazard assessments, when no *in vivo* DNT data is available, the DNT-IVB can be used to determine if and what kind of follow-up testing (e.g. orthogonal assays, alternative models or guideline studies) should be performed. For existing but equivocal *in vivo* DNT data, the DNT-IVB can be implemented to notify the weight-of-evidence (WoE)-based assessment for DNT. If the existing *in vivo* DNT data is negative, but concern exists from new or novel MIE-based or

alternative species assay, a regulatory choice could be to run the DNT-IVB for in-depth clarification (Crofton et al. 2011; Bal-Price et al. 2015a; Fritsche et al. 2017). Over all, it is envisioned that the AOP framework will be the basis of organizing data and developing IATA (OECD 2016, 2020).

During the last decades, several potential assays have been developed for quantitative assessment of chemical effects on neurodevelopmental processes *in vitro* (Fritsche 2017; Bal-Price et al. 2018). These assays are based on a variety of neural cell types derived from human and animal sources and are focused in the measurement of molecular, morphological and electrophysiological endpoints. A recent publication evaluated the readiness of 17 DNT testing methods for use in testing and evaluating chemicals DNT potential (Bal-Price et al. 2018). Thereby, respective scores were assigned on the basis of publicly available information extracted from publications. The ones selected for the current DNT-IVB have been scored with the highest readiness and/or followed the recommendations of Crofton et al. (2011) in their development. Furthermore, the laboratories that developed the selected assays expressed the willingness and had the resources to pursue a large chemical testing (Masjosthusmann et al. 2020). The readiness evaluation was based on several criteria, which have been proposed by the OECD and are clustered in four categories (Tab. 1; OECD 2014).

**Table 1: Example for ranking parameters for *in vitro* methods to detect chemicals.** Ranking parameters were established by the OECD for thyroid-disrupting chemicals to determine readiness of tests for validation (OECD 2014).

<b>CATEGORY 1</b> <b>Initial high priority considerations</b>	<b>CATEGORY 2</b> <b>Method performance considerations</b>
<ul style="list-style-type: none"> <li>- Biological plausibility</li> <li>- Extrapolation to humans or broadly applicable across vertebrates/phyla</li> <li>- Availability of resources</li> <li>- Reference chemicals</li> </ul>	<ul style="list-style-type: none"> <li>- Within-laboratory reproducibility</li> <li>- Between-laboratory reproducibility</li> <li>- Assay variability</li> <li>- Accuracy</li> <li>- Assay specificity/sensitivity</li> </ul>
<b>CATEGORY 3</b> <b>Technical capability</b>	<b>CATEGORY 4</b> <b>Other practical considerations</b>
<ul style="list-style-type: none"> <li>- Dynamic range/concentration test range</li> <li>- Detection/adjustment of confounding factors and/or incorrect/inconclusive measurements and/or other bias</li> <li>- Response characterization</li> </ul>	<ul style="list-style-type: none"> <li>- Technological transferability/proprietary elements</li> <li>- Transparency of the method</li> <li>- Documentation of development and utility of the method</li> </ul>

The criteria implemented in category 1 represent the highest priority. Each criterion within this category is considered to have equal weight and all are essential to demonstrate the readiness of the assay, e.g. the assessment of the biological plausibility is considered to be very important in defining readiness of the method for validation. Many DNT tests cover multiple mechanisms and processes with varying levels of plausibility and data on their *in vivo* relationship. Thus, the practical value of such criteria for DNT methods needs to be considered case-by-case. Whereas criteria in this category are hard to quantify, criteria for category 2 are better defined and quantifiable. They relate to the evaluation of reliability and efficacy of the method. Sufficient positive and negative compounds should be included to assess specificity and sensitivity.

Moreover, the focus should be given to the robustness of the assay. Regarding category 3, the criteria are also relevant to assay performance evaluation. However, the particular performance issues are considered to be of less significance during initial phases of test development and evaluation. The criteria of category 4 are considered as good to meet in order to gain broad acceptance.

Finally, the DNT testing battery proposed under this procurement is the sum of single assays, covering neurodevelopmental processes from the fetal and postnatal phase through different stages of cell development (Fig. 6; Masjosthusmann et al. 2020).

Neurodevelopmental Process	Assay		
	Human		Rat
NPC Proliferation	<i>NPC1</i> Neural Progenitors	<i>hNP1 Prolif</i> Neural Progenitors	hiPSC-derived Neural Progenitors, Radial Glia
NPC Apoptosis	<i>hNP1 Apop</i> Neural Progenitors		
Cell Migration	<i>UKN2</i> Neural Stem line	<i>NPC2a</i> Radial Glia	<i>NPC2b</i> Neurons, <i>NPC2c</i> Oligodendrocytes
NPC Neuronal Differentiation	<i>NPC3</i> Neurons		Neuronal Subtypes, hiPSC-derived Neural Progenitors
Neurite Outgrowth	<i>NPC4</i> Neurons	<i>UKN4</i> NSC line Neurons	<i>UKN5</i> Peripheral Neurons, <i>hN2/iGluta</i> Neurons, <i>Cortical Initiation</i> Primary Neurons
Neuronal Maturation and Synaptogenesis			<i>Cortical Maturation</i> Primary Neurons
NPC Glial Differentiation	<i>NPC5</i> Oligodendrocytes	<i>NPC6</i> Oligodendrocytes (Maturation)	Radial Glia, Astrocytes, Microglia
Myelination (of Axons)			Oligodendrocytes
Neural Network Formation	<i>NFF Assay</i> hiPSC Neurons		<i>Cortical MEA</i> Primary Neurons

IUF – Leibniz Research Institute Düsseldorf | IUF - in progress | IUF/UKN - in progress | UKN – University of Konstanz | US EPA - US Environmental Protection Agency

**Figure 6: Assays of the DNT *in vitro* testing battery.** Respective assays of a DNT *in vitro* testing strategy covering neurodevelopment endpoints during fetal and postnatal stages of brain development. Assays are grouped according to the neurodevelopmental processes (rows, yellow boxes) and test systems (columns). Each box represents the respective assay and its test method name (italics) and the test/cell system used. The home institution of the developer and operators are color-coded: Leibniz Research Institute for Environmental medicine Düsseldorf (IUF Düsseldorf; green), University of Konstanz (red), US Environmental Protection Agency (US EPA; blue). Assays which need further development are identified as gaps (grey boxes). Modified from Masjosthusmann et al. 2020.

These test methods were previously set up with mainly human-based cell systems, representing different cell types of the developing brain, including human induced pluripotent stem cell (hiPSC)-derived neural crest cells (NCC), lund human mesencephalic (LUHMES) and immature dorsal root ganglia (iDRG) cells, as well as hiPSC-derived or primary NPCs, which have the ability to differentiate into neurons, astrocytes and oligodendrocytes. While most cell systems allow to study at least one neurodevelopmental process, the ‘Neurosphere Assay’ is a multicellular cell system, thus containing cell-cell as well as cell-matrix interactions (NPC2-5) and therefore abundantly represented in the DNT-IVB. During the last years, all cell systems were characterized on molecular and cellular level to ensure that they are the appropriate matrices for neurodevelopmental endpoint evaluation. In case of the ‘Neurosphere Assay’ using NPCs, FACS analyses revealed that these cells are > 98 % NESTIN<sup>+</sup> and > 96 % SOX2<sup>+</sup> confirming their NPC



nature (Hofrichter et al. 2017). During hNPC migration/differentiation, microarray gene expression analyses indicate a transcriptomic change reflecting a multitude of neurodevelopmental processes including cell differentiation, where specific gene expression products for radial glia, neurons, astrocytes and oligodendrocytes increase in their expression during the early differentiation process (Manuscript 2.4 - Masjosthusmann et al. 2018). These findings are underpinned by respective phenotypic descriptions: GFAP<sup>+</sup> and/or NESTIN<sup>+</sup> radial glia migration and differentiation as well as neural and oligodendrocyte differentiation (Fritsche et al. 2005; Moors et al. 2007, 2009, 2012; Baumann et al. 2015; Dach et al. 2017; Masjosthusmann et al. 2018).

As outlined before, the species aspect should be considered when testing proceeds from human *in vitro* to rodent *in vivo* testing. One way of understanding species aspects is given by comparative species-overarching *in vitro* models. The 'Neurosphere Assay' has the capability to enable a direct species comparison as neurospheres can additionally be gained from rat, mouse (Gassmann et al. 2010; Baumann et al. 2014, 2015) and rabbit (Manuscript 2.5 - Barenys et al. 2021) NPCs. This approach allows studying compounds' toxicodynamics in a relatively simple and inexpensive way, and species differences can be revealed directly (Manuscript 2.7 - Klose et al. 2021b; Baumann et al. 2016; Dach et al. 2017). According to the parallelogram approach (Baumann et al. 2016) existing animal-based *in vivo* data can be compared to *in vitro* data of the same species to illustrate *in vivo* – *in vitro* similarities/differences. Moreover, animal-based *in vitro* data can be compared with human *in vitro* data to obtain information regarding interspecies differences and all data then allow an extrapolation to the human *in vivo* situation. However, human-based and/or human-derived test systems are preferred since they minimize interspecies extrapolation issues and due to advances in stem cell biology that have made human cells more accessible, human-derived test methods are becoming more common. Yet, specifically human neural cells can be difficult to culture and in comparison to rodent-derived neural cells, the developmental timeline of human-derived cells may be much longer (Odawara et al. 2016; Barry et al. 2017; Nimtz et al. 2020). Therefore, for some processes (neuronal maturation and synaptogenesis), only assays based on rodent-derived cells are available and currently usable for the DNT-IVB.

In many cases, multiple assays are available to assess a single KE. These assays are used in a complementary manner and are important, due to differences between test systems (e.g. neural stem vs. primary neural cell cultures) and methods (e.g. developmental timing, assay duration, endpoints, exposures), which might lead to the possibility of different outcomes from assays for the same neurodevelopmental process. Within the current DNT-IVB this is the case for two assays that measure migration, the UKN2 and NPC2 assay. The first one is based on hiPSC-derived NCC

and their ability to migrate early during embryogenesis. Once they arrive at their final destination, e.g. tissues outside the central nervous system, they differentiate in many cell types (Mayor and Theveneau 2013). Conversely, the NPC2 assay utilizes radial glia cell migration (NPC2a) as a prerequisite for proper cortex formation (Borrell and Götz 2014) and oligodendrocyte migration (NPC2c) representing a timepoint later in development, since more mature cells have to arise and migrate (Barateiro and Fernandes 2014). Altogether, the interplay of these test systems reflects differences in the biology of migration (Minoux and Rijli 2010; Sild and Ruthazer 2011; Ortega et al. 2012), thus providing different targets and pathways for feasible chemical interactions. Another example for complementarity is given for the endpoint neuronal network formation (NNF). Both assays (cortical MEA and NNF assay) are based on the same basic cell types, neurons and astrocytes, and suitable for assessing NNF and its activity, but from different species. Whereas the well-established US EPA assay is based on rat mixed primary cortical cultures containing neurons and glia cells (Frank et al. 2017; Shafer et al. 2019), the human-based NNF assay applies hiPSC-derived excitatory and inhibitory neurons as well as human primary astrocytes and is recently under development at the IUF, yet unpublished. However, assay results may be different due to differences in developmental timing as well as differences in the pathways and proteins expressed in both species (Saavedra et al. 2021).

Recently, the DNT-IVB was assembled to test 119 compounds (e.g. carbamates, metals, neonicotinoids, organochlorines/fluorines, organophosphates pyrethroids and flame retardants (Manuscript 2.6 - Klose et al. 2021a)) in the test methods NPC1-5 and UKN2,4,5, that were performed by the Institute for Environmental Medicine (IUF) Düsseldorf and the University of Konstanz, respectively (Masjosthusmann et al. 2020). This study concluded that the applied DNT testing strategy is a promising approach for hazard assessment and compound prioritization since its performance demonstrated a sensitivity of 82.7 % and a specificity of 88.2 % using selected known human DNT positive and negative compounds as benchmark. As shown in Fig. 6, US EPA added possibly redundant assays for proliferation, apoptosis, neurite outgrowth and maturation as well as NNF and synaptogenesis to the battery. Currently, the US EPA aims at contributing data for all of these 119 compounds as well.

Knowing that this battery is not complete, i.e. endpoints still needing test method development and endpoints not being represented at all, gaps in the testing battery are pointed out (Fig. 6). For example, *in vitro* assays permitting evaluation of glia specific processes, such as radial glia proliferation and differentiation, astrocyte development or myelin formation, as well as neuronal subtype development or human-based synaptogenesis, and especially functional response to an exposure to chemical(s) are still not well developed or missing. Taking these gaps into

consideration the European Chemical Industry Council (CEFIC) has recently published a call titled “Expansion of a regulatory accepted *in vitro* testing battery for developmental neurotoxicity (DNT) evaluation”, that aims to deliver missing *in vitro* assays that could be incorporated into the existing DNT *in vitro* testing battery (Sachana et al. 2021b), like radial glia-, astrocyte- and microglia-based/enhanced test systems. This project (LRI AIMT 11) is recently under development at the IUF and UKN.

Thus, it is important to note that an *in vitro* assay, which is not listed as part of this battery, might still be able to provide useful data for a decision regarding DNT. However, such an assay needs to be closely evaluated to determine its validity and reproducibility with e.g. known positive and negative control compounds.

## 3.2 From scientific validation to compound classification and prioritization

The interpretation and appropriate use of data derived from individual *in vitro* assays that might comprise the DNT-IVB is based on demonstrating that they have biological and toxicological relevance (e.g. scientific rationale for use of test system, linking endpoints measured to a relevant adverse outcome), acceptable technical qualification (e.g. reproducibility, reliability, predictive capacity) and comparative interpretation of results across different assays (Crofton et al. 2011; Eskes and Whelan 2016).

### 3.2.1 Scientific validation of DNT-*in vitro* assays

The respective cell culture system should be characterized for its ability to accurately quantify chemical-induced changes in one or more specific neurodevelopmental endpoint(s) as well as simultaneous measurement of viability and/or cytotoxicity to distinguish DNT-specific from unspecific effects (Manuscript 2.3 - Nimtz et al. 2019). All research manuscripts included in this thesis contain compound’s impact on viability and/or cytotoxicity assessment. Besides the characterization and identification of the application domain of the alternative model, it should be demonstrated that the model is robust and generates reproducible data. Assay’s dynamic range and reproducibility should include estimates of criteria such as signal-to-background ratio (mean signal / mean background) and signal-to-noise ratio (mean signal – mean background / standard deviation of background). Here, the signal is defined as endpoint measurements under maximal conditions, while the background refers to the endpoint at baseline or solvent control conditions. Both ratios should be determined to provide an indication of the dynamic range of the assay. Although there is no consensus on an acceptable value, it is assumed that larger numbers

generally indicate a better dynamic range (Masjosthusmann et al. 2020). However, such ratios do not adequately take into consideration the assay variability between wells.

The variation between plates and over time (between single experiments) is useful to evaluate reproducibility and can be demonstrated in a medium- to high-throughput testing format by using multi-well plates and by assessing the endpoint response under control and treated (endpoint-specific positive controls) conditions. In case of the 'Neurosphere Assay' (NPC1-5), assay performance in 96-well format in combination with high content image analysis enables such medium- to high-throughput testing strategy (Manuscript 2.3 - Nimitz et al. 2019; Manuscript 2.6 - Klose et al. 2021a; Manuscript 2.8). Endpoint-specific controls are chemicals that are known to alter in a concentration depended manner selectively the endpoint of concern in a particular test system, without affecting the general test system characteristics including cell viability. An endpoint-specific positive control should consistently alter the respective endpoint. For the 'Neurosphere Assay' and thereby for all research manuscripts included in this thesis, endpoint-specific controls were used that demonstrate a consistent modulation of the respective endpoint and the reproducibility of the assay. Among these was the SRC kinase inhibitor PP2 which specifically inhibits the SRC kinase dependent migration (Moors et al. 2007), EGF that significantly inhibits neuronal differentiation (Baumann et al. 2015), BMP7 which significantly reduces oligodendrocyte differentiation and induces the differentiation to astrocytes (Gross et al. 1996; Baumann et al. 2015) as well as NH-3 that inhibits the T3-dependent oligodendrocyte maturation in a significant manner (manuscript 2.7 - Klose et al. 2021b). Endpoint-specific controls for other endpoints, like NPC1 or NPC4, are currently under development.

To further demonstrate the biological relevance and practical ability of the assay to screen moderate numbers of chemicals in a time-efficient manner, the model should be challenged with a set of different test compounds (Crofton et al. 2011). Therefore, compounds with a known MoA, that specifically affect one endpoint and reflecting a 'training set', and known DNT positive and negative compounds, that are used as a 'test set' to determine the performance characteristics of the assay, should be applied to the assay. Whereas the 'training set' is used to determine the ability of an assay to correctly measure an endpoint, the 'test set' analyzes the ability of an assay to correctly identify positives (sensitivity) or negatives (specificity; Kadereit et al. 2012; Mundy et al. 2015; Baumann et al. 2016; Masjosthusmann et al. 2020).

### 3.2.2 *In vitro* data analysis

In order to provide a common metric of comparison across the battery of assays, identical methods for data analysis are indispensable. Data analyses typically start with comparative

---

compound testing design and statistical analyses. Therefore, an assay should include solvent controls and a wide concentration range for a chemical within a multi-well plate over multiple experimental runs. The next step is normalization of data to control wells within a plate to correct for plate-to-plate variability, e.g. setting raw values in percentage to the respective control. The normalized concentration-response data then have to be pooled across all experiments and are subjected to curve fitting using multiple models (linear and non-linear). Finally, the best curve fit can be used to determine a reference point, a point on the concentration-response curve corresponding to an estimate of potency (e.g.  $EC_{50}$ ) or a threshold defining a critical level of response (e.g. 30% change from control). For deriving a reference point the Benchmark Dose (BMD) approach is recommended by the EFSA Scientific Committee (Hardy et al. 2017). For *in vitro* toxicity testing, BMC is comparable to the BMD (Krebs et al. 2020) and defines the concentration that is associated with a specific change in response, the BMR, which is based on the variability of the respective endpoint, thus should be higher than the general variability of the measured endpoint.

All experimental manuscripts of this thesis include respective solvent controls, a wide concentration range (for single compound testing at least 7 concentrations), data normalization (usually percentage or fold-changes to the control), statistical analyses (mostly OneWay ANOVA followed by Bonferroni's post-hoc tests and p-value cut-offs), single experiment pooling and finally respective curve fitting performance (except manuscript 2.4). In case of manuscript 2.6 (Klose et al. 2021a) and 2.7 (Klose et al. 2021b) the BMC model was used ensuring a direct compound and/or species comparison.

### 3.2.3 Compound classification

Ultimately, data from the respective assay must be interpreted for compound classifications. Here, a decision model has to provide an algorithm or established rules to classify chemical activity as 'DNT-specific' (i.e. 'active', 'hit' or 'positive'), as 'DNT-unspecific' (i.e. 'nonspecific' or 'non-selective') or as 'DNT-inactive' (i.e. 'no effect' or 'negative'). Therefore, the respective decision model has to determine whether a compound has affected the neurodevelopmental process assessed in the assay. First of all, the decision model should include an evaluation based on statistical analyses of the data to determine whether a change/threshold (BMR) for a DNT-specific hit has been reached or exceeded. Moreover, the affecting compound concentration on the endpoint of interest needs to be compared to a concurrent measurement of effects on viability and/or cytotoxicity to determine specific effects on neurodevelopmental process versus secondary effects due to loss of viability and cytotoxicity. The decision model would then classify

the compound (i) as 'DNT-specific', when the BMC of viability/cytotoxicity can be separated from the BMC of the specific endpoint; (ii) as 'DNT-unspecific', when both BMCs cannot be separated or overlap, and (iii) as 'DNT-inactive' in case the BMC is not reached for neither the endpoint nor viability/cytotoxicity. In some cases, a fourth category defined as 'borderline-hit' has been used (Delp et al. 2018; Masjosthusmann et al. 2020) specifically for compounds for which the separation between both BMCs is not clear. This category is of great importance for not generating too many false-negatives due to statistical reasons (Leontaridou et al. 2017).

Despite the common goal of assay hit definition, the outcome of decision models that interpret chemical data from individual assays is dependent on variables that are inherent to the assay, like complexity of the test system, measurement technology used and biological variability. This leads to different approaches for different assays.

One approach is to apply a classification model, which is based on overlap of confidence intervals (CI) of the BMCs calculated for the DNT-specific endpoints and the endpoints related to cytotoxicity/viability. This is used for NPC1-5 of the current DNT-IVB (Masjosthusmann et al. 2020; Manuscript 2.6 - Klose et al. 2021a). Thereby a compound is classified as 'DNT-specific' if the CI do not overlap, as 'DNT-unspecific' if the CI overlap is greater than 10 % or as 'borderline' if the lower confidence limit of cytotoxicity/viability overlaps by less than or equal to 10 % with the CI of the specific endpoint. In case no confidence interval is available for cytotoxicity/viability because the BMR is not reached, the lower confidence limit is set as the highest tested concentration (Masjosthusmann et al. 2020). Another approach, applied for the UKN assays, is based on a ratio cutoff for the ratio between the BMC for cell viability and the specific endpoints (Krug et al. 2013b; Hoelting et al. 2016; Nyffeler et al. 2017a). Here, individual fixed BMR levels were set up for the neurodevelopmental and cytotoxicity/viability endpoints which consider differences in the underlying biological process and/or the baseline variability. If a compound does not reach the fixed BMR, its classified as 'no hit' and not followed up with any further testing. In comparison, a specific classification model is applied, when the compound leads to a response above the fixed BMR. To be classified as 'DNT-specific', different criteria for each assay have to be fulfilled: ratio  $BMC_{10} \text{ viability}/BMC_{25} \text{ migration} \geq 1.3$  in UKN2 assay; ratio  $BMC_{25} \text{ viability}/BMC_{25} \text{ neurite area} \geq 4$  in UKN4 assay or  $\geq 3$  in UKN5 assay. In case of an unaffected viability in UKN4/5, the viability can be defined more cautiously with  $BMC_{10}$ . Moreover, if the calculations do not reach the ratio required to define a compound as a specific hit, the lower confidence limit instead of the  $BMC_{25}$  is used for the same calculation. If the ratio cut-off is still not reached, the compound is defined as cytotoxic, otherwise the compound is categorized as 'borderline'.



To date, the procedure for classifying chemicals is not standardized and allows for flexibility in adjusting the decision model for a fit-for-purpose use. However, most decision models set parameters that maximize both sensitivity (the correct prediction of a positive compound) and specificity (the correct prediction of a negative compound) to limit the number of false positives (Hsieh et al. 2015; Filer et al. 2017).

### 3.2.4 Compound prioritization

After generating relevant and reliable data within a DNT-IVB, potency is a crucial factor for hazard characterization and further testing. Compounds can be ranked and prioritized based on comparison of relative potencies across all assays within the DNT-IVB. Therefore, hazard of compounds with potent effects in multiple assays might be ranked higher compared to those that are potent in just one assay. However, in similarity to the classification also consensus-based prioritization models are under development and not standardized. In order to provide an overall compound ranking and clustering, several procedures and tools have been applied for the data currently available for the DNT-IVB (Masjosthusmann et al. 2020) as well as for the manuscript 2.6 included in this thesis (Klose et al. 2021a). For one, BMC values with CI allow distinguishing between DNT-specific and DNT-unspecific hits giving objective potency ranking measures. In addition, compounds can be ranked by using the lowest BMC identified over the whole battery and the assay with the lowest BMC is then defined as the most sensitive endpoint (MSE, Baumann et al. 2016) considered as a relevant endpoint for further targeted testing. Obviously, other endpoints affected in a similar range of the MSE, should be considered, too. Thought, almost all *in vitro* assays, including the 'Neurosphere Assay' deal with nominal medium concentrations and adverse effects are not related to the actual free compound concentration in the cell, which can influence the process of compound prioritization since both values can differ up to two orders of magnitude (Kramer 2010). Therefore, especially the biokinetic behavior of the chemical as well as other conditions (see 3.4) should be considered for prioritization.

The MSE-Prioritization takes only the MSE and not, e.g., the number of affected endpoints into consideration. To address this point, compound effects based on both, the number of endpoints affected and the respective potency can be analyzed by using hierarchical clustering, resulting in a visualized heatmap, which provides a cluster of chemicals with similar effects (Harrill et al. 2018). This method enables identification of chemicals with a common MoA. Another currently propagated compound prioritization instrument is the Toxicological Prioritization Index (ToxPi) tool introduced by the US EPA (Reif et al. 2010; Gangwal et al. 2012; Marvel et al. 2018). This tool yields an explicit, prioritized order of compounds as well as a visualization of the underlying,

weight-of-evidence scheme that specifies the contribution of each data source to a chemical's activity or risk profile (Marvel et al. 2018). Here, the ToxPi tool hierarchically clusters compounds according to their potency and assay hit patterns. It is possible to produce ToxPi information on compound clustering and ranking of a compound class for "general" toxicity (e.g. ToxCast data) and "specific" toxicity (e.g. DNT-IVB data). Comparison of clustering between both gives the first indication whether a substance class produces a DNT-specific effect or if general toxicity of these compounds predicts DNT toxicity well. In case of manuscript 2.6 (Klose et al. 2021a) the ToxPi tool revealed a distinct ranking, suggesting that DNT hazard of FRs is not well predicted by ToxCast assays.

### 3.3 Mechanistical investigations for developing AOPs

The IATA concept has been proposed by the OECD to embed alternative testing strategies into WoE assessment for regulatory decision-making by using data from various information sources, including *in silico*, *in chemico*, *in vitro* and *in vivo* (OECD 2016, 2020). Thereby, the IATA-based chemical hazard characterization relies on an integrated analysis of existing information available for the chemical(s) of interest, e.g. with the optional use of the AOP conceptual framework. The AOP framework connects toxicological mechanistic information to apical endpoints for hazard and risk assessment strategies and regulatory sciences (OECD 2013; Leist et al. 2017). Thereby, AOPs are based on a sequence of measurable KE, that are expected to be triggered by a MIE and finally end up in an AO of regulatory relevance. AOPs assist in structuring the available information in terms of MIE, KEs and AO as well as in the identification of missing data and/or in the design of new testing strategies (Sachana et al. 2021a).

Using an AOP within an IATA appears particularly challenging. To date, the number of putative and reviewed AOPs relevant to DNT is limited (Bal-Price et al. 2017; Barenys et al. 2019; Li et al. 2019; Spinu et al. 2019; Chen et al. 2020; Klose et al. 2021; <http://aopwiki.org>). Most of the assays used for DNT, especially those within the DNT-IVB represent several KEs, but do not measure MIEs. This does not directly impact the use of DNT data in AOP-based IATAs, but this uncertainty impacts the further use of *in silico* models, which are mainly based on chemical interactions with the MIE. This clearly illustrates the need of validated assays in addition to the DNT-IVB, which represent MIEs, e.g. impact on ion channels, neurotransmitter or growth factor receptors, thyroid hormone, cell adhesion molecules to just name a few. Another challenge for creating DNT-AOPs, is based on the understanding of the pathological pathways leading from functional *in vitro* endpoints to behavioral changes at the organism level. The basic hypothesis is that if a chemical affects KEs *in vitro*, it is assumed to have a similar potential *in vivo*. However, in the real-life situation, many

circumstances (biological, genetic, environmental, social) may impact the outcome (Cheroni et al. 2020; Paparella et al. 2020).

So far, the use of *in vitro* data, e.g. just derived from the DNT-IVB is not sufficient for making regulatory decisions. However, it is important to determine the amount of data to be gathered in an AOP-informed IATA, since all uncertainties will decrease as more data are being generated and experience is gained in regulatory use. Therefore, the identification of the most common and/or highly connected KEs and KERs is one of the main aims for developing an AOP network for human DNT.

Oligodendrocyte differentiation was the endpoint most frequently altered in the manuscripts included in this thesis (manuscript 2.6 - Klose et al. 2021a; manuscript 2.8), as well as over the whole DNT-IVB (Masjosthusmann et al. 2020).

Oligodendrocytes are the myelinating cells of the CNS and responsible for axon myelination to facilitate rapid saltatory conduction of action potentials. To properly myelinate, oligodendrocyte development is based on a series of differentiation steps from neural stem/progenitor cells: oligodendrocyte precursor cells (OPCs) → non-myelinating preoligodendrocytes → pre-myelinating, immature oligodendrocytes → myelinating, mature oligodendrocytes (Baumann and Pham-Dinh 2001; Barateiro and Fernandes 2014; Marinelli et al. 2016). OPCs are proliferative cells migrating to different regions of the brain in a highly regulated, fine-tuned process of migration, proliferation, differentiation and myelination that accelerates towards the end of gestation and continues throughout the first two postnatal decades (Emery 2010; Insel 2010; van Tilborg et al. 2018). As a backup pool for oligodendrocyte production, OPCs also reside in the adult brain (reviewed by Insel 2010). Specifically, developing oligodendrocytes can be affected by a large variety of substances through a broad spectrum of MoA. They exert a high susceptibility to stressors like reactive oxygen species and are sensitive to excitotoxicity and endoplasmic reticulum stress (Bradl and Lassmann 2010; Volpe et al. 2011; Marinelli et al. 2016). This vulnerability is due to their high metabolic rate, oxygen consumption and adenosine triphosphate (ATP) production, as they synthesize more than 3-fold their own weight of myelin (Norton and Poduslo 1973) and support membrane production up to 100x the weight of their cell bodies per day (Ludwin 1997; McTigue and Tripathi 2008; Bradl and Lassmann 2010). ROS sensitivity is reinforced by their enormous intracellular stores of iron, which is the largest in the brain (Juurlink 1997; Back et al. 1998; Marinelli et al. 2016). A major constituent of myelin is cholesterol. Therefore, oligodendrocytes possess the highest capacity of *de novo* cholesterol biosynthesis amongst the different brain cell types (Arenas et al. 2017), rendering them extremely susceptible to compounds that interfere with this metabolic pathway (Manuscript 2.7 - Klose et al. 2021b).

This plethora of knowledge has been gained from clinical and disease-related studies on the functional adverse outcomes related to oligodendrocyte toxicity manifesting in neurological disorders, such as the Allan-Herndon-Dudley Syndrome (López-Espíndola et al. 2014; Tonduti et al. 2014) or periventricular leukomalacia (Back et al. 2001). Altogether, this indicates that oligodendrocytes strongly differ from neurons regarding their chemical sensitivity. However, in the toxicological context, oligodendrocytes are an understudied cell type as most studies deal with neurons, eventually followed by astrocytes (Fritsche et al. 2015).

In order to bring the 'Neurosphere Assay' to a higher readiness level for future applications in a regulatory context, phenotypic outcomes were combined with transcriptome analyses, thereby understanding single MoA of selected compounds, which are helpful to develop AOPs for a better comprehension of DNT hazards. The manuscripts included in this thesis mainly focused on the most affected endpoint oligodendrocyte differentiation/oligodendrogenesis.

Different AOPs can cross and overlap when they share one or more KE(s) or have the same AO leading to the formation of complex AOP networks. Thus, one single MIE can cause multiple AOs and the same AO can be caused by more than one MIE. The latter one can be observed in the case of the brominated flame retardant TBBPA (Manuscript 2.7 - Klose et al. 2021b). Using the NPC6 Assay (TH-dependent oligodendrocyte maturation assay) in combination with microarray analyses TBBPA was identified to be a TH disruptor, as it impairs TH-dependent human oligodendrocyte maturation by dysregulation of oligodendrogenesis-associated genes. On the other hand, TBBPA disrupts a gene expression network regulating cholesterol homeostasis, leading to a reduction of oligodendrocyte number independently of TH signaling. Thus, TBBPA targets different KEs of human oligodendrocyte development resulting in two novel AOPs. However, both AOPs converge in the common KE "lower amount of myelin", resulting in one merged AOP with the same AO caused by more than one MIE. Whereas the MIE for the 'Thyroid Hormone Disruption AOP' is known (competitive binding of a chemical to the TH receptor in developing human brain cells; Dach et al. 2017), the MIE explaining how TBBPA interferes with cholesterol-related genes is yet to be identified.

Within manuscript 2.8, also for one of the analyzed CHMs, TM, oligodendrocyte differentiation was identified as the most sensitive endpoint. The underlying molecular mechanisms were unraveled using microarray analysis, thus detecting that TM dysregulates a gene expression network involved in oxidative stress. Since effective oxidative stress response is a requirement for developing oligodendrocytes and their survival, TM exposure might reduce the number of hNPC differentiated oligodendrocytes by inducing the intracellular ROS level. This observation leads to the implementation of a further MIE 'increased reactive oxygen species production' along with

KEs connected to oxidative stress into the AOP network mentioned above for TBBPA-induced disturbance of oligodendrocyte development. This work demonstrates that including a so far unknown new KE may expand an existing AOP.

Another approach to place data in an AOP-context is the application of an already existing AOP as a basis for chemicals' hazard assessment (Manuscript 2.8). By performing the 'Neurosphere Assay' upon cellular LGT exposure, it was possible to identify a specific neurosphere 'gap and arborization' migration endophenotype, that was previously identified upon neurosphere treatment with the flavonoid epigallocatechin gallate (EGCG; Barenys et al. 2017). Based on these data, the working group around Prof. Fritsche generated the putative AOP 'Disrupted laminin- $\beta$ 1-integrin interaction leading to impaired cognitive function' (Bal-Price et al. 2016; Fig. 1E), which was submitted to the OECD in 2019. Keeping that AOP in mind, experiments under influence of LGT were performed, to reconstruct AOP-relevant KEs and especially the MIE. Thus, by comparing special endophenotypes within compound screenings, existing AOPs can be helpful to envision probable MoAs and thereby serve as a basis for hazard assessment.

### 3.4 Moving from hazard characterization to risk assessment

The traditional concept of toxicity testing is to determine safety factors for human exposure based on the evaluation of the outcome of animal tests. For human risk assessment, the dose that has no adverse effect in the animal needs to be extrapolated to the no-effect dose in humans based on the application of uncertainty factors that account for toxicodynamic and toxicokinetic inter-species differences as well as inter-individual susceptibilities (EFSA 2012; Konietzka et al. 2014). Toxicity screening based on *in vitro* methods can efficiently identify the potential biological activity of chemicals. However, adverse effect concentrations observed in human *in vitro* assays cannot be used to directly evaluate the safety factor for human exposure. Once an effect concentration has been obtained *in vitro*, a translation to relevant *in vivo* exposure is necessary. The usual procedure for this is an *in vitro*-to-*in vivo* extrapolation (IVIVE; Blaauboer 2010; Basketter et al. 2012).

One requirement for this extrapolation is the knowledge of the biokinetic behavior of the chemical. Commonly, adverse effects found *in vitro* are related to the nominal medium concentrations. Certainly, this medium concentration can substantially deviate from the actual free compound concentration in the cell system due to evaporation, cell density imbalances, active vs. passive uptake into cells or multi-cellular tissues, as well as binding to the plastics of cell plates and/or to medium serum proteins (Paini et al. 2019), the latter being a rather critical issue for lipophilic compounds (e.g. PBDEs; Glden and Seibert 2003). For some compounds free cellular

concentrations can differ up to two orders of magnitude from the nominal concentrations, showing the importance of understanding, measuring and modeling *in vitro* biokinetics (Kramer 2010; Croom et al. 2015). Important to note is that actual analytical measurement of medium and cellular concentrations of a substance in *in vitro* DNT studies, including the DNT-IVB, are very rarely done.

Another tool complementing IVIVE is physiologically based biokinetic (PBBK) modelling. This model is essential for effect prediction, as it incorporates relevant information on physiology and requires knowledge on barrier passage, metabolism, and excretion. For example, measuring the DNT potential of a compound without considering the ability of the compound to pass the blood-placenta or blood-brain barrier and reach the fetus may lead to incorrect conclusions (Prieto et al. 2004). In many cases these specific data for compounds are not available. Therefore, computational methods, such as quantitative structure-property and structure-activity (QSPR and QSAR) relationships can be addressed to find structurally similar and comparable compounds with known physiological properties (Berhanu et al. 2012).

Another approach for a very first estimation and crude risk assessment could be the comparison from studied *in vitro* hazards to biomonitoring data, similar to the way described for the case study of FRs (Manuscript 2.6 - Klose et al. 2021a). It is to note, that such superficial comparisons do not account for *in vitro* kinetics or for actual fetal brain concentrations *in vivo*. Nevertheless, extrapolating the DNT-IVB BMCs to children's FR exposure via breast milk suggests a low risk for the here tested individual compounds. However, it raises concern, as humans are generally exposed to compound mixtures including FRs, pesticides, pharmaceuticals, toxic metals and other environmental contaminants. Therefore, individual compound effects easily add up to mixtures at relevant human exposure concentrations that might exert additive, synergistic or antagonistic effects, especially when the same converging endpoint is affected. Yet, mixture experiments as well as sophisticated IVIVE are needed to substantiate these concerns.

Overall, without addressing IVIVE, a toxicological risk assessment on the basis of *in vitro* methods cannot be performed. In the future, regulatory agencies will more and more be forced to utilize alternative *in vitro* and *in silico* NAMs as discussed here due to the increasing ethical pressure on reducing animal experiments and the accompanying need for a higher throughput in chemical testing.





## 4 Abstract

Human brain development is based on complex and spatiotemporally orchestrated processes, which make it highly sensitive towards toxic chemicals. Only few compounds are known to be developmentally neurotoxic (DNT) in humans, whereas the DNT potential for the majority of chemicals is unknown. Currently used DNT *in vivo* guideline studies are not suitable for large scale testing as they need high amounts of animals, time, and money and bear the issue of species extrapolation. Therefore, regulators, academia, and industry agreed on a need for a mechanistically informed, fit-for-purpose and human-relevant DNT testing strategy, which allows fast and cheap DNT hazard assessment, while at the same time meeting regulatory requirements. The three reviews included in this thesis summarize the development (manuscript 2.1) and availability (manuscript 2.2) of alternative human stem/progenitor cell-based assays, that can be used to set up a DNT *in vitro* testing battery (DNT-IVB) covering key neurodevelopmental processes. A well-suited model for this purpose is the 'Neurosphere Assay', which employs human, rodent and rabbit neural progenitor cells (NPC) grown as 3D neurospheres and allows the assessment of distinct neurodevelopmental key events (KE), including NPC proliferation, migration and differentiation into neural effector cells (astrocytes, neurons and oligodendrocytes), as well as thyroid hormone (TH)-dependent oligodendrocyte maturation (manuscript 2.3). Two research manuscripts included in this thesis are focused on the characterization of the 'Neurosphere Assay'. One manuscript (manuscript 2.4) deals with the biological and molecular characterization of developing neural progenitor cells in a species comparative manner, whereas the other one (manuscript 2.5) is focused on the establishment of rabbit neurospheres illustrating the usefulness as a complementary method to the rodent-based 'Neurosphere Assay'. Furthermore, this thesis contains two case studies of data-poor substance classes on their DNT hazard. One is dealing with the screening and prioritization of flame retardants (FRs) using a DNT-IVB (manuscript 2.6), and the other one characterizes the DNT potential of two Chinese Herbal Medicines (CHMs) using the 'Neurosphere Assay' (manuscript 2.8). Differentiation into oligodendrocytes was identified to be the endpoint affected by most tested chemicals, indicating that oligodendrocytes represent a crucial cellular target for compounds during neurodevelopment. By incorporation of large-scale transcriptomic analyses, I provide further insight into the mode(s)-of-action (MoA) of selected compounds (manuscript 2.7 + 2.8). Additionally, data generated in this thesis are placed in an adverse outcome pathway (AOP)-context by applying and extending putative DNT-AOPs.

In summary, this thesis demonstrates that the combination of endophenotypes with transcriptome analyses builds a powerful tool for understanding a compounds' MoA and applying/extending AOPs for a better perception of the DNT hazard in a regulatory context.

## 5 Zusammenfassung

Die Entwicklung des menschlichen Gehirns besteht aus einer Vielzahl streng zeit- und räumlich kontrollierter und komplexer Prozesse, welche durch ihre große Plastizität breite Angriffsflächen für Toxine bieten. Für eine Vielzahl der sich im Umlauf befindlichen Chemikalien ist das entwicklungsneurotoxische (DNT) Potential nicht bekannt. Derzeit verwendete DNT-*in-vivo*-Richtlinienstudien eignen sich nicht für Tests in großem Maßstab, da sie viele Tiere, Zeit und Geld benötigen. Zusätzlich bergen sie das Problem der inter-Spezies-Extrapolation. Daher sind sich Aufsichtsbehörden, Wissenschaft und Industrie einig, dass eine mechanistisch informierte, zweckmäßige und für den Menschen relevante DNT-Teststrategie erforderlich ist, die eine schnelle und kostengünstige Bewertung des DNT-Gefährdungspotentials ermöglicht und gleichzeitig die regulatorischen Anforderungen erfüllt werden müssen.

Die drei in dieser Dissertation enthaltenen Übersichtsarbeiten fassen die Entwicklung (Manuskript 2.1) und Verfügbarkeit (Manuskript 2.2) alternativer Assays auf der Basis menschlicher Stamm- / Vorläuferzellen zusammen, welche Schlüsselprozesse (KE) der neurologischen Entwicklung zum Einsatz in einer DNT-*in-vitro*-Testbatterie (DNT-IVB) abbilden können. Ein gut geeignetes Modell für diesen Zweck ist der "Neurosphären Assay", bei dem neurale Vorläuferzellen (NPC) von Menschen, Nagern und Kaninchen in 3D kultiviert werden und die Analyse verschiedener KE der Gehirnentwicklung, einschließlich der Proliferation und Migration von NPCs, sowie Differenzierung in neurale Effektorzellen (Astrozyten, Neuronen und Oligodendrozyten) und die von Schilddrüsenhormon (TH) abhängige Oligodendrozyten-Reifung (Manuskript 2.3) ermöglichen. Zwei Manuskripte befassen sich mit der Charakterisierung des „Neurosphären Assays“, indem sie sich mit der biologischen und molekularen Charakterisierung sich entwickelnder neuronaler Vorläuferzellen auf speziessvergleichende Weise befassen (Manuskript 2.4) und Kaninchen-Neurosphären als ergänzendes Zellsystem beschreiben (Manuskript 2.5). Darüber hinaus enthält diese Arbeit zwei Fallstudien von Substanzklassen, für welche nur eingeschränkte Informationen über ihr DNT-Potential verfügbar sind. Eine befasst sich mit dem Screening und der Priorisierung von Flammschutzmitteln (FRs) unter Verwendung einer DNT-*in vitro* Batterie (Manuskript 2.6), und das zweite charakterisiert das DNT-Potential zweier traditioneller chinesischer pflanzlicher Arzneimittel (CHMs) unter Verwendung des „Neurosphären Assays“ (Manuskript 2.8). Die Differenzierung zu Oligodendrozyten wurde als der am häufigsten beeinflusste Endpunkt identifiziert, was darauf hinweist, dass Oligodendrozyten während der neuralen Entwicklung ein entscheidendes zelluläres Angriffsziel für Chemikalien darstellen. Die Einbeziehung von Transkriptomanalysen ermöglichte es, die Wirkungsweise ausgewählter Chemikalien näher zu analysieren (Manuskript 2.7 + 2.8). Darüber hinaus werden die in dieser Arbeit generierten Daten durch Anwenden und Erweitern putativer DNT-AOPs (Adverse Outcome Pathways) in einen AOP-Kontext eingebettet.

Zusammenfassend zeigt diese Dissertation, dass die Kombination aus phänotypischen Endpunkten des „Neurosphären Assays“ mit transkriptionellen Analysen einen vielversprechenden und leistungsstarken Ansatz bietet, welcher zum Verständnis des DNT-Gefährdungspotentials von Substanzen beiträgt und für zukünftige Risikobewertungen geeignet ist.



---

## Abbreviations

2D	Two-dimensional
3D	Three-dimensional
ABCA1	ATP-binding cassette (ABC) subfamily-A transporter 1
AC <sub>50</sub>	Half maximal activity concentration
ACTB	Beta actin
ADGRL2	Adhesion G Protein-Coupled Receptor latrophilin 2
ADGRL3	Adhesion G Protein-Coupled Receptor latrophilin 3
ADHD	Attention Deficit Hyperactivity Disorder
ADME	Absorption, Distribution, Metabolism and Excretion
aFR	Alternative flame retardant
AHDS	Allan-Herndon-Dudley syndrome
ANOVA	Analysis of variance
AO	Adverse outcome
AOP	Adverse outcome pathway
APOE	Apolipoprotein E
BBB	Blood Brain Barrier
BBOEP	Bis-(2-butoxyethyl) phosphate
BDE-47	2,2',4,4'-tetrabromodiphenylether
BDE-99	2,2',4,4',5-pentabromodiphenylether
BDNF	Brain derived neurotrophic factor
BFRs	Brominated flame retardants
BG	Background control
BGRFR	Multiple bandpass emission filter and excitation filters
BMC	Benchmark concentration
BMD	Benchmark dose
BMP2	Bone morphogenetic protein 2
BMP7	Bone morphogenetic protein 7
BMR	Benchmark response
BP	Basal progenitor
BrdU	Bromodeoxyuridine
BSA	Bovines serum albumin

## Abbreviations

---

C. elegans	Caenorhabditis elegans
CAAT	Johns Hopkins Center for Alternatives to Animal Testing
CADH6	Cadherin-6
CAS	Chemical Abstracts Service
cDNA	Complementary deoxyribonucleic acid
CDON	Cell-adhesion molecule-related/down-regulated by Oncogenes
CEFIC	European Chemical Industry Council
CHD3	Chromodomain helicase DNA binding protein
CHMs	Chinese Herbal Medicines
CI	Confidence intervals
cMINC/UKN2	Neural Crest Cell Migration Assay
CN	Copy numbers
CNN	Convolutional neural network
CNPase	Cyclic-nucleotide-phosphodiesterase
CNS	Central nervous system
CNTN1	Contactin-1
cRNA	Complementary ribonucleic acid
CRYM	Cyrystallin Mu
CTB	CellTiter-Blue
d	Days
DA	Dopaminergic
DAPT	n-[n-(3,5-difluorophenacetyl)-L-alanyl]-S-phenylglycine t-butyl ester
DCFDA	2',7'-Dichlorofluorescein diacetate
DDE	Dichlorodiphenyldichloroethylene
DDT	Dichlorodiphenyltrichloroethane
DEX	Differential gene expression
DHCR24	24-dehydrocholesterol reductase
DHCR7	7-dehydrocholesterol reductase
DIO3	Iodothyronine deiodinase 3
DIV	Days in vitro
DMEM	Dulbecco's modified Eagle's medium
DMSO	Dimethyl sulfoxide
DNA	Deoxyribonucleic acid
DNT	Developmental neurotoxicity

---

DNT-IVB	Developmental neurotoxicity in vitro testing battery
EC <sub>50</sub>	Half maximal effective concentration
ECM	Extracellular matrix
ECVAM	European Centre for the Validation of Alternative Methods
EdU	Ethynyldeoxyuridine
EFSA	European Food Safety Authority
EGCG	Epigallocatechin gallate
EGF	Epidermal growth factor
EGFR	Epidermal growth factor receptor
EGR1	Early growth response 1
EHDPPH	2-ethylhexyl diphenyl phosphate
EPA	Environmental Protection Agency
EtOH	Ethanol
EU	European Union
FACS	Fluorescence-activated cell scanning
FCS	Fetal calf serum
FDA	US Food and Drug Administration
FDFT1	Farnesyl-diphosphate farnesyltransferase 1
FDPS	Farnesyl diphosphate synthase
FDR	False discovery rate
FGF	Fibroblast growth factor
FGFR	Fibroblast growth factor receptor
FRs	Flame retardants
GALC	Galactosylceramidase
GCLM	Glutamate-cystein ligase modifier subunit
GFAP	Glia fibrillary acidic protein
GO	Gene Ontology
GPCRs	G protein-coupled receptors
GS	Goat Serum
GSH	Glutathione
GW	Gestational week
h	Hours
H <sub>2</sub> O <sub>2</sub>	Hydrogen peroxide
HCA	High content image analysis



## Abbreviations

---

HCl	Hydrochloric acid
HDL	High density lipoprotein
HDLBP	High density lipoprotein binding protein
hESC	Human embryonic stem cell
hiPSC	Human induced pluripotent stem cell
HMGCR	3-hydroxy-3-methylglutaryl-CoA reductase
HMGCS1	Hydroxymethylglutaryl-CoA synthase
HMOX1	Heme oxygenase 1
hNPC	Human neural progenitor cell
HPLC	High-performance liquid chromatography
HTA	High-throughput assay
hUCBSC	Human umbilical cord blood mesenchymal stem cell
IATA	Integrated Approaches to Testing and Assessment
ICC	Immunocytochemical
IDDPHP	Isodecyl diphenyl phosphate
iDRG	Dorsal root ganglia (induced)
IGFBP4	Insulin like growth factor binding protein 4
IL33	Interleukin 33
IPC	Intermediate progenitor cells
IPHP	Triphenyl isopropylated phosphate
IPs	Intermediate progenitors
IQ	Intelligence quotient
IST-NET	International Stakeholder NETwork
ITGB5	Integrin beta-5
IUF	Leibniz Research Institute for Environmental Medicine
IUGR	Intrauterine growth restriction
IVIVE	In vitro-to-in vivo extrapolation
KE	Key event
KER	Key event relationships
KLF9	Krüppel-like factor 9
KR	Key regulators
KSR	Knock-out serum replacement
LC	Lysis control
LD50	Medium lethal dose

---

LDH	Lactate dehydrogenase
LGT	Lei Gong Teng
LUHMES	Lund human mesencephalic cell
MAGI2	Membrane-associated guanylate kinase
MBP	Myelin basic protein
MCT-8	Monocarboxylate transporter 8
MD	Media control
ME1	Malic enzyme 1
MEA	Microelectrode Array
MeHgCl	Methylmercury chloride
MeOH	Methanol
mESC	Mouse embryonic stemm cells
MIE	Molecular initiating event
min	Minutes
mNPC	Mouse neural progenitor cell
MoA	Mode-of-action
MOBP	Myelin-associated oligodendrocytic basic protein
Mog	Myelin oligodendrocyte glycoprotein
mRNA	Messenger ribonucleic acid
MSE	Most sensitive endpoint
NAMs	New approach methodologies
N-CAM	Neural cell adhesion molecule
NCC	Neural Crest Cell Migration Assay
NEP	Neuroepithelial precursor
NeuriTox/UKN4	Neurite Outgrowth of CNS (LUHMES) Neurons Test
NH-3	Thyroid hormone receptor antagonist NH-375
NMB	Neuromedin B
NNF	Neuronal network formation
NOAEL	No Observed Adverse Effect Level
NPC	Neural progenitor cell
NPC1a	Primary hNPC Proliferation Assay by Area
NPC1b	Primary hNPC Proliferation Assay by BrdU
NPC2a	Primary hNPC Migration Assay
NPC2b	Primary hNPC Neuronal Migration Assay

## Abbreviations

---

NPC2c	Primary hNPC Oligodendrocyte Migration Assay
NPC3	Primary hNPC Neuronal Differentiation Assay
NPC4a	Primary hNPC Neuronal Morphology (neurite length) Assay
NPC4b	Primary hNPC Neuronal Morphology (neurite area) Assay
NPC5	Primary hNPC Oligodendrocyte Differentiation Assay
NPC6	Primary hNPC Oligodendrocyte Maturation Assay
NQO1	NAD(P)H dehydrogenase quinone 1
NRC	US National Research Council
NSCs	Neural stem cells
NSPCs	Multipotent neural stem/progenitor cells
NT	Neurotoxicity
NT4	Neurotrophin 4
NTP	National Toxicology Program
O4	Oligodendrocyte marker O4
OECD	Organization for Economic Co-operation and Development
OLs	Oligodendrocytes (immature and mature)
OPCs	Oligodendrocyte precursor cells
OPFRs	Organophosphorus flame retardants
ORA	Overrepresentation analyses
oRG	Outer radial glia
OSGIN1	Oxidative stress induced growth inhibitor 1
OSVZ	Outer subventricular zone
PBBK	Physiologically based biokinetic
PBDEs	Polybrominated diphenyl ethers
PBS	Phosphate-buffered saline
PBS-T	Phosphate-buffered saline containing Triton X-100
PC	Positive control
PCA	Principle component analysis
PCBs	Polychlorinated biphenyls
PCW	Post conceptual weeks
PDGFR $\alpha$	Platelet-derived growth factor receptor A
PDL	Poly-D-lysine
PeriTox/UKN5	Neurite Outgrowth of PNS Neurons (hiPSC-derived) Test
PFA	Paraformaldehyde

---

PFOA	Perfluperfluorooctanoic
PLO	Poly-L-ornithine
PLP	Proteolipid protein
PND	Postnatal day
Poly-HEMA	Polyhydroxyethylmethacrylate
PP2	Inhibitor for Src-family kinases
pre-OLs	Pre-myelinating oligodendrocytes
PTPRT	Receptor-type tyrosine-protein phosphatase T
PVL	Periventricular leukomalacia
QM	Maturation quotient
QSAR	Quantitative structure relationships
QSPR	Quantitative structure-property
REACH	Registration, Evaluation, Authorization, and Restriction of Chemical substances
ReNcell CX	Immortalized human neural progenitor cell line
RFU	Relative fluorescence unit
RG	Radial glia
RIN	RNA integrity number
RNA	Ribonucleic acid
RNASeq	Ribonucleic acid sequencing
rNPC	Rat neural progenitor cell
ROI	Region of interest
ROS	Reactive oxygen species
RS	Rabbit Serum
RT-qPCR	Quantitative real-time polymerase chain reaction
SC	Solvent Control
SD	Standard deviation
SEM	Standard Error of the Mean
SEMA3E	Semaphorin 3E
SERPINE 2	Serpin family E member 2
Shh	Sonic hedgehog
SNVs	Somatic single nucleotide variants
SVZ	Subventricular zone
T3	L-triiodothyronine
T4	Thyroxine

## Abbreviations

---

TBBPA	Tetrabromobisphenol A
TBOEP	Tris (2-butoxyethyl) phosphate
t-BPDPHP	Tert-butylphenyl diphenyl phosphate
TCEP	Tris (2-chloroethyl) phosphate
TCIPP	Tris (1-chloro-isopropyl) phosphate
TCM	Traditional Chinese Medicine
TCP	Tricresyl phosphate
TDCIPP	Tris (1,3-dichloro-isopropyl) phosphate
TH	Thyroid hormone
THR	Thyroid hormone receptor
TLC	Thin-layer chromatography
TM	Tian Ma
TOCP	Tri-O-cresyl phosphate
ToxCast	Toxicity Forecaster (EPA)
ToxPi GUI	Toxicological Prioritization Index Graphical User Interface
TPHP	Triphenyl phosphate
TPM	Transcript per KilobaseMillion
TREs	Thyroid hormone response elements
TSHR	Thyroid stimulating hormone receptor
TUBB3	Beta-III-tubulin
TXNIP	Thioredoxin interacting protein
US	United States
US EPA	United States Environmental Protection Agency
vs	Versus
VZ	Ventricular zone
WHO	World Health Organization
WoE	Weight-of-evidence

---

## References

- Alépée N (2014) State-of-the-art of 3D cultures (organs-on-a-chip) in safety testing and pathophysiology. *ALTEX* 441–477. <https://doi.org/10.14573/altex.1406111>
- Alzualde A, Behl M, Sipes NS, et al (2018) Toxicity profiling of flame retardants in zebrafish embryos using a battery of assays for developmental toxicity, neurotoxicity, cardiotoxicity and hepatotoxicity toward human relevance. *Neurotoxicol Teratol* 70:40–50. <https://doi.org/10.1016/j.ntt.2018.10.002>
- Andersen SL (2003) Trajectories of brain development: Point of vulnerability or window of opportunity? *Neurosci Biobehav Rev* 27:3–18. [https://doi.org/10.1016/S0149-7634\(03\)00005-8](https://doi.org/10.1016/S0149-7634(03)00005-8)
- Ankley GT, Bennett RS, Erickson RJ, et al (2010) Adverse outcome pathways: A conceptual framework to support ecotoxicology research and risk assessment. *Environ Toxicol Chem* 29:730–741. <https://doi.org/10.1002/etc.34>
- Annunziata P, Federico A, D'Amore I, et al (1983) Impairment of human brain development: glycoconjugate and lipid changes in congenital athyroidism. *Early Hum Dev* 8:269–278. [https://doi.org/10.1016/0378-3782\(83\)90009-9](https://doi.org/10.1016/0378-3782(83)90009-9)
- Arenas F, Garcia-Ruiz C, Fernandez-Checa JC (2017) Intracellular cholesterol trafficking and impact in neurodegeneration. *Front Mol Neurosci* 10:. <https://doi.org/10.3389/fnmol.2017.00382>
- Aschner M, Ceccatelli S, Daneshian M, et al (2017) Reference compounds for alternative test methods to indicate developmental neurotoxicity (DNT) potential of chemicals: example lists and criteria for their selection and use. *ALTEX* 34:49–74. <https://doi.org/10.14573/altex.1604201>
- Azevedo FAC, Carvalho LRB, Grinberg LT, et al (2009) Equal numbers of neuronal and nonneuronal cells make the human brain an isometrically scaled-up primate brain. *J Comp Neurol* 513:532–541. <https://doi.org/10.1002/cne.21974>
- Baas D, Bourbeau D, Sarliève LL, et al (1997) Oligodendrocyte Maturation and Progenitor Cell Proliferation are Independently Regulated by Thyroid Hormone. *Glia* 19:324–332
- Bacaloni A, Cacaliere C, Foglia P, et al (2007) Liquid chromatography/tandem mass spectrometry determination of organophosphorus flame retardants and plasticizers in drinking and surface waters. *Rapid Commun Mass Spectrom* 21:1123–1130. <https://doi.org/10.1002/rcm.2937> Liquid
- Back SA, Gan X, Li Y, et al (1998) Maturation-dependent vulnerability of oligodendrocytes to oxidative stress-induced death caused by glutathione depletion. *J Neurosci* 18:6241–53
- Back SA, Luo NL, Borenstein NS, et al (2001) Late oligodendrocyte progenitors coincide with the developmental window of vulnerability for human perinatal white matter injury. *J Neurosci* 21:1302–1312. <https://doi.org/10.1523/jneurosci.21-04-01302.2001>
- Bal-Price A, Crofton KM, Leist M, et al (2015a) International STakeholder NETwork (ISTNET): creating a developmental neurotoxicity (DNT) testing road map for regulatory purposes. *Arch Toxicol* 89:269–287. <https://doi.org/10.1007/s00204-015-1464-2>
- Bal-Price A, Crofton KM, Sachana M, et al (2015b) Putative adverse outcome pathways relevant to neurotoxicity. *Crit Rev Toxicol* 45:83–91. <https://doi.org/10.3109/10408444.2014.981331>

## References

---

- Bal-Price A, Hogberg HT, Crofton KM, et al (2018) Recommendation on test readiness criteria for new approach methods in toxicology: exemplified for developmental neurotoxicity. *ALTEX* 35:306–352. <https://doi.org/10.14573/altex.1712081>
- Bal-Price A, Lein PJ, Keil KP, et al (2016) Developing and applying the adverse outcome pathway concept for understanding and predicting neurotoxicity. *Neurotoxicology*
- Bal-Price A, Meek ME (2017) Adverse outcome pathways: Application to enhance mechanistic understanding of neurotoxicity. *Pharmacol Ther* 179:84–95. <https://doi.org/10.1016/j.pharmthera.2017.05.006>
- Barateiro A, Fernandes A (2014) Temporal oligodendrocyte lineage progression: In vitro models of proliferation, differentiation and myelination. *Biochim Biophys Acta - Mol Cell Res* 1843:1917–1929. <https://doi.org/10.1016/j.bbamcr.2014.04.018>
- Barenys M, Gassmann K, Baksmeier C, et al (2017) Epigallocatechin gallate (EGCG) inhibits adhesion and migration of neural progenitor cells in vitro. *Arch Toxicol* 91:827–837. <https://doi.org/10.1007/s00204-016-1709-8>
- Barenys M, Illa M, Hofrichter M, et al (2021) Rabbit neurospheres as a novel in vitro tool for studying neurodevelopmental effects induced by intrauterine growth restriction. *Stem Cells Transl Med* 10:209–221. <https://doi.org/10.1002/sctm.20-0223>
- Barenys M, Reverte I, Masjosthusmann S, et al (2019) Developmental neurotoxicity of MDMA. A systematic literature review summarized in a putative adverse outcome pathway. *Neurotoxicology* 78:209–241. <https://doi.org/10.1016/j.neuro.2019.12.007>
- Barry C, Schmitz MT, Jiang P, et al (2017) Species-specific developmental timing is maintained by pluripotent stem cells ex utero. *Dev Biol* 423:101–110. <https://doi.org/10.1016/j.ydbio.2017.02.002>
- Basketter DA, Clewell H, Kimber I, et al (2012) A Roadmap for the Development of Alternative (Non-Animal) Methods for Systemic Toxicity Testing. *Altex-Alternatives to Anim Exp* 29:1–91
- Baumann J, Barenys M, Gassmann K, Fritsche E (2014) Comparative human and rat “neurosphere assay” for developmental neurotoxicity testing. *Curr Protoc Toxicol* 1:1–24. <https://doi.org/10.1002/0471140856.tx1221s59>
- Baumann J, Dach K, Barenys M, et al (2015) Application of the Neurosphere Assay for DNT Hazard Assessment : Challenges and Limitations. <https://doi.org/10.1007/7653>
- Baumann J, Gassmann K, Masjosthusmann S, et al (2016) Comparative human and rat neurospheres reveal species differences in chemical effects on neurodevelopmental key events. *Arch Toxicol* 90:1415–1427. <https://doi.org/10.1007/s00204-015-1568-8>
- Baumann N, Pham-Dinh D (2001) Biology of oligodendrocyte and myelin in the mammalian central nervous system. *Physiol Rev* 81:871–927. <https://doi.org/10.1152/physrev.2001.81.2.871>
- Behl M, Hsieh JH, Shafer TJ, et al (2015) Use of alternative assays to identify and prioritize organophosphorus flame retardants for potential developmental and neurotoxicity. *Neurotoxicol Teratol* 52:181–193. <https://doi.org/10.1016/j.ntt.2015.09.003>
- Behl M, Ryan K, Hsieh JH, et al (2019) Screening for developmental neurotoxicity at the national toxicology program: The future is here. *Toxicol Sci* 167:258–268. <https://doi.org/10.1093/toxsci/kfy278>



- Bellanger M, Pichery C, Aerts D, et al (2013) Economic benefits of methylmercury exposure control in Europe: Monetary value of neurotoxicity prevention. *Environ Heal A Glob Access Sci Source* 12:1–10. <https://doi.org/10.1186/1476-069X-12-3>
- Bellinger DC (2012) Comparing the population neurodevelopmental burdens associated with children's exposures to environmental chemicals and other risk factors. *Neurotoxicology* 33:641–643. <https://doi.org/10.1016/j.neuro.2012.04.003>
- Bennett D, Bellinger DC, Birnbaum LS, et al (2016) Project TENDR : Targeting Environmental Neuro-Developomental Risks. The TENDR Consensus Statement. *Environ Health Perspect* 124:118–122
- Bergman Å, Rydén A, Law RJ, et al (2012) A novel abbreviation standard for organobromine, organochlorine and organophosphorus flame retardants and some characteristics of the chemicals. *Environ Int* 49:57–82. <https://doi.org/10.1016/j.envint.2012.08.003>
- Berhanu WM, Pillai GG, Oliferenko AA, Katritzky AR (2012) Quantitative structure-activity/property relationships: The ubiquitous links between cause and effect. *Chempluschem* 77:507–517. <https://doi.org/10.1002/cplu.201200038>
- Blaauboer BJ (2010) Biokinetic modeling and in vitro-in vivo extrapolations. *J Toxicol Environ Heal - Part B Crit Rev* 13:242–252. <https://doi.org/10.1080/10937404.2010.483940>
- Blum A, Behl M, Birnbaum LS, et al (2019) Organophosphate Ester Flame Retardants: Are They a Regrettable Substitution for Polybrominated Diphenyl Ethers? *Environ Sci Technol Lett* 6:638–649. <https://doi.org/10.1021/acs.estlett.9b00582>
- Borrell V, Götz M (2014) Role of radial glial cells in cerebral cortex folding. *Curr Opin Neurobiol* 27:39–46. <https://doi.org/10.1016/j.conb.2014.02.007>
- Bradl M, Lassmann H (2010) Oligodendrocytes: Biology and pathology. *Acta Neuropathol* 119:37–53. <https://doi.org/10.1007/s00401-009-0601-5>
- Bronner M, Hatten ME (2013) Chapter 15 - Neurogenesis and Migration. In: *Fundamental Neuroscience* (4th edition). pp 339–361
- Buc-Caron MH (1995) Neuroepithelial progenitor cells explanted from human fetal brain proliferate and differentiate in vitro. *Neurobiol Dis* 2:37–47. <https://doi.org/10.1006/nbdi.1995.0004>
- Burke RD, Todd SW, Lumsden E, et al (2017) Developmental neurotoxicity of the organophosphorus insecticide chlorpyrifos: from clinical findings to preclinical models and potential mechanisms. *J Neurochem* 142:162–177. <https://doi.org/10.1111/jnc.14077>
- Butt CM, Hoffman K, Chen A, et al (2016) Regional comparison of organophosphate flame retardant (PFR) urinary metabolites and tetrabromobenzoic acid (TBBA) in mother-toddler pairs from California and New Jersey. *Environ Int* 94:627–634. <https://doi.org/10.1016/j.envint.2016.06.029>
- Carusi A, Davies MR, De Grandis G, et al (2018) Harvesting the promise of AOPs: An assessment and recommendations. *Sci Total Environ* 628–629:1542–1556. <https://doi.org/10.1016/j.scitotenv.2018.02.015>
- CAS Registry 2021 Registry 2021. <https://www.cas.org/support/documentation/chemical-substances>
- Ceresna (2018) Flame retardant market report. <https://www.ceresana.com/en/market-studies/chemicals/flame-retardants/ceresana-market-study-flame-retardants.html>

## References

---

- Chalmers-Redman RME, Priestley T, Kemp JA, Fine A (1997) In vitro propagation and inducible differentiation of multipotential progenitor cells from human fetal brain. *Neuroscience* 76:1121–1128. [https://doi.org/10.1016/S0306-4522\(96\)00386-7](https://doi.org/10.1016/S0306-4522(96)00386-7)
- Chao HR, Wang SL, Lee WJ, et al (2007) Levels of polybrominated diphenyl ethers (PBDEs) in breast milk from central Taiwan and their relation to infant birth outcome and maternal menstruation effects. *Environ Int* 33:239–245. <https://doi.org/10.1016/j.envint.2006.09.013>
- Chen H, Chidboy MA, Robinson JF (2020) Retinoids and developmental neurotoxicity: Utilizing toxicogenomics to enhance adverse outcome pathways and testing strategies. *Reprod Toxicol* 96:102–113. <https://doi.org/10.1016/j.reprotox.2020.06.007>
- Cheroni C, Caporale N, Testa G (2020) Autism spectrum disorder at the crossroad between genes and environment: Contributions, convergences, and interactions in ASD developmental pathophysiology. *Mol Autism* 11:1–18. <https://doi.org/10.1186/s13229-020-00370-1>
- Chupeau Z, Bonvallet N, Mercier F, et al (2020) Organophosphorus flame retardants: A global review of indoor contamination and human exposure in Europe and epidemiological evidence. *Int J Environ Res Public Health* 17:1–24. <https://doi.org/10.3390/ijerph17186713>
- Claudio L, Kwa WC, Russell AL, Wallinga D (2000) Testing methods for developmental neurotoxicity of environmental chemicals. *Toxicol Appl Pharmacol* 164:1–14. <https://doi.org/10.1006/taap.2000.8890>
- Coghlan ML, Maker G, Crighton E, et al (2015) Combined DNA, toxicological and heavy metal analyses provides an auditing toolkit to improve pharmacovigilance of traditional Chinese medicine (TCM). *Sci Rep* 5:1–9. <https://doi.org/10.1038/srep17475>
- Collins FS, Gray GM, Bucher JR (2008) Transforming environmental health protection. *Science* (80-) 319:906–907. <https://doi.org/10.1126/science.1154619>
- Crofton K, Fritsche E, Ylikomi T, Bal-Price A (2014) International STakeholder NETwork (ISTNET) for creating a Developmental Neurotoxicity Testing (DNT) roadmap for regulatory purposes. *ALTEX* 31:223–224. <https://doi.org/10.14573/altex.1402121>
- Crofton KM, Mundy WR, Lein PJ, et al (2011) Developmental neurotoxicity testing: Recommendations for developing alternative methods for the screening and prioritization of chemicals. *ALTEX* 28:9–15. <https://doi.org/10.14573/altex.2011.1.009>
- Crofton KM, Mundy WR, Shafer TJ (2012) Developmental neurotoxicity testing: a path forward. *Congenit Anom (Kyoto)* 52:140–146. <https://doi.org/10.1111/j.1741-4520.2012.00377.x>
- Croom EL, Shafer TJ, Evans M V., et al (2015) Improving in vitro to in vivo extrapolation by incorporating toxicokinetic measurements: A case study of lindane-induced neurotoxicity. *Toxicol Appl Pharmacol* 283:9–19. <https://doi.org/10.1016/j.taap.2014.11.006>
- Dach K, Bendt F, Huebenthal U, et al (2017) BDE-99 impairs differentiation of human and mouse NPCs into the oligodendroglial lineage by species-specific modes of action. *Sci Rep* 7:1–11. <https://doi.org/10.1038/srep44861>
- Darnerud PO, Eriksen GS, Jóhannesson T, et al (2001) Polybrominated diphenyl ethers: Occurrence, dietary exposure, and toxicology. *Environ Health Perspect* 109:49–68. <https://doi.org/10.1289/ehp.01109s149>
- Davis JA, Gift JS, Zhao QJ (2011) Introduction to benchmark dose methods and U.S. EPA's benchmark dose software (BMDS) version 2.1.1. *Toxicol Appl Pharmacol* 254:181–191. <https://doi.org/10.1016/j.taap.2010.10.016>

- De Felice A, Ricceri L, Venerosi A, et al (2015) Multifactorial origin of neurodevelopmental disorders: Approaches to understanding complex etiologies. *Toxics* 3:89–129. <https://doi.org/10.3390/toxics3010089>
- De Hoz L, Simons M (2015) The emerging functions of oligodendrocytes in regulating neuronal network behaviour. *BioEssays* 37:60–69. <https://doi.org/10.1002/bies.201400127>
- Delp J, Gutbier S, Klima S, et al (2018) A high-throughput approach to identify specific neurotoxicants/ developmental toxicants in human neuronal cell function assays. *ALTEX* 35:235–253. <https://doi.org/10.14573/altex.1712182>
- Dix DJ, Houck KA, Martin MT, et al (2007) The ToxCast program for prioritizing toxicity testing of environmental chemicals. *Toxicol Sci* 95:5–12. <https://doi.org/10.1093/toxsci/kfl103>
- Dorman DC, Allen SL, Byczkowski JZ, et al (2001) Methods to identify and characterize developmental neurotoxicity for human health risk assessment. I: Behavioral effects. *Environ Health Perspect* 109:101–111. <https://doi.org/10.1289/ehp.01109s179>
- EFSA (2013) Scientific Opinion on the developmental neurotoxicity potential of acetamiprid and imidacloprid. *EFSA J* 11:1–47. <https://doi.org/10.2903/j.efsa.2013.3471>
- EFSA (2012) Guidance for establishing the safety of additives for the consumer. *EFSA J* 10:1–12. <https://doi.org/10.2903/j.efsa.2012.2537>
- Egeghy PP, Sheldon LS, Isaacs KK, et al (2016) Computational exposure science: An emerging discipline to support 21st-century risk assessment. *Environ Health Perspect* 124:697–702. <https://doi.org/10.1289/ehp.1509748>
- Emery B (2010) Regulation of oligodendrocyte differentiation and myelination. *Science* (80- ) 330:779–782. <https://doi.org/10.1126/science.1190927>
- EPA (1998) Health Effects Test Guidelines OPPTS 870.6300 Developmental Neurotoxicity Study
- Eskenazi B, Chevrier J, Rauch SA, et al (2013) In utero and childhood polybrominated diphenyl ether (PBDE) exposures and neurodevelopment in the CHAMACOS study. *Environ Health Perspect* 121:257–262. <https://doi.org/10.1289/ehp.1205597>
- Eskes C, Whelan M (2016) *Validation of Alternative Methods for Toxicity Testing*, Advances in Springer
- Fernández V, Llinares-Benadero C, Borrell V (2016) Cerebral cortex expansion and folding: what have we learned? *EMBO J* 35:1021–1044. <https://doi.org/10.15252/embj.201593701>
- Filer DL, Kothiya P, Woodrow Setzer R, et al (2017) Tcpl: The ToxCast pipeline for high-throughput screening data. *Bioinformatics* 33:618–620. <https://doi.org/10.1093/bioinformatics/btw680>
- Flaws B (2005) *Chinese Medical Obstetrics*, First Edit. Blue Poopy Press, Boulder, CO
- Frank CL, Brown JP, Wallace K, et al (2017) Developmental neurotoxicants disrupt activity in cortical networks on microelectrode arrays: Results of screening 86 compounds during neural network formation. *Toxicol Sci* 160:121–135. <https://doi.org/10.1093/toxsci/kfx169>
- Frederiksen M, Vorkamp K, Thomsen M, Knudsen LE (2009) Human internal and external exposure to PBDEs - A review of levels and sources. *Int J Hyg Environ Health* 212:109–134. <https://doi.org/10.1016/j.ijheh.2008.04.005>

## References

---

- Fritsche E (2016) Report on Integrated Testing Strategies for the identification and evaluation of chemical hazards associated with the developmental neurotoxicity (DNT), to facilitate discussions at the Joint EFSA/OECD Workshop on DNT. OECD Guidel Test Chem
- Fritsche E (2017) Report of the OECD/EFSA Workshop on developmental neurotoxicity (DNT): The use of non-animal test methods for regulatory purposes. OECD Environ Heal Saf. [https://doi.org/Unclassified ENV/JM/MONO\(2017\)4/ANN1](https://doi.org/Unclassified ENV/JM/MONO(2017)4/ANN1)
- Fritsche E, Alm H, Baumann J, et al (2015) Literature review on in vitro and alternative Developmental Neurotoxicity (DNT) testing methods. EFSA Support Publ 12:1–186. <https://doi.org/10.2903/sp.efsa.2015.en-778>
- Fritsche E, Barenys M, Klose J, et al (2018a) Current availability of stem cell-Based in vitro methods for developmental neurotoxicity (DNT) testing. Toxicol Sci 165:21–30. <https://doi.org/10.1093/toxsci/kfy178>
- Fritsche E, Barenys M, Klose J, et al (2018b) Development of the concept for stem cell-based developmental neurotoxicity evaluation. Toxicol Sci 165:14–20. <https://doi.org/10.1093/toxsci/kfy175>
- Fritsche E, Cline JE, Nguyen NH, et al (2005) Polychlorinated biphenyls disturb differentiation of normal human neural progenitor cells: Clue for involvement of thyroid hormone receptors. Environ Health Perspect 113:871–876. <https://doi.org/10.1289/ehp.7793>
- Fritsche E, Crofton KM, Hernandez AF, et al (2017) OECD/EFSA workshop on developmental neurotoxicity (DNT): The use of non-animal test methods for regulatory purposes. ALTEX 34:311–315. <https://doi.org/10.14573/altex.1701171s>
- Fritsche E, Grandjean P, Crofton KM, et al (2018c) Consensus statement on the need for innovation, transition and implementation of developmental neurotoxicity (DNT) testing for regulatory purposes. Toxicol Appl Pharmacol 354:3–6. <https://doi.org/10.1016/j.taap.2018.02.004>
- Fromme H, Lahrz T, Kraft M, et al (2014) Organophosphate flame retardants and plasticizers in the air and dust in German daycare centers and human biomonitoring in visiting children (LUPE 3). Environ Int 71:158–163. <https://doi.org/10.1016/j.envint.2014.06.016>
- Gangwal S, Reif DM, Mosher S, et al (2012) Incorporating exposure information into the toxicological prioritization index decision support framework. Sci Total Environ 435–436:316–325. <https://doi.org/10.1016/j.scitotenv.2012.06.086>
- Gasperini RJ, Pavez M, Thompson AC, et al (2017) How does calcium interact with the cytoskeleton to regulate growth cone motility during axon pathfinding? Mol Cell Neurosci 84:29–35. <https://doi.org/10.1016/j.mcn.2017.07.006>
- Gassmann K, Abel J, Bothe H, et al (2010) Species-specific differential ahr expression protects human neural progenitor cells against developmental neurotoxicity of PAHs. Environ Health Perspect 118:1571–1577. <https://doi.org/10.1289/ehp.0901545>
- Gaylord A, Osborne G, Ghassabian A, et al (2020) Trends in neurodevelopmental disability burden due to early life chemical exposure in the USA from 2001 to 2016: A population-based disease burden and cost analysis. Mol Cell Endocrinol 502:110666. <https://doi.org/10.1016/j.mce.2019.110666>
- Gibb S (2008) Toxicity testing in the 21st century: A vision and a strategy. Reprod Toxicol 25:136–138. <https://doi.org/10.1016/j.reprotox.2007.10.013>

- Ginsberg GL, Fedinick KP, Solomon GM, et al (2019) New toxicology tools and the emerging paradigm shift in environmental health decision-making. *Environ Health Perspect* 127:1–7. <https://doi.org/10.1289/EHP4745>
- Giordano G, Costa LG (2012) Developmental Neurotoxicity: Some Old and New Issues. *ISRN Toxicol* 2012:1–12. <https://doi.org/10.5402/2012/814795>
- Glover DD, Amonkar M, Rybeck BF, Tracy TS (2003) Prescription, over-the-counter, and herbal medicine use in a rural, obstetric population. *Am J Obstet Gynecol* 188:1039–1045. <https://doi.org/10.1067/mob.2003.223>
- Grandjean P, Landrigan P (2006) Developmental neurotoxicity of industrial chemicals. *Lancet* 368:2167–2178. [https://doi.org/10.1016/S0140-6736\(06\)69665-7](https://doi.org/10.1016/S0140-6736(06)69665-7)
- Grandjean P, Landrigan PJ (2014) Neurobehavioural effects of developmental toxicity. *Lancet Neurol* 13:330–338. [https://doi.org/10.1016/S1474-4422\(13\)70278-3](https://doi.org/10.1016/S1474-4422(13)70278-3)
- Gross RE, Mehler MF, Mabie PC, et al (1996) Bone Morphogenetic Proteins Promote Astroglial Lineage Commitment by Mammalian Subventricular Zone Progenitor Cells. *17:595–606*
- Gülden M, Seibert H (2003) In vitro-in vivo extrapolation: Estimation of human serum concentrations of chemicals equivalent to cytotoxic concentrations in vitro. *Toxicology* 189:211–222. [https://doi.org/10.1016/S0300-483X\(03\)00146-X](https://doi.org/10.1016/S0300-483X(03)00146-X)
- Hardy A, Benford D, Halldorsson T, et al (2017) Update: use of the benchmark dose approach in risk assessment. *EFSA J* 15:1–41. <https://doi.org/10.2903/j.efsa.2017.4658>
- Harrill JA, Freudenrich T, Wallace K, et al (2018) Testing for developmental neurotoxicity using a battery of in vitro assays for key cellular events in neurodevelopment. *Toxicol Appl Pharmacol* 354:24–39. <https://doi.org/10.1016/j.taap.2018.04.001>
- Hemminki E, Mantyranta T, Maili M, Paivikki K (1991) A survey on the use of alternative drugs during pregnancy. *J Mich Dent Assoc* 66:63–67
- Hoelting L, Klima S, Karreman C, et al (2016) Stem Cell-Derived Immature Human Dorsal Root Ganglia Neurons to Identify Peripheral Neurotoxicants. *Stem Cells Transl Med* 5:476–487. <https://doi.org/10.5966/sctm.2015-0108>
- Hofrichter M, Nimtz L, Tigges J, et al (2017) Comparative performance analysis of human iPSC-derived and primary neural progenitor cells (NPC) grown as neurospheres in vitro. *Stem Cell Res* 25:72–82. <https://doi.org/10.1016/j.scr.2017.10.013>
- Hogberg HT, de Cássia da Silveira E Sá R, Kleensang A, et al (2020) Organophosphorus flame retardants are developmental neurotoxicants in a rat primary brainsphere in vitro model. *Arch Toxicol*. <https://doi.org/10.1007/s00204-020-02903-2>
- Hollyer T, Boon H, Georgousis A, et al (2002) The use of CAM by women suffering from nausea and vomiting during pregnancy. *BMC Complement Altern Med* 2:1–6. <https://doi.org/10.1186/1472-6882-2-5>
- Hsieh JH, Sedykh A, Huang R, et al (2015) A data analysis pipeline accounting for artifacts in Tox21 quantitative high-throughput screening assays. *J Biomol Screen* 20:887–897. <https://doi.org/10.1177/1087057115581317>
- <https://aopwiki.org/>
- Hu D (2015) *Traditional Chinese Medicine*. Tsinghua University Press

## References

---

- Hutter HP, Haluza D, Piegler K, et al (2013) Semivolatile compounds in schools and their influence on cognitive performance of children. *Int J Occup Med Environ Health* 26:628–635. <https://doi.org/10.2478/s13382-013-0125-z>
- Huttner WB, Kosodo Y (2005) Symmetric versus asymmetric cell division during neurogenesis in the developing vertebrate central nervous system. *Curr Opin Cell Biol* 17:648–657. <https://doi.org/10.1016/j.ceb.2005.10.005>
- Insel TR (2010) Rethinking schizophrenia. *Nature* 468:187–193. <https://doi.org/10.1038/nature09552>
- Jung AB, Bennett JP (1996) Development of striatal dopaminergic function. III: Pre- and postnatal development of striatal and cortical mRNAs for the neurotrophin receptors trkBTK+ and trkC and their regulation by synaptic dopamine. *Dev Brain Res* 94:133–143. [https://doi.org/10.1016/S0165-3806\(96\)80004-6](https://doi.org/10.1016/S0165-3806(96)80004-6)
- Juurlink BH (1997) Response of glial cells to ischemia: roles of reactive oxygen species and glutathione. *Neurosci Biobehav Rev* 21:151–66
- Kadereit S, Bastian Z, Van Thriel C, et al (2012) Compound selection for in vitro modeling of developmental neurotoxicity Suzanne. *Front Biosci* 17:2442–2460. <https://doi.org/10.2741/4064>
- Kandel ER, Schwartz JH, Jessell TM (2000) Principles of neural science 4th edition, 4th edn. McGraw-Hill, New York
- Kaufmann W (2003) Current status of developmental neurotoxicity: An industry perspective. *Toxicol Lett* 140–141:161–169. [https://doi.org/10.1016/S0378-4274\(02\)00503-9](https://doi.org/10.1016/S0378-4274(02)00503-9)
- Kimbrough RD (1995) Polychlorinated biphenyls (PCBs) and human health: An update. *Crit Rev Toxicol* 25:133–163. <https://doi.org/10.3109/10408449509021611>
- Kimbrough RD, Krouskas CA (2003) Human exposure to polychlorinated biphenyls and health effects: A critical synopsis. *Toxicol Rev* 22:217–233. <https://doi.org/10.2165/00139709-200322040-00004>
- Klose J, Pahl M, Bartmann K, et al (2021a) Neurodevelopmental toxicity assessment of flame retardants using a human DNT in vitro testing battery. *Cell Biol Toxicol* 1–27. <https://doi.org/10.1007/s10565-021-09603-2>
- Klose J, Tigges J, Masjosthusmann S, et al (2021b) TBBPA targets converging key events of human oligodendrocyte development resulting in two novel AOPs. *ALTEX* 38:215–234. <https://doi.org/10.14573/altex.2007201>
- Knapen D, Angrish MM, Fortin MC, et al (2018) Adverse outcome pathway networks I: Development and applications. *Environ Toxicol Chem* 37:1723–1733. <https://doi.org/10.1002/etc.4125>
- Knudsen TB, Kleinstreuer NC (2011) Disruption of embryonic vascular development in predictive toxicology. *Birth Defects Res Part C - Embryo Today Rev* 93:312–323. <https://doi.org/10.1002/bdrc.20223>
- Konietzka R, Schneider K, Ritter L (2014) Extrapolation Factors and Safety Factors in Toxicology. *Regul Toxicol* 431–438. [https://doi.org/10.1007/978-3-642-35374-1\\_59](https://doi.org/10.1007/978-3-642-35374-1_59)
- Kramer NI (2010) Dissertation: Measuring, Modeling, and Increasing the Free Concentration of Test Chemicals in Cell Assays. University of Utrecht

- Krebs A, Nyffeler J, Karreman C, et al (2020) Determination of benchmark concentrations and their statistical uncertainty for cytotoxicity test data and functional in vitro assays. *ALTEX* 37:155–163. <https://doi.org/10.14573/altex.1912021>
- Krewski D, Andersen ME, Mantus E, Zeise L (2009) Toxicity testing in the 21st century: implications for human health risk assessment. *Risk Anal* 29:474–479. <https://doi.org/10.1111/j.1539-6924.2008.01150.x>
- Krewski D, Andersen ME, Tyshenko MG, et al (2020) Toxicity testing in the 21st century: progress in the past decade and future perspectives. *Arch Toxicol* 94:. <https://doi.org/10.1007/s00204-019-02613-4>
- Krug AK, Balmer N V., Matt F, et al (2013a) Evaluation of a human neurite growth assay as specific screen for developmental neurotoxicants. *Arch Toxicol* 87:2215–2231. <https://doi.org/10.1007/s00204-013-1072-y>
- Krug AK, Kolde R, Gaspar JA, et al (2013b) Human embryonic stem cell-derived test systems for developmental neurotoxicity: a transcriptomics approach. *Arch Toxicol* 87:123–143. <https://doi.org/10.1007/s00204-012-0967-3>
- Kuhn S, Gritti L, Crooks D, Dombrowski Y (2019) Oligodendrocytes in Development, Myelin Generation and Beyond. *cells* 1424:1–23. <https://doi.org/10.3390/cells8111424>
- Law RJ, Covaci A, Harrad S, et al (2014) Levels and trends of PBDEs and HBCDs in the global environment: Status at the end of 2012. *Environ Int* 65:147–158. <https://doi.org/10.1016/j.envint.2014.01.006>
- Lein P, Silbergeld E, Locke P, Goldberg AM (2005) In vitro and other alternative approaches to developmental neurotoxicity testing (DNT). *Environ Toxicology Pharmacol* 19:735–744. <https://doi.org/10.1016/j.etap.2004.12.035>
- Leist M, Ghallab A, Graepel R, et al (2017) Adverse outcome pathways: opportunities, limitations and open questions. *Arch Toxicol* 91:3477–3505. <https://doi.org/10.1007/s00204-017-2045-3>
- Leist M, Hartung T (2013) Inflammatory findings on species extrapolations: Humans are definitely no 70-kg mice. *Arch Toxicol* 87:563–567. <https://doi.org/10.1007/s00204-013-1038-0>
- Leontaridou M, Urbisch D, Kollé SN, et al (2017) The borderline range of toxicological methods: Quantification and implications for evaluating precision. *ALTEX* 34:525–538. <https://doi.org/10.14573/altex.1606271>
- Li J, Settivari R, LeBaron MJ, Marty MS (2019) An industry perspective: A streamlined screening strategy using alternative models for chemical assessment of developmental neurotoxicity. *Neurotoxicology* 73:17–30. <https://doi.org/10.1016/j.neuro.2019.02.010>
- Li L, Leung PC, Chung TKH, Wang CC (2013) Systematic review of Chinese Medicine for miscarriage during early pregnancy. *Evidence-based Complement Altern Med* 2014:. <https://doi.org/10.1155/2014/753856>
- Linderkamp O, Janus L, Linder R, Skoruppa D (2009) Time table of normal foetal brain development. *Int J Prenat Perinat Psychol Med* 21:4–16
- Lipscomb ST, McClelland MM, MacDonald M, et al (2017) Cross-sectional study of social behaviors in preschool children and exposure to flame retardants. *Environ Heal A Glob Access Sci Source* 16:1–10. <https://doi.org/10.1186/s12940-017-0224-6>



## References

---

- López-Espíndola D, Morales-Bastos C, Grijota-Martínez C, et al (2014) Mutations of the thyroid hormone transporter MCT8 cause prenatal brain damage and persistent hypomyelination. *J Clin Endocrinol Metab* 99:E2799–E2804. <https://doi.org/10.1210/jc.2014-2162>
- Ludwin SK (1997) The Pathobiology of the Oligodendrocyte. *J Neuropathol Exp Neurol* 56:111–124. <https://doi.org/10.1097/00005072-199702000-00001>
- Luttrell WE, Olajos EJ, Pleban PA (1993) change in Hen Sciatic Nerve Calcium after a Single Oral Dose of Tri-O-Tolyl Phosphate. *Environ Res* 60:290–294
- Ma J, Zhu H, Kannan K (2019) Organophosphorus Flame Retardants and Plasticizers in Breast Milk from the United States. *Environ Sci Technol Lett* 6:525–531. <https://doi.org/10.1021/acs.estlett.9b00394>
- Ma Y, Salamova A, Venier M, Hites RA (2013) Has the Phase-Out of PBDEs Affected Their Atmospheric Levels? Trends of PBDEs and Their Replacements in the Great Lakes Atmosphere. *Environ Sci Technol* 47:11457–11464. <https://doi.org/dx.doi.org/10.1021/es403029m>
- Makris SL, Raffaele K, Allen S, et al (2009) A retrospective performance assessment of the developmental neurotoxicity study in support of OECD test guideline 426. *Environ Health Perspect* 117:17–25. <https://doi.org/10.1289/ehp.11447>
- Marinelli C, Bertalot T, Zusso M, et al (2016) Systematic review of pharmacological properties of the oligodendrocyte lineage. *Front Cell Neurosci* 10:1–19. <https://doi.org/10.3389/fncel.2016.00027>
- Marvel SW, To K, Grimm FA, et al (2018) ToxPi Graphical User Interface 2.0: Dynamic exploration, visualization, and sharing of integrated data models. *BMC Bioinformatics* 19:1–7. <https://doi.org/10.1186/s12859-018-2089-2>
- Masjosthusmann S, Becker D, Petzuch B, et al (2018) A transcriptome comparison of time-matched developing human, mouse and rat neural progenitor cells reveals human uniqueness. *Toxicol Appl Pharmacol* 354:40–55. <https://doi.org/10.1016/j.taap.2018.05.009>
- Masjosthusmann S, Blum J, Bartmann K, et al (2020) Establishment of an a priori protocol for the implementation and interpretation of an in-vitro testing battery for the assessment of developmental neurotoxicity. *EFSA J* 17:1938e. <https://doi.org/10.2903/sp.efsa.2020.EN-1938>
- Masjosthusmann S, Siebert C, Hübenthal U, et al (2019) Arsenite interrupts neurodevelopmental processes of human and rat neural progenitor cells: The role of reactive oxygen species and species-specific antioxidative defense. *Chemosphere* 235:447–456. <https://doi.org/10.1016/j.chemosphere.2019.06.123>
- Mayor R, Theveneau E (2013) The neural crest. *Dev a glance* 140:2247–2251. <https://doi.org/10.1242/dev.091751>
- McTigue DM, Tripathi RB (2008) The life, death, and replacement of oligodendrocytes in the adult CNS. *J Neurochem* 107:1–19. <https://doi.org/10.1111/j.1471-4159.2008.05570.x>
- Mie A, Rudén C, Grandjean P (2018) Safety of Safety Evaluation of Pesticides: Developmental neurotoxicity of chlorpyrifos and chlorpyrifos-methyl. *Environ Heal A Glob Access Sci Source* 17:1–5. <https://doi.org/10.1186/s12940-018-0421-y>

- Minoux M, Rijli FM (2010) Molecular mechanisms of cranial neural crest cell migration and patterning in craniofacial development. *Development* 137:2605–2621. <https://doi.org/10.1242/dev.040048>
- Mizouchi S, Ichiba M, Takigami H, et al (2015) Exposure assessment of organophosphorus and organobromine flame retardants via indoor dust from elementary schools and domestic houses. *Chemosphere* 123:17–25. <https://doi.org/10.1016/j.chemosphere.2014.11.028>
- Moors M, Bose R, Johansson-Haque K, et al (2012) Dickkopf 1 mediates glucocorticoid-induced changes in human neural progenitor cell proliferation and differentiation. *Toxicol Sci* 125:488–495. <https://doi.org/10.1093/toxsci/kfr304>
- Moors M, Cline JE, Abel J, Fritsche E (2007) ERK-dependent and -independent pathways trigger human neural progenitor cell migration. *Toxicol Appl Pharmacol* 221:57–67. <https://doi.org/10.1016/j.taap.2007.02.018>
- Moors M, Rockel TD, Abel J, et al (2009) Human Neurospheres as Three-Dimensional Cellular Systems for Developmental Neurotoxicity Testing. 117:1131–1138. <https://doi.org/10.1289/ehp.0800207>
- Mundy WR, Padilla S, Breier JM, et al (2015) Expanding the test set: Chemicals with potential to disrupt mammalian brain development. *Neurotoxicol Teratol* 52:25–35. <https://doi.org/10.1016/j.ntt.2015.10.001>
- Nimtzt L, Hartmann J, Tigges J, et al (2020) Characterization and application of electrically active neuronal networks established from human induced pluripotent stem cell-derived neural progenitor cells for neurotoxicity evaluation. *Stem Cell Res* 45:101761. <https://doi.org/10.1016/j.scr.2020.101761>
- Nimtzt L, Kloese J, Masjosthusmann S, et al (2019) The Neurosphere Assay as an In Vitro Method for Developmental Neurotoxicity (DNT) Evaluation. In: *Cell Culture Techniques, Neuromethods*. pp 141–168
- Noctor SC, Martinez-Cerdeño V, Ivic L, Kriegstein AR (2004) Cortical neurons arise in symmetric and asymmetric division zones and migrate through specific phases. *Nat Neurosci* 7:136–144. <https://doi.org/10.1038/nn1172>
- Nordeng H, Havnen GC (2004) Use of herbal drugs in pregnancy: A survey among 400 Norwegian women. *Pharmacoepidemiol Drug Saf* 13:371–380. <https://doi.org/10.1002/pds.945>
- Norton WT, Poduslo SE (1973) Myelination in Rat Brain: Changes in Myelin Composition During Brain Maturation. *J Neurochem* 21:759–773. <https://doi.org/10.1111/j.1471-4159.1973.tb07520.x>
- NRC (2007) *Toxicity Testing in the 21st Century: A Vision and a Strategy*. <https://doi.org/10.17226/11970>
- Nyffeler J, Dolde X, Krebs A, et al (2017a) Combination of multiple neural crest migration assays to identify environmental toxicants from a proof-of-concept chemical library. *Arch Toxicol* 91:3613–3632. <https://doi.org/10.1007/s00204-017-1977-y>
- Nyffeler J, Karreman C, Leisner H, et al (2017b) Design of a high-throughput human neural crest cell migration assay to indicate potential developmental toxicants. *ALTEX* 34:75–94. <https://doi.org/10.14573/altex.1605031>

## References

---

- Odawara A, Katoh H, Matsuda N, Suzuki I (2016) Physiological maturation and drug responses of human induced pluripotent stem cell-derived cortical neuronal networks in long-term culture. *Sci Rep* 6:1–14. <https://doi.org/10.1038/srep26181>
- OECD (2007) OECD Guideline for the Testing of Chemicals OECD 426 Developmental Neurotoxicity Study
- OECD (2020) Overview of Concepts and Available Guidance related to Integrated Approaches to Testing and Assessment (IATA), Series on Testing and Assessment No. 329. *Environ Heal Safety, Environ Dir OECD*
- OECD (2016) Guidance Document for the Use of Adverse Outcome Pathways in Developing Integrated Approaches to Testing and Assessment (IATA), Series on Testing & Assessment No. 260. *OECD Guidel Test Chem*
- OECD (2015) Report of the Workshop on a Framework for the Development and Use of Integrated Approaches to Testing and Assessment (IATA), Series on Testing & Assessment No. 215. 215:1–154
- OECD (2014) Guidance Document for Describing Non-Guideline In Vitro Test Methods: Series on Testing and Assessment No. 211. *OECD Environ Heal Saf Publ*
- OECD (2013) Revised Guidance Document on Developing and Assessing Adverse Outcome Pathways. *IOMC*
- Ortega MC, Bribián A, Peregrín S, et al (2012) Neuregulin-1/ErbB4 signaling controls the migration of oligodendrocyte precursor cells during development. *Exp Neurol* 235:610–620. <https://doi.org/10.1016/j.expneurol.2012.03.015>
- Paini A, Leonard JA, Joossens E, et al (2019) Next generation physiologically based kinetic (NG-PBK) models in support of regulatory decision making. *Comput Toxicol* 9:61–72. <https://doi.org/10.1016/j.comtox.2018.11.002>
- Paparella M, Bennekou SH, Bal-Price A (2020) An analysis of the limitations and uncertainties of in vivo developmental neurotoxicity testing and assessment to identify the potential for alternative approaches. *Reprod Toxicol* 96:327–336. <https://doi.org/10.1016/j.reprotox.2020.08.002>
- Pardridge WM (1998) *Introduction to the Blood-Brain Barrier*. School of Medicine, University of California, Los Angeles
- Patlewicz G, Simon TW, Rowlands JC, et al (2015) Proposing a scientific confidence framework to help support the application of adverse outcome pathways for regulatory purposes. *Regul Toxicol Pharmacol* 71:463–477. <https://doi.org/10.1016/j.yrtph.2015.02.011>
- Piper DR, Mujtaba T, Keyoung H, et al (2001) Identification and characterization of neuronal precursors and their progeny from human fetal tissue. *J Neurosci Res* 66:356–368. <https://doi.org/10.1002/jnr.1228>
- Pistollato F, Madia F, Corvi R, et al (2021) Current EU regulatory requirements for the assessment of chemicals and cosmetic products: challenges and opportunities for introducing new approach methodologies. *Springer Berlin Heidelberg*
- Pollesch NL, Villeneuve DL, O'Brien JM (2019) Extracting and Benchmarking Emerging Adverse Outcome Pathway Knowledge. *Toxicol Sci* 168:349–364. <https://doi.org/10.1093/toxsci/kfz006>

- Poma G, Sales C, Bruyland B, et al (2018) Occurrence of Organophosphorus Flame Retardants and Plasticizers (PFRs) in Belgian Foodstuffs and Estimation of the Dietary Exposure of the Adult Population. *Environ Sci Technol* 52:2331–2338. <https://doi.org/10.1021/acs.est.7b06395>
- Prieto P, Blaauboer BJ, Boer AG De (2004) Blood – Brain Barrier In Vitro Models and Their Application in Toxicology. *Altern to Lab Anim* 37–50. <https://doi.org/10.1177/026119290403200107>
- Radonjic M, Cappaert NLM, de Vries EFJ, et al (2013) Delay and impairment in brain development and function in rat offspring after maternal exposure to methylmercury. *Toxicol Sci* 133:112–124. <https://doi.org/10.1093/toxsci/kft024>
- Reif DM, Martin MT, Tan SW, et al (2010) Endocrine profiling and prioritization of environmental chemicals using toxcast data. *Environ Health Perspect* 118:1714–1720. <https://doi.org/10.1289/ehp.1002180>
- Reubinoff BE, Itsykson P, Turetsky T, et al (2001) Neural progenitors from human embryonic stem cells. *Most* 19:1134–1140. <https://doi.org/10.1038/nbt1201-1134>
- Reynolds BA, Tetzlaff W, Weiss S (1992) A multipotent EGF-responsive striatal embryonic progenitor cell produces neurons and astrocytes. *J Neurosci* 12:4565–4574. <https://doi.org/10.1523/jneurosci.12-11-04565.1992>
- Rovida C, Hartung T (2009) Re-evaluation of animal numbers and costs for in vivo tests to accomplish REACH legislation requirements for chemicals - A report by the transatlantic think tank for toxicology (t4). *ALTEX* 26:187–208. <https://doi.org/10.14573/altex.2009.3.187>
- Roze E, Meijer L, Bakker A, et al (2009) Prenatal exposure to organohalogens, including brominated flame retardants, influences motor, cognitive, and behavioral performance at school age. *Environ Health Perspect* 117:1953–1958. <https://doi.org/10.1289/ehp.0901015>
- Russell WMS, Burch RL (1959) *The Principles of Humane Experimental Technique*. London Methuen Co LTD
- Saavedra L, Kathleen W, Freudenrich TF, et al (2021) Comparison of Acute Effects of Neurotoxic Compounds on Network Activity in Human and Rodent Neural Cultures. *Toxicol Sci* 180:295–312. <https://doi.org/10.1093/toxsci/kfab008>
- Sachana M, Bal-Price A, Crofton KM, et al (2019) International regulatory and scientific effort for improved developmental neurotoxicity testing. *Toxicol Sci* 167:45–57. <https://doi.org/10.1093/toxsci/kfy211>
- Sachana M, Shafer TJ, Terron A (2021a) Toward a better testing paradigm for developmental neurotoxicity: Oecd efforts and regulatory considerations. *Biology (Basel)* 10:1–11. <https://doi.org/10.3390/biology10020086>
- Sachana M, Willett C, Pistollato F, Bal-Price AK (2021b) The potential of mechanistic information organised within the AOP framework to increase regulatory uptake of the developmental neurotoxicity (DNT) in vitro battery of assays. *Neurodev Toxic.* <https://doi.org/10.1016/j.reprotox.2021.06.006>
- Schettler T (2001) Toxic threats to neurologic development of children. *Environ Health Perspect* 109:813–816. <https://doi.org/10.1289/ehp.01109s6813>
- Schmidt BZ, Lehmann M, Gutbier S, et al (2016) In vitro acute and developmental neurotoxicity screening: an overview of cellular platforms and high-throughput technical possibilities. *Arch Toxicol* 91:1–33. <https://doi.org/10.1007/s00204-016-1805-9>

- Schmidt C (2013) Beyond Uncertainty Factors: Protecting the tails of the bell curve. *Environ Health Perspect* 121:A26–A29. <https://doi.org/10.1289/ehp.121-a26>
- Schmuck MR, Temme T, Dach K, et al (2017) Omnisphero: a high-content image analysis (HCA) approach for phenotypic developmental neurotoxicity (DNT) screenings of organoid neurosphere cultures in vitro. *Arch Toxicol* 1–12. <https://doi.org/10.1007/s00204-016-1852-2>
- Shafer TJ, Brown JP, Lynch B, et al (2019) Evaluation of Chemical Effects on Network Formation in Cortical Neurons Grown on Microelectrode Arrays. *Toxicol Sci* 169:436–455. <https://doi.org/10.1093/toxsci/kfz052>
- Shaw SD, Kannan K (2009) Polybrominated diphenyl ethers in marine ecosystems of the American continents: Foresight from current knowledge. *Rev Environ Health* 24:157–229. <https://doi.org/10.1515/REVEH.2009.24.3.157>
- Shy C-G, Huang H-L, Chang-Chien G-P, et al (2011) Neurodevelopment of infants with prenatal exposure to polybrominated diphenyl ethers. *Bull Environ Contam Toxicol* 87:643–648. <https://doi.org/10.1007/s00128-011-0422-9>
- Sidman RL, Rakic P (1973) Neuronal Migration, with Special Reference to Developing Human Brain: A Review. *Brain Res* 62:1–35. [https://doi.org/10.1016/0006-8993\(73\)90617-3](https://doi.org/10.1016/0006-8993(73)90617-3)
- Silbereis JC, Pochareddy S, Zhu Y, et al (2016) The Cellular and Molecular Landscapes of the Developing Human Central Nervous System. *Neuron* 89:248. <https://doi.org/10.1016/j.neuron.2015.12.008>
- Sild M, Ruthazer ES (2011) Radial glia: Progenitor, pathway, and partner. *Neuroscientist* 17:288–302. <https://doi.org/10.1177/1073858410385870>
- Sjödén A, Patterson DG, Bergman Åke Å (2003) A review on human exposure to brominated flame retardants - Particularly polybrominated diphenyl ethers. *Environ Int* 29:829–839. [https://doi.org/10.1016/S0160-4120\(03\)00108-9](https://doi.org/10.1016/S0160-4120(03)00108-9)
- Spinu N, Bal-Price A, Cronin MTD, et al (2019) Development and analysis of an adverse outcome pathway network for human neurotoxicity. *Arch Toxicol* 93:2759–2772. <https://doi.org/10.1007/s00204-019-02551-1>
- Stiles J, Jernigan TL (2010) The basics of brain development. *Neuropsychol Rev* 20:327–348. <https://doi.org/10.1007/s11065-010-9148-4>
- Sugeng EJ, Leonards PEG, van de Bor M (2017) Brominated and organophosphorus flame retardants in body wipes and house dust, and an estimation of house dust hand-loadings in Dutch toddlers. *Environ Res* 158:789–797. <https://doi.org/10.1016/j.envres.2017.07.035>
- Svendsen CN, Fawcett JW, Bentlage C, Dunnett SB (1995) Increased survival of rat EGF-generated CNS precursor cells using B27 supplemented medium. *Exp Brain Res* 102:407–414. <https://doi.org/10.1007/BF00230645>
- Svendsen CN, Skepper J, Rosser AE, et al (1997) Restricted growth potential of rat neural precursors as compared to mouse. *Dev Brain Res* 99:253–258. [https://doi.org/10.1016/S0165-3806\(97\)00002-3](https://doi.org/10.1016/S0165-3806(97)00002-3)
- Svendsen CN, Ter Borg MG, Armstrong RJE, et al (1998) A new method for the rapid and long term growth of human neural precursor cells. *J Neurosci Methods* 85:141–152. [https://doi.org/10.1016/S0165-0270\(98\)00126-5](https://doi.org/10.1016/S0165-0270(98)00126-5)

- Terron A, Bennekou Hougaard S (2018) Towards a regulatory use of alternative developmental neurotoxicity testing (DNT). *Toxicol Appl Pharmacol* 354:19–23. <https://doi.org/10.1016/j.taap.2018.02.002>
- Tohyama C (2016) Developmental neurotoxicity test guidelines: problems and perspectives. *J Toxicol Sci* 41:Sp69-sp79. <https://doi.org/10.2131/jts.41.SP69>
- Tollefsen KE, Scholz S, Cronin MT, et al (2014) Applying Adverse Outcome Pathways (AOPs) to support Integrated Approaches to Testing and Assessment (IATA). *Regul Toxicol Pharmacol* 70:629–640. <https://doi.org/10.1016/j.yrtph.2014.09.009>
- Tonduti D, Vanderver A, Berardinelli A, et al (2014) MCT8 Deficiency: Extrapyraxidal Symptoms and Delayed Myelination as Prominent Features. *Child Neurol Psychiatry* 28:795–800. <https://doi.org/10.1177/0883073812450944.MCT8>
- Tsuji R, Crofton KM (2012) Developmental neurotoxicity guideline study: Issues with methodology, evaluation and regulation. *Congenit Anom (Kyoto)* 52:122–128. <https://doi.org/10.1111/j.1741-4520.2012.00374.x>
- US EPA (2020) Chemical Safety for Sustainability - Strategic Research Action Plan. US EPA Office of Research and Development. Off Res Dev 2019–2022:
- van der Veen I, de Boer J (2012) Phosphorus flame retardants: Properties, production, environmental occurrence, toxicity and analysis. *Chemosphere* 88:1119–1153. <https://doi.org/10.1016/j.chemosphere.2012.03.067>
- van Tilborg E, de Theije CGM, van Hal M, et al (2018) Origin and dynamics of oligodendrocytes in the developing brain: Implications for perinatal white matter injury. *Glia* 66:221–238. <https://doi.org/10.1002/glia.23256>
- Villeneuve DL, Crump D, Garcia-Reyero N, et al (2014) Adverse outcome pathway (AOP) development I: Strategies and principles. *Toxicol Sci* 142:312–320. <https://doi.org/10.1093/toxsci/kfu199>
- Vinken M, Knapen D, Vergauwen L, et al (2017) Adverse outcome pathways: a concise introduction for toxicologists. *Arch Toxicol* 91:3697–3707. <https://doi.org/10.1007/s00204-017-2020-z>
- Volpe JJ (2000) Overview: Normal and abnormal human brain development. *Ment. Retard. Dev. Disabil. Res. Rev.* 6:1–5
- Volpe JJ, Kinney HC, Jensen FE, Rosenberg PA (2011) The developing oligodendrocyte: Key cellular target in brain injury in the premature infant. *Int J Dev Neurosci* 29:423–440. <https://doi.org/10.1016/j.ijdevneu.2011.02.012>
- Waaijers SL, Kong D, Hendriks HS, et al (2013) Persistence, Bioaccumulation, and Toxicity of Halogen-Free Flame Retardants. In: *Reviews of Environmental Contamination and Toxicology*. pp 1–71
- Walter KM, Dach K, Hayakawa K, et al (2019) Ontogenetic expression of thyroid hormone signaling genes: An in vitro and in vivo species comparison. *PLoS One* 14:1–26. <https://doi.org/10.1371/journal.pone.0221230>
- Wang CC, Li L, Tang LY, Leung PC (2012) Safety evaluation of commonly used Chinese herbal medicines during pregnancy in mice. *Hum Reprod* 27:2448–2456. <https://doi.org/10.1093/humrep/des180>

## References

---

- Wang R, Tang J, Xie Z, et al (2015) Occurrence and spatial distribution of organophosphate ester flame retardants and plasticizers in 40 rivers draining into the Bohai Sea, north China. *Environ Pollut* 198:172–178. <https://doi.org/10.1016/j.envpol.2014.12.037>
- Workman AD, Charvet CJ, Clancy B, et al (2013) Modeling transformations of neurodevelopmental sequences across mammalian species. *J Neurosci* 33:7368–7383. <https://doi.org/10.1523/JNEUROSCI.5746-12.2013>
- World Health Organization (2008) The global burden of disease: 2004 update. WHO Press 1–160
- Yamada KM, Cukierman E (2007) Modeling Tissue Morphogenesis and Cancer in 3D. *Cell* 130:601–610. <https://doi.org/10.1016/j.cell.2007.08.006>
- Yogui GT, Sericano JL (2009) Polybrominated diphenyl ether flame retardants in the U.S. marine environment: A review. *Environ Int* 35:655–666. <https://doi.org/10.1016/j.envint.2008.11.001>

### References for pictures included in Figure 2:

- <https://www.noldus.com/blog/inhibitory-avoidance-learning-zebrafish>
- <https://biotium.com/technology/cellular-stains/>
- <https://www.abcam.com/protocols/phalloidin-staining-protocol>
- <https://science.discoveryplace.org/stay-at-home-science/binary-bracelets>







## Danksagung

An dieser Stelle möchte ich mich bei allen Personen bedanken, die meine Promotion ermöglicht und mich währenddessen unterstützt und motiviert haben.

Ein besonderer Dank gilt Frau Prof. Dr. Ellen Fritsche, die die Anfertigung dieser Arbeit durch die Bereitstellung des sowohl sehr interessanten als auch zukunftsversierten Themas ermöglicht hat. Durch ihre umfassende Betreuung, Unterstützung und Förderung während der gesamten Promotionszeit konnte ich mich beruflich und auch persönlich sehr weiterentwickeln.

Bei Frau Prof. Dr. Vlada Urlacher bedanke ich mich besonders für die fakultätsübergreifende Betreuung und die Übernahme der Mentorenschaft, durch die meine Dissertation erst ermöglicht wurde.

Ein weiterer Dank geht an meine Betreuerin Dr. Julia Tigges, die mich jederzeit unterstützt hat. Danke für das ganze Diskutieren meiner vielen Daten, den dazugehörigen Durchblick, das schnelle und kompetente Korrigieren aller Schriftstücke und vor allem danke für die Hilfsbereitschaft.

Vielen Dank an all meine ehemaligen und derzeitigen Arbeitskollegen der AG Fritsche für die Hilfe und Unterstützung bei dem ein oder anderen Experiment und besonders für die super Arbeitsatmosphäre mit jeder Menge Spaß und Gesprächsstoff.

Ein großer Dank geht an diejenigen, die die Konferenzen in Texas, Brüssel, Hannover, Düsseldorf und Helsinki (besonders durch Alkohol, speziell Rotwein) unvergesslich gemacht haben. Es waren unfassbar tolle Tage und eine großartige Zeit. Nicht zu vergessen sind natürlich die feuchtfröhlichen Weihnachtsfeiern und Grillabende, welche durch die AG Fritsche besonders lebhaft gestaltet wurden. Zusätzlich möchte ich die kulinarischen Donnerstage erwähnen.

Außerhalb der wissenschaftlichen Arbeit bedanke ich mich besonders bei Farina, Laura und Kristina. Danke für eure ständig offenen Ohren und tiefgründigen Gespräche. Aus Arbeitskollegen sind Freunde geworden!

Speziell möchte ich mich bei Farina für all die Urlaube, Trips und vielen Cocktailabende bedanken, die in den letzten Jahren für die nötige Abwechslung gesorgt haben.

Zuletzt und mit besonderer Ehre bedanke ich mich bei meinen Eltern und meiner großen Schwester für die unermüdliche Unterstützung in jeglicher Hinsicht, für die ständige Motivation und Geduld und vor allem für den nötigen Rückhalt während des gesamten Studiums und der Promotion. Danke für das kommentarlose Hinnehmen der vielen pessimistischen Phasen.

Vielen, vielen Dank für alles!

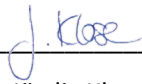


## Eidesstattliche Erklärung/Declaration

Hiermit versichere ich an Eides statt, dass die vorliegende Dissertation „Phenomik und Transkriptomik angewendet in Wirkmechanismus-Analysen für die Entwicklungsneurotoxizität mehrerer Substanzklassen *in vitro*“ von mir selbständig und ohne unzulässige fremde Hilfe unter Beachtung der „Grundsätze zur Sicherung guter wissenschaftlicher Praxis and der Heinrich-Heine-Universität Düsseldorf“ erstellt worden ist. Die Dissertation wurde in der vorgelegten oder einer ähnlichen Form noch bei keiner anderen Institution eingereicht. Ich habe bisher keine erfolglosen Promotionsversuche unternommen.

I declare that I have developed and written the enclosed thesis ‘Phenomics and transcriptomics applied in mode-of-action analyses for developmental neurotoxicity of several compound classes *in vitro*’ completely by myself, and have not used sources or means without declaration in the text. Any thoughts from others or literal quotations are clearly marked. The thesis was prepared in compliance with the principles of ‘Good Scientific Practice at the Heinrich-Heine-University Dusseldorf’. The thesis was not used in the same or in a similar version to achieve an academic grading elsewhere.

Düsseldorf, den ..... 22.06.2021 .....

  
\_\_\_\_\_  
Jördis Klose